NUCLEAR ASTROPHYSICS

by

A.G.W. Cameron

Second Edition

Based on Lectures Given at Yale University
1965 - 66

Compiled by:

S. Edelstein
W. Langer
D.W. Watkins

This is an extensive revision of the first edition which was based on lectures given at Yale University, 1962-63, and compiled by

W.D. Arnett
C.J. Hansen
J.W. Truran

Nuclear Astrophysics

A. G. W. Cameron

Table of Contents

Preface 1

Part A. NUCLEAR PHYSICS 2

1. Nuclear Forces 2
2. Nuclear Masses 18
3. Particle Orbits in Nuclear Potential Wells 47
4. Nuclear Level Densities 79
5. Nuclear Reactions 109
   - Nuclear Reaction Channels 110
   - Cross Section 112
   - The Logarithmic Derivative 124
   - Reciprocity Theorem for Nuclear Reaction 137
   - Compound Nucleus, Continuum Theory 142
   - Determination of Cross Sections, Continuum Theory 146
   - Decay of Compound Nucleus; Competition Evaporation Model 151
   - Nuclear Resonances 156
   - Particle Widths 163
6. Gamma Ray Transitions 166
   - Selection Rules 169
   - Probability of Multipole Emission and Absorption 172
   - Transition to Quantum Mechanics 175
   - Emission and Application 177
   - The Matrix Elements 178
   - Transitions Between Low-Lying States of Nuclei 181

Transitions Involving Highly Excited States 186
Sum Rules 187
Estimates of Matrix Elements Involving Highly Excited Nuclear States 190
Radiative Capture of Neutrons 197
7. Nuclear Beta Decay 204
History and Introduction 204
The Neutrino Hypothesis and the Shape of the Beta Spectrum 210
Orbital Electron Capture 230
Half-Lives of Beta Emitters 236
The Nuclear Matrix Element 244

Part B. STELLAR PHYSICS 1

8. Introduction 1
9. The Virial Theorem and Some Consequences 19
10. Physical Conditions in Stellar Interiors 46
General Remarks 46
Electron Degeneracy 61
Polytropes 70
11. Thermonuclear Reaction Rates 75
Non-resonant Reactions 75
Resonant Reactions 82
Application of Dispersion Theory of Nuclear Reactions 84
Electron Screening 98
Weak Screening 103
Strong Screening 105
Pycnonuclear Reactions 108
Temperature Sensitivity 114
12. Hydrogen Thermonuclear Reactions 116
The $D^2(p,\gamma)\,He^3$ Reaction 119
Neutron Production During Deuterium Burning 129
Proton-Proton Chains 136
The Remaining Reactions 149

Energy Generation Rates 153

CNO Cycles 157

Ne-Na Cycle 160

13. Stellar Models and Evolution 170

Boundary Conditions 171

Theory of Convection 176

Gravitational Energy Source 179

Characteristics of Stars on The Main Sequence 192

Evolution off the Main Sequence 196

Evolution of Massive Stars 201

Evolution of Stars of About One Solar Mass 204

Mass Loss in Evolving Stars 207

14. Helium Thermonuclear Reactions 209

The C^{12} $(\alpha,\gamma)O^{16}$ Reaction 219

O^{16} $(\alpha,\gamma)Ne^{20}$ 223

Pycnonuclear Reactions 245

Minor Reactions 253

15. Neutron Capture on a Slow Time Scale 262

Solution of the Abundance Equations 263

16. A New Table of Abundances of the Elements in the Solar System 276

17. Photobeta Reactions 313

18. Heavy Ion Thermonuclear Reactions 331

19. Photonuclear Reactions 336

Preface

The second edition of these nuclear astrophysics notes has been divided into two parts:

A. Nuclear Physics

B. Stellar Physics

Since the first edition of these lecture notes was compiled, a series of lecture notes and reprints of recent work on the advanced stages of stellar evolution has been published (A.G.W. Cameron, W.D. Arnett, A. Gilbert, C.J. Hansen, J.W. Truran, and S. Tsuruta, "High Density Astrophysics," in High Energy Astrophysics, Vol. III, ed. by C. DeWitt, E. Schatzman, and P. Veron, Gordon and Breach, New York, 1967). The present set of lecture notes is intended to supplement these and deals with basic nuclear physics and the earlier stages of stellar evolution. Part A is entirely new and Part B is selected from the first edition with substitution of new material for the chapter on abundances. Since most of Part B is now several years old, it should be read only for the benefit of the basic ideas involved. More recent literature should be consulted for the best values of nuclear reaction rates, stellar models, and similar material.

Attention is also called to a survey paper: "Stellar Evolution: A Survey With Analytic Models," by Robert F. Stein, in Stellar Evolution, ed. by R.F. Stein and A.G.W. Cameron, Plenum Press, New York, 1966. This is very useful for obtaining an understanding of the basic nature of stellar evolution where there is not too much concern for accurate numerical details.

Part A. NUCLEAR PHYSICS

1. Nuclear Forces

Much work has been done in the last few decades in connection with nuclear forces. Some of it has been an intensive study into the kinds of interactions into which individual nucleons can enter in collisions at high energy. These techniques have been rather successful, considering the difficulties in accounting for some of the detailed properties of nuclear matter and even of nuclei themselves. In the main, one puts into such considerations the measured interaction properties of nuclear collisions at high energies, the different phase shifts that correspond to the various partial waves which can participate in the interactions, and so on. So in no sense can we say that we understand and can easily predict the properties of nuclear forces in the same sense that we say we understand electromagnetic field phenomena, where we believe that we know the basic laws, even if perhaps we don't understand the deepest meaning of the laws as well as we might like. Thus in the case of nuclear forces we don't know even what the basic laws are; so the subject is necessarily on a largely empirical basis which perhaps will disappear gradually as

high energy experiments continue to be performed. Nevertheless, it is not likely that any very simple description of nuclear forces will be developed, because nuclear forces depend on so many different things, as we shall see.

At low energies, principal sources of information come from the measured properties of the deuteron and from n-p and p-p scattering experiments; so first we examine some properties of the deuteron. The magnetic moment of the proton is $\mu_p = 2.79270$ nuclear magnetons. The nuclear magneton, M_N, is similar to the Bohr magneton defined for the electron, $M_B = \frac{e\hbar}{2m_e c}$, but with m_p, the mass of the proton, replacing m_e, the mass of the electron. The magnetic moment of the neutron is $\mu_n = -1.91316\ M_N$ and adding these together, we have

$$\mu_p + \mu_n = 0.87975\ M_N \quad .$$

Adding μ_p and μ_n together this way assumes that the spin of the neutron and proton are parallel. The measured magnetic moment of the deuteron turns out to be $0.857395\ M_N$, and even though this is not exactly $\mu_p + \mu_n$, it is nearly the same. Also, the spin of the deuteron is known from experiment to be 1, in units of $\hbar$, and from these two considerations we may say that the ground state of the deuteron is given to a good approximation by a neutron and

proton bound together with their spins parallel. Then, to a good approximation, one can describe the state in standard spectroscopic notation as a $^3S_1$ state. We denote the state by "S" because the orbital angular momentum, L, of the neutron and proton in the deuteron is zero; the "1" means that the total angular momentum, the vector sum of the spin and orbital angular momenta, is 1 in units of $\hbar$, and the "3" is twice the nuclear spin plus 1: 2x1+1 = 3. We say that the neutron-proton system has no orbital angular momentum because we have accounted for all the measured angular momentum of the deuteron in terms of the spin of the neutron and proton, leaving no room for orbital angular momentum.

However the situation is not quite this simple because the deuteron has been found to have a quadrupole moment $Q = 2.74 \times 10^{-27}$ cm^2. The quadrupole moment measures the departure from spherical symmetry of the charge distribution of an object. It is worthwhile to compare this with the area to be associated with the deuteron. Using some decent wave function for the ground state, the deuteron radius is found to be relatively large, $R \sim 4.31 \times 10^{-13}$ cm and so the cross-sectional area, πR^2 is about 600×10^{-27} cm^2,

and so even though the measured quadrupole moment is finite, it is relatively small. But the fact that a quadrupole moment exists for an apparently simple two body system indicates that the nuclear forces acting cannot be completely central forces: there must be some noncentral character to these nuclear forces.

To account for the existence of Q, one finds that it is necessary to mix into the deuteron ground state a fraction of noncentral forces, called tensor forces, which would correspond to a non-zero angular momentum of the deuteron. Since parity conservation is violated in nuclear physics only in weak interactions, such as beta decay, we cannot allow any admixture of L = 1 or P state into the ground state. If we had some fraction of P wave, then we could represent the ground state wave function for the deuteron as

$$\psi = \varphi_s + \varphi_p$$

but the parity of φ_s is even, while that of φ_p is odd; so ψ has no definite parity and is not a suitable wave function for the ground state of deuterium. Thus we are compelled to go up to L = 2, or D wave, in this case $^3D_1$, and the

deuteron ground state turns out to be about 96% of $^3S_1$ and 4% $^3D_1$.

Now the deuteron has only one bound state, the ground state; no bound excited states exist. It is easy to imagine a simple neutron-proton state other than the ground state; one example is a neutron and proton with spins opposed, a $^1S_0$ state. But the singlet state of the deuteron is not observed to be bound, and therefore corresponds to a state in the continuum of the neutron-proton states. The fact that these two states of the deuteron behave quite differently, one being bound and the other unbound, indicates that nuclear forces are spin dependent. This leads to the inclusion of such objects as spin exchange operators into nuclear theory.

Apart from the deuteron, considering nucleon-nucleon forces in general, one significant feature emerging from nuclear studies is that for the same quantum state, nuclear forces are charge independent. Typical examples of mirror nuclei include the pairs

$$_{10}Ne^{21},\ _{11}Na^{21};$$
$$_{11}Na^{23},\ _{12}Mg^{23};$$
$$_{12}Mg^{25},\ _{13}Al^{25};$$

etc.

These pairs are mirror in the sense that whatever configuration the neutrons and protons one of the pairs has, the other has the reverse configuration. For example ${}_{10}Ne^{21}$ has ten protons and eleven neutrons; ${}_{11}Na^{21}$ has eleven protons and ten neutrons. We can get ${}_{11}Na^{21}$ from ${}_{10}Ne^{21}$ by replacing a neutron with a proton in the same quantum state which is a part of the ground state configuration.

One of the things which contributes to the mass of a nucleus is the electrostatic energy corresponding to confinement of the nuclear protons within nuclear dimensions. This energy is called the electrostatic or Coulomb energy of the nucleus: one must do work in bringing charges up from infinity into the nucleus and the total work done is the Coulomb energy of the nucleus. It is apparent that mirror nuclei will differ due to the fact that one has one more proton than the other. To a first approximation, the difference in energy between these pairs of mirror nuclei, which can result in the beta decay of one nucleus into the other, arises solely from this Coulomb energy difference. When one makes careful measurements, however, one finds that there are slight additional energy differences between these nuclei, but these additional differences that arise

are also due to the difference in charge. The difference is due to the level shift phenomenon. If the neutron replaced has a certain kind of orbit inside the nucleus, then the proton that replaces it will have a similar orbit. The orbit in general will be perturbed by the electrostatic interaction which exists for the proton, but not for the neutron, and the residual energy differences can be precisely understood in terms of the perturbations of the orbits that occur as a result of the electrostatic interaction. These small energy differences or level shifts are closely related to the validity of description of the ground states of the mirror nuclei as that of a nuclear core plus an additional nucleon, proton or neutron, in orbit about that core. The result in every case is that the entire difference in energy between the states arises strictly from the charge differences, not from any intrinsically nuclear force effects; and we therefore conclude that nuclear forces are charge independent.

This charge independence of nuclear forces permits description of the neutron and proton as essentially two different states of some fundamental particle which we shall call the nucleon. The quantum number which is

assigned to mark this difference between the two states is called the isotopic spin or isospin, and the convention is that the proton has an isospin of + $\frac{1}{2}$, the neutron, - $\frac{1}{2}$, and this quantum number suffices to distinguish these two states of the nucleon. It was seen above that a neutron and proton can join together to form a bound system, the deuteron. Since nuclear forces are charge independent, the question naturally arises whether we might have two neutrons paired together to give a bound system called, say, the dineutron, or two protons formed into a diproton, the isotope $_2He^2$. The answer in both cases is negative. The Pauli exclusion principle states that no two fermions, elementary particles of spin $\frac{1}{2}$, may exist in the same quantum state. In the p-n bound state, the deuteron, the spins of p and n are aligned, but their isospin quantum numbers are different; so the Pauli principle admits the $^3S_1$ state as physically acceptable. But in the case of two neutrons, this $^3S_1$ state is forbidden because the neutrons have the same isospin quantum numbers, and if they are placed with their spins aligned, they would have the same set of quantum numbers. The other possible way to fabricate a nuclear system from two neutrons is to place

them with spins opposed, corresponding to the singlet state of the deuteron. In the deuteron, there is no electrostatic repulsion between the neutron and the proton, and neither will there be any electrostatic interaction between the neutrons in the proposed dineutron singlet. Since nuclear forces are charge independent, the specifically nuclear forces between the two neutrons will be the same as those between the proton and neutron. The singlet state of the deuteron is known not to be bound, and therefore neither is the dineutron. For the diproton, similar reasoning prohibits any bound states; in fact, the diproton states lie higher in the continuum of nucleon-nucleon energy levels than the dineutron states because of the added feature of Coulomb repulsion between the two positively charged protons. Mention will be made later about very short-lived "diprotons" when the basic reaction in the proton-proton chain is discussed under nucleosynthesis.

Next consider many-particle systems. It is convenient in discussing nuclear interactions to introduce a scale of length appropriate to the smallness of the nucleus. The characteristic length usually chosen is the fermi (fm) equal to 10^{-13} cm. Scattering experiments show that

particles must come within one or two fermis before they interact significantly. We found before that the approximate radius of the deuteron ground state is about 4.3 fm, and so the neutron and proton forming the ground state of the deuteron are almost beyond the range of nuclear forces. As more nucleons are added, the size of the system decreases and the binding energy per particle increases. The binding energy of the deuteron is only about 2.23 MeV, and if we go up to tritium or He^3, adding one more nucleon, the binding energy increases to about 8 MeV (8.49 MeV for H^3, 7.73 MeV for He^3). Adding one more nucleon to make an alpha particle, He^4, the total binding energy goes up to 28 MeV, 7 MeV per particle. Beyond this point, the nuclear forces begin to saturate. As we continue to assemble nucleons to form heavier and heavier nuclei, the binding energy per particle increases slowly until Fe^{56} where the binding energy per nucleon is about 8.5 MeV. Beyond Fe^{56}, nuclei have somewhat less binding energy per particle; so in the region around iron, the binding energy per nucleon reaches a maximum, a fact which will have far-reaching effects in the discussion of nuclear statistical equilibrium and abundances of nuclei made by processes of nucleosyn-

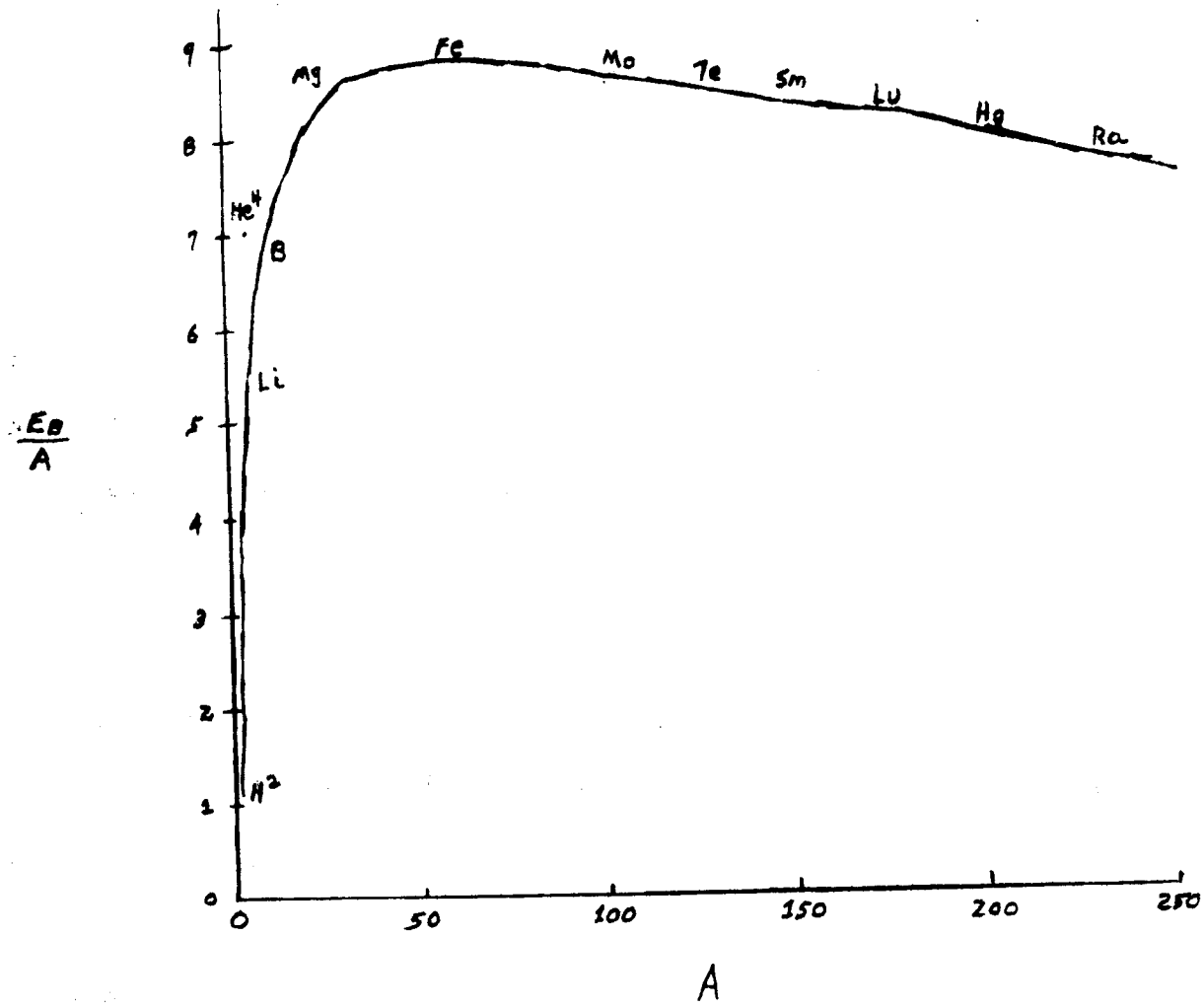

Figure 1.1

The nuclear binding energy per nucleon as a function of the mass number A.

thesis to follow. For the present, however, the essential feature to note is that the nuclear binding forces tend to saturate so that nuclear densities stabilize at about the same value.

Much effort has been made to measure nuclear radii. Experimentally one may attempt measurement in terms of the effective size of the object which undergoes a nuclear interaction with some sort of bombarding particle, or one may instead bombard nuclei with high energy electrons, observe the resultant scattering, and deduce something about the size and charge distribution of the nucleus. Electron scattering experiments indicate a somewhat smaller size for the nucleus than nucleon scattering experiments, and it is easy to see why: nuclear forces have a significant strength over a range of a fermi or two, even though we describe them as being of short range, and so the nucleus looks somewhat larger to a nuclear probe than it does to an electron which interacts only with the Coulomb field of the nucleus. In the main, however, all these experiments indicate that beyond helium the radius of the nucleus goes as the cube root of the number of particles in the nucleus:

$$R = r_o A^{1/3} \tag{1.1}$$

where r_o is a constant, in the neighborhood of 1.2 fm, and A is the nuclear mass number, and this is a good empirical indication that nuclear matter inside the heavier nuclei has approximately constant density from one nucleus to another. Hence nuclear forces are attractive at larger distances but repulsive at short distances.

In recent years, refined electron scattering experiments have indicated that it is not really proper to describe the nucleus as the equation above implies, as a sphere of uniform density which is sharply cut off at some definite radial distance. Rather, it seems, the nucleus has a finite edge in which the nuclear density, ρ, decays from its essentially constant central value down to zero something like this:

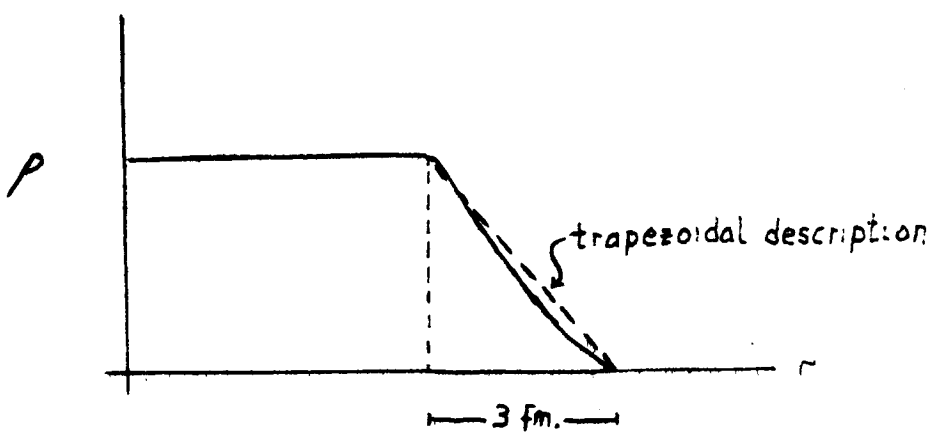

Figure 1.2

One especially useful description of this density variation is the trapezoidal approximation shown in which ρ assumes a constant density out to some value of r and then decays linearly. The radius can then be described as the point at which the density has fallen to half of its central value. The length over which the nuclear density decays is about 3 fermis. The trapezoidal approximation is a fairly good description and will be used in calculations, such as finding the electrostatic energy of the nucleus in the nuclear mass formula.

One might wonder whether the central density remains the same for lighter and medium weight nuclei, where the number of protons and neutrons is about the same and for heavy nuclei where the neutron excess may be rather large, since the nuclear forces might conceivably be somewhat different in the two cases. Experimental evidence is that the nuclear density does stay constant even though the proton-neutron proportion varies. This fact is significant when we wish to discuss the kinetic energy of nucleons as if the nucleons were particles confined to a box. When the neutron-proton proportion is varied, keeping the number of nucleons in the box the same, we have some experimental

assurance that we may regard the volume of the box as unchanged.

The Pauli principle enables one to make a further observation regarding the general properties of nuclear matter. Consider a rather heavy nucleus in its ground state, where the nucleus has the lowest energy available. According to the Pauli principle, all the available nucleon states are filled in order from the lowest state upwards with one particle of given spin per quantum state until all the nucleons have been placed. This means that if we consider any one of these nucleons wandering about inside the nucleus, it is not possible for the nucleon to collide in any meaningful way with any of the other nucleons because there is no unoccupied state nearby into which scattering could take place. Thus the wandering nucleon may journey a long way through nuclear matter without undergoing any scattering interactions with its neighbors. This fact in turn implies that it is valid to consider nucleons in a ground state nucleus as drifting about in some average nuclear potential well, having considerable time to explore fully the boundaries of the well. This picture is the basis for the independent particle model of the nucleus,

which was eventually modified to give the more useful shell model of the nucleus.

References

de Benedetti, S. 1964, Nuclear Interactions, J. Wiley and Sons, Inc., New York.

Blatt, J.M. and Weisskopf, V.F. 1952, Theoretical Nuclear Physics, J. Wiley and Sons, Inc., New York.

Elton, L.R.B. 1959, Introductory Nuclear Theory, Interscience Pub., Inc., New York.

Fermi, E. 1950, Nuclear Physics (compiled by Orear, J., Rosenfeld, A.H., and Schulter, R.A.), University of Chicago Press, Chicago.

Preston, M.A. 1962, Physics of the Nucleus, Addison-Wesley Pub. Co., Reading, Mass.

2. Nuclear Masses

Another useful way to look at the nucleus is given by the Fermi gas model of the nucleus. Later, the same sort of manipulations will be used to treat electrons in building up an equation of state that applies to matter in white dwarf stars. Suppose we have a number of neutrons and protons confined to a box with infinitely high potential walls, and for convenience, let the box be cubic. Inside the box, the wave function, U, describing any one of the nucleons satisfies the Schrödinger equation:

$$-\nabla^2 U = \frac{2mE}{\hbar^2} U = \frac{p_x^2 + p_y^2 + p_z^2}{\hbar^2} U. \qquad (2.1)$$

Outside the box, and at the walls of the box, U = 0. If we agree to put the cube in the first octant with one corner at (0,0,0) and the diagonally opposite corner at (L,L,L), where L is the edge of the cube, then the boundary conditions on U are

$$U = 0 \text{ at } x,y,z = 0,L\ . \qquad (2.2)$$

The solution is

$$U = \left(\frac{2}{L}\right)^{3/2} \sin\frac{p_x x}{\hbar} \sin\frac{p_y y}{\hbar} \sin\frac{p_z z}{\hbar}$$

and to satisfy the boundary conditions on U,

$$\frac{Lp_i}{\hbar} = n_i \pi \qquad i = x,y,z. \qquad (2.3)$$

where n_i are positive integers. We wish now to find the number of states with momentum less than the momentum p that corresponds to the energy E of the particle, that is states for which

$$p_x^2 + p_y^2 + p_z^2 < p^2 \qquad (2.4)$$

or in terms of the allowed values of p_i we found above,

$$(n_x^2 + n_y^2 + n_z^2) < \frac{p^2 L^2}{\pi^2 \hbar^2} \qquad (2.5)$$

Now the n_i are all positive integers and for each triplet (n_x, n_y, n_z), there is a corresponding momentum state; so let us imagine the points (n_x, n_y, n_z) as a lattice network in the first octant of a momentum space where the coordinate axes are n_x, n_y, n_z, and each point of the space corresponds to a possible momentum of the nucleon. For our particle, only certain momenta are allowed and so only a discrete array of points in the space are of interest. The number of states with momentum less than p is the same as the number of

lattice points in the first octant contained within a sphere of radius $\frac{pL}{\pi\hbar}$ in the momentum space:

Figure 2.1

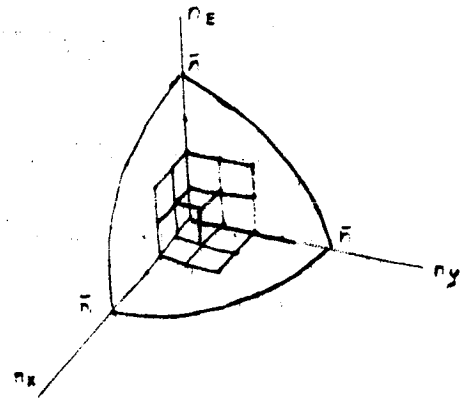

Lattice points representing combinations of integers $n_x n_y n_z$.

$\bar{n} = \frac{pL}{\pi\hbar}$

The number desired is clearly

$$n = \frac{1}{8}\,\frac{4}{3}\,\pi\left(\frac{pL}{\pi\hbar}\right)^3 = \frac{p^3\Omega}{6\pi^2\hbar^3} \qquad (2.6)$$

where $\Omega = L^3$, the volume of the box in which the nucleons are confined. Similarly the number of states dn with momentum between p and p + dp will be

$$dn = \frac{p^2\Omega}{2\pi^2\hbar^3}\,dp\ . \qquad (2.7)$$

This equation says that the number of available states with momentum p is proportional to p^2, and this is also the essential relation which is used in astrophysical applications in calculating the equation of state of a degenerate electron gas. Now nucleons, as well as electrons, are particles with spin $\frac{1}{2}$: they are fermions and obey the Pauli exclusion

principle. If we say that we have complete degeneracy in the available states, we mean that the states are filled to capacity from the bottom upward until the supply of particles has been exhausted and no particles are to be found above a certain level, called the Fermi level, labelled p_F. And one often refers to this maximum momentum that particles in a degenerate gas may have as the Fermi momentum, the corresponding energy as the Fermi energy, or simply the Fermi level of the gas. A careful examination of the problem indicates that the exact shape of the confining box is immaterial.

What is the Fermi momentum for the Z protons in the nuclear gas? Write

$$Z = \int_0^Z dn = \int_0^{p_F} 2 \times \frac{p^2 \Omega}{2\pi^2 \hbar^3} dp = \frac{\Omega p_F^3}{3\pi^2 \hbar^3} \qquad (2.8)$$

allowing for occupation of each momentum state by two protons of opposite spin, one up, one down. Solving (2.8) for p_F, the Fermi momentum for protons is

$$\text{protons} \qquad p_F = (3\pi^2)^{1/3} \hbar \left(\frac{Z}{\Omega}\right)^{1/3} \qquad (2.9)$$

In the same way, for the N = A-Z neutrons in the nuclear

gas, the Fermi momentum for neutrons is

$$\text{neutrons} \qquad p_F = (3\pi^2)^{1/3}\,\hbar\left(\frac{N}{\Omega}\right)^{1/3} \tag{2.10}$$

If now we take $\Omega = \frac{4}{3}\pi r_o^3 A$ as the volume enclosing the gas, the corresponding Fermi energies are

$$\text{protons} \qquad E_F = \frac{p_F^2}{2M} = K\left(\frac{Z}{A}\right)^{2/3} \tag{2.11}$$

$$\text{neutrons} \qquad E_F = \frac{p_F^2}{2M} = K\left(\frac{N}{A}\right)^{2/3} \tag{2.12}$$

where $K = \left(\frac{9\pi}{4}\right)^{2/3} \cdot \hbar^2/2Mr_o^2$, and M is the mass of a nucleon. The assumption made in the calculation above is that the levels for protons and for neutrons fill independently: no exclusion principle forbids occupancy of the same quantum state by two unlike fermions such as protons and neutrons whose isospins are different.

To find the total kinetic energy of all the protons, sum the energy corresponding to each momentum state over all the momentum states:

$$E_Z = \int_o^Z E_n dn = \int_o^{p_F} 2\,\frac{p^2}{2M}\,\frac{p^2\Omega}{2\pi^2\hbar^3}\,dp = \frac{\Omega}{10\pi^2\hbar^3 M}\,p_F^5 \tag{2.13}$$

or

$$E_Z = \frac{3}{5} ZE_F \tag{2.14}$$

and similarly for neutrons,

$$E_N = \frac{3}{5} NE_F \ . \tag{2.15}$$

Now let us consider what happens to the kinetic energy of the nucleons if we have a specific mass number, A, for the nucleus, as we argued before, a corresponding volume, and we vary the relative numbers of neutrons and protons while maintaining the total number of nucleons constant. It is convenient to write this kinetic energy in terms of the excess energy over the case for N = Z; that is, the zero of the energy scale will occur when the number of neutrons is equal to the number of protons. Define

$$\Delta = \frac{1}{2} A-Z \tag{2.16}$$

from which it follows that $N = A-Z = \frac{1}{2} A + \Delta$ (2.17)

and

$$\delta E = E_N(N) + E_Z(Z) - E_N(\tfrac{1}{2}A) - E_Z(\tfrac{1}{2}A) . \tag{2.18}$$

We can evaluate the expression for δE using the relations developed above, equations (2.11), (2.12), (2.14), and (2.15):

$$\delta E = \frac{3K}{5A^{2/3}} \left\{ N^{5/3} + Z^{5/3} - \left(\frac{1}{2} A\right)^{5/3} - \left(\frac{1}{2} A\right)^{5/3} \right\} \quad (2.19)$$

$$= \frac{3K}{5A^{2/3}} \left\{ \left(\frac{A}{2} + \Delta\right)^{5/3} + \left(\frac{A}{2} - \Delta\right)^{5/3} - 2\left(\frac{A}{2}\right)^{5/3} \right\} \quad (2.20)$$

Expanding (2.20) to powers in Δ^2,

$$\delta E = \frac{3K}{5A^{2/3}} \left\{ \left(\frac{A}{2}\right)^{5/3} + \frac{5}{3}\left(\frac{A}{2}\right)^{2/3} \Delta + \frac{5}{9}\left(\frac{A}{2}\right)^{-1/3} \Delta^2 + \left(\frac{A}{2}\right)^{5/3} \right.$$

$$\left. - \frac{5}{3}\left(\frac{A}{2}\right)^{2/3} \Delta + \frac{5}{9}\left(\frac{A}{2}\right)^{-1/3} \Delta^2 - 2\left(\frac{A}{2}\right)^{5/3} \right\} \quad (2.21)$$

$$= \frac{3K}{5A^{2/3}} \cdot \frac{10}{9}\left(\frac{A}{2}\right)^{-1/3} \Delta^2 \quad (2.22)$$

$$\delta E = \frac{2^{4/3}}{3} K \frac{\Delta^2}{A} \quad (2.23)$$

Equation (2.23) states that as we depart from $N = \frac{1}{2} A = Z$, the energy of the nucleus increases as Δ^2; there is an energy advantage to be gained by letting the number of neutrons equal the number of protons in a given confined volume. It is more convenient for discussion to put

$$\delta E = \frac{2}{3} K A \left[\frac{(A-2Z)^2}{A^2} \right] \quad (2.24)$$

and to call the quantity in brackets the symmetry energy

of a nucleon in the nucleus and A times the bracket is then proportional to the symmetry energy of the entire nucleus. This is one of the terms that enters into the mass formula, to be discussed next.

The details of nuclear theory are not sufficiently well understood to permit a calculation of nuclear masses from first principles; so semiempirical formulas, much like the one introduced in 1935 by von Weizsäcker, must be used. These formulas are sums of terms proportional to quantities chosen for physically compelling reasons and coefficients which can be determined from experimental data such as energy differences between mirror nuclei, the position of the valley of beta stability and measured nuclear masses. These formulas, strictly speaking, are atomic, rather than nuclear, mass formulas because the masses of the Z electrons accompanying the nucleus as well as the binding energies of the electrons to the atom are included. But the electron binding energies are negligible on the nuclear scale, and the electron masses are rather small; so virtually all the contributions to the atomic mass formula are of nuclear character.

A remark concerning the atomic unit of mass is in order. Until 1962, the physical unit of mass was 1/16 the mass of the isotope O^{16}. (The chemists used a slightly different unit of mass, defined as 1/16 the average weight of naturally occurring oxygen.) Oxygen has three naturally occurring isotopes, O^{16}, O^{17}, and O^{18}, and oxygen from different sources has slightly differing abundances in the three isotopes, leading to difficulty in making refined measurements. Fluorine has only one naturally occurring isotope, F^{19}, and some people wanted to define the unit of mass as 1/19 the mass of F^{19}, but besides being a vigorous poison, fluorine attacks practically all materials known and so would be inconvenient for use in mass spectrometers. The isotope C^{12} was finally agreed upon for use as the standard, a fortuitous choice because the actual numbers involved resulting from use of the standard C^{12} are only slightly different from the data in the literature based on O^{16}. So the standard now is 1/12 the mass of C^{12} instead of 1/16 the mass of O^{16}.

It is convenient to work not directly in terms of mass, but in terms of mass excess, or mass defect the difference between the actual mass of a nucleus, M, and its

mass number, A, in units of MeV. The mass formula may be written as

$$M-A = 8.07134A - 0.782613Z + E_v + E_s + E_{sym}$$

$$+ E_c + E_{ex} + S(Z,N) + P(Z,N) \qquad (2.25)$$

The first term comes from the mass defect of the neutron in MeV, 8.07134, times the number of nucleons in the nucleus, A. From this, we subtract the energy difference between the neutron and hydrogen atom, 0.782613 MeV, times the number of nuclear protons. This much is straight forward: it is the mass excess that an atom would have if its nucleus were a simple collection of neutrons and protons not disturbed by nuclear forces. But energy is released when nucleons are united in a nucleus: this is the binding energy. For large nuclei the binding energy per nucleon is roughly constant and since the nuclear volume is proportional to atomic number A, we should add a negative volume energy $E_v \propto A$.

The concept of a nuclear volume energy presupposes a nucleon completely immersed in a sea of other nucleons all of which are able to interact equally with it. With a nucleon near the nuclear surface, however, fewer nucleons

are able to interact, and so the binding energy will be reduced for nucleons near the nuclear surface. Thus a surface correction term, called the surface energy, E_s, proportional to $A^{2/3}$ should be added. The surface correction term should clearly have a sign opposite to the volume energy term.

The import of equation (2.23) is that as we put nucleons into the nucleus and induce a departure from N = Z, the kinetic energy of the system will increase and thus we should add a symmetry correction term proportional to δE in equation (2.23) to take account of the energy induced by neutron-proton imbalance.

Next we should take account of the Coulombic characteristics of the Z protons in the nucleus in a term E_c, the Coulomb energy. This represents the work done in bringing up the protons to form the nucleus. Thus E_c may be written as

$$E_c = \frac{1}{2}\left(\frac{3Ze}{4\pi R^3}\right)^2 \int_{\substack{\text{sphere} \\ \text{of radius} \\ R}} \frac{d\tau_1 d\tau_2}{r_{12}} \qquad (2.26)$$

that is, one-half the electrostatic interaction energy between all pairs of protons. We have assumed that the

charge associated with each proton is smeared uniformly over the nucleus of radius R. The factor r_{12} represents the distance between any two protons, τ_1 is the element of volume associated with one proton, τ_2, that associated with the other. The factor 1/2 out front is there because the integration counts every pair twice. The result is

$$E_c = \frac{3}{5} \frac{(Ze)^2}{R} .$$

One frequently finds in the literature a similar expression with Z^2 replaced by Z(Z-1). If one uses a Coulomb exchange energy correction as we do, then replacing Z^2 by Z(Z-1) is not correct. The quantity Z(Z-1) arises from considering Z-1 protons distributed over the nucleus and then bringing up a final proton from infinity and computing the work done. Our process effectively assembles infinitesimal bits of charge, smaller than a proton, in calculation of the Coulomb energy. This procedure, however overestimates the Coulomb energy because there are exchange forces which correlate the motions of the nucleons and in particular prevent a pair of protons from approaching too near one another. These exchange considerations imply that if protons are really not allowed to approach each other as

near as the smearing technique used in calculating E_c implies, we must add a correction which we call the Coulomb exchange energy correction E_{ex}. The form of the correction to the Coulomb interaction because of proton exchange may be written (Bethe and Bacher 1936):

$$A = \sum_{i=1}^{Z} \sum_{k=1}^{Z} \int \psi_i^*(x_1)\psi_i(x_2)\psi_k^*(x_2)\psi_k(x_1) \frac{e^2}{r_{12}} d\tau_1 d\tau_2 \tag{2.27}$$

Here i and k refer to states which the protons may occupy, x_1 refers to the position of one proton, x_2, to the position of the other, r_{12} is the separation of x_1 and x_2, $d\tau_1$ refers to the volume occupied by one proton and $d\tau_2$, to that occupied by the other proton. A is clearly symmetric with respect to interchange of states and position because protons are identical, hence indistinguishable particles. This expression may be reduced using Dirac's mixed density

$$\rho_p(x_1,x_2) = \sum_{i=1}^{Z} \psi_i^*(x_1)\psi_i(x_2) \tag{2.28}$$

so that

$$A = \frac{1}{4} \int \frac{e^2}{r_{12}} |\rho_p(x_1,x_2)|^2 d\tau_1 d\tau_2 \tag{2.29}$$

where the integrations are carried out over a sphere of radius R. The eigenfunctions for the particle in a three dimensional box may be written in the form

$$\psi_i = \left(\frac{1}{L}\right)^{3/2} e^{i(\vec{K}_i \cdot \vec{r})} \tag{2.30}$$

and using this, the mixed density we need to find before calculating A is

$$\rho(\vec{r}_1, \vec{r}_2) = \sum_{i=1}^{N} \psi_i^*(\vec{r}_1)\psi_i(\vec{r}_2) = \frac{1}{L^3} \sum_{i=1}^{N} e^{i\vec{K}_i \cdot (\vec{r}_2 - \vec{r}_1)} \tag{2.31}$$

$$= \frac{1}{L^3} \frac{L^3}{4\pi^3} \int_0^{K_p} dK_x dK_y dK_z \, e^{i\vec{K}\cdot\vec{r}} \tag{2.32}$$

where $\vec{r} = \vec{r}_2 - \vec{r}_1$ and we have used the fact that the states are almost continuously distributed in momentum space. The integration may be done expeditiously by choosing the polar axis in the direction of $\vec{r}$. Then

$$\rho(\vec{r}_1, \vec{r}_2) = \frac{1}{4\pi^3} \times 2\pi \int_{-1}^{1} d\mu \int_0^{K_p} K^2 dK \, e^{iKr\mu}$$

$$= \frac{2}{2\pi^2 r} \int_0^{K_p} KdK \sin Kr$$

$$= \frac{1}{\pi^2 r^3} (\sin K_p r - K_p r \cos K_p r) \tag{2.33}$$

where K_p is $1/\hbar$ times the Fermi momentum of the protons in the nucleus. The probability density, ρ^2, has a pronounced maximum for $r = 0$ and falls off rapidly as $K_p r$ becomes greater than unity. This means that there is practically no correlation between the wave functions at two points whose distance is considerably larger than $\lambda_p = 2\pi/K_p$, the shortest deBroglie wave length of any proton in the nucleus. With this expression for the mixed density and with the additional assumption $K_p R >> 1$ (i.e., large atomic weight), we obtain

$$A = \frac{1}{4}\frac{4\pi}{3} R^3 \int_0^\infty \frac{e^2}{r_{12}} \frac{4\pi r_{12}^2 dr_{12}}{(\pi^2 r_{12}^3)^2} \left(\sin K_p r_{12} - K_p r_{12} \cos K_p r_{12}\right)$$

$$= \frac{e^2 R^3 K_p^4}{3\pi^2} = \frac{3^{5/3}}{2^{8/3}} \pi^{-2/3} \frac{e^2 Z^{4/3}}{R} \tag{2.34}$$

And so the exchange energy may be written

$$E_{ex} = - \left(\frac{3^5}{2^8 \pi^2}\right)^{1/3} \frac{e^2 Z^{4/3}}{R} \tag{2.35}$$

Still, there are departures from any smooth law to the actual run of nuclear masses. These departures are correlated with closed shells of nucleons, to be discussed later with

the shell model of the nucleus, and the departures take place in a more or less regular way. At present, there is no adequate way to calculate from basic principles what these corrections should be; so it is usually done empirically. For the present, we simply note the need for some correction to take account of the energy effects of shell structure, and that it will be a function of the neutron and the proton numbers: S(Z,N).

Finally, there is a pairing correction, P(Z,N), which allows for the fact that the masses of adjacent nuclei are subject to odd-even fluctuations due to the fact that it is energetically favorable to have two nucleons of the same kind in the same quantum state with spins opposed. As illustration, suppose some nucleus to be composed of closed proton shells with one additional proton in an outer shell. The next proton added can go into the same quantum state as the outer proton if we allow their spins to be opposite. We say that the outer protons are paired, and there is an energy associated with the pairing which would not be there if, in violation of the Pauli principle, the two protons could simply sit there in the outer shell without regard to their spins. The same sort of story can be told for

neutrons; so the pairing energy is a function of both proton and neutron number.

In the past, when the nuclear radius R was not well known, it was considered that the entire Coulomb energy $E_c \sim \frac{(Ze)^2}{R}$ should be regarded as uncertain and subject to empirical adjustment. Under such circumstances the exchange term E_{ex}, which is small with respect to E_c, especially for large Z, was ordinarily left out. The shell and pairing corrections were also omitted and one considered

$$M-A = 8.07134A - 0.78261Z + \alpha A + \beta A^{2/3} + \gamma A\left[\frac{(A-2Z)^2}{A^2}\right] + \delta\frac{(Ze)^2}{R} \tag{2.36}$$

with four coefficients, α, β, γ, and δ to be determined. How might one attack the problem of determining the coefficients?

One property about nuclei known independently of their measured masses was their stability against beta decay.

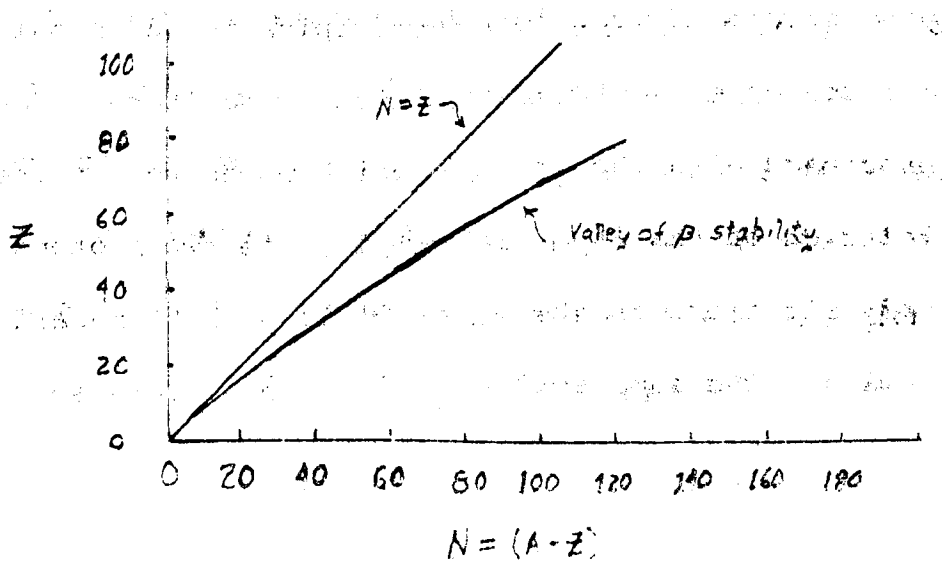

Figure 2.2

Referring to Figure 2.2, lighter nuclei have approximately equal numbers of neutrons and protons and so the stable light nuclei lie close the the 45° line N=Z. As we pass to medium and heavy weight nuclei, we begin getting stable nuclei with larger and larger neutron-over-proton excess, and so the region of stable nuclei gradually curves away from the Z=N line. A line running through the center of the stable nuclei is called the valley of beta stability. It is called a valley because the energies of nuclei to either side of it are higher than those in the valley. To the left of the valley, nuclei are proton rich and tend to undergo positron decay into the valley; to the right the nuclei are neutron rich and tend to decay by electron emission to reduce their energies. Thus the mass excess, M-A, is least in the valley of beta stability. The condition, then, for the valley of beta stability for a given Z is that $\frac{\partial(M-A)}{\partial Z} = 0$. The volume and surface energy terms in (2.36) contain only A and so drop out in the derivative, but both the symmetry energy and Coulomb energy terms survive, and we have the opportunity of determining two coefficients, γ and δ, in the mass formula. For every value of the mass number A for which we know the correspond-

ing Z on the valley of beta stability, we have one approximate solution to the equation $\frac{\partial M}{\partial Z} = 0$; so we have a problem which is greatly overdetermined and which is thus amenable to a least squares solution to determine the coefficients for the symmetry energy and for the Coulomb energy. When these are determined, one may compare the complete mass formula directly with measured masses which constitutes a greatly overdetermined problem for α and β, the coefficients for the volume and surface energy terms. It was this method that was used by von Weizsäcker and others after 1935.

In the middle 1950's the high energy electron scattering experiments which were carried out at Stanford established rather well the size of the nucleus. It was mentioned earlier that the scattering data are accommodated best not by assuming that R is strictly proportional to $A^{1/3}$, but rather by assuming that the central nucleon density is constant. This leads to the expression for nuclear radii, defined as the distances to the half-central-density point in the trapezoidal model:

$$R = 1.112A^{1/3}\left[1 - \frac{0.62025}{A^{2/3}}\right] \text{fm}. \tag{2.37}$$

With the Stanford data, it is no longer necessary to regard R as a poorly known quantity, and therefore the Coulomb energy need no longer be thought of as something which must be determined by variation of parameters as it was above.

This means that the integration for E_c in (2.33) should be altered to conform to the trapezoidal model: we no longer consider the protons to be evenly distributed throughout a spherical volume -- we consider them to have the same trapezoidal distribution as all the nucleons. The results for the Coulomb energy and the exchange energy using the trapezoidal model are

$$E_c = 0.863 \frac{z^2}{r_o A^{1/3}} \left[1 - \frac{5}{6} \frac{z^2}{r_o^2 A^{2/3}} + \frac{1}{2} \frac{z^3}{r_o^3 A} + \frac{4}{9} \frac{z^4}{r_o^4 A^{4/3}} - \frac{5}{14} \frac{z^5}{r_o^5 A^{5/3}} \right]$$

$$E_{ex} = - 0.660 \frac{z^{4/3}}{r_o A^{1/3}} \left[1 - \frac{z}{r_o A^{1/3}} + \frac{4}{3} \frac{z^2}{r_o^2 A^{2/3}} - \frac{13}{15} \frac{z^2}{r_o A} + \frac{10}{9} \frac{z^4}{r_o^4 A^{4/3}} - \frac{3}{5} \frac{z^5}{r_o^5 A^{5/3}} \right] \qquad (2.37a)$$

Where $2z$ is the distance in which the nuclear density falls from its full value to zero. The first terms are like those in (2.34) and (2.35) but the smearing out of the nuclear edge adds correction terms.

With one of the adjustable parameters eliminated by measurement, we may concentrate on other terms. It appeared to Cameron in 1957 that a more consistent view should be taken with respect to the symmetry energy: since the surface energy arises as a correction to the volume energy term, one might investigate a surface symmetry term as a correction to the volume symmetry term already included in the semi-empirical mass formula (Cameron, 1957). This leads to the new term

$$E_{s.sym} \propto \left[\frac{(A-2Z)^2}{A^2}\right] A^{2/3} \quad , \tag{2.38}$$

similar to the volume symmetry term, but with A replaced by $A^{2/3}$ for obvious reasons. The adjustable terms in the mass formula are now written as

$$E_v = \alpha \left[1 - \frac{\beta}{\alpha} \frac{(A-2Z)^2}{A^2}\right] A \tag{2.39}$$

$$E_s = \gamma \left[1 - \frac{\varphi}{\gamma} \frac{(A-2Z)^2}{A^2}\right]\left[1 - \frac{0.62025}{A^{2/3}}\right]^2 A^{2/3} \tag{2.40}$$

where α, β, γ, and φ are variable parameters. The additional term in E_s results from using the trapezoidal model of the nucleus. Work by Seeger ran along similar lines. Subsequently, a study was made to determine the variable parameters for medium weight nuclei, and separately for heavier weight nuclei. Even though the values obtained for α, β and γ were similar, the two values obtained for φ were quite different. Accordingly, it was concluded that a physically meaningful coefficient for the surface symmetry energy could not be obtained.

The results of the thermonuclear detonation "Mike" in 1952 raised questions as to the validity of contemporary mass formulae (Cameron 1959). In the explosion, samples of U^{238} were exposed to a large neutron flux which resulted in multiple neutron capture, up to 17 capture steps away from U^{238}, forming nuclei up to A = 255. The yields of the heavier mass numbers were sufficiently great that it was clear that the basic neutron capture cross sections could not decrease as rapidly as had been predicted as one went from U^{238} to U^{255}. More recent calculations indicate that the neutron capture cross sections decrease by no more than an order of magnitude in the interval mentioned. The

mass formulae considered thus far predict that the neutron binding energy will drop by about a factor of 2 in going from U^{238} to U^{255}, and taking into account the theory of neutron capture, which depends upon such things as neutron binding energy and nuclear level density in the vicinity of the excited state, one expects that the neutron capture cross section will drop about three orders of magnitude, results quite at variance with the observed yield pattern. Since capture of neutrons on a rapid time scale is one of the principal processes involved in making heavy nuclei, the question is clearly of some importance.

It seemed to Cameron that the only possible faulty link in the chain was the determination of the neutron binding energy, and therefore that it seemed unlikely that the conventional form of the mass formula could yield correct predictions of neutron binding energies on the neutron rich side far removed from the valley of beta stability. A number of modifications in the mass formula were tried and their results regarding neutron binding energies examined, but generally the effect of the modifications was found to be negligible. The basic reason for this is that the general coefficients of the terms in the mass

formula must be readjusted to fit the mass surface for each new form of the formula and this readjustment generally compensates for the newly introduced effect, so that the extrapolation of the mass surface away from the valley of beta stability is hardly affected.

But now attention is directed at the volume symmetry term (Cameron and Elkin 1965). Examine the derivation of δE involved the binomial expansion about the condition $N = Z$ in (3.23). Perhaps this technique could be refined to give results valid for neutron rich nuclei. Consider the combined volume and volume-symmetry energy in the following form:

$$E_v = \alpha A \left[1 - \frac{\beta}{\alpha} \frac{(A-2Z)^2}{A^2} \right] . \qquad (2.41)$$

Cameron found that $\alpha = 17.0354$ MeV and $\beta = -31.4506$ MeV. If we extrapolate this expression to the case of a pure neutron gas, then the binding energy per nucleon will change from - 17.0354 MeV for $A = 2Z$ (self-conjugate nuclei) to + 14.4152 MeV for the pure neutron case. Thus our conventional mass formula predicts that a pure neutron gas will be rather violently explosive, having almost as

much positive energy per nucleon as ordinary nuclear matter has negative binding energy per nucleon. This is in disagreement with the theoretical expectation that a pure neutron gas should be only slightly unbound, say with a small fraction of an MeV positive energy per nucleon.

Thus it is clear that higher-order terms in the symmetry energy should be inserted into the mass formula in order to give more realistic masses for neutron rich nuclei. These higher order terms will have the effect of increasing neutron binding energies relative to those predicted by the conventional formula in the neutron-rich region, in conformity with the desired result. However, a failure to obtain a physically realistic value for the coefficient of the surface energy term warns that the usual procedures for determining the coefficients of the mass formula cannot be expected to yield physically realistic values of the higher order symmetry terms either.

Fortunately, there is one very simple form in which higher-order coefficients are included automatically, and in which pure neutron matter is left slightly bound:

$$E_v = \alpha A \exp\left[-\frac{\beta}{\alpha}\frac{(A-2Z)^2}{A^2}\right]. \qquad (2.42)$$

The conventional volume term (3.41) is obtained from the first two terms in the Taylor expansion of this exponential function. With the values of α and β used above, this would leave a pure neutron gas with a binding energy of -2.7 MeV per nucleon, even though theory predicts a slightly unbound neutron gas. It is clear that the true extrapolated behavior lies between the conventional and exponential formulas, but probably closer to the exponential formula.

Retaining the spirit of the surface symmetry correction, combine the volume, surface and symmetry terms into

$$E_{vs} = \alpha A\left[1 - \frac{\gamma}{\alpha A^{1/3}}\left(1 - \frac{z^2}{3r_o^2 A^{2/3}}\right)^2\right] \exp\left[-\frac{\beta}{\alpha}\frac{(A-2Z)^2}{A^2}\right] \tag{2.43}$$

where again 2z is the nuclear surface thickness, and (3.43) is called the exponential form of E_{vs}. Retaining the first two terms in the expansion of the exponential in (3.43), we get the convential form of E_{vs}.

$$E_{vs} = \alpha A\left[1 - \frac{\gamma}{\alpha A^{1/3}}\left(1 - \frac{z^2}{3r_o^2 A^{2/3}}\right)^2\right]\left[1 - \frac{\beta}{\alpha}\frac{(A-2Z)^2}{A^2}\right] .$$

Use of the exponential version of the formula gives satisfactory results for the neutron capture cross sections.

These decrease by less than a factor of ten in going from U^{238} to U^{255} because the neutron binding energy at U^{255} is down only to about 80% of its value at U^{238}. The coefficients α, β and γ for the two cases are found to be as follows:

	Exponential Mass Formula (MeV)	Conventional Mass Formula (MeV)
α	- 17.2928	- 17.4808
β	26.587	27.5121
γ	- 35.939	- 35.8482

The method of solution of the parameters is not so straightforward for the exponential case as it was for the conventional case discussed above because the mass-expression derivative with respect to Z contains α and γ as well as β. Nevertheless this derivative continues to depend most sensitively upon β; so it is possible to determine the coefficients from the conventional input data by an iterative procedure. Basically, trial values for α and γ were assumed wherever they appeared in the exponential factor. The input data consisted of 89 pairs of values of nuclear charge and mass number corresponding to the bottom of the valley of

beta stability. The regions of neutron closed shells $136 \leq A \leq 142$ and $190 \leq A \leq 220$ were excluded. A new value of β was obtained by a numerical procedure in which the quantity $\sum \left[\frac{\partial (M-A)}{\partial Z}\right]^2$ was minimized along the valley of beta stability. With this value of β, new values of α and γ were determined by a least-squares fit to 97 odd-odd nuclei approximately evenly spaced along the valley of beta stability. Odd-odd nuclei were used because the pairing correction P(Z,N) is defined to be zero for such nuclei. Again the closed shell regions where shell corrections S(Z,N) are important were avoided. Previous values for β and α were used in the exponential factor. The process was repeated to improve the values of the coefficients. The calculated coefficients in the two cases are not radically different and they give about the same fit to measured masses in each case. Still the results are imperfect because the measured masses have shell corrections which make them oscillate above and below the calculated masses. This implies that employing least square methods to obtain small energy term coefficients is doomed to failure since the small energy effects in the mass formula considered so far are masked by shell

effects. Still the exponential formula seems to give better results both conceptually and in practice than the conventional one. The shell and pairing refinements will be brought in after the discussion of particle orbits in a nuclear potential well.

References

Bethe, H.A. and Bacher, R.F. 1936, Nuclear Physics. A. Stationary States of Nuclei, Revs. Modern Phys. 8, 82.

Blatt, J.M. and Weisskopf, V.F. 1952, Theoretical Nuclear Physics, J. Wiley and Sons, Inc., New York.

Cameron, A.G.W. 1957, Can. J. Phys., 35, 1021.

Cameron, A.G.W. 1959, Can. J. Phys., 37, 322.

Cameron, A.G.W. and Elkin, R.M. 1965, Can. J. Phys., 43, 1288.

Elton, L.R.B. 1959, Introductory Nuclear Theory, Interscience Pub., Inc., New York.

Fermi, E. 1950, Nuclear Physics (compiled by Orear, J., Rosenfeld, A.H., and Schulter, R.A.), University of Chicago Press, Chicago.

Preston, M.A. 1962, Physics of the Nucleus, Addison-Wesley Pub. Co., Reading, Mass.

3. Particle Orbits in Nuclear Potential Wells

It was mentioned in the discussion of nuclear forces that because nucleons are classified as Fermi particles, the Pauli exclusion principle implies that a nucleon moving through a nucleus in the ground state or at low excitation energy is unable to scatter on other nucleons because of the absence of states into which it could scatter. Consequently nucleons can move relatively long distances through nuclear matter without suffering collisions and this gives them time to explore thoroughly the shape of any potential well in which they find themselves.

The independent particle model of the nucleus is based on the assumption that each nucleon in the nucleus moves independently of all the other nucleons in some common potential field. This common field represents the average effect of all interactions with other nucleons, and it is assumed to be the same for each nucleon. Every nucleon is thus considered to be an independent particle, and the presence of other particles moving in the same field can exert an influence only collectively owing to the Pauli principle discussed in the last paragraph. We would expect this model to be a good approximation if

there were no correlation between nucleon motions. Note that the independent particle model is quite different from the α-particle and liquid drop models, both of which involve a high degree of correlation.

Mathematically the assumption of independent motion of the nucleons means that the wave function for the nucleus as a whole can be written as the product of the wave functions for the A individual nucleons:

$$\psi = \prod_{i=1}^{A} \psi_i(q_i) = \psi_1(q_1)\psi_2(q_2)\ldots\psi_A(q_A) \qquad (3.1)$$

where q_i stands for the coordinates (space, spin, and isospin) of the ith nucleon. Of course this way of writing down the wave function for the nucleus is not entirely satisfactory the way it stands because the Pauli principle we invoked to enable us to write the nuclear wave function as a product of individual wave functions also requires that the nuclear wave function be antisymmetric under exchange of any two sets of nucleon coordinates. For a system of A nucleons, the properly antisymmetrized form is represented by the Slater determinant

$$\psi = \frac{1}{\sqrt{A!}} \begin{vmatrix} \psi_1(q_1) & \psi_1(q_2) & \cdots & \psi_1(q_A) \\ \psi_2(q_1) & \psi_2(q_2) & \cdots & \psi_2(q_A) \\ \vdots & & & \\ \psi_A(q_1) & \psi_A(q_2) & \cdots & \psi_A(q_A) \end{vmatrix} \qquad (3.2)$$

which clearly has the necessary properties; the factor involving A! is present for normalization.[1]

The first essential problem to solve in the discussion of the kinds of orbits nucleons may assume in nuclear potential wells is finding the energy levels of the individual particles in the common or "auxiliary" potentials.[2] It is, of course, necessary to assume some shape for this potential, but one gets much the same sort of levels with a shielded inverse square force, an oscillator force, or a spherical well.

We shall work out the solution for a three dimensional harmonic oscillator potential because it provides familiar ground on which to discuss transitions to other well shapes and because it involves the greatest degree of degeneracy. The assumed potential energy function is

$$V = -V_o + \frac{1}{2} M\omega^2 r^2 \qquad (3.3)$$

where M is the mass of a nucleon and ω is the circular frequency of oscillation of the classical oscillator. The solution is simplest to work out in cartesian coordinates and so we rewrite

$$V = -V_o + \frac{1}{2} M\omega^2 (x^2 + y^2 + z^2). \tag{3.4}$$

The Schrödinger equation is

$$\nabla^2 \psi + \frac{2M}{\hbar^2} \left[E + V_o - \frac{1}{2} M\omega^2 (x^2 + y^2 + z^2) \right] \psi = 0, \tag{3.5}$$

which can be solved by the technique of separation of variables:

$$\psi(x,y,z) = X(x)Y(y)Z(z). \tag{3.6}$$

The Schrödinger equation becomes

$$\left[\frac{1}{X}\frac{d^2X}{dx^2} - (\alpha^2 x)^2\right] + \left[\frac{1}{Y}\frac{d^2Y}{dy^2} - (\alpha^2 y)^2\right] + \left[\frac{1}{Z}\frac{d^2Z}{dZ^2} - (\alpha^2 Z)^2\right]$$

$$= -\frac{2M}{\hbar^2}(E + V_o) \tag{3.7}$$

where $\alpha^2 = (M\omega/\hbar)$. Each bracketed term above is independent of the variables involved in the others, and so each bracketed term must be equal to some constant, say

$$\frac{1}{Q}\frac{d^2Q}{dq^2} - (\alpha^2 q)^2 = -\frac{2M}{\hbar^2}E_q, \quad Q = X,Y,Z; \; q = x,y,z \tag{3.8}$$

Schrödinger's equation now uncouples into three independent simple harmonic oscillator equations, the solutions to which we know well:

$$\frac{d^2Q}{dq^2} + \left[\frac{2ME_q}{\hbar^2} - (\alpha^2 q)^2\right]Q = 0$$

$$E + V_o = E_x + E_y + E_z \; ; \tag{3.9}$$

the energies are

$$E_q = \hbar\omega(n_q + 1/2) \tag{3.10}$$

and hence the total energy is

$$E = -V_o + \hbar\omega(n_x + n_y + n_z + 3/2) \tag{3.11}$$

or

$$E = -V_o + \hbar\omega(N + 1/2) \tag{3.12}$$

where

$$N = n_x + n_y + n_z + 1 \tag{3.13}$$

The degree of degeneracy of an energy level of the oscillator is equal to the number of different ways (N - 1)

can be written as the sum of the three nonnegative integers n_q. For example, even for such a small energy as that corresponding to N = 3, the array

n_x	n_y	n_z
2	0	0
0	2	0
0	0	2
1	1	0
1	0	1
0	1	1

(3.14)

displays the different ways of writing the n_q corresponding to N = 3. The degeneracy, neglecting spin, of the level for N = 3 is therefore 6; so clearly there is considerable room for degeneracy in the solutions for the oscillator potential. The wave functions here are simply the products of the three one dimensional harmonic oscillator eigenfunctions. In normalized form,

$$\psi_{n_x,n_y,n_z}(x,y,z) = \left(\frac{\alpha}{\sqrt{\pi}}\right)^{3/2}\left(\frac{1}{2^{n_x+n_y+n_z}\, n_x!\, n_y!\, n_z!}\right)^{1/2}$$

$$\exp\left[-\frac{1}{2}\alpha^2(x^2+y^2+z^2)\right] H_{n_x}(\alpha x) H_{n_y}(\alpha y) H_{n_z}(\alpha z) \qquad (3.15)$$

where $H_n(\xi)$ is the nth Hermite polynomial. It is a

characteristic of these wave functions that if a given set of ψ's all correspond to the same energy level, any linear combination of this set also belongs to the same energy level. For example, let $\psi_{i,n}$ be the ith member of a set of eigenfunctions belonging to the energy level E_n. It then follows that the wave function $U = \sum_i A_i \psi_{i,n}$, where the A_i are arbitrary constants, also belongs to the level E_n, because

$$HU = H \sum_i A_i \psi_{i,n} = \sum_i A_i H \psi_{i,n} = \sum_i A_i E_n \psi_{i,n} = E_n \sum_i A_i \psi_{i,n}$$

$$= E_n U. \qquad (3.16)$$

In order to compare the results for our oscillator potential with those for other central fields, we wish to write the wave functions in such form as to display their orbital angular momentum explicitly. A simple way to do this is to rewrite the wave function $\psi_{n_x n_y n_z}$ as a function of r times a spherical harmonic. This is always possible by suitable linear combination of the wave functions of (3.15). Putting $\rho^2 = \alpha^2 r^2$, we have the following:

$$N = 1: \quad \psi = \psi_{000} \propto e^{-\frac{1}{2}\rho^2} \propto e^{-\frac{1}{2}\rho^2} Y_{00} \qquad \ell=0,\ 1s \text{ level} \quad (3.17)$$

$$N = 2: \quad \psi = \left\{ \begin{array}{l} \psi_{001} \propto e^{-\frac{1}{2}\rho^2} \rho\cos\theta \propto \rho e^{-\frac{1}{2}\rho^2} Y_{10} \\ \psi_{010} \propto e^{-\frac{1}{2}\rho^2} \rho\sin\theta\sin\varphi \propto \rho e^{-\frac{1}{2}\rho^2} (Y_{11} - Y_{1-1}) \\ \psi_{100} \propto e^{-\frac{1}{2}\rho^2} \rho\sin\theta\cos\varphi \propto \rho e^{-\frac{1}{2}\rho^2} (Y_{11} + Y_{1-1}) \end{array} \right\} \qquad \ell=1,\ 2p \text{ level} \quad (3.18)$$

$$N = 3: \quad \psi = \left\{ \begin{array}{l} \psi_{200} + \psi_{020} + \psi_{002} \propto e^{-\frac{1}{2}\rho^2} (\rho^2 - \frac{3}{2}) \propto e^{-\frac{1}{2}\rho^2} (\rho^2 - \frac{3}{2}) Y_{00} \\ \psi_{002} - \frac{1}{2}(\psi_{200} + \psi_{020}) \propto e^{-\frac{1}{2}\rho^2} \rho^2 (\frac{3}{2}\cos^2\theta - \frac{1}{2}) \propto e^{-\frac{1}{2}\rho^2} \rho^2 Y_{20} \\ \psi_{110} \propto e^{-\frac{1}{2}\rho^2} \sin^2\theta\sin 2\varphi \propto e^{-\frac{1}{2}\rho^2} (Y_{22} - Y_{2-2}) \\ \psi_{011} - i\psi_{101} \propto e^{-\frac{1}{2}\rho^2} \rho^2 \sin 2\theta\ e^{-i\varphi} \propto \rho^2 e^{-\frac{1}{2}\rho^2} Y_{2-1} \\ \psi_{200} - \psi_{020} \propto e^{-\frac{1}{2}\rho^2} \rho^2 \sin^2\theta\cos 2\varphi \propto \rho^2 e^{-\frac{1}{2}\rho^2} Y_{22} \end{array} \right\} \qquad \ell=0,\ 2s \text{ level} \quad (3.19)$$

$$\ell=2,\ 3d \text{ level} \quad (3.20)$$

$$N = 4: \quad \psi = \left\{ \begin{array}{l} \psi_{003} + \psi_{201} + \psi_{021} \propto e^{-\frac{1}{2}\rho^2} (\rho^3 - \frac{5}{2}\rho)\cos\theta \propto e^{-\frac{1}{2}\rho^2} \rho(\rho^2 - \frac{5}{2}) Y_{10} \\ \qquad \text{and two similar functions} \\ \psi_{003} - \frac{3}{2}(\psi_{201} + \psi_{021}) \propto e^{-\frac{1}{2}\rho^2} \rho^3 (\frac{5}{2}\cos^3\theta - \frac{3}{2}\cos\theta) \propto \rho^3 e^{-\frac{1}{2}\rho^2} Y_{30} \\ \qquad \text{and six similar functions} \end{array} \right\}$$

$$\ell=1,\ 3p \text{ level} \quad (3.21)$$

$$\ell=3,\ 4f \text{ level} \quad (3.22)$$

$$\vdots$$

Note first of all that oscillator levels with even N correspond to odd azimuthal quantum numbers ℓ because the wave functions for even N are all odd functions of the coordinates xyz, and vice versa. There is considerable degeneracy of levels, the second s level, 2s, coinciding with the first d level, 3d, in energy, and so on. The levels are designated by the usual spectroscopic notation, giving the lowest level of the azimuthal quantum number ℓ and the principal quantum number $n = \ell + 1$ and numbering consecutive levels of like ℓ by successive values of n. Thus the lowest level with $\ell = 0$ (occurring for N = 1) is called 1s, the next higher level with $\ell = 0$ (occurring at N = 3) is called 2s, and if we had written down the scheme for N = 5, the $\ell = 0$ level there would be called 3s.

The general relation between the principal quantum number n in polar coordinates, the azimuthal quantum number ℓ, and the "energy quantum number" N is

$$N = 2n - \ell - 1$$

which follows from the examples given above, and can be demonstrated generally. For a given energy (given N) we have $\frac{1}{2}$ N or $\frac{1}{2}$ (N+1) different quantum levels in the $n\ell$

scheme, according to whether N is even or odd. These levels have the azimuthal quantum numbers ℓ = N-1, N-3, N-5, ..., and the principal quantum numbers n = N, N-1, N-2, ..., respectively. The total statistical weight of the energy level N is N(N+1), taking account of the spin (which introduces a factor of 2 into the statistical weight). Thus the weight of the levels N = 1,2,3,4,5,6,7, is 2,6,12,20,30,42,56, respectively. The total number of quantum states having an N smaller or equal to N_o is 2,8,20,40,70,112,168 for N_o = 1 to 7. Gathering all these things together, we can write down the contributions to these various energy levels, or, as we shall call them, shells. The j value, which is the orbital angular momentum ℓ plus or minus the intrinsic spin of a nucleon 1/2, is written as a subscript.

Table 1

Oscillator Shell (N)	ℓ Value	Terms	Number of Particles in Shell	Number of Particles up to and including Shell
1	0	$1s_{1/2}$	2	2
2	1	$2p_{3/2}, 2p_{1/2}$	6	8
3	2,0	$3d_{5/2}, 3d_{3/2}, 2s_{1/2}$	12	20
4	3,1	$4f_{7/2}, 4f_{5/2}, 3p_{3/2}, 3p_{1/2}$	20	40
5	4,2,0	$5g_{9/2}, 5g_{7/2}, 4d_{5/2}$ $4d_{3/2}, 3s_{1/2}$	30	70
6	5,3,1	$6h_{11/2}, 6h_{9/2}, 5f_{7/2}, 5f_{5/2},$ $4p_{3/2}, 4p_{1/2}$	42	112
7	6,4,2,0	$7i_{13/2}, 7i_{11/2}, 6g_{9/2}, 6g_{7/2},$ $5d_{5/2}, 5d_{3/2}, 4s_{1/2}$	56	168

Above, all the states for a given value of N have the same energy. But if the oscillator potential is deformed toward a square well, the degeneracy is lifted and the ordering of the energies of the various states for a compromise between an oscillator and a square well

potential is shown in the table. For example, in the second shell, the $2p_{1/2}$ level lies higher in energy than the $2p_{3/2}$ level; similarly in the third shell the $2s_{1/2}$ is highest in energy and the $3d_{5/2}$ lowest.

One might hope that nuclei having neutron or proton numbers given by the figures in the column on the far right above would be especially stable. For light nuclei the agreement is fairly good: we know that an alpha particle, N = Z = 2 is particularly stable. Similarly O^{16} with eight neutrons and eight protons is unusually stable and so is Ca^{40} with twenty protons and twenty neutrons; so there is some indication that among the lighter nuclei this shell scheme does bear some relation to the facts. For larger mass numbers, we find no special stability associated with forty neutrons or protons, or with seventy. But there are numbers for which special stability does occur; nuclei with these special numbers of neutrons and protons have masses which are definitely less than the masses of neighboring nuclei. Experimental data first indicated the existence of these numbers which were called "magic numbers". With the advent of the shell model, numbers were associated

with closed shells of nucleons. These numbers are 2,8, perhaps 14,20, perhaps 28,50,82 and 126. Nuclei which happen to have a magic number of neutrons and also a magic number of protons are exceptionally stable. Near the upper end of the periodic table, we find Pb^{208}, having 82 protons and 126 neutrons which has such unusual properties it behaves almost like a light nucleus.

Even though deformation of an oscillator potential into a square well does not give the observed features of nuclear shell structure for heavy nuclei, it is valid for light nuclei, and so we ask whether we might not be able to maneuver our model for large proton or neutron numbers into agreement with experiment.

Haxel, Suess, and Jensen, and M. Mayer developed a fruitful modification of the straightforward model developed above which was so successful that Jensen and Mayer were eventually awarded the Nobel Prize for their work. Their idea was to assume a coupling between the spins of the nuclei and their orbital motion in such fashion that if the spin angular momentum vector is aligned with the orbital angular momentum vector, then the nucleon orbit is particularly stable. Such orbits

lie lower than that indicated in Table 1. Conversely, if $\vec{s}$ and $\vec{\ell}$ are opposed, then the energy of the level lies higher than that indicated in Table 1 and the orbit is said to have less stability. Put another way, if $\vec{\ell}$ and $\vec{s}$ are aligned, $\vec{j}$ has its maximum value, and the nucleon binding energy is increased; so the $2p_{3/2}$ level is depressed and the $2p_{1/2}$ level raised. In addition this effect of splitting the $j = \ell + \frac{1}{2}$ and $j = \ell - \frac{1}{2}$ terms is assumed to increase with increasing values of ℓ.[4] The p levels are not greatly split, but in the case of the $3d_{5/2}$ and the $3d_{3/2}$ levels, one might expect the $3d_{3/2}$ level to be shifted to just above the $2s_{1/2}$ level in Table 1. Further down the table, we expect to find not simple spreading of shells, but the shifting of lowest levels down into the preceding shell. Thus, for example the $5g_{9/2}$ level for N = 5 would be shifted down into the level for N = 4, and the $6h_{11/2}$ would find itself at the top of the N = 5 shell. The result of such a rearrangement is shown in Table 2.

Table 2

Nuclear Shell	Terms ℓ_j	Number of Particles in Shell	Number of Particles up to and including Shell
I	$s_{1/2}$	2	2
II	$p_{3/2}, p_{1/2}$	6	8
IIa	$d_{5/2}$	6	14
III	$s_{1/2}, d_{3/2}$	6	20
IIIa	$f_{7/2}$	8	28
IV	$p_{3/2}, f_{5/2}, p_{1/2}, g_{9/2}$	22	50
V	$g_{7/2}, d_{5/2}, d_{3/2}, s_{1/2}, h_{11/2}$	32	82
VI	$h_{9/2}, f_{7/2}, f_{5/2}, p_{3/2}, p_{1/2}, i_{13/2}$	44	126
VII	$i_{11/2}, g_{9/2}, g_{7/2}, d_{5/2}, d_{3/2}, s_{1/2}, j_{15/2}$	58	184

In shell VII, experimental data is incomplete since no nuclei with 184 neutrons have been studied, let alone 184 protons, but one might hope that multiple neutron capture experiments could someday indicate whether a closed shell

exists at 184 nucleons. The first two shells are unchanged since the spin-orbit coupling is weak for $\ell = 1$. The depression of the $d_{5/2}$ term in the third shell is assumed to produce an intermediate shell between II and III, called IIa. The same effect is assumed to occur between shells III and IV. Thereafter the depression of the term of highest j is so strong that it does not form an intermediate shell but must be incorporated into the previous shell. Note that this arrangement does give the magic numbers.

We are now in a position to discuss the shell correction term S(Z,N) in the empirical mass formula of section 2. One could hope for a simple shell correction relation such as S(Z,N) = S(Z) + S(N) with no coupling between the shell corrections for the neutrons and protons, and this turns out to be reasonably successful. The numbers S(Z) and S(N) are determined independently by applying a least squares technique to all available mass data.[5] Whether the resulting functions of Z and N have any meaning can be seen by observing whether the functions vary smoothly. In practice, it is useful to plot not S(Z) and S(N), but

$\frac{dS(Z)}{dZ}$ and $\frac{dS(N)}{dN}$ which is an even stronger test of physical meaningfulness: any erratic behavior in S(i) will be greatly magnified in dS(i)/di. The results are given for protons in Figure 3.1 and for neutrons in Figure 3.2 One can see from Figure 1 that generally the function behaves in a reasonable fashion. There are strong breaks in S'(Z), one at Z = 20, others at Z = 28, 50, 82, 126, (The last break is hypothetical; no data are available for nuclei with atomic numbers nearly that large.) giving a graphic demonstration of the tendency to get exceptional behavior in nucleon binding energies at these closed shell positions. Note the rise in nucleon binding energy just before an abscissa corresponding to a closed shell and the sharp drop thereafter. In adding nucleons to a shell which is almost complete, the last nucleons interact strongly with one another, which means that their binding energy is greater than the average binding energy per particle, explaining the sharp increase in nucleon binding energy as a shell is closed. The first nucleons added to a new shell do not interact either with themselves or with the core of the nucleus as strongly as average and so their binding energy at

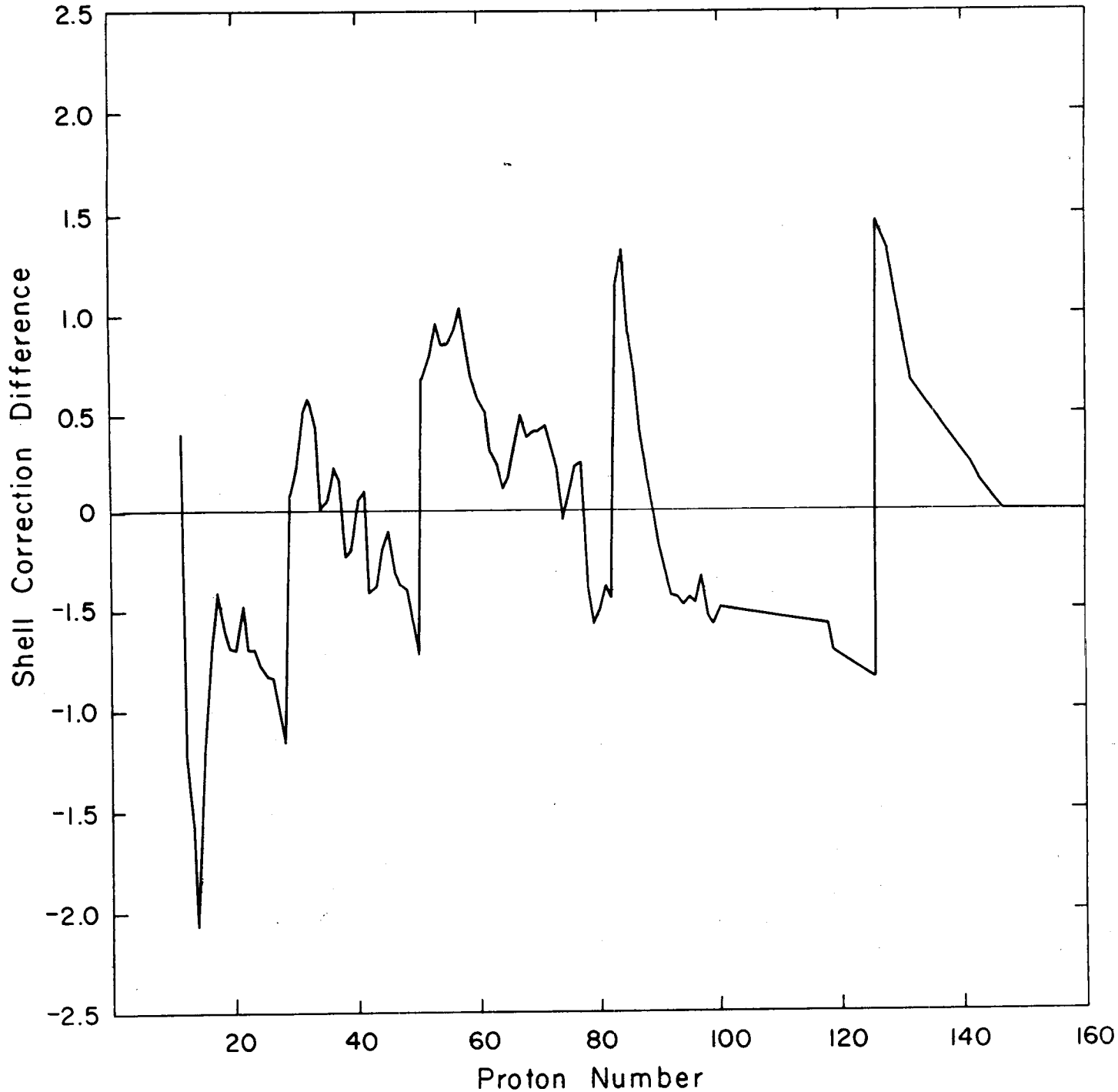
2.5
2.0
1.5
1.0
0.5
0
-1.5
-1.0
-1.5
-2.0
-2.5
Shell Correction Difference
20
40
60
80
100
120
140
160
Proton Number

Figure 3.1

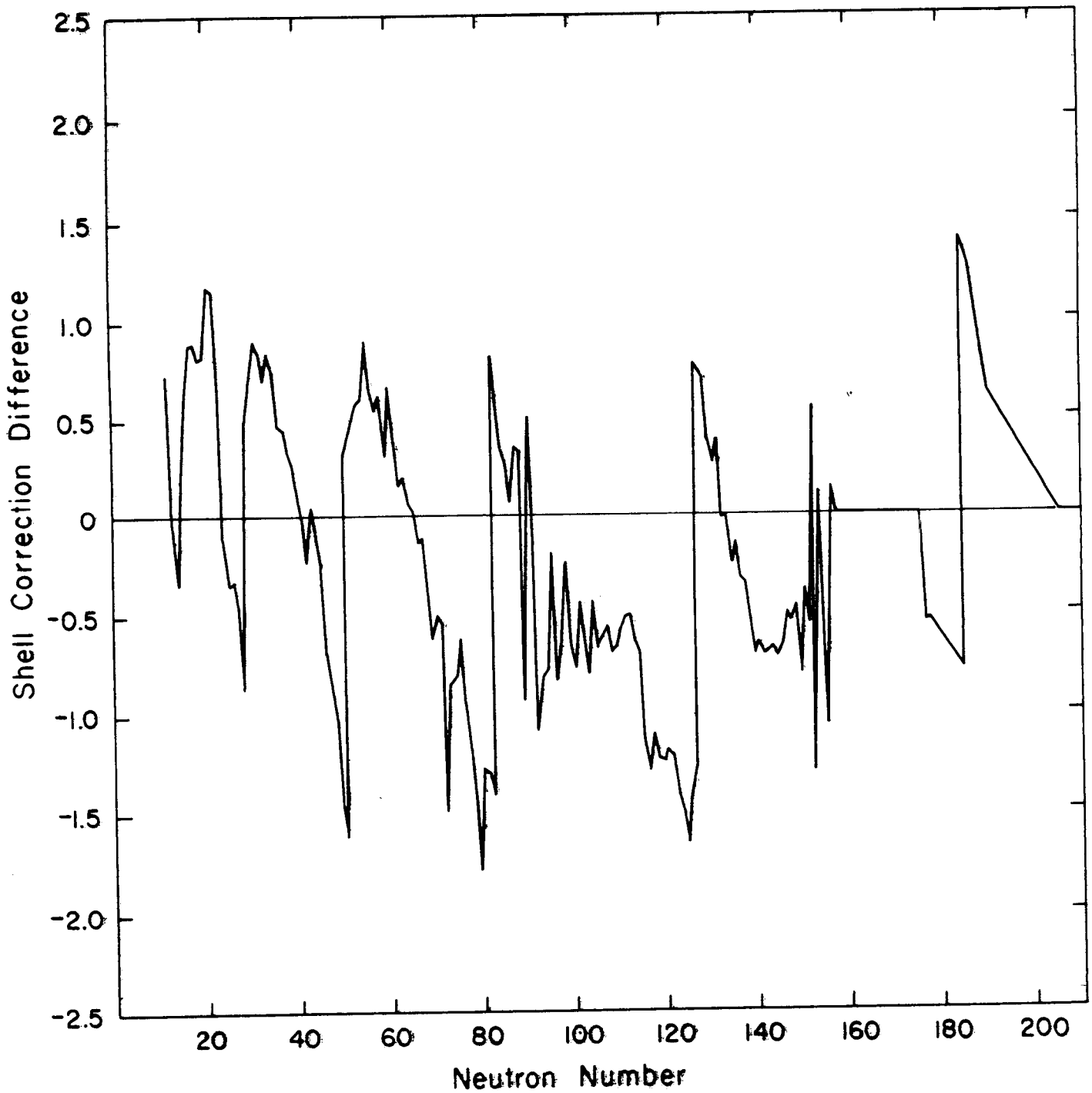
2.5
2.0
1.5
1.0
0.5
0
-0.5
-1.0
-1.5
-2.0
-2.5
Shell Correction Difference
20
40
60
80
100
120
140
160
180
200
Neutron Number

Figure 3.2

first is less than average, explaining the sharp drop in binding energy just as a new shell is begun. Figure 3.. has the same features, but the break at 126 nucleons is a measured one for neutrons.

One might expect a steady increase in binding energy as the shell is filled, corresponding to a more or less smooth decline of the graph between the breaks at closed shells. But we see some wiggles between closed shells. Between most of the closed shells on both the neutron and proton plots the tendency is a general increase in energy with some local oscillations. In some regions, however, the oscillation is about a rather steady value; in such regions the shell model fails and we must instead use a collective nuclear model where the shell model particle orbits are completely wiped out due to nuclear deformation. More will be added on this score later. As a refinement, it should be added that there may be a slight energy difference between the energy of a given orbit when it is occupied by neutrons and when it is occupied by protons, but the difference is so small it is not usually vexing. Anyway, in the range of the heavy nuclei, it is usual that quite different mass

numbers are associated with a given number of protons and the same number of neutrons, and other effects swamp the small energy difference.

One can discuss other nuclear properties within the context of the shell model if one assumes that an even number of nucleons of the same type in a state of given j will always arrange themselves to give a spin zero. We can justify this assumption by noting that nuclear forces are mainly attractive and hence favor states symmetric in space coordinates; hence lowest energy states must be antisymmetric in the spins. This means that to a good approximation, such pairs of particles of the same type contribute zero net angular momentum to the nucleus, and roughly zero net magnetic moment. Because pairing is preferred, one loses energy in making these pairs, and nuclei having last neutrons and protons paired have lower masses and are hence more stable than nuclei in which the last nucleon is unpaired. This reasoning is the basis for the pairing correction term P(Z,N) in the semi-empirical mass formula in section 2. When the coefficients were calculated for that mass formula, data for odd-odd nuclei were used since the

pairing energy for odd-odd nuclei is defined to be zero. This means something must be subtracted from the mass for even-odd or even-even nuclei to allow for pairing. Thus we define essentially three separate mass surfaces: one for odd-odd nuclei, on which P is identically zero; one for odd-even nuclei, where there is one contribution of a negative sign; one for even-even nuclei, for which there are two negative contributions to P. These mass surfaces are important in considering stability against beta decay.

Near the valley of beta stability the plot of proton number and mass defect is roughly parabolic:[6]

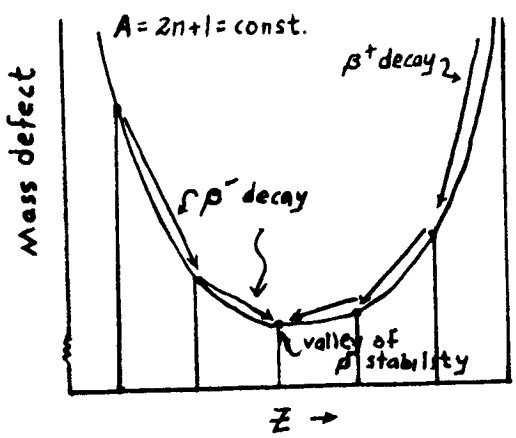

Isobars Odd-A

Figure 3.3

(The value of Z corresponding to $\frac{\partial (M-A)}{\partial Z} = 0$ may not be an integer.) Beta decay chains are represented diagramatically. It is easy to see that in all but extremely exceptional cases there is only one nucleus stable against beta decay. Exceptions can occur when two nuclei lie nearly symmetric above the bottom of the valley of beta stability or when an unstable nucleus has such a small energy difference from its daughter that the lifetime for beta decay is comparable to or longer than the lifetime of the galaxy.

In the case for even mass numbers, we have odd-odd and even-even nuclei, and two mass parabolas must be considered:

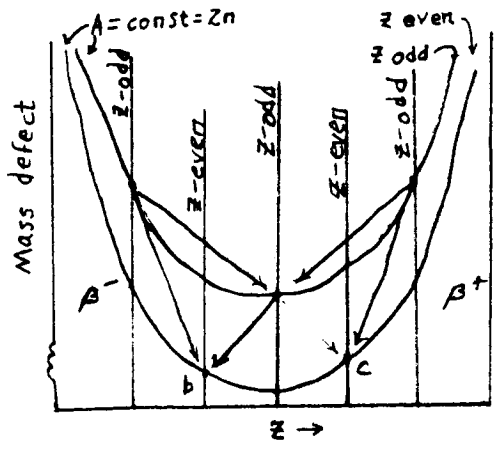

Isobars, Even-A

Figure 3.4

Possible decay modes are indicated in this more complicated situation. The figure suggests that even-A, odd-Z nuclei are unstable, and should not be found in nature. Actually there are a few, but none heavier than $_7N^{14}$ except for $_{19}K^{40}$ (which is radioactive) and $_{23}V^{50}$. As the figure is drawn, there would be two nuclei, b and c, with mass number A (A even) that are stable against beta decay, and in most circumstances there are only two isobars stable against beta decay, though instances of three can occur between closed shells where the mass surface is strongly deformed.

Another feature of the pairing phenomenon is that the pairing tendency is larger for high values of orbital angular momentum. From Figure 3.2, we note that near the tops of shells there are some orbits with low ℓ; for example in shell VI we go from $i_{13/2}$ to $p_{1/2}$ and then $p_{3/2}$. Now suppose we have just finished filling the $p_{1/2}$ level and added an $i_{13/2}$ particle. Does the ground state of the nucleus have a spin 13/2? In fact we find spins no higher than 9/2 for nuclei in the ground state. The reason is that it is energetically favorable for the nucleus to take one of the $p_{1/2}$ nucleons, pair it

with the $i_{13/2}$ particle, and the pairing energy depresses the pair leaving the remaining particle in $p_{1/2}$ unpaired. The ground state of the nucleus then has spin $I = 1/2$, not 13/2, and the state in which $p_{1/2}$ is filled and a nucleon is left in $i_{13/2}$ will appear as a low excited state. In the same way, the nucleus As^{75} has 33 protons, 5 of them in the unfilled shell IV. If pairing energies were not important, we would have four protons in $p_{3/2}$ and the remaining one in $f_{5/2}$; the nuclear spin would be $I = 5/2$. But it is found that the protons form two pairs in the $f_{5/2}$ state, leaving an unpaired proton in the $p_{3/2}$ state; the nuclear spin is $I = 3/2$. The difference between the pairing energy for a pair with low ℓ and a pair with high ℓ is not very large. The states in which the unpaired nucleon is in the level of high spin are therefore observed among the first few excited states.

The pairing phenomenon explains the existence of islands of isomerism. Experimentally it is found that for certain ranges of proton or neutron numbers, there are nuclei which may have rather long lived excited states. The islands are found for N or Z between 39 and

49 and between 69 and 81, and a less well pronounced group for N between 111 and 125. These ranges correspond to N or Z near the end of a nucleon shell and the explanation via pairing considerations is as follows. Near the tops of the closed shells in Table 2, we have depressed a high spin orbit from the shell next higher up by spin-orbit coupling and are filling states of lower spin with nucleons. At the top of the shell, then, we have close-lying levels differing greatly in spin. A nucleon in a lower spin state may take an appreciable time to pair with one in a higher spin state, thus decaying to ground, and this is how the islands of isomerism occur.

Pairing also explains why, without exception, even-even nuclei have ground state spins of zero, and why, with only two known exceptions, their first excited state is I = 2.

The shell model of the nucleus has had many successes, but it is not always sufficient. If we fill a subshell completely, we sensibly have a spherical distribution of nucleons; but if the orbit is only partially filled, the nucleon distribution tends not to be

spherically symmetric. In heavier nuclei, where there may be many particles in an orbit, the asymmetry may be considerable. Consequently, there is some tendency to deform the nuclear well itself away from a spherical shape in order to accommodate the aspherical form the wave functions assume. If a nucleus is deformed away from its spherical shape, then the degeneracy shown in Table 2 is lifted and the shell structure we had before tends to be obliterated. Calculations for deformed wells were carried out by Nilsson and Figures 3.5 and 3.6 are parts of the resulting Nilsson diagram. The dashed line in the center of the figures represents zero deformation. To the right, deformation is toward a football shape; to the left, a bun shape. It is easy to see that before very high energies are reached, the gaps which before allowed us to have a shell structure disappear and one must discuss the angular momentum and parity associated with individual orbits rather than of the properties of a nuclear shell. In the upper regions of Figure 3.6 is clear that what nucleon configuration forms the ground state depends strongly on whether it is energetically advantageous for the nucleus simply to add nucleons

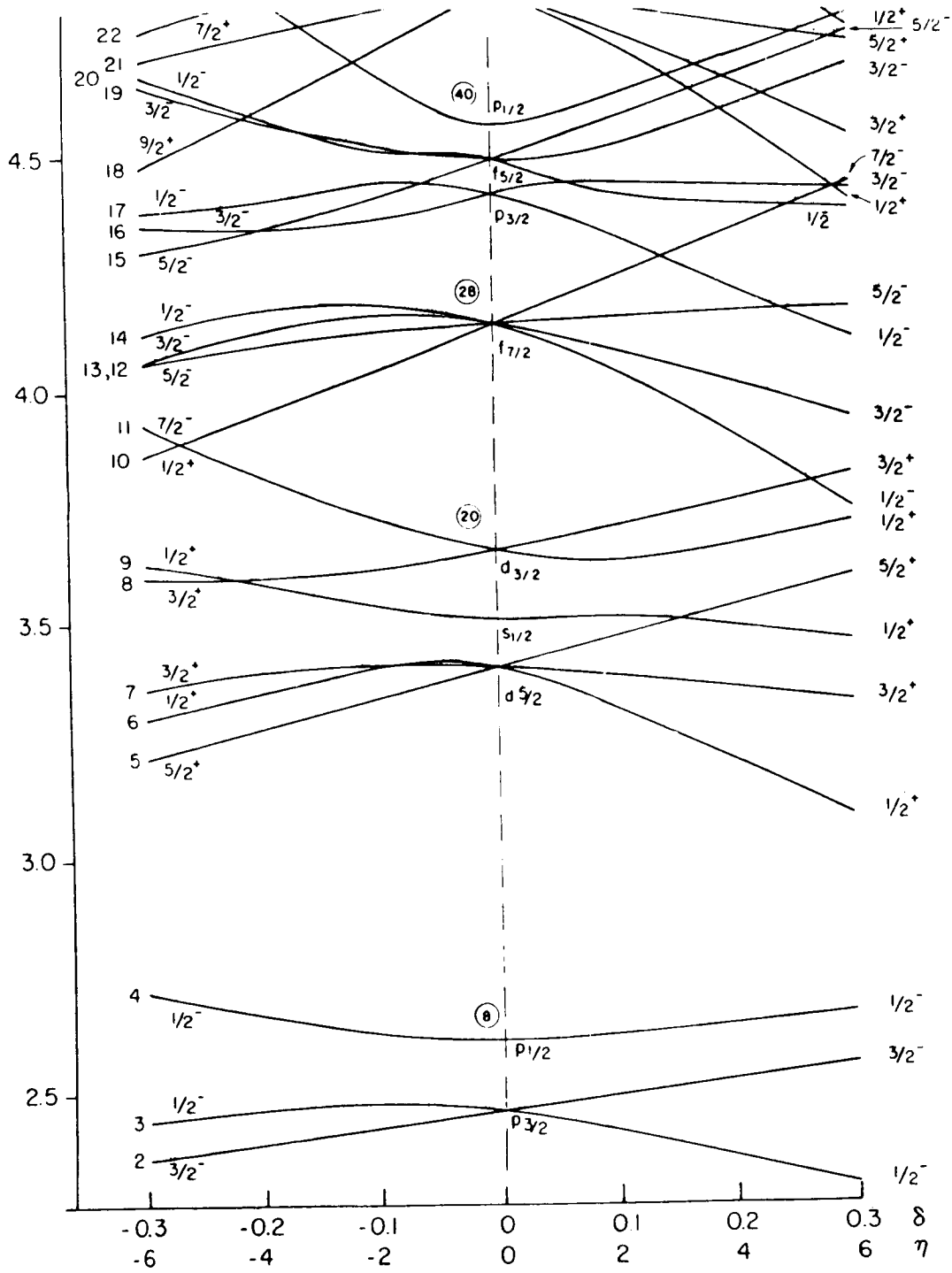

Fig. 11. The energy levels of a single particle in an axially symmetric deformed well with spin orbit coupling [21]). The parameter δ is defined in (110) and (111). Nilsson's parameter η is defined in terms of δ and the spin orbit coupling constant. The number at the left of each curve is Nilsson's label for the orbit. The Ω value for each orbit is given at the right.

Figure 3.5

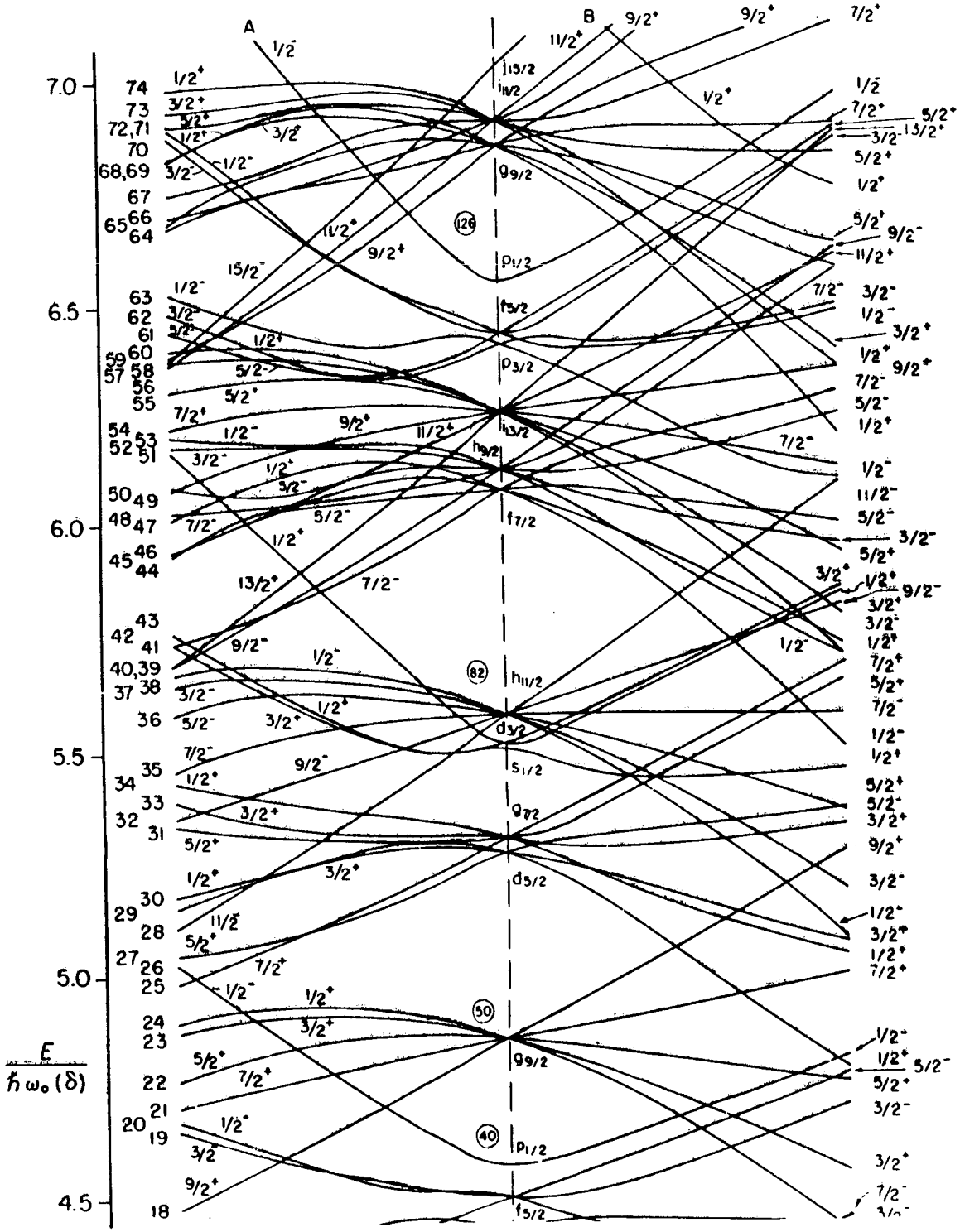
A
B
7.0
6.5
6.0
5.5
5.0
4.5
E / ħω₀(δ)
126
82
50
40
i13/2
i11/2
g9/2
p1/2
f5/2
p3/2
i13/2
h9/2
f7/2
h11/2
d3/2
s1/2
g7/2
d5/2
g9/2
p1/2
f5/2

Figure 16

to higher states or to change the character of its deformation and thereby alter the ordering of energy levels; the confusion also extends to the ordering of excited states.

The reason for the rather constant level of oscillations in regions between closed shells is easily seen at this point. In regions of highly deformed nuclear wells, prone to occur mostly between closed shells, the figures show that the shell structure is so smeared out that the levels available for nucleons increase in energy in a rather steady fashion, and so the derivative of nucleon binding energy with respect to nucleon number is expected to be roughly constant. The flat regions of Figures 3.1 and 3.2 seem to confirm our expectations.

Another feature which may complicate life is the fact that more than two particles may be involved in spin-spin coupling. For example, suppose we place three nucleons in the $g_{9/2}$ orbit. From what has been said previously, we expect two of the particles to assume a spin opposed configuration leaving the unpaired nucleon to give a net spin of 9/2. Occasionally one observes a spin of 7/2 instead of 9/2, and the reason is that the

three nucleons find it energetically favorable to combine their spins to give the 7/2 spin. The spin 9/2 state would then lie somewhat above the spin 7/2 state.

When the nucleus shows deformation, it frequently exhibits other collective features as well. Low-lying excited states can be produced by setting a deformed nucleus into gross rotation, and we may gain one or two units or orbital angular momentum entirely as a result of this collective motion. This produces well-known sequences of states in which a ground state is surmounted by excited states of increasing spin with regular increases in the space between them. In addition, recognizable features of collective motion in the form of vibrations can be observed in some low-lying states.

References

[1] Eisberg, R.M., 1961, Fundamentals of Modern Physics, J. Wiley and Sons, Inc., New York.

[2] Bethe, H.A. and Bacher, R.F., 1936, Nuclear Physics. A. Stationary States of Nuclei, Revs. Modern Phys., 8, 82.

[3] Haxel, O., Jensen, J.H.D., and Suess, H.E., 1949, Phys. Rev. 7[illegible], [illegible].

[4]Blatt, J.R. and Weisskopf, V.F., 1952, Theoretical Nuclear Physics, J. Wiley and Sons, Inc., New York.

[5]Cameron, A.G.W. and Elkin, R.M., 1965, Can. J. Phys., 43, 1288.

[6]Fermi, E., 1950, Nuclear Physics (compiled by Orear, J., Rosenfeld, A.H., and Schulter, R.A.), University of Chicago Press, Chicago.

4. Nuclear Level Densities

Our previous treatment of the nucleus as a fermi gas assumed the nucleus to be in its ground state, corresponding to a completely cold fermi gas. For such a cold gas, the occupation number for states up to the fermi level is 1 and beyond that, 0. If some excitation energy is supplied, some states above the fermi energy will be occupied, with a corresponding depopulation of states just below the fermi level which were occupied in the completely cold gas.

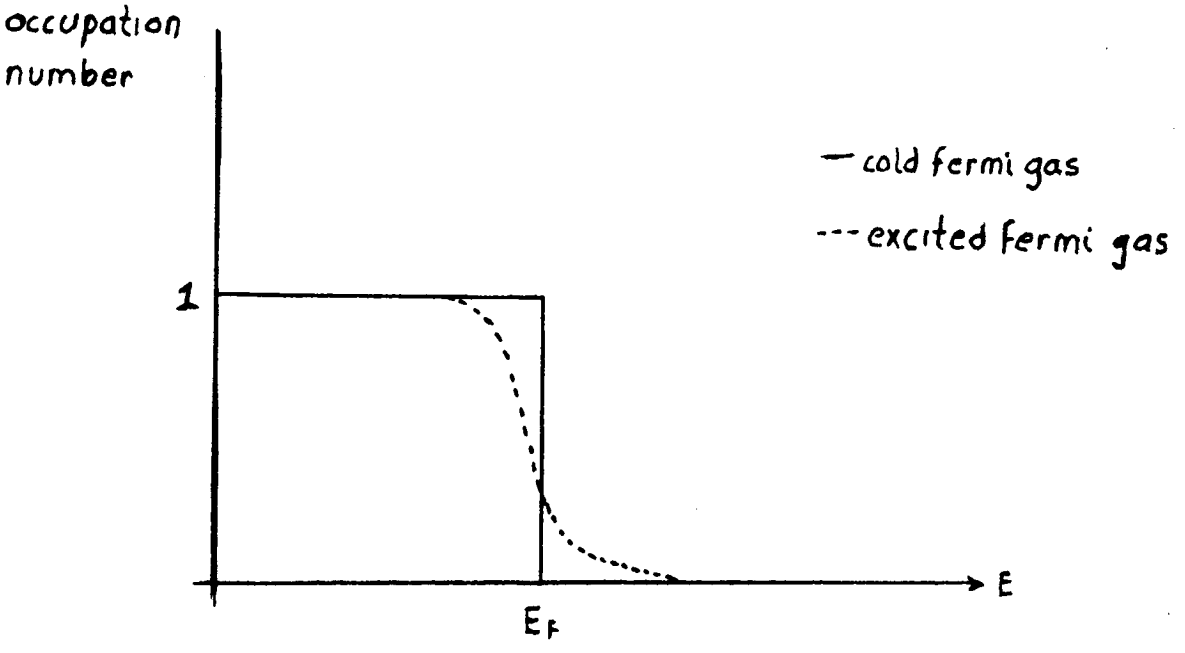

Figure 4.1

The precise shape of the dashed curve in Figure 4.1 depends on the degree of excitation or temperature of the gas; as the excitation is increased, the rounding of the sharp corner becomes more and more pronounced. But as long as excitation is not so large as to destroy the shape of the dashed curve shown, one can show from the properties of fermi statistics that the total energy of the gas is

$$E_{total} = \frac{3}{5} \eta E_F \left[1 + \frac{5\pi^2}{12} \left(\frac{KT}{E_F}\right)^2 + \ldots \right] \qquad (4.1)$$

where η is the number of fermi particles in the gas, E_F is the fermi energy, and T is the temperature of the gas. The first term is just the total energy of the cold fermi gas. The excitation energy can be put into the form

$$E = a(kT)^2$$

where

$$a = \frac{\pi^2}{4} \frac{N}{E_F} \qquad (4.2)$$

For nonrelativistic fermi momenta,

$$E_F = \frac{p_F^2}{2M}$$

with

$$p_F = (3\pi^2)^{\frac{1}{3}} \hbar \left(\frac{N}{\Omega}\right)^{\frac{1}{3}} \qquad (4.3)$$

where Ω is the spatial volume to which the gas is confined. Considering the nucleus to be a fermi gas of two types of nucleons, the excitation energy due to neutrons is

$$E_n = \left(\frac{\pi^2}{72}\right)^{\frac{1}{3}} \frac{\Omega M}{\hbar^2} \left(\frac{N}{\Omega}\right)^{\frac{1}{3}} (kT)^2 \qquad (4.4)$$

where N is the number of neutrons present in the gas. For protons, with Z the number of protons in the gas, or atomic number of the nucleus,

$$E_p = \left(\frac{\pi^2}{72}\right)^{\frac{1}{3}} \frac{\Omega M}{\hbar^2} \left(\frac{Z}{\Omega}\right)^{\frac{1}{3}} (kT)^2 \qquad (4.5)$$

In (4.4) and (4.5) M is the mass of a nucleon. The total energy of excitation for the nucleus is the sum of (4.4) and (4.5),

$$E = E_n + E_p = \left(\frac{\pi^2}{72}\right)^{\frac{1}{3}} \frac{\Omega^{\frac{2}{3}} M}{\hbar^2} \left[N^{\frac{1}{3}} + Z^{\frac{1}{3}}\right] (kT)^2. \qquad (4.6)$$

We now connect the entropy of the nucleus with the number of accessible states by the fundamental relation encountered in statistical mechanics

$$S(T) = k\,[\ln \rho(T) - \ln \rho(0)] \qquad (4.7)$$

where $\rho(T)$ is the number of states available to the system at a given temperature, or, as we shall see, the nuclear level density at temperature T. If a system is in its

ground state, we have perfect order, and we say therefore that the entropy is zero for the system in its ground state. Ordinarily any excitation energy injected into the system can be shared among a number of states, and clearly there is a fairly large number of ways in which the energy may be shared among the states. With excitation, then, the disorder of the system has increased, and so the entropy has also increased. We have the usual thermodynamic relation

$$S(T) = \int_0^T \frac{dE}{T} \tag{4.8}$$

$$= \int_0^T 2ak^2 dT \tag{4.9}$$

where we have used equation (4.2). Here a is suitably modified for use with a gas of two types of fermi particles

$$a = \left(\frac{\pi^2}{72}\right)^{\frac{1}{3}} \frac{\Omega^{\frac{2}{3}} M}{\hbar^2} \left(N^{\frac{1}{3}} + Z^{\frac{1}{3}}\right).$$

Then

$$S(T) = 2ak^2 T \tag{4.10}$$

and

$$S(T) = 2\sqrt{ak^2 E}. \tag{4.11}$$

So that

$$\frac{\rho(T)}{\rho(0)} = e^{S/k} = e^{2\sqrt{ak^2 E}/k} \; e^{2\sqrt{aE}} \tag{4.12}$$

relates the level densities for excited states to those for ground states. We have used a grossly simplified argument, and so (4.12) can be expected to give only qualitative features.

In (4.12), we have a relation for the total density of all levels, but what is really needed is the density of levels for a given J (angular momentum) value. This requires consideration of the combinatorial problem of counting the number of states available for a given excitation energy and counting the number of ways particles can be taken from below the fermi level and placed in these excited states, consistent with conservation of energy.

Suppose neutrons have single-particle orbits with energy a_s, occupation number n_s, magnetic quantum number m_{1s}, and protons correspondingly have b_s, z_s, m_{2s}. A single state of the whole system is defined by four constants of the motion

$$N = \sum n_s \tag{4.13}$$

$$Z = \sum z_s \tag{4.14}$$

$$E = \sum n_s a_s + \sum z_s b_s \tag{4.15}$$

$$M = \sum n_s m_{1s} + \sum z_s m_{2s}. \tag{4.16}$$

The total angular momentum is also a constant of the motion, but one chooses to work with the M values and to extract J values at the end by looking at the distribution of M values and taking the differences between the total number of states with successive M values.

A more careful treatment of nuclear level densities, originally given by Bethe, leads to the level density formula

$$\rho(E,J) = \frac{\sqrt{\pi}}{12} \exp\left[2\sqrt{aE} \right] \frac{(2J+1)\exp\left[-(J+\frac{1}{2})^2/2\sigma^2\right]}{2a^{1/4}E^{5/4}\sqrt{2\pi}\,\sigma^3} \qquad (4.17)$$

where $\rho(E,J)$ is the density in MeV^{-1} of levels of given angular momentum J (both parities included) at an energy E above the fully degenerate state, and σ is the spin dependence parameter.[1] The observable level density is

$$\rho(E) = \sum_J \rho(E,J) \simeq \frac{\sqrt{\pi}}{12} \frac{\exp(2\sqrt{aE})}{\sqrt{2\pi}\,\sigma\, a^{1/4}E^{5/4}}. \qquad (4.18)$$

The spin dependence parameter σ is given by

$$\sigma = g \langle m^2 \rangle t \qquad (4.19)$$

where g is the sum of the neutron and proton single-particle level spacings, the number of proton and neutron orbits in a nuclear potential well per unit energy interval at the

fermi level, and is related to a by

$$a = \frac{1}{6}\pi^2 g \tag{4.20}$$

and t is the thermodynamic temperature of the nucleus given by

$$t = \sqrt{\frac{E}{a}} . \tag{4.21}$$

The quantity $\langle m^2 \rangle$ is the mean-square magnetic quantum number for single-particle states. Jensen and Luttinger found that the succession of shell - model states implies that

$$\langle m^2 \rangle \approx 0.146\ A^{2/3} \tag{4.22}$$

with fluctuations of 10% due to shell effects. Combining, we obtain

$$\sigma^2 = 0.0888 \text{ at } A^{2/3}. \tag{4.23}$$

This means that the spin parameter varies like $E^{1/4}$, a relatively slow variation which can often be neglected. It is useful to define the nuclear temperature τ as

$$\frac{1}{\tau} \equiv \frac{d(\ln\rho)}{dE} = \sqrt{\frac{a}{E}} - \frac{3}{2}E;$$

at high energies τ tends toward the thermodynamic temperature t of equation (4.21).

For most nuclei the only good information on neutron

resonances is obtained from s-wave neutron resonances. Suppose we are observing s-wave resonances on a target nucleus with ground-state spin and parity I^{π}. The only states of the compound nucleus which will be seen are those with spin $I + \frac{1}{2}$ or $I - \frac{1}{2}$ and parity π. Assuming equal probabilities for both parities, the level density for s-wave neutron resonances is

$$\rho_0 = \frac{1}{2} \sum_{J=I-\frac{1}{2}}^{I+\frac{1}{2}} \rho(E,J). \qquad (4.24)$$

If we use equations (4.17), (4.23) and (4.24) to fit the neutron resonance data, we have in effect two free parameters, a and E_0' (energy of the fully degenerate state). One might think that E_0' was simply the ground state so that E could be simply the excitation energy. The remaining parameter a could then be fitted to match theoretical predictions with observed neutron resonance spacings.

If this is done, there will be systematic differences in the values of a for neighboring even-even, odd-A, and odd-odd nuclei. These discrepancies could be removed by subtracting the pairing energy from the excitation energy to obtain an effective excitation energy. Suppose, for

example, we wish to consider excitation of an even-even nucleus. In excitation we break up the particles in orbits near the fermi level and place them into higher orbits, and in so doing we destroy some of the pair bonding. Much of the energy expended in the excitation goes into breaking the pairing. We therefore should replace E by

$$U = E - P(N) - P(Z) \tag{4.25}$$

where P(N) and P(Z) are pairing energies for neutrons and protons, zero for odd values of N or Z, this procedure has the empirical justification that it removes systematic even-odd effects in the values of a.

Figures 4.2 and 4.3 show a typical run of nuclei for which the total number of neutron resonances is plotted versus neutron energy E_n. Most of the plots seem to have roughly straight line portions near ground and in all cases the curvature away from the straight line is in the same direction, suggesting levels are being missed at high energies. Experimentalists often determine neutron energies by the time of flight method, and higher energy means shorter time of flight so that a loss of resolution can be expected at high energies, accounting for our missed levels. By evaluating (4.18) at the neutron binding energy and compair-

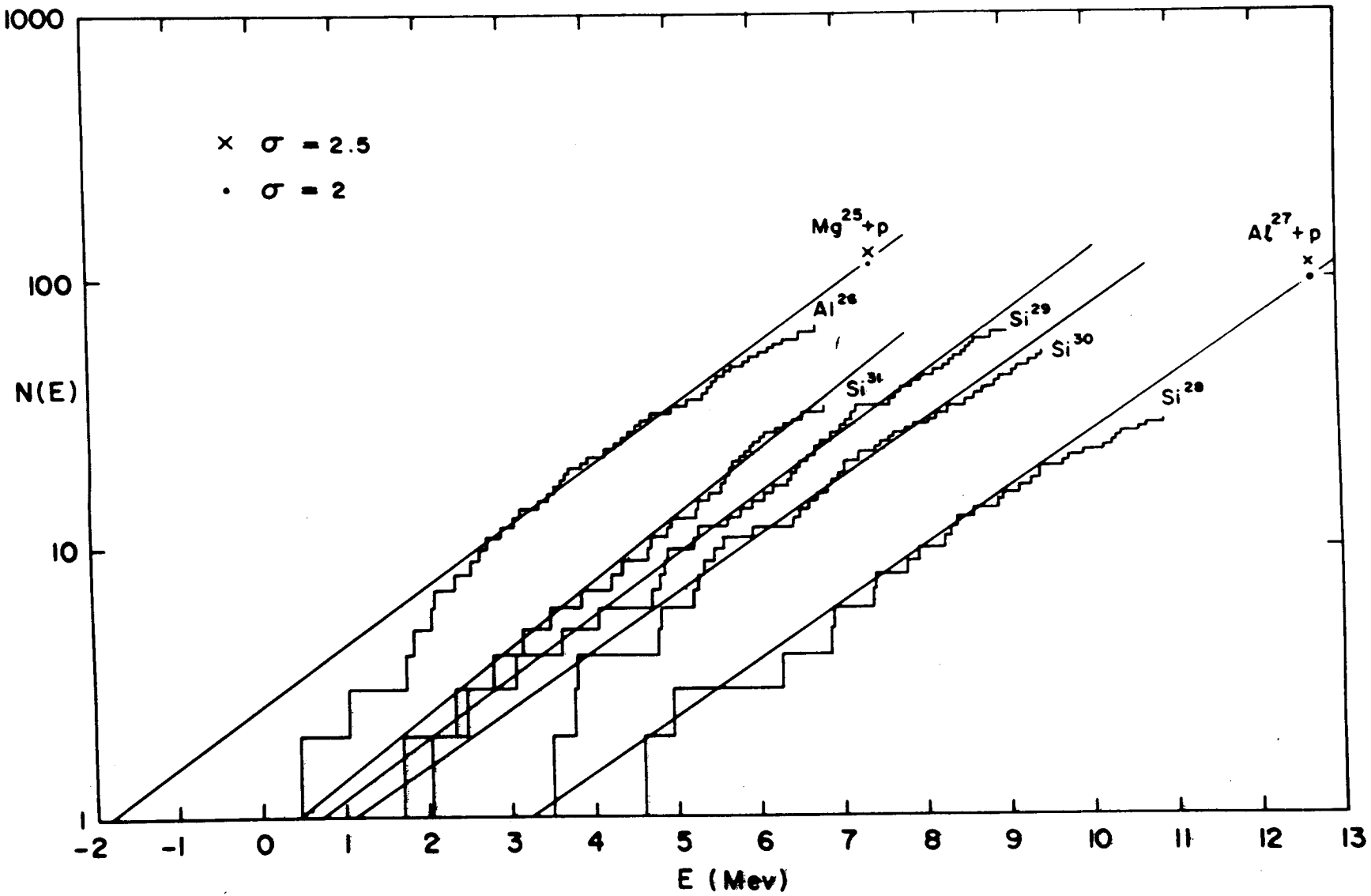
1000
100
10
1
N(E)
× σ = 2.5
• σ = 2
Mg25+p
Al26
Si31
Si29
Si30
Si28
Al27+p
-2
-1
0
1
2
3
4
5
6
7
8
9
10
11
12
13
E (Mev)

Figure 4.2

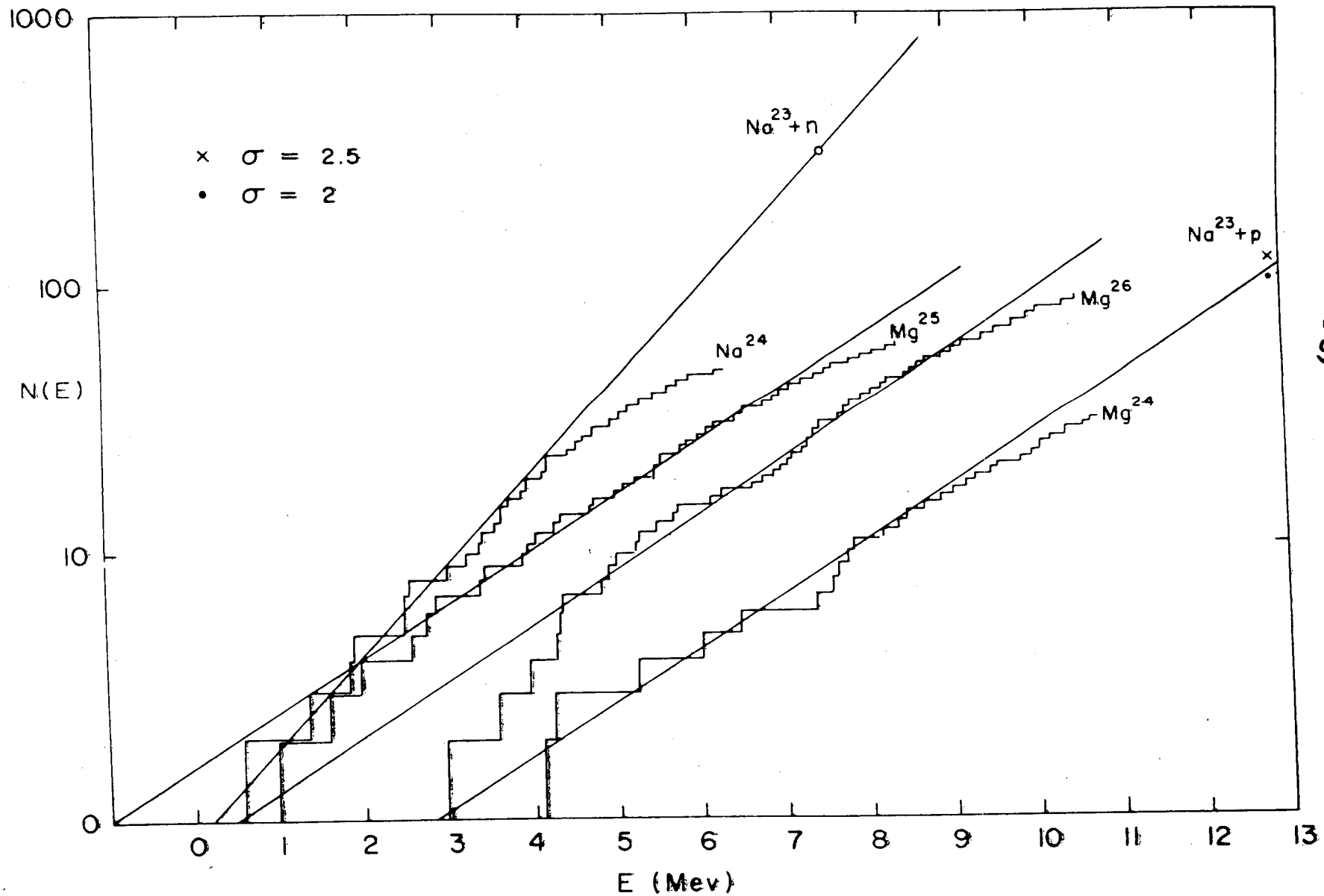
1000
100
10
0
N(E)
× σ = 2.5
• σ = 2
Na23+n
Na24
Mg25
Mg26
Mg24
Na23+p
0
1
2
3
4
5
6
7
8
9
10
11
12
13
E (Mev)

Figure 4.3

ing the corresponding level density expected at the neutron binding energy from the approximately linear portions of the N vs. E plots, one can check whether levels are being missed. In order to use (4.18) one must have a value for the spin dependence parameter. S-wave capture or scattering gives information for only two spin values, $I - \frac{1}{2}$ and $I + \frac{1}{2}$, so that the numbers of levels are known only for these two spin values, not the total number of levels. In order to correct this for the total number of levels one must guess at a reasonable value for the spin parameter, and Figures 4.2 and 4.3 show results for two values of σ appropriate to the nuclei considered. In all the cases shown the indication is that the curvature away from the straight line is indeed due to experimentally missed levels.

Straight line relationships like these suggest asking whether the proper formula is $N = \exp\,(2\sqrt{aU})$ or instead $N = \exp\,(\frac{1}{T}U)$ where T is some constant. One way to test the two propositions is to make plots of representative data. This is done in Figures 4.4 and 4.5. Figure 4.4 tests the $\exp\,(2\sqrt{aU})$ relationship by plotting $\ln^2 N$ as a function of the effective excitation energy. In the lower energy region the fit is quite good, but the discrepancy at the neutron binding energy is huge. Figure 4.5 tests $\exp\,(\frac{U}{T})$

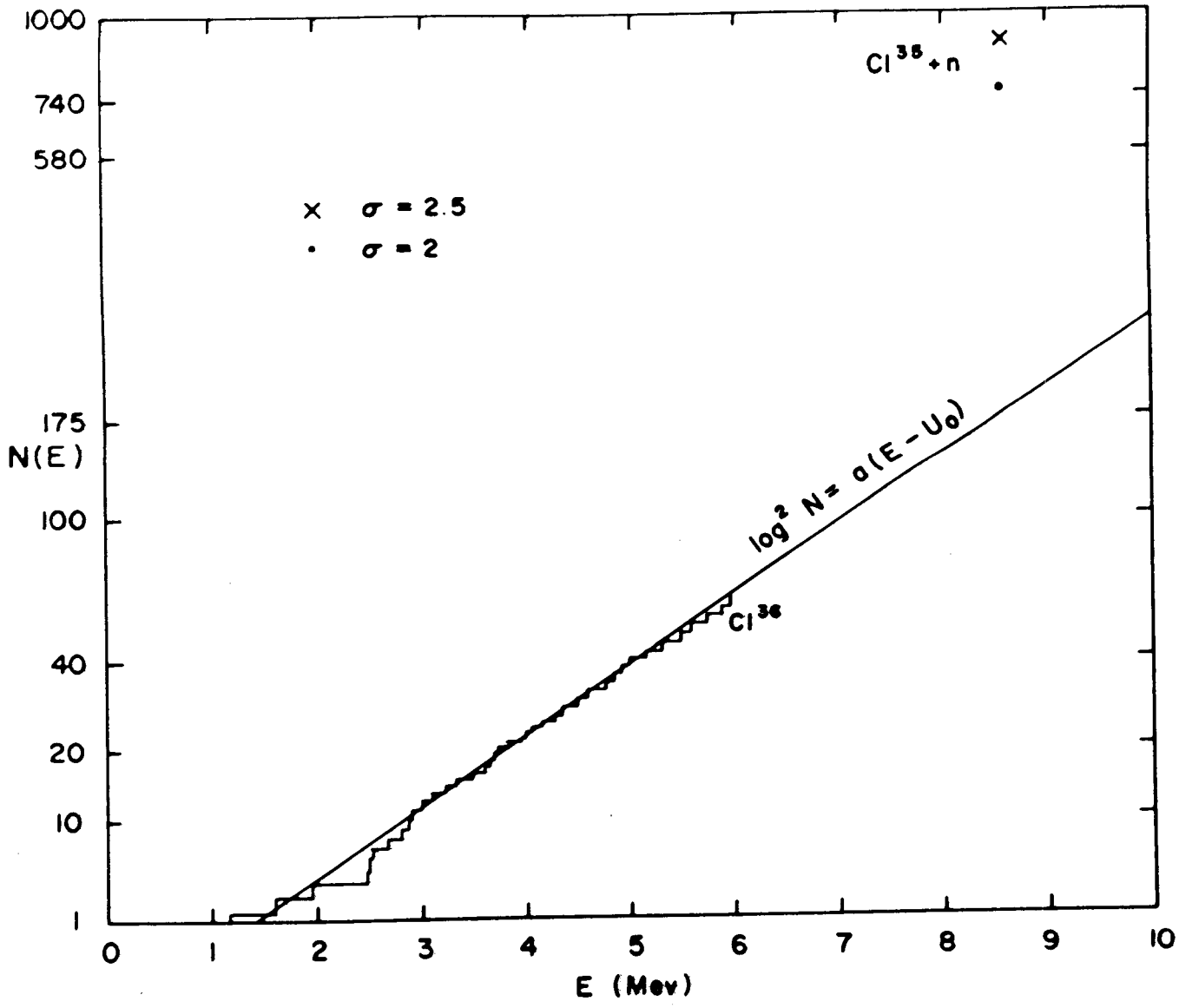
1000
740
580
175
N(E)
100
40
20
10
1
0
1
2
3
4
5
6
7
8
9
10
E (Mev)
Cl35+n
× σ = 2.5
• σ = 2
log² N = a(E − U₀)
Cl36

Figure 4.4

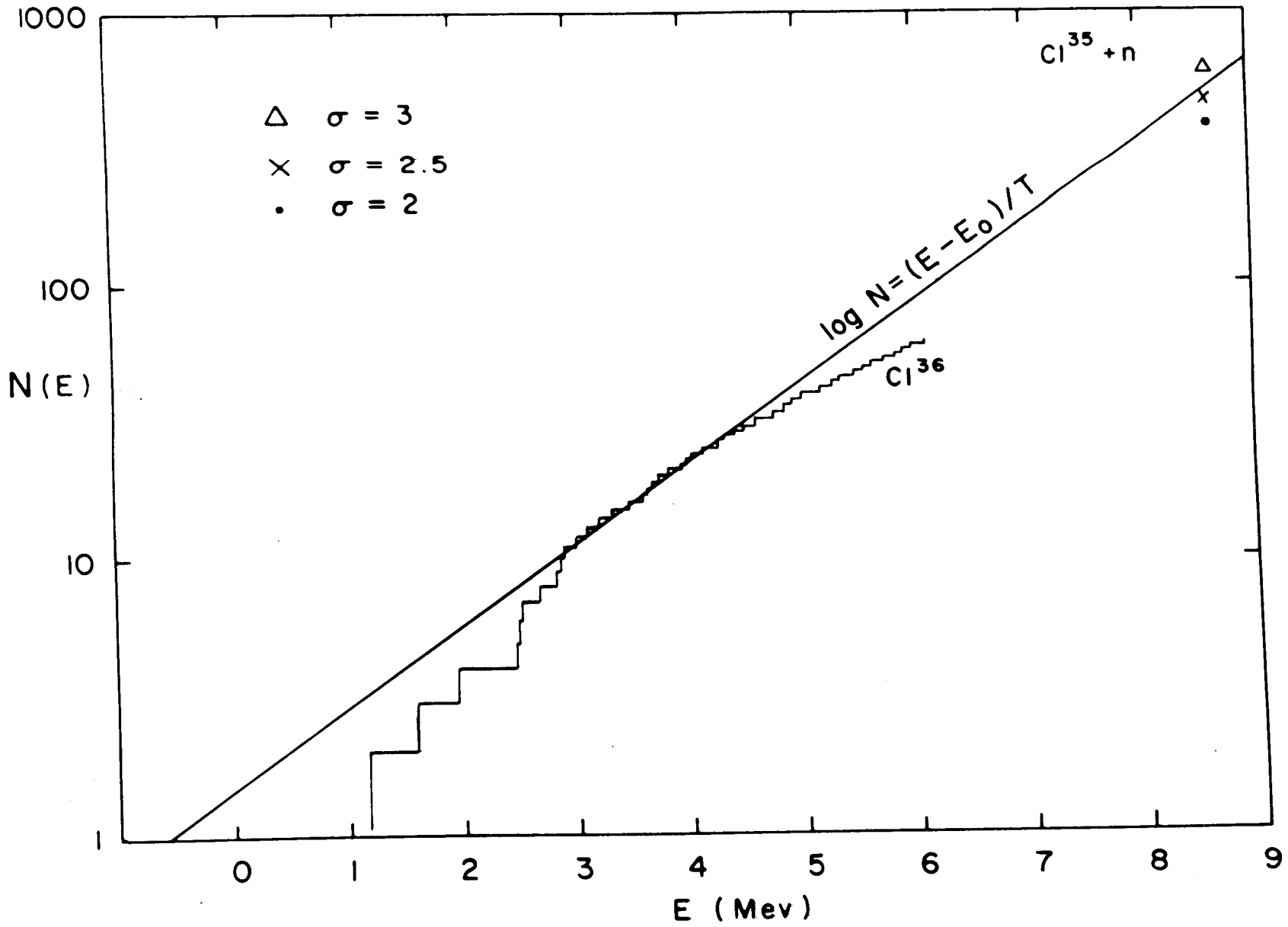
1000
100
10
1
N(E)
0
1
2
3
4
5
6
7
8
9
E (Mev)
Cl35 + n
Δ σ = 3
× σ = 2.5
• σ = 2
log N=(E−E0)/T
Cl36

Figure 4.5

which looks very poor at lower energies, but does fit the neutron binding energy reasonably well. We must be missing some levels. The basic behavior at low excitation energies is not that given by the fermi gas model, exp $(2\sqrt{aU})$, but instead something like exp (U/T). The fermi gas model is useful for supplying a complete set of levels which may then be reordered in energy due to other effects such as the pairing and collective corrections. At high enough excitation energies, we believe the gas model must be valid. From this evidence it seems better to use an empirical form like exp (U/T) near the ground state, and the fermi gas model at high energies. We shall need some prescription for finding out how to join these two prescriptions smoothly.

Bethe's treatment of the nucleus as a fermi gas of free neutrons and protons confined to the nuclear volume and gives

$$a/A = \text{constant} \tag{4.26}$$

The value of a can be determined from a consideration of the level densities at neutron binding energy, and this value then divided by mass number. In fact we do not find

a constant ratio. Nuclear level densities are subject to strong shell influences and near closed shells nuclei have much smaller level densities at the neutron binding energy than nuclei well away from closed shells, and so it is easy to see why a/A is not constant. The question is, Is there a way to allow for the existence of the shells? Figure 4.6 shows the run of data for a/A versus total shell corrections for $Z \geq 30$. We consider the nuclei in the regions

$$54 \leq Z \leq 78 \qquad 86 \leq N \leq 122$$

$$86 \leq Z \leq 122 \qquad 130 \leq N \leq 182$$

to be deformed. Nuclei are not generally considered to be deformed when they are close to closed shells. In Figure 4.6 the crosses correspond to undeformed nuclei and the dots to deformed nuclei. The undeformed nuclei seem to cluster around line I while the deformed nuclei seem to fit the parallel line II. For the undeformed nuclei of line I

$$a/A = 0.00917\ S + 0.142,$$

and for deformed nuclei

$$a/A = 0.00917\ S + 0.120.$$

Figure 4.7 shows a/A vs. the total shell correction

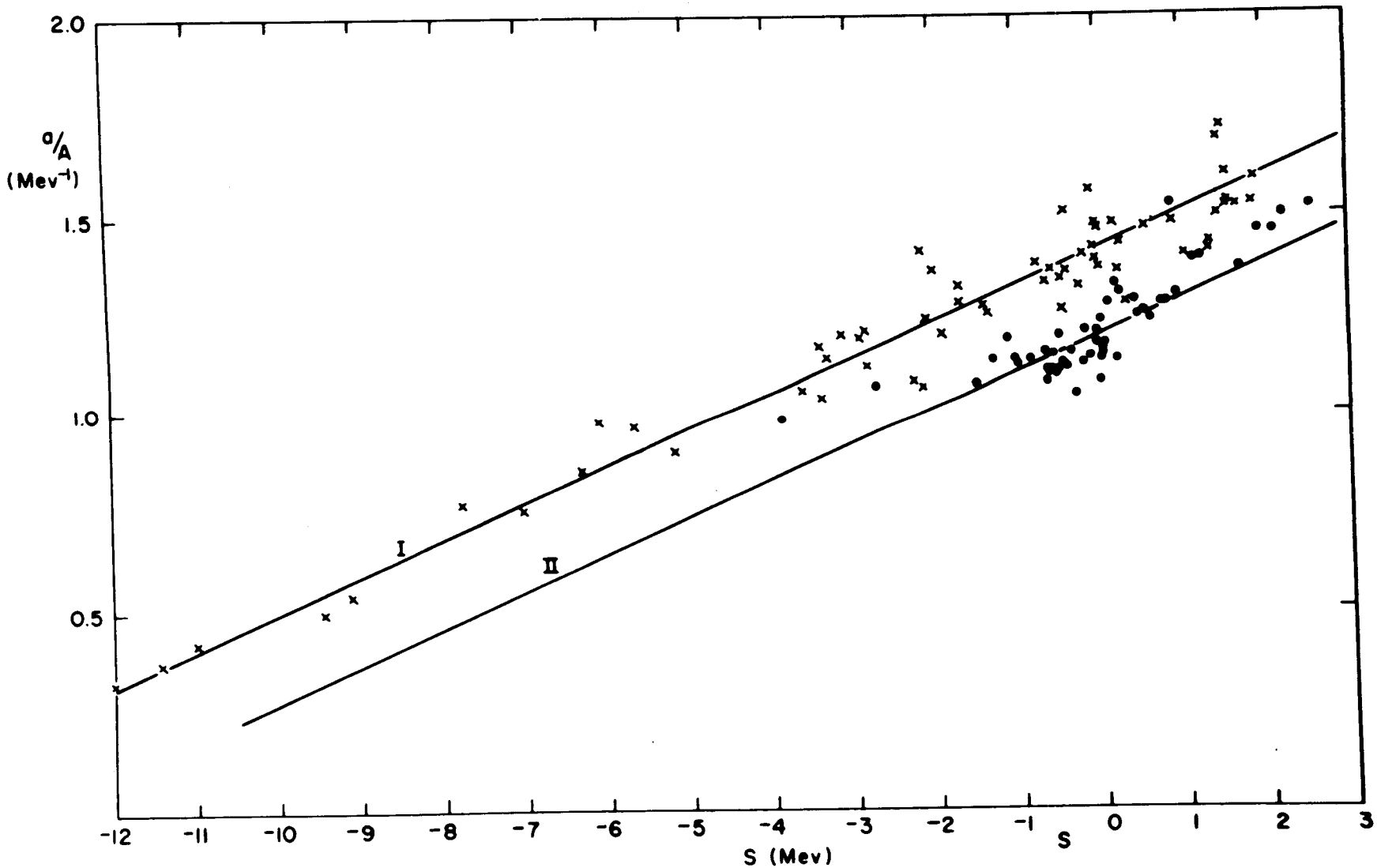

Figure 4.6

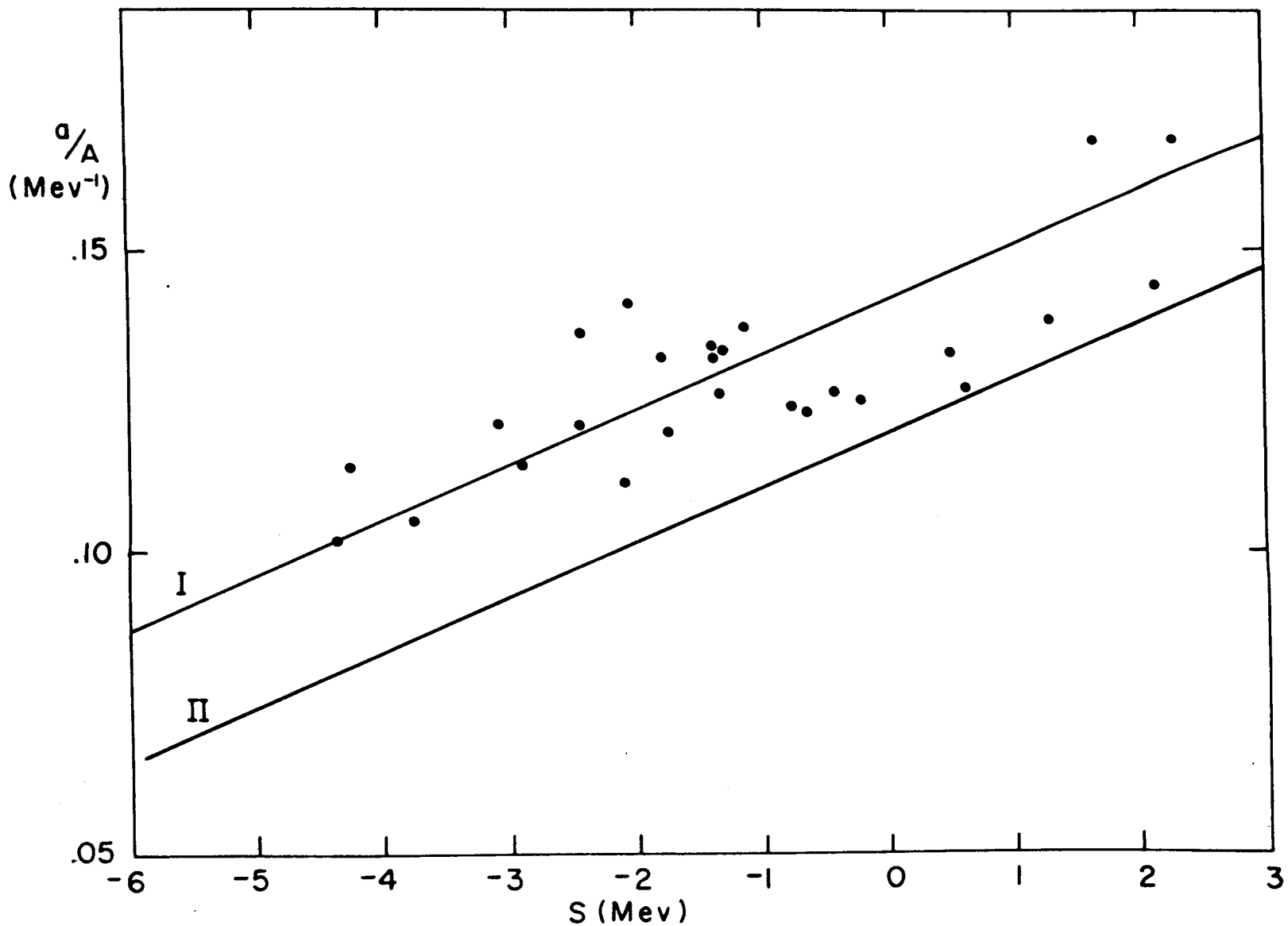

Figure 4.7

$S = S(N) + S(Z)$, for $20 \leq Z \leq 29$. In this region the correlation is still close to line I, which is the correlation for undeformed heavy nuclei, though the scatter is rather more than one would like. Figure 4.8 shows a/A vs. total shell correction for nuclei with $11 \leq Z \leq 19$. These nuclei no longer scatter about the correlation line for undeformed heavy nuclei. Some of them might fall below the line because of deformation or some other collective effect (e.g., Na and Mg isotopes). It must also be pointed out that the mass formula is not very good in this region; the shell corrections are less accurate. Nevertheless, the nuclei do seem to follow approximately the correlation for deformed heavy nuclei (line II) and so we shall use it to get values of a/A for nuclei with a few known lower levels.

Figure 4.9 shows level data for Sm^{148}. We have levels measured near ground and also near the neutron binding energy. The solid line is calculated from the composite level density relation. Above the cross, the dashed line is an extrapolation of the low energy formula and below it, the high energy formula. To determine fits to data, we choose a point P in some region near ground where the levels are practically linear and demand that our straight

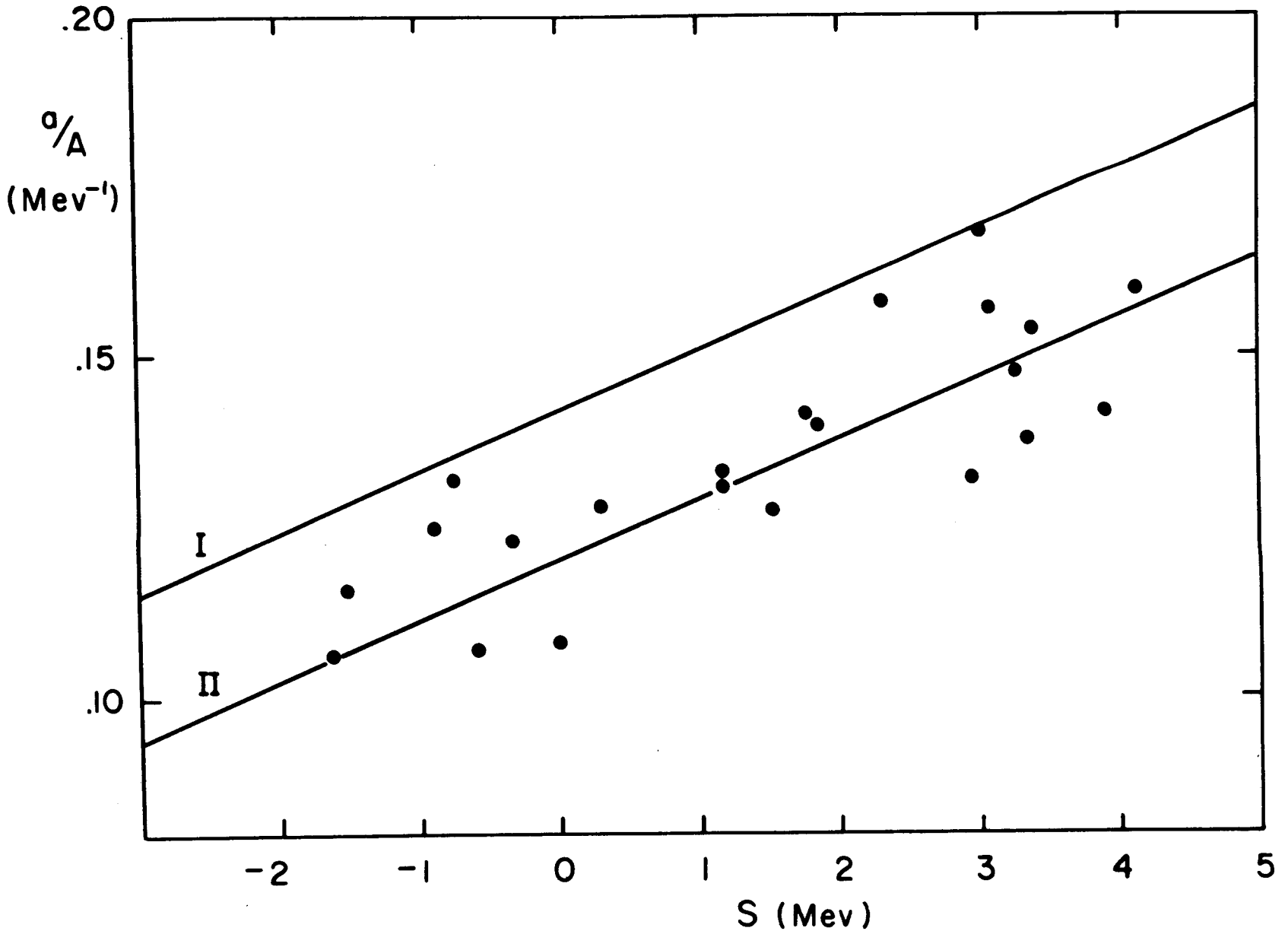

Figure 4.8

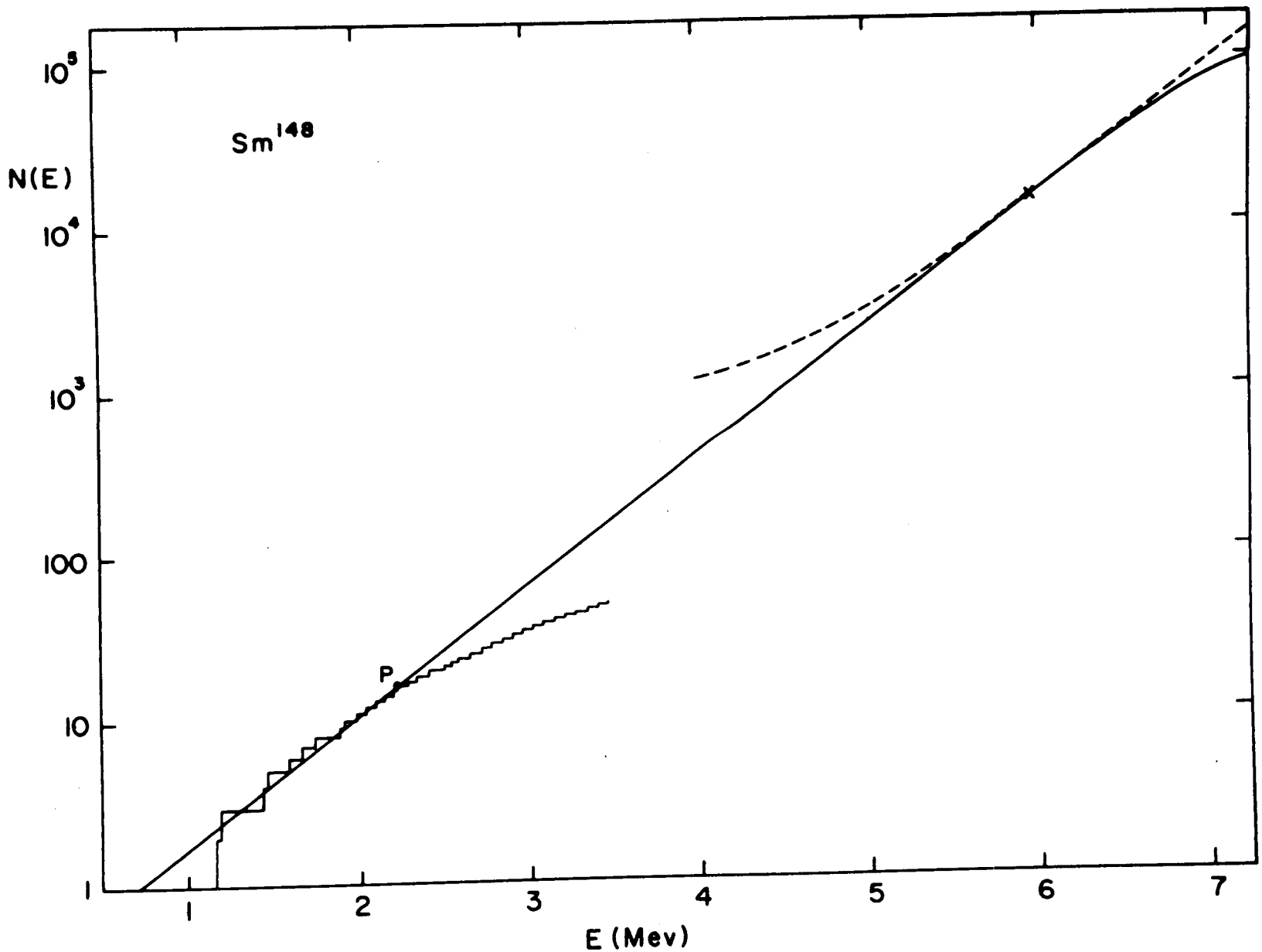

Figure 4.9

line pass through it. The line through the pivot point P is then rotated until it meets the high energy calculated line tangentially. We then believe the low energy form up to the point of tangency and the high energy formula above it.

We can write

$$N = \exp\left[\frac{E_p - E_o}{T}\right] \tag{4.27}$$

where E_p is the energy of the point of tangency described above and E_o its intercept, T is called the nuclear temperature. T effectively gives the slope of the low-energy formula straight line. Figure 4.10 is the resulting set of nuclear temperatures, which has a smooth dependence on mass number. There is no systematic difference due to even-odd effects and so all nuclei are represented in the same way. Generally, T decreases with increasing A and superimposed on this are marked shell effects, particularly near the double closed shell nucleus Pb^{208}, these effects are visible to a lesser extent near the N = 82, N = 50, and N = 28 shells. The Z = 50 shell does not show up in this manner, however, nor does it cause a fluctuation in a. The rise of T near closed shells makes N smaller there as it

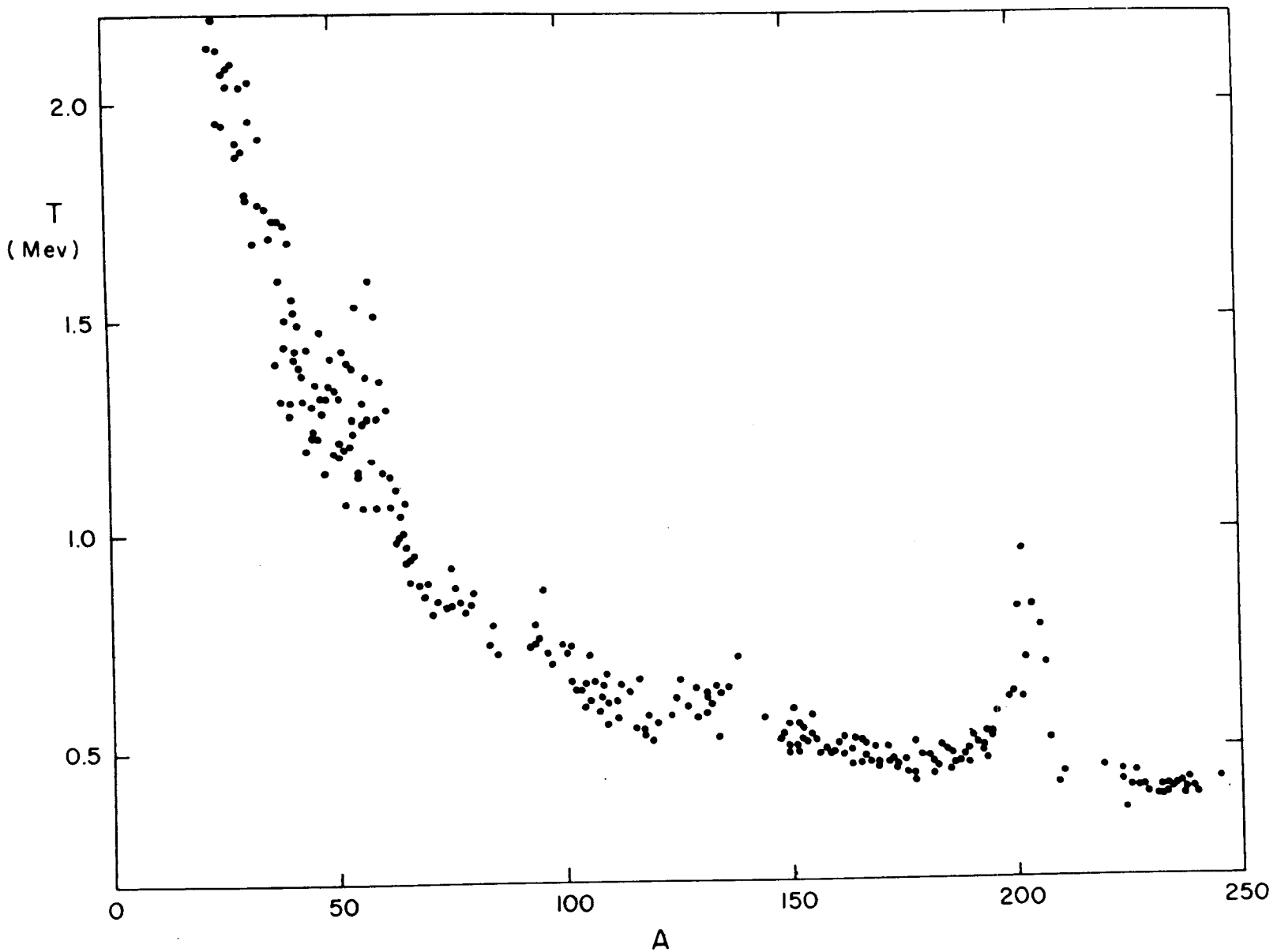

Figure 4.10

should.

One may attempt plotting E_x, the excitation energy of the tangency point, vs. A. When this is done, systematic odd-even effects are visible, but these can be substantially removed by subtracting the relevant pairing energies. A plot of $U_x = E_x - U_o$ vs. A is shown in Figure 4.11. Generally there are no shell effects, except possibly for some nuclei with Z or N within two units of a closed shell. Overall, U_x decreases with decreasing A. The spread in U_x also decreases with increasing A. The three curves drawn are

(1) The average value, $U_x = 2.5 + \frac{150}{A}$

(2) The upper limit, $U_x = 2.7 + \frac{200}{A}$

(3) The lower limit, $U_x = 2.1 + \frac{120}{A}$.

The uncertainty in U_x at first seems large, but this is not critical, as one can see by reinspection of Figure 4.9. The point of tangency, marked x, is at an energy $E_x = 6.0$ MeV. There is a region, about 1 MeV wide, where the two curves are virtually indistinguishable. An uncertainty in U_x of about 0.5 MeV would therefore not affect the slope and intercept of the lower protion of the curve significantly. The size of this region, where the two curves almost coincide, increases as A decreases becoming about 2 MeV for nuclei with $A \sim 50$. Hence the fact that the uncertainty in U_x also increases as A decreases should not be critical.

A graph of E_o vs. A is shown in Figure 4.12, there are quite obvious odd-even effects here. For odd A nuclei, the average value of E_o is about

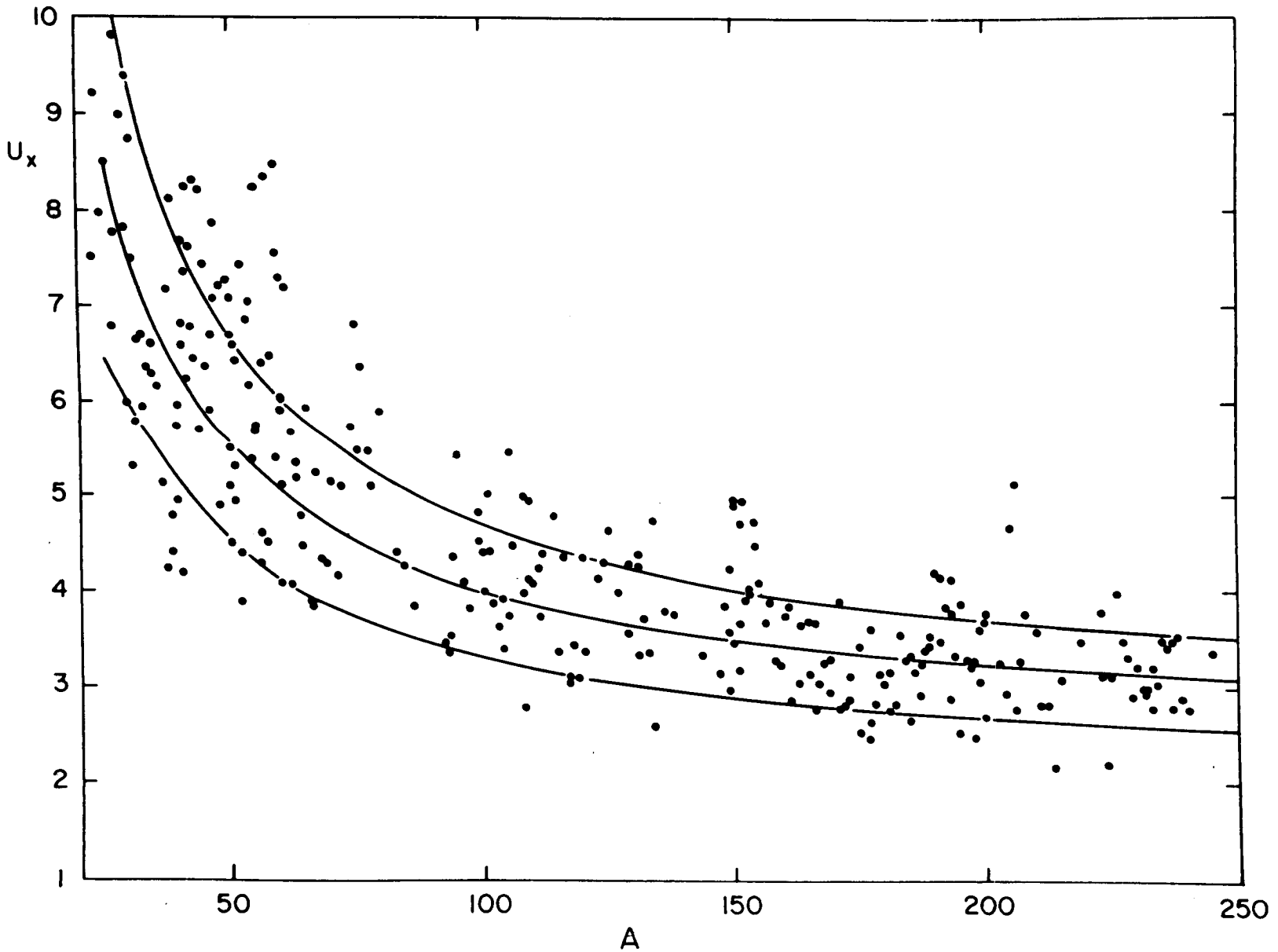

Figure 4.11

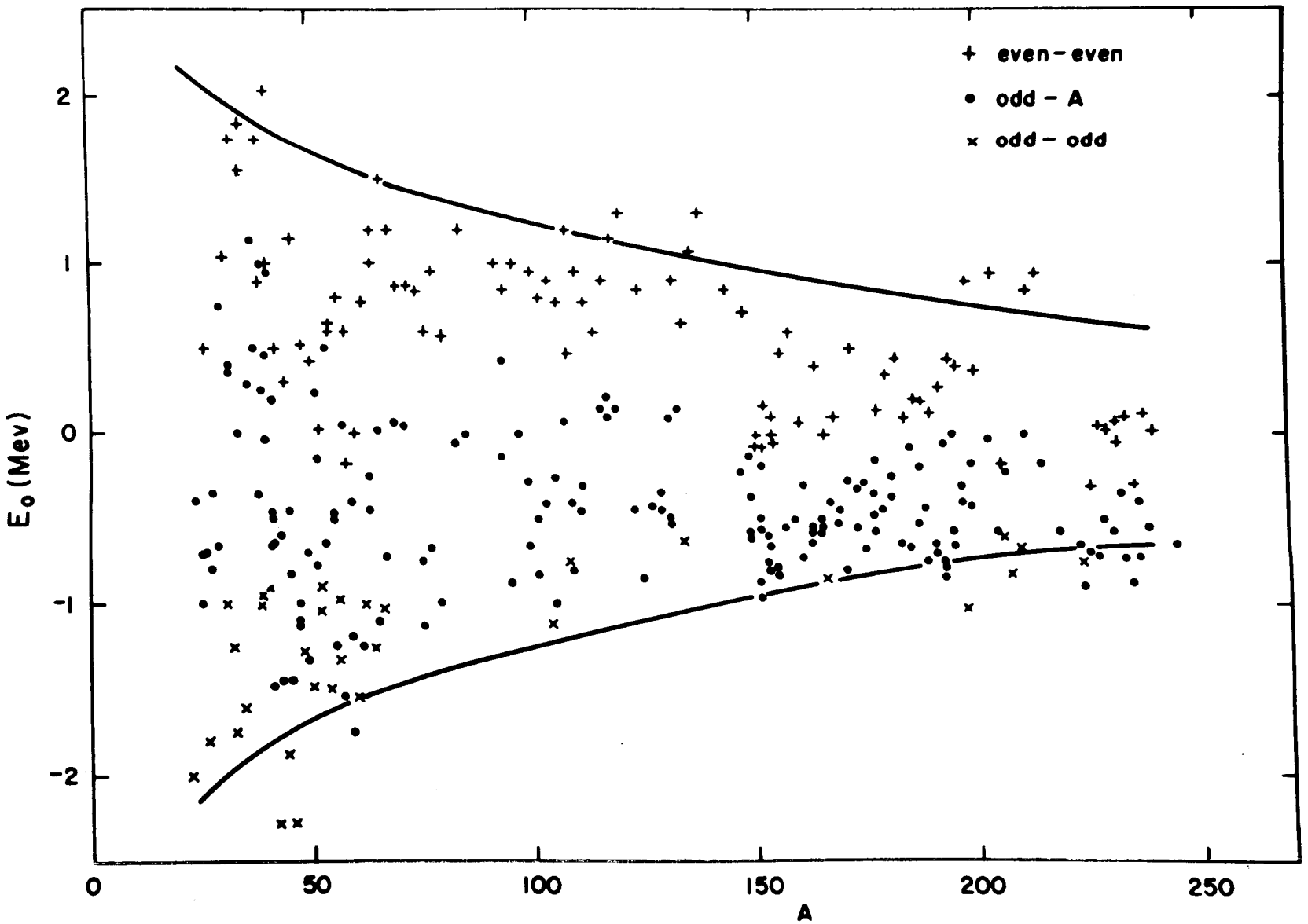

Figure 4.12

-0.5 MeV and the spread becomes larger as we go to smaller values of A, which is hardly unexpected since this is the region where nuclei assert their individuality most prominently. The separation between neighboring even-even and odd-odd nuclei is of the order of the pairing energy. The curves drawn are $\pm \langle P \rangle$ where $\langle P \rangle$ is an average of $\frac{1}{2}[P(N)+P(Z)]$ with local fluctuations smoothed out. These give outer envelopes for the intercepts of even-even and odd-odd nuclei, respectively. Most values of E_o are inside the region bounded by the two curves. For deformed even-even nuclei the intercepts seem to be systematically lower than $\langle P \rangle$, particularly for the deformed nuclei on either side of the region of the double closed shell nucleus Pb^{208}. The odd A values tend to cluster in the middle, but with a fair amount of scatter. Anyway, it is reasonable to take the pairing energy lines as rough measures of where these intercepts should go.

Let ρ_c be the calculated value of the neutron resonance density from (4.17), (4.23), and (4.24), and let ρ_{obs} be the observed value of the neutron resonance density. The ratio ρ_c/ρ_{obs} vs. A is shown in Figure 4.13. The scatter is appreciable, the logarithmic mean expectation value for the error in calculating the level density being 1.75. It is likely that this is the best that can be done in the near future because to do better, refined techniques must be devised to take account of shell and pairing effects and so on for specific nuclei.

We can summarize the composite prescription for a complete representation of the nuclear level density when we have no experimental information about the nucleus in question as follows.

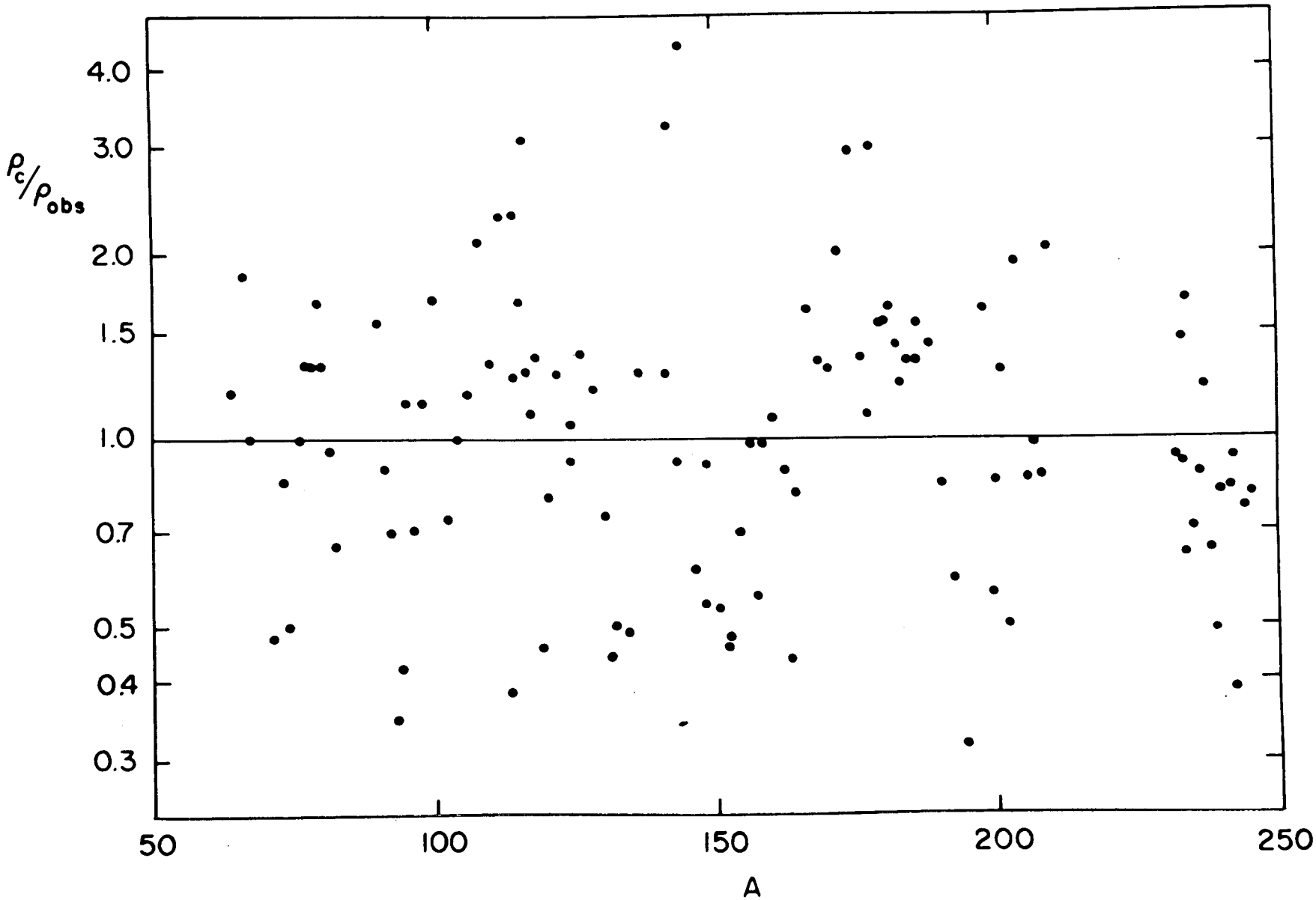

Figure 4.13

At high energies the density of levels at energy E of given J (of either parity) is

$$\rho_2(E,J) = \frac{\sqrt{\pi}}{12} \frac{\exp(2\sqrt{aU})}{a^{1/4}\, U^{5/4}} \frac{(2J+1)\exp[-(J+\frac{1}{2})^2/2\sigma^2]}{2\sqrt{2\pi}\,\sigma^3} \ (\mathrm{MeV}^{-1}) \qquad (4.17)$$

where

$$U = E - U_o = E - P(Z) - P(N) \qquad (\text{in MeV}) \qquad (4.25)$$

$$\sigma^2 = 0.0888\ (aU)^{\frac{1}{2}}\ A^{2/3}\ , \qquad (4.23)$$

P(Z) and P(N) being tabulated pairing energies. a is obtained from the appropriate correlation of a/A with S, the total shell correction S = S(Z) + S(N). For undeformed nuclei

$$a/A = 0.00917S + 0.142 \quad (\mathrm{MeV}^{-1}),$$

and for deformed nuclei

$$a/A = 0.00917S + 0.120 \quad (\mathrm{MeV}^{-1}) \quad ,$$

S(N) and S(Z) being tabulated shell corrections. The density of levels of all J is

$$\rho_2(E) = \frac{\sqrt{\pi}}{12} \frac{\exp(2\sqrt{aU})}{a^{1/4}\, U^{5/4}} \frac{1}{\sqrt{2\pi}\,\sigma} \qquad (4.18)$$

The nuclear temperature is given by

$$\frac{1}{\tau} = \sqrt{\frac{a}{U}} - \frac{3}{2U} \ .$$

This ρ_2 is valid for all energies greater than E_x, where

$$U_x = 2.5 + \frac{150}{A} \quad (\text{MeV}) \tag{4.28}$$

$$E_x = U_x + P(Z) + P(N).$$

Below this the level density is

$$\rho_1(E) = \frac{1}{T} \exp[(E-E_o)/T] \quad . \tag{4.29}$$

The parameters T and E_o are determined by fitting ρ_2 and ρ_1 at $E = E_x$, i.e.,

$$T = \tau(U_x)$$

$$\rho_1(E_x) = \frac{1}{T} \exp[E_x-E_o)/T] = \rho_2(U_x), \tag{4.30}$$

$$E_o = E_x - T \ln[T \rho_2(U_x)] \quad .$$

These level densities are the quantities to which things like particle reaction rates or particle reaction cross sections are most sensitive, and so when we wish to calculate nuclear reaction rates under stellar conditions, especially under extreme stellar conditions in which the very heaviest nuclei will be involved in the reactions, it is particularly important to have a reliable prescription for the nuclear level densities.

References

Gilbert, A., and A.G.W. Cameron. 1965. Can. J. Phys. 43, 1446.

Gilbert, A., F.S. Chen and A.G.W. Cameron. 1965. Can. J. Phys. 43, 1248.

5. Nuclear Reactions

We have already considered some of those aspects of nuclei concerned with the static properties, the particle orbits, level densities and mass. We now turn our attention to some of the changes that can take place in nuclei, specifically nuclear reactions.

To begin with we will consider some general properties of nuclear reactions. If we want to make a realistic calculation of nuclear reaction rates we will require some idea of the basic principles involved, and some quantitative knowledge of the functions involved. Our treatment will follow that in Theoretical Nuclear Physics by J. M. Blatt and V.F. Weisskopf.

We represent a nuclear reaction as follows:

$$\underline{a} + \underline{X} \rightarrow \underline{Y} + \underline{b} \tag{5.1}$$

where, $\underline{a}$ is a particle interacting with some nucleus $\underline{X}$, producing a transition to some nucleus $\underline{Y}$ and an emitted particle $\underline{b}$. The emitted particle $\underline{b}$ may be another nucleus, and more than one particle may be emitted. Strictly speaking $\underline{a}$ or $\underline{b}$ may be a γ-ray, but such transitions will always be considered separately.

Some possible types of reactions are

$$\underline{a} + \underline{X} \rightarrow \underline{X}^* + \underline{a} \quad \text{(inelastic scattering)}$$

$$\underline{a} + \underline{X} \rightarrow \underline{X} + \underline{a} \quad \text{(elastic scattering)}$$

$$\underline{a} + \underline{X} \rightarrow \underline{Y} + \underline{b}$$

Nuclear Reaction Channels

The particle $\underline{a}$ and the nucleus $\underline{X}$ are in the ground state. The combination of these will be one channel for the reaction which we will call the entrance channel or the initial channel. Elastic scattering then involves a re-emission of particles into the entrance channel. Inelastic scattering defines an entirely different channel even though the nucleus and the projectile may be the same.

Similarly $\underline{Y} + \underline{b}$ (with $\underline{Y}$ and $\underline{b}$ in ground states) is an exit channel. Any similar reaction in which $\underline{Y}$ is in any one of its excited states corresponds to a different channel. We will denote channels by Greek letters. Consider the channel α. The state of the nucleus involved in this channel is indicated by α', and the state of the particle involved is indicated by α''. Thus we can write a reaction as follows:

$$a_{\alpha''} + X_{\alpha'} \rightarrow X_{\beta'} + a_{\beta''} \qquad (5.2)$$

where β indicates another channel.

When we have a nuclear reaction there are certain basic physical laws that we expect to be obeyed. We expect that there will be conservation of energy, linear momentum, angular momentum and parity in a reaction, as long as we are not talking about weak interactions. We can always insist upon conservation of parity in strong nuclear reactions since the extent to which parity is not conserved in these reactions is small.

The reaction energy in a nuclear reaction is known as the Q-value. If we define the channel energy as the sum of the kinetic energies of the particle and nucleus in that channel, then

$$\epsilon_\beta = \epsilon_\alpha + Q_{\alpha\beta} \tag{5.3}$$

where

$$Q_{\alpha\beta} = E_{\alpha'} + E_{\alpha''} - E_{\beta'} - E_{\beta''} \tag{5.4}$$

If ϵ_β is less than zero then conservation of energy requires that the reaction cannot take place and we describe the reaction channel as being closed.

For the channels we are considering, all particles are in the ground state of the nucleus. In any particular

reaction, such as an α entrance channel and a γ exit channel, with $Q_{\alpha\beta} > 0$ (so that the reaction is exothermic) the limit in which the channel energy in α goes to zero gives the definition of the ordinary nuclear Q value (i.e. the ordinary reaction energy for the reaction). Similarly if the reaction is endothermic, so that we must have some energy in the α channel which just leaves the outgoing particles with zero energy in the γ channel, then the entrance channel energy ϵ_α is just the negative of the Q value.

Cross Section

Define the cross section σ

$$\sigma = \frac{\text{number of events of specified type per unit time per nucleus}}{\text{number of incident particles per unit area per unit time}}$$

Consider a plane wave of particles of type A incident on a nucleus X in the entrance channel α. We will separate the events involving the entrance channel from the other events by writing the total cross section for the entrance channel α as the sum of a scattering cross section in α plus the reaction cross section corresponding to α.

$$\sigma_t(\alpha) = \sigma_{sc}(\alpha) + \sigma_r(\alpha) \qquad (5.5)$$

The scattering cross section includes only elastic scattering. The inelastic scattering will be regarded as part of the reaction cross section.

In order to get the qualitative features of the reaction we assume that both the projectile a and the nucleus X have zero spins. We divide each channel α into different orbital angular momenta so that we can talk about sub-channels of type α and orbital angular momenta ℓ. To treat the problem of angular momentum we consider a plane wave of incident particles which can be decomposed into spherical harmonics $Y_{\ell,0}$ where each $Y_{\ell,0}$ corresponds to a different spherical wave carrying a different amount of angular momentum. This means that we can decompose the cross sections into sub-channels.

$$\sigma_{sc}(\alpha) = \sum_{\ell=0}^{\infty} \sigma_{sc,\ell} \tag{5.6}$$

$$\sigma_{r}(\alpha) = \sum_{\ell=0}^{\infty} \sigma_{r,\ell} \tag{5.7}$$

where σ_{sc} and $\sigma_{r,}$ are total cross sections in that they have been integrated over all emerging angles. If we were going to talk about the angular distribution of the outgoing particles we would have to consider the angular dependence

of the cross sections. We will not in general consider angular distribution because in the application to thermonuclear reaction rates we are only interested in total cross sections.

Now we would like to place some limits on the reaction cross sections from rather simple geometrical arguments. To do this we divide the incoming plane wave into a number of zones, as follows:

Figure 5.1

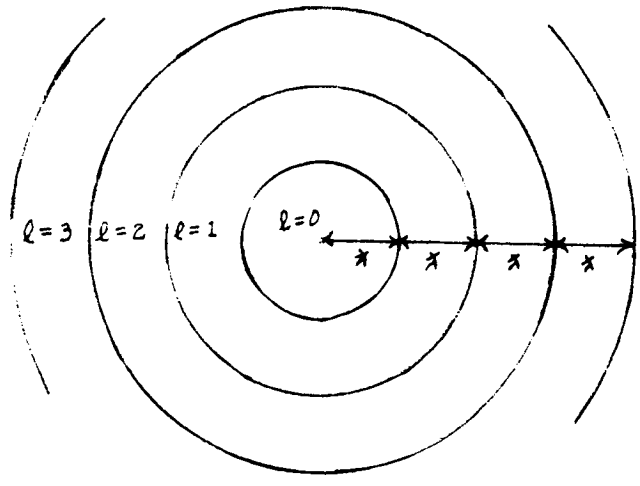

The innermost zone will contain particles with impact parameters less than the de Broglie wave length divided by 2π. The next zone will contain particles of impact parameters between $\lambda\!\!\!^{-}$ and $2\lambda\!\!\!^{-}$ etc.

In classical mechanics the angular momentum of an incident particle is the mass times the velocity times the impact parameter p. Thus in the $\ell^{\underline{th}}$ zone the incident particles

will have angular momenta between $mv\ell\lambda\!\!\!^{-}$ and $mv(\ell+1)\lambda\!\!\!^{-}$. From the definition of the deBroglie wavelength the angular momenta lie between $\ell\hbar$ and $(\ell+1)\hbar$. We would now like to quantize this classical picture by assuming that the particles with angular momentum ℓ are the ones which move in the $\ell^{\underline{th}}$ zone (to a crude approximation). The cross-sectional area of the $\ell^{\underline{th}}$ zone is

$$\pi(\ell+1)^2 \lambda\!\!\!^{-2} - \pi\ell^2\lambda\!\!\!^{-2} = (2\ell+1)\pi \lambda\!\!\!^{-2} \qquad (5.8)$$

We will consider this to give an upper limit to the reaction cross section for the particles incident on the nucleus in this zone. So $\sigma_{r,\ell} \leq (2\ell+1)\pi \lambda\!\!\!^{-2}$
This relation does not apply to the scattering cross section.

We have not yet said anything about nuclear size. When $\ell\lambda\!\!\!^{-}$ starts to exceed the nuclear radius we say that the cross sections farther out for higher angular momenta fall off very rapidly because the chance of hitting anything beyond the nuclear edge is small. On the other hand when $\ell\lambda\!\!\!^{-}$ is less than the nuclear radius the chance of hitting the nucleus is very high and we say that the partial cross section for such angular momenta is likely to approach the upper limit.

We can now proceed in a more formal fashion to find

some of these cross section limits. We will represent the incident beam by a plane wave in the entrance channel, and we will define a channel coordinate $\vec{r}_\alpha$ as the vector between the center of the target nucleus and the projectile. The plane wave can be written in the following form

$$\exp(i\,\vec{k}_\alpha \cdot \vec{r}_\alpha) = \exp(ikz) \tag{5.9}$$

where k is the wave number and we have chosen the z axis parallel to the vector $\vec{k}_\alpha$. We define $\vec{k}_\alpha$ as

$$\vec{k}_\alpha = \frac{M_\alpha \vec{V}_\alpha}{\hbar} \tag{5.10}$$

where $M_\alpha = \frac{M_a M_x}{M_a + M_x}$, the reduced mass,

We define the channel wave number $|\vec{k}|$

as

$$|\vec{k}_\alpha| = k_\alpha = \frac{1}{\lambda\!\!\!^{-}_\alpha} = \frac{(2M_\alpha \epsilon_\alpha)^{\frac{1}{2}}}{\hbar} \tag{5.11}$$

From now on we will omit the index α as we will rarely need to refer to specific channels.

The plane wave has to be expanded in spherical harmonics in which the coefficients of the various multipole orders will involve spherical Bessel functions. We only want to

concern ourselves with incoming and outgoing waves at large distances from the scattering nucleus located at the center of the coordinates. So we take the asymptotic forms of the spherical Bessel functions for large values of the argument and get for a plane wave expansion

$$e^{ikz} \approx \frac{\pi^{\frac{1}{2}}}{kr} \sum_{\ell=0}^{\infty} (2\ell+1)^{\frac{1}{2}} \, i^{\ell+1} \left\{ e^{-i(kr-\frac{1}{2}\ell\pi)} - e^{+i(kr-\frac{1}{2}\ell\pi)} \right\} Y_{\ell,0} \tag{5.12}$$

This expression describes an undisturbed plane wave. The reactions taking place will only disturb the outgoing plane wave. We now change the outgoing plane wave by modifying only the coefficient representing this wave in the above. Thus we write

$$\psi(\vec{r}) \cong \frac{\pi^{\frac{1}{2}}}{kr} \sum_{\ell=0}^{\infty} (2\ell+1)^{\frac{1}{2}} \, i^{\ell+1} \left\{ \exp[-i(kr-\tfrac{1}{2}\ell\pi)] - \zeta_\ell \exp[i(kr-\tfrac{1}{2}\ell\pi)] \right\} Y_{\ell=0} \tag{5.13}$$

The scattered wave is the difference between the actual wave and the incident wave. Thus,

$$\psi_{sc} = \psi(\vec{r}) - \exp(ikz) \tag{5.14}$$

or

$$\psi_{sc} = \frac{\pi^{1/2}}{kr} \sum_{\ell=0}^{\infty} (2\ell+1)^{1/2}\, i^{\ell+1}\, (1 - \zeta_\ell)\, \exp[i(kr - \tfrac{1}{2}\ell\pi)]\, Y_\ell \tag{5.15}$$

The scattering cross section is obtained by dividing the number of scattered particles per second by the number of incident particles per square centimeter per second. Define N_{sc} as the number of scattered particles and N as the number of incident particles. To find N_{sc}, the origin is enclosed by a large sphere of radius r, and we equate ψ_{sc} (the flux going through the sphere) to N_{sc}. The quantum mechanical probability current is:

$$I = \frac{\hbar}{2iM} \left(\psi^* \nabla \psi - \psi \nabla \psi^* \right) \tag{5.16}$$

Thus,

$$N_{sc} = \frac{\hbar}{2iM} \int \left(\frac{\partial \psi_{sc}}{\partial r} \psi^*_{xc} - \frac{\partial \psi^*_{sc}}{\partial r} \psi_{sc} \right) r_o^2 \sin\theta \, d\theta \, d\varphi \tag{5.17}$$

$$= \frac{\hbar}{2iM} \int \frac{\pi}{k^2} \sum_{\ell=0}^{\infty} (2\ell+1) \left| 1 - \zeta_\ell \right|^2 Y^2_{\ell,0} \left(\frac{2ik}{r_o^2} \right) r_o^2 \sin\theta \, d\theta \, d\varphi \tag{5.18}$$

We then have $\int Y^2_{\ell,0} \sin\theta \, d\theta \, d\varphi = 1$

Then

$$\frac{\pi\hbar}{Mk} = \frac{\pi}{k^2} \frac{(2M\epsilon)^{\frac{1}{2}}}{\hbar} \frac{\hbar}{M} = \frac{\pi}{k^2} \frac{(2M\frac{1}{2}Mv^2)^{\frac{1}{2}}}{M}$$

$$= \frac{\pi v}{k^2} \tag{5.19}$$

Thus

$$N_{sc} = \frac{v\pi}{k^2} \sum_{\ell=0}^{\infty} (2\ell+1) \; (1 - \zeta_\ell)^2 \tag{5.20}$$

The v which appears in these equations is the channel velocity.

The incident flux is given by

$$N = \frac{\hbar}{2iM} \left[\frac{\partial}{\partial z} \exp ikz \exp(-ikz) - \frac{\partial}{\partial z} \exp(-ikz) \exp(ikz)\right] \tag{5.21}$$

$$= \frac{\hbar}{2iM} \cdot 2ik = \frac{\hbar k}{M} = \frac{\hbar}{M} \cdot \frac{(2M\frac{1}{2}Mv^2)^{\frac{1}{2}}}{\hbar} \tag{5.22}$$

or N = v

The scattering cross section is

$$\sigma_{sc,\ell} = \frac{N_{sc}}{N} = \pi \lambda^2 \; (2\ell+1) \; |1 - \zeta_\ell|^2 \tag{5.23}$$

Na determines the reaction cross section which is

the number of particles removed from the beam per second i.e. the number of particles entering a sphere of radius r_o, but which do not leave again through the entrance channel. Thus it is the net flux into the sphere as computed from the complete wave function $\psi(\vec{r})$.

$$N_A = \frac{-\hbar}{2iM} \int \left(\frac{\partial\psi}{\partial r} \psi^* - \frac{\partial\psi^*}{\partial r} \psi \right) r_o^2 \sin\theta \, d\theta \, d\varphi \qquad (5.24)$$

The minus sign is taken in order that N_A come out positive. Equation (5.24) gives

$$N_A = \frac{v\pi}{k^2} \sum_{\ell=0}^{\infty} (2\ell+1) \left(1 - |\zeta_\ell|^2\right) \qquad (5.25)$$

So

$$\sigma_{r,\ell} = \frac{N_A}{N} = \pi \lambda^2 (2\ell+1) \left(1 - |\zeta_\ell|^2\right) \qquad (5.26)$$

And these results constitute a formal proof of the geometrical limits which were previously discussed only qualitatively. We should have $|\zeta_\ell|^2 \leq 1$ to prevent the outgoing wave from exceeding the incoming wave. For different values of ζ_ℓ we can get different expressions for the reaction and scattering cross sections. Suppose $\zeta = -1$

then

$$\left.\begin{aligned} \sigma_{sc,\ell} &= 4\pi \lambda\!\!\!^{-2} (2\ell+1) \\ \sigma_{r,\ell} &= 0 \end{aligned}\right\} \qquad (5.27)$$

which gives a maximum value for the scattering cross section. On the other hand if $\zeta_\ell = 0$ then

$$\left.\begin{aligned} \sigma_{sc,\ell} &= \pi \lambda\!\!\!^{-2} (2\ell+1) \\ \sigma_{r,\ell} &= \pi \lambda\!\!\!^{-2} (2\ell+1) \end{aligned}\right\} \qquad (5.28)$$

which is the limiting value for the reaction cross section. Qualitatively the reaction and scattering cross sections are essentially equal to the geometric area.

Suppose, apart from angular momentum arguments, one just considers a disc absorbing particles and that this leads to a reaction when the particles strike within the actual geometrical area. But when particles just miss the edge of the disc they do not react but can still be diffracted by wave effects. This diffraction can give a scattering cross section which is equal to the geometrical area of the disc.

Choosing different ζ_ℓ's we can make a plot as follows.

Figure [illegible]

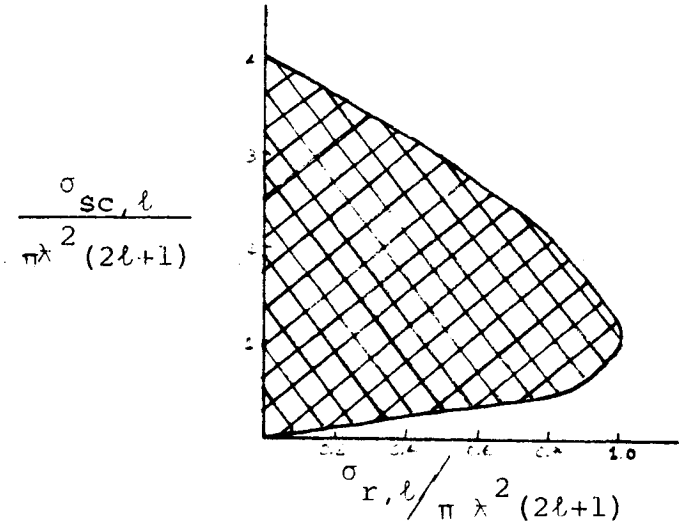

We may have any combination of scattering and reaction cross sections within the shaded area. Thus we may have pure scattering but we can never have pure reactions without scattering. The reason for this is that in order to get absorbtion the outgoing part of the plane wave must be weakened and that means we have to add an outgoing wave of opposite phase. It is this outgoing wave which corresponds to some scattering. We can obtain pure scattering by simply making a change in phase. The scattering cross section can be as much as four times the reaction cross section because the scattering cross section involves the phase of ζ_ℓ, but the reaction cross section involves only the absolute value of ζ_ℓ. This means that in elastic scattering the incoming

and outgoing waves are coherent and therefore they can interfere both constructively and destructively. It is the constructive interference which can give rise to a factor of four. The reaction cross section does not contain the possibility of interference and so the maximum value for it is one.

We must now relate the size of the nucleus to the de Broglie wave length. As the energy of the incoming particle is increased its de Broglie wave length decreases, i.e. $\lambda\!\!\!^{-}$ goes to zero, and consequently at some energy, $\lambda\!\!\!^{-}$ will become small compared to the nuclear radius. So the ideal case might be obtained for a nucleus, with R very much greater than $\lambda\!\!\!^{-}$, which absorbs all the particles incident on the nucleus which lead to reactions, and does not interact with particles that miss the edge. The critical value of ℓ is $R/\lambda\!\!\!^{-}$ and all particles with $\ell \leq \ell_{critical}$ will strike the nucleus.

$$\therefore \quad \text{if } \zeta_\ell = 0, \ell\lambda\!\!\!^{-} \leq R \qquad (5.29)$$

$$\text{if } \zeta_\ell = 1, \ell\lambda\!\!\!^{-} \geq R \qquad (5.30)$$

Thus we have

$$\sigma_r = \sigma_{sc} = \sum_{\ell=0}^{R/\lambda\!\!\!^{-}} (2\ell+1)\pi \lambda\!\!\!^{-}{}^2 \qquad (5.31)$$

$$\approx \int_0^{R/\lambda\!\!\!^{-}} 2\ell \, \pi \, \lambda\!\!\!^{-}{}^2 \, d\ell$$

$$\approx \pi R^2 \qquad (5.32)$$

In the limit of high energies the total cross section is

$$\sigma_t = \sigma_{sc} + \sigma_r = 2\pi R^2 \qquad (5.33)$$

twice the cross sectional area of the nucleus. This points out that diffraction of particles by the edge of the nucleus gives a contribution to σ_{sc} equal to the geometric area.

The Logarithmic Derivative

Now we want to see what the relations are between the external wave functions for the incoming and outgoing waves and the conditions in the nucleus. Ordinarily we know very little about what is going on in the nucleus. However, we know that the wave function that corresponds to the nucleus must join on smoothly with the wave functions in the external channels. Therefore we have to deal with the conditions at the nuclear surface, the

value and derivative of the wave function. All the necessary information concerning scattering and reaction cross sections are contained in the magnitude of ζ_ℓ.

For simplicity consider neutrons at the surface with zero angular momentum. We must make the assumption that the nucleus has a well defined surface, although we know that it does not. The nuclear edge is fuzzy, the density falling off in a smooth manner. Thus there is a great deal of arbitrariness in talking about the nuclear surface. We define the channel radius R as follows:

$$R = R_x + R_A, \text{ where}$$

$$r > R \text{ outside the nucleus}$$

$$r < R \text{ inside the nucleus}$$

Consider an incoming neutron of zero angular momentum, which we shall call an S wave neutron. We describe the relative motion of the neutron and nucleus in the external region by a wave function $\psi(r)$ which corresponds to the relative motion of two particles having no interaction between them.

$$\nabla^2\psi + k^2\psi = 0 \qquad \text{for} \qquad r > R \tag{5.34}$$

where k is the entrance channel wave number. Now this equation will not hold inside the nucleus.

For large values of r, ψ is a superposition of incident plane waves exp(ikz) and an outgoing spherical wave. Our previous analysis was based on the asymptotic behavior at infinity for large values of r, and now we have to consider the behavior for smaller values of r right down to the channel radius.

We write $\psi(\vec{r})$ as

$$\psi(\vec{r}) = \psi(r,\theta) = \sum_{\ell=0}^{\infty} \frac{U_\ell(r)}{r} Y_{\ell,0}(\theta) \qquad (5.35)$$

where we only consider m = o since exp(ikz), the incident wave, is independent of azimuthal angle ϕ.

For S wave neutrons we have

$$\frac{d^2U_o}{dr^2} + k^2U_o = 0 \qquad r \geq R \qquad (5.36)$$

The general solution of this equation is

$$U_o(r) = a \exp(-ikr) + b \exp(ikr), \quad r \geq R \qquad (5.37)$$

and for a complete specification we need boundary conditions. We shall consider the behavior of the wave function at large distances. At large r the asymptotic form for ψ is

$$\psi \cong \frac{\pi^{\frac{1}{2}}}{kr} \sum_{\ell=0}^{\infty} (2\ell+1)^{\frac{1}{2}} \, i^{\ell+1} \left\{ \exp[-i(kr-\tfrac{1}{2}\ell\pi)] - \zeta_\ell \exp[i\,(kr-\tfrac{1}{2}\ell\pi)] \right\} \tag{5.38}$$

So the constants are

$$a = \frac{i\sqrt{\pi}}{k} \qquad b = -\zeta_0 \, a \tag{5.39}$$

The only limitation put on ζ_0, which gives the coefficient of the outgoing wave, by the asymptotic conditions at infinity, is that the absolute value of ζ_0 should be less than or equal to unity. The coefficient must be obtained from the theory of nuclear reactions and it therefore depends upon conditions in the nuclear interior; thus we must connect ζ_0 with conditions at the nuclear surface. We describe the behavior of $U_0(r)$ just outside the nuclear surface in terms of the logarithmic derivative,

$$f_0 = R \left[\frac{dU_0/dr}{U_0}\right]_{r=R} \qquad (5.40)$$

We argue that the logarithmic derivative immediately outside the nucleus must be equal to the logarithmic derivative inside, which is in turn determined from the conditions inside the nucleus. Thus if we know what the logarithmic derivative is at the nuclear surface we can then determine the quantity ζ_0.

$$f_0 = R \left[\frac{1}{U_0} \left\{-ika \exp(-ikr) + ikb \exp(ikr)\right\}\right]_{r=R}$$

$$= ikR \left[\frac{-\exp(-ikR) - \zeta_0 \exp(ikR)}{\exp(-ikR) - \zeta_0 \exp(ikR)}\right] \qquad (5.41)$$

$$\therefore -f_0 + f_0 \zeta_0 \exp(2ikR) = ikR + \zeta_0 ikR \exp(2ikR)$$

or

$$\zeta_0 = \frac{f_0 + ikR}{f_0 - ikR} \cdot \exp(-2ikR) \qquad (5.42)$$

This gives the necessary relationship between the scattering functions ζ_0 and the logarithmic derivative for this special case of S-wave neutrons. We see that if the logarithmic derivative is a real number then $|\zeta_0|^2 = 1$

and $\sigma_{r,0} = 0$.

We now proceed to evaluate the scattering cross section.

$$\sigma_{sc,0} = \pi \lambda\!\!\!^{-2} \left|1-\zeta_0\right|^2 \tag{5.43}$$

$$= \pi \lambda\!\!\!^{-2} \left|1- \left(\frac{f_0 + ikR}{f_0 - ikR}\right) \exp(-2ikR)\right|^2$$

$$= \pi \lambda\!\!\!^{-2} \left| \frac{-2ikR}{f_0-ikR} + \exp(2ikR)-1\right|^2$$

$$\sigma_{sc,0} = \pi \lambda\!\!\!^{-2} \left|A_{res} + A_{pot}\right|^2 \tag{5.44}$$

where

$$A_{res} = \frac{2ikR}{f_0-ikR} \quad \text{:Resonance Amplitude} \tag{5.45}$$

$$A_{pot} = \exp(2ikR) -1 \quad \text{:Potential Amplitude} \tag{5.46}$$

If the nucleus were to be regarded as a perfectly reflecting sphere of radius R, then the wave function would have to vanish at the nuclear surface. This implies that

$$f_0 = R\left(\frac{dU_0}{dr}\right) \frac{1}{U_0}\Bigg|_{r=R} \Rightarrow \infty \qquad (5.47)$$

and thus $\sigma_{sc,0}$ is determined by A_{pot}. In practice one gets contributions from both terms at the nuclear surface, and thus the potential scattering term is only approximated in some special cases.

The contribution to the reaction cross section can be written in the following form

$$\sigma_{r,0} = \pi \lambda\!\!\!^{-2} (1- |\zeta_0|^2) \qquad (5.48)$$

$$= \pi \lambda\!\!\!^{-2} \frac{-4kR \text{ Im } f_0)}{(R_e \ f_0)^2 + (\text{Im } f_0 - kR)^2} \qquad (5.49)$$

Since the reaction cross section is inherently positive it must be that Im $f_0 \leq 0$.

We will now extend the previous discussion for S-wave neutrons to charged particles of arbitrary angular momentum. Consider an arbitrary ℓ so that in the entrance channel we have

$$\nabla^2 \psi + \left[k^2 - \frac{2M}{\hbar^2} V(r)\right] \psi = 0 \qquad (5.50)$$

where we again assume

$$\psi(\vec{r}) = \psi(r,\theta) = \sum_{\ell=0}^{\infty} \frac{U_\ell(r)}{r} \; Y_{\ell,0}(\theta)$$

and the radial wave equation is

$$\frac{d^2U_\ell(r)}{dr^2} + \left[k^2 - \frac{\ell(\ell+1)}{r^2} - \frac{2M\ V(r)}{\hbar^2}\right] U_\ell(r) = 0 \qquad (5.51)$$

We will take the potential V(r) to be

$$V(r) = \frac{Z_A\ Z_x\ e^2}{r} \qquad \text{for } r > R \qquad (5.52)$$

and this is the Coulomb wave equation. For the Coulomb wave equation there are two linearly independent solutions

$F_\ell(r)$ the regular solution

$G_\ell(r)$ the irregular solution

It is customary to adapt the following notation, which is standard in most literature

$$k = \frac{Mv}{\hbar} \qquad \rho = kr \qquad \eta = \frac{Z_A\ Z_x\ e^2}{\hbar v} \qquad (5.53)$$

so the wave equation reduces to

$$\frac{d^2 U_\ell}{d\rho^2} + \left[1 - \frac{2\eta}{\rho} - \frac{\ell(\ell+1)}{\rho^2}\right] U_\ell = 0 \qquad (5.54)$$

The regular solution is chosen with the following asymptotic behavior at zero and infinity

$$\left.\begin{array}{lll} & F_\ell(\rho,\eta) = 0 & \text{for} \quad \rho=0 \\ \text{Amplitude of} & F_\ell \to 1 & \text{as} \quad \rho\to\infty \end{array}\right\} \qquad (5.55)$$

The behavior for large ρ is given by

$$F_\ell \sim \sin\left[\rho - \eta \log 2\rho - \tfrac{1}{2}\ell\pi + \xi_\ell\right] = \sin \theta_\ell \qquad (5.56)$$

the Coulomb phase shift is given by ξ_ℓ is

$$\exp(2i\xi_\ell) = \frac{(\ell+i\eta)!}{(\ell-i\eta)!} = \frac{(\ell+i\eta)(\ell-1+i\eta)\cdots(1+i\eta)e^{2i\xi_0}}{(\ell-i\eta)(\ell-1-i\eta)\cdots(1-i\eta)} \qquad (5.57)$$

The asymptotic behavior of the irregular solution is

$$G_\ell \sim \cos \theta_\ell \qquad \text{for} \quad \rho\to\infty \qquad (5.58)$$

where

θ_ℓ is defined in equation (5.56).

The following recursion relations will be useful (where U_ℓ stands for either F_ℓ or G_ℓ):

$$(\eta^2 + \ell^2)^{\frac{1}{2}} U_{\ell-1} / \ell = (\eta/\ell + \ell/\rho) U_\ell + U_\ell' \qquad (5.59)$$

$$[\eta^2 + (\ell+1)^2]^{\frac{1}{2}} \frac{U_{\ell+1}}{\ell+1} = \left[\frac{\eta}{\ell+1} + \frac{\ell+1}{\rho}\right] U_\ell - U_\ell' \qquad (5.60)$$

$$[\eta^2 + (\ell+1)^2]^{\frac{1}{2}} \frac{U_{\ell+1}}{\ell+1} + (\eta^2 + \ell^2)^{\frac{1}{2}} \frac{U_{\ell-1}}{\ell} =$$

$$(2\ell+1)\,[\eta/\ell(\ell+1) + 1/\rho] U_\ell \qquad (5.61)$$

Note: A dash represents differentiation with respect to ρ.

The Wronskian relation $F_e' G_e - F_e G_e'$ is independent of ρ as implied by the Coulomb equation, and thus it can be determined from the asymptotic behavior of the functions, and that establishes it as being equal to unity.

We will not concern ourselves with any of the approximate forms that the Coulomb wave function can have but will be satisfied with the Coulomb wave equation and the general behavior of the two types of solutions.

For neutrons (η=0) we can use Bessel functions to write the solutions:

$$F_\ell(\rho) = (\tfrac{1}{2}\pi\rho)^{\frac{1}{2}} \; J_{\ell+\frac{1}{2}}(\rho) \qquad (5.62)$$

$$G_\ell(\rho) = -(\tfrac{1}{2}\pi\rho)^{\frac{1}{2}} \; N_{\ell+\frac{1}{2}}(\rho) \qquad (5.63)$$

with J and N the Bessel and Neuman functions respectively.

We describe outgoing and incoming spherical waves in terms of linear combinations of these functions. For neutrons

$$U_\ell^{(+)}(r) = G_\ell(\rho) + i \; F_\ell(\rho) \qquad (5.64)$$

and for charged particles

$$U_\ell^{(+)}(r) \equiv \exp(-i\,\xi_\ell)\,[G_\ell(\rho) + i\,F_\ell(\rho)] \qquad (5.65)$$

where $U_\ell^{(-)}(r) \equiv$complex conjugate of $U_\ell^{(+)}(r)$.

For large ρ the asymptotic behavior is

$$U_\ell^{(+)}(\rho) \sim \exp[i(\rho - \tfrac{1}{2}\,\ell\pi)] \qquad (\rho \gg \ell) \qquad (5.66)$$

For the external region,

$$U_\ell(r) = a\,U_\ell^{(-)}(r) + b\,U_\ell^{(+)}(r) \qquad (5.67)$$

This form can be compared to equation (5.13).

$$\psi(r) \simeq \frac{\pi^{\frac{1}{2}}}{\rho} \sum_{\ell=0}^{\infty} (2\ell+1)^{\frac{1}{2}} \, i^{\ell+1} \left\{ \exp[-i(\rho-\tfrac{1}{2}\ell\pi)] - \zeta_\ell \exp[i(\rho-\tfrac{1}{2}\ell\pi)] \right\} Y_{\ell,0} \qquad (5.68)$$

$$\left.\begin{aligned} \text{Thus, } a &= i^{\ell+1} (2\ell+1)^{\frac{1}{2}} \frac{\sqrt{\pi}}{k} \\ b &= -\zeta_\ell \, a \end{aligned}\right\} \qquad (5.69)$$

Now we connect ζ_ℓ to the logarithmic derivative f_ℓ.

$$f_\ell \equiv kR\left[\frac{dU_\ell^{(+)}/d\rho}{U_\ell^{(+)}}\right]_{r=R} \equiv \Delta_\ell + iS_\ell \qquad (5.70)$$

Δ_ℓ and S_ℓ are real numbers determined by the external conditions. It follows from the definition of $U_\ell^{(+)}$ that,

$$\Delta_\ell = kR\left[\frac{G_\ell G_\ell' + F_\ell F_\ell'}{F_\ell^2 + G_\ell^2}\right]_{r=R} \qquad (5.71)$$

$$S_\ell = kR\left[\frac{G_\ell F_\ell' - F_\ell G_\ell'}{F_\ell^2 + G_\ell^2}\right]_{r=R} \qquad (5.72)$$

From the Wronskian relation, $G_\ell F_\ell' - F_\ell G_\ell' = 1$ we denote the common factor in Δ_ℓ and S_ℓ as

$$P_\ell \equiv \frac{1}{F_\ell^{\,2}(R) + G_\ell^{\,2}(R)} \tag{5.73}$$

P_ℓ is identified with the penetrability of the potential barrier by charged particles. We can now write

$$S_\ell = kRP_\ell \tag{5.74}$$

The phase of $U_\ell^{(-)}(R)$ is represented by X where,

$$\exp(2iX_\ell) = \frac{U_\ell^{(-)}(R)}{U_\ell^{(+)}(R)} = \frac{G_\ell(R) - iF_\ell(R)}{G_\ell(R) + iF_\ell(R)} \exp(2i\xi_\ell) \tag{5.75}$$

The relation between ζ_ℓ and the other quantities is:

$$\zeta_\ell = \frac{f_\ell - \Delta_\ell + iS_\ell}{f_\ell - \Delta_\ell - iS_\ell} \exp(2iX_\ell) \tag{5.76}$$

If f_ℓ is real then $|\zeta_\ell|^2 = 1$ which is scattering without reaction. The maximum scattering cross section involves taking $\zeta_\ell = -1$ and thus

$$f_\ell = \Delta_\ell + S_\ell \tan X_\ell \tag{5.77}$$

Using the relations for $\sigma_{sc,\ell}$ and $\sigma_{r,\ell}$ we have

$$\sigma_{sc,\ell} = (2\ell+1)\pi \lambda\!\!\!^{-2} \; |A^{\ell}_{res} + A^{\ell}_{pot}|^2 \quad .$$

where

$$\left.\begin{aligned} A^{\ell}_{res} &= \frac{-2iS_\ell}{(Ref_\ell-\Delta_\ell) + i(Imf_\ell-S_\ell)} \\ A^{\ell}_{pot} &= \exp(-2i\chi_\ell) - 1 \end{aligned}\right\} \qquad (5.79)$$

and

$$\sigma_{r,\ell} = (2\ell+1)\pi \lambda\!\!\!^{-2} \left[\frac{-4S_\ell \; Imf_\ell}{(R_e f_\ell-\Delta_\ell)^2 + (Imf_\ell-S_\ell)^2} \right] \qquad (5.80)$$

and $Imf_\ell \leq 0$ as before.

<u>Reciprocity Theorem for Nuclear Reactions</u>

We have so far dealt only with the reaction cross section $\sigma_r(\alpha)$ which does not specify how the nuclear reaction is to proceed after entry of particle a (into the target nucleus X) in the entrance channel α. There are many channels β through which the reaction can proceed. We write:

$$\sigma_r(\alpha) = \sum_{\beta\neq\alpha} \sigma(\alpha,\beta) + \sigma_{cap}(\alpha) \qquad (5.81)$$

which is the reaction cross section in channel α. σ_{cap} denotes radiative capture.

We now develop a relation between $\sigma(\alpha,\beta)$ and the inverse reation $\sigma(\beta,\alpha)$ by first introducing the differential cross section:

$$\sigma(A,B) = \sigma(\alpha,\beta,\theta,\varphi)\,d\Omega \qquad (5.82)$$

The process represented by this cross section is one in which the incident particle a travels in the z direction, while the outgoing particle b moves within solid angle $d\Omega$ the direction of which is given by the polar angles θ & φ. The differential cross section for the inverse process is:

$$\sigma(-B,-A) = \sigma(\beta,\theta,\varphi,\alpha)\,d\Omega \qquad (5.83)$$

in which all the direction are reversed.

Consider states A and B of a quantum mechanical system, where state A contains particle a in channel α'' and nucleus X in channel α' (both a and X being free particles): The interval ϵ_α to $\epsilon_\alpha + \Delta\epsilon$ contains the channel energy. The direction of a is within $d\Omega$, in the z direction, toward X. State B contains particle b in

channel B' and nucleus Y in B' (both b and Y being free particles). The interval ϵ_B to $\epsilon_B + \Delta\epsilon$ contains the channel energy. The direction of b is within $d\Omega$, in the z direction, away from Y.

To understand the connection between the processes $A \rightarrow B$ and $-B \rightarrow -A$ we enclose the system in a large volume V and consider probabilities per unit time P(A,B) and P(-B, -A) of the transitions. (It is understood that the minus sign denotes "reversed time.") P(A,B), P(-B,-A) are given by:

$$P(A,B) = v_\alpha \frac{\sigma(A,B)}{V} \qquad (5.84a)$$

$$P(-B,-A) = v_\beta \frac{\sigma(-B,-A)}{V} \qquad (5.84b)$$

where the v's are the relative velocities in the respective channels. These relations can be understood by thinking of the particle which induces the reaction as bouncing around inside V so that it periodically has a chance of striking the nucleus and the flux for one particle is just the velocity of the target area, which gives the probability of having a reaction take place per unit time of a general quantum mechanical system

has two single non-degenerate states (which we can designate by p and q which have the same energy, then the transition rate T_{pq} for $p \to q$ equals the rate $T_{-q,\,-p}$ for $-q \to -p$ where again the minus is taken to mean time reversal. These states can now be made degenerate, which means they acquire some statistical weights. If the statistical weight of the degenerate state P is g_P and g_Q for degenerate state Q the transition probabilities obey the relation:

$$\frac{T_{p,Q}}{g_Q} = \frac{T_{-Q,-P}}{g_P} \qquad (5.85)$$

g_A and g_B are given by the number of free particle states with energy and direction in the intervals $\Delta\epsilon$ and $d\Omega$, respectively.

$$g_A = \frac{Vp_\alpha^{\,2}dp_\alpha d\Omega}{(2\pi\hbar)^3} \qquad (5.86a)$$

$$\text{Now} \quad E = p^2/2M \quad \Rightarrow \quad dE = \frac{pdp}{M} \qquad (5.86b)$$

$$\therefore p^2dp = MpdE \qquad (5.86c)$$

$$\therefore \quad g_A = \frac{V(2M_\alpha^3\epsilon_\alpha)^{\frac{1}{2}}}{(2\pi\hbar)^3}\,\Delta\epsilon d\Omega \qquad (5.86d)$$

and similarly

$$g_B = \frac{V(2M_\beta^{\,3}\epsilon_\beta)^{\frac{1}{2}}\Delta\epsilon d\Omega}{(2\pi\hbar)^3} \qquad (5.86e)$$

Hence

$$\frac{P(A,B)}{\dfrac{V(2M_\beta{}^3\epsilon_\beta)^{\frac{1}{2}}\Delta\epsilon d\Omega}{(2\pi\hbar)^3}} = \frac{P(-B,-A)}{\dfrac{V(2M_\alpha\epsilon_\alpha)^{\frac{1}{2}}\Delta\epsilon d\Omega}{(2\pi\hbar)^3}} \qquad (5.87)$$

$$\therefore \quad M_\alpha{}^{3/2}\,\epsilon_\alpha{}^{\frac{1}{2}}\,P(A,B) = M_\beta{}^{3/2}\,\epsilon_\beta{}^{\frac{1}{2}}\,P(-B,-A) \qquad (5.88a)$$

$$\therefore \quad V_\alpha\,M_\alpha{}^{3/2}\,\epsilon_\alpha{}^{\frac{1}{2}}\,\sigma(A,B) = V_\beta\,M_\beta{}^{3/2}\,\epsilon_\beta{}^{\frac{1}{2}}\,\sigma(-B,-A) \qquad (5.88b)$$

Now $$\frac{1}{\lambda\!\!\!^{-}_\alpha} = \frac{(2M_\alpha\epsilon_\alpha)^{\frac{1}{2}}}{\hbar} = \frac{M_\alpha v_\alpha}{\hbar} \qquad (5.89)$$

$$\therefore \quad \frac{\sigma(A,B)}{\lambda_\alpha{}^2} = \frac{\sigma(-B,-A)}{\lambda_\alpha{}^2} \qquad (5.90)$$

<u>i.e.</u> $$\frac{\sigma(\alpha,\beta,\theta,\varphi)}{\lambda_\alpha{}^2} = \frac{\sigma(\beta,\theta,\varphi,\alpha)}{\lambda_\alpha{}^2} \qquad (5.91)$$

Now $$\int \sigma(\alpha,\beta,\theta,\varphi)\,d\Omega = \sigma(\alpha,\beta) \qquad (5.92a)$$

$$\int \sigma(\beta,\theta,\varphi,\alpha)\,d\Omega = \sigma(\beta,\alpha) \qquad (5.92b)$$

$$\therefore \quad \frac{\sigma(\alpha,\beta)}{\lambda_\alpha{}^2} = \frac{\sigma(\beta,\alpha)}{\lambda_\alpha{}^2} \qquad (5.93)$$

This is the reciprocity theorm.

The Compound Nucleus, Continuum Theory

We now consider a certain kind of average over resonances which is called continuum theory or compound nucleus theory. The original suggestion for this treatment was due to N. Bohr and is known as the Bohr assumption. This says that when a particle enters a nucleus its energy is quickly shared among all the nucleons, while energy, angular momentum and parity are conserved in the reaction. The subsequent decay of the compound nucleus is independent of the way in which it was formed. This assumption thus considers that there are strong interactions between the nucleons. This does not contradict the independent particle model where interactions are prevented by the Pauli principle. The incoming particles generally have ample energy to knock nucleons into unoccupied states, so that strong interactions are possible. Calculations of nuclear mean free path Λ ($\Lambda = (\sigma\rho)^{-1}$ where σ is the collision cross section and ρ is the nucleon density within the nucleus) indicate that

$$\Lambda \simeq .4 \times 10^{-13} \text{ cm}, \quad \epsilon \lesssim 20 \text{ MeV}$$

$$\Lambda \simeq 1.8 \times 10^{-15} \times E(\text{in MeV}) \text{ cm}, \quad \text{for higher}$$

energies. These distances are less than nuclear dimensions if the incident energies are less than ~100 MeV. Thus such particles can be expected to interact with the nucleus and be captured. This will impart an average energy ϵ/A to each nucleon. If this is smaller than the separation energy of a nucleon then a thorough mixing of the energy will occur and it will be a long time befor enough energy is statistically concentrated on one nucleon to allow it to escape. The length of this mixing time is the reason for the assumption that the compound nucleus forgets how it was formed.

The Bohr assumption is written mathematically as follows:

$$\sigma(a,b) = \sigma_C(a)\ G_C(b) \qquad (5.94)$$

in which particle a is incident upon the nucleus X and $\sigma_C(a)$ is the cross section for the formation of a compound system C, $G_C(b)$ is relative probability that the compound nucleus will emit the particle. Since the nucleus must decay somehow, the sum over all such probabilities is unity

i.e. $$\sum_b G_C(b) = 1$$

We consider radiation to be a possible mode of decay.

We can write the reaction in greater detail by specifying channels α (entrance channel) and β (exit channel).

$$\sigma(\alpha,\beta) = \sigma_C(\alpha)G_C(\beta) \tag{5.95}$$

The disintegration depends only on energy, angular momentum and parity (we exclude $G_C(\alpha)$). We will here neglect all dependences on the angular momentum and parity, and only obtain relations for the conservation of energy.

We make use of the mean lifetime $\tau(E_C)$ to define the reaction width:

$$\Gamma(E_C) = \hbar\tau(E_C) \quad \text{(units of energy)} \tag{5.96}$$

Since there are several nodes of decay available to C we can divide Γ into reaction widths:

$$\Gamma(E_C) = \sum_\beta \Gamma_\beta(E_C) \tag{5.97}$$

The sum is over all exit channels available to C.

We can get a useful relation from the reciprocity theorm.

$$\frac{\sigma(\alpha,\beta)}{\lambda\!\!\!^{-}_{\alpha}{}^2} = \frac{\sigma(\beta,\alpha)}{\lambda\!\!\!^{-}_{\beta}{}^2} \tag{5.98a}$$

$$\frac{\sigma_C(\alpha)G_C(\beta)}{\lambda\!\!\!^{-}_{\alpha}{}^2} = \frac{\sigma_C(\beta)G_C(\alpha)}{\lambda\!\!\!^{-}_{\beta}{}^2} \tag{5.98b}$$

therefore,

$$\frac{\sigma_C(\alpha)}{\Gamma_\alpha \lambda\!\!\!^{-}_{\alpha}{}^2} = \frac{\sigma_C(\beta)}{\Gamma_\beta \lambda\!\!\!^{-}_{\beta}{}^2} = U(E_C) \tag{5.98c}$$

It will be noted that $\frac{\sigma_C(\alpha)}{\Gamma_\alpha \lambda\!\!\!^{-}_{\alpha}{}^2}$ is independent of the channel α and can be written as a function $U(E_C)$ of the compound nucleus energy.

Then,

$$\Gamma_\beta = \frac{\sigma_C(\beta)}{\lambda_\beta^2\ U(E_C)} = \frac{k_\beta^2\ \sigma_C(\beta)}{U(E_C)} \tag{5.99}$$

and

$$G_C(\beta) = \frac{\Gamma_\beta}{\Gamma} \tag{5.100a}$$

$$G_C(\beta) = \frac{k_\beta^2\ \sigma_C(\beta)}{U(E_C)} \Big/ \sum_\gamma \frac{k_\gamma^2\ \sigma_C(\gamma)}{U(E_C)} \tag{5.100b}$$

$$G_C(\beta) = \frac{k_\beta^2\ \sigma_C(\beta)}{\sum_\gamma k_\gamma^2\ \sigma_C(\gamma)} \tag{5.100c}$$

Thus the different probabilities for decay of the compound nucleus can be computed if the cross sections $\sigma_C(\nu)$ for the formation of the compound system by all possible channels are known.

Determination of Cross Sections, Continuum Theory

As a first approximation we may guess that the reaction cross section is $\pi(R + \lambda\!\!\!^{-})^2$. This combines our previous estimates for high and low energies. Actually, however, barrier effects will reduce this as will sudden changes in the potential to which the particle is subjected. This gives rise to a reflection of the incoming wave at the nuclear surface which will be strongest for low energies.

Figure 5.3

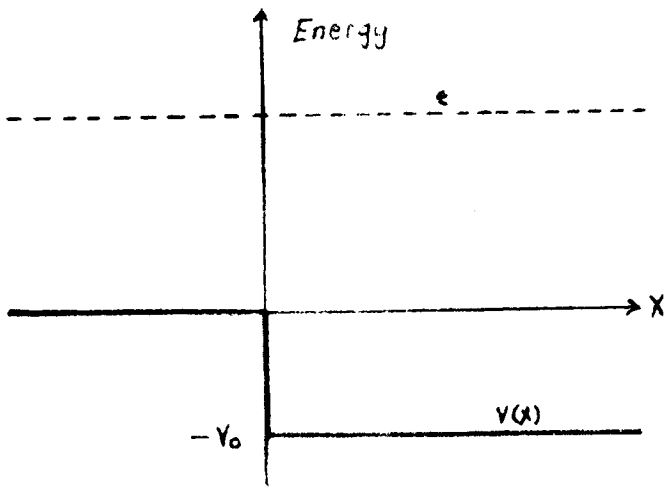

We can determine the consequence of such a reflection with a simple two dimensional example. A beam of particles of energy ϵ is incident from the left, traveling in the positive X direction in a potential given by:

$$V(x) = 0, \quad \text{for } x < 0$$

$$V(x) = -V_0, \quad \text{for } x > 0$$

Particles which come along from the left will be partially reflected at the jump in the potential at x = 0 and we can calculate the transmission coefficient

$$\left(\text{i.e. } \frac{\text{number of particles penetrating into } x > 0}{\text{number of incident particles}}\right)$$

in the usual way that one does in quantum mechanics. The wave function $\Psi(x)$ will be:

$$\Psi(x) = Ae^{ikx} + Be^{-ikx}, \quad \text{for } x < 0 \qquad (5.101a)$$

$$\Psi(x) = Ce^{iKx}, \quad x > 0 \qquad (5.101b)$$

where:

$$k = \frac{(2M\epsilon)^{\frac{1}{2}}}{\hbar}, \quad x < 0 \qquad (5.102a)$$

$$K = [2M(\epsilon + V_0)]^{\frac{1}{2}}, \quad x > 0 \qquad (5.102b)$$

and

$$T = \frac{|A|^2 - |B|^2}{|A|^2} \qquad (5.103)$$

By matching $\Psi(x)$ and the deviative of $\Psi(x)$ at $x = 0$ we obtain

$$A + B = C \tag{5.104a}$$

$$ik(A - B) = iKC \tag{5.104b}$$

$$\therefore 2kA = C(k + K) \tag{5.104c}$$

$$\therefore 2kB = C(k - K) \tag{5.104d}$$

$$\therefore \left(\frac{k}{k + K}\right) A = \left(\frac{k}{k - K}\right) B \tag{5.104e}$$

$$\tag{5.104f}$$

or

$$B = \left(\frac{k - K}{k + K}\right) A \tag{5.104g}$$

thus

$$T = \frac{|A|^2 - \left[\frac{(k - K)^2}{(k + K)^2}\right] |A|^2}{(A)^2} \tag{5.104h}$$

and after some rearranging.

$$T = \frac{4kK}{(K + k)^2} \tag{5.104i}$$

This transmission coefficient is actually the same for particles incident from either direction. If $k \ll K$, T will be small i.e. low energy limit. In the high energy limit, $K \sim k$ and $T \to 1$.

T can be taken to approximate the transmission coefficient of neutrons into a nucleus. Actually the

neutron in higher angular momentum states will be further impeded by the centrifugal barrier.

We now take the capture cross section for neutrons to be:

$$\sigma_C(n) \approx \pi(R + \lambda\!\!\!^{-})^2 \frac{4kK}{(k + K)^2} \qquad (5.105)$$

Note that this approaches the classical value πk^2 at high energies. At low energies we have

$$\sigma_C(n) \sim \lambda\!\!\!^{-2} k \sim \lambda\!\!\!^{-} \sim \epsilon^{-\frac{1}{2}} \sim \frac{1}{v} \qquad (5.106)$$

This is the $\frac{1}{v}$ law for slow neutron absorption. Again, these estimates are too large due to the centrifugal and coulomb barriers.

The partial formation cross sections can be written as:

$$\sigma_{C\,\ell}(\alpha) = (2\ell + 1)\pi \lambda\!\!\!^{-2} T_\ell(\alpha) \; + \qquad (5.107)$$

It then becomes necessary to sum the partial cross sections over the ℓ values. We can generally indicate the

---

+ See Blatt and Weisskopf for derivation of expressions for the transmission coefficients for these barriers.

$$f_0 = R\left(\frac{dU_0}{dr}\right) \frac{1}{U_0}\Bigg|_{r=R} \Rightarrow \infty \qquad (5.47)$$

and thus $\sigma_{sc,0}$ is determined by A_{pot}. In practice one gets contributions from both terms at the nuclear surface, and thus the potential scattering term is only approximated in some special cases.

The contribution to the reaction cross section can be written in the following form

$$\sigma_{r,0} = \pi \lambda\!\!\!^{-2} \left(1 - |\zeta_0|^2\right) \qquad (5.48)$$

$$= \pi \lambda\!\!\!^{-2} \frac{-4kR \ \mathrm{Im}\ f_0)}{(R_e\ f_0)^2 + (\mathrm{Im}\ f_0 - kR)^2} \qquad (5.49)$$

Since the reaction cross section is inherently positive it must be that $\mathrm{Im}\ f_0 \leq 0$.

We will now extend the previous discussion for S-wave neutrons to charged particles of arbitrary angular momentum. Consider an arbitrary ℓ so that in the entrance channel we have

$$\nabla^2 \psi + \left[k^2 - \frac{2M}{\hbar^2} V(r)\right] \psi = 0 \qquad (5.50)$$

account of the Pauli exclusion principle it will be the Fermi distribution inside the nucleus Blatt and Weisskopf estimate:

$$K_0 \approx 1 \times 10^{-13}\ \mathrm{cm}^{-1} \tag{5.109}$$

for thermal particles. In general

$$K = \sqrt{K_0^2 + k^2} \tag{5.110}$$

Decay of Compound Nucleus; Competition, Evaporation Model

We have succeeded in getting particles into the nucleus. We now wish to find how particles can get out of it. We recall from the reciprocity theorm that this is related to the process of putting all the various possible exit particles into the nucleus. Thus it is necessary to make some sort of estimate about the various exit channels.

We therefore want the energy distribution of the emitted particles. The kinetic energy in channel β is $\epsilon_\beta = \epsilon_\alpha + Q_{\alpha\beta}$. Only a small amount of the energy is imparted to the residual nucleus Y. Most of it goes into kinetic energy of the emitted particle b. Thus

we can consider the kinetic energy of b to be ϵ_β. So,

$$\epsilon_\beta = \epsilon_{bY} - E_\beta^* \qquad (5.111)$$

in which ϵ_Y is the maximum value of ϵ_β when the nucleus Y will have an excitation energy E_β^* after the reaction. We neglect the possibility of the particle be being left in an excited state. Thus the emitted spectrum depends on the levels E_β^* available in the reaction. In general these increase in density with increasing nuclear excitation, a process which favors emission of particles with low energies. Hence the actual distribution will represent a compromise between these tendencies and will have some sort of peak. We will consider only averages over individual levels.

The number of particles b emitted between ϵ and $\epsilon + d\epsilon$ has a distribution function $G_b(\epsilon)d\epsilon$ given by:

$$G_b(\epsilon)d\epsilon = \sum_{\epsilon<\epsilon_\beta<\epsilon+d\epsilon} G_C(\beta) \qquad (5.112)$$

where the sum is over the channels whose energy is within the interval $d\epsilon$. The number of terms in the sum determined by the number of levels of Y having an

excitation energy E_β^* between E and E - dE, with $E = \epsilon_{bY} - \epsilon$. This number is called $\omega_Y(E)dE$ where $\omega_Y(\epsilon)$ is the "level density".

We had:

$$G_C(\beta) = \frac{k_\beta^2 \, \sigma_C(\beta)}{\sum_\gamma k_C^2 \, \sigma_C(\gamma)} \qquad (5.113)$$

The denomination is a sum over all channels and does not depend on ϵ_β. We get the relative intensity distribution of the outgoing particle by taking only the numerator of (6.93).

$$b(\epsilon)d\epsilon = \text{constant} \times \epsilon \, \sigma_C(\beta)\omega_Y(\epsilon_{bY} - \epsilon)d\epsilon. \qquad (5.114)$$

$\sigma_C(\beta) = \sigma_C(\epsilon)$ is a function $\epsilon = \epsilon_\beta$, the channel energy. $\epsilon\sigma_C(\beta)$ is an increasing function of ϵ, whereas $\omega_Y(\epsilon_{bY} - \epsilon)$ is a strongly decreasing function. Thus the intensity distribution which is a product of two factors described is a peaked distribution.

Let $S(E) = \log \omega(E)$

and expand in a Taylor series aroung the maximum energy ϵ_{bY}.

$$S(\epsilon_{bY} - \epsilon) = S(\epsilon_{bY}) - \epsilon \left(\frac{dS}{d\epsilon}\right)_{E = \epsilon_{bY}} + \ldots \qquad (5.115)$$

$$I_b(\epsilon)d\epsilon = \text{const.} \times \epsilon\sigma_C(\epsilon)e^{-\epsilon/\Theta(\epsilon_{bY})}d\epsilon \times e^{S(\epsilon_{bY})} \qquad (5.116)$$

Let

$$\frac{1}{\Theta(\epsilon)} = \frac{dS}{dE} \qquad (5.117)$$

and absorb $e^{S(\epsilon_{by})}$ into the constant.

Hence

$$I_b(\epsilon)d\epsilon = \text{const.}\ \epsilon\sigma_c(\epsilon)e^{-\epsilon/\Theta(\epsilon_{bY})}d\epsilon \qquad (5.118)$$

Θ can be interpreted as a nuclear "temperature" and has the dimension of an energy. We consider S(E) as analagous (apart from the Boltzman constant k) to the entropy of the residual nucleus in the energy range dE near E. The definition of Θ is then equivalent to the thermodynamic relation dS - dQ/T.

The function $\sigma_C(\epsilon)$ is slowly varying for neutrons (except at very low energies) and this term can be neglected. This leaves

$$I_b(\epsilon)d\epsilon = \text{const.} \times \epsilon\ e^{-\epsilon/\Theta(\epsilon_{bY})}d\epsilon. \qquad (5.119)$$

This is precisely the Maxwell distribution of molecule energies which would be evaporated from a surface at

temperature Θ. The maximum of $I_\beta(\epsilon)$ lies at $\epsilon = \Theta$ which should be small compared to ϵ_Y to make the Taylor expansion valid. The average energy of the emitted neutrons is, $\epsilon = 2\Theta$. For charged particles the factor $\sigma_C(\epsilon)$ distorts the distribution and the maximum shifts to higher particle energies. We thus think of the neutrons as being evaporated from the nucleus. However, it should be noted that the temperature characteristic of the evaporation is that of the residual nucleus, since evaporation of one particle accounts for a relatively large loss thus reducing the temperature a good deal. Since the average neutron energy is low, the residual nucleus will usually be left excited by almost ϵ_{bY}, so that ϵ_{bY} is the energy which characterizes the temperature associated with the process.

Since it is not usually possible to distinguish an exit channel for a particle b (in an experiment) or to determine the energy of b we need only consider the cross section of reaction (a,b) without considering the specific channels leading to emission of b. We define

$$F_b = \sum_\beta k_\beta^2 \sigma_C(\beta) \qquad (5.120)$$

or expressing the sum as an integral, we have:

$$F_b = F_b(\epsilon_{bY}) = \frac{2M_r}{\hbar^2} \int_0^{\epsilon_{by}} \epsilon_\beta \, \sigma_C(\epsilon_\beta) \omega_Y(\epsilon_{bY} - \epsilon_\beta) d\epsilon_\beta \tag{5.121}$$

The cross section then becomes;

$$\sigma(a,b) = \frac{\sigma_C(a) F_b}{\sum_C F_C} \tag{5.122}$$

Thus if we know level densities we could calculate reaction cross sections.

Nuclear Resonances

We saw that the nucleus contains levels both above and below particle separation energies, when we were looking at the theory of alpha decay. It was apparent that for certain values of the excitation energy the wave function of a space particle outgoing from the potential will joins to a large wave function inside (on resonance). At other energies the interior wave function is small (off resonance).

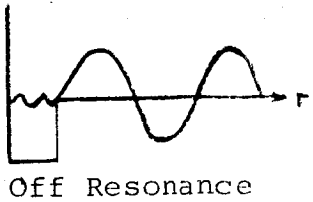

Off Resonance

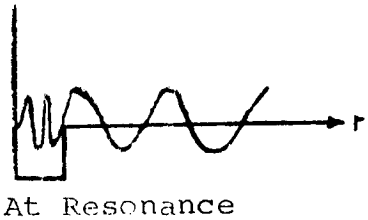

At Resonance

Thus it would appear that for certain values of the incident particle energy the incoming particle can penetrate into the nucleus with a large probability, which is much less probable at other energies. These are the nuclear resonances which we have previously averaged out.

It is evident in order for a resonance to have meaning, the width of the resonance Γ^s must be less than the distance between resonances D_s.

i.e.
$$\Gamma^s < D_s \tag{5.123}$$

We can make a classical picture in order to think about the lifetimes of these states. Consider the period D of the motion of a nucleon inside the nucleus (or more properly, the period of a maximum in the square of the wave function). D is the time taken for a configuration to recur. Consider a number of states with equal spacing D:

$$E_n = E_0 + nD \tag{5.124}$$

The wave function Ψ is then written as a linear combination of N states.

$$\Psi = \sum_{n=1}^{N} a_n \varphi_n \; e^{-iE_n t/\hbar} = e^{-iE_0 t/\hbar} \sum_{n=1}^{N} a_n \varphi_n \, e^{-inDt/\hbar} \qquad (6.12)$$

where φ_n gives the space dependence. From (6.19) it is clear that:

$$\left|\Psi\left(t + \frac{2\pi\hbar}{D}\right)\right|^2 = \left|\Psi(t)\right|^2 \qquad (6.120)$$

Thus

$$P = \frac{2\pi\hbar}{D}$$

Consider a state created by a particle "a" entering into the residual nucleus by the channel α, and the question: How long does it take the particle to re-appear at the nuclear surface such that the remaining constituents of the nucleus are arranged so that a can leave through its original entrance channel? This time is of the order of $2\pi\hbar/D$, the period of the motion. If the particle now does leave the nucleus the lifetime of the state would have been of order P and the width of the state:

$$\Gamma^s \approx \frac{\hbar}{P} \approx \frac{D}{2\pi} \sim D \qquad (6.121)$$

i.e. width is of order of level spacing and a state is not well defined. However the lifetime of a state will be greatly increased if there is a large reflection coefficient at the nuclear boundary, and then the state will be well defined.

Γ_α^s is the probability for decay through channel α and $\Gamma_\alpha^s/\hbar$ the probability per unit time that the system will decay via channel α when all other channels are artificially closed the lifetime τ_s of the state with only channel α open is then $\tau_\alpha = \hbar/\Gamma_\alpha^s$, which must be of order P. Define $T(\alpha)$ as the transmission coefficient toward the outside so that:

$$\tau_\alpha \sim \frac{P}{T(\alpha)} \tag{5.128}$$

$$\Gamma_\alpha^s \sim T(\alpha)\ \frac{D}{2\pi} \tag{5.129}$$

It should be noted that in these considerations the spacing D is that between levels with the same J and π (for which integrals of the notion are the same except for the energy.)

We shall not try to derive the shape of the cross section curve in the neighborhood of a resonance, but

we will write it in analogy with the dispersion of light. We have in the vicinity of a resonance:

$$\sigma_{C\ell}(\alpha) \cong (2\ell + 1)\pi \lambda_\alpha^{\,2} \frac{\Gamma_\alpha^{\,s}\,\Gamma^s}{(\epsilon_\alpha - \epsilon_{\alpha s}) + (\frac{1}{2}\Gamma^s)^2} \tag{7.10}$$

where Γ_α^s is the probability of decay of the compound nucleus into channel α and $\epsilon_{\alpha s}$ is the energy of the resonance. For a particular type of reaction we multiply by $G_c(\beta) = \Gamma_\beta^s/\Gamma^s$ and use excitation energies E:

$$\sigma(\alpha,\beta) \approx (2\ell + 1)\pi \lambda\alpha^2 \frac{\Gamma_\alpha^{\,s}\,\Gamma_\beta^{\,s}}{(E-E_s) + (\frac{1}{2}\Gamma^s)^2} \tag{5.130}$$

This is the Breit-Wigner one level formula.

This is not correct for the case of elastic scattering, because there can be interference effects between the re-emission of the particle "a" by the compound nucleus and the scattering at the nuclear surface as well as at the potential outside the nucleus. The corresponding cross section for elastic scattering is

$$\sigma_{sc,\ell} = \sigma_\ell(\alpha,\alpha) = (2\ell + 1)\pi \lambda\alpha^2 \left[\frac{i\Gamma_\alpha^{\,s}}{(\epsilon_\alpha - \epsilon_{\alpha s} + \frac{1}{2}i\Gamma^s} + A_{pot}^{\ell}\right]^2 \tag{5.131}$$

The first term is the resonance scattering amplitude and the second the potential scattering amplitude as previously defined. This inteference can often lead to a cross section shape like:

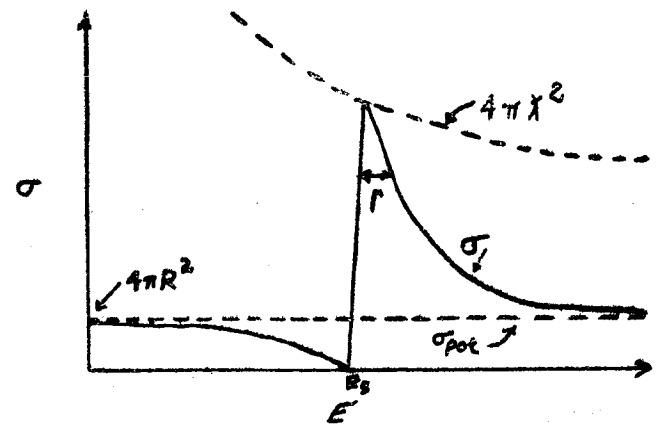

If one is not interested in a precise cross section off resonance but in a sum of the cross sections or an integral of the cross sections over many resonances then interference effects are not of any concern, because if there is constructive interference between a couple of resonances, then in general there will be destructive interference on the other side of both resonances and the integral over energy will be the same. Usually when one is evaluating nuclear cross sections for use in nuclear astrophysics one does not know enough about all of the relevent properties to be able

to make a calculation of the interference effects and we are therefore interested in integrating over resonances.

Thus, let us consider the single-level cross sections:

$$\sigma(ab) = \pi \lambda_a^2 (2\ell + 1) \frac{\Gamma_a \Gamma_b}{(E_a - E_r)^2 + (\Gamma/2)^2} \tag{5.132}$$

For a narrow resonance, we assume that λ_a, Γ_a, Γ_b and Γ_γ vary slowly over the resonance peak. The contribution of this resonance to the average cross section is therefore given by.

$$\sigma(a,b) \cong \pi\lambda^2 (2\ell + 1)\Gamma_a \Gamma_b \int_{-\infty}^{\infty} \frac{1}{(E_a - E_1)^2 + (\Gamma/2)^2} dE_a \tag{5.133}$$

$$\sigma(a,b) \cong 2\pi^2 (2\ell + 1) \left(\frac{\lambda_a^2 \Gamma_a \Gamma_b}{\Gamma} \right)_{E_a = E_1} \tag{5.134}$$

where in order to extend the limits of integration from $-\infty$ to ∞ we have assumed that the contributions from the resonance tails are small. When there are many

resonances within the thermonuclear bombarding region we use non-resonant reaction formula, but write it as that the cross section represents an average over resonances. i.e.

$$\langle \sigma \rangle = 2\pi^2 \lambda\!\!\!^{-2} \left\langle \frac{(2\ell + 1)\, \Gamma_a \Gamma_b}{\Gamma} \right\rangle \qquad (5.135)$$

Particle Widths

From nuclear reaction theory, the particle widths can be written as:

$$\Gamma_\ell = 2P_\ell \gamma_\ell^{\,2}$$

where ℓ specifies the value of the orbital angular monentum. P_ℓ is the nuclear penetrability defined by:

$$P_\ell = \rho / [F_\ell^{\,2}(\rho) + G_\ell^{\,2}(\rho)] \qquad (5.136)$$

and $\rho = k\,R$ where R is the nuclear radius and $F_\ell(\rho)$ and $G_\ell(\rho)$ are the regular and irregular solutions of the coulomb equation. The factor $\gamma_\ell^{\,2}$ is the reduced width for the particle channel and is dependent upon the behavior of the wave function within the nucleus. Generally a detailed knowledge of the form of the reduced

width is not available. On the basis of a "black nucleus" nodel we can write γ_ℓ^2 in the form:

$$\gamma_\ell^2 \simeq \frac{2 \times 10^{-14}}{R\ \rho(E,J,\pi)} \qquad (5.137)$$

Now, the above quantities are functions of the nuclear radius at which the coulomb wave functions are evaluated, but there is some ambiguity as to the position we designate as the nuclear radius. From the discussion concerning the use of exterior wave functions in the nuclear boundary and interior wave functions it was determined that one wants the boundary to be placed out reasonably as far as possible because the nuclear forces have finite ranges and will modify the Coulomb potential at the distance of about one fermi or more, outside the position which one would normally designate as the nuclear radius. Besides that the nucleus has a diffuse edge which adds to the confusion and making a small number of nucleous go out rather far giving nuclear potential at a fair distance from the nucleus. Thus there is some advantage to putting the radius out as far as possible.

On the other hand placing the radius out too far leads to difficulties with the interior estimate of reduced particle width Thus we have to achieve some compromise between large and small nuclear radius. This is done by considering the radius to be an adjustable parameter, and varying it to see when a decent companion with experiment is obtained.

The nuclear radius is written as:

$$R = r_o(A_P^{\frac{1}{3}} + A_T^{\frac{1}{3}}) \text{ fermis} \qquad (5.138)$$

where A_P and A_T are the mass numbers of the projectile and target nucleus respectively. One now varies r_o to see what value of r_o gives the best fit to experiment. In the paper "Thermonuclear Reactions in Medium and Heavy Nucleii "by Truran, Hansen, Cameron and Gilbert, a comparison with the experimental points for (p,n) reactions published by Johnson et al (1958), it was concluded that

$$r_o = 1.20$$

provided the best fit to the data.

6. Gamma Ray Transitions

Nuclear gamma ray transitions are not in principle, different from atomic transitions or from transitions in any quantum mechanical system. A convenient approach to this problem is to adapt the results of the classical theory of radiation to the quantum theory. Eventually we will be led to Weisskopf simple estimates of the transition matrix elements, results which have proven to be useful as a standard of comparison in nuclear physics.

The nucleus is a small enough body so that it may be considered as a source small compared to the wavelengths being emitted (this is good for $E_\gamma < 10$ Mev.). The angular momentum $\vec{\ell}$ of the radiation is designated by the same type of quantum numbers as for a particle

$$\ell_z = m \text{ and } |\vec{\ell}|^2 = \ell(\ell + 1) \tag{6.1}$$

Higher values of ℓ are not important as the probability of radiative transition decreases rapidly with increasing ℓ, unless the lower values are expressely forbidden by some selection rule.

There can be both "electric" and "magnetic" radiation emitted for each value of the angular momentum of the light wave emitted from the system. That is, the radiation may result from either changes in the distribution of charge, or from changes in the distribution of currents in the system. We can also see this by considering a current distribution near the origin to be emitting spherical outgoing waves. Maxwell's equation for the magnetic field $\vec{\mathcal{H}}$ alone is unchanged when we change the sign of the coordinates. Hence we can separate the magnetic field into two parts, even and odd, each of which is a solution of Maxwell's equation. We have an even parity wave for which

$$\vec{\mathcal{H}}(-r) = +\vec{\mathcal{H}}(r) \tag{6.2}$$

and an odd parity wave for which

$$\vec{\mathcal{H}}(-r) = -\vec{\mathcal{H}}(r) \tag{6.3}$$

If we have an even parity $\vec{\mathcal{H}}(\vec{r})$ we have an odd parity for the electric part of the wave $\vec{\mathcal{E}}(\vec{r})$, and vice versa for odd parity $\vec{\mathcal{H}}(\vec{r})$ (This follows from the free space solution to Maxwell's equations $-i\omega\vec{\mathcal{E}} = c\,\nabla \times \vec{\mathcal{H}}$). Consequently for the Poynting vector (which describes the flow of energy

$$\vec{S} = \frac{c}{4\pi}\,\vec{\mathcal{E}} \times \vec{\mathcal{H}} \tag{6.4}$$

if we change $\vec{r} \to -\vec{r}$ either $\vec{\mathcal{E}}$ or $\vec{\mathcal{H}}$ (but not both) will change sign and then $\vec{S}$ will change sign. Hence we have the condition that the Poynting vector always points away from the origin.

The fields can be written in the following general form

$$\vec{\mathcal{E}}(\vec{r},t) = \vec{\mathcal{E}}(\vec{r})\,e^{-i\omega t} + \vec{\mathcal{E}}^{*}(\vec{r})e^{i\omega t} \tag{6.5}$$

$$\vec{\mathcal{H}}(\vec{r},t) = \vec{\mathcal{H}}(\vec{r})e^{-i\omega t} + \vec{\mathcal{H}}^{*}(\vec{r})e^{i\omega t} \tag{6.6}$$

and if there are several frequencies present they may be considered separately.

The fields can be expanded as electric and magnetic multipoles. The electric multipole field of order ℓ,m will be designated by $\vec{\mathcal{E}}_E(\ell,m,\vec{r})$ and $\vec{\mathcal{H}}_E(\ell,m,\vec{r})$ and the magnetic multipole field of order ℓ,m will be designated by $\vec{\mathcal{E}}_M(\ell,m,\vec{r})$ and $\vec{\mathcal{H}}_M(\ell,m,\vec{r})$. The same angular momentum is carried away by electric and magnetic multipole radiation of the same order ℓ,m, but the two field types differ in their intrinsic parity. We can determine the parity as follows:

Electric multipole, $\pi = (-1)^{\ell}$ (6.7)

Magnetic multipole, $\pi = -(-1)^{\ell}$ (6.8)

This means that the parity carried away by electric radiation is the same as that carried away by an emitted particle with orbital angular momentum ℓ the same as the radiation order ℓ. We have the additional result that the multipole field for $\ell = 0$ is identically zero; that is, the system cannot emit an electromagnetic wave carrying away zero angular momentum.

As the radiation fields can be multiplied by arbitrary amplitudes, and since multipole fields form a complete set, we can expand any field satisfying Maxwell's equations as follows:

$$\vec{\mathcal{E}}(\vec{r}) = \sum_{\ell=1}^{\infty} \sum_{m=-\ell}^{\ell} A_E(\ell,m)\vec{\mathcal{E}}_E(\ell,m,\vec{r}) + A_M(\ell,m)\vec{\mathcal{E}}_M(\ell,m,\vec{r}) \tag{6.9}$$

$$\vec{\mathcal{H}}(\vec{r}) = \sum_{\ell=1}^{\infty} \sum_{m=-\ell}^{\ell} A_E(\ell,m)\vec{\mathcal{H}}_E(\ell,m,\vec{r}) + A_M(\ell,m)\vec{\mathcal{H}}_M(\ell,m,\vec{r}) \tag{6.10}$$

The amplitude of the multipole radiation is determined by the coefficients $A_E(\ell,m)$ and $A_M(\ell,m)$ which in turn are determined by the characteristics of the source. And the fundamental problem in determining the radiation transitions is to relate the amplitude coefficients to the properties of the source.

Selection Rules

The selection rules which apply to nuclear radiation are the same as those which apply to radiation from any other quantum system. The total angular momemtum of the system must be constant during the transition from the state ψ_b, that is

$$\vec{J}_a = \vec{J}_b + \vec{\ell} \tag{6.11}$$

As this is a vector relationship it puts the following restrictions on the quanta emitted,

$$|J_a - J_b| \leq \ell \leq J_a + J_b \tag{6.12}$$

$$M_a - M_b = m \tag{6.13}$$

It was previously stated that $\ell = 0$ transitions are prohibited and thus, from equation 6.12 transitions for which $J_a = J_b = 0$ are forbidden. In the practical case of the nucleus it is possible to have these transitions take place by indirect processes. An example is internal conversion (which is the interaction between the nucleus and the outer electrons causing a transition emitting an electron instead of a photon) for which it is possible to have $\ell = 0$ transitions. Once can also emit a pair of photons, or a pair of electrons in a zero-to-zero transition. But in astrophysical circumstances we are not ordinarily concerned with double photon emission, nuclear pair emission or internal conversion, and we shall not go into the theory here.

There are also selection rules arising from the conservation of parity. While parity is not conserved in weak interactions it only fails in electromagnetic interactions to an extremely small extent.

The following table* is a summary of the selection rules for the lowest possible value of ℓ, $\ell_{min} = L$

(A) $\underline{J_a \neq J_b}$

	Electric Radiation	Magnetic Radiation
Parity favored $\pi_a \pi_b = (-1)^{J_a - J_b}$	$L = \lvert J_a - J_b \rvert$	$L = \lvert J_a - J_b \rvert + 1$ except J_a or $J_b = 0$
Parity Unfavored $\pi_a \pi_b = (-1)^{J_a - J_b + 1}$	$L = \lvert J_a - J_b \rvert + 1$ except J_a or $J_b = 0$	$L = \lvert J_a - J_b \rvert$

(B) $\underline{J_a = J_b \neq 0}$

$\pi_a = \pi_b$	$L = 2$ except $J_a = J_b = \frac{1}{2}$	$L = 1$
$\pi_a = -\pi_b$	$L = 1$	$L = 2$ except $J_a = J_b = \frac{1}{2}$

---

* From Theoretical Nuclear Physics by Blatt and Weisskopf, pg. 589.

Therefore for all practical purposes it remains useful to talk about conservation of parity in electromagnetic transitions. The transiton probability between two states ψ_a and ψ_b is proportional to the matrix element H'_{ab}.

$$H'_{ab} = \frac{1}{2}\int \psi^*_b \, (\vec{j} \cdot \vec{A}) \, \psi_a \, d\tau \tag{6.14}$$

where $\vec{j}$ is the current operator and $\vec{A}$ is the vector potential of the emitted radiation. Now, $\vec{A}$ is proportioned to $\vec{\mathcal{E}}$ and $\vec{j}$ is a polar vector (hence odd parity) therefore the parity of $(\vec{j}\cdot\vec{A})$ is opposite to $\vec{\mathcal{E}}$ and thus the same as $\vec{\ell}$. From the integral in equation 14 we see that H'_{ab} vanishes unless

$\pi_a = \pi_b$ for "even" parity radiation, where $\pi_a = \pi_b$ refer to the parities of their respective ψ's.

In referring to these transitions we will characterize an electric transition of multipole order ℓ by $E\ell$, i.e., E1 for an electric dipole, E2 for an electric quadruple; and similarly for magnetic radiation, M1, M2, etc.

In atoms the only important selection rule is that for electric dipole transitions. The higher multipoles are retarded relative to electric dipole transitions and excitation by collisions takes place sooner. In astrophysics there are cases of special interest where the atomic source of radiation is at a low density such that collisions are unimportant, in this case one has to be concerned with higher multipole emissions.

We will see that for the same ℓ value the probability of electric radiation is much greater than magnetic radiation. Consequently if we have a parity-favored situation then electric radiation is generally more important than the allowed magnetic radiation. For the parity-unfavored transitions closer estimates of the transition probabilities are needed, and it can happen that the E and M transition probabilities are of the same order of magnitude.

Probability of Multipole Emission and Absorption

We want to relate the coefficients $A_E(\ell,m)$ and $A_M(\ell,m)$ to the source producing the multipole radiation. To do this we consider the source as a classical system of currents with periodic variations in time:

$$\vec{j}\,(\vec{r},t) = \vec{j}\,(\vec{r})e^{-i\omega t} + \vec{j}^{\,*}(\vec{r})e^{i\omega t} \tag{6.15}$$

We will suppose that this distribution of currents is associated with a small region of space having linear dimensions of order d. Similarly the charge density associated with the current distribution in equation 6.15 is

$$\rho(\vec{r},t) = \rho(\vec{r},t)e^{-i\omega t} + \rho^*(\vec{r})e^{i\omega t} \tag{6.16}$$

and by the continuity equation we have

$$i\omega\rho(\vec{r}) = \nabla\cdot\vec{j}\,(\vec{r}) \tag{6.17}$$

The radiation emitted by this system is treated as a classical problem

in several texts, we will use the results derived in appendix B of Blatt and Weisskopf

$$A_E(\ell,m) = \frac{-4\pi}{(2\ell+1)!!} \left(\frac{\ell+1}{\ell}\right)^{\frac{1}{2}} \varkappa^{\ell+2} Q_{\ell m} \tag{6.18}$$

where $(2\ell+1)!! = 1\ (3)(5)\ (7)\ldots(2\ell-1)\ (2\ell+1)$ (6.19)

$$\varkappa = \frac{w}{c} = \frac{2\pi\nu}{c} \tag{6.20}$$

and $Q_{\ell m} = \int r^{\ell} Y^{*}_{\ell m}\ (\theta,\phi)\ \rho(\vec{r})dV$ (6.21)

with the approximation in this equation subject to $\varkappa d \ll 1$ (6.22)

Equation (6.22) merely says that the wavelength is long compared to the dimensions of the system. $Q_{\ell m}$ is what we will call the electric multipole moment of order ℓ,m. The integration of dV extends over the volume of the charge distribution, and the normalized spherical harmonics are:

$$Y_{\ell m}(\theta,\phi) = \frac{(-1)^{\ell+m}}{(2\ell)!!} \left[\frac{(2\ell+1)\ (\ell-m)!}{4\pi\ (\ell+m)!}\right]^{\frac{1}{2}} (\sin\theta)^m \quad \times$$

$$\frac{d^{\ell+m}}{(d\cos\theta)^{\ell+m}} \left[(\sin\theta)^{2\ell}\right] \exp(im\Phi) \tag{6.23}$$

and $Y^{*}_{\ell m} = (-1)^m\ Y_{\ell,-m}$ (6.24)

Similarly one obtains for A_M

$$A_M\ (\ell,m) = \frac{4\pi}{(2\ell+1)!!} \left(\frac{\ell+1}{\ell}\right)^{\frac{1}{2}} \varkappa^{\ell+2}\ M_{\ell m} \tag{6.25}$$

where $M_{\ell m} \approx -\int r^{\ell} Y^{*}_{\ell m}(\theta,\phi) \frac{\nabla\cdot(\vec{r} \times \vec{j})}{c(\ell + 1)} dV$ (6.26)

and $\varkappa d \ll 1$

These are not the only sources of radiation that can arise from the system. There are intrinsic magnetic moments associated with the spins of the nucleons; thus we must consider the classical analogue of radiation resulting from a density of magnetization which varies in a periodic fashion (corresponding to different spin orientations of the nucleons). We write this as

$$\vec{M}(\vec{r},t) = \vec{M}(\vec{r})e^{-i\omega t} + \vec{M}^{*}(\vec{r})e^{i\omega t} \tag{6.27}$$

The transition probability amplitudes are the same as before except that we must define two new moments denoted by primes:

$$Q'_{\ell m} = \frac{-i\varkappa}{\ell+1} \int r^{\ell} Y^{*}_{\ell m}(\theta,\phi)\, \nabla\cdot(\vec{r} \times \vec{M})\, dV \tag{6.28}$$

$$M'_{\ell m} = -\int r^{\ell} Y^{*}_{\ell m}(\theta, \phi)\, (\nabla\cdot\vec{M})\, dV \tag{6.29}$$

We can now write for the dipole moment with m = 0 :

$$Q_{1,0} = \left(\frac{3}{4\pi}\right) \int z\, \rho(\vec{r})\, dV \tag{6.30}$$

$$M_{1,0} = \left(\frac{3}{4\pi}\right)^{\frac{1}{2}} \frac{1}{2c} \int \left(xj_y - yj_x\right) dV \tag{6.31}$$

$$Q'_{1,0} = \left(\frac{3}{4\pi}\right)^{\frac{1}{2}} \frac{\varkappa}{2} \int (\vec{r} \times \vec{M})_z\, dV \tag{6.32}$$

$$M'_{1,0} = \left(\frac{3}{4\pi}\right)^{\frac{1}{2}} \int M_z \, dV \tag{6.33}$$

A useful observation can be made by noting that the current $\vec{j}$ is of the order of magnitude of the velocity of the charges times the charge density, $\rho \vec{v}$ where $\bar{v}$ is a typical velocity. Neglecting the spin part of the radiation we have

$$\frac{M_{1,0}}{Q_{1,0}} \approx \frac{v}{c} \tag{6.34}$$

and this is generally true for all multipoles, at least an an approximation. Since the speed of the nuclear charges in the nucleus is usually much less than that of light, and as these amplitudes have to be squared to get the intensities, one can see that the instrinsic magnetic multipole moment will be significantly less than the intrinsic electric multipole moments.

Transition to Quantum Mechanics

We gradually make the transition to quantum mechanics by first classically calculating the energy emitted per second and the angular distribution resulting from the radiation. We divide the Poynting vector by the energy contained in a single quantum in order to find the rate of emission specified quanta. We have

$$\vec{S} = \frac{c}{4\pi} \vec{\mathcal{E}} \times \vec{\mathcal{H}} \tag{6.35}$$

and $$|\vec{S}| \simeq \frac{c}{4\pi} \mathcal{E}^2 \simeq \frac{c}{4\pi} \mathcal{H}^2 \tag{6.36}$$

where the approximation is used because the waves are not completely transverse. If we consider a large sphere of radius R around the source, the absolute value of $\vec{S}$ will give the energy escaping per square centimeter per second. The energy emitted into a solid angle $d\Omega$ is

$$|\vec{S}|\ R^2\ d\Omega = U(\Omega)d\Omega \tag{6.37}$$

where U is the energy. As $\mathcal{E}^2$ and $\mathcal{H}^2$ vary rapidly with time we will average them

$$\left.\begin{aligned} \langle \mathcal{E}^2(\vec{r},t)\rangle &= 2\ \vec{\mathcal{E}}^*(\vec{r})\cdot \vec{\mathcal{E}}(\vec{r}) \\ \langle \mathcal{H}^2(\vec{r},t)\rangle &= 2\ \mathcal{H}^*(\vec{r})\cdot \vec{\mathcal{H}}(\vec{r}) \end{aligned}\right\} \tag{6.38}$$

We can write the energy for pure electric multipole radiation of order ℓ, m as

$$U_E\ (\ell,m;r) = \frac{c}{2\pi\kappa^2}\quad Z_{\ell m}\ (\theta,\phi)\ |A_E(\ell,m)^2| \tag{6.39}$$

Where $Z_\ell\ (\theta,\phi) = \frac{1}{2}\left[1 - \frac{m(m+1)}{\ell(\ell+1)}\right]\ |Y_{\ell,m+1}|^2$

$$+ \frac{1}{2}\left[1 - \frac{m(m+1)}{\ell(\ell+1)}\right]\ |Y_{\ell,m-1}|^2 + \frac{m^2}{\ell(\ell+1)}\ |Y_{\ell,m}|^2 \tag{6.40}$$

The magnetic multipole has a similar expression

$$U_M(\ell,m;r) = \frac{c}{2\pi\kappa^2}\ Z_{\ell m}\ (\theta,\phi)\ |A_M(\ell,m)|^2 \tag{6.42}$$

What we are actually interested in is the total energy emitted per

second which we obtain by integrating equations 6.39 and 6.41 over $d\Omega$. The results are:

$$\text{Electric radiation, } U_E(\ell,m) = \frac{c}{2\pi\varkappa^2} \left|A_E(\ell,m)\right|^2 \tag{6.42}$$

$$\text{Magnetic radiation, } U_M(\ell,m) = \frac{c}{2\pi\varkappa^2} \left|A_M(\ell,m)\right|^2 \tag{6.43}$$

And the total value for U will be a sum over all ℓ and m.

$$U = \sum_{\ell=1}^{\infty} \sum_{m=-\ell}^{\ell} \left[U_E(\ell,m) + U_M(\ell,m)\right] \tag{6.44}$$

Emission and Application

We make the transition to quantum mechanics by dividing the classical rate of energy emission by the energy of the quantum to give us the rate of quantum emission. The total probability of emission for the electric radiation is:

$$T_E(\ell,m) = \frac{U_E(\ell,m)}{\hbar\omega} = \frac{c}{2\pi\varkappa^2\hbar\omega} \left|A_E(\ell,m)\right|^2 \tag{6.42}$$

$$= \frac{c}{2\pi\varkappa^2\omega} \left[\frac{-4\pi}{(2\ell+1)!!} \left(\frac{\ell+1}{\ell}\right)^{\frac{1}{2}} \varkappa^{\ell+2} \left|Q_{\ell m} + Q'_{\ell m}\right|\right]^2 \tag{6.46}$$

And similarly for $T_M(\ell,m)$:

$$T_M(\ell,m) = \frac{8\pi}{\ell} \frac{(\ell+1)}{[(2\ell+1)!!]^2} \frac{\varkappa^{2\ell+1}}{\hbar} \left|M_{\ell m} + M'_{\ell m}\right|^2 \tag{6.47}$$

We can make some crude estimates of the size of the multipole moments by writing

$$Q_{\ell m} = \int r^{\ell}\ Y_{\ell}{}^{*}{}_{m}\ (\theta,\phi)\ \rho(r)dV \tag{6.48}$$

$$\sim \epsilon \int r^{\ell}\ dV = \epsilon d^{\ell} \tag{6.49}$$

where ϵ = total charge. Hence

$$T_E(\ell,m) \sim (\varkappa d)^{2\ell} \tag{6.50}$$

and, with our previous assumption that $\varkappa d \ll 1$, higher multipoles become less probable.

<u>The Matrix Elements</u>

Up until now we have treated the source as a classical system of charges and currents. To calculate the matrix elements we have to describe the source in quantum mechanical terms. The quantum mechanical analogue of this current is

$$\vec{j}\ (a,b;\vec{r}) = \frac{e}{2M}\ [\psi_b^{*}\ (\vec{P}\psi_a) + (\vec{P}\psi_b)^{*}\psi_a] \tag{6.51}$$

where $\vec{P} = -\ i\hbar\ \nabla$ is the operator for the linear momentum of a particle and M is its mass. The charge density is

$$\rho(a,b;\vec{r}) = e\psi_b^{*}\ (\vec{r})\ \psi_a(\vec{r}) \tag{6.52}$$

Using equations 6.51 and 6.52 we can write the multipole moments as:

$$Q_{\ell m}(a,b) = e\int r^{\ell}\ Y_{\ell m}^{*}\ (\theta,\phi)\ \psi^{*}{}_b(\vec{r})\psi_a(\vec{r})d\tau \tag{6.53}$$

$$M_{\ell m}(a,b) = \frac{-e}{2Mc(\ell+1)}\int r^{\ell} Y_{\ell m}^{*}\ (\theta,\phi)\ \nabla\cdot[\ \vec{r}\ \times\ \vec{j}(a,b;\vec{r})]\ d\tau \tag{6.54}$$

Equation 6.54 can be integrated by parts to show that the two terms in

$\vec{j}$ give equal results. Using the definition

$$\vec{L} = -i\,\vec{r} \times \nabla \tag{6.55}$$

one gets

$$M_{\ell m}(a,b) = \frac{-e\hbar}{Mc(\ell+1)} \int r^{\ell}\, Y^{*}_{\ell m}(\theta,\phi)\, \nabla\cdot\, (\psi^{*}_{b}\, \vec{L}\, \psi_{a})\, d\tau \tag{6.56}$$

We also have to have expressions for the spin magnetization. The spin of each particle is $\hbar/2$ and the wave functions ψ_a and ψ_b are functions of spin coordinates as well as $\vec{r}$. For the spin coordinates we have to specify whether the spin is up or down (± 1). The spin gives rise to a magnetization density $\vec{M}(a,b;\vec{r})$ and this result in radiative transitions from ψ_a to ψ_b as follows:

$$\vec{M}(a,b;\vec{r}) = \frac{e\hbar}{2Mc}\, \mu\, \{\psi^{*}_{b}\, \vec{\sigma}\, \psi_{a}\} \tag{6.57}$$

where μ is the magnetic moment in Bohr magnetons and $\vec{\sigma}$ is the Pauli spin operator with components,

$$\sigma_x = \begin{pmatrix} 0 & 1 \\ 1 & 0 \end{pmatrix}, \quad \sigma_y = \begin{pmatrix} 0 & -i \\ i & 0 \end{pmatrix}, \quad \sigma_z = \begin{pmatrix} 1 & 0 \\ 0 & -1 \end{pmatrix} \tag{6.58}$$

The use of { } here indicates a sum over the spins alone. Expression 6.57 must be inserted into the formulas for $Q'_{\ell m}$ and $M'_{\ell m}$ to get the multipole moments: When one does this one finds that $M'_{\ell m}(a,b)$ and $M_{\ell m}(a,b)$ are of the same order of magnitude, that is

the magnetic radiation resulting from currents is comparable to magnetic radiation resulting from spin variations. However, the electric radiation resulting from spin variations is small compared to that resulting from charge variations.

We apply our expressions to a system containing many particles by summing over the particles. In doing this one has to remember that protons have a charge and neutrons do not, but all neutrons have a mass. When you have charges of only one kind you can have an effect called giant dipole resonance, which is an induced resonance resulting in a very strong absorption peak for high energy photons. The classical picture of this resonance is a collective oscillation of the proton gas in the nucleus against the neutron gas. The proton charge distribution undergoes an oscillation and can give rise to radiation emission, or alternatively, radiation can set this oscillation into effect. Hence the neutrons can play a role in radiation even though they have no charge.

Using the subscript k to designate the kth proton or kth nucleon, depending on which we sum over, we arrive at a final set of expressions for the multipole moments.

$$Q_{\ell m}(a,b) = e \sum_{k=1}^{Z} \int r_k^{\ell} Y^*_{\ell m}(\theta_k, \phi_k) \psi_b^* \psi_a \, d\tau \tag{6.59}$$

$$M_{\ell m}(a,b) = \frac{-1}{(\ell+1)} \frac{e\hbar}{Mc} \sum_{k=1}^{Z} \int r_k^{\ell} Y^*_{\ell m}(\theta_k, \phi_k) \nabla \cdot (\psi_b^* \vec{L}_k \psi_a) d\tau \tag{6.60}$$

$$Q'_{\ell m}(a,b) = \frac{-i\kappa}{(\ell+1)} \quad \frac{e\hbar}{2Mc} \sum_{k=1}^{A} \mu_k \int r_k^{\ell} \; Y^*_{\ell m}(\theta_k,\phi_k) \; \nabla\cdot(\psi_b^* \; \vec{r}_k \times \vec{\sigma}_k \psi_a) \; d\tau \qquad (6.61)$$

$$M'_{\ell m}(a,b) = \frac{-e\hbar}{2Mc} \sum_{k=1}^{A} \mu_k \int r_k^{\ell} \; Y^*_{\ell m}(\theta_k,\phi_k) \; \nabla\cdot(\psi_b^* \; \vec{\sigma}_k \psi_a) d\tau \qquad (6.62)$$

This is a formalistic summary of what is involved in emitting radiation from the nucleus and it is necessary to emphasize that it is not a complete description of what is possible. For example if nuclear forces consist partly of exchange forces, arising from the exchange of charge between neutrons and protons, then we should have exchange currents and exchange magnetic moments. Formally we should have included these here, but since we are going to approximate our existing results to arrive at usable numbers it is not necessary to include it.

Transitions Between Low-Lying States of Nuclei

We want to make some estimates of what the multipoles in equations 6.59-6.62 are likely to be for transitions near the ground state. Now if the wave functions ψ_a and ψ_b overlapped perfectly the maximum value for $Q_{\ell m}$ would be of the order of ZeR^{ℓ} where R is the nuclear radius. Our expressions for the transition probabilities are,

$$T_E(\ell,m) = \frac{8\pi(\ell+1)}{\ell[(2\ell+1)!!]^2} \; \frac{\kappa^{2\ell+1}}{\hbar} \; |Q_{\ell m} + Q'_{\ell m}|^2$$

$$T_M(\ell,m) = \frac{8\pi(\ell+1)}{\ell[(2\ell+1)!!]^2} \; \frac{\kappa^{2\ell+1}}{\hbar} \; |M_{\ell m} + M'_{\ell m}|^2$$

For electric radiation the transition probability amplitudes are approximately proportional to $\varkappa^{\ell} Q_{\ell m}$, which is at most equal to $Ze(KR)^{\ell}$. Since we are assuming $\varkappa R \ll 1$ for the energies we are concerned with about 1 Mev.), the transition probabilities decrease rapidly with increasing multipole order.

We wish to make a more general estimate of $M_{\ell m} / Q_{\ell m}$ than was derived in equation 6.34. We can use R^{-1} as a first approximation the "div" operator in $M_{\ell m}$, and the operator $\vec{L}$ will generate a factor ℓ which approximately cancels $(\ell+1)^{-1}$. With these approximations we have

$$\frac{M_{\ell m}}{Q_{\ell m}} \simeq \frac{\hbar}{McR} \tag{6.63}$$

Similarly for some other ratios we have

$$\frac{M'_{\ell m}}{M_{\ell m}} \simeq \frac{|u\,\vec{\sigma}|}{|\vec{L}/\ell+1|} \simeq 2 \text{ or } 3 \tag{6.64}$$

Since $|M| > 1$

$$\frac{Q'_{\ell m}}{Q_{\ell m}} \simeq \left| \frac{\varkappa}{(\ell+1)} \frac{\hbar}{Mc} u \frac{\vec{r} \times \vec{\sigma}}{R} \right| \simeq \frac{\varkappa \hbar}{Mc} = \frac{\hbar \omega}{Mc^2} \simeq 10^{-3} \tag{6.65}$$

The ratio $Q_{\ell m}'$ can be neglected with respect to the other ratios estimated. These correspond to the previous statements that the magnetic moment due

to spin changes is comparable to the magnetic moment due to currents, but the electric moment due to spin changes is negligible compared to the electric moment due to charges. We may estimate that

$$\frac{|M_{\ell m} + M'_{\ell m}|^2}{|Q_{\ell m}|^2} \approx 10 \left(\frac{\hbar}{McR}\right)^2 \tag{6.66}$$

One must remember that equation 6.66 is an extremely crude estimate and that it can be change drastically by selection rules, details of nuclear motion and details of nuclear structure.

We still need an estimate of one of the moments in order to establish some absolute values. To do this we must assume some nuclear model and a good choice is an independent particle model. One familiar version of this model is the shell model, which gives a good description of most aspects of nuclear matter.

In the independent particle model the quantum numbers of individual nucleons describe the state of the nucleus. Only if the two states a and b differ in the quantum numbers of only one nucleon will we have multipole moments which are nonzero. For this reason we think of our transitions as involving a basically unchanged nuclear core coupled to one nucleon changing its state.

Let us focus attention on one of the protons as it changes its state. We assume that in its final state the proton has zero angular momentum and in its initial state has angular momentum ℓ. In addition we assume that the transition is parity-favored, which means that in the initial

state the proton's spin is parallel to $\vec{\ell}$. The wave functions for this proton can be written as,

$$w_a = U_a(r)\ Y_{\ell m}(\theta,\phi)\alpha \tag{6.67}$$

$$w_b = U_b(r)\ (4\pi)^{-\frac{1}{2}}\ \alpha \tag{6.68}$$

where α is a spin function corresponding to spin up, and U_a, U_b depend only on the radial distance $|\vec{r}|$

So $Q_{\ell m}(a,b)$ is now written as,

$$Q_{\ell m}(a,b) = e \sum_{k=1}^{Z} \int r_k^{\ell}\ Y^*_{\ell m}\ (\theta_k,\phi_k)\ \psi^*_b\ \psi_a\ d\tau \tag{6.69}$$

$$= e \int r_1^{\ell}\ Y^*_{\ell m}\ (\theta_1,\phi_1)\ \ |\psi_2 \cdots_Z(a,b)|^2\ \ Y_{\ell m}(\theta_1,\phi_1)$$

$$x(4\pi)^{-\frac{1}{2}}\ \ U_a(r)\ U_b^*\ (r)\ \ |\alpha|^2\ d\tau \tag{6.70}$$

where we have taken only the first term in the sum because we require in our model that the rest of the nucleus remain unchanged.

On integration for the first proton the overlap wave functions and the angular dependent parts become unity. Therefore

$$Q_{\ell m} = (4\pi)^{-\frac{1}{2}}\ e\ J_{\ell} \tag{6.71}$$

where $J_{\ell} = \int_0^{\infty} r^{\ell}\ \ U_a(r)\ U_b(r)\ r^2 dr$ (6.72)

We do not know how the wave function for this proton is distributed

over the nucleus and we must therefore be satisfied with an order of magnitude estimate for J_ℓ. Our simplest assumption will be to consider the wave functions to be uniformly spread over the nucleus, or

$$\left.\begin{aligned} U_a(r) &= U_b(r) = \text{constant}, \quad r \leq R \\ U_a(r) &= U_b(r) = 0 \qquad\qquad , \quad r > R \end{aligned}\right\} \tag{6.73}$$

By normalizing the wave function the constant becomes $(3/R^3)^{\frac{1}{2}}$, hence

$$J_\ell = \int_0^R r^\ell \frac{3}{R^3} r^2 dr = \frac{3}{(\ell+3)} R^\ell \tag{6.74}$$

The matrix elements for radiative transitions have been reduced to the evaluation of a simple integral which involves the wave functions of the particles in the nucleus. Though the estimate is rough it contains all of the essential energy and radial variations. Therefore it is a suitable standard for comparison when we want to take out well known variations such as the energy dependencies of different transitions.

Actually U_a and U_b are not constant but oscillate for $r < R$ and exponentially go to zero for $r > R$. Therefore J_ℓ should be smaller than our calculations, sometimes by factors up to 30, and occasionally by several orders of magnitude. These large deviations can occur in electric dipole radiation where protons oscillate in a collective manner against the neutrons, or in certain types of quadruple emission where the nuclear surface is oscillating in some favorable fashion, or by

collective rotation of the nucleus.

When we put our estimate obtained in equation 6.74 into the transition probability formula we obtain:

$$T_E(\ell) \simeq \frac{2(\ell+1)}{\ell[(2\ell+1)!!]^2} \left(\frac{3}{\ell+3}\right)^2 \frac{e^2}{\hbar c} (\varkappa R)^{2\ell} \omega$$

$$= \frac{4.4(\ell+1)}{\ell[(2\ell+1)!!]^2} \left(\frac{3}{\ell+3}\right) \left(\frac{\hbar\omega}{197 \text{ Mev}}\right)^{2\ell+1} (R \text{ in } 10^{-13} \text{ cm})^{2\ell} \, 10^{21} \text{sec}^{-1} \qquad (6.75)$$

$$T_M(\ell) \simeq \frac{20(\ell+1)}{\ell[(2\ell+1)!!]^2} \left(\frac{3}{\ell+3}\right)^2 \frac{e^2}{\hbar c} \left(\frac{\hbar}{McR}\right)^2 (\varkappa R)^{2\ell} \omega$$

$$= \frac{1.9(\ell+1)}{\ell[(2\ell+1)!!]^2} \left(\frac{3}{\ell+3}\right)^2 \left(\frac{\hbar\omega}{197 \text{ Mev}}\right)^{2\ell+1} (R \text{ in } 10^{-13} \text{cm})^{2\ell-2} \, 10^{21} \text{sec}^{-1} \qquad (6.76)$$

The actual lifetimes must be obtained from the transition probabilities that have been corrected for internal conversions. Often the internal conversion coefficient is known experimentally and then the results can be corrected without requiring any knowledge of the parity or multipole order of the transition. Monograms for the relations (75) and (76) are published by R. Montalbetti in Canadian Journal of Physics; 30, 660 (1952).

Transitions Involving Highly Excited States

We will be considering two basic reactions, emissions of gamma rays following the capture of a particle by a nucleus, and the absorption of high energy gamma rays by the nucleus. These reactions will usually

involve high energies (5-25 Mev.). When a high energy particle is incident on the nucleus ($\sim$ 8 Mev) and forms a compound nucleus there will be a large number of lower lying levels, and our calculation of the outgoing radiation must involve the sum over all those lower lying levels.

Sum Rules

There are relations called sum rules which limit the size of the matrix elements for radiative transitions in nuclei. The sum rules apply to the sum of the square of the transition matrix elements between one state "a" of the nucleus and all other stationary states "b". As the sums are found to be finite they place limits on the total transition probabilities into and out of any state. One result is that when the cross section for photon absorption (from the ground state) is integrated over all photon energies we get a finite value.

An interesting consequence of the sum rules is that if some particular transition is inhibited by the reaction mechanism in some energy range, then that type of transition will have to be stronger in some other energy range to satisfy the sum rules.

From Blatt and Weisskopf we note the following sum rules:

$$\frac{2M}{\hbar^2} \sum_b (E_b - E_a) \, |Q_{1,0}(a,b)|^2 = \frac{3}{4\pi} \frac{NZ}{A} e^2 \qquad (6.77)$$

where M = mass of nucleon

$E_b < E_a$ are transition states

$Q_{1,0}$ is the E_1 matrix element with $m=0$

N = number of neutrons

Z = number of protons

A = mass number

e = electronic charge

and similar rules exist for $Q_{1,-1}$ and $Q_{1,1}$.

This sum rule is independent of the details of the nuclear structure as it involves only natural constants. However, this is an oversimplification because the sum over b is supposed to be over the stationary states of the system. In reality the nuclear states are not stationary but decay by photon emission, or (at higher energies) by particle emission. In particular, in heavy nuclei when the excitation is $\sim$ 15 Mev. the widths of the nuclear states become greater than the distances between states and we have a continuum. In addition to these errors, the electric dipole matrix elements can be augmented by charge exchange forces acting between the nucleons. The exchange force means that the position of the charge is changing more rapidly then that of the nucleons. Now the charge velocities are greater than the nucleon velocities, and since the nucleon velocities were used to obtain the sum rules the rules must be modified in accord with the charge velocities (though we will not go into this here).

Another dipole sum rule is,

$$\sum_b (E_b - E_a)^2 \; |Q_{1,0}(a,b)|^2 = \frac{3}{4\pi} \left(\frac{\hbar}{M}\right)^2 \langle (\sum_{k=1}^{A} e_k' \, p_{kz})^2 \rangle_a \qquad (6.78)$$

which depends on the expectation value of the operator $(\sum_{k=1}^{A} e_k' \, p_{kz})^2$ in the state a, as well as the natural constants.

We also define the effective charge of the nucleons

$$\left.\begin{aligned} e_k' &= e\,(1 - \tfrac{Z}{A}) \text{ for protons} \\ &= -e\,\tfrac{Z}{A} \qquad \text{for neutrons} \end{aligned}\right\} \qquad (6\ 79)$$

and $p_{kz}(a,b) = \frac{iM}{\hbar} (E_b - E_a \; z_k(a,b)$ (6.80)

the momentum operator, where $z_k(a,b)$ is the position operator of the transition from $a \rightarrow b$.

We can evaluate this expectation only if the wave function of the state is known. Instead we will estimate the expectation by assuming no correlation between the momenta of the nucleons, i.e., $\langle p_{kz} \; p_{k'z} \rangle = 0$ for $k \neq k'$, and by letting all the squares of the momenta components be equal, $\langle p^2_{kz} \rangle_a \cong P^2/3$, where P^2 represents the average square of momenta of a representative nucleon in the nucleus. Hence,

$$\sum_b (E_b - E_a)^2 \; |Q_{1,0}(a,b)|^2 \sim (4\pi)^{-1} e^2 \; \frac{NZ}{A} \left(\frac{\hbar P}{M}\right)^2 \qquad (6.81)$$

since $\sum_{k=1}^{A} (e'_k)^2 = Ze^2 \; \frac{N^2}{A^2} + \frac{Ne^2Z^2}{A^2}$

$$= e^2 \frac{NZ}{A^2} (N + Z) \doteq e^2 \frac{NZ}{A} \tag{6.82}$$

In the two sum rules discussed one involves $(E_b - E_a)$ to the first power, the other to the second power. With both sum rules it is possible to say something about the mean energy of the transitions.

In a similar manner we can express sum rules for higher multipole transitions:

$$\sum_b |Q_{\ell m}(a,b)|^2 = e^2 \langle |\sum_{k=1}^{Z} r_k^{\ell} Y_{\ell m}(\theta_k, \phi_k)|^2 \rangle_a \tag{6.83}$$

The average value of this general sum rule can be estimated by again neglecting correlations, and assuming a uniform distribution for the nucleons within the nucleus. As an extremely rough estimate we have,

$$\sum_b |Q_{\ell m}(a,b)|^2 \sim \frac{3}{(2\ell+3)} \frac{Ze^2}{4\pi} R^{2\ell} \tag{6.84}$$

where R is the nuclear radius. For additonal sum rules the reader is referred to Austern and Sachs, Physical Review 81, 706, 710 (1951).

Estimates of Matrix Elements Involving Highly Excited Nuclear States

Our previous estimates of the matrix elements for the transition probabilities between low-lying levels, were based on two simple but extreme models: The independent particle model and the liquid drop model. For high energy regions of nuclei (75 Mev) we find a large

number of nuclear levels, greater in number than either model predicts. The large number of levels leads us to suspect that the previous transition probabilities would be too large if applied to levels differing greatly in energy. In addition, since the nuclei have densities which increase exponentially with energy, the transition probabilities arising out of the ground state would very rapidly diverge when integrated to ∞. A diverging result contradicits the sum rules, hence we conclude that the matrix elements for transitions to highly excited states are much less than our previous estimate for low-lying states. It is this reduction in the intrinsic matrix elements which will concern us here.

We will consider two oversimplified models in our attempt to find the new matrix elements for transitions. Assume that the nucleus is composed of only one charged particle and that the other particles are all neutrons. In model I there is no interaction between nucleons; they all move independently of each other in a common potential V. This is similar to a problem in virtual level theory where it is found that α - particles in a potential well give rise to equally space virtual levels. Hence model I has equidistant quantum states with energy spacing ∇. Because the total energy $N\nabla$ can be constructed in many ways from the energies $n\ \nabla$ of the individual nucleons ($n \leq N$ are integers), the levels of the system will be highly degenerate.

In model II we introduce interactions between the nucleons, where the interactions are weak. By weak we mean that a level of the

system at energy E will have a wave function which is a linear superposition of the wave functions in model I for levels $E' = N\nabla$ near E.

In model I radiative transitions are assumed to take place between states which differ solely in the state of the proton, but which are identical as to the states of all the neutrons. Let us consider two energy levels, A and B, which are degenerate to different amounts and where $E_A > E_B$.

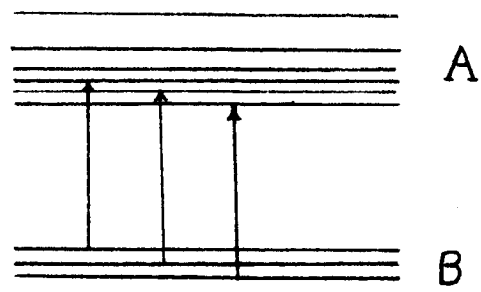

For every component in B (the lower level) we can find a combining level in A (the upper group) by raising the proton up by $(E_A - E_B)/\nabla$ steps. The figure above illustrates how we can combine every level in the lower group with one level in the upper group, but not viee-versa.

Let the matrix element for some given type of transition be called Q_o. We assume that Q_o is the same for all possible transitions in model I, regardless of energy difference $(E_A - E_B)$, or selection rules. These assumptions will help us to single out the basic principles of the problem.

We now consider model II with its weak interaction between the nucleons. As it is a weak interaction the degenerate levels at A are

split by amounts small compared to ∇, the energy spacing. The other aspect of this model is that the wave function for each level is a linear combination of the corresponding degenerate levels in model I. One the average each component level of group A will be assumed to to contribute equally to the combination similarly for B Now there will be transitions between all pairs of levels in the two groups, since each energy level in A contains a small part of that level of model I which combines with a specific level in group B. We call the degeneracy (or number of levels) of group A, g_A ; that is, g_A is a statistical weight of the levels. We can write for the transitions between the specific levels a in A and b in B the relation,

$$|Q(a,b)|^2 \sim \frac{Q_o^{\,2}}{g_A} \tag{6.85}$$

Notice that the matrix element squared is inversely proportional to the degeneracy of the upper group of levels and that the degeneracy in group B does not matter.

In model II we now let the interactions between the nucleons increase. Qualitatively expression (85) should still hold in that $|Q(a,b)|^2$ should be inversely proportioned to the number of levels near the transition level. By near we mean a constant energy interval about the level in which we are interested. We can restate this rule in Blatt and Weisskopf terms: The square of the matrix element between two levels E_a and E_b is approximately proportional to $D(E_>)$, the average level distance at the upper level. We formulate this law as,

$$\langle |Q_{\ell m}(a,b)|^2 \rangle_{av} = q_{\ell m}\,(E_a,E_b)\; D_\ell(E_>) \tag{6.86}$$

where the left hand side is an average between the lower level and a large number of upper levels near $E_>$, the upper energy. $D_\ell(E_>)$ is the spacing between the levels, near $E_>$, which are combining with the lower level to form the transitions which we are evaluating. Consequently we concentrate most of our uncertainty into the function $q_{\ell m}(E_a, E_b)$, which should be a slowly varying function of E_a and E_b, at least compared to the exponential behavior of $D(E_>)$.

We can obtain some useful information about $q_{\ell m}(E_a, E_b)$ from our previous sum rule estimate,

$$\sum_b |Q_{\ell m}(a,b)|^2 \sim \frac{3}{2\ell+3} \frac{Ze^2}{4\pi} R^{2\ell}$$

For simplicity we assume that E_a is the ground state, $E_a = 0$. We can now replace the sum over b by an integral,

$$\sum_b |Q_{\ell m}(0,b)|^2 \cong \int_0^\infty \langle |Q_{\ell m}(0,b)|^2 \rangle \text{ av } \frac{dE_b}{D_\ell(E_b)} \tag{6.87}$$

$$= \int_0^\infty q_{\ell m}(0, E_b)\, dE_b \tag{6.88}$$

Now from the sum rule the integral in equation 6.88 must converge, hence $q_{\ell m}(E_a, E_b)$ cannot be a constant but must decrease at high energies E_b. We can roughly estimate equation 6.88 by assuming maximum energy $E_{max,\ell}$, and zero for $E_b > E_{max,\ell}$. We can get a relation for $q_{\ell m}(E_a, E_b)$ over this range from the sum rule:

$$\int_0^\infty q_{\ell m}(0,E_b)dE_b = \int_0^{E_{max,\ell}} q_\ell(0,E_b)\, dE_b = q_\ell\, E_{max,\ell} \tag{6.89}$$

hence from equation (84)

$$q_\ell\, E_{max,\ell} \sim \frac{3}{(2\ell+3)} \frac{Ze^2}{4\pi} R^{2\ell} \tag{6.90}$$

We can now go back and evaluate q_ℓ in terms of the matrix element estimates made in connection with the independent particle estimates of transition probabilities between low-lying states. We had,

$$Q_{\ell m} = \frac{1}{\sqrt{4\pi}}\, e\, J_\ell$$

$$J_\ell = \int_0^\infty r^\ell\, U_a(r)\, U_b(r)\, r^2 dr$$

and if $U_a(r)$ and $U_b(r)$ are constant inside the nucleus and zero outside,

$$J_\ell \sim \frac{3R^\ell}{(\ell+3)} \tag{6.91}$$

Now we let the distance among the combining low-lying levels be D_0. Then

$$q_\ell \sim \langle |Q_{\ell m}(a,b)|^2 \rangle av/D_0 \tag{6.92}$$

$$\sim \left[\frac{3eR^\ell}{(\ell+3)\sqrt{4\pi}}\right]^2 \frac{1}{D_0}$$

$$q_\ell = \left(\frac{3}{\ell+3}\right)^2 \frac{e^2 R^{2\ell}}{4\pi D_0} \tag{6.93}$$

We can now solve for $E_{max,\ell}$ from equation 6.90

$$E_{max,\ell} \sim \left(\frac{3}{2\ell+3}\right) \frac{Z e^2}{4\pi} R^{2\ell} \frac{1}{q_\ell}$$

$$\sim \left(\frac{3}{2\ell+3}\right) \frac{Z e^2}{4\pi} R^{2\ell} \left(\frac{\ell+3}{3}\right)^2 \frac{4\pi D_0}{e^2 R^{2\ell}}$$

$$= \left(\frac{3}{2\ell+3}\right) \left(\frac{\ell+3}{3}\right)^2 Z D_0 \tag{6.94}$$

letting $(\ell+3)^2/3(2\ell+3) \sim 1$

$$\frac{E_{max,\ell}}{D_0} \sim Z \tag{6.95}$$

We make a sample calculation for medium weight nuclei ($Z \sim 50$); letting $D_0 \sim 0.5$ Mev. we get $E_{max,\ell} \sim 25$ Mev. By our previous assumptions q_ℓ can be considered a constant up to energies of the order of 25 Mev. Actually our results are highly uncertain because our assumptions were highly simplified. Our estimate of the wave functions for the independent particle model were crude; we neglected both correlations between nucleon motions and the oscillatory character of the wave functions inside the nucleus. In addition the estimates for the sum rule neglected correlations. While it is possible that these omissions may partially cancel each other, it is more likely that the estimate for the maximum energy is off by a large factor in either direction. These difficulties

may cause us to seriously question the validity of the estimate for E1 transitions, but it represents the best that we can do.

So far our estimates have referred to electric multipole radiation. As we have shown before we can take $10(\hbar/_{McR})^2$ as an estimate of the ratio of the magnetic to electric transition probability. An important point is that this ratio is independent of the energy transition. Some results of Goldhaber and Sungar suggest that one should empirically modify this ratio so that it becomes $(\hbar/_{McR})^2$ for the magnetic to hypothetical electric transition probabilities. At the same time we would also make a rough estimate that the ratio of the real to hypothetical electric is of the order of 10^{-2}. In any case the upper limit to q_ℓ will apply to magnetic radiation as well as to electric radiation.

Radiative Capture of Neutrons

We assume that a neutron enters a nucleus and forms a compound state E_c, with a mean lifetime τ (E_c) before disintegration. We define the width of the state as,

$$\Gamma(E_c) = \hbar/\tau(E_c) \tag{6.96}$$

This relationship is similar to the uncertainty principle and expresses Γ as an energy. $\Gamma(E_c)$ describes the energy half-width of the state c

and is $\hbar$ times the decay rate. We can write Γ as a sum of partial probabilities of decay by different processes; hence we can represent the total probability of disintegrated as,

$$\Gamma(E_c) = \sum_i \Gamma_i \quad (E_c) \tag{6.97}$$

Since we are considering cases where radiation is emitted by various electric and magnetic multipoles we write Γ_{rad} as:

$$\Gamma_{rad} = \sum_{\ell=1}^{\infty} \left(\Gamma_{E\ell} + \Gamma_{M\ell}\right) \tag{6.98}$$

and each of these, in turn, are the sums of partial radiation widths for the various lower levels,

$$\Gamma_{E\ell} = \sum_b \Gamma_{E\ell} \quad (c,b) \qquad , E_b < E_c \tag{6.99}$$

where $\Gamma_{E\ell}$ (a,b) is non-zero only if the parity and spin differences of c,b allow a transition. A similar relation holds for the magnetic transitions.

The radiation width will exhibit a smoother behavior than a particle emission width, because the total radiation width does not vary greatly when going from one compound level to another within a given energy region. The observed radiation widths do not vary much because they are made up of a large number of partial widths for individual multipole transitions to individual lower levels.

We will now estimate the partial radiation width for electric radiation of order ℓ between an upper state "a" and a lower state "b".

Starting with equation 6.46, (which we rewrite),

$$T_E(\ell,m) = \frac{8\pi(\ell+1)}{\ell[(2\ell+1)!!]^2} \quad \frac{\varkappa^{2\ell+1}}{\hbar} \left|Q_{\ell m} + Q_{\ell m}'\right|$$

and using equation 6.86,

$$\langle |Q_{\ell m}(a,b)|^2 \rangle_{av} = q_{\ell m}(E_a, E_b)\, D_\ell(E_a)$$

and equation 6.98

$$q_\ell \sim \left(\frac{3}{\ell+3}\right)^2 \quad \frac{e^2 R^{2\ell}}{4\pi D_0}$$

we get,

$$\langle \Gamma_{E\ell}(a,b)\rangle_{av} \sim \frac{18(\ell+1)\ (2\ell+1)}{\ell(\ell+3)^2[(2\ell+1)!!]^2} \quad \frac{e^2}{\hbar c} \quad \frac{\hbar\omega}{D_0} \left(\frac{\omega R}{c}\right)^{2\ell} D_\ell(E_a) \qquad (6.100)$$

where a factor $(2\ell+1)$ has been included in the numerator to make a rough correction for statistical weights; by which we mean that for each ℓ value the multipole radiation can have $2\ell+1$ different m values. While this correction is not exact it is a simplified correction and is better than no correction. And, as usual, the partial radiation width for magnetic transitions, $\Gamma_{M\ell}(a,b)$, is estimated to be smaller than $\Gamma_{E\ell}(a,b)$ by the factor $\sim 10\ (\hbar/McR)^2$.

We can now find the spectrum of the initially emitted gamma rays But because there exists a series of lower energy intermediate states which emit gamma rays, the observed spectrum is not the same as the one we estimate. We obtain the initial spectrum by multiplying the partial widths by the energy level density of the final states, $[D_\ell(E_b)]^{-1}$. The emitted radiation of order ℓ then has the following energy distribution,

$$U_\ell(\hbar\omega)\,d(\hbar\omega) = C_\ell(\hbar\omega)^{2\ell+1}\,[D_\ell(E_a - \hbar\omega)]^{-1} \tag{6.101}$$

where C_ℓ is a constant derived from the factors in the previous formula and is independent of $\hbar\omega$. This distribution favors the emission of high energy quantum radiation due to the presence of the factor of $(\hbar\omega)^{2\ell+1}$. D_ℓ is a rapidly decreasing function of the energy

$E_b = E_a - \hbar\omega$, and this factor favors the emission of low energy quantum radiation. If we assume the level density to be,

$$W(E) = D^{-1}(E) = C \exp\,[2\sqrt{aE}\,] \tag{6.102}$$

and use appropriate values for $\vec{a}$, then we find that the emitted spectrum has the following form,

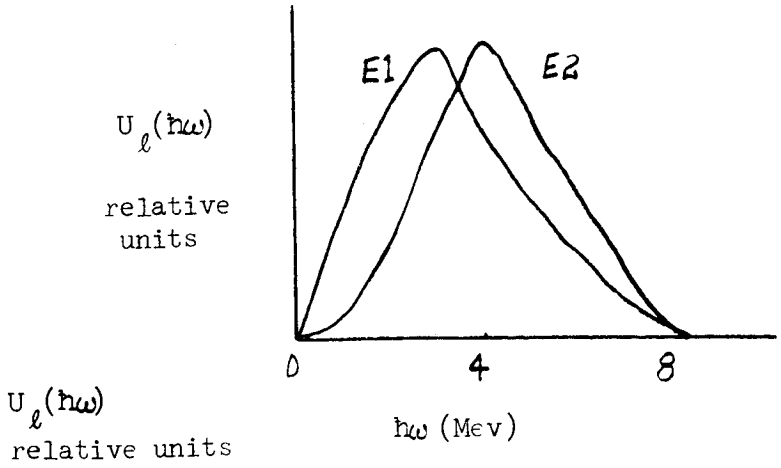

These distributions are smooth whereas they should be discontinuous peaks. However, the peaks are only important for transitions going to states near the ground, where they would be widely spaced. Hence for most regions we can use the smooth curves.

We now estimate the absolute value for $\Gamma_{M\ell}$. We replace the sum over the partilce emission widths by an integral,

$$\Gamma_{E\ell} \sim \frac{18(\ell+1)\ (2\ell+1)}{\ell(\ell+3)^2\ [(2\ell+1)!!]^2} \quad \frac{e^2}{\hbar c} \left(\frac{R}{\hbar c}\right)^{2\ell} \frac{1}{D_0} \int_0^{E_a} (\hbar\omega)^{2\ell+1} \frac{D_\ell(E_a)}{D_\ell(E_a - \hbar\omega)} \, d(\hbar\omega) \tag{6.103}$$

and, according to our usual estimates of magnetic versus electric multipole strength,

$$\Gamma_{M\ell} \sim 10 \left(\frac{\hbar}{McR}\right)^2 \Gamma_{E\ell} \tag{6.104}$$

These formulas can be applied to the case of capture of slow neutrons ($E_n = .025$ ev) followed by γ-ray emission, where the energy of excitation, E_a, is equal to the neutron binding energy (about 8 Mev.). There are measurements for the radiation widths of slow neutrons to which the theory can be compared.

We present some results arrived at by C. J. Hansen for the E1 Γ_{rad} calculations. When we have many excited states to sum over, in general, we need only consider those excited states which can be reached by electric dipole transitions in order to estimate the total radiation width.

We saw earlier that the electric dipole transitions are most likely to be strongest, with magnetic dipoles and electric quadrupoles less strong. For certain nuclei, called self-conjugate nuclei, in which the number of protons is equal to the number of neutrons, the electric dipole transitions are hindered. They are hindered for transitions between those states with the same isotopic spin and for these states we must go beyond the electric dipole to get results.

We write equation 6.100 with $\ell = 1$ and get,

$$\Gamma_\gamma^{E1}(J\pi) = \frac{3}{4} \frac{e^2}{\hbar c} \left(\frac{R}{\hbar c}\right)^2 A^{2/3} \sum_{\substack{\text{suitable}\\ \text{levels}}} \frac{D(U)E^3}{D_0 D(U-E)} \qquad (6.105)$$

We rewrite this with all quantities in Mev., but Γ_γ in ev.,

$$\Gamma_\gamma^{E1}(J\pi) = .296 \frac{A^{2/3}}{D_0} \sum_{J\pi} D(U, J,\pi) \int_0^U \frac{E^3}{D(U-E,J,\pi)} dE \qquad (6.106)$$

The term D_0 acts as a normalization factor, although it can also be interpreted as the single particle level spacing. If we assume the equality of the parity distributions and neglect the exponential form of the J dependence of the level density then the sum over J and π is simple. Summing over all allowed values of J,π of the daughter levels consistent with the electric dipole selection rules ($\nabla J = \pm 1,0$; no $0 \rightarrow 0$; parity change) we get the term

$$\frac{[2(J+1)+1] + [2(J-1)+1]}{2J+1} = \frac{6J+3}{2J+1} = 3$$

hence

$$\Gamma_\gamma = 0.89 \; A^{2/3} \; \frac{D(U)}{D_0} \int_0^U \frac{E^3 dE}{D(U-E)} \tag{6.103}$$

This result was used in a paper by J. Truran, C. Hansen, A. G. W. Cameron and A. Gilbert, Thermonuclear Reactions in Medium and Heavy Nuclei. They calculated these widths and compared them with experimental values for a large number of nuclei with $A > 50$. Their estimates for D_0 were; $D_0 \simeq 230$ Mev for $A > 50$, $D_0 \simeq 400$ Mev for $A > 50$.

7. Nuclear Beta Decay

History and Introduction

Experimental evidence that beta rays are identical with ordinary electrons and positrons is compelling. The charge-to mass ratios for the two agree within experimental limitations, and so do the charges. The observation of orbital electron capture as an alternative process to β^+ emission indicates that the nucleus can accept an ordinary electron in order to accomplish the same transition, and this is taken as confirmation that the β^+ emission is just emission of an ordinary positron. Furthermore, β^- particles are not captured into occupied orbits, showing via the exclusion principle that they are identical with the electrons already occupying those orbits.

Emission of electrons from nuclei suggests that electrons are a permanent part of nuclear matter. Before the discovery of the neutron in 1932, a proton-electron theory of the nucleus was popular. Accordingly, ${}_7N^{14}$ was thought to consist of 14 protons and 7 electrons, 21 nuclear particles in all.

Strong arguments against this theory can be made. Both protons and electrons are fermions, particles of

spin ½. So $_7N^{14}$ would have an odd half-integral spin since its nucleus contains an odd number of fermions. But the measured angular momentum of $_7N^{14}$ is J = 1, and similar results hold for other typical odd-odd nuclei.

Another argument against the proton-electron nuclear theory is presented by the uncertainty principle. If we are to confine an electron to a nuclear volume of dimension R, we must necessarily have a momentum distribution extending to momenta of magnitude $P_{max} \sim \hbar/R$. In the extreme relativistic approximation, the corresponding kinetic energy is $E_{max} \sim \hbar c/R$. Since $R \sim 10^{-12}$cm, $E_{max} \sim 20$ MeV. In order to keep the electron within the nucleus, the potential energy of attraction between electrons and protons must be sufficiently strong to overcompensate this large kinetic energy, but from measurements, there is evidence against such a strong interaction.

It seems that electrons emerge from nuclei yet cannot exist within nuclei, and this apparent contradiction is reminiscent of the situation encountered in atomic structure in the theory of emission and absorption of light from atoms. Electromagnetic radiation does not seem to be an integral part of atomic structure, but electro-

magnetic radiation emerges from atoms, according to the theory, when an atom changes its energy state. One may say that a light quantum is created at the moment of emission, but it is well to note that the electromagnetic field and the atom are in interaction all the time. This continuous interaction shows up in steady disturbances such as the Lamb shift and natural level width, and thus while electromagnetic radiation is not an integral part of atomic structure as such, it has a kind of latent existence in the atom.

Before we become too enthusiastic about the analogy of emission of beta rays from nuclei with extra-nuclear transitions, there are some additional difficulties to be confronted. These concern the apparent lack of conservation of energy, momentum, and angular momentum in beta decay.

Atomic transitions consist of the change of the electron structure outside the nucleus from one well-defined state to another with the emission of a quantum of electromagnetic radiation. The emitted quantum carries away the energy and momentum and angular momentum liberated in the transition; consequently the energy $\hbar\omega$ of the light quantum

is determined, and its momentum is equal and opposite to the momentum of the recoiling atom. By analogy, we should expect that a beta particle is emitted when a nucleus changes from one well-defined state to another and that the beta particle should carry away a definite amount of energy and its momentum should be equal and opposite to the momentum of the recoiling nucleus.

This is not observed. Instead electrons are emitted with a continuous distribution of energies smaller than some maximum total energy E_{max}. The electron does not

Figure 7.1

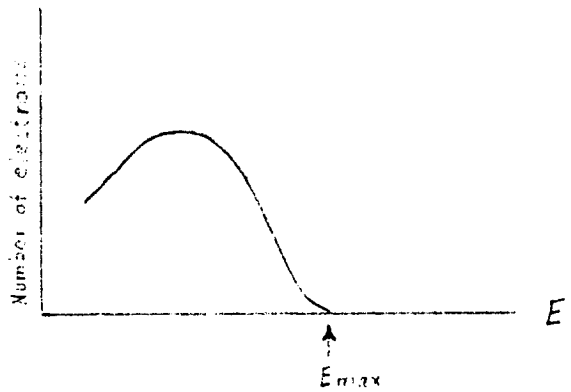

always leave in the opposite direction from the recoil nucleus. Furthermore, angular momentum is not conserved if we consider only the two body nucleus-electron problem. For example, the beta decay of ${}_6C^{14}$ into ${}_7N^{14}$ has been observed, and the nuclear spin of ${}_6C^{14}$ has been measured

as 0, that of $_7N^{14}$, as 1. For the transition, the change in nuclear angular momentum is $\Delta J = 1$, an integral amount. The electron, a fermion, has spin ½, and conservation of angular momentum is apparently violated.

Pauli proposed the neutrino hypothesis, developed largely by Fermi, which effectively resolves these grave difficulties. The neutrino hypothesis assumes the existence of a neutral particle of small mass and half integral spin emitted simultaneously with the observed beta particle. Beta decay is then a three body problem instead of two, and the three particles share the energy, momentum, and angular momentum available from the nuclear transition. The maximum momentum exhibited by the recoil nucleus is in accord with the momentum calculated under the assumption that an electron of energy E_{max} is emitted in the opposite direction. Thus the beta particle gets its maximum energy E_{max} when the neutrino is emitted with zero momentum (hence zero kinetic energy), in effect returning to our dynamical two body problem, which has a unique solution in classical mechanics.

Conservation of energy requires that the difference between the maximum energy E_{max} of the beta particle and the total available energy E_o of the nuclear transition

gives a value for the rest energy $m_\nu c^2$ of the neutrino. Experiments have put an upper limit of 25 kev on the rest mass of the neutrino, zero within experimental error, and it is demanding theoretically that the neutrino rest mass be identically zero. Conservation of angular momentum can be achieved by assigning some half-integral spin to the neutrino, but calculations carried out with neutrino spin $3/2\ \hbar$ do not give the observed shape of the beta ray spectrum; so a neutrino spin $1/2\ \hbar$ is most attractive. This makes the neutrino a zero rest mass fermion, analagous to the photon which is a zero rest mass boson. Being a fermion, the neutrino should have an antiparticle - the antineutrino. The estimated cross section for neutrino induced beta decay is extremely small, $\sim 10^{-44}$ cm^2, and so experimental detection is difficult. Nevertheless, Reines and Cowan (1953) were able to detect antineutrinos from the beta decay of fission fragments in a nuclear reactor.[1] A significant negative experiment bearing on the distinctness of the neutrino and antineutrino was carried out by Davis who showed that

$$Cl^{37} + \bar{\nu} \rightarrow A^{37} + e^- \qquad (7.1)$$

does not occur, but he expects to see

$$Cl^{37} + \nu \rightarrow A^{37} + e^{-} \qquad (7.2)$$

using neutrinos from the sun using a 100,000 gallon tank of tetrachlorethylene (C_2Cl_4, a common cleaning fluid) deep in a South Dakota mine, thus establishing experimentally the existence of the neutrino itself. In addition to the neutrinos and antineutrinos associated with electrons, there appear to be distinct neutrinos and antineutrinos associated with muons, making four altogether. Because of the neutrino's phenomenal penetrating ability (mean free path about a light year in solid lead), massive detection systems coupled with sensitive coincidence circuitry are being assembled to scan the universe as the new field of neutrino astronomy takes form. The neutrino has come a long way since Pauli.

The Neutrino Hypothesis and the Shape of the Beta Spectrum.

Selection Rules for Allowed Transitions

Suppose as a typical case we have a nucleus in which a neutron is converted into a proton and an electron and an

antineutrino is emitted:

$$n \rightarrow p + e^- + \bar{\nu} \qquad (7.3)$$

We wish to predict the shape of the energy spectrum of the emitted electrons which we can compare with experiment. We shall first make the simplifying assumptions that the Coulomb interaction between electron and residual nucleus can be neglected and that the recoil energy of the nucleus can be neglected. The latter approximation is a good one since the mass of the nucleus is always much larger than the electron mass, but the neglect of Coulomb interaction is reasonable only for the lightest nuclei ($Z \lesssim 10$) and sufficiently high electron energies.

We begin, as Fermi did, by using a simple phase space argument, assuming all possible divisions of energy between neutrino and electron are equally likely. Consider the phase space for the two particles, electrons and neutrino. Not all of this phase space is accessible since the sum of the energies is constrained by the law of conservation of energy

$$E_e + E_\nu = E_o \qquad (7.4)$$

We postulate that the probability of a disintegration leading to a specified accessible volume of phase space is directly proportional to that volume. After the disintegration, the electron is contained in the volume element dV_e and has a momentum with magnitude between p_e and $p_e + dp_e$ in a direction within the solid angle element $d\Omega_e$. Similar statements hold for the neutrino, denoted with the subscript ν instead of e. We express the volume of this state in six dimensional phase space in its natural units, $h^6 = (2\pi\hbar)^6$. This gives volume in phase space =

$$(2\pi\hbar)^{-6} \; (p_e{}^2 dp_e d\Omega_e dV_e) \; (p_\nu{}^2 dp_\nu d\Omega_\nu dV_\nu) \qquad (7.5)$$

Now (7.4) states, if we hold electron momentum (and energy) constant, that we can write

$$dE_o = dE_\nu \qquad (7.6)$$

and if we assume a zero rest mass for the neutrino (we shall return to this point later), we can write also

$$E_\nu{}^2 = p_\nu{}^2 c^2 \qquad (7.7)$$

so that

$$E_\nu dE_\nu = E_\nu dE_o = p_\nu c^2 dp_\nu \qquad (7.8)$$

Now we can write the neutrino momentum as

$$dp_\nu = \left(\frac{\partial p_\nu}{\partial E_o}\right)_{p_e} dE_o = \frac{E_\nu}{c^2 p_\nu} dE_o \qquad (7.9)$$

where the subscript p_e means electron momentum is kept constant during the differentiation. With (7.9), and using (7.4) and (7.7),

$$p_\nu^2 dp_\nu = \frac{E_\nu}{c^2} p_\nu dE_o = \frac{E_\nu^2}{c^3} dE_o = \frac{(E_o-E_e)^2}{c^3} dE_o \qquad (7.10)$$

With (7.10), the phase space volume (7.5) assumes the form $\rho(E_o)dE_o$, where $\rho(E_o)$ is the density of final states per unit range of total energy familiar from perturbation theory and we can write

$$\rho(E_o) = (2\pi\hbar)^{-6} c^{-3} (E_o-E_e)^2 p_e^2 dp_e d\Omega_e dV_e d\Omega_\nu dV_\nu \qquad (7.11)$$

According to our assumptions, $\rho(E_o)$ is proportional to the probability that the beta-decay leads to this particular final state.

Equation (7.11) predicts that the emission of the electron and the neutrino into all directions is equally

likely; in particular there is no angular correlation between the directions of emission of the two particles. And, if we imagine that the whole system is enclosed within a large box of volume V, we are equally likely to find the electron and neutrino in any region of the box. These statements result from the extreme simplifications used so far and will be modified later.

Since we are not interested just now in the position of the emitted particles within our imaginary box, we integrate over dV_e and dV_ν. We shall also not be concerned with the absolute direction of emission of the electron, but only with possible angular correlations between electron and neutrino. We therefore measure the neutrino directions with respect to the direction of the electron, that is, replace $d\Omega_\nu$ by $d\Omega_{e\nu}$, where $\theta_{e\nu}$ is the angle between the electron and neutrino momenta. Integrating over the angles for the electrons gives the final phase space factor

$$\rho(E_o) = \frac{V^2}{16\pi^5\hbar^6c^3} \; p_e^2(E_o-E_e)^2 dp_e d\Omega_{e\nu} \qquad (7.12)$$

If the direction of the neutrino (or, more practically, the direction of the nuclear recoil) is not observed in the experiment, we must integrate over $d\Omega_{e\nu}$ also, which

gives an additional factor of 4π. The appearance of the volume V is purely formal, and will drop out later.

The main result contained in (7.12) is the desired shape of the beta-spectrum. The distribution-in-momentum of the emitted electrons is given by

$$P(p_e)dp_e = Cp_e^2(E_o-E_e)^2dp_e \qquad (7.13)$$

where C is a constant. For small momenta, $E_e \ll E_o$, and this distribution is proportional to p_e^2; for large momenta, $E_e \sim E_o$, it is proportional to $(E_o-E_e)^2$. It vanishes at both limits and has a maximum in the middle somewhere. Such a curve is shown in figure 2. Note that figure 2 does resemble the experimental curve in figure 1. Equation (7.13) is the basis for a method of analysis of beta ray spectra to determine end points, called the method of Kurie plots. In making a Kurie diagram, one takes data from a measured beta spectrum and plots the expression $[P(p_e)/p_e^2c]^{1/2}$, where $P(p_e)$ is a measured quantity, versus E_e. Motivation for this selection is easily seen by writing (7.13) as

$$[P(p_e)/p_e^2C]^{1/2} = (E_o-E_e) \qquad (7.14)$$

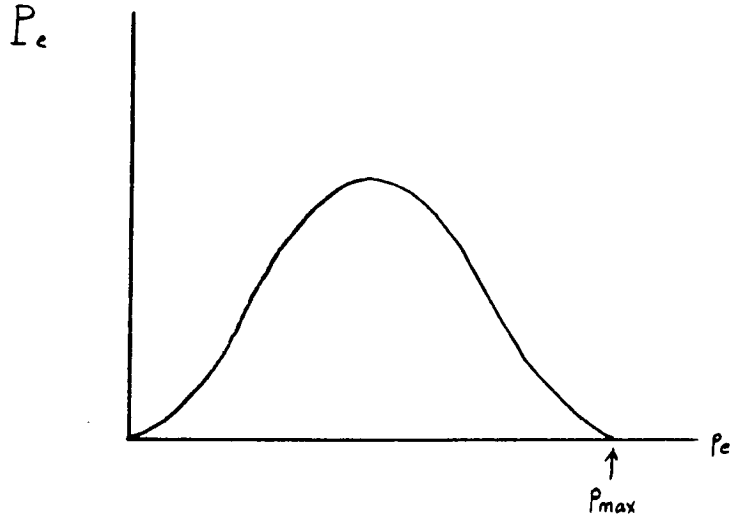

Figure 7.2

This should yield a straight line, in our first approximation, with intercept E_o, the end point of the spectrum. This method was long used to determine all the beta decay end points, and in fact it is by determining how well the measured spectrum goes <u>linearly</u> to zero on the Kurie diagram that one may determine upper limits on the neutrino mass. One can see that if the plot did not go linearly down to the axis, but instead curled over and fell short as shown in figure 3, one would conclude that a portion of the total energy available in the beta decay was being taken up in the finite rest mass of the neutrino. We have assumed, of course, that only one neutrino is emitted.

Even though we have predicted the rough features of beta ray spectra with the neutrino hypothesis and our simple phase space argument, before comparing our results for the detailed spectrum with experiment, we

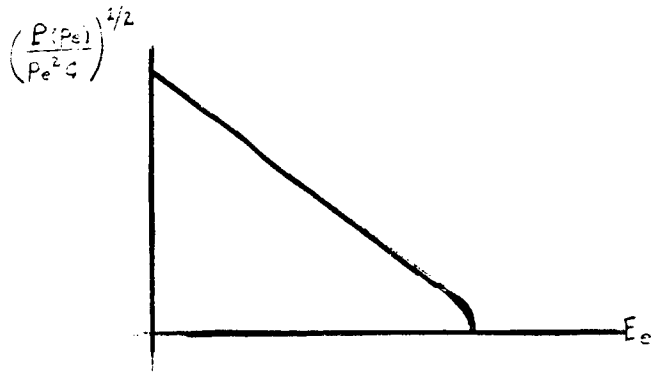

Figure 3

must include the effect of the Coulomb force between the beta particle and the daughter nucleus.

We shall assume that the decay probability is a product of four factors:

1) The a priori probability, $\rho(E_o)$, in equation (7.12).

2) The probability of finding the electron within the nuclear volume, i.e., $\int|\psi_e|^2 dV_e$ extended over the interior of the nucleus.

3) The probability of finding the neutrino within the nuclear volume, i.e., $\int|\psi_\nu|^2 dV_\nu$ over the interior of the nucleus.

4) A specifically nuclear factor which we will describe as the nuclear matrix element which governs the rate of the beta decay.

We can understand the need for factors (2) and (3) by considering the inverse process where an electron and neutrino are put into a box of volume V together with

the decay product nucleus Y. The rate of the inverse beta-decay, $Y+e+\nu = X$, is proportional to the probability of having Y interact with e and ν at the same time. Hence the factors (2) and (3) follow for the inverse beta-decay if we assume that the interactions involved are essentially point interactions. Since the beta-decay and the inverse beta-decay are related by the general reciprocity law for inverse processes, we can conclude that factors (2) and (3) apply also to the beta decay itself.

Now consider the orbital angular momenta ℓ_e and ℓ_ν which the electron and the neutrino may have after emission from the nucleus. For the energies we are considering, the wavelengths of the electron and the neutrino will be much larger than the nuclear radius and so we can write approximately

$$\int_{\substack{\text{nuclear}\\ \text{interior}}} |\psi_e|^2 dV_e \approx |\psi_e(o)|^2 V_N \tag{7.15}$$

and

$$\int_{\substack{\text{nuclear}\\ \text{interior}}} |\psi_\nu|^2 dV_\nu \approx |\psi_\nu(o)|^2 V_N \tag{7.16}$$

where V_N is the nuclear volume and $\psi(o)$ is the wave function evaluated at the center of the nucleus. The wave function ψ_e for a free electron of wave number $K_e = p_e/\hbar$ emitted with orbital angular momentum ℓ_e, can be written

$$\psi_e \propto (K_e r_e)^{-\frac{1}{2}} J_{\ell_e+1} (K_e r_e) \qquad (7.17)$$

where J is a Bessel function. The wave function ψ_e for the first few values of ℓ_e looks something like figure 4 where r_e is the distance of the electron from the nuclear center. We see that $\psi_e(o)$ vanishes except for S wave electrons, those emitted with zero orbital angular momentum. The same consideration holds for the neutrino. We conclude therefore that the electron and neutrino are emitted only with zero orbital angular momentum as long as the approximations which we have introduced are valid. This rule is in agreement with the intuitive notion that the emitted electron must appear to come from the emitting nucleus. Zero orbital angular momentum means zero impact parameter, i.e., an electron direction straight away from the center

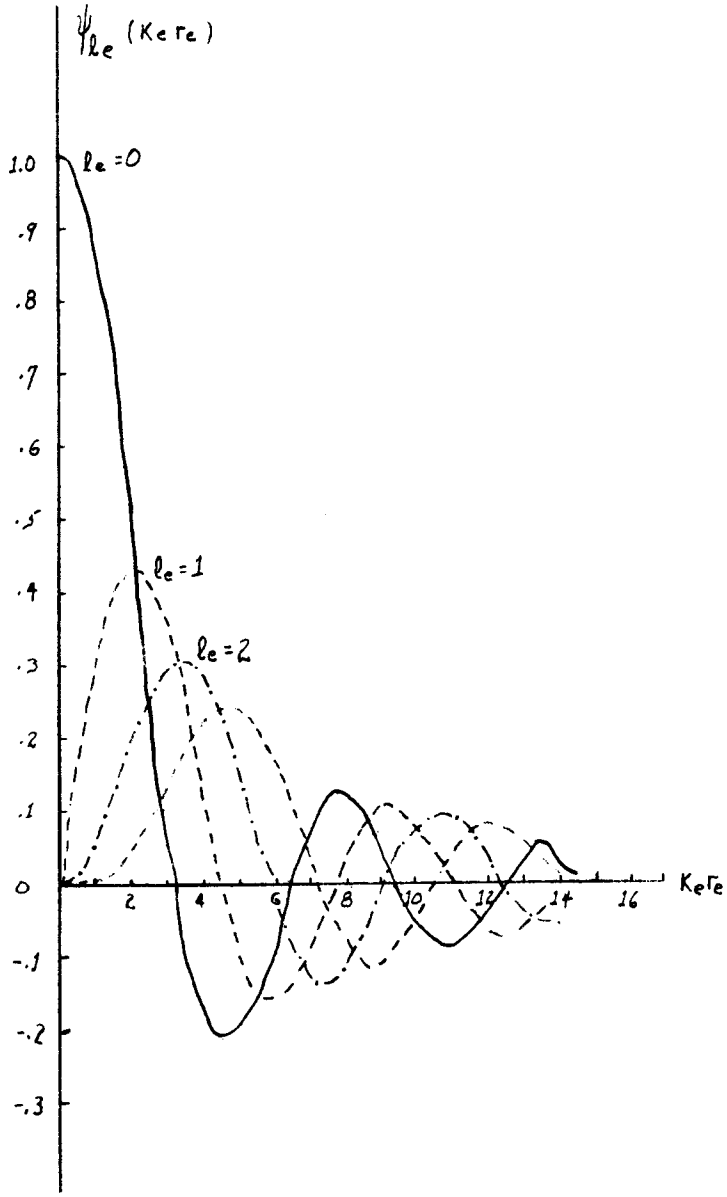
$\psi_{\ell_e}(K_e r_e)$
$\ell_e = 0$
$\ell_e = 1$
$\ell_e = 2$
1.0
.9
.8
.7
.6
.5
.4
.3
.2
.1
0
-.1
-.2
-.3
2
4
6
8
10
12
14
16
$K_e r_e$

Figure 7.4

of the emitting nucleus. This statement is subject, of course, to the qualifications imposed by the Heisenberg uncertainty principle.

Of course the average values of $|\psi_e(r)|^2$ and $|\psi_\nu(r)|^2$ are not exactly equal to their respective values at $r = 0$, and an emission of the light particles with an orbital angular momentum different from zero is possible, although its probability is relatively much smaller. We shall call "allowed transitions" the transitions in which the electron and neutrino are emitted with zero orbital angular momentum, and "forbidden transitions" the relatively weaker ones in which the particles are emitted with an orbital angular momentum different from zero.

Now consider the intrinsic spin of the emitted particles. Both have a spin ½. These two spins can combine to a total intrinsic spin 0 (the singlet case) or 1 (the triplet case).

If electron and neutrino are emitted in the singlet spin state, the only angular momentum carried away by the two light particles is the orbital angular momentum, and that is zero for allowed transitions. Hence the angular momentum of the daughter nucleus must equal the angular

momentum of the parent nucleus. Furthermore, since both the electron and the neutrino are emitted in S states ($\ell = 0$), and S states have even parity, there cannot be any change in the parity of the nuclear wave functions. We therefore get for the case of singlet emission, the Fermi selection rules for allowed transitions:

$$\Delta J = 0; \text{ no change of parity} \tag{7.18}$$

(We have previously discussed the nonconservation of parity in weak interactions, but in the present context it is still useful to consider parity in this way because we are talking not about the relative parity of the electron and the neutrino between themselves, but rather with the parity of the nuclear state to which they are linked; so in this simple approach we say the spins of the two nuclei are the same and that there is no parity change.)

If the electron and neutrino are emitted in the triplet spin state, that is, with parallel spins, we obtain a different selection rule. No orbital angular momentum is involved in allowed transitions; so the total angular momentum carried away by the two particles is just their spin angular momentum which is now unity. Since the parity

operation does not involve the spins, the parity selection rule is as before. The selection rule for triplet emission, the Gamow-Teller selection rule for allowed transitions is

$$\Delta J = \pm 1 \text{ or } 0 \text{ (except no } 0 \rightarrow 0 \text{ transitions); no change of parity} \qquad (7.19)$$

Since the spin change is a vector spin change we surely could not start with a zero nuclear spin, emit one unit of spin angular momentum, end with a nuclear spin zero, and conserve angular momentum.

The selection rules (7.18) and (7.19) were made using a nonrelativistic treatment of the electron and neutrino, but of course the neutrino is always relativistic. It turns out, however, that (7.18) and (7.19) correspond to the selection rules which actually come out when one makes a proper relativistic analysis of the situation.

If we have the case where the nuclear spin does not change, nor the nuclear parity, and the nuclear spins are not zero then both the Fermi and Gamow-Teller selection rules can apply and we can have a contribution to the beta decay of both singlet and triplet states and the contributions must somehow be untangled. Conversely, the transitions

which do not fulfill the conditions for either the singlet or triplet states involve the emission of a light particle with an orbital angular momentum different from zero. They are therefore forbidden in some degree, and it is expected that, other things being equal, allowed beta decays have larger transition probabilities than forbidden decays. This fact can be used to attempt an experimental decision between the two possibilities.

We now turn to the influence of the factors (2) and (3) on the shape of the beta spectrum for allowed transitions. First, we show that these two factors have no influence on the spectrum shape as long as the Coulomb force between the electron and the product nucleus can be neglected. Imagine that the electron is confined within a box of volume V. Then

$$\int |\psi_e|^2 dV_e \cong |\psi_e(o)|^2 V_N = \frac{V_N}{V} \qquad (7.20)$$

which is an energy independent factor. We put $|\psi_e(o)|^2 = \frac{1}{V}$ assuming the probability of finding the electron in the center of the box is the same as finding it anywhere else inside the box. There is a similar argument for the neutrino. We get then two factors V^{-1} and so the

v^2 in (7.12) drops out as one would expect. Since the factors obtained from (2) and (3) are energy independent, the spectrum shape is completely determined by the statistical factor $\rho(E_o)$ in equation (7.13).

If we take the Coulomb force on the escaping electron into account, then the quantity $|\psi_e(o)|^2$ becomes energy dependent. We can get an approximate expression for the Coulomb correction to the spectrum shape by treating the electron nonrelativistically. Using the result of typical non-relativistic Coulomb wave function calculations for this, such as that given by Yost, Wheeler, and Breit, Physical Review, 49, 174, (1936), we get

$$F(Z,E) = \frac{|\psi_e(o)|^2_{coulomb}}{|\psi_e(o)|^2} = \frac{2\pi\eta}{1 - \exp(-2\pi\eta)} \tag{7.21}$$

where the parameter $\eta = Ze^2/\hbar v$ for electrons, $\eta = -Ze^2/\hbar v$ for v for positrons, v being the speed of the beta particle outside the Coulomb field (that is, at large distances), and Z, the atomic number of the product nucleus formed as a result of the beta decay. Let us consider some properties of the Coulomb correction factor or Fermi function F(Z,E). If v is small, then η is large,

and for electrons, the exponential in the denominator is negligible, so that F becomes large compared to unity. If instead v is large, η is small, and expanding the exponential, F approaches unity. So for large velocities (corresponding to high energies) of the emitted electrons, the Coulomb force loses its effect on the spectrum shape and the spectrum approaches that computed without the Coulomb corrections. For positrons, the limits are the other way around. This means that since the F is a factor multiplying the probability of decay, the Fermi function enhances the probability of electron emission and decreases the probability of positron emission, especially at low energies. For both positrons and electrons at high energies the Coulomb force loses its effect on the spectrum shape.

The behavior of the spectrum at very low electron or positron energies can be obtained directly from (7.13) and (7.21). For no Coulomb force, the distribution in momentum is proportional to p^2. For electron emission with low momentum p the Coulomb correction factor F(Z,E) becomes inversely proportional to the electron momentum. Hence the electron distribution in momentum is proportional

to p rather than to p^2 for energies low enough so that $2\pi\eta >> 1$. For positron emission, F(Z,E) becomes proportional to $p^{-1}\exp(-c/p)$ where c is a constant. Hence the distribution-in-momentum of low energy positrons is proportional to $p^{-1}\exp(-c/p)$ and so drops to zero very rapidly. These results are depicted schematically in figure 7.5.

Sometimes one prefers to look at the distribution-in-energy rather than the distribution-in-momentum. Since

$$c^2 pdp = EdE, \tag{7.22}$$

the former distribution is obtained from the latter by multiplication by E/pc^2. In particular, at energies close to the rest energy $m_e c^2$ the energy spectrum for no Coulomb field is proportional to p. If the Coulomb field is taken into account, the energy spectrum at low energies approaches a constant finite value for electrons and it is proportional to exp(-c/p) for positrons. (figure 7.6)

The Coulomb effect can be understood qualitatively in the following way: the energy distribution for positive

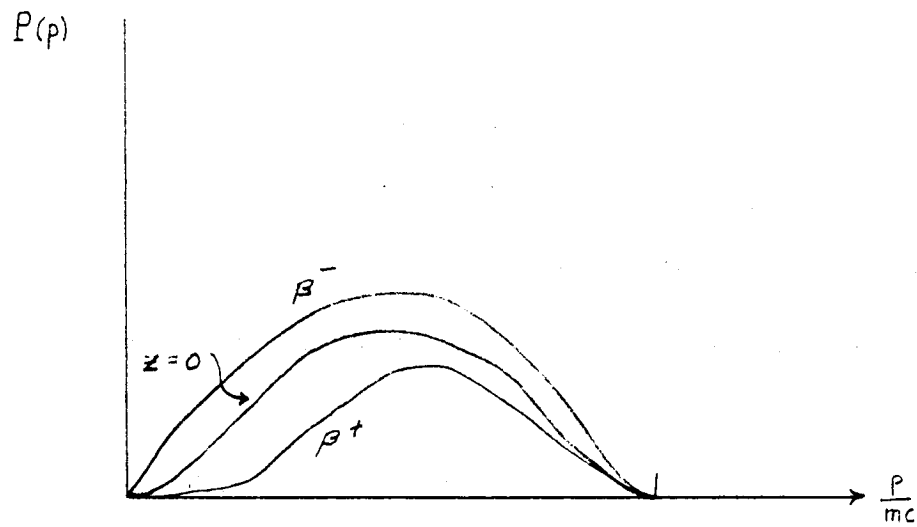

Figure 7.5

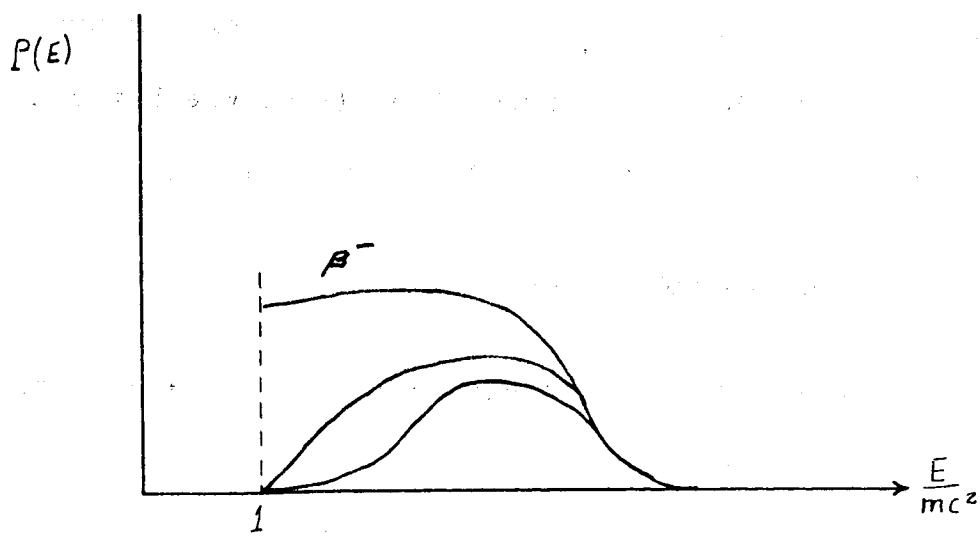

Figure 7.6

and negative electrons is the same at the moment of leaving the nucleus. The Coulomb field accelerates the positive electrons and decelerates the negatrons. Hence the positron spectrum has fewer slow particles and the negatron spectrum has more than they would have in absence of the Coulomb effect.

Better results require a proper relativistic calculation of F(Z,E) and still more accuracy requires allowance for the screening of the field of the residual nucleus by the atomic electrons, [3]

Kurie plots of $[P(p)/F(Z,E)p^2]^{\frac{1}{2}}$ versus E, where F here has the proper relativistic form plus shielding corrections are used widely by experimentalists both to determine end points E_o and to test whether a measured beta ray spectrum has the allowed shape (i.e. whether the experimental points fall on a straight line).

Orbital Electron Capture

Since the nucleus of any atom, radioactive or not, is always surrounded by orbital electrons under laboratory conditions, a nucleus unstable against positron decay can instead capture one of its orbital electrons.

In general, the probability of orbital electron capture depends not only on the properties of the nucleus, but also on the properties of the electron cloud surrounding the nucleus, and so the same nuclear transformation occurs with different decay probabilities if the nucleus is surrounded by somewhat different electron clouds (for example by being part of different molecules).

We can take over some of the statistical considerations for orbital electron capture which were used above. The statistical factor is different now, though, since the electron is in a quite definite quantum state before its capture, and the phase space volume is therefore determined entirely by the energy of the emitted neutrino. This volume is equal to

$$(2\pi\hbar)^{-3} p_\nu^{\ 2} dp_\nu d\Omega_\nu dV_\nu \equiv \rho'(E_\nu) dE_\nu \qquad (7.23)$$

As before, we get the statistical factor $\rho(E_\nu)$ from $\rho'(E_\nu)$ by integrating over all the possible positions inside the box, i.e., over dV_ν. Since the neutrino is always emitted in a direction opposite that of the nuclear recoil, there is no question of angular correlation here, and we can integrate over the angles $d\Omega_\nu$ also. We have

now

$$p(E_\nu)dE_\nu = \frac{V}{2\pi^2\hbar^3} p_\nu^2 dp_\nu \tag{7.24}$$

and since $$E_o + m_e c^2 = E_\nu + E_B \tag{7.25}$$

where E_B is the binding energy of the captured electron,

$$dE_o = dE_\nu \tag{7.26}$$

and $$E_\nu = (E_o + m_e c^2 - E_B) \tag{7.27}$$

If we take the rest mass of the neutrino to be zero as before,

$$c^2 p_\nu dp_\nu = E_\nu dE_\nu = E_\nu dE_o \tag{7.28}$$

and

$$\rho(E_\nu)dE_o = \frac{V}{2\pi^2\hbar^3} \frac{1}{c^2} p_\nu E_\nu dE_o \tag{7.29}$$

$$= \frac{V}{2\pi^2\hbar^3} \frac{E_\nu^2}{c^3} dE_o \tag{7.30}$$

$$\rho(E_\nu) = \frac{V}{2\pi^2\hbar^3 c^3} (E_o + m_e c^2 - E_B)^2 \tag{7.31}$$

Again we shall assume that the decay probability is given by the four factors previously discussed. Factor

(1) is given by (7.31) for electron capture, and for simplicity we restrict ourselves here to allowed electron capture transitions. Then the probability of finding the neutrino inside the nuclear volume [our factor (3)] is equal to V_N/V as before, but the probability of finding the electron inside the nuclear volume [factor (2)] is completely different, no longer proportional to 1/V. The electron before capture is bound to the nucleus, hence the probability of finding it inside the nuclear volume is independent of the size of the box in which the system is imagined to be enclosed. The probability depends on the electron state: it is small for electrons in outlying orbits, and comparatively large for electrons in the inner shells of the atomic structure. By far the largest proportion of the total electron capture is due to the capture of electrons from the innermost shell in the atom, the K shell. If we neglect relativistic corrections, the probability of finding the K electron inside the nuclear volume is the ratio of this volume, V_N, to the volume enclosed by the first Bohr orbit:

$$\int |\psi_e|^2 dV_e \cong \frac{1}{\pi} \left(\frac{Zme^2}{\hbar^2}\right)^3 V_N \qquad (7.32)$$

This probability must be multiplied by two because there are two electrons in the K shell, both of which are equally likely to be captured by the nucleus.

We choose to write the K capture probability in the form

$$\text{capture probability} = \frac{\ln 2}{t_K} = Cf_K \qquad (7.33)$$

where t_K is the half-life of the radioactive nucleus if K capture is the only mechanism by which it can disintegrate, i.e., if the energy E_o liberated by the nuclear transition lies between the limits

$$-(mc^2 - E_B) < E_o < mc^2 \qquad (7.34)$$

and this factor f_K will be defined so that the constant C is the same as it would be for the electron emission case,

$$C = \frac{V_N{}^2}{4\pi 4\hbar^6 c^3} \qquad (7.35)$$

The K shell binding energy is

$$E_B = \frac{1}{2}\left(\frac{Ze^2}{\hbar c}\right)^2 \qquad (7.36)$$

in the nonrelativistic approximation. We find then that

$$f_K = \frac{1}{c}\cdot 2 \int_{\text{nucleus}} |\psi_e|^2 dV_e \int_{\text{nucleus}} |\psi_\nu|^2 dV_\nu \cdot P(E_\nu) \qquad (7.37)$$

$$= \frac{4n^4\hbar^6c^3}{V_N^2}\,\frac{2}{\pi}\left(\frac{Ze^2}{\hbar^2c^2}\right)\frac{V_N^2}{V}\;\frac{V}{2\pi^2\hbar^3c^3}\left[E_o+1-\frac{1}{2}\left(\frac{Ze^2}{\hbar c}\right)^2\right]^2 \qquad (7.38)$$

$$= 4\pi\left(\frac{Ze^2}{\hbar c}\right)^3\left[E_o + 1 - \frac{1}{2}\left(\frac{Ze^2}{\hbar c}\right)^2\right]^2 \qquad (7.39)$$

where the energies E_o and E_B are measured in units m_ec^2. Since the spin directions of electron and neutrino are not observed in practice, the phase space factor must be multiplied by the statistical weights of the final states. This statistical weight is 2 for electron capture (emission of one particle of spin ½), but 4 for ordinary beta decay because both an electron and a neutrino are emitted and because of this difference in the statistical weights, we choose to homogenize the definitions of the small f_K's for the two cases, capture and emission, by dividing (7.39) by 2 to give

$$f_K = (2\pi)\left(\frac{Ze^2}{\hbar c}\right)^3\left[E_o + 1 - \frac{1}{2}\left(\frac{Ze^2}{\hbar c}\right)^2\right]^2 \qquad (7.40)$$

It should be emphasized that the Z used in these equations is the Z which interacts with the electron and so the Z

for electron capture is different from that for the emission case because for capture, the interaction is with the parent rather than the product nucleus.

To find a better value for f_K, corrections for relativistic effects and for nuclear shielding by the atomic electrons must be taken into account[4].

Half-Lives of Beta Emitters

What we have found before can be expressed by

$$P(p) = CF(Z,E)p^2(E_o-E)^2dp \qquad (7.41)$$

which gives the momentum spectrum of the beta-particles in allowed transitions. We may obtain the total probability per unit time that a beta-active nucleus will decay by integrating $P(p)dp$ over all electron momenta in the beta spectrum. This probability also defines the half-life t_- for the decay:

$$\beta^- \text{ decay probability} = \frac{\ln 2}{t_-} = Cf_-(Z,E_o) \qquad (7.42)$$

where

$$f_-(Z,E_o) = \int_o^{p_o} F(Z,E)p^2(E_o-E)^2\,dp \qquad (7.43)$$

with $p_o = (E_o^2 - 1)^{\frac{1}{2}}$, the maximum momentum in the spectrum, in units of mc. For arbitrary Z, the integral must be evaluated numerically, but for Z=0, an explicit evaluation is possible. (This amounts to making the crude approximation that the Coulomb interaction can be neglected.) The result is

$$f_-(0,E_o) = \frac{1}{60}(E_o^2 - 1)^{\frac{1}{2}}(2E_o^4 - 9E_o^2 - 8) + \frac{1}{4}E_o \ln\left[E_o + (E_o^2 - 1)^{\frac{1}{2}}\right] \tag{7.44}$$

If E_o is very large, f_- is proportional to E_o^5. But in the energy region of interest, $1.1 \leq E_o \leq 10$, the dependence on E_o is less strong and more complicated. It turns out, however, that this E_o^5 (strong dependence of the lifetime on the endpoint energy) feature remains if one considers more complicated expressions with $Z \neq 0$, which is necessary, since in most cases the Coulomb effects on the lifetime cannot be ignored.

For positron decay, the story is similar, and we write

$$\beta+ \text{ decay probability} = \frac{\ln 2}{t_+} = Cf_+(Z,E_o) \tag{7.45}$$

where f_+ is the same integral as in (7.43), except that

the Coulomb correction factor is the one appropriate to positron emission ($\eta = -Ze^2/\hbar v$). It is found that f_+ has a similar E_o^5 dependence for large end point energies. But whenever positron emission is energetically possible, K capture also occurs and shortens the half-life, so the observed half life of a positron emitter is not equal to the t_+ in (7.45).

The factors f_-, f_+, and f_K depend on the conditions outside the nucleus since they are determined by phase space considerations and by the effect of the Coulomb field on the electron. Hence the strictly nuclear properties are folded into the coefficient C which has the dimensions of an inverse time. It is useful to define the "comparative half-life" of a simple beta-transition, ft, by

$$ft \equiv \begin{cases} f_-(Z,E_o)t & \text{(for } \beta^- \text{ decay)} \\ [f_+(Z,E_o)+f_K(Z,E_o)]t & \text{(for } \beta^+ \text{ decay)} \\ f_K(Z,E_o)t & \text{(for K capture without } \beta^+ \text{ decay)} \end{cases} \qquad (7.46)$$

where t is the half-life of the transition measured in

seconds. (Recall that the positron emitted in positron decay will eventually be annihilated with a negatron with the liberation of $2m_e c^2$ of energy in the form of photons; therefore the beta decay end point must be at least 1.02 MeV or $2m_e c^2$ before positron emission is possible, otherwise the only possible transition would be K capture alone.) The quantity ft is then what we call the comparative half-life, and if we have an allowed spectrum shape then we have the basic relation

$$ft = \frac{\ln 2}{C} \qquad (7.47)$$

What is the observed frequency distribution for comparative half-lives? A crude representation is shown in Figure 7. We see that there seems to be a definite grouping of decays around 3.5, then many cases around log ft=5, and another, poorly defined, rise around 6 or 7, after which the curve drops rapidly. The small number of decays for large values of ft corresponds to the fact that these decays are highly forbidden, usually involving large spin changes, and that there are not many cases available for measurement in nature. This is because nature seems to make unusual amounts of energy available for the decay

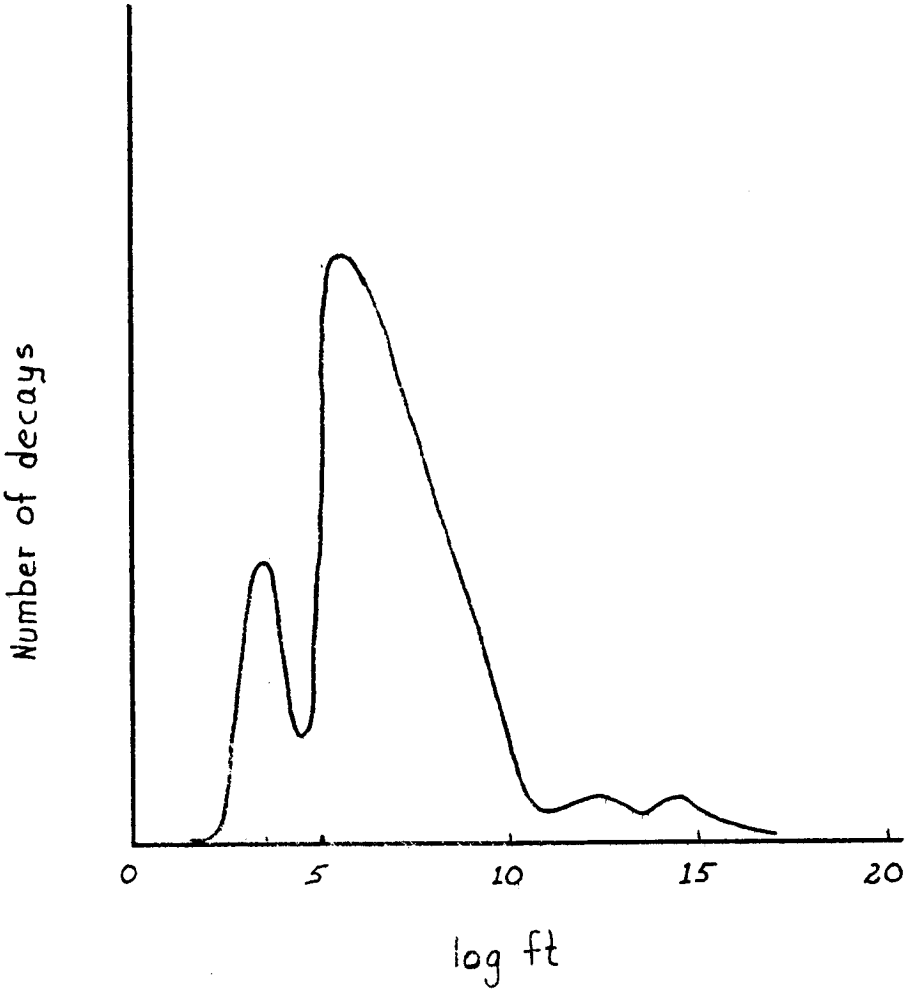

Figure 7.7

Frequency distribution of comparitive half lives.

in such cases, enough energy so that the beta decay goes through an excited state involving a smaller spin, and most of the observed transitions in the complex decay are then associated with the second (smaller spin change) branch. The cluster around 3.5 corresponds to what are called superallowed transitions, the weak grouping around 5 and 6, to allowed transitions, and the weak grouping around 6 or 7 to 8, to first forbidden transitions.

These superallowed transitions are just allowed transitions for which the nuclear matrix element [(4) in the previous list of factors] is particularly large. Most are in very light nuclei where the nuclear states have a particularly simple structure. Clearly the superallowed transitions obey the same selection rules as we found for the allowed transitions, (7.18) and (7.19), summarized as

$$\text{(Allowed)} \quad \Delta J = 0, \pm 1; \; N_0 \tag{7.48}$$

When one does the proper relativistic calculations, the rule (7.48) survives, but we can no longer distinguish Fermi and Gamow-Teller selection rules.

What, now, can we say about selection rules for the

forbidden transitions? First forbidden transitions presumably involve the emission of the electron-neutrino combination with one unit of orbital angular momentum, not zero units as we had for allowed transitions. The spins of the electron-neutrino combination can combine to give 0 or $\pm$ 1, and so the total angular momentum change for first forbidden transitions can be 0, ± 1, or ± 2 units of $\hbar$. What about the relative parities of initial and final nuclei? Since one unit of orbital angular momentum is carried away, we say there must be a parity change. So the selection rules are

$$\text{(first forbidden)} \quad \Delta J = 0, \pm 1, \pm 2; \quad \text{Yes.} \qquad (7.49)$$

For second forbidden transitions, the orbital angular momentum carried away by the light particles is two units of $\hbar$, and so the total angular momentum change can be ± 1, ± 2, ± 3, and since an orbital angular momentum of two is associated with positive parity, the selection rules are

$$\text{(second forbidden)} \quad \Delta J = \pm 1, \pm 2, \pm 3; \quad \text{No.} \qquad (7.50)$$

one can extend this treatment in the obvious way.

In the early stages of development of the subject, it was thought that the value ft for a transition was a good indication of the degree of forbiddenness, but as data accumulated, it became apparent that the ft value was not an entirely reliable guide. One can make the generalization, however, that if the transition is, for example, first forbidden, ft must be 6 at very least, but it is not true that an ft value 6 or larger makes the transition forbidden: there are some cases of allowed transitions with ft $\geq$ 6. This spread is linked to the vagaries of the individual nuclear matrix elements which connect initial and final nuclear states. In general, the more complicated the matrix element, the smaller one would expect the overlap integral connecting the initial and final states of the nucleus to be. Still, it is sometimes useful to utilize the crude classification of degrees of forbiddenness according to ft values in dealing with excited nuclear states in nuclear astrophysical applications. We give the approximate values as

Superallowed	ft $\sim$ 3.5	
Allowed	$\sim$ 5-6	Table 1
First forbidden	$\sim$ 6-7	
Second forbidden	$\sim$ 8-12	

The Nuclear Matrix Element

A thorough treatment of the nuclear matrix element would require a discussion of the Dirac equation to an extent unwarranted here. We content ourselves with noting some of the forms that the expressions take. The probability per unit time for the beta transition can be written as

$$P = \frac{2\pi}{\hbar}|H'_{if}|\rho(E) \qquad (7.51)$$

where H'_{if} is the matrix element of the interaction responsible for the transition, and $\rho(E)$ density of final states, the number of final states of the "emitted particle" per unit range of energy. The formalism of the theory of beta decay was originally written down by Fermi, in complete analogy to the Dirac theory of the emission of light; a photon in Dirac's theory is the electron-neutrino system in Fermi's theory.

A quantity conserved in beta decay which we have not mentioned previously is lepton number. Both electrons and

neutrinos are classified as leptons, or light particles. If we create a negative electron (lepton number +1), we create an antineutrino (-1) to accompany it so the lepton number does not change in the transition. Similarly, if we emit a positron (-1), we also emit a neutrino (+1) and again the lepton number on both sides of the transformation equation is the same. So we are thinking then of emitting this combination with a total lepton number zero as analogous to the emission of a photon in atomic physics.

In the case of photon emission we have an interaction or perturbation Hamiltonian matrix element

$$H'_{if} = \int \psi_f^* H' \psi_i d\tau = \int \psi_f^* (\text{electric moment}) \psi_i d\tau \qquad (7.52)$$

where the H' is the perturbing term in the total Hamiltonian for the system. For light photon emission, the total Hamiltonian consists of the energy of the electrons which form the initial and final states of this system, plus the energy of the free electromagnetic field, and the interaction energy between the field and electrons, H'. Because the interaction energy is small, perturbation

methods of quantum mechanics are especially appropriate. This is even more true in the case of the weak interaction governing beta decay because the weak interaction is only about 10^{-20} times as strong as the electromagnetic interaction.

We might ascribe many different properties to the interaction operator, but whatever else it does, it surely must change the charge of the nucleon involved in the decay process, that is, converting a neutron into a proton or vice-versa. Let us denote the charge exchange operator by Q. In Fermi's original form of the theory, this charge exchange was the main effect of the perturbation so that

$$H'_{if} = \int g(\psi_f{}^* Q \psi_i)(\psi_e{}^* \psi_\nu)_h d\tau \qquad (7.53)$$

where the subscript h indicates $\psi_e{}^*$ and ψ_ν are to be evaluated at the position of the heavy particle involved in the process, and g represents the strength of the coupling giving rise to the emission and is a universal constant. The integral is essentially the matrix element of Q between initial and final nuclear states multiplied by a term denoting the probability amplitudes of having the

electron and neutrino at the position of the nucleon which undergoes the charge exchange. We can also write

$$|H'_{if}|^2 = g^2 \left| \int (\psi_f{}^* Q \psi_i)(\psi_e{}^* \psi_\nu)_h d\tau \right|^2 \qquad (7.54)$$

We previously made the assumption that ψ_e and ψ_ν varied slowly in the region where ψ_i and ψ_f are nonzero, so we could say

$$|H'_{if}|^2 = g^2 \left| \int \psi_f^* Q \psi_i d\tau \right|^2 \; |\psi_e(o)|^2 \; |\psi_\nu(o)|^2 \qquad (7.55)$$

The last two factors are the same ones separated out before. The transition probability is then given by Fermi's Golden Rule as

$$P = \frac{2\pi}{\hbar} g^2 |\psi_e(o)|^2 \; |\psi_\nu(o)|^2 \; |M|^2 \; \rho(E) \qquad (7.56)$$

where $M = \int \psi_f{}^* Q \psi_i d\tau$ (7.57)

This is the form first written down by Fermi, but one correctly anticipates that other operators than Q may be used and still get β decay, and a full investigation of theory must consider these. In fact when one considers nonconservation of parity in weak interactions, and the most general form of the neutrino wave function, which is

of 4-component form, one finds 20 different versions of this interaction. But if one takes the neutrino to be a particle which exhibits polarization so that its spin always lies along its direction of motion, this gives the neutrino a 2 component form and the 20 different integral expressions reduce to 10. One can relate the 10 in pairs to one another so that really there are only 5 independent cases. It is then a matter of experiment to discover which of the five forms are possible. The five forms are called scalar, vector, tensor, axial-vector, and pseudo-scalar, and for a variety of reasons the combinations which can go together are the scalar-tensor, scalar - pseudo-scalar, and vector - axial-vector. It has been found experimentally that it is in fact the vector - axial-vector combination which actually contributes to beta decay, and they enter with such relative phases that one writes the interaction as V - A, where V represents the vector and A the axial-vector interaction. There are interaction coupling constants that go with both of these and $g_V \sim 1.41 \times 10^{-49}$ in cgs units, and $g_A/g_V = -1.19$. Let us now write down the forms the various interactions must take, writing the relatively

large terms on the left and the small ones on the right.

	Large	Small	
Scalar:	$S = (\psi_f{}^*\beta Q\psi_i)(\psi_e{}^*\beta\psi_\nu)$	$+0$	(7.58)
Vector:	$V = (\psi_f{}^*Q\psi_i)(\psi_e{}^*\psi_\nu)$	$-(\psi_f{}^*\vec{\alpha}Q\psi_i)(\psi_e{}^*\vec{\alpha}\psi_\nu)$	(7.59)
Tensor:	$T = (\psi_f{}^*\beta\vec{\sigma}Q\psi_i)(\psi_e{}^*\beta\vec{\sigma}\psi_\nu)$	$+(\psi_f{}^*\beta\vec{\alpha}Q\psi_i)(\psi_e{}^*\beta\vec{\alpha}\psi_\nu)$	(7.60)
Axial Vector:	$A = (\psi_f{}^*\vec{\sigma}Q\psi_i)(\psi_e{}^*\vec{\sigma}\psi_\nu)$	$-(\psi_f{}^*\gamma_5 Q\psi_i)(\psi_e{}^*\gamma_5\psi_\nu)$	(7.61)
Pseudo Scalar:	$P = 0$	$+(\psi_f\beta\gamma_5 Q\psi_i)(\psi_e{}^*\beta\gamma_5\psi_\nu)$	(7.62)

With the notation that is standard for Dirac operators,

β is a "mass" operator (represents $\sqrt{1-v^2/c^2}$)

σ is a "spin" operator (the Pauli matrices) (7.63)

α is a "velocity" operator (represents $\vec{v}/c$

$\gamma_5 = i\alpha_1\alpha_2\alpha_3$

This list represents an exhaustive set of the basic interactions which are possible within the full Dirac electron theory to bring about the transformation of beta decay. The "small" terms are those which involve the velocity of the nucleon, which is small in relativistic units for a nucleon bound in the nucleus. Hence for a first approxi-

mation we could consider only the large terms, except of course for P, which has no large term. Also since $v/c \ll 1$ for the nucleons, the operator $\beta \sim 1$ in S and T. Besides S, V, T, A, and P separately, any linear combination of them is permissible, and the general expression for the perturbation energy operator is

$$H' = C\ (g_S S + g_V V + g_T T + g_A A + g_P P) \tag{7.64}$$

where C is the generalized Fermi coupling constant. For connection with the previous work following Fermi we presented, note that the large term in the vector interaction is just the term Fermi got with only a charge exchange operator. And since experimentally it turns out that the linear combination

$$H' = g_V V + g_A A \tag{7.65}$$

describes nature, we see that the term Fermi wrote down survives.

The beta decay transition interests the astrophysicist for several reasons. We are of course, interested in certain fundamental beta decays like that which occurs in the proton-proton chain without which we could have no

thermonuclear reactions at all, assuming that only hydrogen was present in the universe. And our ability to calculate what goes on in a proton-proton reaction is based strictly on our understanding of this weak interaction theory. Direct laboratory observation of the proton-proton chain reaction is impractical because of its slowness; so we need to have especial confidence in our ability to make calculations for this primary stellar generating reaction. Secondly, many of the reactions which occur in more advanced stages of stellar evolution involve beta decays, many of which are familiar from laboratory experience. But if multiple neutron capture occurs extremely rapidly so that all the product nuclei lie well away from the valley of beta stability then we usually are again faced with the problem of having beta-decay rates that are not measured in the laboratory, and which must therefore be calculated if we are to have any information at all. A typical situation in such rapid neutron capture problems is that we have a daughter nucleus with many excited states and the ground state of a nucleus that could be formed by neutron capture lying above the excited states of the daughter nucleus sum the decays from the ground state or ground and first

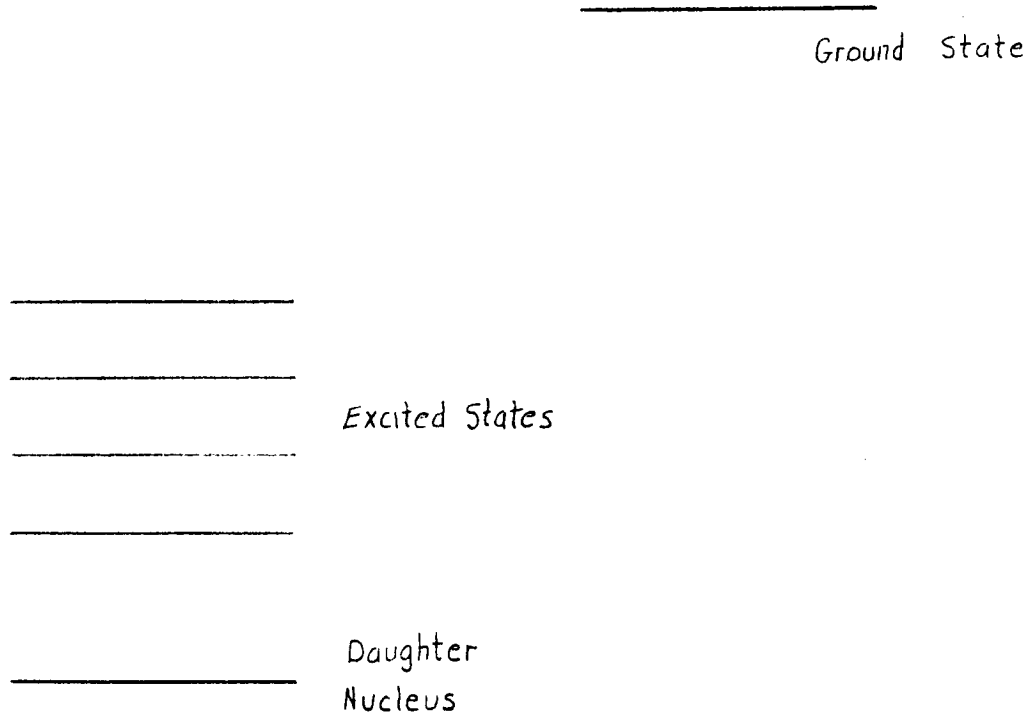

Figure 7.8

few excited states of this nucleus to all the energy accessible states of the daughter nucleus (fig. 7.8). This summing raises the question as to whether there may be some beta decay sum rules that enter to diminish the value of the nuclear matrix element for these transitions to the more highly excited nuclear states. One can make arguments similar to those we made for captured gamma rays where we had to reduce the size of the nuclear matrix element for the photon transitions involving highly excited states. A similar reduction ought to be possible in the case of beta decays to highly excited states; but in the case of beta decay, in general, one does not deal with direct overlap-type integrals, but instead integrals involving wave functions that have been operated on in various ways. The operations may well perturb the overlap of the functions, for instance, by changing their phase. This means that our present situation is not really equivalent to gamma decay between low lying states, where we can have a great purity of a single particle type transition. In the case of beta decay, the only thing that is at all equivalent to a single particle transition are those classed as superallowed; everything else tends to cut down

the size of the matrix element.

Another situation involving beta decay which is of astrophysical interest is in matter at extremely high densities. The Fermi level of the electrons becomes very large, and we must consider what sort of electron capture rates are induced in the nuclei, which are continually bombarded with electrons having energies all the way up to the Fermi level, often many MeV. At the same time under such circumstances, we are dealing with a highly degenerate electron gas, and the electrons are already occupying all the lower cells in phase space. Consequently nuclei which ordinarily emit electrons in beta decay may have no phase space available into which they can emit their decay electrons, and so will not be able to decay in the ordinary way . If we tamper with the occupancy of phase space, the f functions entering into the comparative half-life are modified, and so on. These specialized applications will be encountered later.

References

Blatt, J.M. and Weisskopf, V.F., 1952, Theoretical Nuclear Physics, Chapter X, Section 2.

Ibid., p. 682.

Ibid., p. 687.

Blatt, J.M. and Weisskopf, V.F., op. cit., Chapter XIII.

Fermi, E., 1950, Nuclear Physics, (compiled by Orear, J., Rosenfeld, A.H. and Schulter, R.A.), University of Chicago Press, Chicago.

Semat, H., Introduction to Atomic and Nuclear Physics, Third Edition, 1958, p. 460, Rinehart, New York.

Part B. STELLAR PHYSICS

8. Introduction

Astrophysics, as you can gather from the title, primarily means the physics of the stars. The meaning of the term has been broadened a great deal in recent years. It has been applied to the physics of the planets, of the sun, and of interplanetary medium as well.

The first development in astrophysics consisted of looking at the spectra of the stars that were photographed, and of trying to deduce from these the conditions at the surfaces of the stars. When a gas is heated to a high temperature, it will emit light of certain characteristic wavelengths. However, if you shine black body radiation corresponding to a temperature that is higher than the gas through the gas then, instead of seeing bright emission lines you will see dark lines due to the absorption of characteristic wave-lengths by the gas. In the case of stars it is found that the outer layers have a temperature gradient that decreases as we go outwards, so that the gas at the very edge is generally cooler than the gas which is emitting the light. The usual effect is then a spectrum which contains dark absorption lines. By looking at these, determining which elements produce them, and seeing how much the elements are excited, one finds that certain of the lines arise from absorption by atoms in excited states. From statistical mechanics it is known that the populations of atoms in excited states depend upon the usual Boltzmann factor. Thus the relative

numbers of lines that arise from absorption in various excited states of an atom can be determined. From these considerations the composition, temperature, density and pressure in the outer layers can to some extent be determined. The density is somewhat less sensitively determined than the temperature, but nevertheless the relative abundances of ionized and neutral forms of certain elements depend at a given temperature on the density.

One of the first things done that could be called astrophysics then was to make use of empirical classifications of stellar spectra to determine what these meant in terms of temperature. On this basis were obtained the traditional spectral classes of the stars. These are arranged according to the surface temperatures of the stars. These temperatures may vary from slightly less than 2000°K to more than 500,000°K. The spectra of most stars (and hence the composition at the surface) can be arranged in the following continuous sequence. (Each class is further subdivided in ten subclasses labeled 0 through 9, e.g. A0.)

Class O: Temperatures of 25,000°K up. Lines of ionized helium.

Class B: 25,000 - 11,000°K. The lines of hydrogen and neutral helium are conspicuous at B0. Ionized oxygen and ionized carbon become strong at B3.

Neutral helium is strongest at B5. Hydrogen lines become progressively stronger in the higher numbered subdivisions of the class.

Class A: At A0 hydrogen and ionized magnesium lines are strongest, while the helium and ionized oxygen lines have disappeared. Hydrogen lines weaken in the higher subdivisions, while ionized metals (Fe, Ti, Ca) strengthen. 10,700 - 7500°K.

Class F: Class F0 is rich in lines of the ionized metals, the strongest being the H and K lines of singly ionized Ca. Metallic lines strengthen and hydrogen lines weaken as we pass through this class. 7500 - 6000°K.

Class G: In this class the lines of the neutral metals become strong while the hydrogen lines continue to weaken. Molecular bands of CN and CH appear. 6000 - 4910°K. Our sun is class G2.

Class K: In general molecular bands and lines of neutral metals become much stronger while the lines of hydrogen and ionized metals continue to weaken. At K5 the lines of TiO are weakly visible. 4910 - 3500°K.

Class M: The characteristic feature is the complex spectrum of molecular oxide bands, of which the TiO bands

are strongest. 3500 - 2200°K.

Some stars do not fit into this sequence of spectral classes. Therefore some additional spectral classes have been established which parallel the above classes in temperature. These classes include the following:

Class S: A low temperature class parallel to Class M. This is still characterized by molecular oxide bands but the most prominent feature is the ZrO bands. Certain elements such as Zr, Y, Ba, La and Sr give strong atomic lines and oxide bands. Lines of neutral technetium are usually seen.

Classes R and N (or Class C): Parallel in temperature to the ordinary classes K and M. The spectrum is characterized not by oxide but by molecular carbide bands, such as those of CN, C_2, and CH.

Class W: Extremely high temperature objects called Wolf-Rayet stars with bright, broad, hazy emission lines of ionized helium and highly ionized carbon, oxygen, and nitrogen. Two sequences exist the WC stars have strong carbon lines and weak nitrogen lines; in the WN class the reverse is true. These stars are generally found to be ejecting gas rapidly into space.

One of the main things we will be concerned with is the understanding of how the relative abundances of the various elements

came to be what they are. As noted above, some of the stars have an abnormal composition due to nuclear reactions occurring in their interior, and in fact, it was these abnormal compositions that gave some of the initial clues as to the kind of thermonuclear reactions that are taking place in stellar interiors. From this, we are able to go on to deduce many things about the general formation of the elements.

As an example, consider the peculiar spectra of the R and N class stars. Normally, the oxygen abundance in a star is greater than the carbon abundance, so that in statistical equilibrium the molecule with the highest binding energy, that is carbon monoxide, will be formed and there will be oxygen left over to form oxide compounds which give prominent features of the spectrum. In the R and N stars it appears that carbon predominates over oxygen and when the oxygen is used up in forming carbon monoxide, the residual carbon combines to form C_2, CN, etc. Thus, some factors in the evolutionary life of R and N stars must give rise to an overabundance of carbon relative to oxygen.

In summary then, the astrophysicist takes spectra, examines the relative intensities of the lines, deduces from this the temperature and density in the photospheric surface layers of the stars, and hence, if he knows from some other means also the total luminosity of the star, then he can deduce the radius

from the usual Planck emission law for radiation. From a knowledge of the conditions at the surfaces of stars, one can go on to formulate a picture of the interiors.

It was apparent long ago that the stars are composed entirely of gas. Therefore if the star is a structure which is in hydrostatic equilibrium we know that at every point in the interior the pressure must be sufficient to hold up the weight of the overlying layers. We therefore have essentially four things -- pressure, temperature, density and composition that we can vary. The pressure, temperature, and density are related by a gas law, but one still has a certain degree of freedom in specifying what the actual structure of the star will be. For example, if the star has a certain radius and roughly a certain kind of structure then you can say how much the pressure has to be at the center in order to hold up all the overlying layers. Now, you do not know whether you have obtained that pressure by having a high density and relatively low temperature at the center, or by having a lower density and a higher temperature at the center. Much of the more refined aspects of the study of stellar interiors is the determination of the combination of temperature and density in the interior in order that we should have hydrostatic equilibrium.

Rather early in this century, Emden developed the properties of what were called polytropic spheres. We will talk more

about these later, but essentially Emden's contribution was to say there is a relation of a given kind between the pressure and density in the interior of a gas sphere so as to maintain it in hydrostatic equilibrium. Hence, the temperature distribution in the interior could be whatever is required to actually produce that relation between pressure and density. Starting from an assumption of that kind, investigators had an idea of just what kind of temperature and density conditions must be obtained in the interior of a star for hydrostatic equilibrium. These were the kinds of conditions that had to be studied in determining a number of other properties of the star. For example, how does a star manage to transport energy from the interior out to the surface? Emden's idea was that this transport took place by convection. As you know, there are three ways in which we can transport heat: convection, radiation, and conduction. Ordinarily, the thermal conductivity in a stellar interior is very small and conduction is not important. (We shall find some exceptions to that rule, but this is the usual case in ordinary stars.) The choice really lay between whether it was convection, the actual mixing of gases which would enable heat to be transported from one place to another in the star, or whether it was radiation which would give energy transport by a process of emitting energy at one spot, absorbing it at a cooler spot, and re-emitting

it, and so on, in this way gradually letting the energy filter from a hot spot to a cool spot along a temperature gradiant according to the laws of emission and absorption of radiation. Emden's idea in setting up some of the theory of polytropes was that probably the heat transport took place by convection, and in this case there would be a specific relation between the pressure and the density everywhere. This is why the polytropic spheres were studied very early.

Later on in the 1920's it was felt that convection was probably not the actual means by which energy was transported, but rather it was by radiative transfer. Eddington[1] made very great contributions in working out the conditions necessary to transport energy by radiation with small temperature gradiants and by working out the opacity of the material which absorbs the radiation. The position towards the end of the 1920's was that one could understand the kind of pressures, temperatures and densities that had to obtain in the center of a star, and the conditions under which energy transport from the interior to the surface could occur.

It was thus possible to understand generally what the structure was, what the conditions in the interior were, and how the energy transport occurred, but it was not possible to understand where the energy came from. This was

1) A. S. Eddington, The Internal Composition of the Stars, Cambridge, England

the major question that faced people in the late 1920's and early 1930's --- what was the source of energy in the stellar interiors? Of course, this question was not then asked for the first time, but it was the last of the major puzzles.

People had been thinking about the possible energy sources for quite some time. If one goes back to the last century, one encounters some pretty fantastic suggestions, e.g. the suggestion that perhaps meteors are continually falling into the sun and heating it, because, of course, meteors were observed to fall into the earth's atmosphere and when they did, they obviously became very hot. That idea did not last very long. Helmholtz and Kelvin made what seemed to be the best suggestion that anyone could think of for a long time, namely, that the stars obtained their energy strictly by gravitational contraction. However, when they calculated how long the sun could have been shining at its present luminosity, and how long it would have taken for it to have contracted to its present radius, it turned out, depending upon precisely what assumption one had to make for the interior distribution of mass and hence the exact gravitational potential energy of the model, that the sun could shine in that way for a few tens of millions of years. These figures did not agree with those of the geologists who at the same time were studying the ages of the rocks on the surface of the earth. Without question,

these rocks appeared to be at least a billion years old.

The way out of this dilemma appeared in the form of the mass-energy relationship. The science of nuclear physics had progressed to the point where it was known that the conversion of only a small fraction of the solar mass to energy would supply enough heat to allow the sun to shine for extremely long periods of time. The question was then how was the mass converted? A simple process like the combining of four hydrogen atoms (with two beta decays) to form one helium atom would, in theory, release a considerable amount of energy. The difficulty was, however, that the Coulomb barriers were well known and these seemed to be high enough so as to prohibit two hydrogen nuclei from approaching near enough together in order to combine. The Coulomb barrier heights were known to be of the order of 10^5 or 10^6 electron volts for the very simplest nuclei. These energies are much higher than the thermal energies of the particles themselves, even at temperatures of 10-15 million degrees, which was a rough figure for the temperature at the center of the sun. These difficulties were finally surmounted by Gamow and other investigators who calculated the quantum mechanical penetration probabilities for charged particles through potential barriers and found that these penetration probabilities, though

small, were still non-zero. Atkinson and Houtermans then applied these calculations to an astrophysical problem and calculated the rate at which the penetration of the Coulomb barrier would occur by the bombarding of one charged particle by another in the high energy tails of the Maxwell velocity distributions of those particles. Their important contribution was to show that even though the average thermal energies of the particles lay far below the top of the Coulomb barrier, nevertheless penetration through the barrier can take place at a very definite rate.

Once we knew in general what the essential nature of a thermonuclear reaction had to be, the next step was to find just what are the nuclear reactions that are responsible for nuclear energy generation. It was evident that a four-way collision of hydrogen atoms occurring simultaneously with two beta decays was a rather improbable way to make helium. In the late 1930's, Bethe, and independently, von Weizsäcker discovered the carbon-nitrogen cycle by means of which hydrogen could be converted into helium. At the same time Bethe and Critchfield found a sequence of reactions by means of which four hydrogen atoms could come together and be converted into helium; that is, they found a set of nuclear reactions involving a certain sequence of intermediate products which would allow the

conversion of hydrogen into helium without the use of 'catalyst nuclei' to promote this transformation. On this basis, then, the essential nuclear reactions responsible for maintaining the luminosity of most stars became known. At the same time investigators were beginning to study the problem of the evolution of the stars.

As an introduction to a study of stellar evolution, we will consider some aspects of the relation between the total energy released by a star and its surface temperature. One of the most remarkable properties of stars is the wide range of their luminosities. The brightest stars known emit about 10^6 as much energy per second as the sun; the faintest known emit only 10^{-6} as much energy per second as the sun. The logarithm of the total rate of energy emission of a star is called its absolute bolometric magnitude. Astronomical magnitudes form a logarithmic scale with a factor 2.512 between magnitude classes. Because of the limited spectral transmission of the earth's atmosphere and the even more limited spectral sensitivity of most recording instruments, it is difficult to translate measurements into bolometric magnitudes. Hence in practice there are many systems of practical magnitudes which are based on specific spectral ranges. These magnitudes include the visual, photographic,

and photoelectric magnitudes in various colors. The difference between the photographic and visual magnitudes of a star is called its color index. This gives a measure of the surface temperature of the star. The absolute magnitude of a star is equal by definition to the apparent magnitude it would have if it were placed 10 parsecs away from us. (The parsec is a unit of astronomical distance equal to 3.258 light years.) As an example of the above, the bolometric magnitude of the sun is +4.63, its luminosity is 3.78×10^{33} erg/sec and its effective surface temperature is 5760°K.

Certain startling relations between the effective surface temperatures (or color index B-V, or spectral class) and the absolute magnitudes of the stellar population became immediately apparent when these two quantities were plotted against one another for a large number of stars. Such a plot is called a "Hertzsprung-Russell" or "H-R" diagram. A schematic representation is shown in Figure 8.1. The area of greatest population for the majority of stars consists of a long diagonal slash in the diagram called the "main sequence". Another well defined region is that labled "red giants". These are large, luminous red stars. In the bottom left-hand corner of the diagram is a region populated by very small blue white stars of mass usually less than that of

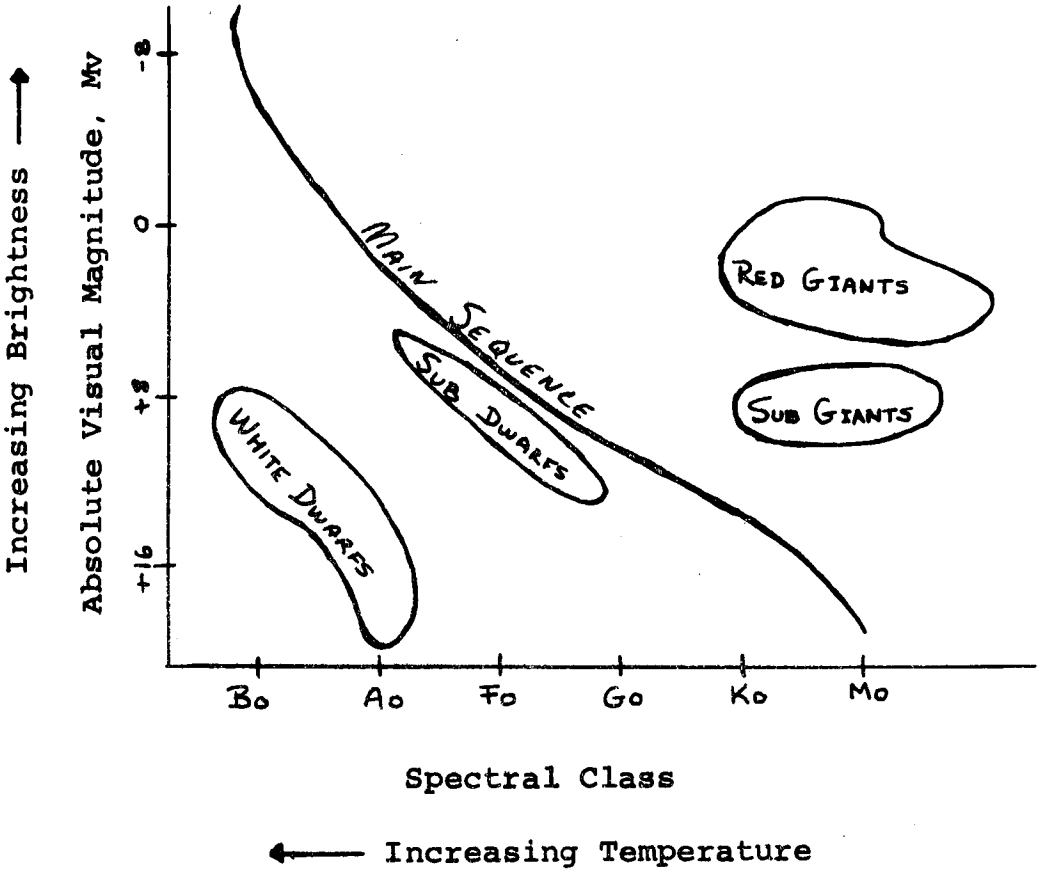

Figure 8.1 Schematic H-R Diagram

the sun called "white dwarfs". As will be shown, these stars constitute the "stellar graveyard" in that they represent the end of stellar evolution. These stars consist of highly degenerate matter in which the density is so high that electrons have effectively filled up all available cells in momentum space. This results in extremely high internal pressures which in turn support the outer layers of these very dense stars. They have no in-

ternal energy sources so that their residual supply of internal heat is being gradually radiated to space. That is to say, they are cooling off with no future expectations of an active stellar life.

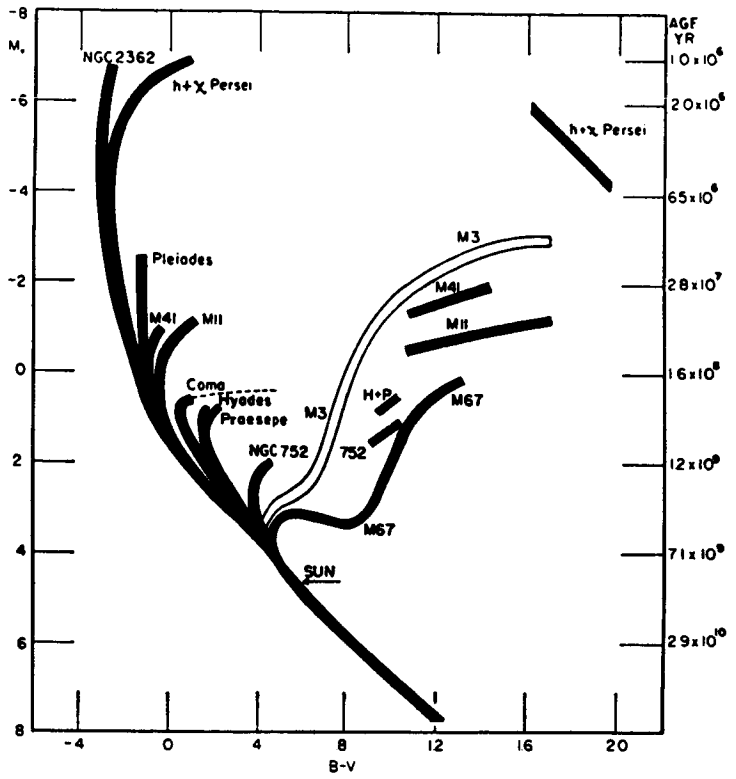

Figure 8.2

A composite color-magnitude diagram for galactic clusters. In this diagram visual magnitudes are plotted against the difference of the photoelectric magnitudes measured in blue and visual light. For comparison, the giant branch of the globular cluster M3 is also included. The lengths of time required for stars to evolve away from the main sequence are shown on the right.

A more specific example of an H-R diagram is shown in Figure 8.2, where the star population data for several ga-

lactic clusters (associations of bright, relatively newly formed stars coexisting with large amounts of gas) have been plotted in the same fashion as Figure 8.1. We note the presence of the main sequence common to all the clusters. At the same time however there are sequences of stars originating in the main sequence which tail off into the region of the red giants. The point of origin of a sequence is characteristic of the cluster and in fact is an indication of the age of the individual cluster. This may be seen from the following considerations: the luminosity of a star is a strong function of its mass. For stars such as the sun, the luminosity varies approximately as the fourth power of the mass so that the larger stars are releasing far more energy per unit mass than lighter ones. We expect then that the larger the mass of a star the more rapidly will its evolution take place. It is also known that a star originally "born" onto the main sequence will remain at its point of birth until the hydrogen in the vicinity of its center becomes transformed into helium. The length of time that this process takes turns out to be about two-thirds of its total active lifetime. Once the core hydrogen is exhausted the star heads out into the red giant region. If we now assume that all stars in a given galactic cluster were formed at the same time, then

the point on the main sequence at which the sequence branches off into the red giant region will occur at that point for which all stars of a given age in the cluster are just evolving off the main sequence. This age is then just the age of the cluster. These ages are indicated on the right-hand ordinate of Figure 8.2.

We also note in Figure 8.2 that for many of the clusters (e.g. H+χ Persei, M41, M11) the sequence leading to the red giant region has a break in it. The region of the gap contains variable stars, that is, stars whose magnitude varies regularly with time.

When the star leaves the main sequence and arrives in the red giant region it remains there until helium thermonuclear reactions start to take place. At this point the details of the evolution are not well known except that the star moves off down into the region of the white dwarfs. In transit, however, it is known that it must reduce its mass below a certain value known as the "Chandrasekhar limit". To do this, it either emits mass regularly or spectacularly as in a nova or supernova explosion, or both.

The history of a star before its arrival on the main sequence is that of a large cloud of gas which contracts while releasing half its gravitational potential energy as radiation. Recent models place this protostar in the red

giant region where it then comes down and settles on the main sequence. The time for such a contraction is approximately 2-3 million years. We may compare this to the main sequence age of 10 billion years for a star like the sun.

After heading back to the red giant region its thermonuclear processes continue with the subsequent building up of small amounts of the heavy elements. Some fraction of the stellar mass is then ejected into the interstellar medium as the star trims down to the Chandrasekhar limit for white dwarfs. This gas, now enriched with heavy elements, can be used for new star formation. We expect then that the heavy element concentration in the interstellar gas will increase. One of our tasks will be to examine the details of stellar evolution in order to explain the compositions of stars with peculiar spectra, and the relative abundances of elements as found in the solar system with particular attention to meteorites.

9. The Virial Theorem and Some Consequences

One of our primary objectives in dealing with stellar interiors is to have some idea of what temperature and density combination will be involved in the calculation of certain nuclear reaction rates. These temperature and density conditions and other interesting consequences may be determined by the application of the Virial Theorem.

To prove this Theorem let us consider a self-gravitating system of particles. By this we mean that the particles under consideration are so dilute that the only forces between them are gravitational forces. Consider any one of these particles, of mass m with coordinates (x,y,z), subject to a force with components (X,Y,Z). Applying Newton's Third Law to this particle we can write the following reactions to this force:

$$m \frac{d^2x}{dt^2} = X$$

$$m \frac{d^2y}{dt^2} = Y$$

$$m \frac{d^2z}{dt^2} = Z \tag{9.1}$$

We note the identity:

$$\frac{1}{2} \frac{d^2}{dt^2} (mx^2) = m\left(\frac{d}{dt} x \frac{dx}{dt}\right) = mx \frac{d^2x}{dt^2} + m\left(\frac{dx}{dt}\right)^2 \tag{9.2}$$

Therefore we can rewrite equations (9.1) as:

$$\frac{1}{2}\frac{d^2}{dt^2}(mx^2) = m\left(\frac{dx}{dt}\right)^2 + xX$$

$$\frac{1}{2}\frac{d^2}{dt^2}(my^2) = m\left(\frac{dy}{dt}\right)^2 + yY$$

$$\frac{1}{2}\frac{d^2}{dt^2}(mz^2) = m\left(\frac{dz}{dt}\right)^2 + zZ$$

(9.3)

Summing these expressions we find:

$$\frac{1}{2}\frac{d^2}{dt^2}(mr^2) = m\left[\left(\frac{dx}{dt}\right)^2 + \left(\frac{dy}{dt}\right)^2 + \left(\frac{dz}{dt}\right)^2\right] + (xX + yY + zZ)$$

(9.4)

Now, summing over all the particles in the system, we note:

$$I = \sum_i m_i r_i^2$$

(9.5)

$$K = \sum_i \frac{m}{2}\left[\dot{x}^2 + \dot{y}^2 + \dot{z}^2\right]$$

(9.6)

where I is the moment of inertia of the system and K the kinetic energy. Therefore equation (9.4) becomes:

$$\frac{1}{2}\ddot{I} = 2K + \sum_i (x_i X_i + y_i Y_i + z_i Z_i)$$

(9.7)

The last term in equation (9.7) is called the virial of Clausius.

In order to evaluate the virial term let us consider now the interaction between any two of the particles, denoted by subscripts 1 and 2. Let that force exerted by particle m_2 on m_1 have components (A,B,C); thus the force exerted by particle m_1 on m_2 has components (-A, -B, -C). The contribution these forces make to the virial expression is, then:

$$A(x_1 - x_2) + B(y_1 - y_2) + C(z_1 - z_2) \tag{9.8}$$

Thus, for the system as a whole, the virial term is just equal to the double summation over all pairs of expression (9.8), i.e.:

$$\text{Virial} = \Sigma\ \Sigma \left[A(x_1 - x_2) + B(y_1 - y_2) + C(z_1 - z_2)\right] \tag{9.9}$$

Thus far, our arguments have been quite general. Now we recall that our system is such that only the gravitational forces are significant. In this case (A, B, C) are just the components of $Gm_1 m_2/r_{12}^2$ directed from particle m_2 to m_1. Hence we have

$$A = -\left(\frac{Gm_1 m_2}{r_{12}^2}\right)\left(\frac{x_1 - x_2}{r_{12}}\right) \tag{9.10}$$

and similar expressions for the other components.

The Virial is then:

$$\text{Virial} = \Sigma\Sigma \left(\frac{-Gm_1 m_2}{r_{12}^3}\right) [(x_1 - x_2)^2 + (y_1 - y_2)^2 + (z_1 - z_2)^2]$$

$$= -\Sigma\Sigma \frac{Gm_1 m_2}{r_{12}} \qquad (9.11)$$

Now we note that the term $(Gm_1 m_2/r_{12})$ is just the gravitational potential of the two particles m_1 and m_2; in other words it is just the work required to separate m_1 to infinity from m_2. The double summation over all pairs of the system of this quantity is then just the work required to separate all the particles in the system to infinity; that is, the gravitational potential energy. This means that, writing Ω as the gravitational potential energy, we obtain the form of the virial theorem:

$$\frac{1}{2} \frac{d^2 I}{dt^2} = 2K + \Omega \qquad (9.12)$$

There are more general forms in which we could write the virial theorem. K is the thermal energy of the system, which simply means it is the sum of the energies of the particles in thermal motion. Now it may be that some of the energies of particles in motion may not be truly expressible in terms of a temperature. That is to say, we might have mass motions in the system in the form of turbulence

or in the form of the rotation of the system as a whole. So it is useful to recognize the possibility of splitting the kinetic energy of the particles into mass motions and thermal motions. Let us, then, write the Virial Theorem more generally as:

$$\frac{1}{2}\frac{d^2 I}{dt^2} = 2K + 2K_T + 2K_R + \mathcal{M} + \Omega - 3pV \tag{9.13}$$

Here K_T is the kinetic energy of mass motions or turbulence, K_R is the kinetic energy of rotation of the system, K remains the thermal kinetic energy, and $\mathcal{M}$ is the energy due to any magnetic fields contained within the system. Chandrasekhar and Fermi first proved the form of the virial theorem which contained the term due to the magnetic field. It is further possible to consider that the system has a boundary on which pressure is exerted, hence we have included a term (-3pV), where p is the pressure exerted on the boundary of the system having a volume V.

Now, returning to our statement of the virial theorem in equation (9.12) we can seek the meaning of this theorem. If the moment of inertia of the system is not changing, i.e., if the system is truly in equilibrium, we would have:

$$2K + \Omega = 0 \tag{9.14}$$

In other words, for a system of this sort in equilibrium, we see that twice the internal thermal energy must be equal to the gravitational potential energy, and right here we see a very important aspect of stellar evolution. A star can be considered as a system in which the moment of inertia is not changing very rapidly, so that the left-hand side of this expression is zero to a very good approximation. Hence, twice the internal thermal energy of the star will be equal to the absolute value of the gravitational potential energy. We must remember that Ω is intrinsically a negative quantity. The star of course does shrink during those periods in which nuclear energy sources are not supplying the energy necessary to maintain it in a given position of equilibrium. Hence, as a star shrinks, and as the magnitude of the gravitational potential energy increases, twice the internal thermal energy must stay equal to it or, in other words, half of the gravitational potential energy that is released is stored as internal thermal energy and half must be radiated away.

Here we have perhaps our greatest clue to understanding the general nature of stellar evolution. A star

is a sphere of gas in space that shrinks as long as there are no nuclear reactions available in the interior to supply the energy that is radiated into space. As long as it continues to shrink, it releases gravitational potential energy, of which half goes into thermal energy and half is radiated away.

Thus far we have not specified what the particles in the system are. The Virial Theorem, in its general form could as well be applied to a cluster of stars which is self-gravitating. Let us now suppose that the particles in the system are molecules in a gas. Consider an element of mass dm at a temperature T. Each molecule has a mean kinetic energy of 3/2 kT. If the element contains dN molecules, the thermal energy contained within this element is:

$$dK = \frac{3}{2} kT\, dN = \frac{3}{2} RT\, dm$$

$$= \frac{3}{2} (c_p - c_v)\, T\, dm \qquad (9.15)$$

Here R is the gas constant, and is simply the difference between the specific heat at constant pressure c_p, and the specific heat at constant volume c_v. Now the internal energy of such a gas is simply:

$$dU = c_v\, T\, dm \qquad (9.16)$$

Writing, as is customary, $\gamma = C_p/C_v$, equation (9.15) for the thermal energy in an element dm becomes:

$$dK = \frac{3}{2}\left(\frac{C_p}{C_v} - 1\right)C_v \; Tdm = \frac{3}{2}\,(\gamma-1)\; dU \tag{9.17}$$

thus, for the entire system we can write:

$$K = \frac{3}{2}\,(\gamma-1)U \tag{9.18}$$

The Virial Theorem then becomes:

$$\frac{1}{2}\frac{d^2 I}{dt^2} = 3(\gamma-1)U + \Omega \tag{9.19}$$

Now, letting $E = U + \Omega$ be the total energy of the system, for the equilibrium case we have

$$3(\gamma-1)U + \Omega = 0 \tag{9.20}$$

$$E = -(3\gamma-4)U$$
$$= \left[\frac{3\gamma-4}{3(\gamma-1)}\right]\Omega \tag{9.21}$$

We are now in a position to note several important consequences of the Virial Theorem. Consider first an ideal gas for which $\gamma = 5/3$. From equations (9.21) we find:

$$E = \frac{1}{2}\,\Omega$$
$$U = -\frac{1}{2}\,\Omega \tag{9.22}$$

Thus for a star which can be considered as a perfect gas in equilibrium, half of the gravitational potential released in contraction is stored as internal energy and half is radiated away.

Now, let us consider the case for radiation or extremely degenerate relativistic matter, for which $\gamma = 4/3$. For such a gas we find:

$$E = 0$$

$$U = -\Omega \tag{9.23}$$

This corresponds to a sort of a transition region. The fact that the total energy of the system is zero implies that we could expand or contract the system at will without change of energy. Therefore this value of γ represents the threshhold of instability in a system. Now it so happens that astrophysical systems can undergo phase changes in which the compression of a gas does not lead to a temperature rise because the gas is absorbing energy and converting matter from one form into another. Ionizing hydrogen in the gas would be one such form of phase change. Under such circumstances, γ falls less than 4/3 and such systems become unstable against gravitational collapse.

We now wish to form an approximate idea of conditions in stellar interiors. Let us apply the Virial Theorem to a uniform by dense sphere of gas at a temperature T. Although this does not constitute a system in hydrostatic equilibrium we will treat it as such to obtain results which are at least of the right order of magnitude. In this case we have

$$\gamma = 5/3 \quad \text{and:}$$

$$2U + \Omega = 0 \tag{9.24}$$

Now, the gravitational potential energy for a uniform sphere is given by:

$$\Omega = -\frac{3}{5}\,\frac{GM^2}{r} \tag{9.25}$$

We assume a mean molecular weight per particle μ, in amu. For example, in the case of ionized hydrogen we have two particles (a proton and an electron) for every unit of atomic mass; hence we would have $\mu = 1/2$. The number of molecules is, then, equal to MN_0/μ where N_0 is Avogadro's number.

Thus for the internal energy we have

$$U = \frac{3}{2}\,kT\,\frac{MN_0}{\mu} \tag{9.26}$$

Thus from equation (9.24) relating U and Ω we have:

$$T = \frac{GM\mu}{5RkN_o} \tag{9.27}$$

Now, for the uniform gas sphere we have

$$M = \frac{4}{3}\pi\rho R^3 \tag{9.28}$$

Equation (9.27) then becomes

$$T = \frac{(4\pi\rho)^{1/3}\, GM^{2/3}\, \mu}{5(3^{1/3})\, kN_o}$$

$$= (4.1 \times 10^6) M^{2/3} \rho^{1/3} \mu \ {}^oK \tag{9.29}$$

Here M is in solar mass units, and ρ is gm/cm^3.

Now let us see just how good our result is. We will find that a temperature of approximately 15×10^6 ^oK is required to convert hydrogen to helium in the sun. With M = 1, and assuming $\mu \approx 2/3$ we find that this would require a density $\rho \approx 165$ gm/cm^3. This agrees with the results one finds for the sun's density from more precise models to within a factor of two.

We note one further important conclusion that can be drawn from this relation. It is this: as a star contracts or expands the factor $\frac{T}{\mu\rho^{1/3}}$ remains constant.

Thus far we have considered the consequences of the virial theorem under conditions in which the dimensions of the system are not changing. Let us now consider a body which is nearly in equilibrium and ask under what conditions it can become unstable against gravitational equilibrium, and thus suffer a gravitational collapse. This problem is of particular interest in considerations of the formation of galaxies out of clouds of gas in intergalactic space and of the formation of stars from interstellar gas.

If we begin with a gas cloud in equilibrium we know that the second derivative of the moment of inertia with respect to time is zero. If we wish the cloud to become unstable against gravitational collapse, then the second time derivative must become negative, forcing the first derivative to become negative. Thus the condition that a gas cloud will become unstable against gravitational collapse is:

$$\frac{d^2 I}{dt^2} < 0 \tag{9.30}$$

If we consider a gas for which $\gamma = 5/3$ we then have that twice the internal energy must be less than the absolute

value of the gravitational potential energy, i.e.

$$2U < |\Omega|$$

(9.31)

for the case of a spherical gas cloud this becomes:

$$kT < \frac{GM\mu}{5RN_0}$$

(9.32)

$$M > \frac{5RN_0 kT}{G\mu} = 5\left[\frac{3M}{4\pi\rho}\right]^{1/3} \frac{N_0 kT}{G\mu}$$

$$M^{2/3} > 5\left[\frac{3}{4\pi}\right]^{1/3} \frac{N_0 kT}{G\mu\rho^{1/3}}$$

Finally:

$$\frac{M}{M_\odot} > 1.2 \times 10^{-10} \frac{T^{3/2}}{\mu^{3/2}} \rho^{1/2}$$

(.33)

Now let us consider the conditions that might be typical of the gas in intergalactic space or in a dense interstellar cloud and ask what this relation implies.

We will assume for the intergalactic medium that $\mu = 1$, $T = 10^4$ °K and $\rho = 10^{-28}$ gm/cm^3. Here we assume that the temperature is at least high enough to ionize hydrogen. The value of the density is an approximate smoothed out density of all the matter in the universe. Under these conditions we find that instability against gravitational contraction implies:

$$\frac{M}{M_\odot} > 1.2 \times 10^{10}$$

This is an interesting result in that observational evidence places the ranges of galactic mass between 10^9 and 10^{11} solar masses, although extreme cases do exist of 10^{12} solar masses. This result leads us to believe that perhaps the galaxies are themselves products of a gravitational instability in an intergalactic medium possessing approximately these general characteristics.

Now that we have established order of magnitude estimates of the mass of galaxies, let us consider their development in more detail, following the method of Hoyle (1953). His theory is outlined briefly below.

The key to Hoyle's galactic evolutionary theory lies in the thermal properties of hydrogen gas. Let us consider a hydrogen gas cloud with an initial density $\rho_0 = 10^{-27}$ gm./cm.^{3}. To estimate the temperature of the gas, we must realize that most cosmic objects have very large Reynold's numbers and hence the gas is likely to be turbulent, i.e. to develop mass motions. The energy of the mass motions becomes converted into heat. Hoyle estimates that certainly more than 10^{12} ergs/gm. and possibly more than 10^{14} ergs/gm. is made available in this way.

The thermal energy of atomic hydrogen is $\frac{3}{2}$ RT per gram, where R is the gas constant and T is the temperature (°K). Hence somewhat more than 10^{12} ergs/gm. is required to heat hydrogen from 0°K to 10,000°K. At this point ionization of the hydrogen sets in, and more than 10^{13} ergs/gm. is required to ionize hydrogen.

Hydrogen gas can radiate energy in three ways: (1), line emission, which will be neglected, (2), free-free transitions, in which unbound electrons make transitions between two states of the continuum, and (3), free-bound transitions, in which electrons are captured from a state of the continuum into a bound state of the hydrogen atom. The rate of hydrogen radiation from the latter two processes is

$$1.45 \times 10^{-27}\ T^{1/2} \left[1 + \frac{3.85 \times 10^{5}}{T}\right] N^{2}\ \text{ergs/cm}^{3}\ \text{sec.},$$

where N is the number of hydrogen atoms per cm.^{3} and T is the kinetic temperature in °K. This formula holds well only for T >25,000 °K. We see that the rate of radiation decreases until very large temperatures are reached.

From these properties of hydrogen gas we can see that the large mass of hydrogen gas with which we have to deal is likely to have a temperature of either close to

10,000 ^{o}K or greater than 10^5 ^{o}K. The reason for these two temperature calsses is that the time of development of a galaxy is of the order to 10^{17} seconds, and in this time hydrogen initially at temperatures $<10^5$ ^{o}K can cool by radiation until most of the hydrogen atoms have recombined with electrons.

Let us reconsider the case of a gas cloud at a temperature of 10,000^{o}K. The necessary condition for a gas cloud of uniform composition to be in thermal equilibrium, in the case where radiation pressure is negligible so that gravitational forces are balanced by gradients in the gas pressure, is that the total gravitational potential energy Ω (taken as positive) must be equal to twice the thermal energy of the gas. If Ω is greater than this then a spherical could will contract.

This inequality gives a lower limit to the mass of a gas of neutral hydrogen which can condense. For $M = \rho_o V = 10^{-27}V$, $M > 10^{10}$ solar masses is the minimum mass of hydrogen gas which can condense. During such condensation the thermal energy is quickly radiated away and the temperature remains at 10,000 ^{o}K. Hence the contraction of the gas takes place under isothermal conditions.

The thermal energy released in a uniform isothermal contraction from a volume V to a volume V' is

$$MRT \ln\left(\frac{V}{V'}\right) \tag{9.34}$$

The gravitation energy released by the contraction is of the order of

$$\frac{GM^2}{V^{1/3}} \left[\left(\frac{V}{V'}\right)^{1/3} - 1\right] \tag{9.35}$$

Now if the initial mass of the hydrogen gas cloud is large compared to the minimum, then it follows that (9.35) is large compared to (9.34), regardless of the value of V'. Hence in the contraction of such a cloud only a small part of the gravitational potential energy is converted into thermal energy, and the rest must go into mass motions which will be adequate to expand the cloud back to nearly its original dimensions. Such a cloud therefore cannot undergo appreciable contraction. However, such a cloud is also unstable to the fragmentation into subcondensations which have about the minimum mass consistent with (9.33). We may identify such a fragmentation process with the formation of a cluster of

galaxies, the subcondensations having a mass $\sim 10^{10}$ solar masses as noted above. These are about the masses of elliptical galaxies.

Let us now consider the condensation of a galaxy of this minimum mass. Expressions (9.34) and (9.35) remain comparable for $V' = 0.1V$; the former is still 30 percent of the latter for $V' = 10^{-3}V$, and it has fallen to 5 percent of the latter $V' = 10^{-6}V$. Hence there can be an almost complete dissipation of the energy of contraction for a decrease of linear dimensions of a factor 2 or 3, but further contraction is then prevented by the development of mass motions. However, after a contraction of linear dimensions by about a factor of 3, the galaxy is then unstable to a fragmentation into further subcondensations. These in turn can contract in linear dimensions by about a factor of 3, followed by further fragmentation, and so on. As the density of the subcondensations increases, the rates of contraction and radiation also increase. If a subcondensation contracts by a factor of $k^{2/3}$, and then divides into k equal masses having a radius equal to $1/k$ of that of the original subcondensation, and if many such stages of condensation

take place, then Hoyle points out that the time for all stages of condensation is, in units of that required for the first stage,

$$1 + \frac{1}{k} + \frac{1}{k^2} + \frac{1}{k^3} + \ldots = \frac{k}{k-1}$$

For $k^{2/3} \approx 3$, $k \approx 5$, and the time required for an infinity of steps is only 25 per cent longer than that required for the first step. Hoyle postulates that the condensation of the first step will take a time of the order of 10^{17} seconds, and since the fragmentation will really be a continuous process, very small subunits will be formed over the whole of this time scale.

The process of fragmentation will stop when the density of the subunits has become so large that they are opaque to their own radiation. Hoyle shows that such final subunits have masses which generally should lie in the range 0.3 to 1.5 solar masses, with some dispersion which will extend outside this mass range. After a galaxy has been fragmented into a hierarchical structure of subcondensations, these must fall toward the galactic center of gravity where the hierarchical structure will be broken up by mutual interactions. This causes a shrinkage of the dimensions of the galaxies. Occasionally certain

subcondensations will resist disruption, and it is tempting to identify these with the globular clusters.

Let us now consider a gas cloud which has a temperature initially in excess of 10^5 °K. The minimum mass required for condensation of this gas cloud is given by (9.33), with the effect of fully ionized hydrogen taken into account.

For $M = 10^{-27} V$ the minimum mass is 5×10^{11} solar masses. As contraction occurs the rate of radiation starts to exceed the rate of release of thermal energy, and eventually a point of temperature instability must be reached that swiftly reduces the temperature to 10,000 °K. Assuming that the linear dimensions have decreased by a factor of 5 before this occurs, then the first fragmentation of this gas cloud will be into dwarf galaxies with masses of about 3×10^8 solar masses. Further fragmentation will then occur as described above. These dwarf galaxies will collide with one another and most will be disrupted; some will escape into intergalactic space. We may identify the massive spiral galaxies with a formation process of this type.

Not all the gas in these galaxies will be formed into stars; there will be less tendency for condensation

in regions of smaller gas density. Such gas will contract to the center of the galaxy, or, if the galaxy has a fairly large amount of total angular momentum, then the residual gas will contract to a disk passing through the center of the galaxy. Further star formation can then take place.

Let us now consider what are the typical conditions in the interstellar medium. Again, for convenience, we choose $\mu = 1$. Now for the temperature of this gas we choose $T = 10^2$ °K, a figure that can be obtained both observationally and theoretically for a neutral gas. There are regions in the galaxy, particularly in the neighborhood of extremely hot stars, where the radiation from the star ionizes the hydrogen ($T \sim 10^4$ °K), but generally our figure is correct. Taking a value for the density, $\rho = 10^{-22}$ gm/cm^3 (equal to that in some of the denser interstellar clouds), we find that the condition for gravitational collapse becomes:

$$\frac{M}{M_\odot} > 1.2 \times 10^3$$

This result gives us a very basic clue to the understanding of the formation of stars. We cannot

expect any of the interstellar gas with a mass of the order of that of the sun to become gravitationally unstable and to contract to form a star. Single star formation is not to be expected. However, gas clouds of masses of the order of 10^3 or 10^4 solar masses can become unstable. By some means we must form stars of this gas.

Here is what might happen once such a cloud does begin to collapse. We know that the typical star in space does not have a mass of 1,000 or 10,000 solar masses. The largest that are known seem to lie somewhere in the range of 50-100 solar masses. We also know that there are clusters of stars in space; so it is not surprising that this model could give rise to dense clusters of stars. We also see associations of stars in space which have a few very bright stars included among them (O and B stars according to the spectral classification). These associations are observed to be expanding, that is, the O and B stars are usually observed to be leaving some central region. If their motions are projected back one finds that in a typical case the stars in an association may have been

at a common point approximately 1 to 3 million years ago. This time also happens to be comparable to the lifetime of the O and B stars on the main sequence. Thus observationally one can see that stars do form in clusters which are not stable. Once having formed, the stars then expand into space. One obvious way in which a star cluster might be unstable is if all of the original gas does not form stars. If some stars are formed and their surface temperature rises enough so that they can ionize the residual gas in the cluster and cause that gas to become hot enough to expand out of the region of the cluster, then the remaining mass in the form of stars would no longer be gravitationally bound. If, however, most of the gas went into stars, those stars would be gravitationally bound for the very reason that the initial gas cloud out of which they were formed became gravitationally bound. Thus, if most of the gas goes into stars there results a stable star cluster. If only a part of the gas goes into stars, then an unstable cluster results, that is, an association that will expand resulting in the presence of individual stars in space as in fact we observe most of the stars to be.

The essential point in the formation of single stars of mass comparable to that of the sun out of a cloud that starts out with a large mass is the following. Once such a cloud of gas begins to contract, the density increases; the rate of collisions between constituents also increases, approximately as the square of the density. It is these collisions which provide all the cooling mechanisms in that cloud. Consequently as the cloud contracts the cooling becomes more efficient and we will prevent the temperature from rising during the collapse itself. It can be seen that when we apply the virial theorem to a subunit of this cloud, keeping the internal energy in the form of heat about the same per gram, and increasing the gravitational potential energy in absolute magnitude per gram as the contraction continues, then smaller and smaller subunits of the gas will themselves become gravitationally bound. Hence, as contraction continues and as the temperature does not rise appreciably, the cloud can be expected to fragment into smaller and smaller masses each of which will individually become gravitationally stable. In principle this fragmentation will continue until the individual fragments become

so opaque to their own radiation that, despite the increased efficiency of the cooling-radiative processes, the radiation produced will not be able to escape and the temperature must start rising. Once that condition is satisfied, i.e., once the gas comes opaque to its own radiation, then we might expect the fragmentation process to stop. When one examines the relevant numbers one finds that the fragments should become opaque to their own radiation when their mass is approximately equal to that of the sun. In this way we can account for the major features of observational astronomy in the form of galaxies, clusters of stars, and individual stars.

There is one last aspect which involves a consideration of the virial theorem. When a final fragment has formed which is opaque to its own radiation, the central temperature must rise more and more. When the temperature exceeds 1800°K the hydrogen molecules forming this fragment start to become dissociated for the most part. Quite a bit of energy is necessary to dissociate these hydrogen molecules, which means that the temperature cannot rise very much above 1800° until those hydrogen molecules have been dissociated. The amount of energy required to

dissociate the hydrogen molecules forming any final fragment is in general, much more than the gravitational potential energy that is available. This leads to a region of gravitational instability entirely apart from the conditions we had previously. Instead of getting rid of most of energy gained from the contraction by radiating it away into space, it is now being used to dissociate hydrogen molecules and hence the collapse must continue. During the time that the dissociation of the hydrogen molecules is going on, the γ for the gas falls below 4/3. This is then an example for the other condition for gravitational instability, namely that in a case where γ is less than 4/3, the contraction of a body does not raise the pressure at a rate rapid enough to allow that body to remain in hydrostatic equilibrium.

Actually we do not achieve stability when we have finished dissociating the hydrogen molecules because we find that by this time the temperature has approached 5,000 to 8,000° K and we have started to ionize the hydrogen atoms. This requires even more energy. Furthermore, by the time we have really stopped ionizing the hydrogen atoms throughout most of the volume of our

fragment, the temperature is high enough to start ionizing helium in the first stage. By the time helium is singly ionized throughout most of the fragment, it is doubly ionized at the center. We do not really have a star formed until the hydrogen and helium are almost completely ionized throughout most of the fragment.

In the case of a body such as the sun, it turns out from some models that have recently been calculated that the radius must become less than 57 times the present radius of the sun before a final body can be formed and be stable in hydrostatic equilibrium.

10. Physical conditions in Stellar Interiors

General Remarks

Efforts have been made for many years to determine the physical conditions at various points in stellar interiors. These attempts have improved with the passage of time and the more realistic inclusion of various physical effects in the theory. The development of the subject has been governed by the fact that the differential equations describing the stellar interior are non-linear. Thus some elegant mathematical analyses have been developed which enable stellar models to be computed using analytic approximations to certain physical properties; these models have the nice property that computations for one assumption of mass and luminosity can be transformed to other values of mass and luminosity by using certain dimensionless variables in the calculations.

There are four basic differential equations which govern the conditions in stellar interiors. The first of these is that concerned with the condition of hydrostatic equilibrium. In most main sequence stars atoms in the interior are largely stripped of electrons and hence the gas may be said to obey perfect gas laws, except under conditions of very high densities ($>10^4$ gm/cm^3) where electron degeneracy sets

in. Let us consider, then, a thin spherical shell of radius r, thickness dr about the center of the star. Spherical symmetry will be assumed. Let P be the pressure at r and let the increment in P as we proceed from r to r + dr be dP. The difference in pressure dP represents a force, -dP, acting on a mass element of unit cross-section, in the direction of increasing r. This force must be balanced by the force of gravitational attraction to which the mass element is also subjected. If we define M(r) as the mass included within a radius r and $\rho(r)$ as the density in the layer in question then by Newton's Law, the attractive force between the mass element $\rho(r)dr$ and M(r) is given by $G\,M(r)\rho dr/r^2$. Hence, the condition for hydrostatic equilibrium may be written:

$$-dP = \frac{G\,M(r)\rho dr}{r^2}$$

$$\frac{dP}{dr} = -\frac{G\,M(r)\rho}{r^2} \qquad (10.1)$$

Now, from our definition of M(r) we can write:

$$M(r) = \int_0^r 4\pi r^2\,\rho(r)\,dr$$

Hence, the conservation of mass within the star may be written in the form:

$$\frac{d\,M(r)}{dr} = 4\pi r^2\ \rho(r) \qquad (10.2)$$

This is the second of the differential equations which govern conditions in stellar interiors.

The energy flow at the surface, or more generally at a radius r, for a star, as measured by the luminosity of the star, is provided by the release of energy in the various nuclear reactions going on within the interior, or by gravitational contraction. Thus, if ε is the energy released per unit mass per unit time, the energy loss through a spherical shell at radius r is given by:

$$L(r) = \int_0^r \varepsilon\ \rho(r)\ 4\pi r^2\ dr$$

Thus, the conservation of energy within a star may be written in the form:

$$\frac{dL(r)}{dr} = 4\pi r^2\ \rho\ r)\varepsilon \qquad (10.3)$$

where L(r) is the net outward energy flux.

The fourth differential equation we wish to obtain is

one which describes the transport of energy in the stellar interior. In general there are three methods by which energy transport might take place; by conduction, convection, and radiation. All of these modes of energy transport are of importance in some aspect of the theory of stellar interiors. Conduction is, however, only important in cases of electron degeneracy. We will not be concerned with this problem at the present. Radiation is important in situations in which the temperature gradient is not very great, while convection becomes increasingly important as the temperature gradient is increased.

Energy transport by radiation takes place more rapidly for large temperature gradients than for small. It is impeded by high densities and high opacities of the material through which it must pass. These conditions are expressed in an equation for the temperature gradient necessary to transport a given flux of energy (Chandrasekhar 1939, Schwarzschild 1958):

$$\frac{dT}{dr} = -\frac{3}{4ac}\frac{K\rho(r)}{T^3}\frac{L(r)}{4\pi r^2} \qquad (10.4)$$

In this expression T is the temperature in ^{o}K, a is Stefan's

radiation constant, c is the velocity of light and K is the opacity of the material, that is, the mass absorption coefficient in cm^2/gm.

Let us now consider when energy transport by convection will take place. For this, consider a volume element of the gas which we will take to be large enough that adiabatic conditions will hold if we give this element a sudden upward displacement. In this displacement pressure equilibrium will be maintained. But under adiabatic conditions we have

$$\rho \propto P^{1/\gamma}$$

where γ is the ratio of the specific heats. Thus as this element of gas rises within the star it must expand to remain in pressure equilibrium with its surroundings. If the density of the mass element is less than its surroundings as it rises the element will continue to rise and hence that region of the star will be unstable to the onset of convection. If, on the other hand, the rising mass element becomes more dense than its surroundings, clearly there will be a downward force exerted on it and the element will return to its initial position. The condition for stability against convection then is that the actual pressure gradient in the star must be less than that corresponding to a density gradient in adiabatic equilibrium. The steeper one makes

the temperature gradient, the more one goes from the situation in which the rising mass element is denser than its surroundings to that where it is lighter than its surroundings. Once the adiabatic temperature gradient is exceeded by the actual temperature gradient within the star, then the structure becomes unstable against convection.

Now, under adiabatic conditions the temperature varies with the pressure according to the relation

$$T \propto P^{(\gamma-1)/\gamma}$$

A rising volume element having a smaller density than its surroundings will thus have a temperature excess. At higher levels it loses its excess heat by viscous effects and by radiation. This energy transport will very quickly reduce a very steep temperature gradient until it is close to the limiting adiabatic gradient. Hence, it may be seen that for steep temperature gradients, nearly all transport of energy is by convection; while for temperature gradients lower than the adiabatic value the energy transport is entirely by radiation. Thus for the case of convective equilibrium we have the adiabatic condition holding in the star to a good approximation:

$$\frac{1}{P}\frac{dP}{dr} = \frac{\gamma}{\rho}\frac{d\rho}{dr} \tag{10.5}$$

In general we can expect convection to be important near the centers of stars where thermonuclear energy generation, which often varies as a high power of the temperature, tries to establish a steep temperature gradient. Farther away from the center of a star where energy generation is not important the temperature gradient becomes less and energy transport is by radiation. However, convection can also set in in a region where a major constituent of the gas is partly ionized. As a volume element of the gas rises in such a region recombination takes place. This heats the volume element which continues to rise until the major constituent has become nearly all recombined. This process is responsible for establishing outer convection zones in stars where hydrogen is partly ionized.

Convection is an extremely efficient means of transporting energy because, with the typical velocities for convection in stellar interiors, we may bring matter through distances of the order of the radius of a star in a matter of hours to days. Because of this tremendous efficiency of convection in general, in our calculations concerning stellar structure we can usually assume that the temperature gradient is that which corresponds to an adiabatic displacement. Actually, if the temperature gradient were exactly

equal to that for an adiabatic displacement, the rising element would remain in both density and pressure equilibrium with its surroundings, and clearly would carry no energy. If, however, we make the temperature gradient just very slightly super-adiabatic, then the element when it reaches the top of its motion would be hotter than its surroundings. It would then cool by radiation. Thus we see we have transported energy from the center of the star rather efficiently.

At the surface of stars there must be a transition from energy transport by convection to energy transport by radiation, as obviously energy cannot be transported by convection into space. In the transition region we must somehow take into account energy transport by radiation and convection simultaneously. The equation governing this situation must demand that the flux remain constant, where the flux is calculated from the sum of that carried by radiation and of that carried by convection.

We now need to consider some auxiliary equations--first of all is the Gas Law. Normally, matter in the laboratory, achieves a density of a few grams per cm^3, and then becomes very resistant to compression, simply because the electron structures of the atoms become so close together that they

are essentially touching. Deep in the interior of a star, the atoms are completely ionized and the typical dimensions of the nuclei which are thus exposed are something closer to 10^{-13} cm. rather than the roughly 10^{-8} cm. which are typical of atoms. Hence, there is plenty of room for the electrons and the ions, and the perfect gas law becomes valid until we reach very high densities; the condition that negates use of the perfect gas law is the setting in of electron degeneracy. For the perfect gas case

$$P = \frac{kN_0 \rho T}{\mu}, \tag{10.6}$$

where μ is the mean molecular weight.

If the star in question is sufficiently massive, radiation pressure may become important in which case,

$$P_r = \frac{1}{3} aT^4 . \tag{10.7}$$

In order to apply equation (10.4), that is the equation governing L(r), one must know the form for the mass absorption coefficient. For the case of absorption and emission due to atomic processes, one must consider the energy level structure of the atom, that is, the sequence of bound discrete states merging into the continuous spectrum past the ionization

limit. In this case we may talk about transitions between bound states (bound-bound), and between the continuum and bound states (bound-free, free-bound). Clearly the bound-bound transitions that can absorb energy within the stellar interiors must be exceedingly hard to calculate, because there are so many different bound states and different atoms. There is no easy way to generalize the energy level spacing. One must resort to computer techniques; by knowing all the atoms and all the bound states under consideration, fixing a temperature and density, one may calculate the distribution of atoms in their bound states and among the various degrees of ionization by statistical equilibrium considerations, and then calculate what all the transitions are within this array. People are actually doing this, because of their desire to get these opacities as accurately calculated as possible, but clearly it is exceedingly difficult to do from a numerical point of view, and this effect is not the most important source of opacity, but is a correction to the opacity which one gets from the other processes. In the deep interior of the star, most of the opacity seems to come from bound-free transitions, not of hydrogen and helium which are completely ionized, but of some of the heavier atoms, such as the carbon-nitrogen-oxygen series or the still heavier atoms

of silicon, sulfur, argon, calcium, iron and so on. The importance of heavy ions is emphasized by the fact that the cross section varies as Z^4 for bound-free transitions.

The free-free transitions are those which occur in the continuous state. The cross section for free-free transitions is largest when involving those states which lie closest to the ionization edge, varies as Z^2, and is largest for small energies.

There are other processes which contribute to the opacity, such as electron scattering (Compton, Thompson scattering), the cross section for which is

$$\sigma = \frac{8\pi e^4}{3m^2c^4}$$

The above are the processes that are of greatest importance for opacity deep in the interior of the star. As we get closer to the surface, other things can become of much greater importance. For example, when the temperature becomes low enough so that we can have molecules, we can then have absorption by molecular lines, molecular bands, etc., which is once again a complicated calculational process. We can also have Rayleigh scattering by the atoms. There also are a number of other minor processes, the most important one is the scattering by the negative hydrogen

ion, H^-, that is, an ordinary hydrogen atom to which an extra electron has become attached, very loosely bound. There can be both bound-free and free-free transitions of the negative hydrogen ion. These account for the majority of the absorption processes at temperatures around a few tens of thousands of degrees. The importance of the process really goes with the abundance of the negative hydrogen ions that one can have. Though hydrogen is the most abundant constituent of the stellar interior, the amount of H^- we can have depends upon the availability of the electrons. If we have too high a temperature, then not only do we prevent any appreciable amount of H^- from existing in equilibrium, but we even start to ionize the hydrogen itself. If we have the temperature too low, then all the heavier metals with low ionization potentials (the most important of which, for example, is potassium which has an ionization potential of only 4 electron volts) all become neutral and there are not extra electrons around which can be captured by the hydrogen atoms. There is thus clearly a peak in the temperature range at which negative hydrogen ion absorption is most important.

Much of the classical analysis of stellar interiors makes use of an approximate formula that fits many of the processes at higher temperatures. This formula was developed by Kramers and reads

$$K = \text{constant} \times \rho T^{-3.5} \tag{10.8}$$

The form is adequate for a first look at problems in stellar structure but does not do for more realistic calculations.

Figure 10.1 shows the behavior of the opacity in a stellar interior for various densities and temperatures. The peak in the opacity curves tends to come in the region where many stars have outer convection zones. The low temperature end is shown in more detail in Figure 10.2. These figures contain the results of fairly elaborate calculations carried out with a computer code developed at the Los Alamos Scientific Laboratory by A.N. Cox and his collaborators. The composition assumed in the calculations is approximately the solar composition discussed in section 10 of these notes.

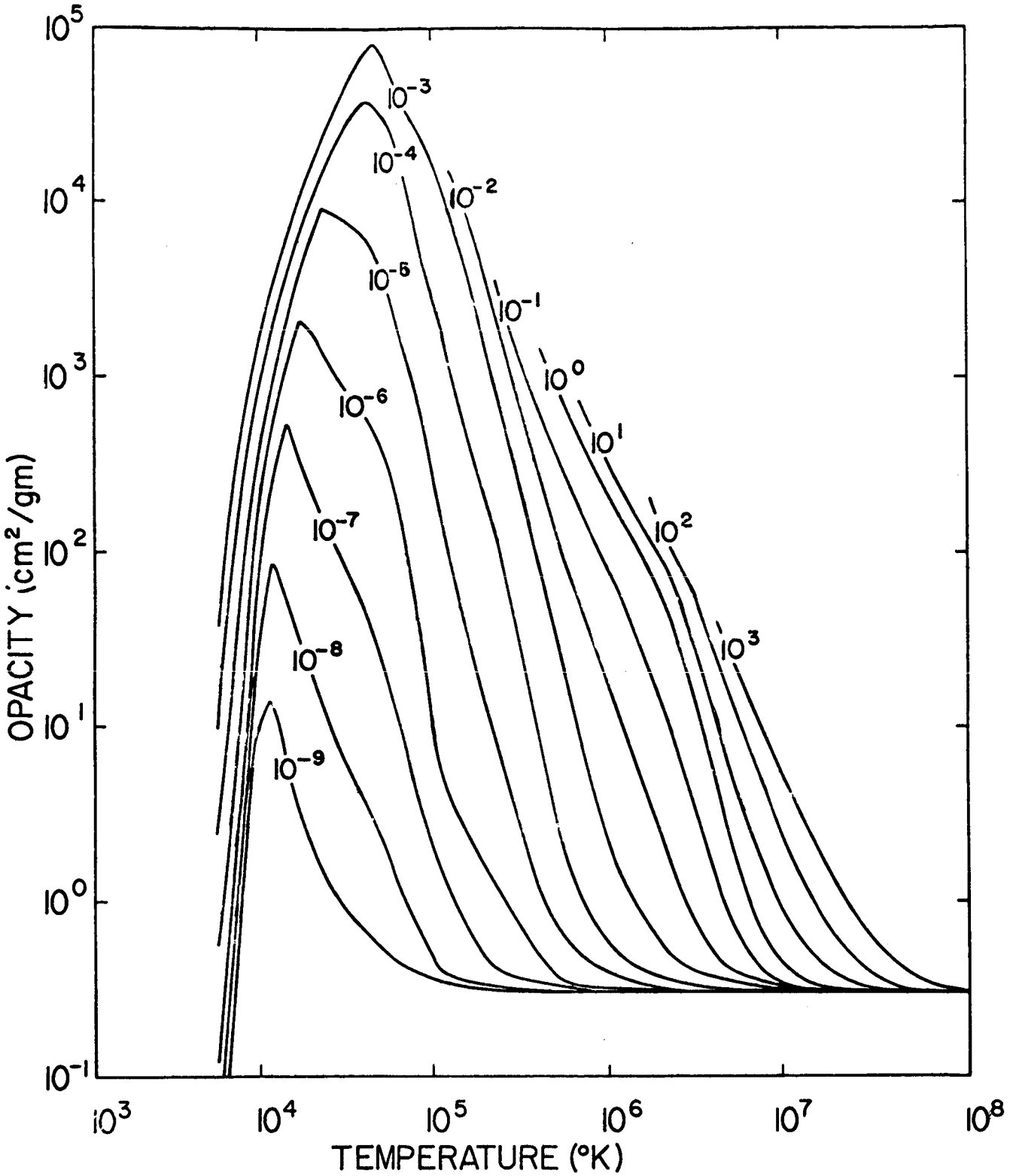
OPACITY (cm²/gm)
TEMPERATURE (°K)
10⁵
10⁴
10³
10²
10¹
10⁰
10⁻¹
10³
10⁴
10⁵
10⁶
10⁷
10⁸
10⁻³
10⁻⁴
10⁻²
10⁻⁵
10⁻¹
10⁰
10⁻⁶
10¹
10⁻⁷
10²
10⁻⁸
10³
10⁻⁹

Figure 10.1

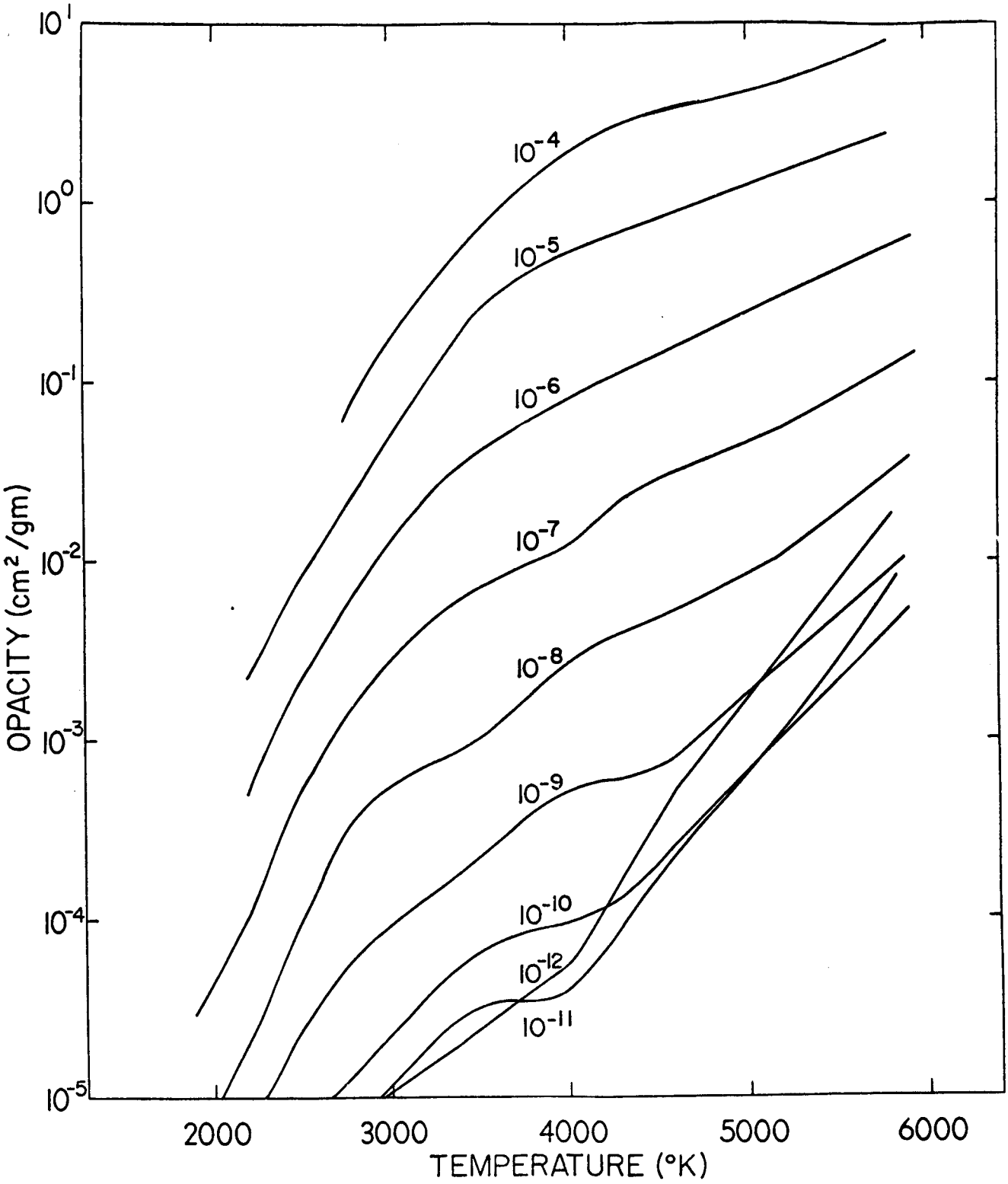
10^1
10^0
10^{-1}
10^{-2}
10^{-3}
10^{-4}
10^{-5}
OPACITY (cm²/gm)
10^{-4}
10^{-5}
10^{-6}
10^{-7}
10^{-8}
10^{-9}
10^{-10}
10^{-12}
10^{-11}
2000
3000
4000
5000
6000
TEMPERATURE (°K)

Figure 10.2

Electron Degeneracy

As mentioned before, the use of the perfect gas law becomes inappropriate when high densities are encountered (e.g. 10^6 gm/cc at temperatures $\sim 10^7$ °K). For a perfect gas one expects the usual Maxwell-Boltzmann distribution law to hold for both ions and electrons present in the stellar mixture. This assumes that there are no explicit restrictions on the energy or momentum of a given particle. For the case of a very dense electron gas, however, the Pauli exclusion principle put an upper limit on the number of electrons which may occupy a given "volume" of momentum space. This restriction is expressed as follows:

$$N(p)\ dp = \left(\frac{2}{h^3}\right) 4\pi p^2 dp \tag{10.9}$$

where N(p) is the number of electrons per unit volume of space in the momentum interval p to p + dp. The factor of two arises from the two possible spin orientations. The constant h is Planck's constant.

We may compare this to the equivalent Maxwellian distribution,

$$N(p)\ dp = \frac{N_e}{(2\pi mkT)^{3/2}}\ e^{-p^2/2mkT}\ 4\pi p^2\ dp \tag{10.10}$$

where N_e is the number density of electrons, and

$$N_e = \frac{\rho N_o}{\mu_e} \tag{10.11}$$

where μ_e is the mean molecular weight per electron.

If the exponential factor in equation 10.10 is not too different from unity, and

$$\frac{N_e}{(2\pi mkT)^{3/2}} > \frac{2}{h^3}$$

then there is a violation of the Pauli principle and the perfect gas law will not hold. This condition may be rewritten as,

$$\rho > \frac{2(2\pi mkT)^{3/2}}{h^3} \quad \frac{\mu_e}{N_o} = 8.1\text{x}10^{-9} \ \mu_e T^{3/2} \tag{10.12}$$

As an example consider the case when $\mu_e = 2$ which holds for mixtures of predominately heavy elements, and $T=10^8$ °K. We then have a violation when $\rho > 1.62\text{x}10^4$gm/cc.

An important case arises when the temperature of the electron gas is zero. In this case all the electrons will have completely filled all the lowest energy states available. Clearly then there is some maximum momentum p_o such that no electrons will have moments above p_o. That is

$$N(p)dp = \left(\frac{2}{h^3}\right) 4\pi p^2 dp \qquad , \quad p \leq p_o$$

$$N(p) = o \qquad , \quad p > p_o .$$

If N(p) is integrated from p=o to $p=p_o$ the result will be N_e, that is

$$N_e = \frac{8\pi}{h^3} \int_o^{p_o} p^2 dp = \frac{8\pi}{3h^3} p_o^3 \quad , \text{ or}$$

$$p_o = \left[\frac{3h^3}{8\pi} N_e\right]^{\frac{1}{3}}$$

(10.13)

The energy corresponding to p_o is called the Fermi energy. The pressure due to this completely degenerate gas is given by

$$P = \frac{\pi m^4 c^5}{2h^3} f(x) = 6.01 \times 10^{22} f(x),$$

(10.14)

where

$$f(x) = x(2x^2-3)(x^2+1)^{1/2} + 3 \sinh^{-1} x,$$

(10.15)

and

$$x = \frac{p_o}{mc} .$$

For $x \to \infty$ (extreme relativistic momenta),

$$f(x) \sim 2x^4 - 3x^2 + \ldots \qquad , \quad (x \to \infty).$$

(10.16)

For $x \to o$ (non-relativistic)

$$f(x) \sim \frac{8}{5} x^5 - \frac{4}{7} x^7 + \frac{1}{3} x^9 - \frac{5}{22} x^{11} + \ldots \quad (x \to o)^*.$$

Chandrasekhar (page 393, loc. cit.) finds that a necessary and sufficient condition for the setting in of degeneracy is

$$\frac{4\pi^2}{(mc^2/kT)^2} \quad \frac{x(x^2 + 1)^{1/2}}{f(x)} << 1$$

In a crude sense let the boundary between degenerate and nondegenerate matter be given by,

$$\frac{4\pi^2}{(mc^2/kT)^2} = \frac{f(x)}{x(x^2+1)^{1/2}} \quad .$$

As an example of how the above considerations affect the course of stellar evolution, consider the evolutionary track for stars whose internal pressure was given by the perfect gas law which was found earlier, and was given (for a uniform gas sphere) by,

$$T = 4.1 \times 10^6 \; M^{2/3} \; \rho^{1/3} \mu \quad {}^\circ K,$$

where M is solar mass units. If the star is in some relatively late stage of evolution we may expect large abundances of nuclear reaction products to be present.

---

* For a more complete treatment and derivations of the above, along with a tabulation of f(x) see Chandrasekar, Introduction to Study of Stellar Structure, Chapter 10.

Let us suppose this is the case. An approximate form for μ is given by

$$\mu = \frac{1}{(X/\mu_x) + (Y/\mu_y) + (Z/\mu_z)}$$

$$= \frac{2}{1 + 3X + 0.5Y} \qquad (10.17)$$

where

X = abundance of hydrogen by weight

Y = abundance of helium by weight

Z = 1-X-Y = abundance of heavier elements by weight.

For the case under consideration, X = Y = 0, and $\mu = 2$.

An approximate form for μ_e is

$$\mu_e = \frac{2}{1 + X} ,$$

which for our case equals two*.

We thus have $N_e = \frac{\rho N_o}{2}$.

The evolutionary track given does not hold for those stars whose internal pressures are predominately governed by the pressure of radiation. We define the boundary line between stars whose internal conditions obey the

---

* See Chandrasekhar loc. cit. p 254 et. seq. for a fuller treatment of the μ's.

perfect gas law and those whose internal conditions are regulated by radiation by an equality of pressures for the two cases, i.e.,

$$\frac{1}{3} aT^4 = kNT = \frac{kN_o T}{\mu} ,$$

or

$$T = 2.55 \times 10^7 \rho^{1/3} .$$

The track line corresponding to this condition occurs at 5.5 solar masses. For stars heavier than this, radiation pressure is predominant. In such a case we say $\gamma = 4/3$ and the relation $U = -\Omega$ is valid. Thus,

$$U = VaT^4 = \frac{3}{5} \frac{GM^2}{R} ,$$

and making the appropriate substitutions the track equation becomes,

$$T = 1.92 \times 10^7 \times M^{1/6} \rho^{1/3} .$$

We note that the temperature depends on density as before (to the 1/3 power) but the effect of mass is less pronounced.

The relevant tracks are plotted in Figure 10.3 and illustrate the behavior derived above. Again, the cutoff between perfect gas and radiation occurs at a mass of 5.5 solar masses.

We now continue with our analysis of the degenerate case.

The value of p_0 can be computed and thus f(x) ascertained. The boundary of degeneracy in terms of ρ and T can be found from

$$T = \left(\frac{f(x)}{x(x^2 + 1)^{1/2}}\right)^{1/2} \frac{mc^2}{4\pi^2 k} \quad .$$

If this boundary is plotted on the same graph as the evolutionary tracks for stars of various mass Figure 10.3 is obtained. We note that stars of mass less then about 1.3 enter the degenerate region. For these stars the pressure due to degenerate electrons is so high that further compression is not then possible. This is essentially the end point in the evolution of a star of small mass. It settles down to become a white dwarf, achieving in this process some maximum temperature which depends specifically on its mass. For example, a star of one solar mass might achieve a maximum temperature of 10^9 °K.

For a completely degenerate white dwarf there is an upper limit on the mass of about 1.4 solar masses. This comes about because for degenerate stellar configurations above the mass limit it is found that the gravitational force will always exceed the pressure force due to degeneracy independent of the radius of the star. The

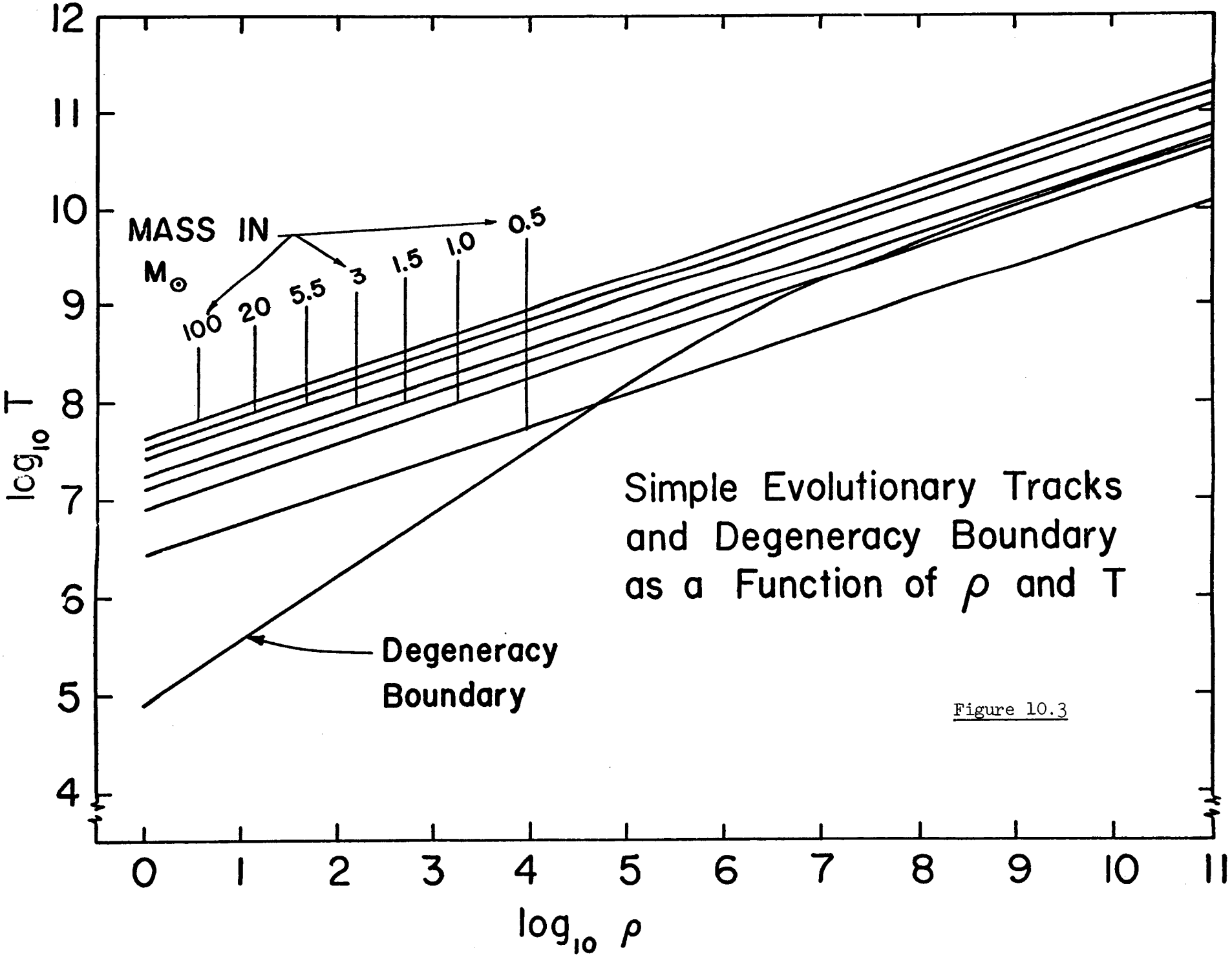

Simple Evolutionary Tracks and Degeneracy Boundary as a Function of ρ and T

Figure 10.3

star will then be unable to attain an equilibrium configuration unless it rids itself of some mass. The limiting mass condition is given roughly by,

$$M < \frac{5.756}{\mu_e^2}$$

solar masses. Thus, for $\mu_e = 2$, $M < 1.44$. For the case of large stars such as red giants it is observed that many are ejecting mass. If these stars are to become white dwarfs they must reduce to the white dwarf limit. This is a potential source of stellar catastrophe.

A further point in connection with Figure 10.3 is the form of the degenerate boundary curve. One notes that there appear to be two asymptotes - one for low ρ and one for high ρ. These are related to the form of the gas law for large and small x, i.e.,

$$P = \frac{1}{20}\left(\frac{3}{\pi}\right)^{\frac{2}{3}} \frac{h^2}{m} N_e^{5/3} \qquad (x \to o)$$

$$P = \frac{1}{8}\left(\frac{3}{\pi}\right)^{1/3} hc \; N_e^{4/3} \qquad (x \to \infty) \quad .$$

A more complete treatment of some of the above problems requires a more sophisticated picture of stellar structure.

Polytropes

As was discussed in previous sections the pressure at the center of a star is usually very high. This high pressure may be obtained by having a high density and low temperature or a low density and a high temperature at the center. Which one of these two combinations holds in the center is a matter for detailed investigation. One can, nevertheless, make a considerable investigation of the properties of stellar interiors by assuming a specific relation between the pressure and the density, and saying that the temperature must be whatever is necessary to satisfy that relation throughout the star according to whatever gas law holds.

The theory of polytropes was built up early in the century by making the assumption that the pressure P is related to the density at any point by

$$P = K \rho^{\gamma} \quad .$$

We associate γ with the polytropic index n by the relation $n = \frac{1}{\gamma-1}$. From the above we have

$$\frac{1}{P} \frac{dP}{dr} = \frac{\gamma}{\rho} \frac{d\rho}{dr} \quad ,$$

which is the equation for convective equilibrium.

For the case n = 3, one finds that this leads to conditions which closely resemble the case of stars in radiative equilibrium.

If we now consider two of the equations for equilibrium as

$$\frac{dP}{dr} = -\frac{GM(r)}{r^2}\rho$$

with,

$$M(r) = \int_0^r 4\pi r^2 \rho dr,$$

then we find

$$\frac{1}{r^2}\frac{d}{dr}\left(\frac{r^2}{\rho}\frac{dP}{dr}\right) = -4\pi G\rho \quad .$$

If we let $\rho = \lambda\theta^n$, where λ is a constant and θ plays the role of a temperature, then

$$P = K\rho^{(1+n)/n} = K\lambda^{(1+n)/n}\theta^{n+1} \quad .$$

Making the appropriate substitutions we find,

$$\left[\frac{(n+1)K}{4\pi G}\lambda^{\frac{1}{n}-1}\right]\frac{1}{r^2}\frac{d}{dr}\left(r^2\frac{d\theta}{dr}\right) = -\theta^n ,$$

If we define the dimensionless variable ξ as

$$r = \xi\alpha \quad , \text{ where}$$

$$\alpha = \left[\frac{(n+1)K}{4\pi G}\lambda^{\frac{1}{n}-1}\right]^{\frac{1}{2}} ,$$

then we obtain the "Lane-Emden equation of index n",

$$\frac{1}{\xi^2} \frac{d}{d\xi}\left(\xi^2 \frac{d\theta}{d\xi}\right) = -\theta^n \quad .$$

The boundary conditions are given by letting λ be the density at the center of the star so that θ is equal to unity at the origin. If we substitute

$$P = K\lambda^{1+\frac{1}{n}} \theta^{n+1}$$

into the equilibrium condition for the pressure we find

$$\lambda^{1+\frac{1}{n}} (n+1) \frac{d\theta}{dr} \theta^n = -\frac{GM(r)}{r^2} \rho \quad ,$$

so that at the origin,

$$\theta = 1, \qquad r = o = \xi$$

and

$$\frac{d\theta}{dr} = 0 \qquad , \qquad r = o = \xi \quad .$$

The condition at the stellar boundary is that the radius of the star is given by the smallest value of ξ for which ρ and hence θ is equal to zero.

The actual solutions for arbitrary n must, in general be carried out numerically*.

The numerical solutions are usually started by considering a series solution for $\xi<1$, that is

$$\theta = 1 - \frac{1}{6}\xi^2 + \frac{n}{120} \xi^4 - \ldots, \qquad \xi \ll 1.$$

---

* An exhaustive discussion of the Lane-Emden equation and its solutions are given in Chandrasekhar's book on stellar structure.

For a polytrope in hydrostatic equilibrium one finds that the gravitational potential energy is given by

$$-\Omega = \frac{3}{5-n} \frac{GM^2}{R}$$

In the case n=0 this corresponds to the a uniform sphere as discussed before. The maximum value of n is that corresponding to a sphere which is infinitely condensed, that is n=5. Values between zero and five therefore represent possible configurations. The polytropic index is then a measure of density distribution of the sphere. For two values of n, namely 1.5 and 3 one obtains the following for the ratio of the central density to the average density;

$$\rho_c/\bar{\rho} = 5.99 \quad , \quad n=1.5$$

$$\rho_c/\bar{\rho} = 54.18 \quad , \quad n=3 \quad .$$

Some interesting conditions obtain at stellar centers for the convective equilibrium (n=1.5) and approximate radiative equilibrium (n=3) cases.

In the case of convective equilibrium, n=1.5 and $\gamma = \frac{5}{3}$, which is the case for a perfect gas. Thus

$$P = K\rho^{5/3} = NkT \quad .$$

At the center this becomes,

$$P_c = K\rho_c^{5/3} = NkT_c \quad ,$$

or,

$$K = Nk \frac{T_c}{\rho_c^{5/3}} = \frac{N_o kT_c}{\mu \rho_c^{2/3}}$$

The pressure at the center may also be related to the mass and radius of the star*. These relations yield,

$$T_c = 9.62 \times 10^6 \rho^{1/3} M^{2/3} ,$$

where M is in solar masses and T_c is the temperature at the center. This is to be compared with the results obtained previously for the case of a uniform star. In this instance we note that the dependence of T_c on ρ and M is the same except that the numerical factor is somewhat greater.

Similarly, if the star in question is in radiative equilibrium then

$$T_c = 1.98 \times 10^7 M^{1/6} \rho^{1/3} ,$$

which is practically the same as for the case of a uniform star derived previously.

---

* Chandrasekhar, loc.cit., p 99, equations 79 - 81.

11. Thermonuclear Reaction Rates

As indicated in the introduction the energy source for stellar interiors is due to thermonuclear reactions. These are of many types and involve the many species of nuclides found in stellar interiors. This section will discuss some preliminary aspects of thermonuclear reactions which will be needed for detailed studies.

The ions in stellar interiors are found to be non-degenerate in almost all cases. That is, they have a velocity distribution which is Maxwellian. Some degenerate cases have been postulated ("neutron stars") but these have not been observed to date. We shall find that reactions take place at energies of 5 - 10 kT or more.

We shall be primarily concerned with two kinds of reactions, namely resonant and non-resonant thermonuclear reactions.

Non-resonant Reactions

Given two nuclear species, denoted by subscripts 1 and 2, with number densities n_1 and n_2, the number of reactions per unit volume per second r is given by

$$r = n_1 \, n_2 \, \langle \sigma v \rangle \, ,$$

where $< \sigma v >$ is the average value of the product of the reaction cross section (as a function of velocity) and the relative velocities of the nuclei.

The quantity $< \sigma v >$ is then given by

$$< \sigma v > = \frac{\int_0^\infty \sigma(v)\ v\ N(v)dv}{\int_0^\infty N(v)dv},$$

where $N(v)$ is the number density of nuclei having relative velocities v.

For reaction rates between like species,

$$r = \tfrac{1}{2}n^2 < \sigma v >.$$

If $n_1(\vec{v})$ and $n_2(\vec{v})$ are the velocity distribution functions for the two types, then the reaction rate may be expressed as,

$$r = \iint n_1(\vec{v})\ n_2(\vec{v})\ |\vec{v}_1 - \vec{v}_2|\ \sigma(\vec{v}_1 - \vec{v}_2)\ d^3\vec{v}_1\ d^3\vec{v}_2\ ,$$

where the integrals are over both velocity spaces.

If we assume a Maxwell distribution of velocities, that is

$$N(v)dv = \left(\frac{m}{2\pi kT}\right)^{3/2} \exp\left(-\frac{mv^2}{2kT}\right) 4\pi v^2 dv,$$

then

$$r = n_1 n_2 \frac{(m_1 m_2)^{3/2}}{(2\pi kT)^3} \iint d^3\vec{v}_1\ d^3\vec{v}_2\ |\vec{v}_1 - \vec{v}_2|\ \sigma(\vec{v}_1 - \vec{v}_2) \times$$

(cont.)

$$\times \exp - \left[\frac{m_1 v_1^2 + m_2 v_2^2}{2kT} \right]$$

It is convenient to change to center of mass coordinates at this point, that is

let $\vec{v} = \vec{v}_1 - \vec{v}_2$ for the relative velocity

and (the center of mass velocity)

$$\vec{V} = \frac{m_1 \vec{v}_1 + m_2 \vec{v}_2}{m_1 + m_2}$$

so that

$$\vec{v}_1 = \vec{V} + \frac{m_2}{m_1 + m_2} \vec{v}, \text{ and}$$

$$\vec{v}_2 = \vec{V} - \frac{m_1}{m_2 + m_1} \vec{v} .$$

Therefore we may write,

$$\frac{m_1 v_1^2 + m_2 v_2^2}{2kT} = \frac{(m_1 + m_2) V^2}{2kT} + \frac{1}{2kT} \frac{(m_1 m_2) v^2}{(m_1 + m_2)} .$$

The integral over $d^3\vec{V}$ and over the solid angle in $d^3\vec{v}$ can be carried out immediately. This gives

$$r = n_1 n_2 \, 4\pi \left(\frac{m_1 m_2}{2\pi kT \, (m_1 + m_2)} \right)^{3/2} \int_0^\infty dv \, v^3 \, \sigma \, (v) \exp - \left(\frac{m_1 m_2}{m_1 + m_2} \right) \frac{v^2}{2kT} .$$

At low bombarding energies and far away from resonances nuclear reaction cross sections can be expressed in the form:

$$\sigma = \frac{S}{E} \exp\left(- \frac{2\pi e^2 Z_1 Z_2}{hv}\right)$$

where E is the relative energy which corresponds to the velocity v, e is the electronic charge and Z_1 and Z_2 are the atomic numbers of the colliding particles. We write $E = (1/2)\, mv^2$, where $m = \frac{m_1 m_2}{m_1 + m_2}$. S is a slowly varying function of the bombarding energy which is considered to be constant in the present formulation of the problem. The reaction rate becomes:

$$r = 2n_1 n_2 \left(\frac{2}{\pi m}\right)^{1/2} \frac{S}{(kT)^{3/2}} \int_0^\infty dE \exp - \left(\frac{E}{kT} + \frac{B}{E^{1/2}}\right),$$

where $\frac{B}{E^{1/2}} = \frac{2\pi Z_1 Z_2 e^2}{\hbar v}$.

For convenience in later discussions we will define

$$\eta = \frac{Z_1 Z_2 e^2}{\hbar v} .$$

The integrand of the last expression is a sharply peaked function and reflects the fact that the cross section increases as the energy increases (because the probability for penetration of the coulomb barriers increases) whereas the Maxwell distribution falls off exponentially at high energies. The product of the Maxwell distribution and the cross section will therefore exhibit a marked maximum.

The integration indicated cannot be done to yield a closed solution, so that it is expedient to approximate the strongly peaked function of the integrand by a Gaussian form which is integrable. This is done by matching the Gaussian and the integrand at the maximum so that the curvatures are the same.

If the integrand and Gaussian are written as

$$\exp[-(x+ax^{-\frac{1}{2}})] \cong c\exp[-(x-b)^2/\sigma^2],$$

then we find that $b = (\frac{a}{2})^{2/3}$, $c = \exp[-3(\frac{a}{2})^{2/3}]$, and $\sigma^2 = \frac{4}{3}(\frac{a}{2})^{2/3}$

whereas $$c\int_0^\infty dx \exp[-(x-b)^2/\sigma^2] \approx c\sigma\sqrt{\pi},$$

for b reasonably far from the origin.

Therefore,

$$\int_{-\infty}^{\infty} dx \exp[-(x+ax^{-\frac{1}{2}})] \approx 2\left(\frac{\pi}{3}\right)^{1/3} \left(\frac{a}{2}\right)^{1/3} \exp[-3\left(\frac{a}{2}\right)^{2/3}].$$

If we let $n_i = \frac{N_0 \rho x_i}{A_i}$, where x_i is the fraction by weight of constituent i, then the number of reactions per second per nucleus of type 2 is

$$p = \frac{4.34 \times 10^5 \ \rho x_i \ (A_1+A_2) \ S\tau^2 e^{-\tau}}{A_1^2 A_2 \ Z_1 \ Z_2}, \quad (\sec^{-1})$$

where

$$\tau = 42.48 \left[\frac{Z_1^2 Z_2^2 \ A_1 A_2}{A_1 + A_2}\right]^{\frac{1}{3}} \quad T_6^{-\frac{1}{3}},$$

$$S = \sigma E \exp\left[31.28 \ Z_1 Z_2 \left(\frac{A_1 A_2}{(A_1+A_2)E}\right)^{\frac{1}{2}}\right].$$

σ is in barns, and T_6 is in 10^6 °K, E in kev. in the center of mass system of the particles.

The quantity S can sometimes be determined for a specific reaction by measuring the reaction cross section at the lowest possible bombarding energy and putting the measured value into the equation for S. In other cases S must be calculated from resonance theory or from the statistical properties of nuclear resonances. This will be discussed in greater detail later on.

Salpeter has made calculations indicating correction factors which must be applied to the expression for p (the reaction rate per nucleon) which correct for the approximation of the integrand by a Gaussian. This factor is

$$F(\tau) = 1 + \frac{5}{12\tau} - \frac{35}{288\tau^2} + \ldots$$

A further modification must be taken into account if the colliding particles have relative energies approaching the Coulomb penetration energies. S will then be given by

$$S = \sigma E \exp\left[2\pi\eta + E\left(\frac{MR^3}{Z_1 Z_2}\right)^{\frac{1}{2}} \times 1.2150\times10^{-4}\right]$$

where R is the nuclear radius of interaction in 10^{-13} cm, M is the reduced mass in a.m.u., E is in kev., and S is in

kev-barns.

For future reference we compute the energy at which the maximum number of interactions is liable to take place. This number is just the maximum of the function

$$\exp -\left(\frac{E}{kT} + \frac{B_{\frac{1}{2}}}{E^{\frac{1}{2}}}\right) \quad ,$$

which occurred in the integrand of the integral discussed previously. The maximum energy E_m turns out to be,

$$E_m = 1220 \left[Z_1^2 Z_2^2 \frac{A_1 A_2}{A_1 + A_2} T_6^2 \right]^{\frac{1}{3}} \quad \text{in electron volts.}$$

The half-width (ΔE) of the Gaussian obtained previously, that is, the energy width corresponding to one half the height of the Gaussian is given by

$$\Delta E_{\frac{1}{2}} = 17.9 \, (T_6 E_m)^{\frac{1}{2}} \quad \text{electron volts.}$$

The energy spread corresponding to a 1/e reduction rather than ½ is

$$\Delta E_{1/e} = 21.5 \, (T_6 E_m)^{\frac{1}{2}} \quad \text{ev.}$$

The above may also be expressed as,

$$\Delta E_{\frac{1}{2}} = 625 \left[Z_1^2 Z_2^2 \frac{A_1 A_2}{A_1 + A_2} T_6^5 \right]^{\frac{1}{6}} \quad \text{ev., and}$$

$$\Delta E_{1/e} = 750 \left[Z_1^2 Z_2^2 \frac{A_1 A_2}{A_1 + A_2} T_6^5 \right]^{\frac{1}{6}} \quad \text{ev.}$$

The peak in the integrand considered is called the "Gamow" peak.

Resonant Reactions

The results obtained for non-resonant reactions were based on the assumption that the nuclear cross section involves essentially only the barrier penetration probability factors. If there are some additional factors of a purely nuclear character which cause the nuclear cross section as a function of energy to have local maxima in the form of resonances, the thermonuclear reaction rates can be very much altered.

A useful expression describing the cross section at resonance for a reaction involving an incoming particle a and an outgoing particle b is the Breit-Wigner single level formula which is,

$$\sigma(a,b) = \frac{\pi \lambda\!\!\!^{-}_a{}^2 g \Gamma_a \Gamma_b}{(E-E_n)^2 + \frac{1}{4}\Gamma^2} ,$$

where $\lambda\!\!\!^{-}_a$ is the de Broglie wavelength for particle a divided by 2π, E_r is the energy at the resonance peak, Γ_a and Γ_b are the full widths at half maximum for the emission of particle a or b from the compound nucleus, Γ is the sum of all partial widths, where for most reactions that we will consider $\Gamma \cong \Gamma_a + \Gamma_b$. The quantity g is the so called statistical factor

$$g = \frac{2J + 1}{(2S+1)(2I+1)} ,$$

where J is the spin of the compound state, S is the spin of the bombarding particle and I is the spin of the target nucleus.

Since the resonance cross section at resonance is so large we may assume essentially all the reactions take place at E_r. One then obtains,

$$r = 4\pi m_1 m_2 \left[\frac{m_1 m_2}{2\pi kT(m_1+m_2)} \right]^{3/2} v_r^3$$

$$\times \exp\left[-\left(\frac{m_1 m_2}{m_1+m_2}\right) \frac{v_r^2}{2kT} \right] \int_0^\infty \sigma(v)\,dv$$

The integration over the cross section may be done over the range from $-\infty$ to ∞ with little effect on the final answer since the contribution of the far tails of the resonance contributes little to the integral. Thus,

$$\int_{-\infty}^{\infty} \sigma(v)\,dv \cong 2\pi\lambda_a^2 g \frac{\Gamma_a \Gamma_b}{\Gamma} ,$$

where λ_a^2 is evaluated at E_r. The reaction rate per nucleus is then,

$$p = 4.81\times10^9 \frac{\rho x_1 g}{A_1 T_6^{3/2}} \frac{\Gamma_1 \Gamma_b}{\Gamma} \left(\frac{A_1+A_2}{A_1 A_2}\right)^{3/2} \exp-\left[\frac{0.0116E_r}{T_6}\right] \sec^{-1} ,$$

when E_r is in ev.

Application of Dispersion Theory of Nuclear Reactions

We have written down the probability of getting a certain number of reactions which depend on the two assumed forms for the nuclear cross section curve, and the nuclear physics involved concerns these two assumptions regarding the form of the curve. Now, let us consider the formulation involved in the dispersion theory of nuclear reactions, which is due to Wigner and Eisenbud*.

Let us assume a potential of the sort shown in figure 11.1

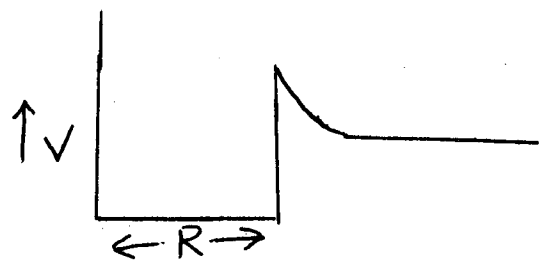

With this oversimplification we are making use of a "black box" procedure. We are not attempting to understand in detail the actions of particles in this "black box" but rather the behavior of particles at all points exterior to the "black box". If we consider the probability that a particle can escape our potential, we see that this probability may be

*E.P.Wigner, L.Eisenbud, Phys. Rev., 72, 29(1947)

written as the product of an internal and external probability. By internal probability we mean the probability that a particle in the well will come to the surface, and by external we mean the probability that a particle at the surface will escape to regions outwards where we think we understand something about the behavior of the interaction because it is electrostatic in nature. Thus we write

$$\Gamma = 2\ k\ P\ \gamma^2$$

where k is the wave number of the particle,

$$k = \frac{m_1 m_2}{m_1 + m_2} \frac{v}{\hbar} = 2.19\text{x}10^9 \frac{A_1 A_2 E^{\frac{1}{2}}}{A_1 + A_2}\ \text{cm}^{-1}$$

P is the probability for penetrating the Coulomb and centrifugal barriers and has the form

$$P = \frac{1}{F^2 + G^2} \quad .$$

γ^2 is the reduced width of the particle in the level under consideration. F and G are the regular and irregular solutions to the Schrödinger equation for particles in a Coulomb field. These solutions are usually carried out in terms of the variables ρ and η, where

$$\rho = kR, \qquad \eta = \frac{Z_1 Z_2 e^2}{\hbar v} = 157.4\ Z_1 Z_2 \left(\frac{A_1 A_2}{[A_1 + A_2]E} \right)^{\frac{1}{2}}$$

R is being the distance from the origin represented by the boundary of our "black box". This method of representing

nuclear reaction rates has certain deficiences which are associated with the assumption that there is an infinitely sharp boundary within which the forces are nuclear and outside which the forces are electrostatic. Actually nuclear forces don't stop abruptly; instead they decay fairly rapidly, but smoothly. The Coulomb forces always remain effective, even inside the nucleus.

Using our simplified representation it has been found best to take the value of R somewhat larger than the actual radii that would be expected for nuclei. Furthermore, since we are calculating the probability of barrier penetration of one charged particle through the Coulomb barrier with respect to a second charged particle, we take R as being the sum of the radii of the two particles. The results are fairly good if we take a large value of R, that is

$$R = 1.45 \times 10^{-13} \quad (A_1^{1/3} + A_2^{1/3})\,\text{cm}.$$

This involves the assumption that nuclear matter is incompressible and the radius of a nucleus may be written as proportional to the mass number to the 1/3 power. We note in passing that measurements of the nuclear radius (obtained, for example, bombarding a nucleus with high energy electrons,

which have no nuclear interaction properties) indicate that the proportionality constant one should normally use for the radius would be smaller, about 1.1×10^{-13} cm. Our value is found to work best within the famework of this series of approximations, however.

We do not develop all the properties of Coulomb wave functions in detail. The reader seeking a quick summary is referred to a paper by Block, et al, in Reviews of Modern Physics, 23, p.147, (1951), and for a collection of methods for calculating the values of Coulomb wave functions for all regions of the $\rho - \eta$ plane, there is another paper which was written by Fröberg, Reviews of Modern Physics, 27, p.399 (1955).

As far as thermonuclear reactions are concerned, we are primarily interested in the bombardment of particles of very low relative velocities, or very low relative energies. Consider what this means in terms of ρ and η. Now,

$$\rho = k R$$

where k is proportional to the velocity, hence the value of k will tend to be unusually small for the region of the $\rho - \eta$ plane in which we are interested. Similarly, η is inversely proportional to the velocity; the velocity is

unusually small; hence η will be unusually large for the particular bombarding energies in which we are interested. For these restrictions on ρ and η we may use the Bessel-Clifford expansion to calculate the coulomb wave functions. This expansion is discussed in more detail in Fröberg, loc. cit.

For low bombarding energies, G^2 is much greater than F^2. F is the regular solution to the Coulomb wave equation, and approaches zero near the origin. G is the irregular solution, and diverges near the origin. Hence, since we are approaching the origin,

$$G^2 \gg F^2 \quad .$$

Therefore, $P \approx G_L^{-2} = \dfrac{\rho^{2L}}{D_L^2 \; \theta_L^2}$, where we now indicate the angular momentum dependence by the subscript L,

and

$$\frac{1}{D_L^2} = \frac{2^{2L}}{[(2L)!]^2} \; [(L^2+\eta^2)([L-1]^2+\eta^2)\ldots(1^2+\eta^2)] \; \frac{2\pi\eta}{(e^{2\pi\eta}-1)}$$

Let us write, for convenience,

$$q = \frac{2^{2L}}{[(2L)!]^2} \; [(L^2+\eta^2)(L-1)^2 + \eta^2)\ldots \; (1^2+\eta^2)]$$

Because η is large,

$$e^{2\pi\eta} \gg 1,$$

thus,

$$\frac{1}{G_L^2} \approx \frac{2\pi\eta \; q \; \rho^{2L}}{\theta_L^2} \; \exp\,(-2\pi\eta) \; .$$

For L = 0, q = 1. Now, we use the Bessel-Clifford expansion. In the low energy limit,

$$\theta_L = -\left[\frac{2}{(2L)!}\right]\left(\frac{x}{2}\right)^{2L+1} K_{2L+1}(x)$$

where $x = (8\rho\eta)^{\frac{1}{2}}$.

Note that velocity dependence cancels out of the product $(\rho\eta)$. Thus $(8\rho\eta)^{\frac{1}{2}}$ is a number that is characteristic of the reaction. It depends upon the properties of the target nucleus and the bombarding particle only. θ, however, depends quite strongly upon the angular momentum. $K_{2L+1}(x)$ is the modified Bessel function of the second kind*.

If $(8\rho\eta)$ is a large number, then one may use the asymptotic expansions for the K's. Thus we have outlined the evaluation of barrier penetration factors for low bombarding energies in these thermonuclear reactions.

Another approach, using the WKB approximation, has been used by Burbidge, Burbidge, Fowler, and Hoyle (Rev. Mod. Phys., 29, 547 (1957)).

Unfortunately, the conditions that ρ is small and η is large are not always met in thermonuclear ractions; for example, considering such reactions as those between two

*See British Association Tables, or Watson, G.N., "Treatise on the Theory of Bessel Functions", Cambridge, New York.

carbon or two oxygen nuclei, one finds that the optimum thermonuclear bombarding energy is not in the region of the $\rho - \eta$ plane where we can use the Bessel-Clifford expansion. Another method is necessary. Fröberg's paper is particularly useful in this respect -- it plots those boundaries in the $\rho - \eta$ plane which separate regions of validity for proper approximation for the Coulomb wave functions.

Consider again

$$\Gamma_L = 2\ k\ P_L\ \gamma_L^2 \quad .$$

P, the part we have just evaluated, is external. The internal part depends on nuclear structure. In any individual case, γ_L^2 might be large or small depending on the accident of nuclear structure involved. We can make some general statements about it, however. If we do not know the nuclear properties for a reaction adequately, we must resort to these general statements sometimes if we wish to estimate the thermonuclear reaction rate.

The sum rule limit due to Teichman and Wigner is given by

$$\gamma_L^2 \lesssim \frac{3}{2}\ \frac{\hbar^2}{mR}$$

where m is the reduced mass of the two particles. In some light nuclei, for reactions involving protons, neutrons, and alpha particles, one can find values of γ_L^2 which are

close to this limit. In general, the values of γ_L^2 are much below this, but for some particular nuclear reactions involving certain resonances of the compound nucleus, γ_L^2 is near the sum rule limit. This expression was derived for the emission of protons or neutrons; alpha particles seem to obey this same rule. There are alpha particle reduced widths which are near the sum rule limit, none much greater, and many much smaller.

The reduced width, γ_L^2, is the measure of the probability that a particle within the nucleus will arrive at the surface*. In more specific terms, γ_L^2 is a measure of the wave function for the particle at the nuclear surface.

While it may be useful to have a maximum value for the reduced widths, the fact that most are much less than this maximum leaves us in a somewhat nebulous position. Some sort of average value, at least, would be useful. To clarify this, let us consider a single particle interaction with a nucleus. Consider a single particle moving in a potential

---

*For tabulated values of γ_L^2, see the periodically revised reviews by Ajzenberg and Lauritsen, and Nuclear Data Sheets.

well; at the moment the other particles in the nucleus act on our single particle only in the sense that they do provide a potential well in which that single particle can move. If the particle is in a stationary state, then the wave function for the particle must satisfy certain boundary conditions. This requires that the energies taken by the particle in the well can have only certain discrete values (quasi-stationary states exist above the bound part of the well which decay with the emission of the single particle into the external region).

Now, let us take a different case. We bombard the nucleus by our single particle, gradually raising the energy of our particle. In this approximation nothing happens until the energy is raised to the first single particle excited state of the nucleus, which is an eigenvalue for the particle in this potential well. There is now a resonance in which the particle is captured by the well.

Actually, the resonances are not absolutely sharp because the shape of these resonances is governed by the Breit-Wigner formula. There would be a very small probability for capture of the particle by the well at energies that do not coincide with a resonance. The cross section for a

reaction of the single particle with this well is small, except in the vicinity of a resonance, in which case there is a peak value. In a typical case these peaks are about 15 Mev apart. In fact, however, resonances for nuclear bombardment by a proton or some other single particle do not occur just every 15 Mev or so. There are many more. This indicates that our model of the nucleus as just a potential well containing these few single particle states is an oversimplification. Actually the nucleus has a much larger number of states of the same spin and parity; the few states that are formed by the single particle are a small subset of this number. These other states represent various other modes of excitation of the compound nucleus which happen to have the same spins and parities but which differ in the internal motion of nucleons in the nucleus.

We never have this very pure situation. The single particle character of the pure states becomes mixed into these other states to some extent, and the characteristics of these other states also become mixed into the single particle state. The purity of levels is degraded. When we bombard the nucleus by a particle, we find that the properties of a pure

state mix most strongly with the other states in its vicinity, and less strongly in the region between the pure states. This is essentially the point of view given by the "cloudy crystal ball" model of the nucleus. We would expect that in a region near one of the characteristic energies the reduced width γ_L^2 would be large; otherwise, small.

In very light nuclei mixing of states does not occur to such a degree. In cases where the reduced width is close to the sum rule limit, the resonance formed is very nearly the kind of resonance described by an eigenvalue for the interaction of a single particle with a potential well. In the pure model, the reduced widths would equal the sum rule limits at these special states, and be zero in between. In the other extreme, one may say that on the average γ_L^2 is a constant, that is, there is no dependence on the position of characteristic resonance energies. Thus, on the average, the cross-section for interaction of a single particle with the nucleus would be independent of energy.

Now we consider the "black nucleus" model; by "black nucleus" we mean one which will absorb any incident particle rapidly because it possesses states close at hand in which

there is a mixture of the wave function for the interaction of that particle with the nuclear potential well. We also require that there be a great individual fluctuation in the values of the reduced width at any given narrow energy interval. A distribution function for these variations was given by Porter and Thomas* which appears to work well. Their distribution function for reduced widths is of the form

$$N(y) = \frac{\exp(-y/2)}{(2\pi y)^{\frac{1}{2}}}$$

where

$$y_L = \gamma_L^2 / \langle \gamma_L \rangle^2$$

The probability of having a small reduced width (including zero) is much larger than the probability of having a large reduced width.

If we have a "black" nucleus and nuclear reactions that do represent a good average , then we can relate the reduced widths to the average spacing between levels of a given spin and parity by

$$\frac{\gamma_L^2}{D} \approx 2\text{x}10^{-14} \text{ cm.}$$

*C.F. Porter, R.G. Thomas, Phys. Rev., 104, 483 (1956)

If our nuclear reaction involves the properties of any one nuclear level, then we must be very uncertain as to the intrinsic nuclear factors that enter into the determination of the influence of that level on the reaction rate. But if we are concerned with heavy nuclei so that we may average over many resonances, then the ratio $\frac{\gamma_\ell^2}{D}$ is approximately the value quoted. We call this ratio the nuclear strength function.

In terms of these quantities, we can write our cross-section factor S:

$$S = 2.84\text{x}10^{15} \quad \frac{q\rho^{2\ell}}{\theta_\ell^{\,2}} \quad \frac{Z_1 Z_2 (2J+1)}{(2s+1)(2J+1)} \left[\frac{\gamma_a^2 \; \Gamma_b}{(E-E_r)^2 + \Gamma^2/4}\right] \text{ kev barns}$$

This is usually valid if we are reasonably close to a particular level whose properties dominate the nuclear cross section. If the energy being considered is about half-way between two levels of the same spin and parity, each of which might influence the nuclear cross-section, interference (constructive or destructive) takes place between these two resonances. The cross section might easily be raised or lowered by a factor of 10 relative to the prediction of the Breit-Wigner formula.

Suppose there are many resonances within the thermonuclear bombarding region so that we may use the nonresonant reaction

formula, but write it so that the cross section factor S represents an average over resonances.

$$\langle \sigma \rangle = 2\pi^2 \lambda\!\!\!^{-2} \left\langle g \frac{\Gamma_a \Gamma_b}{\Gamma D} \right\rangle$$

This is the form for the average cross section. It is obtained by integrating the Breit-Wigner formula, then averaging that cross section over the interval between such resonances.

This is the average cross section for interaction of a particle in states of a given spin and parity. We would have similar expressions for each spin and parity of interest. Let's write

$$\langle \sigma \rangle = \frac{4\pi^2 g P}{k} \left\langle \frac{\gamma_a^2 \Gamma_b}{\Gamma D} \right\rangle$$

Suppose

$$\Gamma_a << \Gamma_b \approx \Gamma .$$

This corresponds (for charged particles) to interaction with the Coulomb barrier at a low energy. Then

$$\langle \sigma \rangle = \frac{4\pi^2 g P}{k} \left\langle \frac{\gamma_a^2}{D} \right\rangle$$

where γ_L^2/D is the nuclear strength function. This gives a means of estimating an average cross section (in a case where we have an average of many resonances in the bombarding

energy region) if we use some average value of the nuclear strength function (such as 2×10^{-14} cm.).

$$\langle \sigma \rangle \approx 8\pi^2 \times 10^{-14} \frac{gP}{k}$$

One may obtain an average over (σ v) by remembering that $k \propto v$, and absorbing this v dependence in the cross section term. So

$$\langle \sigma v \rangle \approx 8\pi^2 \times 10^{-14} \frac{gP}{m/\hbar}$$

for nonrelativistic values of v.

We expect these expressions to be correct at least to a general order of magnitude.

Electron Screening:

All of the formulae for thermonuclear reaction rates that we have considered involve the assumption that we are dealing with the interaction of bare nuclei. The coulomb repulsion energy between any two nuclei was then considered to be the complete repulsion between the positive charges of the nuclei; i.e. $Z_1 Z_2 e^2/r$. This, we observe, is a valid approximation in the study of thermonuclear reaction rates in stellar interiors where the atoms are ionized by the high temperatures known to exist therein, and where the density is relatively low.

However, in general in stellar interiors the gas density is high and the average distances between the nuclei and the neighboring electrons is small. The electrostatic potential of the bare nucleus therefore tends to attract nearby electrons while repelling the nearby nuclei, thus inducing a spherically symmetric polarization of the neighboring particles. In a collision the two nuclei carry this polarized cloud with them, thus changing the effective interaction energy.

In order to examine the effect of such 'electron screening' let us consider our formula for the thermonuclear reaction rate:

$$r = 4\pi n_1 n_2 \left[\frac{m}{2\pi kT} \right]^{3/2} \int_0^\infty dv\ v^3\ \sigma(v)\ \exp - \left(\frac{m\ v^2}{2kT} \right)$$

Here m is the reduced mass of the system, 'v' is the relative velocity of the two nuclei, $\sigma(v)$ is the nuclear cross section and $[v \exp - (mv^2/2kT)]$ is the Maxwell Boltzmann distribution factor. If we write E, the relative kinetic energy of the two nuclei as:

$$E = \frac{1}{2}\ m\ v^2$$

our equation for the thermonuclear reaction rate becomes

$$r = A \int_0^\infty dE E^{1/2}\ \sigma(E)\ E^{1/2} \exp - \left(\frac{E}{kT} \right)$$

where

$$A = \frac{8\pi n_1 n_2}{m^{\frac{1}{2}}} \left[\frac{1}{2\pi kT} \right]^{3/2}$$

Our formula for the reaction rate is a particular form of the general expression for thermonuclear reaction rates given by:

$$r = A' \int_0^\infty dE \quad P(E)\ \sigma_{nuc}\ (E)\ E^{\frac{1}{2}}\ e^{-E/kT}$$

In this expression P(E) is the barrier penetration factor, σ_{nuc} (E) a purely nuclear factor depending upon the details of the interaction and $E^{\frac{1}{2}}\ e^{-E/kT}$ is, again, the Maxwell Boltzmann distribution factor.

The general expression for the interaction energy may now be written

$$U(r) \quad = \quad \frac{Z_1 Z_2 e^2}{r} + U_s(r)$$

Here $U_s(r)$ is the energy due to the effects of the screening clouds of the two nuclei.

For most reactions known to occur in stellar interiors the integrand of the reaction rate, as we have seen, has a fairly sharp maximum at some energy E_{max}. In all cases of interest E_{max} is known to be large with respect to the mean thermal energy. Now, with the addition of the screening

energy, the particles will behave as if they experienced a relative energy given by U(r). The classical turning point R_c for such a particle occurs for the potential $U(R_c)$ which is equal to E_{max}, the maximum value of the bombarding energy.

$$E_{max} = \frac{Z_1 Z_2 e^2}{R_c} + U_s(R_c)$$

Let R be the radius of the cloud of charge surrounding the nucleus or in other words that radius beyond which an appreciable fraction of the nuclear charge is screened by the electron cloud. Let us consider that case for which R_c is small compared to the radius of the charged cloud. Now $U_s(r)$ must be a function which is small for r>>R and which approaches a constant value + U_0 in the limit r<<R. The value of + U_0 must be of the order of magnitude of $Z_1 Z_2 e^2/R$. Thus, from this and our equation for E_{max}

$$\frac{R_c}{R} \sim \frac{U_0}{E_{max}} \ll 1$$

From this condition we see that U(r) can be replaced by the potential at the origin + U_0 which is independent of both r and E.

Now rewriting our expression for E_{max} we have

$$E_{max} = \frac{Z_1 Z_2 e^2}{R_c} + U_o$$

$$R_c = Z_1 Z_2 e^2 \ (E_{max} - U_o)^{-1}$$

Therefore, as stated previously, the particle is seen to behave as if it were bombarding on ordinary coulomb barriers with an elevated energy $(E - U_o)$. The penetration factor $P(E)$ and the nuclear factor $\sigma_{nuc}(E)$ for energy E without screening are equal to the correct factors with screening for an energy $(E + U_o)$. Since U_o is much smaller than E_{max}, but not necessarily smaller than kT we can write for the thermonuclear reaction rate:

$$r = A \int_0^\infty dE \ P(E) \ \sigma_{nuc}(E) \ E^{\frac{1}{2}} \ e^{-E/kT} \ e^{-U_o/kT}$$

Thus the effect of the screening due to the polarization charge cloud is to multiply the reaction rate with the screening neglected by the factor

$$e^{-U_o/kT}$$

The arguments employed thus far are primarily those due to Salpeter (1954)*. Continuing with him, we will now proceed to calculate the charge distribution and the

*E.E. Salpeter, Austral. J. Phys. 7, 353 (1954).

potential of the screening cloud for the two limiting cases of 'weak' and 'strong' screening. By weak screening is meant that the coulomb interaction energy between the nucleus and the neighboring electrons and nuclei is small compared to the thermal energy. Strong screening assumes that the coulomb interaction between the nucleus Z_1 and neighboring nuclei is strong. In the latter case the screening cloud contains electrons only.

Weak Screening:

Let us first consider the case of weak screening. We will assume here, further, that the electrons are non-degenerate and that the main constituents of the surrounding gas are atoms of charge Z, and atomic weight A. We wish to calculate the interaction energy $U_s(r)$ as defined previously. We now assume that total interaction energy U(r) may be written

$$U(r) = Z_1 Z_2 e^2 \Psi(r);$$

$$\Psi(r) = r^{-1} + \Psi_s(r)$$

$\Psi_s(r)$ is the term due to the screening cloud, which we will consider to be independent of Z_1 and Z_2 of the two interacting particles.

Consider the nucleus Z_1 to be fixed at the origin and let V(r), $\bar{\rho}(r)$ be the electrostatic potential and electric

charge density, averaged over all particles but Z_1. If $U_s(r)$ is defined as above we then have that $V(r)$ is $Z_1 e\Psi_s(r)$. As $V(r)$ and $\bar{\rho}(r)$ are related by Poisson's equation, we may write

$$\nabla^2[Z_1 e\Psi(r)] = -4\pi\bar{\rho}(r) - 4\pi Z_1 e\delta(r)$$

Now, from statistical mechanics we know that in a region in which the particles have potential energy $U_c(r)$, the particle density is simply given by the field-free density times the Boltzmann factor.

$$\bar{\rho}(r) = \left(\frac{\rho N_o ze}{A}\right)\left(\exp\left[-\frac{Z_1 ze^2\Psi(r)}{kT}\right] - \exp\left[\frac{Z_1 e^2\Psi(r)}{kT}\right]\right)$$

Thus the Poisson equation for $V(r)$ may be written:

$$\nabla^2\Psi_s(r) = 4\pi\rho N_o\left(\frac{Z^2 + Z}{A}\right)\frac{e^2}{kT}\Psi(r)$$

Now $\Psi_s(r)$ which represents the screening term in the total interaction potential must be such that it satisfies the bounding condition imposed on the screening potential. Thus as r goes to infinity, $\Psi_s(r)$ approaches $-r^{-1}$ and as r approaches zero, $\Psi_s(r)$ approaches a finite limit. If we define the radius of the charge cloud by the relation

$$R^2 = \left(\frac{kT}{4\pi\rho N_o e^2}\right)\left(\frac{A}{Z^2 + Z}\right)$$

then the Poisson equation for $V(r)$ or $x_s(r)$ becomes:

$$\nabla^2 x_s(r) = \frac{x(r)}{R^2}$$

with solution

$$x_s(r) = r^{-1}\,(e^{-r/R} - 1)$$

which in the limit of $r \to o$ becomes

$$x_s(o) = -\frac{1}{R}$$

In this calculation we have assumed a continuous charge density $\bar{\rho}(r)$, evaluated by the use of the Boltzmann factor. Defining the interparticle distance 'a' by the equation

$$4\pi a^3 \rho\, N_o = 1$$

we observe that our approximation demands that the electrons be contained in a volume of such dimensions that $\bar{\rho}(r)$ and $U_s(r)$ do not vary appreciably over it; in other words $a \ll R$. From our definition of a, our equation for R^2 becomes

$$R^2 = \left(\frac{kT}{e^2/a}\right)\left(\frac{A}{Z^2+Z}\right)\, a^2$$

Thus the condition $a \ll R$ is certainly satisfied for the case of weak screening for which $Z^2 e^2/a \ll kT$.

Thus we may write our final expression for the screening potential between nuclei Z_1 and Z_2 as:

$$U_o = Z_1 Z_2 e^2 x_s(o)$$
$$= -\frac{Z_1 Z_2 e^2}{R}$$

<u>Strong Screening</u>:

Strong screening implies that at the radius R of the

charged cloud, the coulomb repulsion charges between Z_1 and z is large compared to the thermal energy. We will further assume that this coulomb energy is large with respect to the ionization potential. The ratio of the ionization potential of a K shell electron in a hydrogen-like atom to the mean thermal energy is given by:

$$I_{z_1} = \left(\frac{Z_1 e^2}{2a_{0z}}\right) (kT)^{-1} = \frac{(h/a_{0z})^2}{8\pi^2 m} (kT)^{-1}$$

where a_{0z} is the Bohr radius. The conditions we assume to apply are, then:

$$2z I_{z_1} << \frac{Z_1 z e^2}{a} (kT)^{-1} >> \frac{R}{a}$$

From the first of these conditions we have that $a << a_{0z}$ and that

$$\frac{Z_1 e^2}{a} \left(\frac{h}{2\pi a}\right)^2 m^{-1} \sim E_F$$

Thus the coulomb energy of an electron at a distance 'a' or greater from the nucleus is small compared to the Fermi energy, and for an electron at a distance less than 'a' the coulomb energy is small compared to the corresponding uncertainty energy. Thus the electron density in the region of interest differs little from the field free density, and we can consider it as being uniform.

The second of our conditions implies that the Coulomb repulsion of the Z nuclei at distances between a and R is much greater than the thermal energy. Hence the density of these nuclei is extremely small compared to the field free density.

Thus we can consider, in this case, that the nucleus Z_1 is surrounded by electrons with a uniform density up to some radius R_1. Outside of this sphere of charge the nucleus is effectively screened. The total electrostatic energy of the nucleus Z_1 with surrounding electron cloud of charge $- Z_1$ is given by:

$$- \left(\frac{3}{2} - \frac{3}{5}\right) \frac{Z_1{}^2 e^2}{R_1}$$

where the first term corresponds to the energy between the nucleus and the electron cloud, and the second term is the self-energy of the cloud. If we consider another nucleus Z_2 with corresponding electron cloud of charge $-Z_2$, for distances between the nuclei which are small with respect to R_1 and R_2 (in particulars for distances which are of the order of 'a'), the screening contribution is simply the total interaction energy for a nucleus $(Z_1 + Z_2)$ less the sum of the analogous energies for the individual nuclei.

Thus we have:

$$U_o = -\frac{9}{10} e^2 \left[\frac{(Z_1+Z_2)^2}{R_{12}} - \frac{Z_1^2}{R_1} - \frac{Z_2^2}{R_2} \right]$$

Defining ξ as the average number of electrons per a.m.u. in the gas cloud, or

$$\xi = \Sigma_i \frac{x_i Z_i}{A_i}$$

where x_i is the fractional mass abundance of nuclei of charge Z_i and mass A_i, we can write:

$$E_f = \frac{h^2}{8\pi^2 m} (3\pi^2 N_o \xi \rho)^{2/3} = \frac{(h/a)^2}{8\pi^2 m}$$

where E_f is the fermi energy of the gas defined as the thermodynamic potential at zero temperature. We can, then, approximate R_1 by:

$$R_1 = \left(\frac{3Z_1}{\xi}\right)^{1/3} a$$

and U_o becomes:

$$U_o = -\frac{9}{10a} \left(\frac{\xi}{3}\right)^{1/3} \left[(Z_1+Z_2)^{5/3} - Z_1^{5/3} - Z_2^{5/3}) \right]$$

<u>Pycnonuclear Reactions</u>:

As we have observed in our discussion of 'strong' screening, at extremely high densities such that electron degeneracy is realized, electron shielding cuts off nuclear potential barriers quite close to the nuclear surface.

Under such circumstances the classical turning points of low-energy ions are very insensitive to the bombarding energies. Nuclear reaction rates thus become rather insensitive to temperature, but extremely dependent upon density; such nuclear reactions we will term pycnonuclear reactions.

In our discussion of strong screening, (Salpeter(1954)) we assumed that each of the interacting particles Z_1 and Z_2 carried with them an electron cloud, in which the electrons were assumed to be uniformly distributed. In the present case, rather, we assume that the electrons are completely free, and of uniform density. The validity of this approximation requires that the Fermi level of the electrons must be comparable to, or greater than, the electrostatic energy of the electron at the nuclear surface. Thus we write the modified coulomb potential in the following form (Schatzman 1948; Erma 1957):

$$U(r) = \frac{Z_1 Z_2 e^2}{r} \left(1 - \frac{3}{2}\frac{r}{R} + \frac{1}{2}\frac{r^3}{R}\right)$$

where Z_1 and Z_2 are the positive charges between which the potential exists; $Z_2 \geq Z_1$; and R is the radius of the spherical volume containing Z_2 electrons. Thus we are assuming we have the charge Z_1 approaching the charge Z_2. The first term is

the ordinary coulomb potential between two unshielded nuclei; the second term arises from the uniform sea of electrons of radius R about the charge Z_2, and the third term gives the effect of the other nuclei which neutralize the total charge. For simplicity, we shall drop the third term and write

$$U(r) \simeq \frac{Z_1 Z_2 e^2}{r} - \frac{3}{2} \frac{Z_1 Z_2 e^2}{R}$$

We now consider a particle of bombarding energy E. Its classical turning point R_c, corresponding to the point of closest approach at which all of its kinetic energy has been converted into potential energy in the field of the bombarded ion, may then be defined by:

$$E = U(R_c) = \frac{Z_1 Z_2 e^2}{R_c} - \frac{3}{2} \frac{Z_1 Z_2 e^2}{R}$$

Hence:

$$R_c = Z_1 Z_2 e^2 \left(\frac{3 Z_1 Z_2 e^2}{2R} + E \right)^{-1}$$

Therefore the particle behaves as if it were bombarding an ordinary coulomb barrier with an elevated energy:

$$E^* = E + \frac{3 Z_1 Z_2 e^2}{2R}$$

Thus the first effect of shielding is to increase the effective energy of the bombarding particle, and the classical turning

point approaches the nucleus.

In estimating the penetration probability for a barrier U(r) of arbitrary shape, in quantum mechanics, it is usual to take the expression

$$P \approx \exp - 2 \left(\frac{2m}{\hbar^2}\right)^{1/2} \int_{R_n}^{R_c} (U-E)^{\frac{1}{2}} \, dr$$

where m is the reduced mass of the bombarding particle of energy E; R_n is one boundary of the potential which in this case is the nuclear radius; and R_c is the other boundary of the potential which in this case corresponds to the classical turning point. The barrier penetration probability then becomes

$$P \approx \exp - 2 \left(\frac{2m}{\hbar^2}\right)^{\frac{1}{2}} \int_{R_n}^{R_c} \left(\frac{Z_1 Z_2 e^2}{r} - E^*\right)\Big) \, dr$$

This can be integrated by using the WKB approximation (Bethe 1937) giving

$$P \approx \exp - 2 \left(\frac{2m}{\hbar^2}\right)^{\frac{1}{2}} \frac{Z_1 Z_2 e^2}{\sqrt{E^*}} \left[\cos^{-1} x^{\frac{1}{2}} - x^{\frac{1}{2}}(1-x)^{\frac{1}{2}}\right]$$

where

$$x = \frac{E^* R_n}{Z_1 Z_2 e^2}$$

At this point we may further approximate by taking the zero kinetic energy limit, E=0. This may be interpreted as

the limiting case of high densities in which the gas is also infinitely cold: we are neglecting all temperature effects. Under these conditions we have:

$$E^* = \frac{3Z_1 Z_2 e^2}{2R}$$

and

$$x = \frac{3R_n}{2R}$$

In calculating R, one finds

$$\frac{4}{3} \pi R^2 = Z_2 \left(\frac{N_0 \rho}{\mu_e}\right)^{-1}$$

where N_0 is Avogadro's number, ρ is the density and μ_e is the mean molecular weight per electron. Therefore,

$$R = 0.735 \times 10^{-8} \left(\frac{\mu_e Z_2}{\rho}\right)^{1/3}$$

If we define

$$y(x) = \cos^{-1} x^{\frac{1}{2}} - x^{\frac{1}{2}} (1-x)^{\frac{1}{2}}$$

The barrier penetration probability becomes:

$$P \simeq \exp - 116.2\, y(x) \left(\frac{Z_1 Z_2}{A_1} \frac{A_1 A_2}{+ A_2}\right)^{\frac{1}{2}} \left(\frac{\mu_e Z_2}{\rho}\right)^{1/6}$$

The wave number k of the incident particle may be written:

$$k = \frac{mv}{\hbar}$$

Now we have the equation for the cross section $< \sigma >$

as an average over resonances, supposing that many such resonances contribute to the optimum thermonuclear region, given by:

$$< \sigma > = \frac{4\pi^2 g P}{k} \left\langle \frac{\gamma_a^2 \ \Gamma_b}{\Gamma D} \right\rangle$$

for one spin value. Substituting for k we can obtain an approximate expression for $< \sigma v >$ as given by:

$$< \sigma v > \approx \quad 4\pi^2 \hbar \quad \frac{gP}{m} \left\langle \frac{\gamma_a^2 \ \Gamma_b}{\Gamma D} \right\rangle$$

$$= 0.025 \left(\frac{A_1 + A_1}{A_1 A_2}\right) g \ \frac{\gamma_a^2 \ \Gamma_b}{\Gamma D} \quad \exp - 116.2 \ y(x) \left(\frac{Z_1 Z_2}{A_1} \frac{A_1 A_2}{+ A_2}\right)^{\frac{1}{2}} \left(\frac{\mu_e Z_2}{\rho}\right)^{1/6}$$

In normal thermonuclear reactions the function $< \sigma v >$ depends very strongly on the temperature and not at all on the density. From this expression, however, we observe that at very high densities the situation is reversed; $< \sigma v >$ depends sensitively on the density but not on the temperature. Because y(x) does not vary strongly with the density, we may say in a crude approximation that the pycnonuclear reaction rate varies as exp - const. $\rho^{-1/6}$ in the high density limit. Effectively it is the quantum mechanical zero point energy which allows the penetration of the much reduced coulomb barriers, in such cases of high densities and perhaps low temperatures.

The effective density limit, for protons, occurs at

approximately 10^4 - 10^5 gm/cm^3. Most of the helium pycnonuclear reactions will take place at approximately 10^8 - 10^9 gm/cm^3. These are not radically different from the density ranges that one encounters in white dwarfs.

Temperature Sensitivity:

In many cases it is useful to be able to speak of the temperature sensitivity of a thermonuclear reaction. Let us write the reaction rate p as proportional to some constant times T^n.

$$p = p_0 \; T^n$$

Then the power n may be obtained from the relation

$$n = \frac{d(\ln p)}{d(\ln T)}$$

Thus, for non-resonant reactions it follows that:

$$n = \frac{1}{3} \; (\tau - 2)$$

For resonant reactions the power takes the form:

$$n = \frac{0.0116}{T_6} \; E_r \; - \frac{3}{2}$$

For thermonuclear reactions with reasonable cross sections, the reaction rates become interesting for $n \sim 20$. For instance $n \sim 18$ for the reactions in the carbon cycle for temperatures in the range of interest. For the proton-proton

chain, $n \sim 4$. This is due to the fact that the proton-proton reaction is a very special case, taking place at temperatures far above those for which one might expect reactions which involve a pair of single charges. Certain resonant reactions exist for which n is extremely high as, for instance, the triple alpha reactions for which $n \sim 35$ under conditions of interest.

12. Hydrogen Thermonuclear Reactions

We shall now consider in detail one class of reactions which provides stellar energy for main sequence stars, that is the hydrogen thermonuclear reaction series. In effect this reaction series converts four hydrogen nuclei into one helium nucleus with an accompanying energy release of 26.730 Mev. The paths by which this transformation may take place are varied and may involve intermediate elements such as carbon, oxygen, etc. The range of temperatures at which the reactions take place varies from ten to thirty million degrees depending on the mass of the star and its initial composition. Stars on the lower end of the main sequence (yellow to red spectral classes) generally burn hydrogen by a combination of element chains consisting of rather light elements, as heavy as boron or lighter. We shall refer to these chains as the proton-proton series (PP). Upper main sequence stars do the conversion using heavier elements from carbon to oxygen. This is the CNO cycle (or bi-cycle). At very high temperatures of about 50 million degrees isotopes of sodium, neon and magnesium also undergo transformation. These reactions will be discussed at the end of this section.

When the hydrogen in the core has been converted to helium and the central temperatures and pressures are still not high enough to initiate helium burning, the region of hydrogen destruction consists of a thin shell which progresses to the outer layer of the star . It is at this point that the star leaves the main sequence to become a red giant. We shall leave the star here for the time being and defer discussion of the helium burning stages until a later section.

For the moment let us return to the pre-hydrogen burning stage where deuterium destruction is taking place. When the temperature in the contraction stage reaches about 8000 °K we start to burn deuterium. At this point the amount of energy provided by deuterium burning may be of the order of the energy from gravitational contraction.

The main deuterium burning reactions are listed below along with some reactions involving heavier elements which are destroyed as contraction proceeds. Some of these will then be discussed in detail.

D^2 (p,γ) He^3

D^2 (d,n) He^3

D^2 (d,p) H^3

Lithium: $Li^6(p,\alpha)He^3$ (at temperatures of about 3×10^6 °K)

$Li^7(p,\alpha)He^4$ (" " " " 4×10^6 °K)

Beryllium:

$$\left.\begin{array}{l} \left.\begin{array}{l} Be^9(p,d)Be^8(2\alpha) \\ D^2(p,\gamma)He^3 \end{array}\right] \\ \hline \left.\begin{array}{l} Be^9(p,\alpha)Li^6 \\ Li^6(p,\alpha)He^3 \end{array}\right] \end{array}\right\} \text{(at temperatures of about } 5\times10^6 \text{ °K)}$$

Boron:

$$\left.\begin{array}{l} \left.\begin{array}{l} B^{10}(p,\alpha)Be^7 \\ Be^7(e,\nu)Li^7 \\ Li^7(p,\alpha)He^4 \end{array}\right] \\ \hline B^{11}(p,\alpha)Be^8(2\alpha) \end{array}\right\} \text{(at temperatures of about } 8\times10^6 \text{ °K)}$$

The $D^2(p,\gamma)He^3$ reaction is a non-resonant reaction which will be discussed in much more detail immediately following this. The second two reactions compete with one another and the first of the two produces neutrons which will be of some importance as will be discussed later.

After the exhaustion of the deuterium, the star will continue to contract and its central temperature will continue to rise. In rapid succession the elements lithium, beryllium and boron will be destroyed. The abundances of these elements are so very small that the energy produced by their destruction

is negligible compared to the energy released by gravitational contraction. The final temperatures reached will be on the order of 8×10^6 °K or more, after which the star settles down on the main sequence and hydrogen burning commences. The times associated with the above reactions are on the order of 10^4 to 10^6 years.

The $D^2(p,\gamma)He^3$ Reaction

We are now going to consider the theory of the proton capture by H^2. This is a non-resonant reaction. There are no other resonances near the bombarding energy at which we form the compound He^3 nucleus. We shall consider only p-wave* protons in the continuum states. The deuteron enters into the calculation only to the extent that it provides a square well potential for the odd proton in both continuum and bound states.

We may picture the situation as in the diagram.

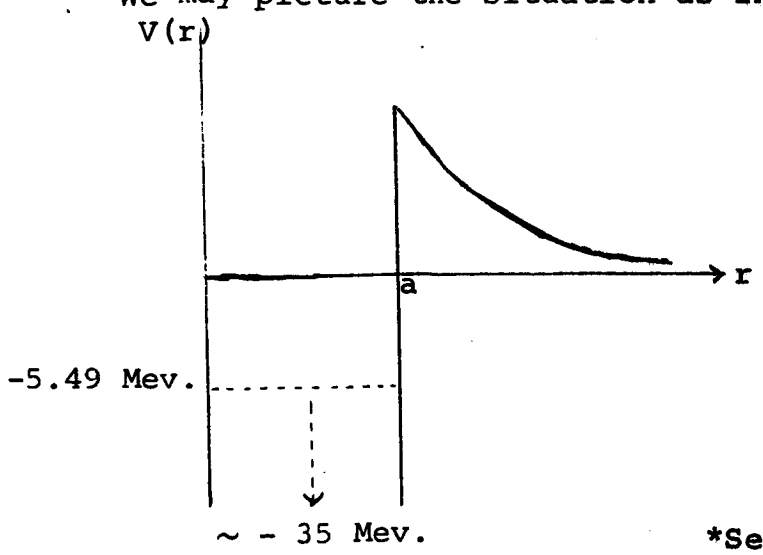

*See page 124 for reason L=1.

Here we observe we have a nuclear potential well surmounted by a repulsive coulomb barrier. The bottom of this barrier which corresponds to that for the deuteron is of the order of - 35 Mev. There is a state within the well corresponding to the ground state of He^3 for which V = - 5.49 Mev. We are interested in the probability that as the proton penetrates the barrier we shall have a transition involving the emission of γ-rays. The method for calculating this probability consists of writing the expressions for the wave functions of both the ground state of the He^3 nucleus and the incident proton. Using these expressions to determine the nuclear matrix elements for emission of electromagnetic radiation, we shall then observe that we get many more transitions outside the nuclear potential well than we do inside.

In order to proceed with this general analysis, we shall first write the Schroedinger equation for a proton in the center of mass system:

$$\nabla^2 \psi + \frac{2\mu}{\hbar^2} (E-V) \psi = 0$$

where (corresponding to our diagram)

$$V = -V_0 \quad \text{for} \quad r < a$$

$$= \frac{Z_1 Z_2 e^2}{r} \quad \text{for} \quad r > a$$

For the ground state of the He^3 atom we then have $E=-\epsilon=-5.49$ Mev, which corresponds to the binding energy of the last proton in He^3. Here the reduced mass μ is given by

$$\mu = \frac{2}{3} M_p = 1.115\text{x}10^{-24}\text{gm}$$

and a is the nuclear radius which we find from the coulomb energy difference to be

$$a \cong 2.26\text{x}10^{-13}\text{cm}.$$

The radial Schroedinger equation may be written as $(R_\ell(r) = NG_\ell(r)/r)$

$$G_\ell''(r) + \frac{2\mu}{\hbar^2}\left[(E-V(r)) - \frac{\ell(\ell+1)\hbar^2}{2\mu\ r^2}\right] G_\ell(r) = 0$$

where V(r) is defined as before. For the bound state of He^3 we have $\ell = 0$, whence

$$G_0''(r) + \frac{2\mu}{\hbar^2}\ (E-V(r))\ \ G_0(r) = 0$$

Consider the region $r < a$. Here we have $E=-\epsilon, V=-V_0$. We can convert the equation above to a dimensionless form by the substitution

$$\frac{2\mu}{\hbar^2}\ (V_0 - \epsilon) = \gamma^2\ ;\quad x = \gamma r$$

whence

$$G_0''(x) + G_0(x) = 0$$

Thus the radial solutions for the region $r < a$ may be

written

$$R_0(r) = N\gamma \frac{G_0(x)}{x} = A \frac{\sin x}{x}$$

Let us consider, now, the region $r > a$. Here we have $V = e^2/r$ and $E = -\epsilon$.

$$G_0'' (r) - \frac{2\mu}{\hbar^2}\left(\epsilon + \frac{e^2}{r}\right) G_0(r) = 0$$

Introducing the parameters

$$\beta = \sqrt{\frac{2\mu\epsilon}{\hbar^2}} = 4.2\text{x}10^{-12}\ \text{cm}^{-1}$$

$$\eta = \frac{e^2}{\hbar}\sqrt{\frac{\mu}{2\epsilon}} = 0.055$$

we can convert our equation to a dimensionless form by the substitution $\rho = \beta r$, yielding

$$G_0'' (\rho) - \left[1 + \frac{2\eta}{\rho}\right] G_0(\rho) = 0$$

To write down the solutions for $G_0(\rho)$ let us consider briefly the more general form of this equation, for non-zero ℓ.

$$G_\ell'' (\rho) - \left[1 + \frac{2\eta}{\rho} + \frac{\ell(\ell+1)}{\rho^2}\right] G_\ell(\rho) = 0$$

The exact solution of this equation in integral form is given by

$$G_\ell(\rho) = W(-\eta, \ell + \tfrac{1}{2}, 2\rho)$$

$$= \frac{\exp(-\rho-\eta \ln 2\rho)}{\Gamma(1 + \ell + \eta)} \int_0^\infty t^{\ell+\eta} e^{-t} \left(1 + \frac{t}{2\rho}\right)^{\ell-\eta} dt$$

Here $W(-\eta, \ell+\frac{1}{2}, 2\rho)$ is the general Whittaker function. For the case of $\ell = 0$, using the WKB approximation one obtains

$$G_0(\rho) = W(-\eta, \tfrac{1}{2}, 2\rho) \simeq \exp - \int [\Phi(\rho) + \frac{1}{2} \ln \Phi(\rho)]\, d\rho$$

where

$$\Phi(\rho) = \sqrt{1 + \frac{2\eta}{\rho}} \quad \text{for} \quad \ell = 0 .$$

Thus the radial wave functions for the region $r > a$ are given by

$$R_0(r) = \frac{N\beta\, G_0(\rho)}{\rho} = \frac{B\, W_0(\rho)}{\rho}$$

Matching logarithmic derivatives at $r = a$ yields the condition:

$$x \cot x \Big|_{r=a} = -\rho \left[\Phi(\rho) + \frac{1}{2\Phi(\rho)}\right] \Big|_{r=a}$$

$$= -1.45$$

Thus, for $a = 2.26 \times 10^{-13}$ cm and using V_0 given by

$$V_0 = \epsilon + \frac{\hbar^2 \gamma^2}{2\mu} = 34 \text{ Mev}$$

we find

$$x_0 = \gamma a = 2.16$$

Now, to determine the constants A and B we recall the two conditions: (i) the solutions for $r < a$ and $r > a$ must have equal amplitudes at the nuclear surface and (ii) the ground state wave-function must be normalized to unity.

The first of these conditions may be written

$$\frac{A\ G_0(\gamma a)}{\gamma a} = \frac{B\ W_0(\beta a)}{\beta a}$$

yielding A = 0.942B. From the second condition, recalling that the angular part of the wave-function is represented by normalized spherical harmonics yields

$$1 = aA^2 \int_0^1 \left| \frac{\sin \gamma r}{\gamma r} \right|^2 r^2 d\left(\frac{r}{a}\right) + aB^2 \int_1^\infty \left| \frac{W(\beta r)}{\beta r} \right|^2 r^2 d\left(\frac{r}{a}\right)$$

Integrating these integrals numerically one finds $B^2 = 0.473 \times 10^{39}$.

Now, to continue we must write down the continuum wave functions for the p-wave proton. The reason for the choice of $\ell = 1$ here is as follows. The transition to the ground state which we are going to consider here is an electric dipole transition. From the selection rules for such transitions one finds that there must be a change of one unit in the orbital angular momentum of the particle that undergoes the radiative process. Thus to end up with a S-wave proton in the ground state of helium we must have a p-wave proton bombarding the nucleus.

To write down the continuum wave functions we must again consider the radial solutions to the Schroedinger equation.

$$\frac{1}{r^2} \frac{d}{dr} \left(\frac{r^2 dR_\ell(r)}{dr} \right) + \left(\frac{2\mu}{h^2} \quad (E-V(r)) - \frac{\ell(\ell + 1)}{r^2} \right) R_\ell(r) = 0$$

For the region $r < a$ we have again $V(r) = -V_0$, substituting

$$k^2 = \frac{2\mu}{\hbar^2}(E+V_0) \; ; \quad \rho = kr$$

we have

$$\frac{d^2R_\ell(\rho)}{d\rho^2} + \frac{2}{\rho}\frac{dR_\ell(\rho)}{d\rho} + \left(1 - \frac{\ell(\ell+1)}{\rho^2}\right) R_\ell(\rho) = 0$$

The solutions of this equation are the spherical Bessel functions $j_\ell(\rho)$. Thus for p-wave protons we may write:

$$R_\ell(r) = \left(\frac{\sin kr}{(kr)^2} - \frac{\cos kr}{kr}\right)$$

Now, for the region $r > a$ we have $V(r) = e^2/r$, $\ell = 1$. Our radial equation then becomes

$$\frac{1}{r^2}\frac{d}{dr}\left(\frac{r^2 dR_\ell(r)}{dr}\right) + \left(\frac{2\mu}{\hbar^2}\left(E - \frac{e^2}{r}\right) - \frac{2}{r^2}\right) R_\ell(r) = 0$$

Writing: $R_\ell(r) = N_1 \frac{u_\ell(r)}{r}$

$$\beta_1 = \sqrt{\frac{2\mu E}{\hbar^2}}$$

$$\eta_1 = \frac{e^2}{\hbar}\sqrt{\frac{\mu}{2E}}$$

$$\rho = \beta r$$

we have finally

$$\frac{d^2u_1(\rho)}{d\rho^2} + \left(1 - \frac{2\eta}{\rho} - \frac{2}{\rho^2}\right) u_1(\rho) = 0$$

The solutions to this equation are linear combinations of

regular and irregular coulomb functions for $\ell = 1$.

$$u_1(\rho) = (F_1(\rho) \cos \delta_1 + G_1(\rho) \sin \delta_1), \quad r > a$$

Here $F_1(\rho)$ is the regular solution defined by insisting that $F_1(0) = 0$ and that its asymptotic oscillations have unit amplitude. The other independent solution $G_1(\rho)$ is chosen to be asymptotically out of phase by $\pi/2$. Here δ_1 is the nuclear phase shift.

If we now also write for $r < a$

$$R_1(r) = \frac{N_2 v_1(r)}{r}$$

we will have

$$v_1(r) = A' \left[\frac{\sin kr}{kr} - \cos kr\right], \quad r < a$$

We can now determine the nuclear phase shift δ_1 by matching logarithmic derivatives at $r = a$,

$$\tan \delta_1 = \frac{F_1 v_1' - F_1' v_1}{G_1' v_1 - G_1 v_1'},$$

where the differentiation is with respect to kr. Now as the coulomb functions are normalized to unit particle density at infinity one can obtain A' at $r = a$.

The phase shift δ_1 is due to the presence of the nucleus. If a pure coulomb field were to exist all the way to the origin, the only solution we would have for the incoming wave

would be the regular solution which vanishes at the origin. For low energies, then, one would expect the phase shifts to be small ($\delta_1 \sim 0$) and we can use only the regular coulomb function. Physically this says that for low bombarding energies the probability of the particles penetrating the coulomb barrier is small; effectively it cannot sense the presence of the nucleus through the coulomb barrier.

We wish, at this point, to calculate the capture cross section for this reaction. In general the capture cross section is defined by

$$\sigma_c = \frac{\text{No. of } \gamma\text{-rays emitted per target nucleus per second}}{\text{No. of incident particles per cm}^2 \text{ per sec.}}$$

$$= \frac{\text{Transition Probability}}{\text{Incident Flux}}$$

The incident flux is simply the density of particles times the velocity of the particles. Since the Coulomb wave functions are normalized to unit particle density at infinity the incident flux is just v particles/ cm^2 sec.

Now for electric multipole emission the general formula for the capture cross section is given by:

$$\sigma(E\ell) = \frac{8\pi(\ell+1)}{\ell[(2\ell+1)!!]^2} \frac{1}{\hbar v} \left(\frac{\omega}{c}\right)^{2\ell+1} \sum_{m=-\ell}^{\ell} |Q_{\ell m}|^2$$

Here $Q_{\ell m}$ is the electric multipole moment defined by

$$Q_{\ell m} = e\int \Psi_f^* \, (r^{\ell} Y_{\ell}^{m*}) \Psi_i d\tau$$

$$= ea^{\ell} \int R_f^* \left(\frac{r}{a}\right)^{\ell} R_i r^2 dr \int \mathcal{Y}_{j\ell s}^{m*} Y_{\ell}^{m*} \mathcal{Y}_{j\ell s}^{m} \sin\theta \, d\theta d\Phi$$

The important consideration here concerns the radial integrand. Here R_f^* is the radial wave function corresponding to the final state which, in our case, is the bound state for the last proton in the well representing the He^3 compound nucleus; R_i is the radial wave function for the incident particle which is a combination of the Coulomb wave functions. We take $\ell = 1$ here corresponding to electric dipole radiation.

The ground state wave function in question has an oscillatory character within the nuclear potential well and dies away rapidly on the exterior of the well. The incoming wave being represented mostly by the regular Coulomb wave function F_1 decreases very rapidly toward the nucleus. The figure on the following page shows the radial integrand plotted for two energies (Lal, Thesis 1961). Here we see that the integrand peaks at several nuclear radii. The matrix element, then, arises almost entirely from transitions taking place outside the nuclear potential well. The actual contribution to the integrand from inside the well, not

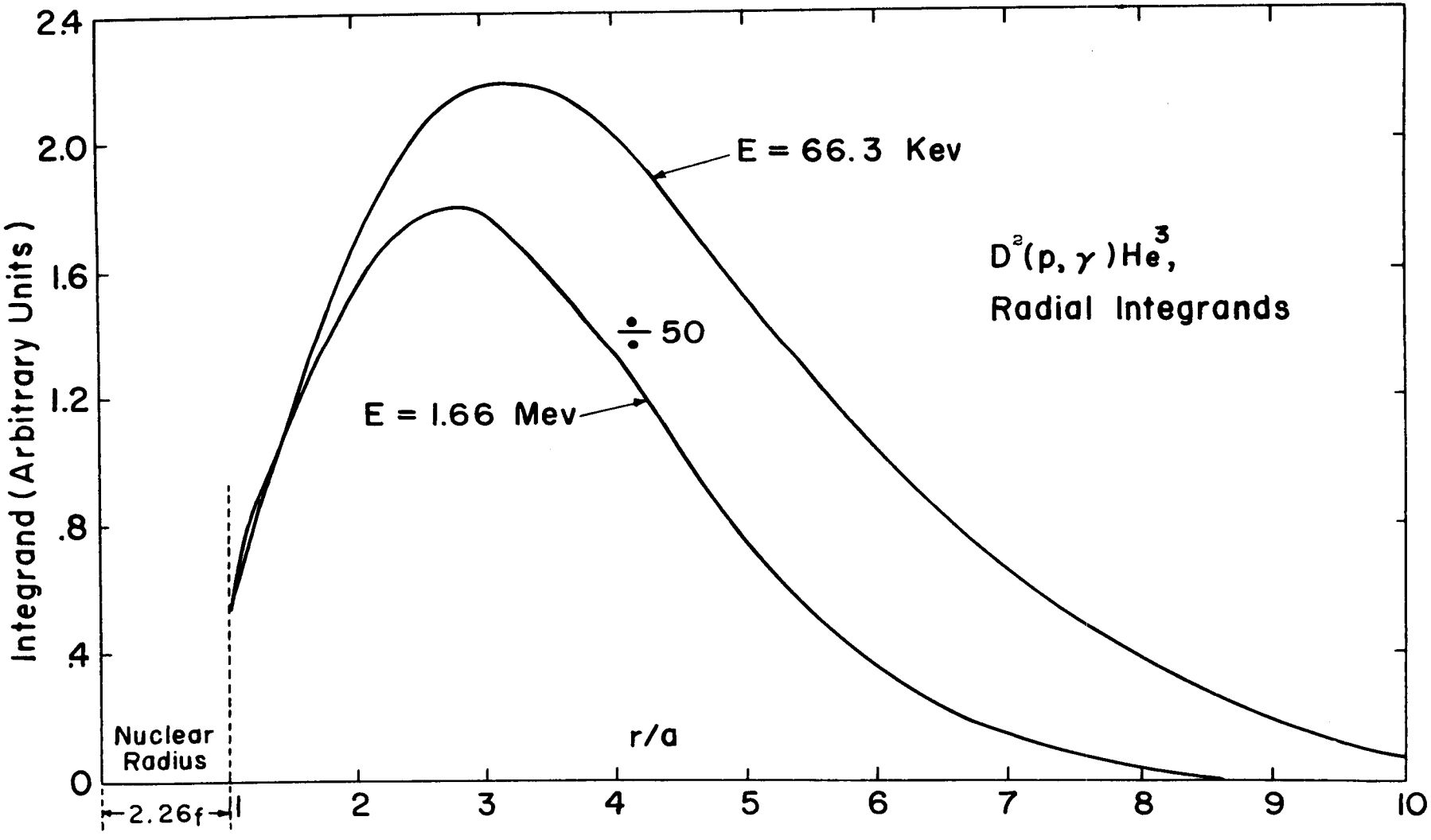
Integrand (Arbitrary Units)
2.4
2.0
1.6
1.2
.8
.4
0
E = 66.3 Kev
÷ 50
E = 1.66 Mev
D²(p, γ)He³,
Radial Integrands
Nuclear Radius
2.26f
r/a
1
2
3
4
5
6
7
8
9
10

plotted by Lal, would be extremely small: comparable to the error made in neglecting the nuclear phase shift of the incoming particle.

This result is typical of such non-resonant reactions. When bombarding such a nucleus at an energy far away from any resonances, one finds generally this direct capture process which will have its amplitude peaked at some distance from the nuclear potential well. Due to this observed behavior we can see that the actual shape of the nuclear potential well is not particularly important. One would then expect that the absolute cross section calculated from this procedure would at least be correct as to order of magnitude. For this reaction the experimental values (Griffiths, Lal, and Scarfe) give

$$S(0) = 2.5 \times 10^{-4} \text{ kev barns}$$

$$\langle dS/dE \rangle = 0.079 \times 10^{-4} \text{ barns}$$

with an uncertainty of the order of 50%.

We shall now discuss some of the consequences of the deuterium burning stage along with a re-examination of some of the other deuterium reactions.

Neutron Production During Deuterium Burning

Neutron production during deuterium burning was

initially discussed by Salpeter (Physical Review, 97, 1237, (1955)). We recall the two reactions

$$D^2(d,n)He^3$$

$$\text{and} \quad D^2(d,p)H^3$$

In the limit of low bombarding energy, these two reactions have equal cross-sections. Salpeter finds for the cross-section factor for the combined reactions

$$S_0 = (2.1 \pm 0.5) \times 10^2 \text{ kev barns.}$$

From this we may find the ratio of the number of neutrons produced relative to the number of protons absorbed in the $D^2(p,\gamma)He^3$ reaction.

$$\frac{P_n}{P_p} = 1.24 \times 10^5 \left(\frac{x_D}{x_H}\right) \exp\left(\frac{-5.4}{T_6^{1/3}}\right)$$

Deuterium burning takes place in the sun at $T_6 = 0.8$, and under those circumstances,

$$P_n/P_p = 0.111$$

There is an error in this figure of the order of 50%, most of which is due to the error in the proton capture reaction. Assuming that the primitive material forming the sun has the same ratio by number of deuterons to protons as does the earth,

$$n_d/n_p \simeq 1.5 \times 10^{-4}$$

we find x by multiplying the number densities by the relative masses, so

$$\frac{x_d}{x_p} = 3 \times 10^{-4} .$$

As deuterium burning goes to completion, the ratio of x_d/x_p will decrease, hence we divide by a factor of 2 to get the total yield of neutrons over the exhaustion of the deuterium. Thus

$$\frac{P_n}{2P_n + P_p} = 0.046$$

averaged over the deuterium burning process.

These neutrons are produced with energies of the order of 2.5 Mev and, for the most part, they collide with the abundant hydrogen. Besides being by far the most abundant constituent of the medium, hydrogen has a rather large scattering cross section for neutrons. Consequently, the medium is an extremely efficient neutron moderator (also, the masses of hydrogen atoms and neutrons are very nearly equal, so on the average half of the neutron energy is lost in each collision). The collisions of the neutrons with the hydrogen atoms or protons will rapidly slow the neutrons until they are in thermal equilibrium with their surroundings. Once this occurs, the neutrons just wander about, with

their energies varying within the rather diffuse bounds allowed by the Maxwell energy distribution, until they are captured. To discover what captures them we are interested in relative capture cross sections multiplied by the relative abundances of the different nuclei present. It happens that we need consider only two nuclei, the dominant neutron-capturing nuclei, which are hydrogen and He^3. The problem is complicated by the fact that the abundance of He^3 varies because He^3 is one of the products of the deuteron destruction reaction.

Both hydrogen and He^3 have neutron capture cross-sections which vary as $^1/_v$, where v is the neutron velocity. Thus it is a simple matter to calculate the effective capture cross-section for any given temperature. One takes the cross section measured in the laboratory (at $\frac{1}{40}$ of an electron volt) and uses the $^1/_v$ dependence to calculate the capture cross section at the temperature of interest.

The relative amounts of He^3 and He^4 cannot be determined in any but exceedingly abnormal stars in which the amount of He^3 is greatly increased. The abundance of helium in the sun cannot be determined at all because of the fact that it is not ionized and all the fundamental lines are

in the far ultraviolet. Eventually its abundance in the sun will be measured from space, but as yet we have no direct measurement. Judging from indirect evidence, the abundance of helium by number is about 15% relative to hydrogen. Some of this indirect evidence is the measured helium-hydrogen ratios in much hotter stars where some helium lines are detectable; the rest comes from the construction of solar models in which some of the properties depend on the ratio of helium to hydrogen.

For $T_6 = 0.8$ (corresponding to 87.6 electron volts) the average cross section for hydrogen is 0.0056 barns. For He^3, the cross section is 91 barns. Note that the capture of neutrons by hydrogen (the $H^1(n,\gamma)D^2$ reaction) regenerates deuterium, which is fed back to the start of the deuterium-burning process. Because few neutrons are produced, this correction is small and will be neglected. The He^3 neutron capture reaction forms tritium: $He^3(n,p)H^3$. In general, exothermic particle reactions have much greater cross sections than simple capture reactions; this reaction is typical of such cases. The tritium formed has a short half life (12.26 years) compared to the time in which deuterium burning is expected to occur in the sun (~300,000

years). The tritium decays back to He^3 with the emission of electrons and anti-neutrinos, so the neutron capture in He^3 does not effectively diminish the amount of He^3 present.

Now, we wish to know the initial relative abundance of He^3. The natural abundance of He^3 is difficult to determine, however, because helium is lost from the earth's atmosphere in a time short compared to a billion years. Occasionally, from some meteorites, apparently primordial gases are extracted - gases which have been frozen in these meteorites for the last 4.5 billion years. This is particularly significant in discussion of cosmochronology because some of the isotope compositions, particularly xenon, differ in these meteorites from that in the earth's atmosphere. However, for the He^3 to He^4 ratio, these meteorites give a remarkably uniform value of about 3×10^{-4}.

For the sun, we take

$$\frac{He^4}{H} = 0.156$$

and therefore

$$\frac{He^3}{H} = 4.7 \times 10^{-5}$$

If we assume that this is characteristic of solar matter, then we may calculate the neutron capture effectiveness of He^3 with respect to hydrogen:

$$4.7 \times 10^{-6} \times \frac{91}{0.0056} = 0.76.$$

The initial He^3 present in the sun in nearly as important as hydrogen for absorbing neutrons.

Because two deuterons are destroyed to form only one He^3 nucleus in some cases, the ratio of deuterons burned to He^3 produced is 0.954. If we assume that the primitive ratio of deuterium to hydrogen in the solar nebula is equal to the terrestrial ratio, we may use

$$\frac{D^2}{H^1} = 1.5 \times 10^{-4}.$$

Now,

$$1.5 \times 10^{-4} (0.954) \frac{91}{0.0056} = 2.32$$

so the additional He^3 formed becomes more than twice as effective as hydrogen for capturing neutrons. The number of neutrons produced per H^1 present is

$$0.046 \ (1.5 \times 10^{-4}) = 6.9 \times 10^{-6}$$

Now we wish to calculate the change in abundance for any other nucleus with average cross section $\langle\sigma\rangle$:

$$f = \frac{6.9 \times 10^{-6}}{0.0056} \langle\sigma\rangle \int_0^1 \frac{dx}{1 + 0.76 + 2.32x}$$

$$= 4.5 \times 10^{-4} \langle\sigma\rangle$$

For typical heavy nuclei with odd mass numbers the

average cross section may be of the order of 10 to 100 barns (averaged over many resonances). Thus a typical heavy nucleus would be depleted from about 0.5 to 5%. This may have observable effects on isotopic composition of heavy elements in the sun as compared to the earth and meteorites. I believe that part of the differences of terrestrial and meteoric xenon is attributable to this.

The next set of reactions to be considered are the proton-proton chains. Again, these represent the main mode of energy production in lower main sequence stars.

Proton-Proton Chains

In a star initially composed of pure hydrogen there is a simple sequence of reactions that leads to the production of He^4 in the interior. The central temperatures at which these reactions occur vary from about 8×10^6 °K in a faint red dwarf star to about 15×10^6 °K in the sun. When less massive stars reach the main sequence they stay at that particular position on H-R a very long time while these processes take place.

The reactions are given below in their entirety where the various designations given the reactions will be discussed in turn.

Proton-Proton Chains

PP I

$H^1(p, \beta^+\nu)D^2$

$D^2(p,\gamma)He^3$

$He^3(He^3, 2p)He^4$

PP II

$He^3(\alpha,\gamma)Be^7$

$Be^7(e^-,\nu)Li^7$

$Li^7(p,\alpha)He^4$

PP III

$Be^7(p,\gamma)B^8$

$B^8(\beta^+\ \nu)Be^8*(2\alpha)$

We start out with the basic proton-proton reaction which is a collision of two protons. Most of the time the protons are re-emitted, but once in a long while a beta-decay takes place which results in the formation of a deuteron. (This reaction will be examined in detail later on.) This process is extremely slow because a beta transformation must take place during the collision which is a very improbable process. The reaction does not proceed at an appreciable rate until the temperature and density become high enough so that Coulomb barrier penetration can take place very easily. Though this reaction will probably

never be observed under laboratory conditions, the theoretical calculation of the reaction rates is well defined and is presumed to be correct.

The deuteron produced from the p-p reaction then captures a proton with the subsequent emission of a γ-ray to form He^3. The abundance of He^3 then builds up until it reaches a concentration high enough for an appreciable rate of He^3-He^3 reactions to take place. This results in the emission of two protons and leaves an alpha particle. Thus He^4 is formed and the proton supply is replenished. This whole reaction chain is referred to as the PP I Chain.

Once the stellar interior contains an appreciable amount of He^4 there is an alternate path by which He^3 can be destroyed. This is the capture of an α-particle by He^3 resulting in Be^7. The Be^7 then undergoes a beta decay to Li^7. The Li^7 will react rather quickly with a proton to form two α-particles. This is the PP II Chain.

An alternate route in the PP II Chain which leads to PP III may take place if the Be^7 formed captures a proton yielding B^8. The B^8 has a half life of 0.78 seconds for beta decay to Be^8 which then decays into two α-particles.

An interesting point is that the end point of the B^8 beta decay is about 14 Mev, so that on the average about 7 Mev per neutrino is lost to the star since the neutrinos stream out from the interior unhindered by intervening material. This process significantly reduces the efficiency of the hydrogen to helium conversion as a means of generating energy in the interior to keep the center of the star heated. One of the things that has been of great interest in the last five years has been to determine the relative importance of these various reactions in the stellar interior.

We shall now discuss the details of the p-p to D^2 reaction. As indicated before this is the thermonuclear reaction which has the least probability of being observed in the laboratory because the cross section is so small.

The approach used here will follow that of Bethe and Critchfield[1], with corrections by Salpeter[2], and Frieman and Motz[3].

To talk about the $H^1(p,\beta^+\nu)D^2$ reaction we must first discuss the process of beta-decay, since we eventually have a proton decaying into a neutron, positron and neutrino,

---

[1]H.A. Bethe, C.L. Critchfield, Phys. Rev. 55, 434
[2]E.E. Salpeter, Phys. Rev. 88, 547
[3]E. Frieman, L. Motz, Phys. Rev. 83, 202

i.e.

$$p \rightarrow n + \beta^{+} + \nu.$$

The usual rules of conservation of energy, and linear and angular momenta including spin still apply. Since this is a weak interaction, parity is in general not conserved. The electron (positron) and antineutrino (neutrino) can have their spins parallel or antiparallel. If the proton is contained in a nucleus then the total spin of the nucleus can change by zero or one unit of spin by arranging the spins of the positron-neutrino pair in either antiparallel or parallel fashion. If the decay does not change the spin, i.e., if $\Delta J = 0$,we then have the so-called Fermi selection rules. If there is a spin change of 0 ± 1, but not zero-to-zero, we then have the Gamow-Teller selection rules. There are also the so-called forbidden transitions in which the spin change is greater than unity. This requires that the positron-neutrino system emitted have some net angular momentum with respect to the nucleus, which in effect means that the pair is emitted some distance from the nucleus. Because the wave functions for the nucleus decrease rapidly with distance from the nucleus we expect that these transitions are relatively improbable.

We are interested in the case of a two (or di-)proton

system decaying to D^2. If each of the protons have come together with zero angular momentum (s-wave), we may then think of the diproton as a nucleus in its ground state. If this is the case, the spins of the two protons must be anti-parallel in order that the Pauli exclusion principle not be violated. The net spin of the diproton is then zero. For the deuteron, however, we do not have two identical particles so that the neutron and proton may have parallel (Triplet, S = 1 state) or antiparallel (Singlet, S = 0 state) spins. It turns out that the triplet state forms the deuteron ground state. The singlet state is so ill-defined that no characteristic energy is ascribed to it. The transitional beta-decay from the diproton to D^2 then involves a spin change of one and obeys the Gamow-Teller selection rules. What we will have to do is form the wave function for the diproton (wave function for two protons in collision) and the wave function for the deuteron, and compute the probability that the transformation can take place during the collision.

In the Fermi theory of beta-decay, the transition probability for decay is given by

$$T = g\ f(W)\,|G|^2\ |M_{sp}|^2$$

where g is the coupling constant

$$g = (6.3 \pm 0.3) \times 10^{-4} \text{ sec}^{-1},$$

W is the endpoint energy of the emitted positron (in units of mc^2) where for zero relative energy of collision,

$$W_o = 1.827 \ (1 \pm .002)$$

f(W) is the Fermi function which gives essentially the probability for emitting the electron or positron into the available phase space. It is given by

$$f(W) = (W^2-1)^{\frac{1}{2}} \left(\frac{W^4}{30} - \frac{2W^2}{20} - \frac{2}{15}\right)$$
$$+ \frac{1}{4} W \log \left[W + (W^2 - 1)^{\frac{1}{2}}\right]$$

The relative velocities of collision we will be concerned with are of the order

$$v \simeq \left(\frac{4\pi e^2 kT}{\hbar M}\right)^{\frac{1}{2}} \text{ cm/sec, which corresponds}$$

to energies in the kev region. (M is the proton mass) These energies are small in comparison to W_o. This leads to an approximate value of f(W) given by[2]

$$f(W) = 0.145 \left[1 + 0.054 \left(\frac{T}{15}\right)^{2/3}\right] (1 \pm 0.03).$$

$|M_{sp}|^2$ is the spin part of the overall matrix element for the transition. This takes care of the summation over the various spin states involved and of the fact that either one of the protons can be the one that gets changed into the neutron. The numerical value of $|M_{sp}|^2$ turns out to be 3/2.

The factor G is the overlap integral between the final and initial states, i.e.,

$$G = \int \Psi_f^* \Psi_i d\tau .$$

The cross section for the reaction is then given by

$$\sigma = \frac{gf(W)}{v} \left| \int \Psi_p \Psi_o d\tau \right|^2 ,$$

where Ψ_p is the wave function for two protons normalized to unit density, and Ψ_d is the deuteron ground state wave function.

We shall follow Bethe and Critchfield and assume a square well potential model for the deuteron. Though seemingly crude, this gives good results since it turns out that the major contribution to the matrix elements come from regions away from the well. That is, the shape of the well itself is not very important. In such a case let the well radius be r_o and its depth be V_o. Then,

$$\Psi_d = \left(\frac{B}{r}\right) \exp\left[-(x-x_o)\right], \text{ for } r > r_o$$

$$= \left(\frac{B}{r}\right) \sin \mu x \,/\, \sin \mu x_o, \text{ for } r < r_o$$

where $x = r/b$, $x_o = r_o/b$

$$b = \frac{\hbar}{\sqrt{M\epsilon}}$$

$$\mu = \left[(V-\epsilon)/\epsilon\right]^{\frac{1}{2}}$$

$$B = (2\pi b)^{-\frac{1}{2}} (1+x_o)^{-\frac{1}{2}} (1+\mu^{-2})^{-\frac{1}{2}}.$$

M is the proton mass and ϵ is the binding energy of the deuteron.

If we insist on continuity in the logarithmic derivatives we find a relation between V_o and r_o, viz.,

$$\mu \cot \mu x_o = -1.$$

The proton wave function at large distances is given by,

$$\Psi_p = \frac{\sin(\rho - \Phi)}{\rho},$$

where $\rho = kr$, $k = \frac{Mv}{2\hbar}$ and
Φ is a phase angle.

Inside the nuclear potential well

$$\Psi_p = \frac{A}{r} \sin \frac{(MD)^{\frac{1}{2}} r}{\hbar} = \frac{w}{r}, \quad r < r_o$$

where D is the depth of the square potential well between two protons. The width is assumed to be the same as that for the deuteron, namely r_o. The constant A is a normalization factor.

Outside the well the wave function is a function of the usual Coulomb wave functions given by,

$$\Psi_p = (e^{iK} \cos K)(F + G \tan K)/kr, \quad r > r_o$$

where K is a phase shift. (This phase shift is what makes Ψ_p different from the usual Coulomb wave function solution.)

At the boundary $r = r_o$ we have

$$\tan K = \frac{F^2 \delta}{1-FG\delta}$$

where

$$\delta = \left(\frac{d \log F}{d\rho} - \frac{d \log w}{dr}\right)_{r_o}.$$

For low proton energies $F(r_o)$ is small which implies K is small also. (For example, for a relative energy of 12.5 kev., K = 0.0017). Thus $e^{iK}\cos K \approx 1$. In such a case we can express the normalization factor as

$$A = \frac{F(r_o) + G(r_o) \tan K}{k \sin (MD)^{\frac{1}{2}} r_o/\hbar}$$

For L = 0 protons (s-wave), $F = C\rho\Phi$, and $G = C^{-1}\Theta$,

where

$$C = (2\pi\eta)^{\frac{1}{2}} e^{-\pi\eta}, \text{ and } \eta = e^2/\hbar v.$$

Φ and Θ are slowly varying functions of r which approach unity as r approaches zero. Thus,

$$\tan K = C^2 k r_o \lambda,$$

where,

$$\lambda = \Phi^2 \zeta/(1 - \Phi\Theta\zeta),$$

and

$$\zeta = \left(\frac{d \log F/w}{d \log \rho}\right) = \left(1 + r \frac{d \log \Phi}{dr} - r \frac{d \log w}{dr}\right)_{r_o}$$

The proton wave functions are then,

$$\Psi_p = C[\Phi(r) + \lambda(r_o/r)\ \Theta(r)],\ r > r_o$$

$$\Psi_p = C\,\frac{r_o}{r}\,[\,\Phi(r_o) + \lambda\Theta(r)\,]\,\frac{\sin \nu r/b}{\sin \nu r_o/b}\ ,\quad r < r_o,$$

where,

$$\nu = (MD)^{\frac{1}{2}}\, b/\hbar = (D/\epsilon)^{\frac{1}{2}}.$$

One notices that the main variation with energy of Ψ_p is the coefficient C which includes the Gamow barrier penetration probability. The function λ represents the effect of the potential well on the wave functions, and in essence this means the effect of any resonance that is associated with the diproton system itself.

We shall now use the Bessel-Clifford expansions (as we did in previous sections) to re-express the functions Φ and Θ:

$$\Phi(y) = y^{-\frac{1}{2}}\, I_1(2y^{\frac{1}{2}}) = 1 + \frac{y}{1!2!} + \frac{y^2}{2!3!} + \frac{y^3}{3!4!} + \ldots,$$

$$\Theta(y) = -2y^{\frac{1}{2}}\, K_1(2y^{\frac{1}{2}}) = 1 + y(\log y + 2\gamma - 1)\,\Phi$$

$$- \sum_{s=1}^{\infty} \frac{y^{s+1}}{2!\,(s+1)!} \sum_{t=1}^{s} \left(\frac{1}{t} + \frac{1}{t+1}\right)\ ,$$

with $y = 2r/a$, $a = 2\hbar^2/Me^2 = 5.75 \times 10^{-13}$ cm.

($\gamma = 0.577\ldots$, Euler's constant).

For a value of η of unity these expansions give the values of Φ and Θ to within 1%.

The cross section for the reaction now reads,

$$\sigma = \frac{gf(W)}{v} C^2 \frac{(4\pi b^2)^2}{2\pi b} \Lambda^2 ,$$

where

$$(1+x_0)^{\frac{1}{2}} (1+\mu^{-2})^{\frac{1}{2}} \Lambda = \Lambda_1 + \Lambda_2 + \Lambda_3 ,$$

$$\Lambda_1 = \frac{x_0[\Phi(r_0)+\lambda\Theta(r_0)]}{\sin \mu x_0 + \sin \nu x_0} \int_0^x \sin \mu x \sin \nu x \, dx,$$

$$\Lambda_2 = \int_{x_0}^{\infty} x \, dx \exp[-(x-x_0)]\Phi(2bx/a),$$

$$\Lambda_3 = \int_{x_0}^{\infty} dx \exp[-(x-x_0)]\Theta(2bx/a) .$$

Before we evaluate these explicitly, Λ is essentially the matrix element for the transition probability. This is split up into a term (Λ_1) which arises from inside the potential well, and two terms Λ_2, Λ_3 which arise from regions outside the well. As will be shown the latter two terms are the dominant ones. Finally, the Λ's become,

$$\Lambda_1 = \frac{\frac{1}{2} x_0^2[\Phi(r_0) + \lambda\Theta(r_0)]}{\sin \mu x_0 \sin \nu x_0} \left[\frac{\sin (\mu-\nu)x_0}{(\mu-\nu)x_0} - \frac{\sin (\mu+\nu)x_0}{(\mu+\nu)x_0}\right]$$

$$\Lambda_2 = 1+x_0 + (2b/a)(1+x_0+\tfrac{1}{2} x_0^2)+\tfrac{1}{2} (2b/a)(1+x_0+\tfrac{1}{2} x_0^2+\tfrac{1}{6} x_0^3)+\ldots,$$

$$\Lambda_3 = \lambda x_0\{1+(2b/a)[\log (2b/a) +2\gamma-1]\Lambda_2$$
$$- [(2b/a)^2 \tfrac{3}{2} (1+x_0+\tfrac{1}{2} x_0^2) + \tfrac{1}{2} \left(\tfrac{2b}{a}\right)^3 \left(\tfrac{7}{3}\right) \left(1+x_0+\tfrac{1}{2} x_0^2+\tfrac{1}{6} x_0^3\right)+\ldots]$$

$$+\sum_{s=1}^{\infty} (2b/a)^3 f_s(x_0)/(s-1)! ,$$

with,

$$f_s(x_0) = (s!)^{-1} \int_{x_0}^{\infty} \exp[-(x-x_0)]x^s \log x \, dx,$$

$$f_1(x_0) = 1+(1+x_0) \log x_0 - Ei(-x_0)\exp(x_0),$$

$$f_2(x_0) = \frac{3}{2} + \frac{1}{2} x_0 + (1+x_0+\frac{1}{2} x_0^2)\log x_0 - Ei(-x_0)\exp(x_0),$$

$$f_3(x_0) = (11/6) + (5/6)x_0 + \left(\frac{1}{6} x_0^2+(1+x_0+\frac{1}{2} x_0^2+\frac{1}{6} x_0^3)\right) \log x_0 - Ei(-x_0) \exp(x_0).$$

If $r_0 = e^2/mc^2$, $\Lambda^2 = 8.08$

" $r_0 = e^2/2mc^2$, $\Lambda^2 = 5.93$

As mentioned before, Bethe and Critchfield find that Λ_2 and Λ_3 are considerably larger than Λ_1 for reasonable assumptions of well depth, etc. Thus the shape of the well turns out to be a relatively minor factor in the cross section.

Salpeter has re-evaluated the matrix element using the theory of effective range and various potential shapes. For $\eta=\infty$ (zero bombarding energy) he finds:

Yukawa well;	$\Lambda^2 = 7.11$
Exponential well;	$\Lambda^2 = 7.00$
Square well;	$\Lambda^2 = 6.92$

Frieman and Motz used explicit wave functions and found $\Lambda^2 = 6.79$. (Salpeter regards this calculation as the most accurate.)

For a reasonable value of $\eta \approx 1.5$, Salpeter adopts

$$\Lambda^2 = 6.82 \ (\pm\ 0.05).$$

We finally obtain a value for the cross section factor S(0) of,

$$S(0) = (3.36 \pm 0.4)\times 10^{-22} \text{ kev. barns,}$$

with

$\langle ds/dE \rangle = 2.7\times 10^{-24}$ barns.[4] (We note that the value of S(0) is presumed known to within 12%.)

The Remaining Reactions

$D^2(p,\gamma)He^3$; This reaction has been discussed in the context of what happens to the deuterium during the contraction phase of a star when the interior temperature (about 800 ,000°C) first rises enough to be able to destroy the deuterium and where the lifetime of the deuterium may be many thousands of years. In the stellar interior, when the proton-proton chain is going, the proton-proton reaction is extremely slow because the relatively few p-p collisions in the high energy tail of the Maxwellian distribution are unable to overcome the great reluctance of the system to beta-decay. Consequently, under typical conditions in the center of a main sequence star, we find that the temperature dependence of the p-p reaction is reduced to about the order of the fourth power

[4] Hubert Reeves, Stellar Energy Sources, (to be published)

of the temperature, in contrast to more usual reactions which tend to vary as about the twentieth power of the temperature. The destruction of deuterons is so drastically faster than the p-p reaction that they will disappear on a time scale of the order of seconds once the deuterium has been formed. This means that we can expect D^2 to H^1 number density ratios on the order of 10^{-17} in stellar interiors.

<u>$He^3(He^3,2p)He^4$</u>: This is a non-resonant exothermic particle emission reaction and therefore goes very readily. The S(0) value is poorly known but is believed to lie between,

$$1.2\times10^3 \leq S(0) \leq 2.4\times10^3 \text{ kev.-barns.}$$

The slope of the S factor with energy is not known at all.

<u>$He^3(\alpha,\gamma)\ Be^7$</u>: This is a non-resonant reaction (Johnson-Holmgren, 1959) with a large cross section corresponding to a direct capture process. It forms the first link in the PP II chain and competes with the $He^3(He^3,2p)He^4$ reaction. The cross section parameters are,

$$S(0) = 0.47\pm0.07 \text{ kev.-barns,}$$

$$\langle dS/dE \rangle = -2.8\times10^{-4} \text{ barns.}$$

Though the cross section is considerably smaller than for the $He^3(He^3,2p)He^4$ reaction of the PP I chain, the amount of He^4 present as compared to He^3 tends to make this an important

reaction under certain conditions of temperature and pressure.

$\underline{Li^7(p,\alpha)He^4}$: This reaction follows the destruction of Be^7 by electron capture. It is one hundred times faster than the "competing" reaction $Li^7(p,\gamma)Be^8$, which in turn is of little interest anyhow since the Be^8 splits into two α-particles. For the reaction in question,

$$S(0) = 100 \pm 25 \text{ kev-barns.}$$

$\underline{Be^7(p,\gamma)B^8}$: This is a non-resonant reaction which starts the PP III chain, with

$$S(0) = 0.020 \pm 0.010 \text{ kev-barns,}$$

(Kavanagh, 1959). This reaction is unimportant at temperatures below 20×10^6 ^{o}K. Above these temperatures it represents an interesting reaction in that about one quarter of the energy released is lost by neutrino emission when the B^8 beta-decays.

$\underline{Be^7(e^-,\nu)Li^7}$: This is the reaction that leads into the PP II chain by capturing an electron. In the laboratory the captured electron is a K electron. In the stellar interior, however, the atom is ionized and a free electron must be captured.

We may estimate the rate for this free-electron capture by multiplying the rate for K-capture by the ratio of the probabilities for finding free and K-electrons in the nucleus.

The probability of finding a K electron inside the nucleus is

$$\int |\psi_e|^2 dV = \frac{1}{\pi}\left(\frac{Zme^2}{h^2}\right) V_n,$$

where Ψ_e is the K electron wave function and the integral is over the nuclear volume V_n. If there were no Coulomb fields, and if the average volume of space associated with one electron is V, the probability of finding the electron in the nucleus is V_n/V. In the presence of a Coulomb field the electrons become concentrated towards the nucleus and we find

$$\int |\psi_e|^2_{free} dV = \frac{V_n}{V} \frac{2\pi\eta}{1 - \exp(-2\pi\eta)},$$

where

$$\eta = \frac{Ze^2}{\hbar v},$$

$$v = \text{velocity of free electron at infinity.}$$

If we set $\mu_e = 1$ for hydrogen and equal to 2 for everything else then

$$V = \frac{3.32 \times 10^{-24}}{\rho(1 + x_H)} \text{ cm}^3,$$

$$\rho = \text{density in gm/cm}^3,$$

and x_H is the concentration of hydrogen by mass. For small v, $\exp(-2\pi\eta) << 1$.

The probability can now be integrated over a Maxwellian velocity distribution to obtain a rate of free electron capture

of

$$p_e = 1.9 \times 10^{-9} \frac{\rho(1 + x_H)}{T_6^{1/2}} \text{ sec}^{-1}.$$

When the calculation is done properly, i.e., including relativistic effects etc., the rate becomes (Bahcall, 1962)

$$p_e = 2.12 \times 10^{-9} \frac{\rho(1 + x_H)}{T_6^{1/2}} \text{ sec}^{-1}.$$

correct to within a few percent.

Energy Generation Rates [5]

Since the first proton-proton reaction starts off the PP series the rate of the proton-proton reaction will determine the energy generation rate in effect. If we put together what we have derived previously we find a reaction rate for the proton-proton reaction of,

$$r = (1.0 \pm 0.1) \times 10^{11} fg\rho x_H^2 \, e^{-33.81 \, T_6^{-1/3}} / T_6^{2/3}$$

where

$$g(T) = 1 + \frac{5}{12\tau} - \frac{35}{288\tau^2} + \ldots + \frac{\langle dS/dE \rangle}{S(0)} \left(E(T) + \frac{35}{36} kT\right)$$

or,

$$g(T) \cong 1 + 1.23\text{x}10^{-2} T_6^{1/3} + 7.8\text{x}10^{-3} T^{2/3} + 6.73\text{x}10^{-4} T$$

[5]This section follows Reeves (loc. cit.) and uses his data.

f = electron screening factor = $1 + 0.25\ \rho^{1/2}/T_6^{3/2}$

$\tau = 33.81\ T_6^{-1/3}$.

At temperatures below about 8×10^6 °K only the $H^1(p,\beta^+\nu)D^2$ and $D^2(p,\gamma)He^3$ (i.e., the p-p and dpγ) reactions can come into equilibrium. For these two reactions combined, the Q value (neglecting the energy lost by the neutrinos) is 6.675 Mev or 1.069×10^{-5} ergs.

The energy generation rate is then

$$\epsilon = (1.1 \pm 0.1) \times 10^6\ fg\rho x_H^2 e^{-33.81T_6^{-1/3}}/T_6^{2/3}$$

ergs/gm-sec

for $T_6 \approx 8$.

If the temperature is sufficiently high the He^3 may react with whatever He^4 is present (leading to the PP II chain) or may react with itself thus completing the PP I. If these reactions do take place the PP I reaction will go faster at lower relative temperatures or when the He^4 to H^1 ratio is lower. We note, however, that the PP I requires two protons for completion whereas the PP II requires only one. When all factors are considered it turns out that the relative energy generations from the three PP cycles can be expressed in terms of the He^4 to H^1 ratios.

The total energy generation for the three PP cycles is

then,

$$\epsilon_{pp} = \epsilon' \Psi \quad \text{ergs/gm -sec,}$$

where

$$\epsilon' = (2.06 \pm 0.2) \times 10^6 f g \rho x_H^2 e^{-33.81 T_6^{-1/3}} / T_6^{2/3}$$

ergs/gm-sec

and Ψ is a function of x_4/x_1 where $x_1 = x_H$ and x_4 is the mass-fraction for He^4. Ψ is plotted for two values of x_4/x_1, on the following figure. ($x_4/x_1 = 1$ corresponds roughly to the present solar composition and $x_4/x_1 = \frac{1}{4}$ corresponds roughly to a primeval sun at the inception of hydrogen burning.)

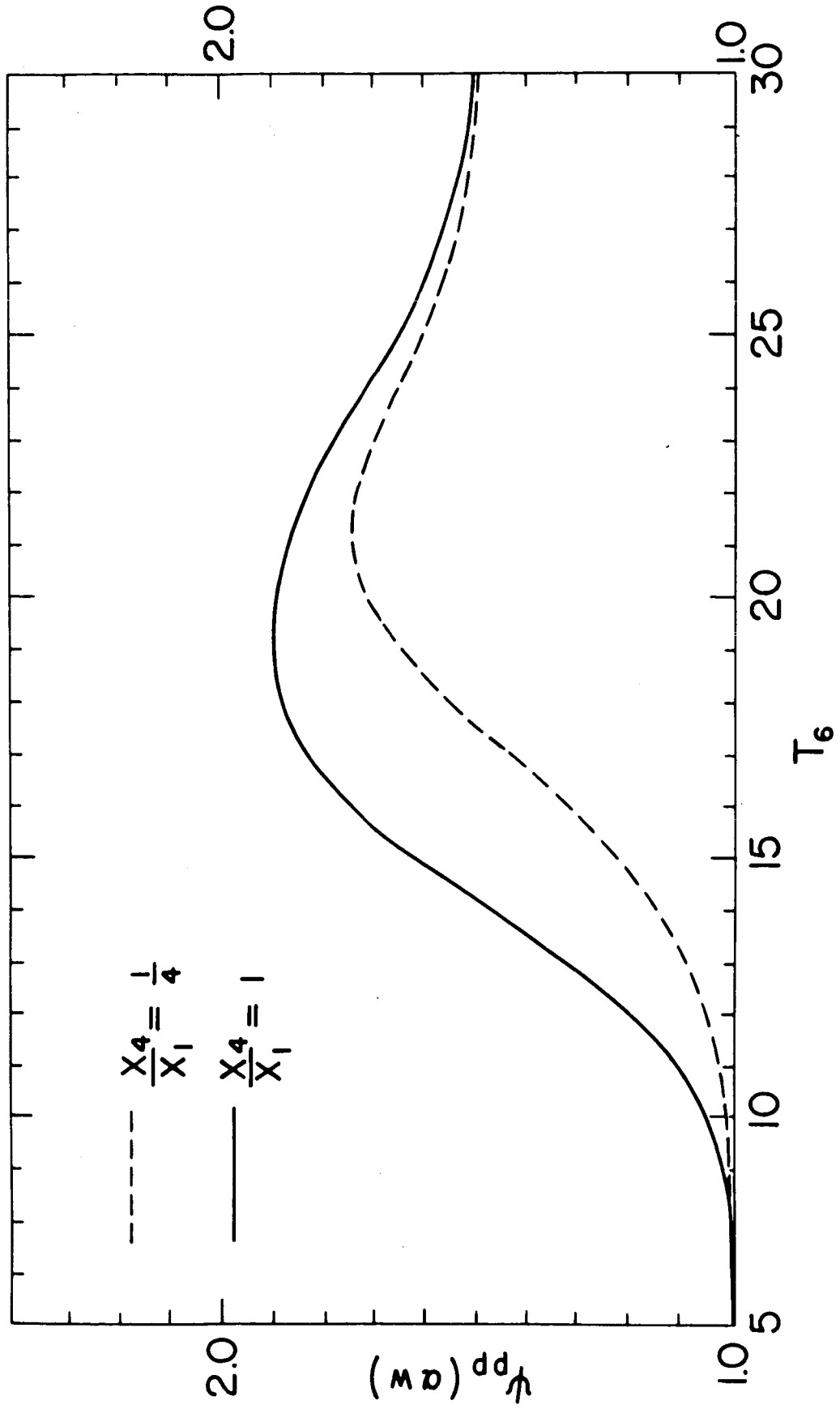
2.0
1.0
2.0
1.0
5
10
15
20
25
30
T_6
ψ_{pp} (α w)
$X^4/X^1 = -\frac{1}{4}$
$X^4/X^1 = 1$

CNO Cycles

As stated before, the hotter stars of the main sequence, with central temperatures of 17 x 10^6 °K or more, convert hydrogen to helium mainly by the CNO cycles. The carbon and nitrogen serve as catalysts for the reaction as can be seen from the following scheme for the cycles:

$$C^{12}(p,\gamma)N^{13}(\beta^+\nu)C^{13}$$
$$C^{13}(p,\gamma)N^{14}$$
$$N^{14}(p,\gamma)O^{15}(\beta^+\nu)N^{15}$$
$$N^{15}(p,\alpha)C^{12}$$
$$N^{15}(p,\gamma)O^{16}$$
$$O^{16}(p,\gamma)F^{17}(\beta^+\nu)O^{17}$$
$$O^{17}(p,\alpha)N^{14}$$
$$O^{17}(p,\gamma)F^{18}(\beta^+\nu)O^{18}$$
$$O^{18}(p,\alpha)N^{15}$$
$$F^{19}(p,\alpha)O^{16}$$

From the above, C^{12} captures a proton and forms N^{13} which beta decays to C^{13} with a half-life of 10.0 minutes. For the $C^{12}(p,\gamma)N^{13}$ reaction, S(0)= (1.20 + 0.15) kev-barns with $\langle dS/dE \rangle$ = 5.81 x 10^{-3} barns.

The C^{13} captures a proton to form N^{14} which is stable (S(0) = 5.52 $\pm$ 0.7 kev barns, $\langle dS/dE \rangle$ = 1.94 x 10^{-2} barns).

The N^{14} then captures a proton to form O^{15} ($S(0) = 3.12 \pm 0.25$ kev barns, $\langle dS/dE \rangle = -2.67 \times 10^{-3}$ barns) which beta decays with a 2.07 minute half-life to N^{15}. The N^{15}, for most of the time undergoes a (p,α) reaction to form C^{12} ($S(0) = 5.34 \times 10^4$ kev barns, $\langle dS/dE \rangle = 8.22 \times 10^2$ barns) thus forming the C^{12} which we started with leaving a He^4. We may expect, however, that if the cycle just illustrated turns over a few thousand times, the N^{15} will take an alternate route and γ-decay into O^{16}. ($S(0) = 2.74 \times 10^1$ kev-barns, $\langle dS/dE \rangle = 1.86 \times 10^{-1}$ barns.) If this happens the cycle continues on as shown. Some of the cross sections for these reactions are unknown. For those of which there is some data; this data is listed at the end of this section.

The reaction rate for the cycle is, as usual, governed by the slowest reaction of the group, and this is the $N^{14}(p,\gamma)O^{15}$ reaction. An important consequence of this in terms of nuclear synthesis is that when the CNO cycle is in equilibrium N^{14} is the most abundant nuclide, O^{16} probably the next most abundant, then C^{12}, C^{13} lower still and N^{15} vanishingly small.

There is an interesting aspect of the C^{12}, C^{13} ratio. Since both these nuclides have the same charge number, their reaction rates differ only slightly as they are affected by

the slightly different reduced mass of the proton for each of the two cases, and their equilibrium abundances are in the ratio of their cross section factors S(E). This ratio (C^{12}/C^{13}) is then about four. The spectra of some red giants whose atmospheres contain carbon molecules indicates that this ratio exists in these atmospheres.

The reaction rate for the $N^{14}(p,\gamma)O^{15}$ reaction is

$$r = 1.98 \times 10^{32}\ fg\rho x_{14} x_H e^{-152.313 T_6^{-1/3}} / T_6^{2/3}\ \mathrm{sec}^{-1}\ \mathrm{gm}^{-1}$$

where

$$g = 1 + 2.74\times10^{-3} T_6^{1/3} - 3.74\times10^{-3} T_6^{2/3} - 7.17\times10^{-5} T_6,$$

$$f = 1 + 1.75\ \rho^{1/2}/T_8^{3/2}$$

and x_{14} is the mass fraction of N^{14}.

The energy released is (for temperatures greater than or equal to about $T_6 = 16$),

$$\epsilon_{CN} = 7.94\times10^{27} fg\rho x_{14} x_H e^{-152.313 T_6^{-\frac{1}{3}}}\ T^{-2/3},\ \mathrm{erg/gm\ sec.}$$

For temperatures below $T_6 = 16$ the period of the cycle is too long to let the O^{16} reach an equilibrium abundance relative to the other nuclides in that portion of the cycle.

Once the elements with atomic masses in the range from twelve to 20 have been built up following reactions as have been discussed, another cycle, the Ne-Na cycle, assumes significance because a byproduct of the cycle is Ne^{21} which is a potential source of neutrons. As will be discussed later,

The formation of neutrons leads to the formation of the very heavy elements (beyond iron) on a slow time scale. We shall only list the reactions for the present with the further comment that the temperature ($T_6 \sim 50$) required to destroy Ne^{20} turns out to be obtained in hydrogen-burning shells of red giant stars.

<u>Ne-Na Cycle</u>

$$Ne^{20}(p,\gamma)Na^{21}(\beta^+\nu)Ne^{21}$$

$$Ne^{21}(p,\gamma)Na^{22}(\beta^+\nu)Ne^{22}$$

$$Ne^{22}(p,\gamma)Na^{23}$$

$$Na^{23}(p,\alpha)Ne^{20}$$

$$\text{or,}\quad Na^{23}(p,\gamma)Mg^{24}$$

(The cross sections for the above, if known, are listed at the end of this section.)

As a summary and aid to computation the remainder of this section is devoted to a listing of the pertinent reactions discussed in this section, cross sections, and miscellaneous useful data.

Table: Proton-Proton Chain

$H^1 + H^1 \rightarrow D^2 + e^+ + \nu$	
$D^2 + H^1 \rightarrow He^3 + \gamma$	PPI
$He^3 + He^3 \rightarrow He^4 + 2H^1$	
$He^3 + He^4 \rightarrow Be^7 + \gamma$	
$Be^7 + e^- \rightarrow Li^7 + \nu$	PPII
$Li^7 + H^1 \rightarrow Be^8 + \gamma$	
$Be^8 \rightarrow 2He^4$	
$Be^7 + H^1 \rightarrow B^8 + \gamma$	
$B^8 \rightarrow Be^8 + e^+ + \nu$	PPIII
$Be^8 \rightarrow 2He^4$	

Table: The CNO BI-CYCLE

$$C^{12} + H^{1} \rightarrow N^{13} + \gamma$$

$$N^{13} \rightarrow C^{13} + e^{+} + \nu$$

$$C^{13} + H^{1} \rightarrow N^{14} + \gamma$$

$$N^{14} + H^{1} \rightarrow O^{15} + \gamma$$

$$O^{15} \rightarrow N^{15} + e^{+} + \nu$$

$$N^{15} + H^{1} \rightarrow C^{12} + He^{4}$$

$$N^{15} + H^{1} \rightarrow O^{16} + \gamma$$

$$O^{16} + H^{1} \rightarrow F^{17} + \gamma$$

$$F^{17} \rightarrow O^{17} + e^{+} + \nu$$

$$O^{17} + H^{1} \rightarrow N^{14} + He^{4}$$

$$O^{17} + H^{1} \rightarrow F^{18} + \gamma$$

$$F^{18} \rightarrow O^{18} + e^{+} + \nu$$

$$O^{18} + H^{1} \rightarrow N^{15} + He^{4}$$

$$F^{19} + H^{1} \rightarrow O^{16} + He^{4}$$

Table: The NEON-SODIUM CYCLE

$$Ne^{20} + H^{1} \rightarrow Na^{21} + \gamma$$

$$Na^{21} \rightarrow Ne^{21} + e^{+} + \nu$$

$$Ne^{21} + H^{1} \rightarrow Na^{22} + \gamma$$

$$Na^{22} \rightarrow Ne^{22} + e^{+} + \nu$$

$$Ne^{22} + H^{1} \rightarrow Na^{23} + \gamma$$

$$Na^{23} + H^{1} \rightarrow Ne^{20} + He^{4}$$

$$Na^{23} + H^{1} \rightarrow Mg^{24} + \gamma$$

From section entitled thermonuclear reaction rates.

Reactions per second per nucleus of type 2:

$$P = \frac{4.34\times10^5 \ \rho x_1 \ (A_1+A_2)}{A_1^{\,2} A_2 \ Z_1 Z_2} \quad S \ \tau^2 \ c^{-\tau} \qquad \sec^{-1}$$

where:

$$\tau = 42.483 \left[\frac{Z_1^{\,2} Z_2^{\,2} \ A_1 A_2}{A_1 + A_2}\right]^{1/3} T_6^{\,-1/3}$$

$$S = \sigma E \exp 31.285 \ Z_1 Z_2 \left(\frac{A_1 A_2}{(A_1+A_2)E}\right)^{1/2}$$

x_1 = concentration by weight of particles of type 1 in the gas

σ = cross section in barns

E = energy in c.m.s. in kev.

T_6 is in 10^6 ^{0}K

defining:

$$A = \frac{4.34\times10^5 \ (A_1+A_2)}{A_1^{\,2} \ A_2 \ Z_1 Z_2} \qquad (\tau T^{1/3})^2$$

$$B = \tau \ T^{1/3}$$

we can write the reaction rate as:

$$p = A \ (\rho x_1) \ T^{-2/3} \ \exp(-B/T^{1/3}) \quad \sec^{-1}$$

Reaction	S(kev-barns)	A	B	⟨dS/dE⟩ (barns)
$H^1(p,\beta^+\nu)D^2$	3.36×10^{-22} ±0.4	3.3×10^{-13} ±0.4	33.810 ± 0.003	2.7×10^{-24}
$D^2(p,\gamma)He^3$	2.5×10^{-4} ±1.3	2.2×10^{5} ±0.4	37.210 ± 0.002	7.9×10^{-6}
$D^2(d,n)He^3$ / $D^2(d,p)H^3$	9.6×10^{1}	3.6×10^{10}	42.6	
$He^3(\alpha,\gamma)Be^7$	0.47 ±0.07	1.2×10^{8} ±0.2	128.277 ± 0.004	-2.8×10^{-4}
$He^3(He^3,2p)He^4$	1.2×10^{3}	4.3×10^{11}	122.774 ± 0.004	
$Li^6(p,\alpha)He^3$	5.06×10^{3}	5.96×10^{12}	84.149 ± 0.005	
$Li^7(p,\alpha)He^4$	100±25	1.2×10^{11}	84.731 ± 0.004	
$Li^7(p,\gamma)Be^8$	~1	$\sim10^{8}$	84.731 ± 0.004	
$Be^7(p,\gamma)B^8$	2×10^{-2} ±1	2.6×10^{7} ±1.3	102.645 ± 0.005	
$Be^9(p,\alpha)Li^6$	3.01×10^{4}	3.84×10^{13}	103.615 ± 0.004	
$Be^9(p,d)Be^8$	3×10^{4}	3×10^{13}	103.615 ± 0.004	
$B^{10}(p,\alpha)Be^7$	1.79×10^{4}	2.45×10^{13}	120.640 ± 0.003	
$B^{11}(p,\alpha)Be^8$	8.99×10^{4}	1.23×10^{14}	120.974 ± 0.003	
$C^{12}(p,\gamma)N^{13}$	1.20 ±0.15	1.7×10^{9} ±0.3	136.926 ± 0.002	5.81×10^{-3}
$C^{13}(p,\gamma)N^{14}$	5.52 ±0.7	8.0×10^{9}	137.200 ± 0.003	1.94×10^{-2}

Reaction	S(kev-barns)	A	B	<dS/dE> (barns)
$N^{14}(p,\gamma)O^{15}$	3.12 ±0.25	4.7×10^{9} ±0.4	152.311 ± 0.002	-2.67×10^{-3}
$N^{15}(p,\alpha)C^{12}$	5.34×10^{4}	8.0×10^{9}	152.538 ± 0.003	8.22×10^{2}
$N^{15}(p,\gamma)O^{16}$	2.74×10^{1}	4.2×10^{10}	152.538 ± 0.003	1.86×10^{-1}
$O^{16}(p,\alpha)F^{17}$	1.06×10^{1} ±0.18	1.7×10^{10} ±0.3	166.958 ± 0.001	-2.81×10^{-2}
$O^{17}(p,\alpha)N^{14}$	2×10^{2}	3×10^{11}	167.154 ± 0.003	
$O^{17}(p,\gamma)F^{18}$				
$O^{18}(p,\alpha)N^{15}$	1×10^{5}	1.5×10^{14}	167.327 ± 0.002	
$F^{19}(p,\alpha)O^{16}$	1×10^{6}	1.5×10^{15}	181.164 ± 0.003	
$Ne^{20}(p,\gamma)Na^{21}$	55±20	9.33×10^{10}	194.510 ± 0.002	
$Ne^{21}(p,\gamma)Na^{22}$	>5.6	$>10^{10}$	194.658 ± 0.004	
$Ne^{22}(p,\gamma)Na^{23}$	≥550	$\geq10^{12}$	194.793 ± 0.002	
$Na^{23}(p,\alpha)Ne^{20}$	3×10^{3}	3×10^{12}	207.704 ± 0.004	
$Na^{23}(p,\gamma)Mg^{24}$	$>10^{4}$	$>10^{13}$		

For the computation of reaction rates and energy generation rates the following are tabulated:[6]

$$g = 1 + UT_6^{\frac{1}{3}} + VT_6^{2/3} + WT_6 \quad ,$$

where g contains correction terms including <dS/dE> and Salpeter's correction series for the integration of the Gaussian of section 4. For the use of g (and the function f, or electron screening correction) refer to the text of this section.

[6] Taken exclusively from Reeves (Op.Cit.).

REACTION	U	V	W	f
	$U=5/12B$	$V=\frac{E_0}{T_6^{2/3}}\frac{\langle dS/dE\rangle}{S(0)}$	$W=\frac{35}{36}\frac{\langle dS/dE\rangle_k}{S(0)}$	Electron Screening Factor (Weak)
$H^1 + H^1 \rightarrow H^2 + e^+ + \nu$	1.23×10^{-2}	7.80×10^{-3}	6.73×10^{-4}	$(1 + 0.25\rho^{1/2}/T_6^{3/2})$
$H^1 + H^2 \rightarrow He^3 + \gamma$	1.12×10^{-2}	3.12×10^{-2}	2.45×10^{-3}	$(1 + 0.25\rho^{1/2}/T_6^{3/2})$
$He^3 + He^3 \rightarrow He^4 + 2H^1$	3.39×10^{-3}			$(1 + 1.0\ \rho^{1/2}/T_6^{3/2})$
$He^3 + He^4 \rightarrow Be^7 + \gamma$	3.25×10^{-3}	-2.15×10^{-3}	-4.90×10^{-5}	$(1 + 1.0\ \rho^{1/2}/T_6^{3/2})$
$Be^7 + e^- \rightarrow Li^7 + \nu$				
$Li^7 + H^1 \rightarrow He^4 + He^4$	4.92×10^{-3}			$(1 + 0.75\rho^{1/2}/T_6^{3/2})$
$Be^7 + H^1 \rightarrow B^8 + \gamma$	4.06×10^{-3}			$(1 + 1.0\ \rho^{1/2}/T_6^{3/2})$
$B^8 \rightarrow Be^8 + e^+ + \nu$				

REACTION	U	V	W	f
	$U=5/12B$	$V=\frac{E_0}{T_6^{2/3}}\frac{\langle dS/dE\rangle}{S(0)}$	$W=\frac{35}{36}\frac{\langle dS/dE\rangle_k}{S(0)}$	Electron Screening Factor (Weak)
$C^{12} + H^1 \rightarrow N^{13} + \gamma$	3.04×10^{-3}	1.90×10^{-2}	4.05×10^{-4}	$(1 + 1.5\ \rho^{1/2}/T_6^{3/2})$
$N^{13} \rightarrow C^{13} + e^+ + \nu$				
$C^{13} + H^1 \rightarrow N^{14} + \gamma$	3.04×10^{-3}	1.38×10^{-2}	2.94×10^{-4}	$(1 + 1.5\ \rho^{1/2}/T_6^{3/2})$
$N^{14} + H^1 \rightarrow O^{15} + \gamma$	2.74×10^{-3}	-3.74×10^{-3}	-7.17×10^{-5}	$(1 + 1.75\rho^{1/2}/T_6^{3/2})$
$O^{15} \rightarrow N^{15} + e^+ + \nu$				
$N^{15} + H^1 \rightarrow C^{12} + He^4$	2.73×10^{-3}	6.74×10^{-2}	1.29×10^{-3}	$(1 + 1.75\rho^{1/2}/T_6^{3/2})$
$N^{15} + H^1 \rightarrow O^{16} + \gamma$	2.73×10^{-3}	2.97×10^{-2}	5.69×10^{-4}	$(1 + 1.75\rho^{1/2}/T_6^{3/2})$
$O^{16} + H^1 \rightarrow F^{17} + \gamma$	2.50×10^{-3}	-1.27×10^{-2}	-2.22×10^{-4}	$(1 + 2.0\ \rho^{1/2}/T_6^{3/2})$
$F^{17} \rightarrow O^{17} + e^+ + \nu$				
$O^{17} + H^1 \rightarrow N^{14} + He^4$	2.50×10^{-3}			

13. Stellar Models and Evolution

Stellar models are almost always calculated on the assumption that the star is spherically symmetric and in hydrostatic equilibrium. We have introduced, in Chapter 10 the set of equations which govern the structure of stellar interiors:

$$\frac{dP(r)}{dr} = -\frac{GM(r)\ \rho(r)}{r^2} \qquad 13.1$$

$$\frac{dM(r)}{dr} = 4\pi r^2\ \rho(r) \qquad 13.2$$

$$\frac{dL(r)}{dr} = 4\pi r^2\ \rho(r)\ \epsilon(r) \qquad 13.3$$

For radiative equilibrium:

$$\frac{dT(r)}{dr} = -\frac{3K}{4ac}\ \frac{\rho(r)}{T^3}\ \frac{L(r)}{4\pi r^2} \qquad 13.4$$

For convective equilibrium:

$$\frac{1}{T}\ \frac{dT(r)}{dr} = \frac{\Gamma-1}{\Gamma}\ \frac{1}{P}\ \frac{dP(r)}{dr} \qquad 13.5$$

In these equations P is the total pressure (gas plus radiation), T is the temperature, M(r) is the mass within a sphere of radius r, L(r) is the energy crossing the surface of a sphere of radius r per second, $\epsilon(r)$ is the energy produced per gram per second, K is the absorption coefficient (cm^2 per gram), and Γ is the effective ratio of the specific heats. Γ differs from $\gamma = c_p/c_v$ through

the inclusion of the effects of dissociation and ionization of the gas, and it will in general vary throughout the convection zone of a star.

In addition to the above equations there are generally explicit relations for the pressure, the absorption coefficient, and the energy generation by nuclear effects as a function of temperature, density and composition.

Boundary Conditions:

The solution of these equations demands a consideration of the appropriate boundary conditions. If the explicit expressions for pressure, absorption coefficient and energy generation are used to eliminate $\rho(r)$, K, and $\epsilon(r)$ we are left with four differential equations in the five variables P(r), M(r), L(r), T and r. A specification of four boundary conditions should enable us to solve for four of these variables in terms of the fifth variable. In general the resulting equations cannot be integrated analytically but must be handled numerically.

In the actual solution of these equations several complications arise. First, as we have, in fact, two sets of boundary conditions to be satisfied (at the center and at the surface) we must in general vary these conditions to

obtain a self-consistent set of boundary conditions. Let us suppose, then, that we have decided upon a set of boundary conditions for the center of a star. We still cannot simply integrate numerically through the stellar interior and expect to arrive at the appropriate conditions at the other boundary. The explanation of this apparent lack of consistency lies in a more careful consideration of the nature of the integration variables. The quantities M(r) and L(r) are seen to be zero at the center and increasing outward from the center; conversely, P(r) and T are seen to decrease outward. In integrating P(r) and T outward from the center to the surface a small variation or error at the center causes a very large variation in the solution at the surface. This may be seen for instance in the $1/T^3$ dependence of equation 13.4. An analogous situation is seen to occur when one attempts to integrate M(r) and L(r) inward from the surface.

Consequently a numerical solution of these equations for a complete stellar model must proceed in the following manner. First the equations are integrated outward to some intermediate radius r_i. The equations are then integrated inward from the surface to that same radius.

Finally, the two solutions are fitted at the chosen r_i by a variation of parameters at the center and at the surface. We can proceed now to a consideration of the central and surface boundary conditions.

At the center of a star we observe from the defining equations that

$$r = 0: \quad M(r) = 0, \quad L(r) = 0$$

Thus at the center the parameters to be specified are T_c and P_c, the density being dependent on these choices through the equation of state.

We have at the surface the choice of a specification of T_s and P_s or, equivalently, of L(R) and R. Let us suppose we can neglect surface temperatures and pressures entirely and assume

$$r = R: \quad T_s = 0, \quad P_s = 0$$

Although this choice quite obviously will not lead to a proper representation of the surface layers it does in many instances result in a reasonable set of solutions for the interior of the star. However, for stars possessing very large envelopes in the red-giant stage these 'zero-boundary conditions' failed in that they resulted in radii which were greater by orders of magnitude than the actual radii, with

accompanying densities so low that the actual radii lay at a distance less than one optical depth. In such cases these become a very unrealistic set of boundary conditions.

Let us rather define the surface as that point at which the actual temperature is equal to the effective temperature ($T_s = T_e$). The luminosity of the star is given here by the product of the surface area and the intensity per unit area:

$$L = (4\pi R^2) \left(\frac{ac}{4} \quad T_e^{\,4}\right)$$
$$= \pi \, ac \, R^2 \, T_s^{\,4} \qquad 13.6$$

Here c is the velocity of light and a is the Stefan-Boltzmann constant.

The atmospheric layers above the surface we have defined have an optical depth as given by:

$$\tau_s = \int_R^\infty K \, \rho(r) \, dr \qquad 13.7$$

An approximate value for τ_s may be taken from the theory of radiative transfer in stellar atmospheres: $\tau_s \simeq 2/3$. A refined atmospheric calculation would necessarily take into account the variation of the absorption coefficient K with both height and wavelength. The variations of K with the wavelength are often termed 'non-grey' effects. In this calculation we will consider K to be independent of both height and wavelength.

$$\tau_s = K \int_R^\infty \rho(r) \, dr = \frac{2}{3} \qquad 13.8$$

Assuming that the height of the atmosphere is small compared to the radius and that the mass is entirely within a radius R, we have from equation 13.1:

$$P_s = \frac{GM}{R^2} \int_R^\infty \rho(r)\, dr \qquad 13.9$$

From equations 13.8 and 13.9 we have then an approximate

value for the surface pressure:

$$P_s = \frac{2}{3} \frac{GM}{KR^2} \qquad 13.10$$

We note again that we could have specified L(R) and R rather than P_s and T_s. These surface boundary conditions are accurate enough for most model-making purposes as, generally, less sophisticated values for internal parameters govern the uncertainties.

In our study of the physical conditions in stellar interiors we have dealt with some of the problems of energy transport in stars. When the temperature gradient is super-adiabatic, convection becomes the dominant process. As energy transport by convection is an extremely efficient process, a temperature gradient which is just barely super-adiabatic can account for high luminosities. As the surface layers must lose energy by radiation, the temperature gradient in the surface layer must be decreased sufficiently to drop below the adiabatic temperature gradient. There must therefore be a transition region in which energy transport by convection gives way to energy transport by radiation. In this region, though the temperature gradient may be super-adiabatic, energy transport by convection and by radiation are comparable. We must develop a physical theory of convection

in order to construct the structure of a star in this transition layer. It is entirely possible that the properties of the stellar interiors will be determined by the properties of this transition region.

Theory of Convection

We begin our study of convection with a discussion of Prandtl's mixing length theory as applied by Erika Bohm-Vitense*. In a region of convective turbulence we consider an element of gas as it forms and moves through a distance termed the 'mixing length' and then dissolves into its surroundings. It is assumed that the element moves adiabatically. In absorption the energy excess is released through ordinary radiative processes. This is clearly a crude picture of such a process; actually the moving turbulent element loses energy continuously as it rises, hence the temperature gradient is not strictly adiabatic.

We can write for the temperature gradient of the structure:

$$\nabla = \frac{d \ln T}{d \ln P} \qquad 13.11$$

The local adiabatic temperature gradient we will write as ∇_{ad}; the local radiative temperature gradient as ∇_{rad}.

*Vitense, E.B. 1958, Zeits. f. Astrophys., 46, 108

The moving element may have a temperature gradient differing from that of the structure due to the fact that it is continuously radiating energy to its surroundings. This temperature gradient we will write:

$$\nabla' = \left(\frac{d\ \ell n\ T}{d\ \ell n\ P}\right)' \qquad 13.12$$

The criterion for instability against convection is that the temperature gradient of the structure is super-adiabatic:

$$\nabla > \nabla_{ad} \qquad 13.13$$

The total energy flux is then given by the sum of the radiative flux and the convective flux:

$$F_{tot} = F_{rad} + F_{conv} = \frac{L}{4\pi R^2} \qquad 13.14$$

The radiative energy flux is given by:

$$F_{rad} = \frac{16\ \sigma\ T^4}{3K\ \rho\ H}\ \nabla \qquad 13.15$$

The convective energy flux is given by:

$$F_{conv} = c_p\ \rho\ T\ \bar{v}\ \frac{\ell}{2H}\ (\nabla - \nabla') \qquad 13.16$$

Here c_p is the specific heat at constant pressure, $H=RT/\beta\mu g$ is the pressure scale height, g is the gravitational acceleration, β is the ratio of gas pressure to total pressure, R is the gas constant, μ is the mean molecular weight, σ is the radiative constant, K is the opacity, and ℓ is the mixing length.

In this theory the mean velocity is given by:

$$\bar{v} = \frac{\ell}{2} \sqrt{\frac{gC}{H}} \quad (\nabla - \nabla')^{\frac{1}{2}} \qquad 13.17$$

Here the factor 'C' accounts for the change of the degree of ionization of matter with temperature and density changes and can be expressed:

$$C = 1 - \frac{\partial \ \ell n \ \mu}{\partial \ \ell n \ T} \qquad 13.18$$

The temperature of the moving element is given by a relation which represents the ratio of the excess energy content of the element to the radiation during its lifetime.

$$\frac{\nabla' - \nabla}{\nabla_{ad} - \nabla'} = c_p \ \rho \ T \ \frac{K \ \rho \ \ell}{24\sigma T^4} \ \bar{v} \qquad 13.19$$

These are the basic equations of this convection theory. We can now consider the relative values of the four temperature gradients we have defined. From equation 13.13 we have the condition for instability against convection. The radiative temperature gradient will necessarily exceed the structure temperature gradient as the structure gradient is in effect a compromise between energy transport by convection and energy transport by radiation. The temperature gradient for the turbulent element must lie in magnitude between the structure gradient and the adiabatic gradient

as the element is moving rapidly and has a temperature excess with respect to its surroundings. Thus we may write:

$$\nabla_{rad} > \nabla > \nabla' > \nabla_{ad} \qquad 13.20$$

It should be stated here that these equations and the development of the theory assume that the mixing length 'ℓ' is a small quantity. In dealing with stellar structures the assumption is generally made that the mixing length is of the same order of magnitude as the pressure scale height. If the mixing length is treated as a parameter which can be adjusted to fit what might be considered appropriate conditions, then we observe that all of the uncertainties in the theory can be lumped into the uncertainty in the value of the mixing length.

Gravitational Energy Source

We shall now consider what would happen in that case in which we assume the energy generation to be entirely due to release of the gravitational potential energy of the contracting solar mass.

The luminosity is

$$L = \int_0^R 4\pi r^2 \rho \, \epsilon(r) \, dr \qquad 13.21$$

where $\epsilon(r)$ is the energy released per gram of material per

second due to contraction of the star and

$$\epsilon(r) = \frac{d\,L(r)}{4\pi r^2 \rho dr} \qquad 13.22$$

If U is the internal energy per gram of material and V is the specific volume, then at each point in the star

$$\frac{\partial U}{\partial t} = -\,\epsilon(r) - P\,\frac{\partial V}{\partial t} \qquad 13.23$$

This states that the change in internal energy is balanced by the energy loss and the work done by the pressure. The internal energy per gram of material at a point inside the star is

$$U = c_V\,T(r) \qquad 13.24$$

Assume that the ideal gas law governs the interior of the star

$$U = \frac{1}{(\Gamma-1)}\,\frac{P(r)}{\rho(r)} \qquad 13.25$$

where Γ is the ratio of specific heats at the point considered. If we replace V by its reciprocal $(V=1/\rho)$ we have

$$-\,\epsilon(r) = \frac{1}{(\Gamma-1)}\,\frac{\partial}{\partial t}\left(\frac{P}{\rho}\right) + P\,\frac{\partial}{\partial t}\left(\frac{1}{\rho}\right)$$

$$= \frac{1}{(\Gamma-1)}\,\frac{1}{\rho}\,\frac{\partial P}{\partial t} - \frac{\Gamma}{(\Gamma-1)}\,\frac{P}{\rho^2}\,\frac{\partial \rho}{\partial t} \qquad 13.26$$

If it is assumed that the star is contracting homologously,

then the rate of change with time of pressure and density at every point is completely determined by the rate of change of the radius of the star in such a way that

$$\frac{1}{R}\frac{dR}{dt} = \frac{1}{r}\frac{dr}{dt} = \text{constant} \qquad 13.27$$

$$-\frac{1}{R}\frac{dR}{dt} = \frac{1}{4P}\frac{\partial P}{\partial t} = \frac{1}{3\rho}\frac{\partial \rho}{\partial t} \qquad 13.28$$

Thus we have from equation 13.26:

$$\epsilon(r) = \left(\frac{3\Gamma-4}{\Gamma-1}\right)\frac{P(r)}{\rho(r)}\left(-\frac{1}{R}\frac{dR}{dt}\right) \qquad 13.29$$

Hence, from equation 13.21:

$$L = 4\pi\left(\frac{-1}{R}\frac{dR}{dt}\right)\int_0^R\left(\frac{3\Gamma-4}{\Gamma-1}\right)P(r)\,r^2\,dr \qquad 13.30$$

We thus have an expression for the luminosity for the case in which the energy generation is entirely due to the release of gravitational energy of the contracting solar mass. For a further discussion of the material the reader is referred to <u>The Early Evolution of The Sun</u>, Ezer, and Cameron, Icarus, 1963. We shall now use some of the results obtained in this paper to illustrate several of the concepts discussed in this chapter.

We have presented in our discussion of the physical conditions in stellar interiors the graphs of opacity for lines of constant density as a function of temperature from

the Los Alamos Opacity Code (pps. 59,60). In constructing models in which the envelope of the star is large, one must obtain a suitable surface boundary condition. This demands that we have a reasonably large value for the opacity in the surface layers. For a star of large radius we must maintain as far as is possible a high density and a high temperature. This will assure a high value for the opacity which means that the distance corresponding to an optical depth of $\tau_s = 2/3$ is a reasonably small quantity, necessary for a self-consistent set of solutions to our equations. The large value for the density means that the temperature gradient must also be large; hence, the star is seen to become entirely convective.

Figure 13.1 shows the Hertzsprung-Russel diagram for the models of the contracting sun calculated under these assumptions, with the mixing length equal to the pressure scale height. Above the indicated threshold of stability the models are of academic interest only since the thermal, ionization and dissociation energies exceed the magnitude of the gravitational potential energy. These stars would be unstable against gravitational collapse. The threshold of stability as indicated in the figure is that point at which

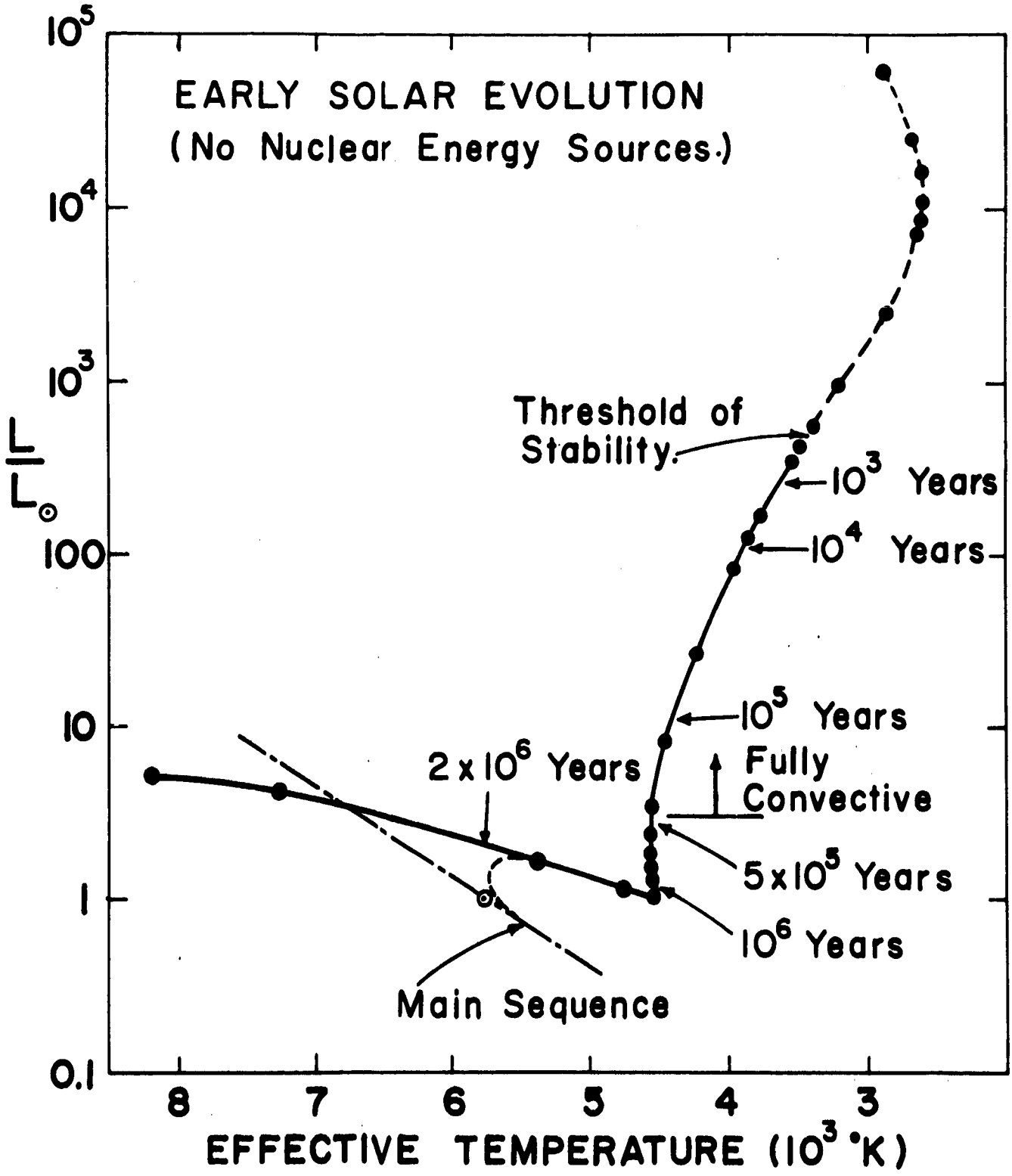
EARLY SOLAR EVOLUTION
(No Nuclear Energy Sources.)
Threshold of Stability
10^3 Years
10^4 Years
10^5 Years
2×10^6 Years
Fully Convective
5×10^5 Years
10^6 Years
Main Sequence
$\frac{L}{L_\odot}$
10^5
10^4
10^3
100
10
1
0.1
8
7
6
5
4
3
EFFECTIVE TEMPERATURE (10^3 °K)

Figure 13.1

the models are just energetically possible. A star formed at this point, because of its high luminosity, would shrink rapidly. The structure remains fully convective down to a certain point as indicated in the figure. Below this point, a radiative central core begins to develop. At the point at which the radiative core contains approximately 55% of the mass, the direction of evolution turns. The dark line shown here indicates the path that would be followed under the assumption, in this model, of no nuclear sources. If these nuclear sources are taken into consideration it can be shown that the star would evolve on to the main sequence approximately in the manner indicated by the broken line in this figure.

Figure 13.2 shows the behavior of the luminosity and radius of the sun as a function of time beyond the threshold of stability.

Figure 13.3 shows the dependence of the luminosity on the ratio of mixing length to pressure scale height for a model in which the radius $R = 20R_{\odot}$. The models shown in Figure 13.1 were all calculated on the assumption that this ratio was unity. We observe that the luminosity is essentially proportional to the ratio of the mixing length to the

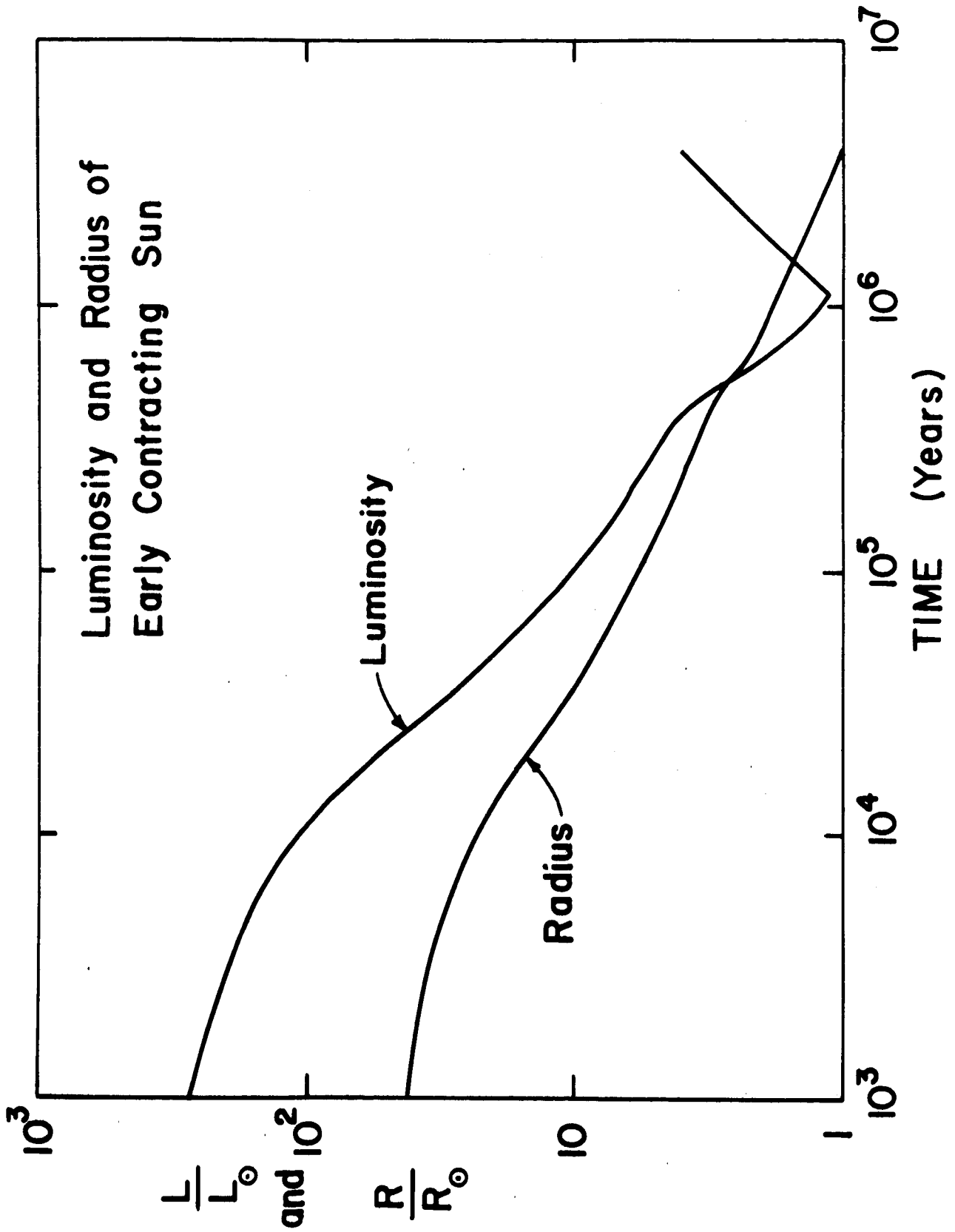
Luminosity and Radius of
Early Contracting Sun
Luminosity
Radius
10^3
10^2
10
1
$L/L_\odot$ and $R/R_\odot$
10^3
10^4
10^5
10^6
10^7
TIME (Years)

Figure 13.2

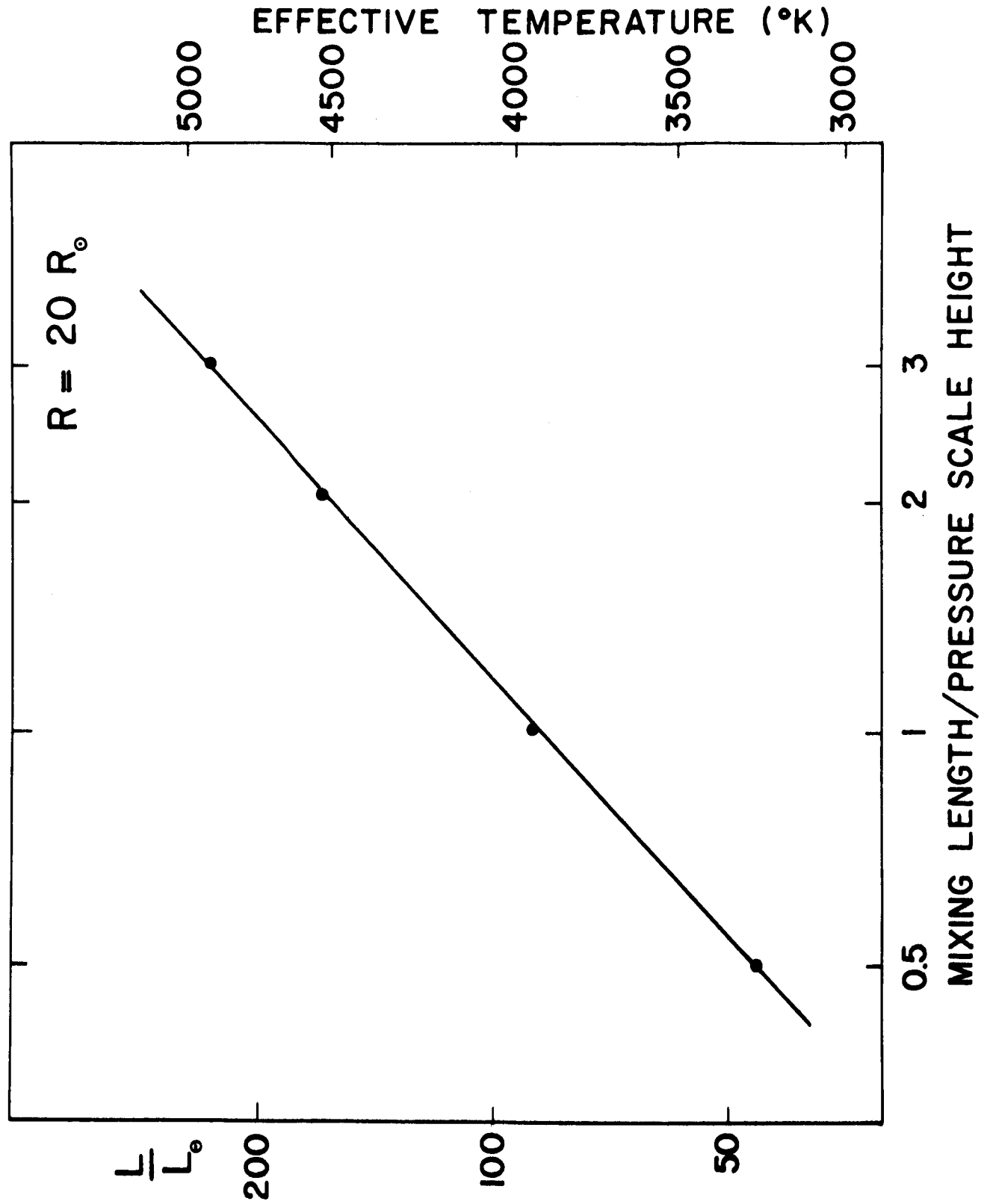
EFFECTIVE TEMPERATURE (°K)
5000
4500
4000
3500
3000
R = 20 R⊙
L/L⊙
200
100
50
0.5
1
2
3
MIXING LENGTH/PRESSURE SCALE HEIGHT

Figure 13.3

pressure scale height.

Figure 13.4 shows the dependence of the luminosity on the ratio of mixing length to pressure scale height for a model in which the radius $R = 2R_{\odot}$.

Figure 13.5 indicates the dependence of the average velocity of the turbulent elements in the outer convective zone on the pressure, for a solar model in which $R = 20R_{\odot}$. Also shown are the sound velocities at various points of the transition layers. The peak in the velocity curve is not realistically determined because the peak structure is narrow compared to the mixing length. The fact that the velocities of the convective elements can become an appreciable fraction of the velocity of sound indicates that some supersonic phenomena may become important in the interiors.

Figure 13.6 shows the variation of the fraction of mass inside the radiative core, and of the temperature at the bottom of the convective zone, with the ratio of mixing length to pressure scale height. The temperature dependence becomes important if one wishes to consider its effect on lithium burning in the outer convection zone.

Figure 13.7 shows the rate of lithium burning averaged

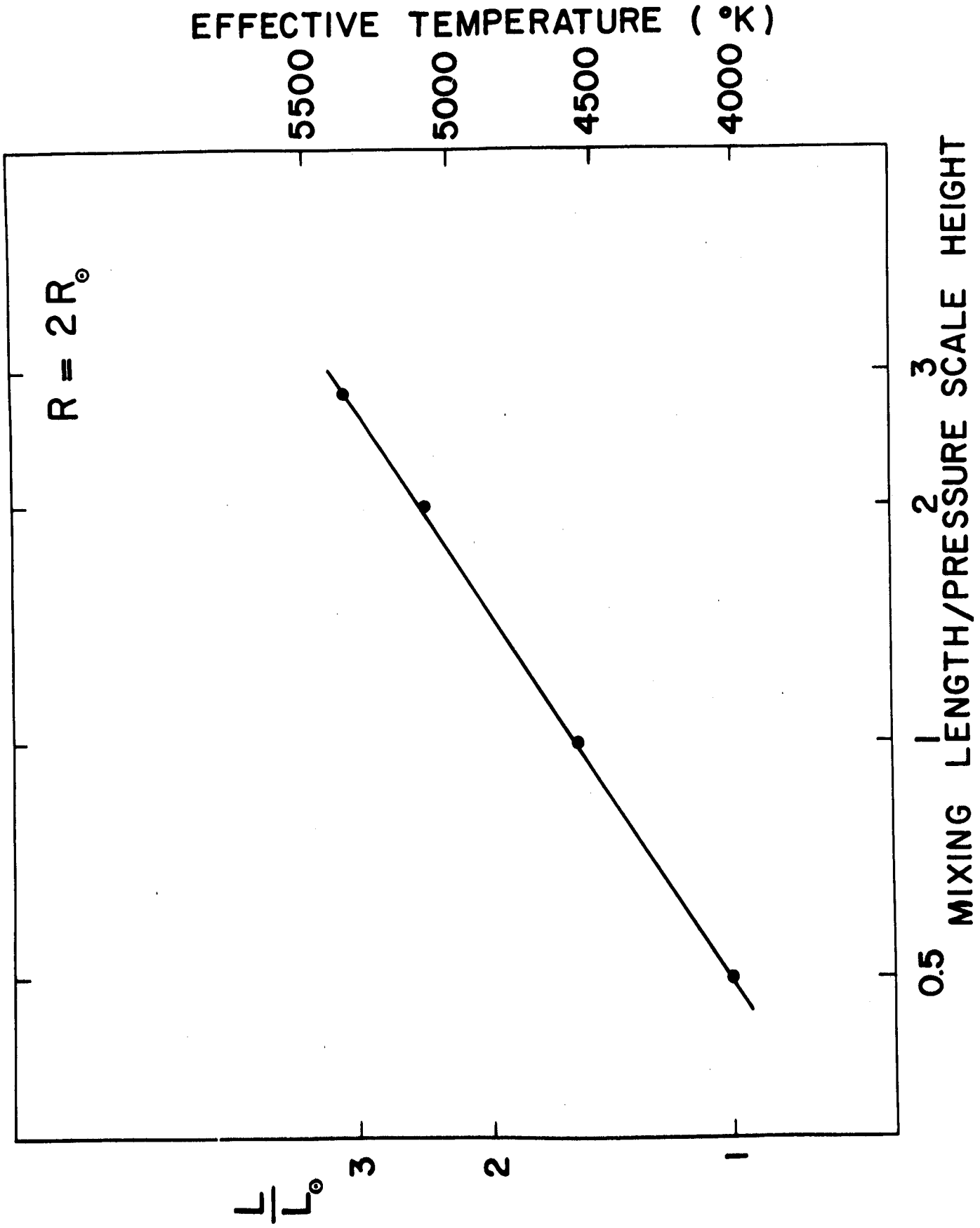
EFFECTIVE TEMPERATURE (°K)
5500
5000
4500
4000
R = 2R⊙
0.5
1
2
3
MIXING LENGTH/PRESSURE SCALE HEIGHT
L/L⊙
3
2
1

Figure 13.4

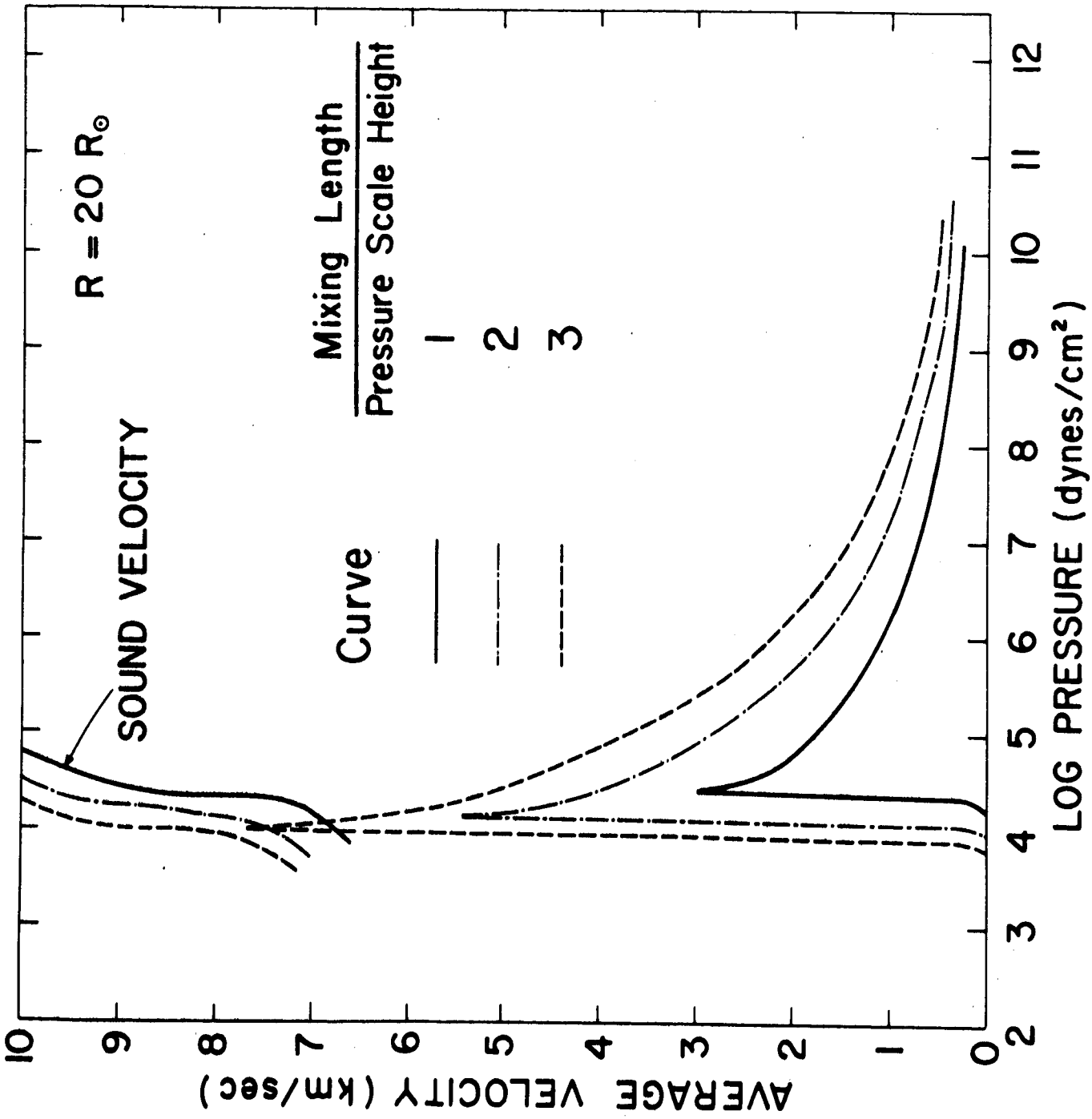
R = 20 R⊙
SOUND VELOCITY
Mixing Length / Pressure Scale Height
Curve
1
2
3
AVERAGE VELOCITY (km/sec)
LOG PRESSURE (dynes/cm²)
0
1
2
3
4
5
6
7
8
9
10
2
3
4
5
6
7
8
9
10
11
12

Figure 13.5

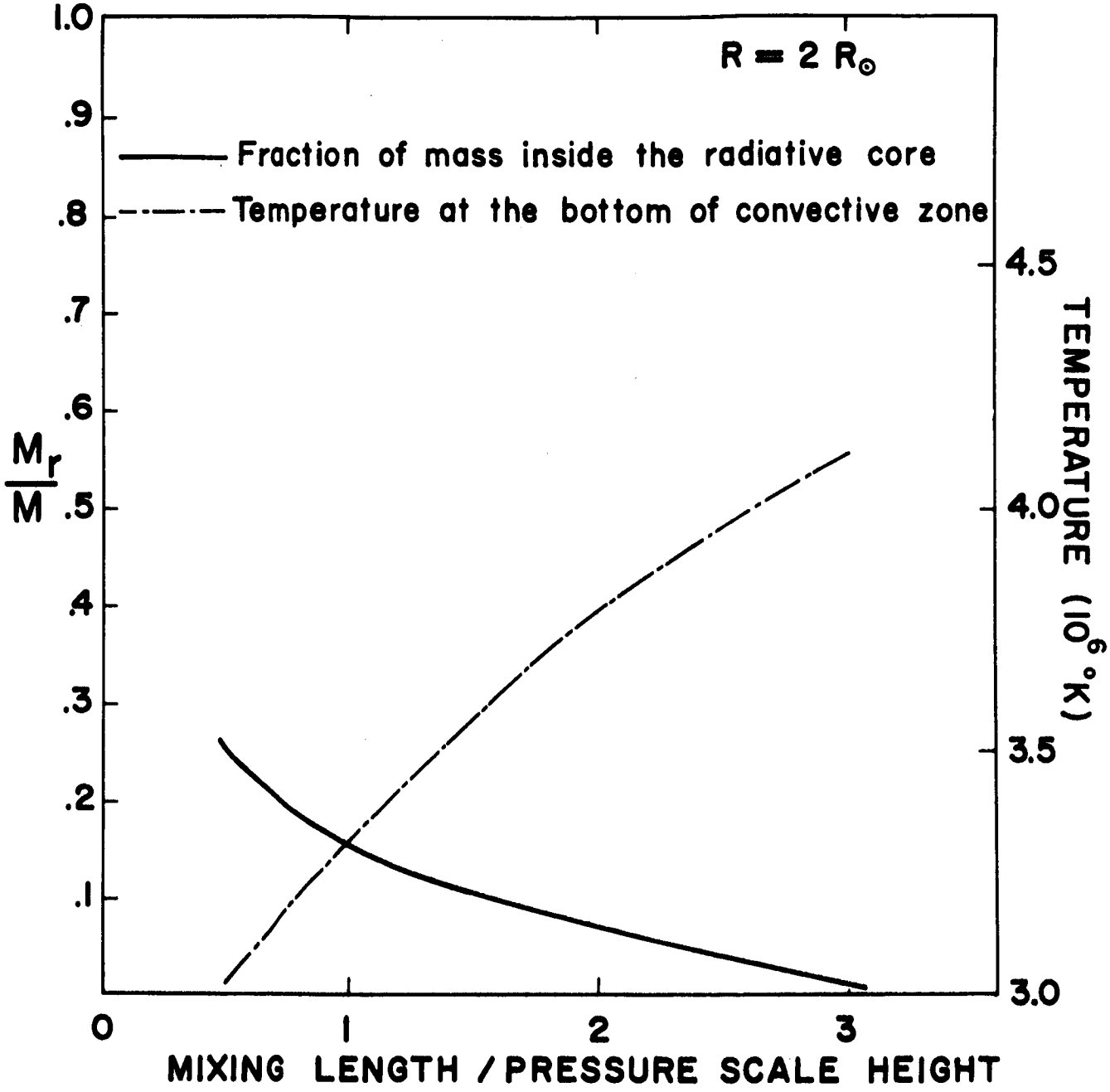
R = 2 R⊙
Fraction of mass inside the radiative core
Temperature at the bottom of convective zone
1.0
.9
.8
.7
.6
.5
.4
.3
.2
.1
Mr/M
4.5
4.0
3.5
3.0
TEMPERATURE (10^6 °K)
0
1
2
3
MIXING LENGTH / PRESSURE SCALE HEIGHT

Figure 13.6

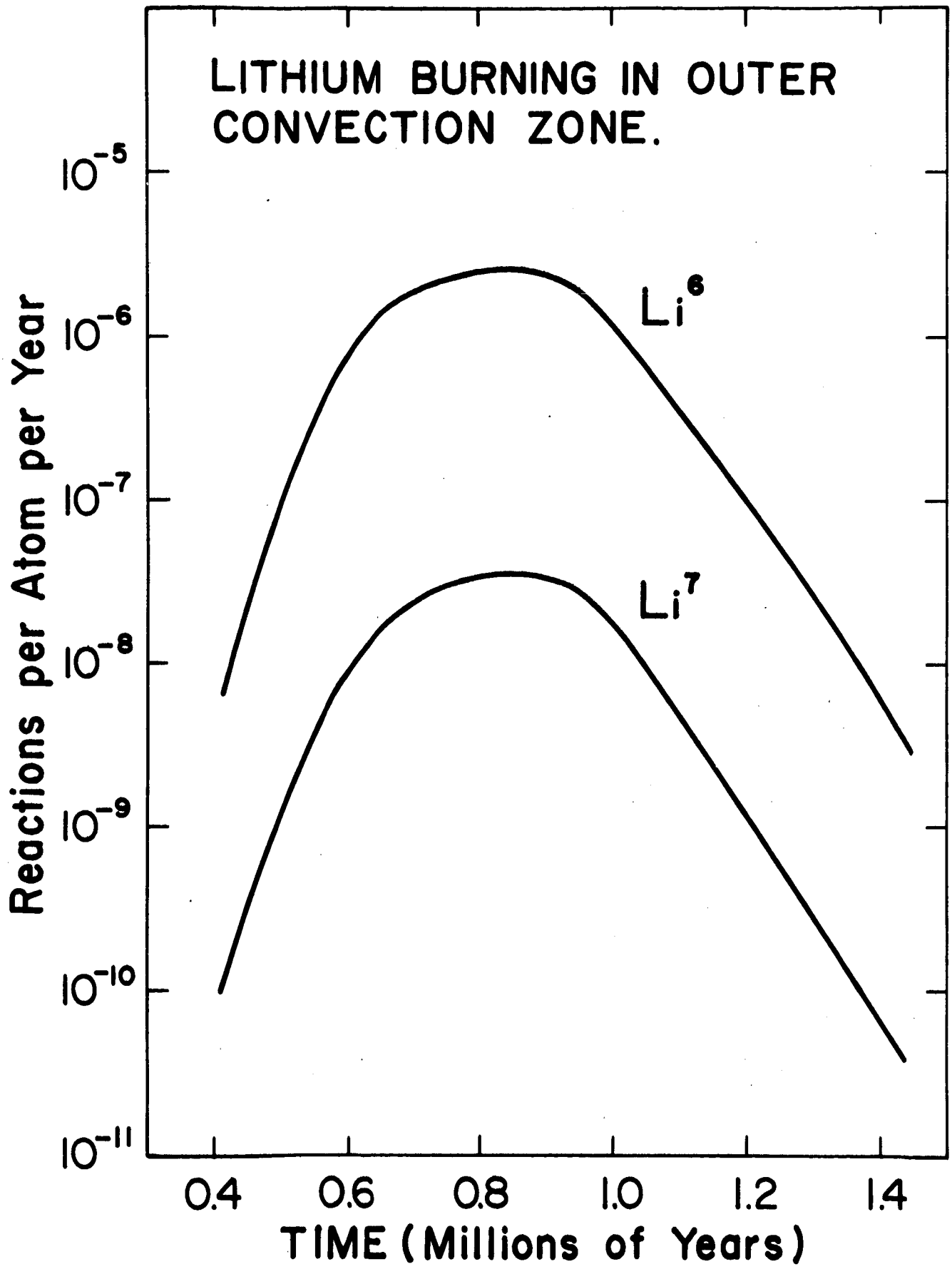
LITHIUM BURNING IN OUTER CONVECTION ZONE.
Reactions per Atom per Year
10^{-5}
10^{-6}
10^{-7}
10^{-8}
10^{-9}
10^{-10}
10^{-11}
Li^6
Li^7
0.4
0.6
0.8
1.0
1.2
1.4
TIME (Millions of Years)

Figure 13.7

throughout the outer convective zone for both isotopes of lithium as a function of the evolutionary time of the solar models, calculated with the mixing length assumed equal to the pressure scale height. The total depletion of the isotopes is obtained by integrating under these curves.

Characteristics of Stars on The Main Sequence

The preceeding section discussed the formation of a star of one solar mass from gas and the subsequent evolution of the star to its place on the main sequence. As was pointed out in that discussion, the energy sources in the final stages of evolution do not derive solely from gravitational contraction of the star, but rather one expects the star to derive some energy from nuclear reactions. In particular, one expects the star to burn out its deuterium once the temperature has risen to about 800,000 degrees, lithium at about 3-4 million degrees, beryllium at about 5 million degrees, boron and primordial He^3 at about 8 million degrees. These energy sources will have the effect of slowing down the rate of descent onto the main sequence to longer times compared to the case of pure gravitational energy release. Once the star reaches the main sequence the

regular conversion of hydrogen to helium will take place.

At the moment, no evolutionary model of the sun has been published which purports to describe exactly the mode of hydrogen to helium conversion, that is, the proper break up of hydrogen burning into the various PP chains possible. (See Section 12) In general however, one can say that in the primordial sun the PP 1 and PP 2 chains would have been of comparable importance. The central temperature at this time was probably about 13 million degrees. As hydrogen was depleted in the central regions the temperature must have gone up and those regions must have contracted in order to maintain the energy production per gram of active material (hydrogen) present. At the present time the central temperature is probably as high as 16 million degrees. (The age of the sun to date is estimated to be about 4.5 billion years). The increase in central temperature and the steady production of helium both favor the PP 2 chain as against the PP 1. Consequently, in the sun at the present time the PP 2 chain is probably dominant near the center, with the PP 1 chain taking over as one leaves the central regions. We note here also that the PP 3 chain may contribute about 1% of the total energy

and the CNO cycles about 2-3% at the present time. It is to be stressed, however, that these statements may require some degree of modification when more exact calculations can be made.

As seen in Section 12 the PP chains have a very small temperature dependence--- about the fourth power in the temperature---so that the interior regions of stars of mass comparable to the sun will not have a very high temperature gradient and consequently the energy generation distribution will not become strongly peaked as we approach the center. In this case we expect that the central regions will not require an efficient means of energy transfer like convection but rather may be able to get along with purely radiative transfer. Toward the less dense outer regions of the sun, on the other hand, the transfer becomes convective (but naturally becomes radiative at its outer boundaries in the photosphere in order to be able to radiate energy into free space). Thus we have a central radiation zone followed by a convection zone and topped by an outer radiative layer. The transition boundary between the central radiation zone and the convection zone is believed to be at a temperature near one million degrees. The total

regular conversion of hydrogen to helium will take place.

At the moment, no evolutionary model of the sun has been published which purports to describe exactly the mode of hydrogen to helium conversion, that is, the proper break up of hydrogen burning into the various PP chains possible. (See Section 12) In general however, one can say that in the primordial sun the PP 1 and PP 2 chains would have been of comparable importance. The central temperature at this time was probably about 13 million degrees. As hydrogen was depleted in the central regions the temperature must have gone up and those regions must have contracted in order to maintain the energy production per gram of active material (hydrogen) present. At the present time the central temperature is probably as high as 16 million degrees. (The age of the sun to date is estimated to be about 4.5 billion years). The increase in central temperature and the steady production of helium both favor the PP 2 chain as against the PP 1. Consequently, in the sun at the present time the PP 2 chain is probably dominant near the center, with the PP 1 chain taking over as one leaves the central regions. We note here also that the PP 3 chain may contribute about 1% of the total energy

and the CNO cycles about 2-3% at the present time. It is to be stressed, however, that these statements may require some degree of modification when more exact calculations can be made.

As seen in Section 12 the PP chains have a very small temperature dependence--- about the fourth power in the temperature---so that the interior regions of stars of mass comparable to the sun will not have a very high temperature gradient and consequently the energy generation distribution will not become strongly peaked as we approach the center. In this case we expect that the central regions will not require an efficient means of energy transfer like convection but rather may be able to get along with purely radiative transfer. Toward the less dense outer regions of the sun, on the other hand, the transfer becomes convective (but naturally becomes radiative at its outer boundaries in the photosphere in order to be able to radiate energy into free space). Thus we have a central radiation zone followed by a convection zone and topped by an outer radiative layer. The transition boundary between the central radiation zone and the convection zone is believed to be at a temperature near one million degrees. The total

volume contained in the two zones is believed to be about equal but because of the vast difference in densities the outer convection zone may contain only a few percent of the total solar mass.

If we now consider a more massive star than the sun we note some startling differences. Here the central temperature may be 20 millions of degrees or higher so that there is a switch from the PP chains to the CNO cycles. The governing reaction in this case is proton capture by N^{14} which is the slowest reaction and goes approximately as the temperature to the 18 power. (See page 114 for the expression of temperature sensitivity <u>but note</u> that for non-resonant reactions the equation for n is $n = \frac{1}{3}(\tau-2)$ and <u>not</u> as stated there. Also see page 159 for the numerics of the CNO cycles.) This temperature sensitivity for massive stars implies a high temperature gradient in the central regions of these stars which in general will exceed the adiabatic gradient so that convection will set in. For a massive star on the main sequence the surface temperature will be higher than that of the sun so that the outer convection zone will decrease in extent. If we went to extremely massive stars we might

have little or no surface convection: (Note that we still require a radiation layer at the photosphere. We will assume this is always the case and not refer to it hereafter.) The central convection zone, however, may grow until it comprises half the mass of the star. Between the inner and outer convection zones there will be in general, a radiative zone for energy transfer. Thus we find three zones in the case of massive stars as compared to two for stars like the sun. (A schematic diagram of the situation is shown in Figure 13.8) If we start with a sun-like star then, and examine stars on the main sequence of steadily increasing mass we find that initially we have no central convection zone and then progressively we obtain one at the expense of the outer convection zone while still maintaining an intermediate radiation zone.

Evolution off the Main Sequence

For very massive stars the luminosity is found to be roughly proportional to the mass. About half of the total mass will be used in the conversion of hydrogen to helium while such a star is on the main sequence so that in effect the total energy available is also proportional to the mass. This implies that the time taken for the star

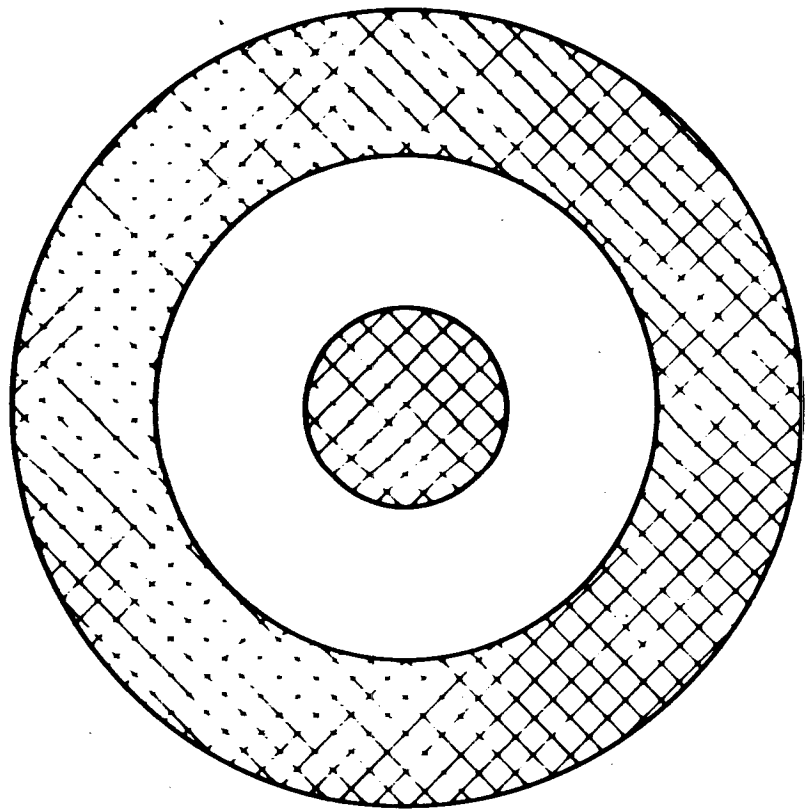

SECTION OF HOT MAIN SEQUENCE STAR

CROSS-HATCHING INDICATES CONVECTIVE REGIONS

Figure 13.8

to convert all the hydrogen at its center to helium, i.e. the time during which it is on the main sequence, must be roughly a constant. This time turns out to be about 3 million years for very massive stars independent of the mass.

As we go to less massive stars we find that the luminosity begins to decrease more rapidly than the mass so that the lifetimes on the main sequence become longer. For stars of about spectral class G or redder the main sequence lifetimes are probably longer than the age of our galaxy (about 10^{10} years).

For the general trend of stellar evolution we refer the reader back to Section 8, page 15, Figure 8.2, where the Hertzsprung-Russel (H-R) diagrams for several stellar clusters are shown. Diagrams such as this represent the observational approach to stellar evolution and are excellent guides to all theoretical studies in the field.

An example of a combined observational and theoretical approach is shown in Figure 13.9. The set of semi-empirical evolutionary tracks shown are due to Sandage* and indicates what paths are taken by stars as they leave the main sequence

*A.R. Sandage, Ap. J., 125, 435, 1957

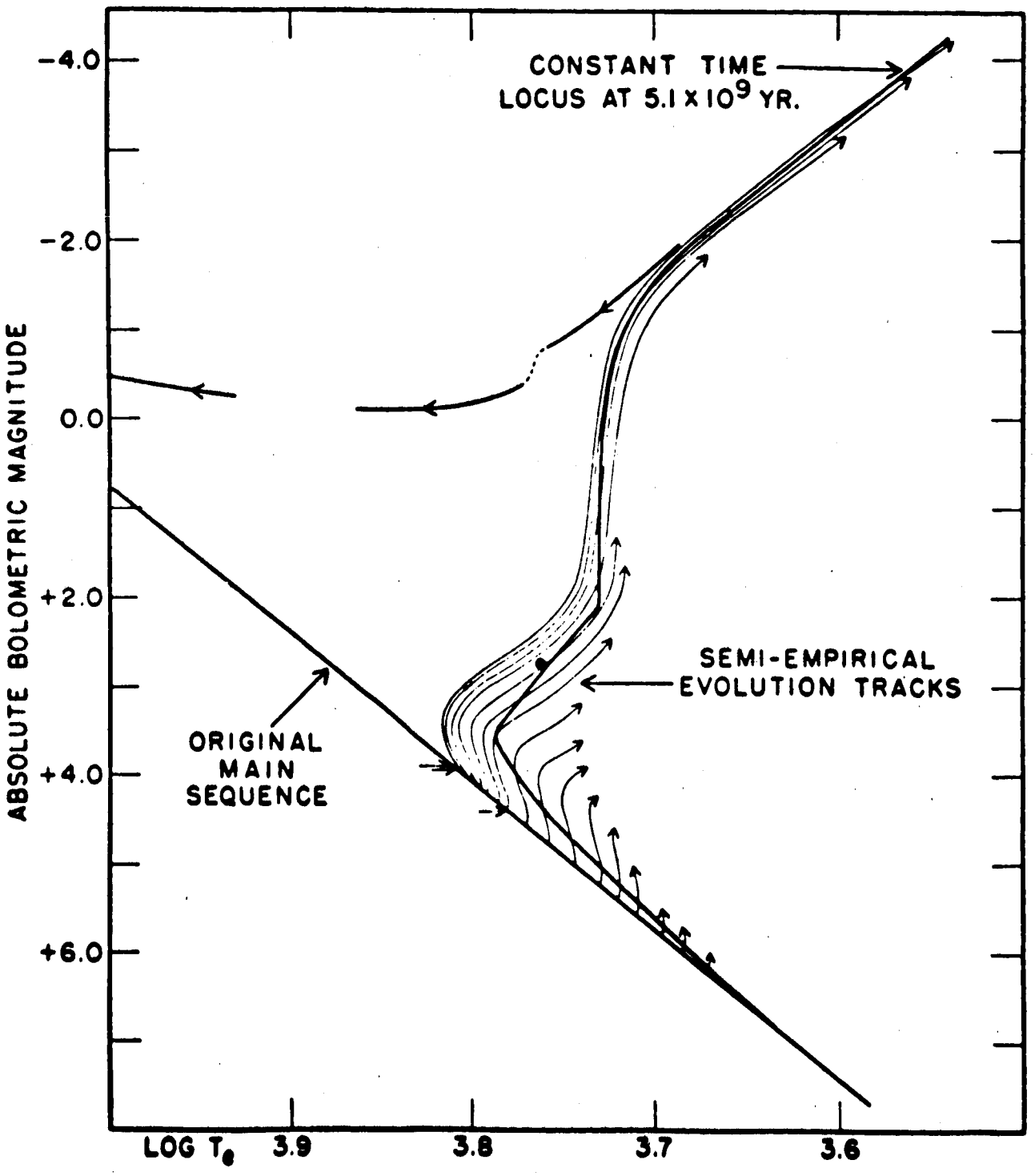
CONSTANT TIME
LOCUS AT 5.1 x 10^9 YR.
SEMI-EMPIRICAL
EVOLUTION TRACKS
ORIGINAL
MAIN
SEQUENCE
ABSOLUTE BOLOMETRIC MAGNITUDE
-4.0
-2.0
0.0
+2.0
+4.0
+6.0
LOG T_e
3.9
3.8
3.7
3.6

Figure 13.9

when the hydrogen at their centers has been exhausted. These tracks have been constructed by the examination of the characteristic H-R diagrams of several globular and galactic clusters coupled with theoretical tracks calculated by Hazelgrove and Hoyle*. One should note the line passing thru the evolutionary tracks labled "constant time locus". This line represents the locus of all stars which have been created at a given time on the main sequence and have subsequently evolved to those positions on the H-R diagram given by that line. Note that the more massive stars, those with the higher initial values of absolute magnitude, have evolved off the main sequence much faster than the less massive stars in agreement with the previous discussion. (A graph of lifetime on the main sequence versus mass is given at the end of this section). Note also the apparent gap in the "horizontal branch" at the left hand portion of the evolutionary track. This corresponds to the location of variable stars as discussed in Section 8.

As discussed before, the ultimate fate of all stars appears to be evolution to the white dwarf stage. Figure 13.10

*C.B. Hazelgrove and F. Hoyle, M.N., 119, 112, (1959)

shows a heavily populated portion of the H-R diagram which seems to consist of faint stars approaching the white dwarf graveyard after leaving the horizonal branch. Little, if anything, is known of the details of evolution from the red giant region (shown in Figure 13.9 as the right hand tip of the orizonal branch) to the white dwarf region.

Evolution of Massive Stars

Though to date the whole course of stellar evolution has not been explained satisfactorily, some phases of evolution, at least to the red giant stage, have been explained in a ~eneral sense. As was discussed before, a massive star sits on the main sequence until about half of its hydrogen in the central convective region has been converted to helium. At the end of the star's lifetime on the main sequence the hydrogen fuel at its center has been exhausted but the star must still continue to radiate. Therefore, the central region must contract releasing gravitational energy, hence maintaining its luminosity. The temperature of the central region will then increase, thereby increasing the rate of hydrogen conversion to helium at distances away from the center.

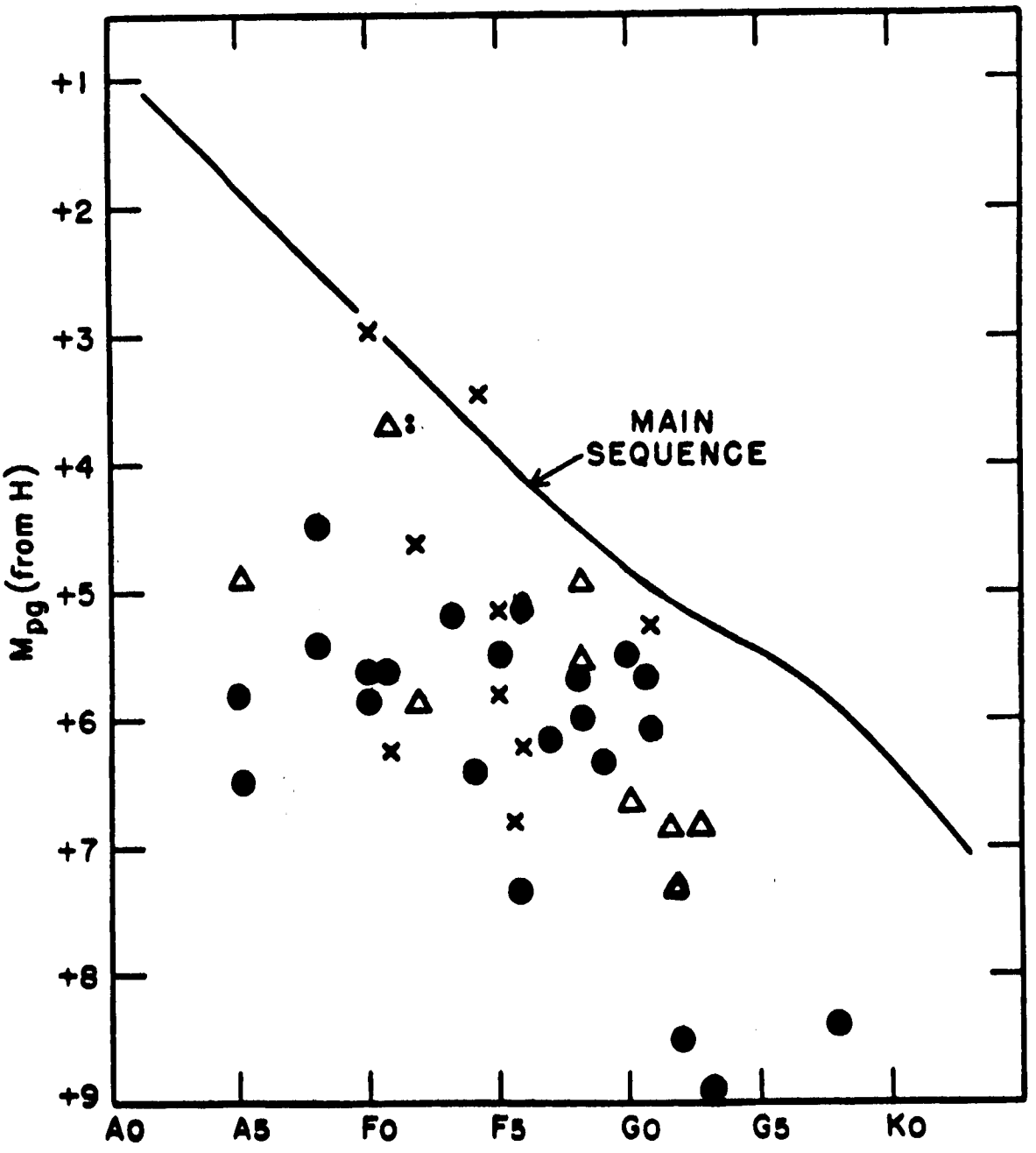

Figure 13.10

As this hydrogen is exhausted the gravitational shrinkage will continue. Finally the bulk of the central region will be exhausted of hydrogen leaving a dense central helium core surrounded by a thin shell of hydrogen-rich material which will provide the energy source. As evolution progresses the central inert core will grow and the hydrogen shell will move out towards the stellar periphery. In order to maintain a high temperature in the hydrogen burning shell the central core must shrink, thereby raising the central temperature to higher and higher values.

The structure of the star becomes rather peculiar as the above process goes on. In the outer regions the material is essentially all ionized hydrogen with a mean molecular weight of one half whereas the helium core has a mean molecular weight of four thirds (one alpha particle and two free, electrons). (Actually the mean molecular weight in the envelope will be somewhat higher than one half, say perhaps two-thirds, since the star may have some helium there.) We thus have a discontinuity in mean molecular weight at the junction of the helium core and the outer regions of the star. On the other hand, there must be a continuity in the physical variables of temperature and pressure. One finds that as a consequence of these facts, the star must develop a very large, tenuous outer envelope surrounding the helium core. In this fashion the

star approaches the red giant stage.

In the case of a very massive star the gravitational contraction of the central region need not progress very far until the central temperature will have risen to the point where helium burning may set in (about 30 million degrees). Thus the star will have two sources of energy, helium burning at the center and a continuation of hydrogen burning in the shell surrounding the core. As the star evolves carbon burning may commence at the center. This process may continue until there are many modes of energy generation taking place in various regions of the star. These later stages of evolution must occur at a very rapid rate since the upper regions of the H-R diagram are sparsely populated.

Evolution of Stars of About One Solar Mass

The evolution of sun-like stars is much like that of more massive stars except that because the centers of stars of one solar mass are in radiative equilibrium rather than convective equilibrium the active energy-producing hydrogen is not in constant circulation within the central core. Thus, we expect the hydrogen will first be exhausted in a much smaller region around the center of

the star. The exhaustion about the center will also take place at a much more even rate. When about ten per cent of the mass of the central radiation region has been converted to helium the star will move off the main sequence.

As in more massive stars a helium core will develop at the center, though of a smaller size. Again, the energy generation will take place in a shell surrounding this core but because of the thinness of the shell the temperature there must be very high in order to sustain an adequate reaction rate. At this point the mode of hydrogen conversion gradually switches from the PP chains to the CNO cycles.

The above processes will take place at a very slow rate during the initial stages of evolution off the main sequence so that, although the core contracts gravitationally and the hydrogen shell rises in temperature, there will be a relatively small temperature gradient between the stellar center and the hydrogen shell. This indicates that an inert, isothermal core will be produced. An even more interesting property of the core is that for less massive stars we expect the inert helium

core to become degenerate as an examination of the arguments leading to the evolutionary tracks shown in Figure 10.3 on page 68 and the discussion on page 73-74 will show. This represents a drastic change in the structure of the star. We also have a large outer envelope forming for the same reasons as in the massive star case. The existence of the isothermal core becomes more apparent now that the core has become degenerate since this material has a very high thermal conductivity.

As evolution proceeds the degenerate core grows and the hydrogen-burning shell moves out. The central temperature rises owing to more rapid gravitational contraction of the core. When the central temperature reaches about 80-100 million degrees we have brought the star to the tip of the red giant branch. Helium reactions begin to take place at the center, but because this region is degenerate, the pressure will not change significantly with the subsequent rise in temperature, so that no expansion takes place and hence the density remains essentially unchanged. The helium reactions then proceed at faster and faster rates because of the high temperature sensitivity of the reactions themselves. This process has been appropriately called the

"Helium Flash" by Schwarzschild. The rapid increase in the helium reaction rate continues until finally kT in the central degenerate region has been raised above the Fermi level and the ideal gas law holds once more, the material no longer being degenerate. The central region thereupon expands due to the increase in temperature until enough helium has been burned so as to replenish the gravitational energy released during the contraction phases of the helium core. About one per cent of the helium will be converted to carbon in the process. As the core gets larger the outer envelope will decrease in size and the star will assume a more normal appearance. This is exemplified by a backtracking of the evolutionary track from the red giant tip (See figure 13.9). The details of evolution past this stage are practically unknown (except for the ultimate end as a white dwarf) and in fact some of the results just discussed must be viewed with caution because of the rapidity of the reactions and more explicitly because dynamic effects have been neglected although the star itself has undergone gross changes in structure in short periods in time.

Mass Loss in Evolving Stars

It has been observed that stars in the red giant phase

seem to be losing mass from their surface at a rapid rate. Some of the more massive stars seem to be losing mass at the rate of one solar mass every million years, indicating that their red giant phase cannot last very long. This process seems to be connected with what has been called the "solar wind" wherein the star develops a corona sufficiently hot to eject the surface materials to infinity. (The sun's corona is believed to be at a temperature of about two million degrees.)

Clearly these effects complicate the whole march of stellar evolution and no calculations have been made to incorporate them. All that can be said here is that mass loss seems to be necessary if a star is to reduce its mass below the Chandrasekhar limit ($\sim 1.4\ M_{\odot}$).

We will leave to a later section the problems associated with the more violent stages of evolution, namely the eruption of stars into novae and supernovae.

Figure 13.11 shows the variation of lifetime τ on the main sequence as a function of mass. The abscissa is in units of the logarithm to the base 10 of the ratio of the star's mass to the mass of the sun. Thus, at a value of this parameter of zero we find the sun's lifetime on the

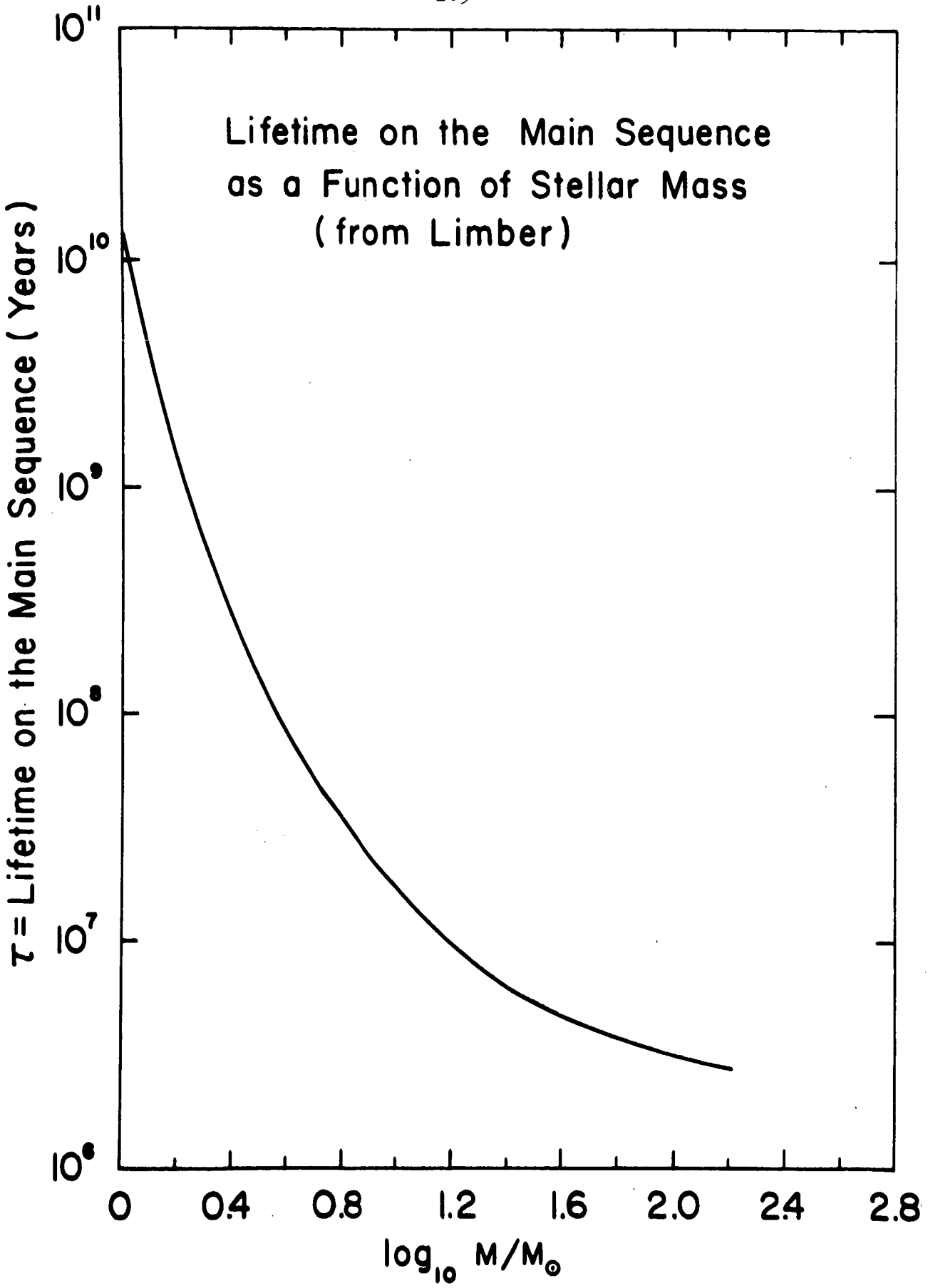
Lifetime on the Main Sequence
as a Function of Stellar Mass
(from Limber)
τ = Lifetime on the Main Sequence (Years)
10^{11}
10^{10}
10^{9}
10^{8}
10^{7}
10^{6}
0
0.4
0.8
1.2
1.6
2.0
2.4
2.8
$\log_{10} M/M_{\odot}$

Figure 13.11

sequence as being 1.2×10^{10} years, about 5×10^{9} years of this having elapsed to date. Note also that for very massive stars ($M/M_{\odot} \sim 100$ and greater) the lifetime curve approaches a value of about 3×10^{6} years as mentioned earlier in this section. The data for this figure is taken from D. Nelson Limber, Ap.J. 131, 169, (1960).

14. Helium Thermonuclear Reactions

In the 1950's, questions arose concerning the later stages of stellar evolution and whether any thermonuclear reactions took place under these conditions. E.J. Öpik, for one, noted that for sufficiently large temperatures, the triple collision of three alpha particles would take place to make C^{12}. At about the same time, F. Hoyle made the interesting observation that we must not only account for the fact that stars generate energy in later stages of their evolution but we must also account for the fact that the products of these thermonuclear reactions are the elements we observe and out of which we are made. The triple collision of alpha particles is a sufficiently rare event that subsequent capture of an alpha particle to form O^{16} would occur with comparative haste. The C^{12} made by the triple collision would almost instantly disappear, making O^{16}.

Hoyle said, since carbon is one of the most significant elements in our total environment, substantial quantities of it must be produced, and the simple triple collision of alpha particles is not the way to do this. If there were a resonance which would make the rate of formation of C^{12} comparable to or greater than the rate of destruction of C^{12} to form O^{16}, then this would help to explain the observed abundance of C^{12}. On this basis, Hoyle predicted that there should be a level in the C^{12} nucleus at about 7.7 Mev. There was some suspicion at that time that a level did exist in this vicinity, but the matter was in dispute and the experimental evidence inconclusive. Hoyle's prediction caused nuclear physicists at the California Institute of Technology to make a new search for such a level. They found one at 7.656 Mev, which is slightly lower than Hoyle's prediction, but not significantly so. This level does have the desired characteristics.

Be^8 plays a role of some importance here. Be^8 is unstable toward break-up into alpha particles by about 94 kev. None the less, we can use statistical mechanics to determine the equilibrium concentration, which will, in general, not be zero. It is a characteristic of any kind of

reaction that it is reversible. If we consider Be^8 as being formed from and breaking-up into two alpha particles, then the basic equation of statistical mechanics relates the equilibrium abundances of the two independent species and the compound by

$$\frac{n_1 n_2}{n_{12}} = \left(\frac{2\pi\, m_1 m_2\, kT}{h^2 (m_1 + m_2)}\right)^{3/2} \left(\frac{\omega_1 \omega_2}{\omega_{12}}\right) \left(e^{\chi/kT}\right)$$

where the n's are number densities, the ω's are statistical weights (which are partition functions if there are several levels in each of the species), and the χ in the Boltzmann factor is the energy of the ground state above the sum of the masses. The equilibirum abundance of Be^8 is

$$n_2 = 9.40\text{x}10^{-31 - 473/T_8} \frac{n_1^2}{T_8^{3/2}}$$

where subscript 1 refers to α particles. Considering the conditions at the beginning of the helium flash, i.e.,

$$T_8 \simeq 1$$

$$\rho \simeq 10^5 \text{ grams/cm}^3$$

then 1 part in 10^8 of the helium will be in the form of Be^8 at equilibrium.

For the formation of C^{12}, there is a 7.656 $\pm$ 0.007 Mev level that acts as a resonance at the second excited state

of C^{12}. It has spin 0 and even parity. To find the excitation energy:

Second excited state	7.656±0.007 Mev
Sum of Masses of 3 α's	7.2753±0.0014
Excitation energy	0.381±0.008 Mev

The energy level diagram of C^{12} looks like this,

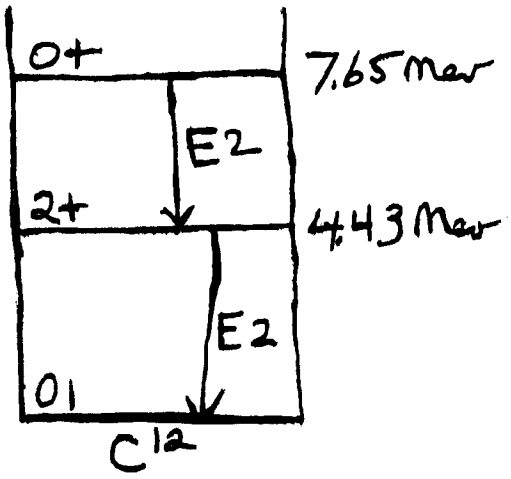

From the first excited state (2+, 4.43 Mev) to ground we have an electric quadrupole (E2) transition. From the second excited state (0+,7.653 Mev) to ground, we have a 0+ to 0+ transition, which cannot take place with the emission of one gamma ray. There could be a simultaneous emission of two gamma rays, but experimental results presently indicate that the probability of this occurrence is too low to be significant. There can be a transition between two spin 0 states by emission of an electron pair, providing

that this channel is energetically possible . Since this is the case, there is an electric monopole transition, E0, that involves the emission of an electron and a positron, which carry away no angular momentum.

In addition, there can be an electric quadrupole transition from 0+ to 2+. The latter level will decay by an E2 transition also.

Finally, the level may decay into three α particles, i.e., the inverse of the formation process.

There have been many fascinating experiments to study the character of these low-lying states of C^{12} and particularly to study the properties of the 7.656 Mev level because of its interest for astrophysics. One of the early experiments of interest was that of Fowler, Cook, Lauritsen, Lauritsen, and Mozer (1956) which showed that the second excited state of C^{12} can be formed by alpha particles. They observed the β-decay of B^{12} which in a certain small fraction of its decays goes to the second excited state of C^{12} instead of the ground state. It was observed that β-decay to this 7.656 Mev state was followed by α-emission. This was a direct demonstration of the inverse of the reaction which we have been discussing. This is important because

it shows that the spin and parity of this level are such that the inverse reaction, which forms C^{12}, is also possible. This indicated that enhancement of the triple-alpha reaction was possible through the Be^8 intermediate stage, using the resonance of the second excited state of C^{12}.

Now, if we consider the expressions for the thermonuclear reaction involving a resonance, we find that we need to know the formation width. In this case it is the sum of the radiation width for transitions to the 2+ state plus the pair emission widths for transitions to the ground state of C^{12}. The alpha-particle width of the state is more than 1000 times the radiation width; hence the radiation width may be neglected with respect to the alpha width. We need absolute, not relative, values for these two widths.

When carbon is bombarded by high energy electrons, peaks appear in the scattering cross section corresponding to excitation of the first excited state, the second excited state, etc. The excitation of these states by inelastic electron scattering is equivalent, in a sense, to the de-excitation of the states by pair emission. In quantum electrodynamics the emission of a positron is equivalent to the

absorption of an electron. Therefore, the matrix element for this transition is essentially the same as it is for the emission of the electric monopole pair.

Alburger and some of his colleagues were able to measure the relative width for pair emission, and found:

$$\frac{\Gamma_{e^\pm}}{\Gamma} = (6.6 \pm 2.2) \times 10^{-6}$$

Alburger also succeeded in measuring the rate of γ-ray decay to the 4.43 Mev first excited state of C^{12}. Eventually the γ-rays themselves were observed, but first it was done indirectly by observing C^{12} recoils. This gave

$$\frac{\Gamma_\gamma}{\Gamma} = (3.3 \pm 0.9) \times 10^{-4}$$

so we find

$$\frac{\Gamma_\gamma}{\Gamma_{e^\pm}} = 50 \pm 22$$

Now, using the pair emission width deduced from the cross section for electron inelastic scattering forming the 7.656 Mev state, as mentioned before, we can find absolute widths. From the calculations of Walecka we have

$$\Gamma_{e^\pm} = 4.5 \times 10^{-5} \text{ ev};$$

therefore,

$$\Gamma_\gamma = 2.5 \times 10^{-3} \text{ ev}$$

Now,

$$\Gamma_\alpha \simeq \Gamma = 7 \text{ ev}$$

This is equal to the sum rule limit for single particles. We can think of the 3α reaction as being equivalent to the Be^8 $(\alpha,\gamma)C^{12}$ reaction. There are other possible ways of completing the reaction, such as a true triple collision, but it does not matter what the details are in view of the fact that the 7.656 Mev state decays overwhelmingly into α's. We can calculate the formation of C^{12} as a slight leakage from full reversibility of $3\,\alpha \rightleftharpoons (C^{12})^*$ calculated according to statistical equilibrium. If n_1, n_8, and n_3 are respectively the number densities of alpha particles, Be^8 nuclei, and C^{12*} excited states, then

$$\frac{n_1 n_8}{n_3} = \left[\frac{2\pi\, m_1 m_8\, kT}{h^2 (m_1 + m_8)}\right]^{3/2} \frac{\omega_1 \omega_8}{\omega_3}\; e^{\chi_{8,3}/kT}$$

where $\chi_{3,8}$ is the energy of $(C^{12})^*$ above $(Be^8 + \alpha)$. Now, n_8 can be obtained from

$$\frac{n_1^2}{n_8} = \left[\frac{2\pi\, m_1^2 kT}{h^2 (2m_1)}\right]^{3/2} \frac{\omega_1^2}{\omega_8}\; e^{\chi_{8,1}/kT}$$

where $\chi_{8,1}$ is the energy of Be^8 above 2 α. Therefore,

$$n_8 = n_1^2 \left[\frac{h^2 (2m_1)}{2\pi\, m_1^2 kT}\right]^{3/2} \frac{\omega_8}{\omega_1^2}\; e^{-\chi_{8,1}/kT}$$

and

$$n_3 = n_1 n_2 \left[\frac{h^2 (m_1 + m_2)}{2\pi\ m_1 m_2\ kT}\right]^{3/2} \frac{\omega_3}{\omega_1 \omega_2}\ e^{-\chi_{3,2}/kT}$$

$$= n_1{}^3 \left[\frac{2\pi\hbar^2}{kT}\right]^3 \left[\frac{2m_1}{m_1{}^2}\right]^{3/2} \left[\frac{3m_1}{2m_1{}^2}\right]^{3/2} \cdot \frac{\omega_3}{\omega_1{}^2}\ e^{-(\chi_{3,2}+\chi_{2,1})/kT}$$

$$= \frac{8\pi^3\ \hbar^6 (3)^{3/2}}{(m_1 kT)^3}\ n_1{}^3\ e^{-\chi\ kT}$$

where $\chi = \chi_{3,2} + \chi_{2,1}$ = energy of C^{12*} above 3 α's, and where $\omega_1 = \omega_3 = 1$. Now, from the uncertainty principle,

$\Gamma\ \tau = \hbar$ where τ is the mean life. The rate of formation of C^{12} per C^{12*} nucleus per second is given by

$$\frac{1}{\tau} = \frac{\Gamma_\gamma}{\hbar}$$

Actually, we should use

$\dfrac{\Gamma_\gamma\ \Gamma_\alpha}{\Gamma_\gamma + \Gamma_\alpha}$ instead of Γ_γ to take account of the fact that there is leakage. Therefore, the amount of C^{12} formed per cubic centimeter per second

$$= \frac{n_3}{\hbar} \left(\frac{\Gamma_\gamma\ \Gamma_\alpha}{\Gamma_\alpha + \Gamma_\gamma}\right)$$

$$= \frac{8\pi^3\ \hbar^5 (3)^{3/2}}{(m_\alpha\ kT)^3} \left(\frac{\Gamma_\gamma\ \Gamma_\alpha}{\Gamma_\gamma + \Gamma_\alpha}\right) n_1{}^3\ e^{-\chi/kT}$$

Suppose we wish to calculate a rate for the formation of C^{12} by an α particle reacting with the system composed of two

other alphas. There are three ways of choosing the odd alpha particle, so the rate is

$$r_{3\alpha} = P_{3\alpha} \frac{n_1}{3} ,$$

and

$$P_{3\alpha} = \frac{8\pi^3 \hbar^5 (3)^{5/2}}{(m_\alpha kT)^3} \left(\frac{\Gamma_\gamma \Gamma_\alpha}{\Gamma_\gamma + \Gamma_\alpha}\right) n_1^2 \quad e^{-\chi/kT}$$

which is the reaction rate per alpha particle. If we write

$$n_1 = \frac{N_0 \rho}{4} = \frac{\rho x_\alpha}{m_\alpha}$$

where N_0 is the Avagodro's number and x_α is the fraction by weight of α-particles in the mixture, then

$$P_{3\alpha} = \frac{8\pi^3 \hbar^5 (3)^{5/2}}{m_\alpha^5 (kT)^3} \left(\frac{\Gamma_\gamma \Gamma_\alpha}{\Gamma_\alpha + \Gamma_\gamma}\right) (\rho x_\alpha)^2 \quad e^{-\chi/kT}$$

$$= 5.92 \times 10^{-7} \frac{(\rho x_\alpha)^2}{T_8^3} \exp\left(-\frac{44.3}{T_8}\right) \sec^{-1}$$

<u>The $C^{12}(\alpha,\gamma)O^{16}$ Reaction</u>

The nonresonant reaction $C^{12}(\alpha,\gamma)O^{16}$ is the means by which C^{12} produced by the triple alpha reaction is destroyed. The energy level diagram of O^{16} is as follows:

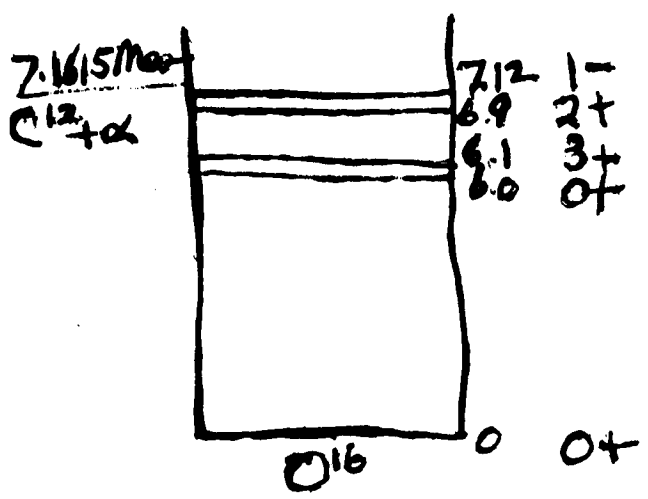

The threshold for the reaction at zero bombarding energy is 7.1615 Mev. While this reaction is nonresonant, it is close to several resonances, all of which, in principle, can be formed by combining an alpha particle with C^{12}. There are restrictions on spin and parity of the compound states that can be formed. The alpha particle and the C^{12} nucleus both have zero spin and even parity; to form a state of odd parity, the parity of motion between the alpha particle and the C^{12} must be odd, i.e., the relative angular momentum must be odd. For example, an s-wave alpha particle bombarding C^{12} would form a state 0+; it could not form any 0- states. If there is one unit of angular momentum in the motion of the bombarding particle, it could form a state 1-. Similarly, states 2+, 3-, 4+, etc. could be formed by bombarding particles possessing larger angular momenta with respect to the target. Only half of all the possible spin-parity combinations are allowed for possible resonances in reactions of this kind. We notice that all the first excited states of C^{12} can be formed in this way, so, in principle, the reaction could take place in the energy region of the tails of these levels. We need consider only the tail of the nearest level (the 1- level) because it has the

largest width for radiative decay to the ground state. Off resonance, the reaction cross section contains the product of the alpha particle width and the gamma ray width. We are interested in which of these levels will have the largest value for this product. For a given energy, the greatest barrier penetrability occurs for the lowest angular momentum; a larger barrier penetrability means a larger alpha width. Also, the 1- state can decay to the ground state of O^{16} by emission of electric dipole radiation, which ordinarily has a greater intrinsic width than any higher multipole radiation. The 2+ state would decay by electric quadrupole and the 3- by electric octupole radiation, and these decays are therefore less probable. The 0+ state cannot decay at all by the emission of a gamma ray, but decays predominantly by the emission of electron-positron pairs, and consequently this decay rate is very slow.

There is another point to consider here; O^{16} is a self-conjugate nucleus, i.e., it has the same number of neutrons as protons. This would not favor the 1- state (7.12 Mev) emitting electric dipole radiation because E1 radiation is intrinsically inhibited in self-conjugate nuclei. However, the radiation width has been measured,

and the E1 transition is stronger than would ordinarily be expected for self-conjugate nuclei. The radiation width for this level is

$$\Gamma_\gamma = 0.066 \pm 30\% \text{ ev.}$$

We now need to know the alpha width for this level to evaluate the reaction rate for nonresonant reactions, and we shall use the alpha particle model to estimate this width. Generally speaking, the alpha particle model is poor, but if it is valid for any nucleus, it is valid for O^{16}. In this model O^{16} is an α-particle tetrahedron for which one can calculate the normal modes of vibration. Fortunately, the 7.12 Mev level is one of the fundamental identifications in this model. J.K. Perring (unpublished, private communication) has developed wave functions for these states. On his model, α emission from the 7.12 Mev state is "allowed", and therefore the α-width is expected to be a large fraction of sum-rule limit. We assume the reduced width is

$$\gamma^2_\alpha = 0.1\ h^2/mR.$$

With this assumption, the number of reactions per cm^2 per sec

$$= \frac{1.33 \times 10^{-13}}{T_8^{\,2}(1+0.16T_8^{\,-2/3})^2}\ n_1 n_3\ \exp\left(-\frac{69.18}{T_8^{\,1/3}}\right)$$

where n_1 is the number density of the alphas and n_3 the number density of the C^{12} nuclei. The slight variation of this expression from the usual nonresonant form represents an allowance for the variation of the nuclear cross section factor with energy due to the nearness of the 7.12 Mev level to the thermonuclear bombarding energy region.

Let us note explicitly that this alpha particle width is the single important parameter that remains to be measured before we have complete knowledge of the behavior of the helium-burning reactions in stellar interiors.

$O^{16}(\alpha,\gamma)Ne^{20}$

The next reaction is the capture of alpha particles by O^{16}, i.e., $O^{16}(\alpha,\gamma)Ne^{20}$. The level diagram is as follows:

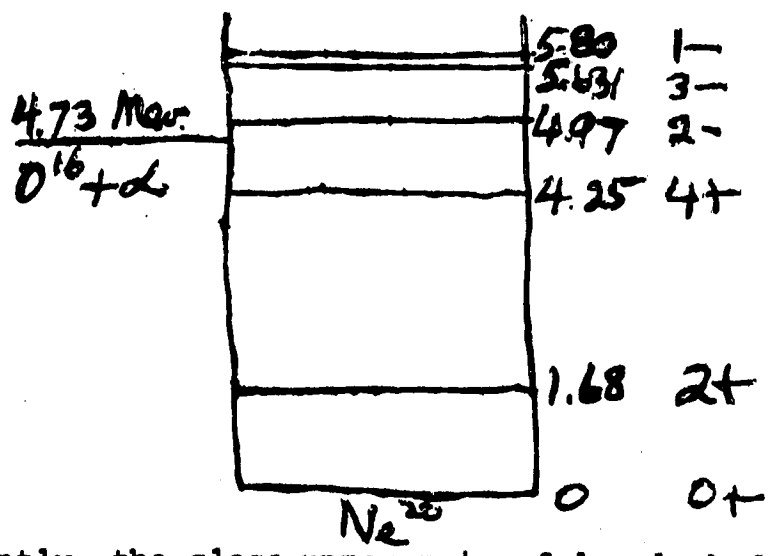

Until recently, the close upper pair of levels had been measured as only one level. The sum of the masses of O^{16}

plus alpha particle is 4.73 Mev; the level at 4.97 Mev is only some 240 kev above this. Calculating the optimum bombarding energy for these alpha particle reactions, we find that it is of the order of 200-300 kilovolts. It would seem that the 4.97 Mev level would give an enormous resonance for this reaction, but recently it was discovered that this state does not have the right spin and parity to be formed by the combination of an α-particle and O^{16}. The next higher states, at 5.6 and 5.8 Mev, do have acceptable spin-parity combinations. For the 5.631 Mev level, we have the following experimental information:

$$(2\ell+1)\ \frac{\Gamma_\alpha \Gamma_\gamma}{\Gamma} = 0.003 \pm 0.002 \text{ ev}$$

and

$$\frac{\Gamma_\gamma}{\Gamma} = 0.07 \pm 0.01$$

Therefore

$$\Gamma_\alpha = 6 \pm 4 \times 10^{-3} \text{ ev}$$

$$\Gamma_\gamma = 4 \pm 3 \times 10^{-4} \text{ ev}$$

For the 5.80 Mev level, we know that

$$\frac{\Gamma_\gamma}{\Gamma} < 0.006$$

and

$$\Gamma_\alpha < 16 \text{ ev (sum rule limit)}$$

$$\sim 2 \text{ ev, probably.}$$

If one assumes that Γ_γ is of the order of 10^{-2} ev, then

$$(2\ell+1) \quad \frac{\Gamma_\alpha \Gamma_\gamma}{\Gamma} \sim 0.03 \text{ ev.}$$

For $T_8 < 2.1$, the nonresonant rate dominates, and

$$p = 4.5 \times 10^{9 - 37.2/T_8^{1/3}} \quad \frac{\rho x_4}{T_8^{2/3}}$$

where x_4 refers to the fractional abundance of O^{16} by weight. For $2.5 < T_8 < 8$, the 5.631 Mev state dominates, and

$$p = 6.3 \times 10^{2 - 45.9/T_8} \quad \frac{\rho x_4}{T_8^{3/2}}$$

Note that there is a gap in which the changeover is occurring. One could proceed to the next step, Ne^{20} (α,γ) Mg^{24}, but, as we shall see, such reactions are not important.

Now let us consider the products of the helium reactions we have discussed. If one has helium gas, compresses it, heats it, and allows these reactions to occur, what is the result? We write the rates of reaction (per cm^3 per sec) as

$3\alpha \rightarrow C^{12}$	$q_1 n_1^3$
$C^{12}(\alpha,\gamma)O^{16}$	$q_3 n_1 n_3$
$O^{16}(\alpha,\gamma)Ne^{20}$	$q_4 n_1 n_4$

Then,

$$q_1 = \frac{8.70 \times 10^{-54}}{T_8^{\,3}} \exp\left(\frac{-44.3}{T_8}\right)$$

$$q_3 = \frac{1.33 \times 10^{-13}}{T_8^{\,2}(1+0.16T_8^{-2/3})^2} \exp\left(\frac{-69.18}{T_8^{\,1/3}}\right)$$

$$q_4 = 1.19\text{x}10^{-14} \frac{n_1 n_4}{T_8^{\,2/3}} \exp\left(\frac{-85.6}{T_8^{\,1/3}}\right), \quad T_8 < 2.1$$

$$= 1.67\text{x}10^{-21} \frac{n_1 n_4}{T_8^{\,3/2}} \exp\left(\frac{-105.5}{T_8}\right), \quad T_8 > 2.5$$

Given these expressions, the differential equations take the following form

$$\frac{dn_1}{dt} = -3q_1 n_1^{\,3} - q_3 n_1 n_3 - q_4 n_1 n_4$$

$$\frac{dn_3}{dt} = q_1 n_1^{\,3} - q_3 n_1 n_3$$

$$\frac{dn_4}{dt} = q_3 n_1 n_3 - q_4 n_1 n_4$$

$$\frac{dn_5}{dt} = q_4 n_1 n_4$$

Each 3α reaction releases $Q = 7.281$ Mev or 1.165×10^{-5} ergs. We shall start with a pure helium gas and relate the various solutions of these equations to the initial rate of energy generation in this gas which is

$$\epsilon = q_1 \; n_{10}^{\,3} \; Q$$

$$= 7.33 \times 10^{64} \; \rho^2 q_1 \text{ erg/gm sec}$$

where n_{10} is the initial abundance of alpha particles.

The helium concentration has been plotted versus product abundances for this helium gas model, in terms of the two parameters $\frac{q_3}{q_1 n_{10}}$ and $\frac{q_4}{q_1 n_{10}}$. The q's are the reaction rates we have been discussing, and are functions only of temperature, not density. We shall consider a wide range of values for the first parameter, and for each value in this range we shall consider two values of the second parameter, i.e., 0.1 and 1.0. These graphs were made using the assumption that the temperature and the density remain the same while helium burning progresses (otherwise the parameters shift slightly during the course of the helium burning). Closer examination reveals that this assumption is not bad.

In Figure 14.1, with the smallest values of the parameters, we note that the C^{12} production is initially linear, but after most of the helium is converted, the C^{12} abundance passes through a maximum and then production of O^{16} and small amounts of Ne^{20} becomes significant.

In Figure 14.2 we change the second parameter to 1.0. The C^{12} curve is hardly altered, but now the end-point concentration of Ne^{20} is greater than O^{16}. The result of helium burning is still essentially the formation of C^{12}.

In Figure 14.3 the first parameter is increased to 1.0 and

the second is again 0.1. The changes are apparent; C^{12} is the dominant nucleus only in the earlier part of helium burning. Later C^{12} destruction is more important and large amounts of O^{16} accumulate.

In Figure 14.4 the parameters are both 1.0. The C^{12} curve is nearly the same as in the previous case, but now O^{16} destruction is more important in the later stages of helium burning, and Ne^{20} is finally the most abundant nucleus.

In Figure 14.5 the first parameter has been increased to 10 and the second is again 0.1. The changes are drastic; C^{12} is the dominant nucleus only in the earliest part of helium burning. C^{12} destruction becomes important and large amounts of O^{16} accumulate until, at the very end of helium burning, the destruction of O^{16} becomes more important and we accumulate some appreciable amounts of Ne^{20}.

As we are beginning to expect, in Figure 14.6 we see that increasing the second parameter to unity changes the C^{12} curve very little, but the larger rate of oxygen destruction means that the amount of O^{16} remaining at the end of helium burning is very small. The formation of Ne^{20} dominates the later stages of helium burning, leaving almost

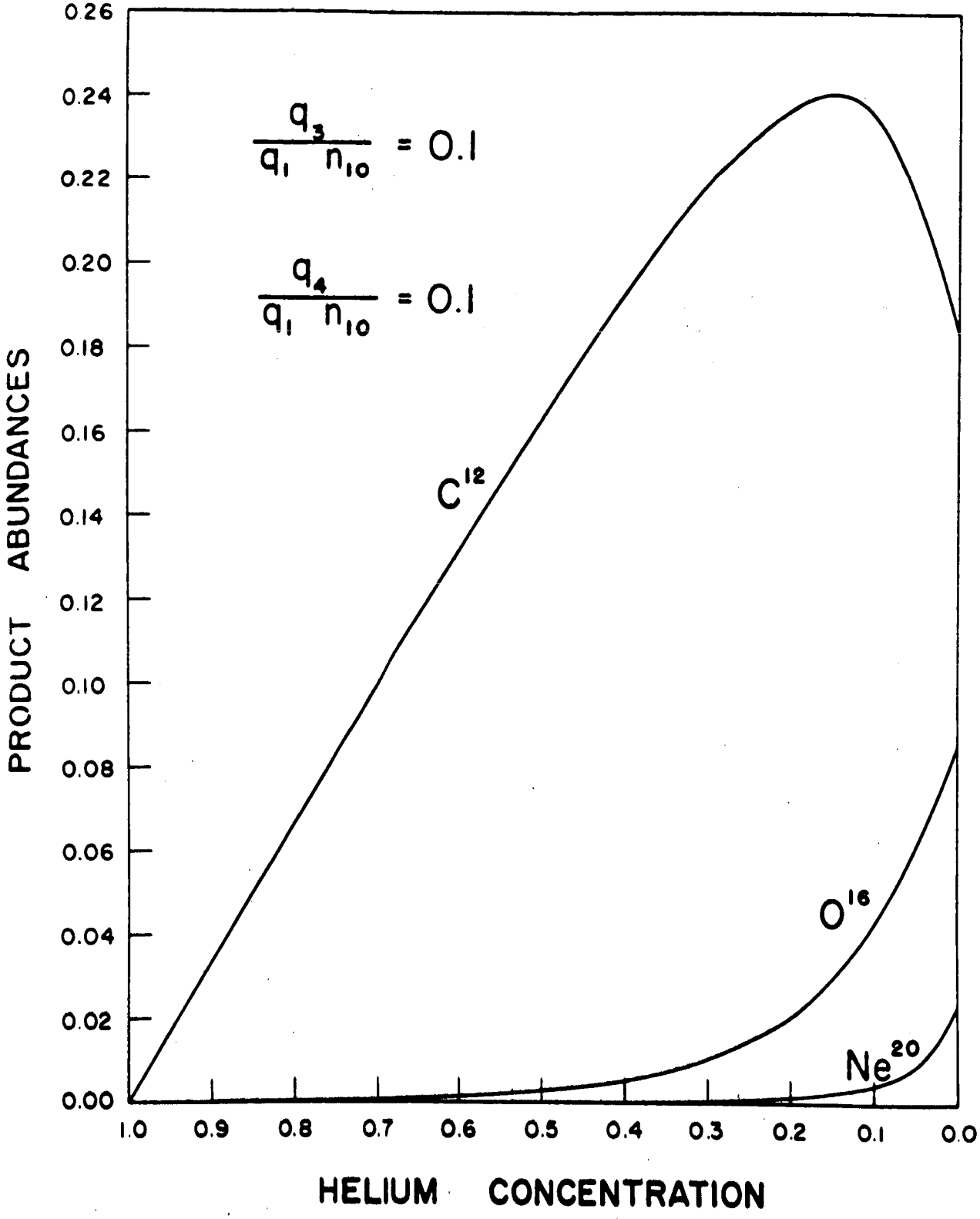
0.26
0.24
0.22
0.20
0.18
0.16
0.14
0.12
0.10
0.08
0.06
0.04
0.02
0.00
PRODUCT ABUNDANCES
$\frac{q_3}{q_1 \; n_{10}} = 0.1$
$\frac{q_4}{q_1 \; n_{10}} = 0.1$
C^{12}
O^{16}
Ne^{20}
1.0
0.9
0.8
0.7
0.6
0.5
0.4
0.3
0.2
0.1
0.0
HELIUM CONCENTRATION

Figure 14.1

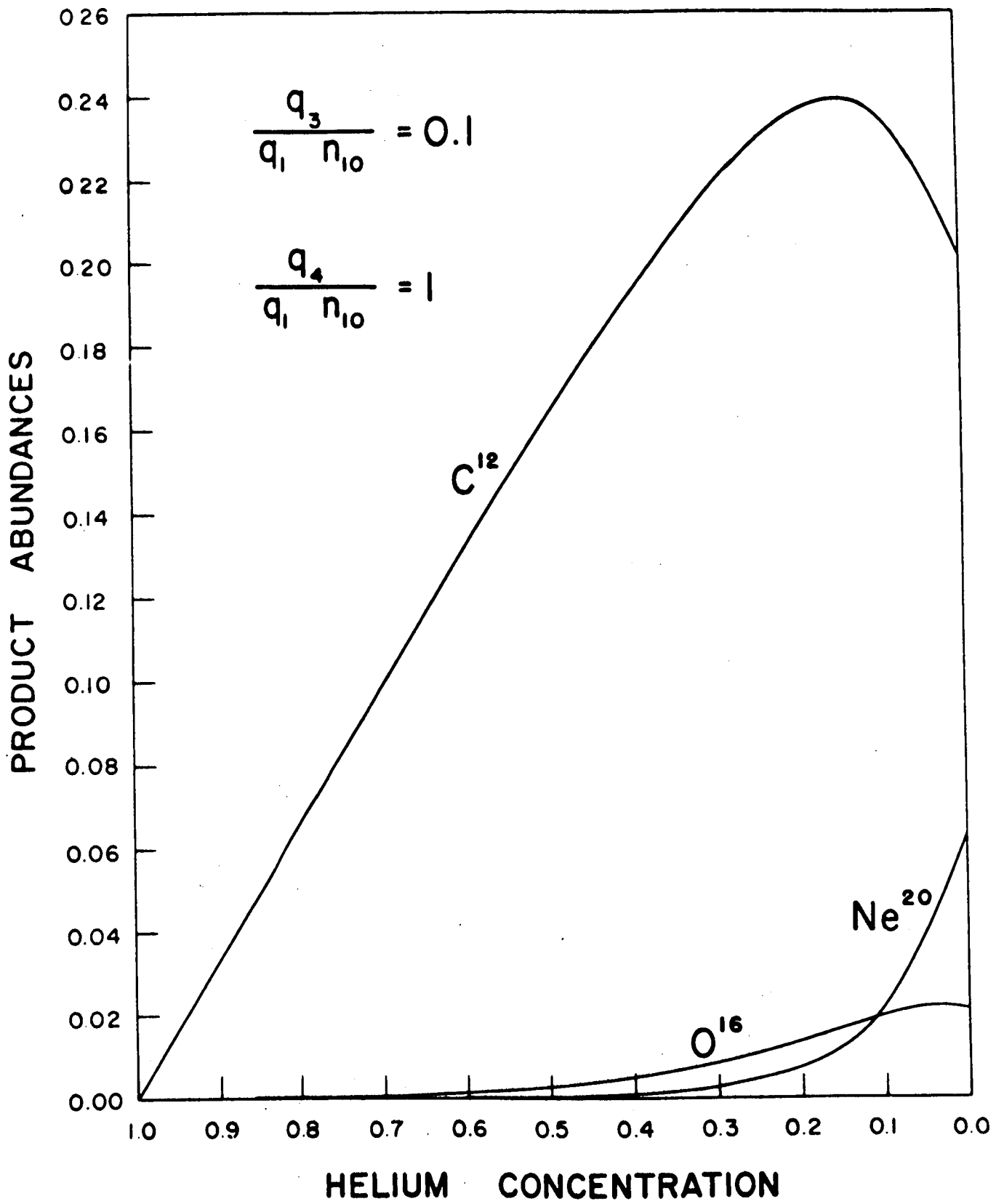
0.26
0.24
0.22
0.20
0.18
0.16
0.14
0.12
0.10
0.08
0.06
0.04
0.02
0.00
PRODUCT ABUNDANCES
$\frac{q_3}{q_1 \; n_{10}} = 0.1$
$\frac{q_4}{q_1 \; n_{10}} = 1$
C^{12}
Ne^{20}
O^{16}
1.0
0.9
0.8
0.7
0.6
0.5
0.4
0.3
0.2
0.1
0.0
HELIUM CONCENTRATION

Figure 14.2

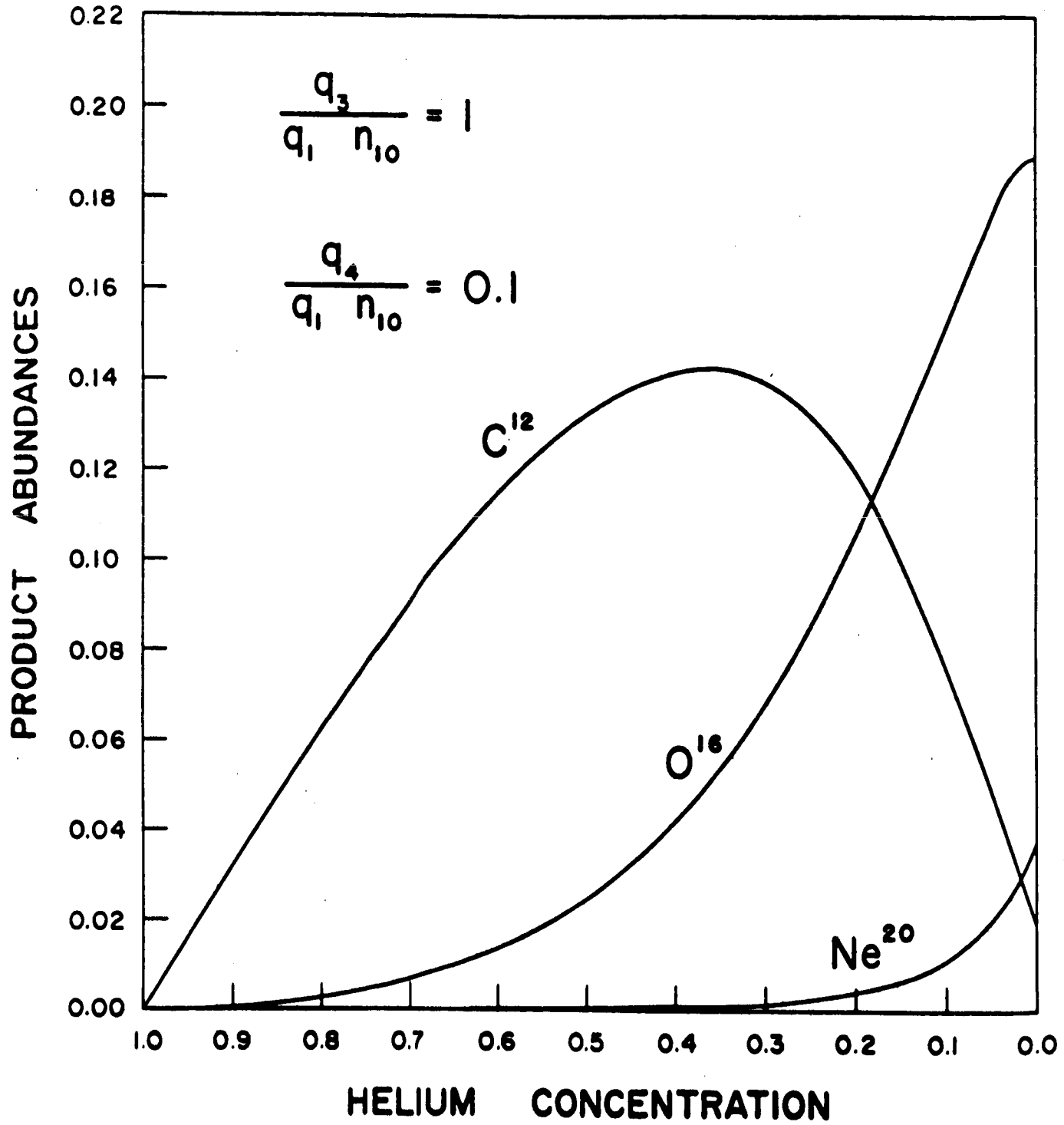
0.22
0.20
0.18
0.16
0.14
0.12
0.10
0.08
0.06
0.04
0.02
0.00
PRODUCT ABUNDANCES
$\frac{q_3}{q_1 \; n_{10}} = 1$
$\frac{q_4}{q_1 \; n_{10}} = 0.1$
C^{12}
O^{16}
Ne^{20}
1.0
0.9
0.8
0.7
0.6
0.5
0.4
0.3
0.2
0.1
0.0
HELIUM CONCENTRATION

Figure 14.3

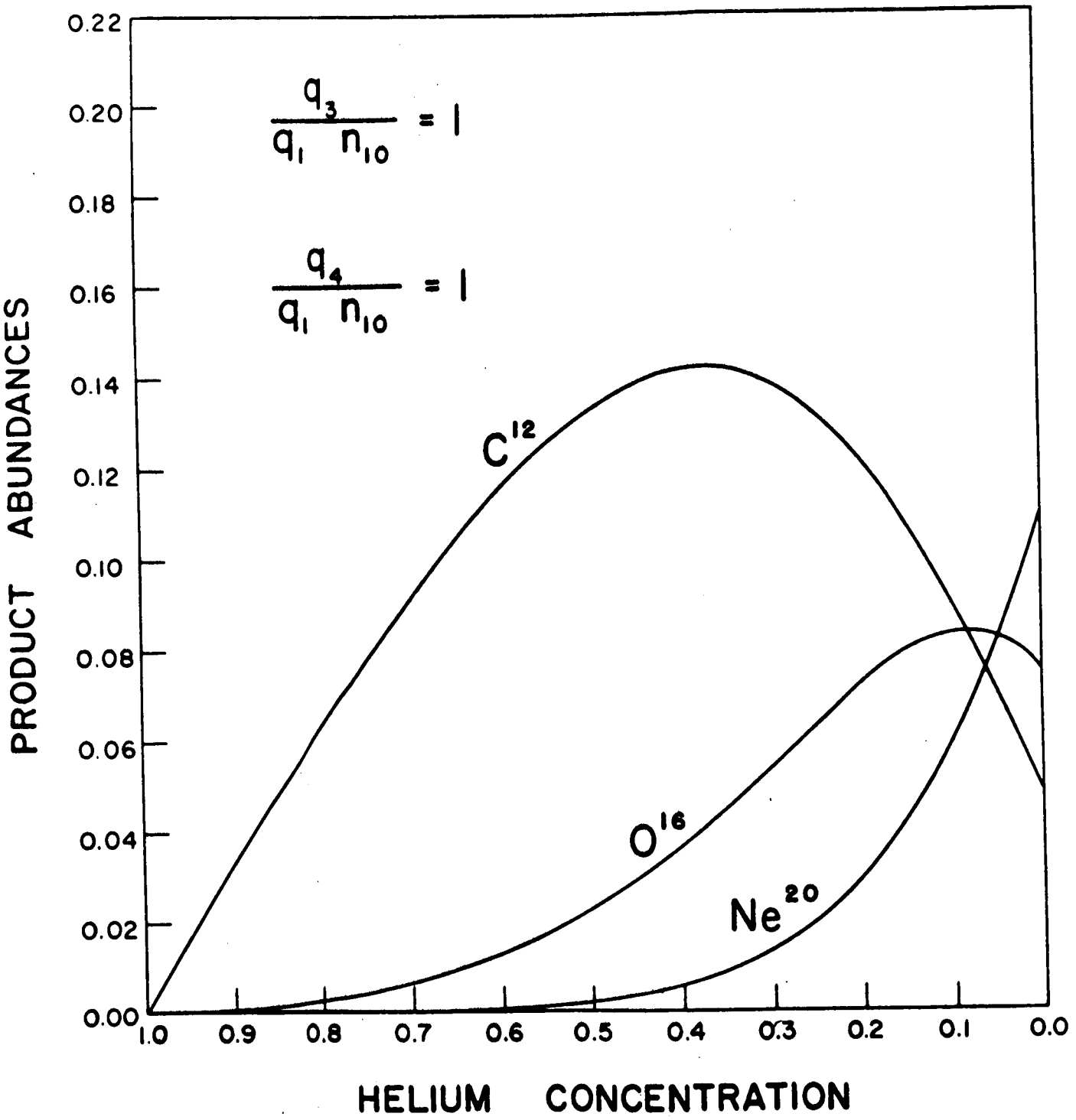
0.22
0.20
0.18
0.16
0.14
0.12
0.10
0.08
0.06
0.04
0.02
0.00
PRODUCT ABUNDANCES
$\frac{q_3}{q_1 \; n_{10}} = 1$
$\frac{q_4}{q_1 \; n_{10}} = 1$
C^{12}
O^{16}
Ne^{20}
1.0
0.9
0.8
0.7
0.6
0.5
0.4
0.3
0.2
0.1
0.0
HELIUM CONCENTRATION

Figure 14.4

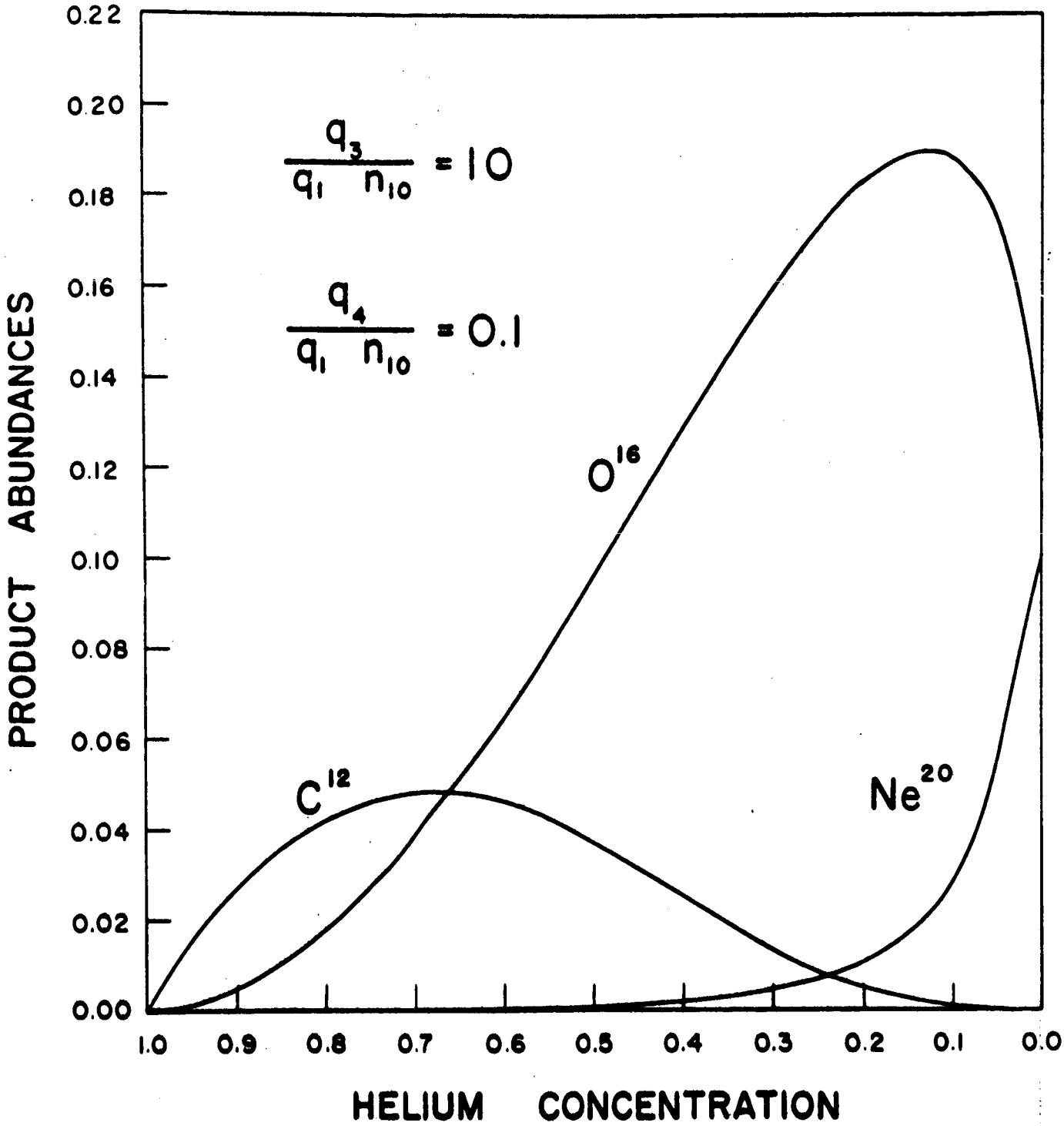
0.22
0.20
0.18
0.16
0.14
0.12
0.10
0.08
0.06
0.04
0.02
0.00
PRODUCT ABUNDANCES
$\frac{q_3}{q_1 \; n_{10}} = 10$
$\frac{q_4}{q_1 \; n_{10}} = 0.1$
O^{16}
C^{12}
Ne^{20}
1.0
0.9
0.8
0.7
0.6
0.5
0.4
0.3
0.2
0.1
0.0
HELIUM CONCENTRATION

Figure 14.5

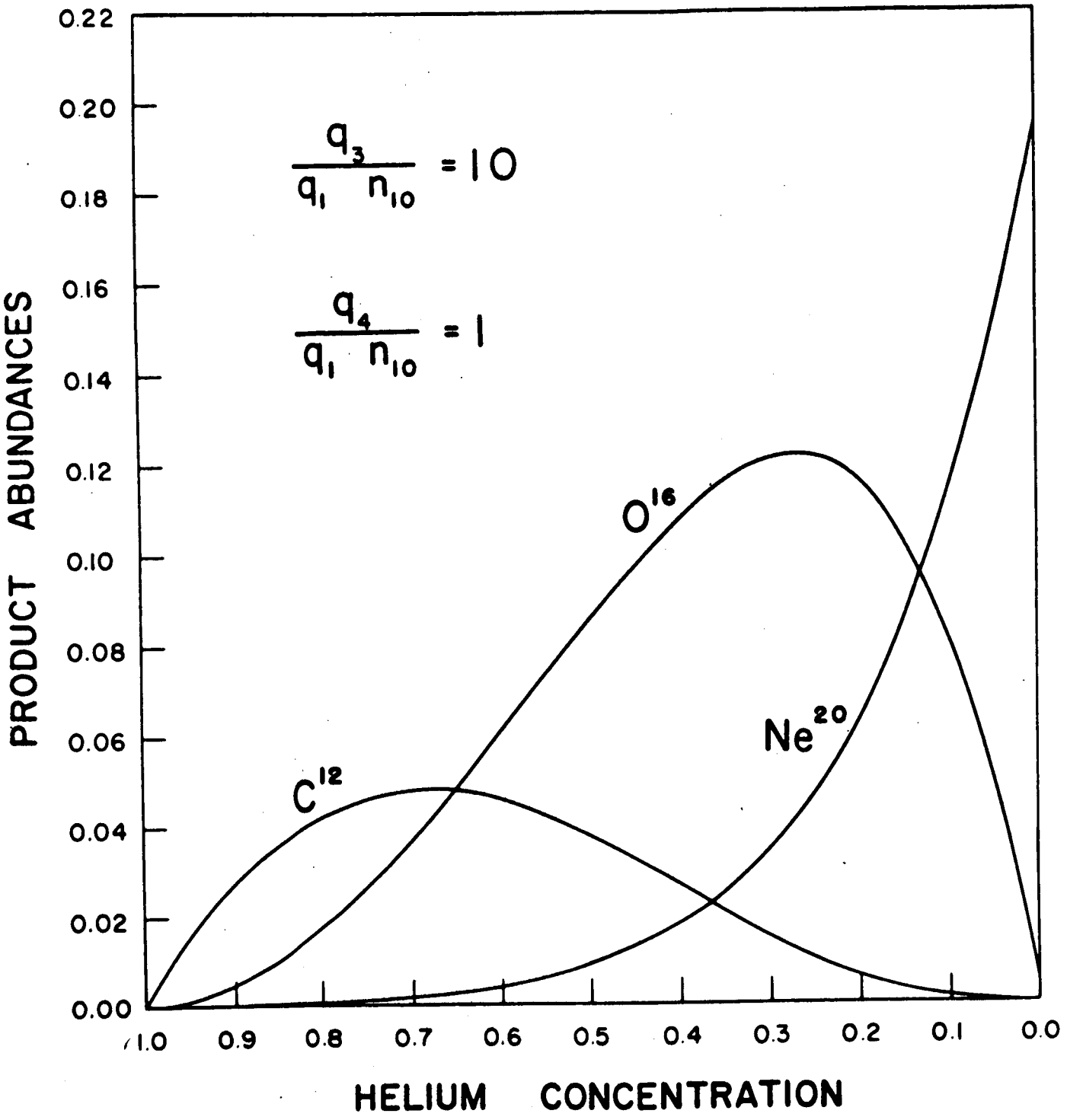
0.22
0.20
0.18
0.16
0.14
0.12
0.10
0.08
0.06
0.04
0.02
0.00
PRODUCT ABUNDANCES
$\frac{q_3}{q_1 \; n_{10}} = 10$
$\frac{q_4}{q_1 \; n_{10}} = 1$
O^{16}
Ne^{20}
C^{12}
1.0
0.9
0.8
0.7
0.6
0.5
0.4
0.3
0.2
0.1
0.0
HELIUM CONCENTRATION

Figure 14.6

all of the material in the form of Ne^{20}.

In Figure 14.7, the upper parameter is increased to 100 and the lower one is down again to 0.1. Destruction of C^{12} rapidly becomes the dominant process and the total abundance of C^{12} never becomes a significant quantity. O^{16} formation dominates, but toward the end of the helium burning process O^{16} destruction becomes important, and finally some significant quantities of Ne^{20} are formed.

In Figure 14.8 the first parameter is again 100 but the second parameter is now unity. There is little difference in the C^{12} curve, but the larger rate of oxygen destruction results in the transformation of essentially all of the helium into Ne^{20} in the last stages of He burning.

Figure 14.9 is a density-temperature diagram which shows under what circumstances we can obtain some values of the parameters which we have just used. The solid lines show the combinations of density and temperature at which a pure He gas would generate a given energy, neglecting any further reactions in the helium burning chains. The dashed lines are evolutionary tracks that we may expect for stars of one solar mass or ten solar masses, according to the relations we derived in an earlier section. (We assume that

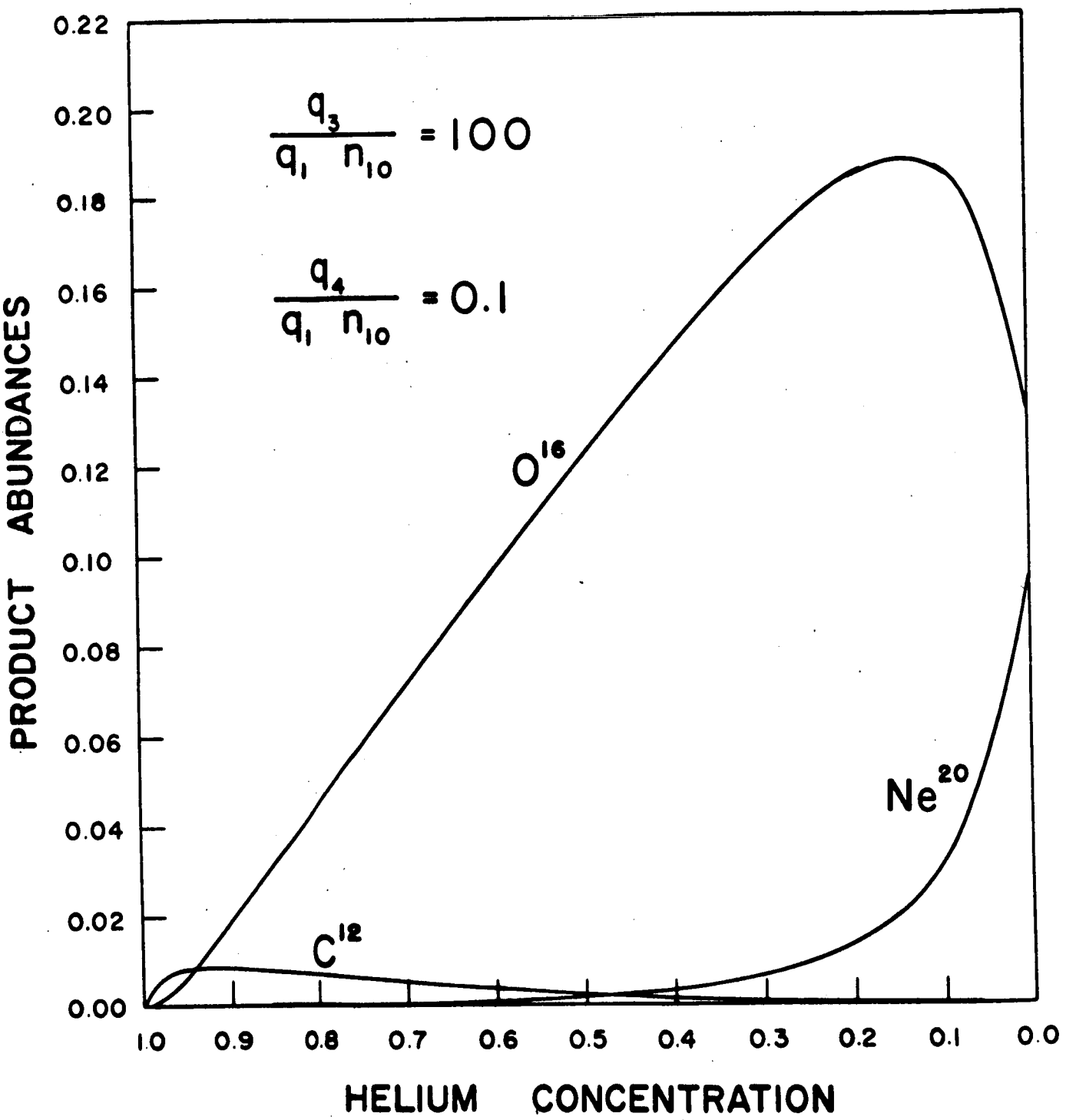
0.22
0.20
0.18
0.16
0.14
0.12
0.10
0.08
0.06
0.04
0.02
0.00
PRODUCT ABUNDANCES
$\frac{q_3}{q_1 \; n_{10}} = 100$
$\frac{q_4}{q_1 \; n_{10}} = 0.1$
O^{16}
Ne^{20}
C^{12}
1.0
0.9
0.8
0.7
0.6
0.5
0.4
0.3
0.2
0.1
0.0
HELIUM CONCENTRATION

Figure 14.7

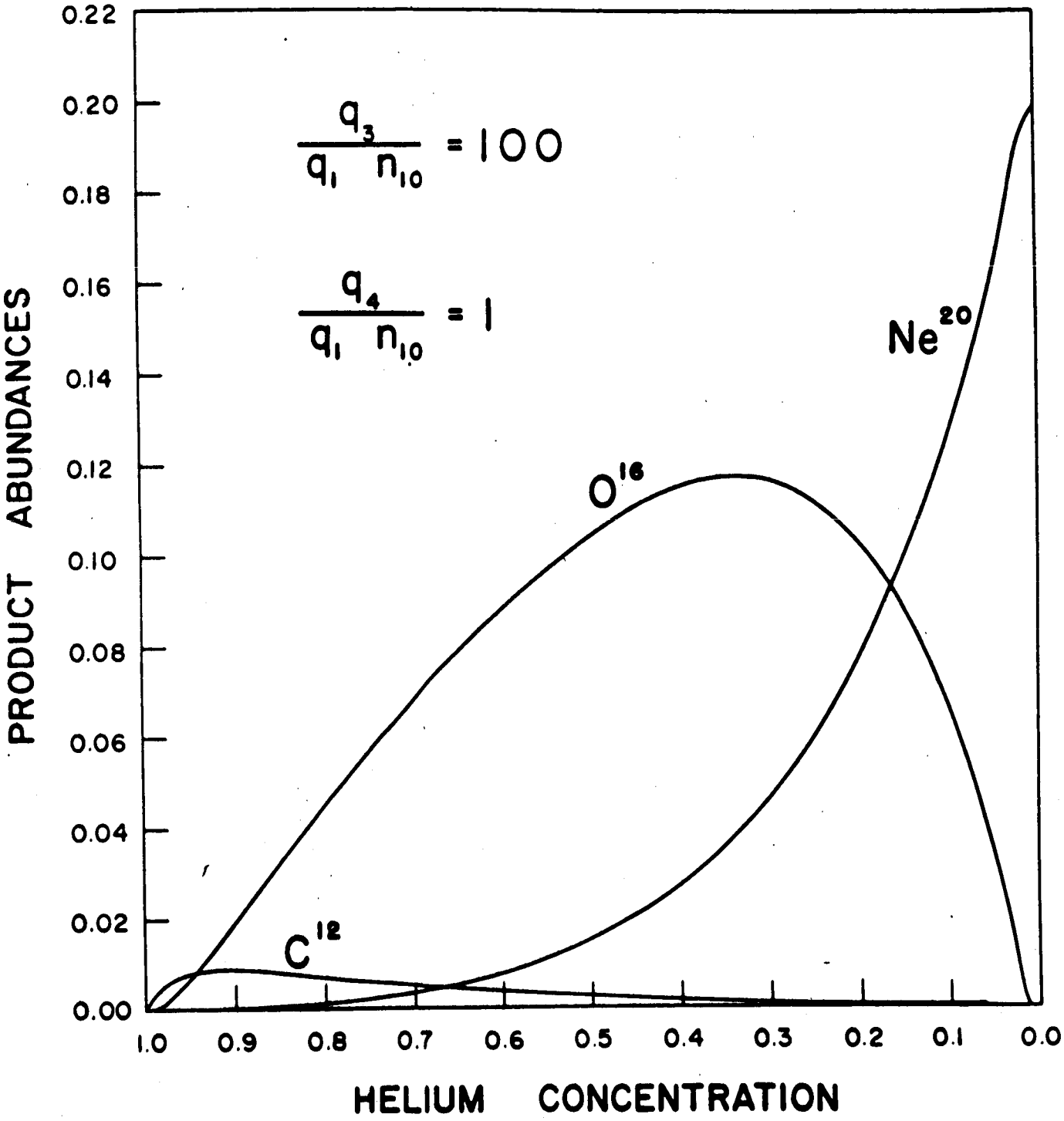
0.22
0.20
0.18
0.16
0.14
0.12
0.10
0.08
0.06
0.04
0.02
0.00
PRODUCT ABUNDANCES
$\frac{q_3}{q_1 \; n_{10}} = 100$
$\frac{q_4}{q_1 \; n_{10}} = 1$
Ne^{20}
O^{16}
C^{12}
1.0
0.9
0.8
0.7
0.6
0.5
0.4
0.3
0.2
0.1
0.0
HELIUM CONCENTRATION

Figure 14.8

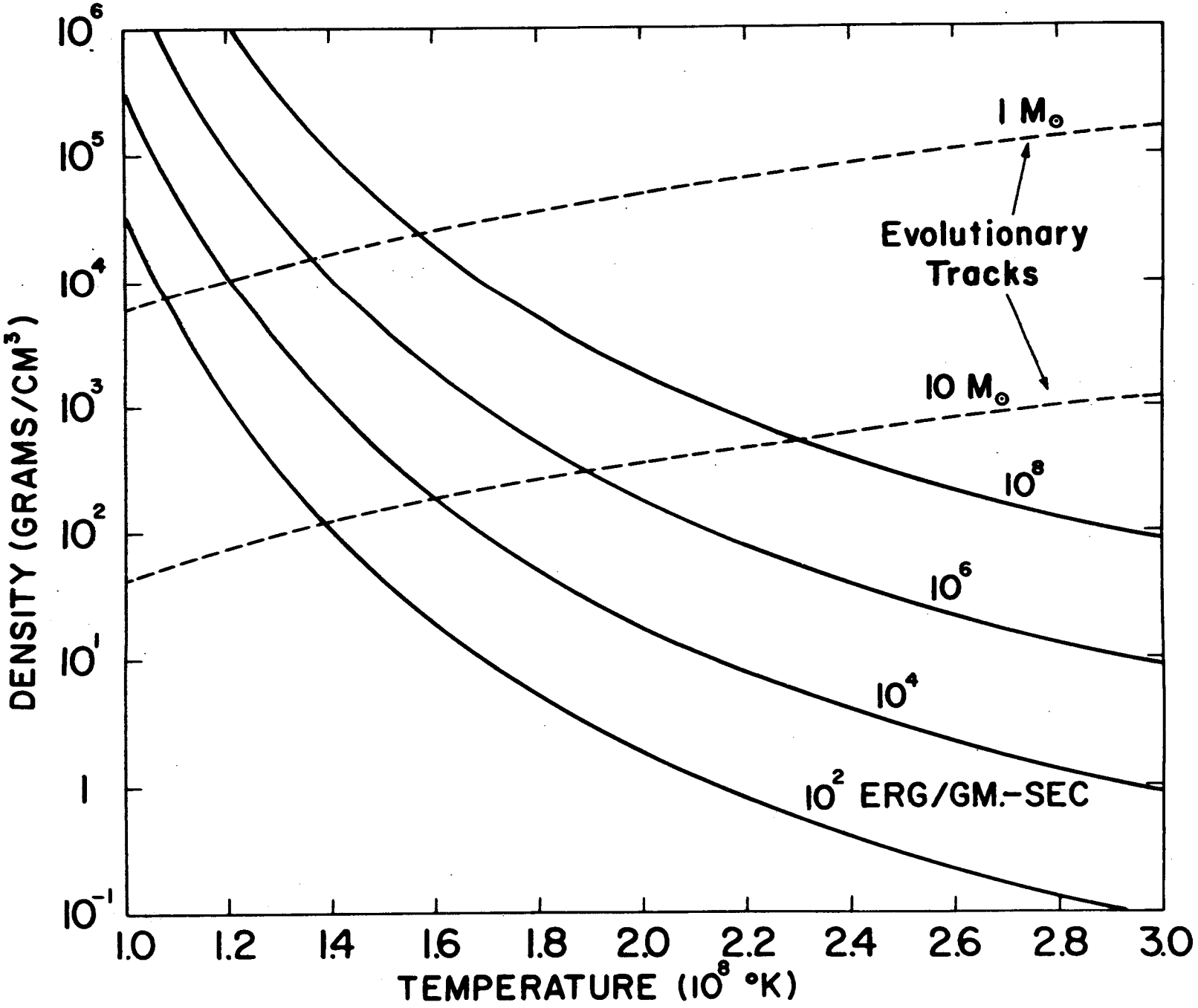
DENSITY (GRAMS/CM³)
10⁶
10⁵
10⁴
10³
10²
10¹
1
10⁻¹
1.0
1.2
1.4
1.6
1.8
2.0
2.2
2.4
2.6
2.8
3.0
TEMPERATURE (10⁸ °K)
1 M⊙
Evolutionary Tracks
10 M⊙
10⁸
10⁶
10⁴
10² ERG/GM.-SEC

Figure 14.9

the densities throughout the star are such that the center does not become highly degenerate). Stars of approximately one solar mass will generally increase in overall luminosity after they burn out hydrogen at the center, and go into the red giant region. Consequently the average energy generation at the center will go from roughly 20 ergs/gm. sec. for the sun into the range of a few hundred ergs/gm. sec. in the helium burning stages. An energy generation range of about 10^2 to 10^4 ergs/gm sec should take place at a density near 10^4 grams per cm^3 and at a temperature rather close to 1.2×10^8 degrees Kelvin. We can further state that a helium burning energy source for a star of one solar mass will depart from these conditions in the direction of higher temperature and lower density. Therefore we can expect to have temperature T_8 of 1.4 to 1.6 with densities of the order of perhaps 10^3 grams/cm^3 or so for such helium burning shell sources.

For a star of 10 solar masses we expect a much higher energy generation rate per gram, perhaps in the range 10^6 or 10^8 ergs/gm. sec; this would mean a temperature somewhere around 2.0 to 2.2×10^8 ^{o}K and a density between 10^2 and

10^3 gm/cm^3. This is the case where we have energy generation at the center of the star. If instead there is a highly condensed core with a shell energy source in the star, we should change these conditions along the diagonal line directed toward the lower right-hand part of the curve; then the temperatures will be around $T_8 = 3$, perhaps, but the density will stay about 10^2 gm/cm^3.

Figure 14.10 shows the values of the first parameter, $\frac{q_2}{q_1 n_{10}}$, corresponding to various rates of energy generation, plotted as a function of temperature. The evolutionary tracks for stars of one solar mass and ten solar masses are shown. For a given energy generation rate, $\frac{q_2}{q_1 n_{10}}$ increases with an increase in temperature.

Let us consider a star of one solar mass. With a temperature of helium burning near 1.2×10^8 degrees Kelvin and an energy generation rate around 10^2 to 10^4 ergs/gm. sec, $\frac{q_2}{q_1 n_{10}}$ should lie in the range of 1 to 10. The previous abundance curves show that in such a case the earlier parts of helium burning will result primarily in the formation of C^{12} but the later parts of helium burning will have an overwhelming production of O^{16}. The range of the parameters is sufficiently uncertain so that one could not say whether

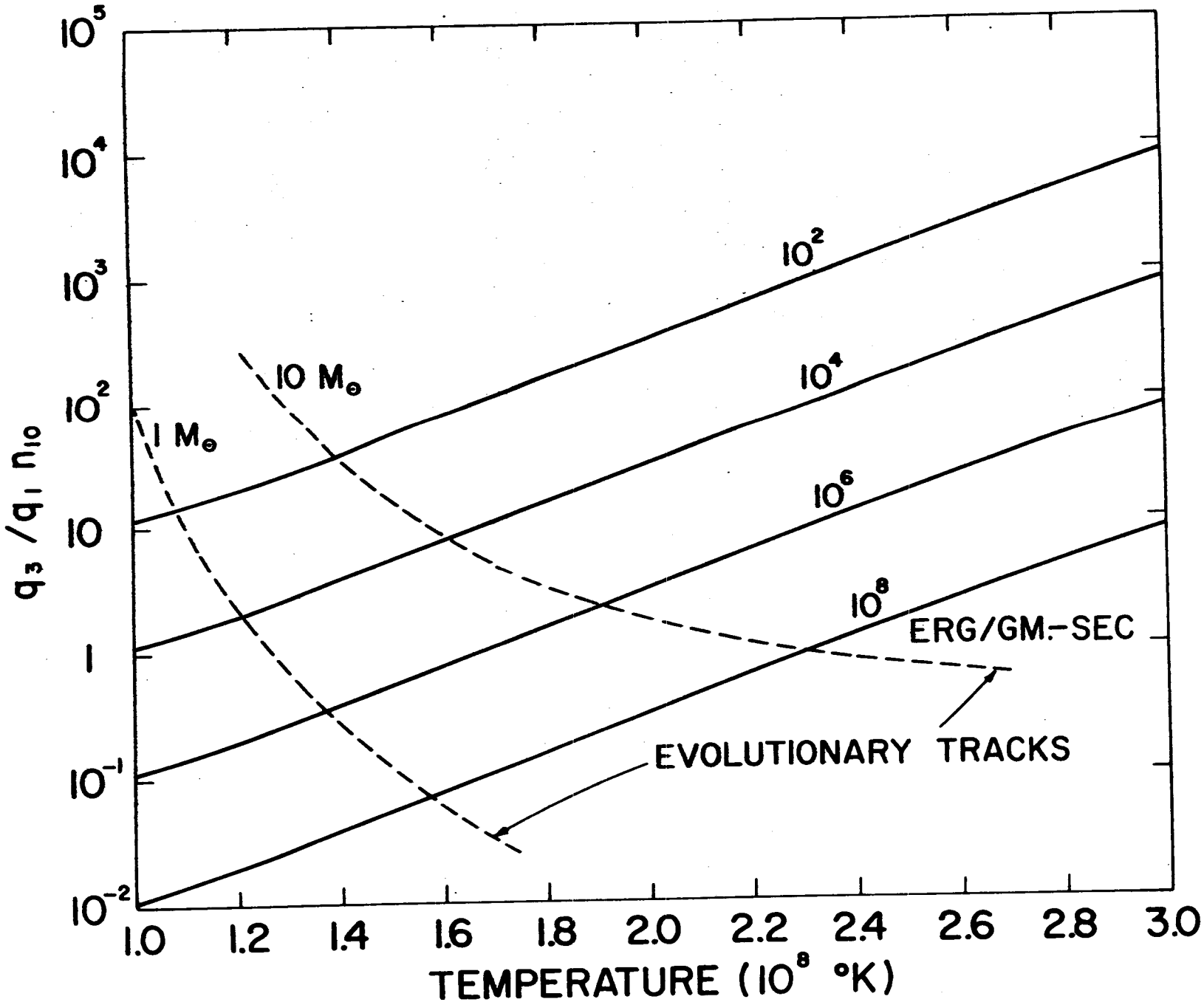
10^5
10^4
10^3
10^2
10
1
10^{-1}
10^{-2}
$q_3 / q_1 n_{10}$
1.0
1.2
1.4
1.6
1.8
2.0
2.2
2.4
2.6
2.8
3.0
TEMPERATURE (10^8 °K)
10^2
10^4
10^6
10^8
ERG/GM.-SEC
10 $M_\odot$
1 $M_\odot$
EVOLUTIONARY TRACKS

Figure 14.10

to expect comparable amounts of C^{12} and O^{16} at the end of the helium burning process or large amounts of O^{16} and negligible amounts of C^{12}. If we recall that for a helium burning shell source the temperature will increase as also will the rate of energy generation per gram, we see that the value of $\frac{q_4}{q_1 n_{10}}$ will remain in the general range of 1 to 10. Thus the results for a helium burning shell are roughly the same as those for helium burning taking place at the center.

In the case of a star of ten solar masses, i.e., energy generation around 10^6 to 10^8 ergs/gm. sec. and temperature T_8 around 2.0 to 2.2, the value of $\frac{q_4}{q_1 n_{10}}$ is close to 0.1. If this second parameter is closer to unity then comparable amounts of C^{12} and O^{16} are left. We shall see that it is probable that the second parameter is small; consequently the best guess we can make at the moment regarding helium burning in a massive star is that it will predominantly form O^{16} but is likely to leave fairly small amounts of C^{12}. In this case also, we do not change the general conclusion much by considering a shell source.

Figure 14.11 shows the second parameter $\frac{q_4}{q_1 n_{10}}$ as a function of temperature for various rates of energy generation.

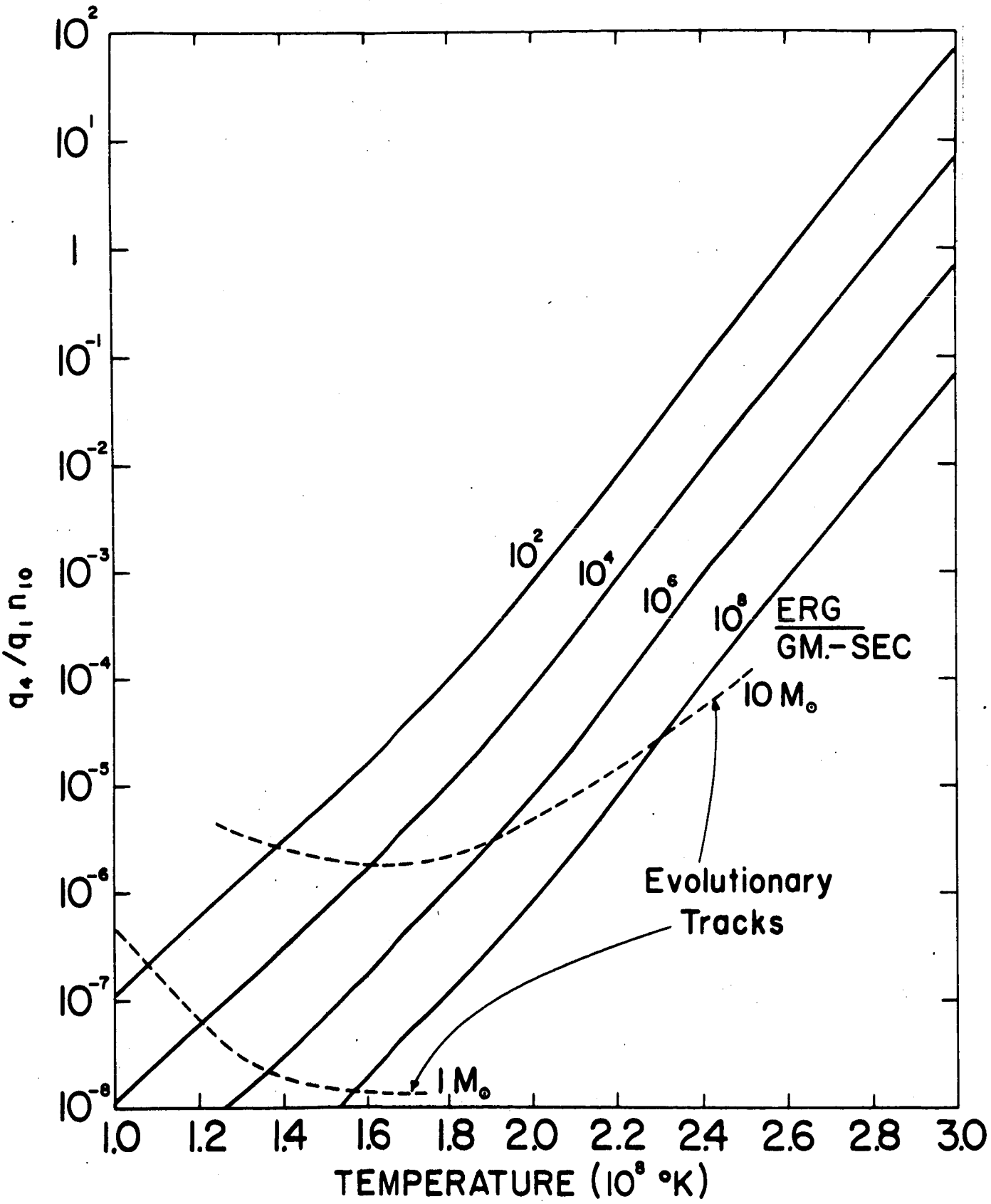
10^2
10^1
1
10^{-1}
10^{-2}
10^{-3}
10^{-4}
10^{-5}
10^{-6}
10^{-7}
10^{-8}
$q_4/q_1 n_{10}$
10^2
10^4
10^6
10^8 ERG / GM.-SEC
$10 M_\odot$
Evolutionary Tracks
$1 M_\odot$
1.0
1.2
1.4
1.6
1.8
2.0
2.2
2.4
2.6
2.8
3.0
TEMPERATURE (10^8 °K)

Figure 14.11

Considering the dotted evolutionary track for stars of one solar mass, we see that for a temperature of 1.2×10^8 °K and a moderate energy generation rate the value of $\frac{q_4}{q_1 n_{10}}$ is close to 10^{-7}. This is truly negligible and indicates that no significant amount of Ne^{20} would be formed under such conditions. If we consider the increase in temperature due to using a shell source, we find the value of $\frac{q_4}{q_1 n_{10}}$ only 10^{-6} or 10^{-5}, and still negligible.

In the case of ten solar masses, the situation is not essentially changed. For a temperature T_8 around 2.0 to 2.2 and an energy generation of 10^6 to 10^8 ergs/gm.sec., then the value of $\frac{q_4}{q_1 n_{10}}$ lies near 10^{-5}. If we now consider a helium burning shell source, the temperature would increase as would the energy generation, and an extrapolation gives values of $\frac{q_4}{q_1 n_{10}}$ of about 10^{-1} by going a bit beyond 3×10^8 °K. Such high temperatures may be obtained in the last stages of helium burning, hence it is possible that under extreme conditions in massive stars with helium burning shell sources, the value of $\frac{q_4}{q_1 n_{10}}$ may rise into the range of 10^{-1} to unity in the later stages, and appreciable amounts of Ne^{20} can be formed. Unless we consider such extreme conditions, it seems

that Ne^{20} formation is small during the helium burning process. This leads us to the general conclusion that, under the great majority of conditions likely to be involved in stellar interiors during the course of evolution of ordinary stars, the helium burning process is likely to form large amounts of O^{16} and negligible amounts of Ne^{20}. It may or may not leave significant amounts of C^{12}.

We must temper these conclusions by the observation that they are based upon an assumption regarding the reduced α-particle width of the 7.1 Mev state of O^{16}; consequently we should be prepared for changes of the order of a factor of 10 in the first parameter $\frac{q_3}{q_1 n_{10}}$ when the reduced width is eventually measured. Using the graphs presented it should be possible to see what changes this will produce in the conclusions we have reached. One remarkable thing that we have learned, however, is that the ratio of C^{12} to O^{16} should not be greatly changed as one goes from typical conditions for helium burning in the center of a star to typical conditions for helium burning in a shell source surrounding the center.

Pycnonuclear Reactions

The general theory of pycnonuclear reactions has

previously been discussed (p. 108-115). Detailed discussion of the calculation of these pycnonuclear reaction rates may be found in the author's paper on the subject (A.G.W. Cameron, Astrophysical Journal, 130, 916).

Figure 14.12 shows numerically calculated reaction rates for $C^{12}(\alpha,\gamma)O^{16}$ at 5×10^6 °K for a variety of densities as function of α-particle energy. The ordinary thermonuclear reaction rates without electron screening corrections of any kind refer to an effective zero matter density; under such circumstances the optimum bombarding energy at which the reaction takes place is many times kT. The arbitrarily normalized curves show $\langle\sigma v\rangle N(v)$ as a function of α-particle energy, where N(v) is the number of particles at that velocity. At zero density the curve peaks around 40 kT; the reaction rate is extremely small so far out in the tail of the Maxwellian distribution. The total rate goes as the integral of these curves; for increasing densities the change in the reaction rate due to the pycnonuclear effect is strongly exhibited. For particles under conditions of high electron screening, the effective bombarding energy is high. At a density of 10^7 it becomes a sizeable contribution all the way down to zero energy, and for higher densities

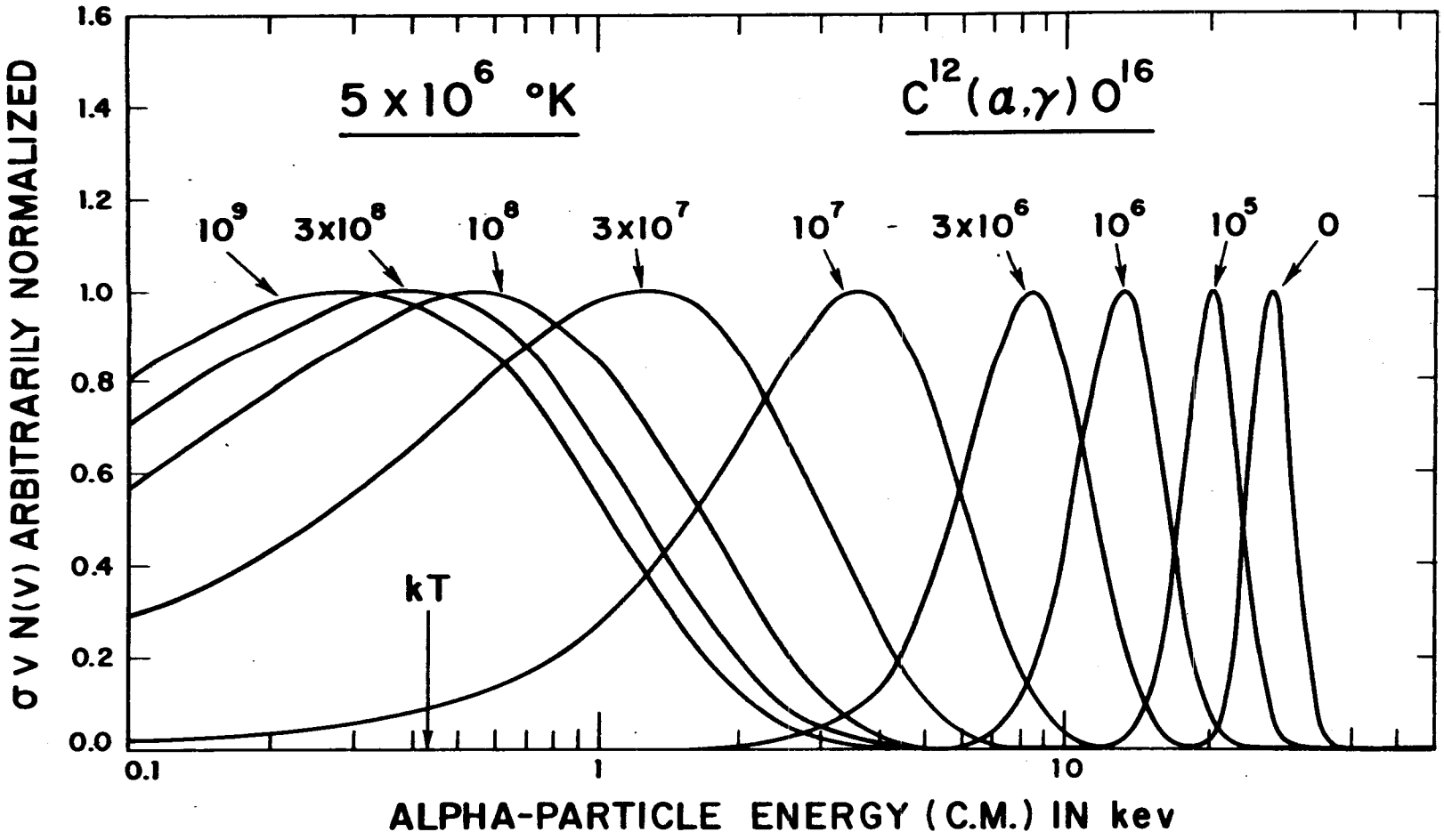
5 x 10^6 °K
C^12(α,γ)O^16
10^9
3x10^8
10^8
3x10^7
10^7
3x10^6
10^6
10^5
0
kT
σ V N(V) ARBITRARILY NORMALIZED
1.6
1.4
1.2
1.0
0.8
0.6
0.4
0.2
0.0
0.1
1
10
ALPHA-PARTICLE ENERGY (C.M.) IN kev

Figure 14.12

the curve starts to approach the Maxwell distribution of velocities. Since v N(v) is the Maxwell velocity distribution, we see that the probability of a reaction taking place is becoming almost independent of bombarding energies. This effect occurs under extreme conditions of high density and low temperature.

Figure 14.13 shows the logarithm of $\langle\sigma v\rangle$, i.e., the logarithm of the reaction rate, for different temperatures as a function of density. Remember that the number of reactions per cm^3 is just the reaction rate times the product of the number densities of the particles involved. The reaction rates increase, especially for lower temperatures, as the density increases.

Figure 14.14 shows the combination of temperature and density that we require in order to have a given rate of energy generation from this reaction. The fact that the curves turn downward at a density of 10^8 gm/cm^3 is due to the assumption that the mixture is half helium and half carbon. Suppose a star is in an advanced stage of evolution and is trying to shrink to a white dwarf state without raising its central temperature too high. For such a range of temperatures, a star could not shrink to much more than

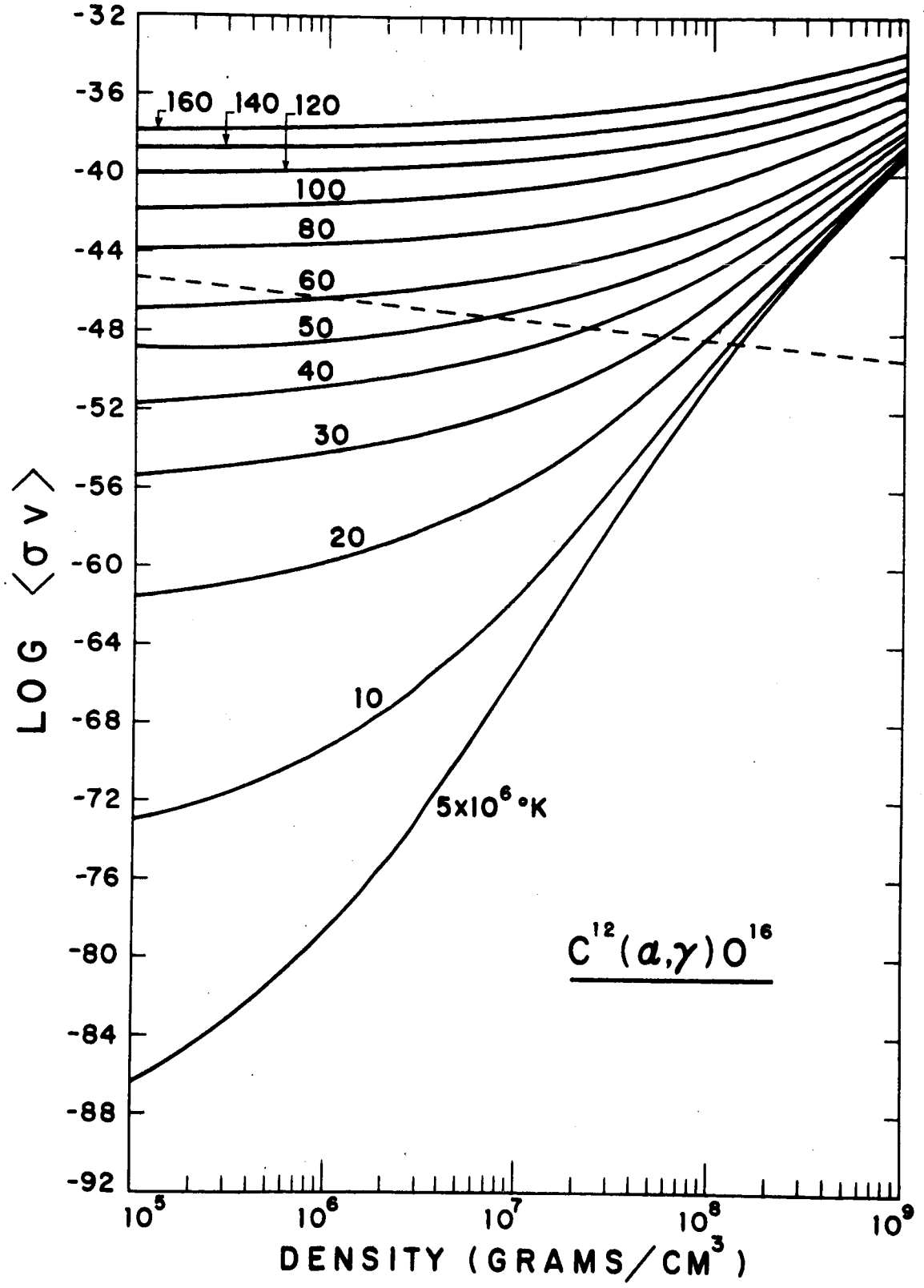
-32
-36
-40
-44
-48
-52
-56
-60
-64
-68
-72
-76
-80
-84
-88
-92
LOG ⟨σv⟩
160
140
120
100
80
60
50
40
30
20
10
5x10^6 °K
C^12(α,γ)O^16
10^5
10^6
10^7
10^8
10^9
DENSITY (GRAMS/CM^3)

Figure 14.13

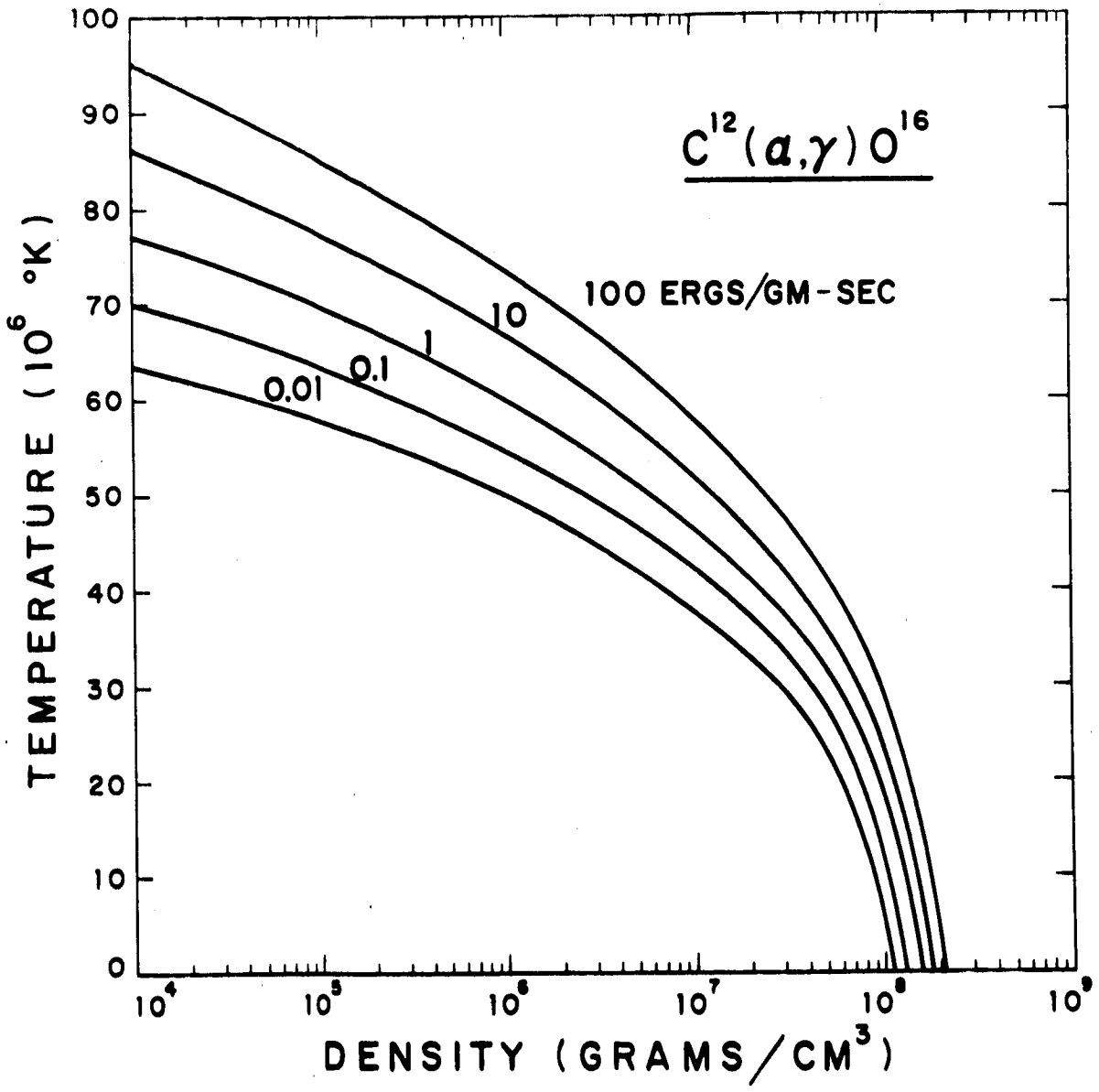
$C^{12}(\alpha,\gamma)O^{16}$
100 ERGS/GM-SEC
10
1
0.1
0.01
TEMPERATURE (10^6 °K)
DENSITY (GRAMS/CM^3)
100
90
80
70
60
50
40
30
20
10
0
10^4
10^5
10^6
10^7
10^8
10^9

Figure 14.14

10^7 gm/cm^3 without trying to burn helium and carbon together, and a central density of 10^7 gm/cm^3 is not atypical of white dwarf stars. Consequently it must always be considered as a possibility that there will be some small amount of energy generation occurring in the interiors of white dwarf stars. The rate of energy generation in such white dwarf stars might not be sufficient to cause disruption but nevertheless it might maintain luminosity in such stars for periods of time longer than the time in which one expects them to cool.

We consider next the $N^{14}(\alpha,\gamma)F^{18}$ $(\beta^+ \nu)O^{18}$ reaction. We do not know the reaction rate for this reaction. There is a level at 4.651 Mev which is 230 kev above the sum of masses; this would be resonant with the proper combination of spin and parity. N^{14} has a spin of 1^+ and the α-particle has a spin of 0^+; consequently by varying the relative orbital angular momentum of the N^{14} and the α-particle, we can form any combination of spin and parity except 0+. Even in the case this level is 0+, there are levels in the F^{18} nucleus which are about 100 kev apart in this region, so that there would be a resonance slightly higher. We shall assume that the 4.6 Mev level is 2+ (not taking the

most favorable case), which gives a thermonuclear reaction rate

$$p = 1.7 \times 10^{-5} \frac{\rho x_\alpha}{T_8^{3/2}} \exp\left(-\frac{26.7}{T_8}\right) \sec^{-1},$$

taking the reduced width

$$\gamma^2 \sim 1\% \text{ of maximum.}$$

Figure 14.15 shows this reaction rate for different temperatures as a function of density. The initial concentration was assumed to be half nitrogen and half helium for calculation, but this is not an especially sensitive restriction. There are quite significant rates of energy generation at 70 or 80 million degrees. This indicates that this reaction may trigger the helium burning reactions in the dense central core of a star of about one solar mass (Schwarzschild helium flash process), rather than the triple α reaction. The dashed line indicates an energy release of 1 erge/gm.sec. in a gas with equal parts of N^{14} and He^4.

Figure 14.16 is the ignition diagram for the $N^{14}(\alpha,\gamma)F^{18}(\beta^+ \nu)O^{18}$ reaction. The temperature is plotted for various energy-generation rates and shown as a function of density. The obvious kink corresponds to the switch from resonant to nonresonant reactions.

Figure 14.17 and 14.18 are corresponding graphs for the

triple-alpha reaction. Note that in this case we have the product of two reaction rates; we consider three cases: the triple α reaction is fully resonant, partially resonant, or completely non-resonant. By fully resonant, we mean the process we have previously discussed; by partially resonant we consider Be^8 in its ground state interacting with an α-particle in the non-resonant tail of the 7.656 Mev level of C^{12}. The dashed line indicates an energy release of 1 erg/gm.sec. in pure helium.

We call the reaction nonresonant if we have Be^8 formed in the tail of the ground state at low bombarding energies, reacting with α-particles in the tail of the 7.656 Mev level of C^{12}. The kinks in Figure 14.18 correspond to transitions between these reaction modes.

The net result of these considerations is that we cannot expect helium gas to endure for long at densities much above 10^8 gm/cm^3, and that N^{14} can probably act as a trigger for the helium flash process.

Minor Reactions

Now we shall consider some of the minor reactions (by minor we mean those which are not on the main line of the helium burning processes). In practically all cases the reactions are multiply-resonant, but we have not sufficient

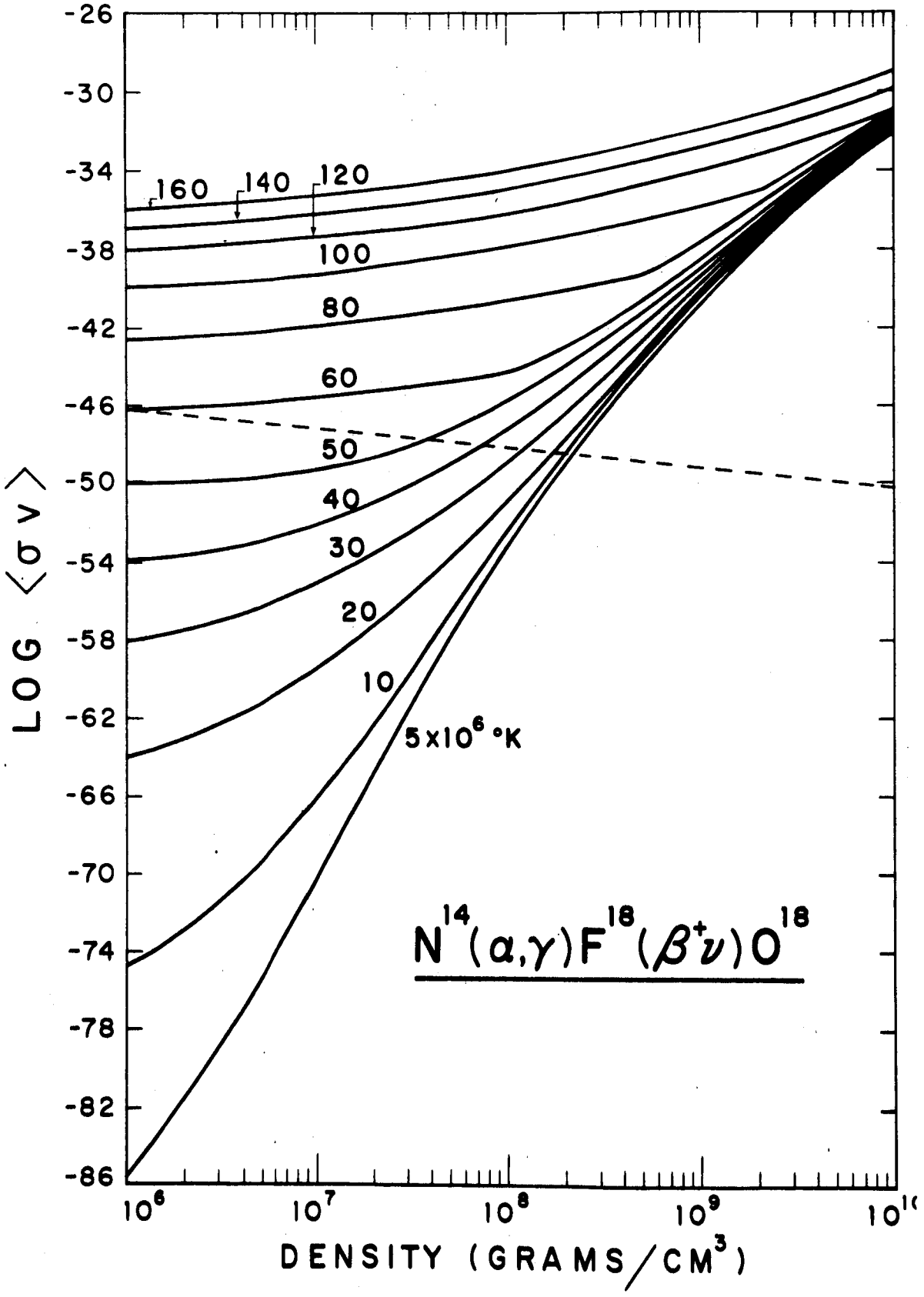
-26
-30
-34
-38
-42
-46
-50
-54
-58
-62
-66
-70
-74
-78
-82
-86
LOG ⟨σv⟩
160
140
120
100
80
60
50
40
30
20
10
5x10^6 °K
N^14(α,γ)F^18(β+ν)O^18
10^6
10^7
10^8
10^9
10^10
DENSITY (GRAMS/CM^3)

Figure 14.15

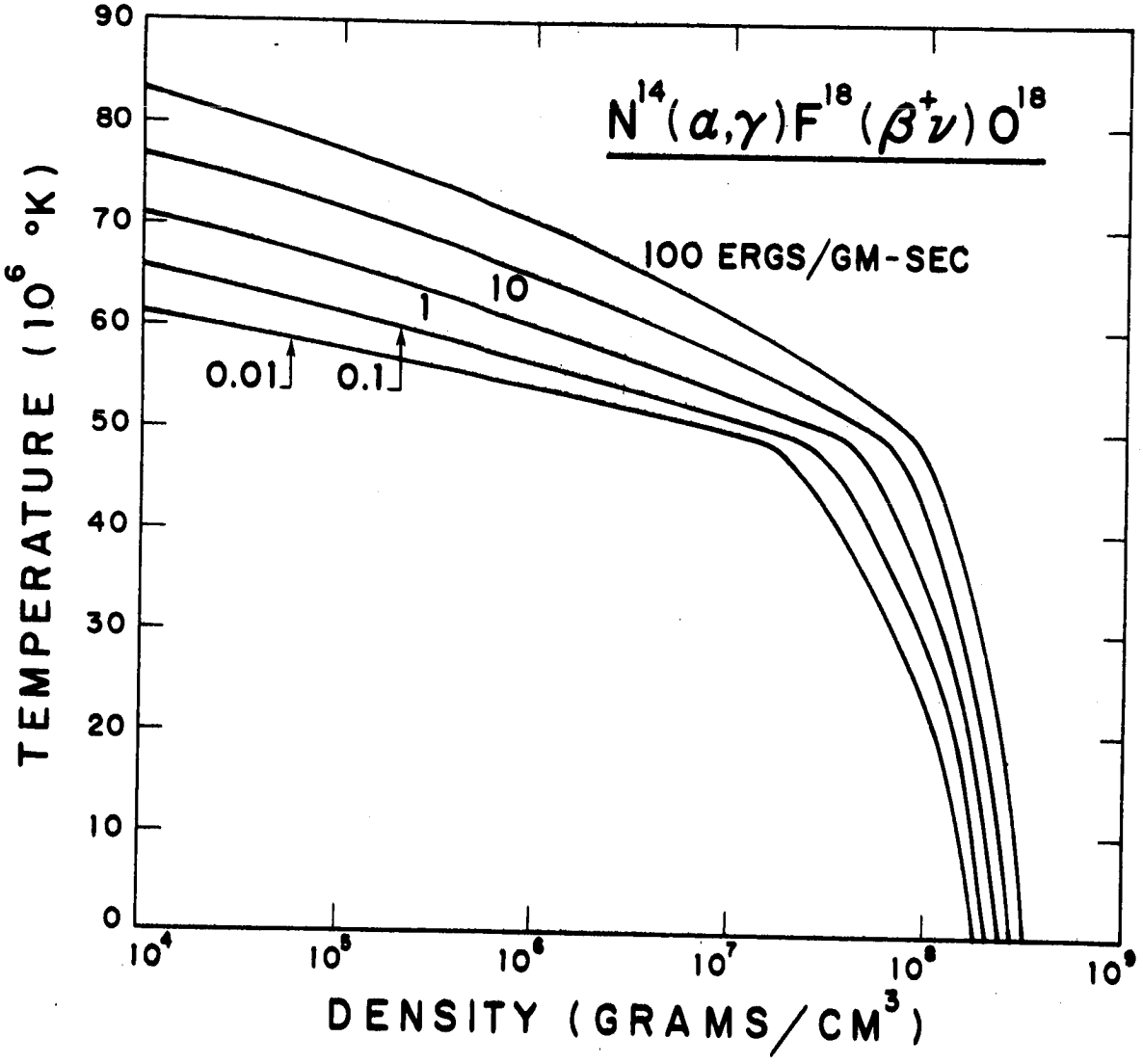
$N^{14}(\alpha,\gamma)F^{18}(\beta^{+}\nu)O^{18}$
100 ERGS/GM-SEC
10
1
0.1
0.01
TEMPERATURE (10^6 °K)
DENSITY (GRAMS/CM^3)
90
80
70
60
50
40
30
20
10
0
10^4
10^5
10^6
10^7
10^8
10^9

Figure 14 16

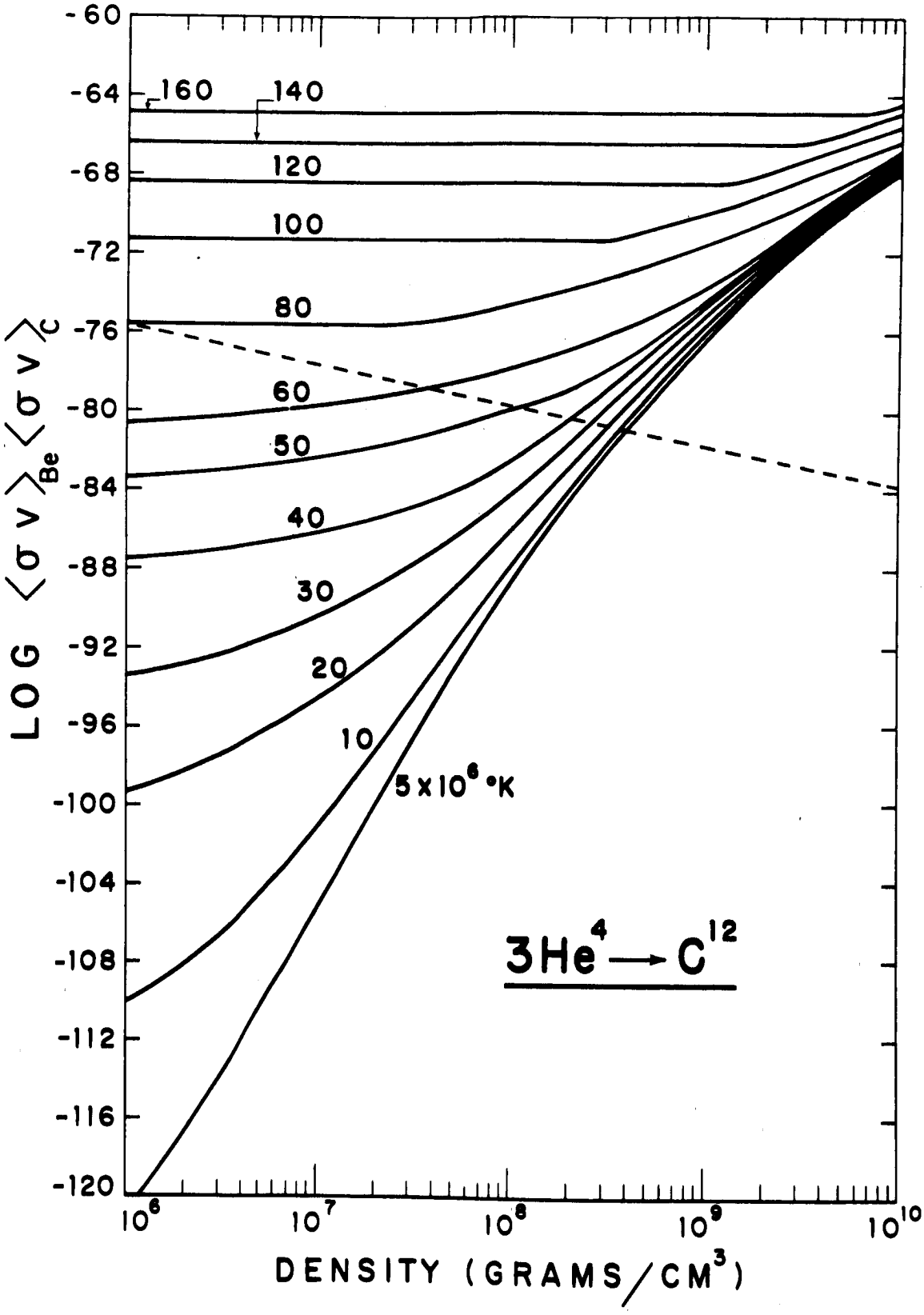
-60
-64
-68
-72
-76
-80
-84
-88
-92
-96
-100
-104
-108
-112
-116
-120
160
140
120
100
80
60
50
40
30
20
10
5 x 10^6 °K
3He^4 → C^12
LOG ⟨σ v⟩Be ⟨σ v⟩C
10^6
10^7
10^8
10^9
10^10
DENSITY (GRAMS/CM^3)

Figure 14.17

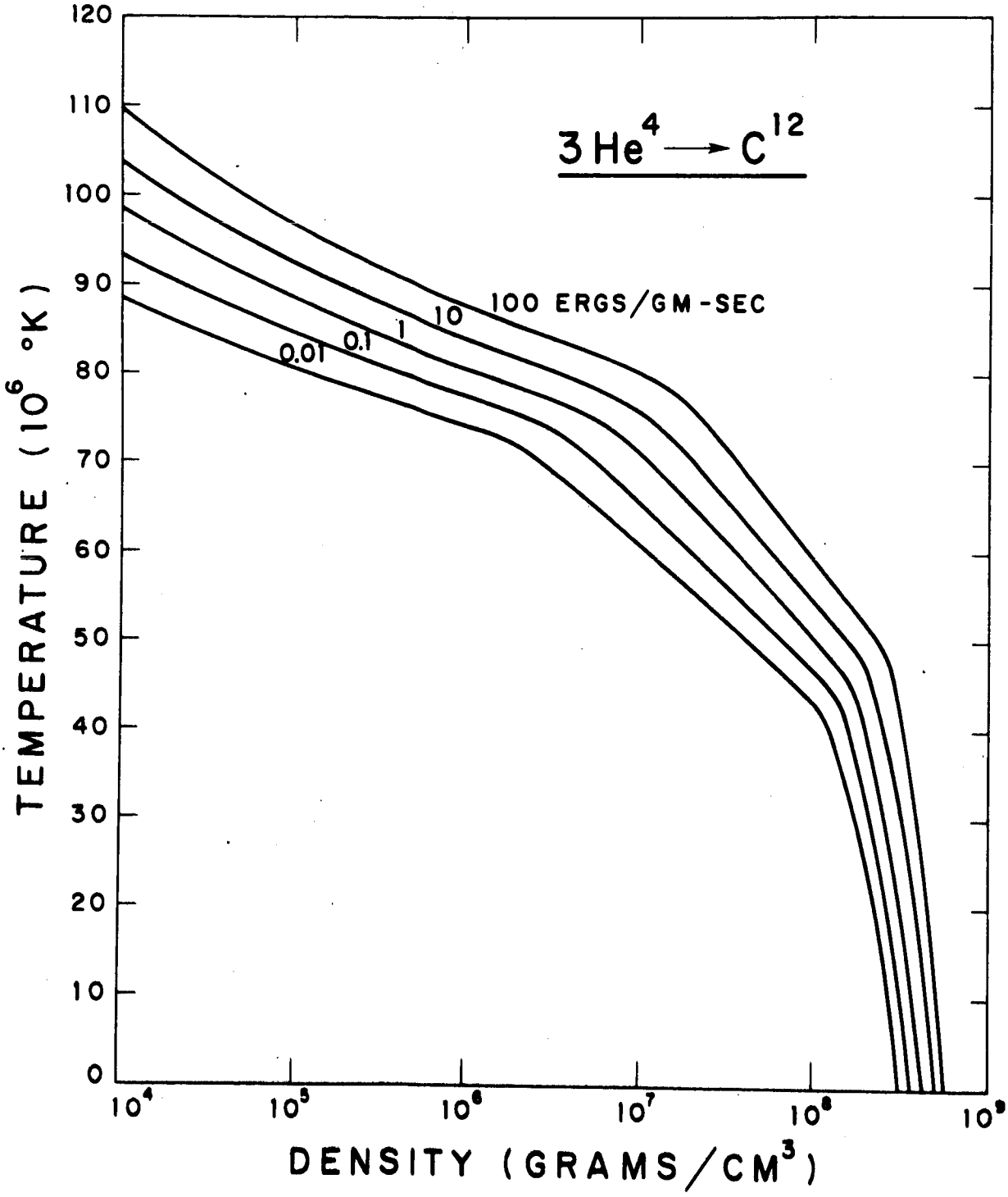
$3He^4 \rightarrow C^{12}$
100 ERGS/GM-SEC
10
1
0.1
0.01
TEMPERATURE (10^6 °K)
DENSITY (GRAMS/CM^3)
120
110
100
90
80
70
60
50
40
30
20
10
0
10^4
10^5
10^6
10^7
10^8
10^9

Figure 14.18

knowledge of the nuclear physics of the relevant nuclei to evaluate in detail these resonant contributions. Nonetheless, the systematics of level densities indicate that there should be several levels in a typical Gamow thermonuclear peak.

Capture of an α-particle by N^{14} led to the production of O^{18}. Then the reaction $O^{18}(\alpha,\gamma)Ne^{22}$ may occur. Indeed this reaction should occur near the middle of helium burning; its reaction rate is probably somewhat faster than $C^{12}(\alpha,\gamma)O^{16}$. One expects it to be multiply-resonant, but our ignorance of the levels does not allow us to evaluate this reaction rate properly. However, the fact that this reaction should take place in the middle of the helium burning process has immense significance for some of the later reactions, as we shall see.

A set of reactions most significant in terms of element formation are the neutron sources:

$C^{13}(\alpha,n)O^{16}$	Q = 2.215 Mev
$O^{17}(\alpha,n)Ne^{20}$	Q = 0.588 Mev
$Ne^{21}(\alpha,n)Mg^{24}$	Q = 2.555 Mev
$\{ Ne^{22}(\alpha,\gamma)Mg^{26}$	Q = 10.616 Mev
$\{ Ne^{22}(\alpha,n)Mg^{25}$	Q = -0.482 Mev

The $C^{13}(\alpha,n)O^{16}$ reaction is nonresonant but fast. However,

at the end of the CNO cycles we expect to have little of the original CNO nuclei left in the form of C^{13}; hence this process should produce a very small yield of neutrons early in the helium burning process. Similarly, the abundance of O^{17} is probably very small at the end of the CNO cycles. Again, the reaction should be reasonably fast, but the neutron yield would be very small. The $Ne^{21}(\alpha,n)Mg^{24}$ reaction is not so fast; it should be multiply-resonant and will take place primarily during the later parts of the helium burning process, particularly if the temperature is as high as 200 million degrees. We have seen that for stars of the order of one solar mass helium burning does not take place above 1.5 or 1.6 x 10^8 degrees. In the more massive stars the helium burning temperature is well beyond 200 million degrees. Insofar as these reactions are concerned, helium burning should proceed with these minor constituents, in the more massive stars, while in the lighter stars, the chance of neon isotopes taking part in helium burning is very considerably reduced. We need a temperature $T_8 \sim 2$ to have α-particles react significantly with Ne^{22}; at that temperature the optimum bombarding energy is in the vicinity of 450 Kev. Three resonances below this and three above are known, but the properties of these levels are unknown.

The significance of these reactions in terms of neutron production is as follows: C^{13} and O^{17} will have low abundances, and Ne^{21} will have a questionable abundance. Significant amounts of Ne^{20} are probably present in the cosmic mixture of elements from which the star is formed. For temperatures the order of 50 million degrees, in hydrogen burning shells, most of the Ne^{20} is depleted into Ne^{21}. It is likely that Ne^{21} may advance further by capturing a proton to make Ne^{22} or even Na^{23}; this being the case, Ne^{21} may or may not be a significant source of neutrons.

However, we do know that the CNO nuclei, the third most abundant group of nuclei present in the natural distribution of the elements, are left primarily in the form of N^{14} at the end of CNO cycles. Alpha capture occurs early, making F^{18} and then O^{18}, and near the middle of helium burning O^{18} should advance up to Ne^{22}. This means that most of the initial CNO nuclei are in the form of Ne^{22} in the later stages of helium burning; this in turn means that the $Ne^{22}(\alpha,n)Mg^{25}$ reaction is probably the principal source of neutrons produced on a slow time scale (the time scale characteristic of thermonuclear reaction times in stellar

interiors under these conditions). We do not know what fraction of the CNO group will actually give up neutrons by these processes, but it would not be surprising to find half or more of the CNO group yielding neutrons.

For completeness we write the remaining reactions:

$N^{15}(\alpha,\gamma)F^{19}$	Q = 4.012 Mev
$F^{19}(\alpha,p)Ne^{22}$	Q = 1.675 Mev
$Na^{23}(\alpha,p)Mg^{26}$	Q = 1.826 Mev

These do not seem to be especially interesting from an astrophysical point of view.

15. Neutron Capture on a Slow Time Scale

We have seen that, as a result of helium burning, neutrons can be produced in stellar interiors at temperatures of the order of 1 to 2 x 10^8°K. In particular the $C^{13}(\alpha,n)O^{16}$ reaction produces neutrons at temperatures near 1 x 10^8°K, and the $Ne^{22}(\alpha,n)Mg^{25}$ reaction near 2 x 10^8°K. We may now inquire as to the period of time in which the neutrons are produced. In a star of roughly one solar mass the helium burning stage may involve something on the order of 10^8 to 10^9 years. The later stages in which most of the neutrons are produced may require 10^7 or 10^8 years or even much less for more massive stars. Under such conditions we observe that the time between successive neutron captures will be large in comparison to other time scales of interest in our study of stellar interiors. The mean time between neutron captures by a typically heavy nucleus can range anywhere from 1 to 10^5 years. Burbidge, Burbidge, Fowler and Hoyle* describe this process as the 's' process of neutron capture, where the 's' simply stands for slow. We will term this process simply neutron capture on a slow time scale.

It is possible to determine a rather unique neutron capture path, provided that we have a

---

* BBFH, Rev. of Mod. Physics, 29, 547 (1957).

knowledge both of the time scale of the capture processes, and of the beta decay half-lives of the nuclei in question. The upper end of the capture path is terminated at Bi^{209}, as neutron capture beyond this nucleus leads to alpha-particle emitters with half-lives very short compared with the neutron capture time scale; hence neutron capture products accumulate as lead and bismuth isotopes.

In order to observe the effects of these neutron captures on a slow time scale, we shall present here the results of a calculation by the author. These results were obtained for a kT energy of 11 kev ($\sim 1 \times 10^{8}$ °K). It should be noted here that the results presented are correct only if one assumes that extra neutron removal reactions such as $N^{14}(n,p)C^{14}$ do not take place. If Ne^{21} or Ne^{22} is the main neutron source this difficulty will probably not arise, because the N^{14} will be destroyed by helium reactions at a lower temperature than that at which the neutrons are produced. In this calculation we consider that all neutrons are captured by nuclei with mass numbers 20 or higher.

Solution of the Abundance Equations

The initial abundances of the nuclei that were assumed for these calculations are shown in Figure 15.1. The capture cross sections that were calculated are shown in Figure 15.2.

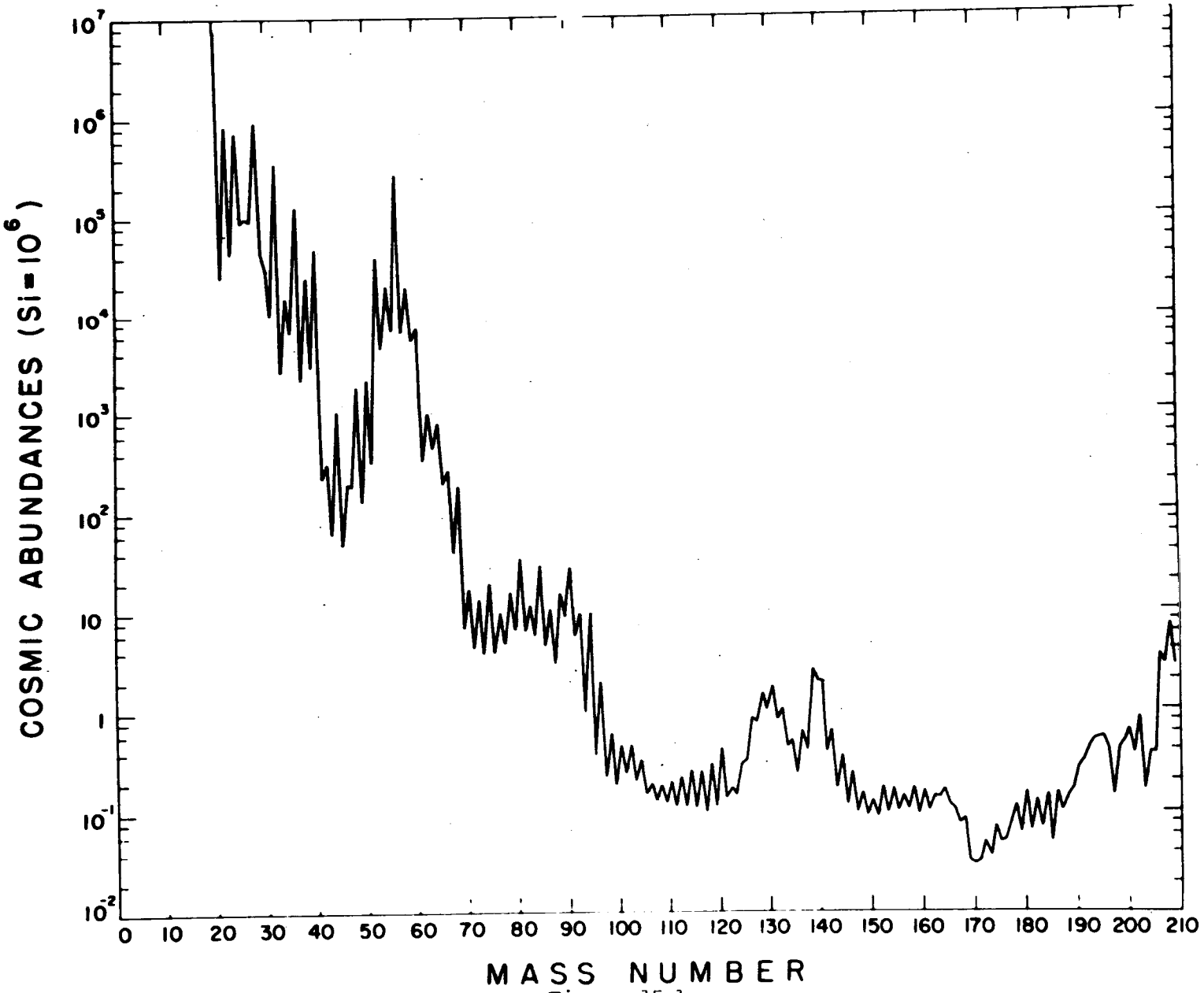

Figure 15.1

The cosmic abundances of Suess and Urey plotted as functions of mass number. This curve has been modified in the iron peak and lead regions to take partial account of the new solar abundance determinations of Goldberg, Muller, and Aller.

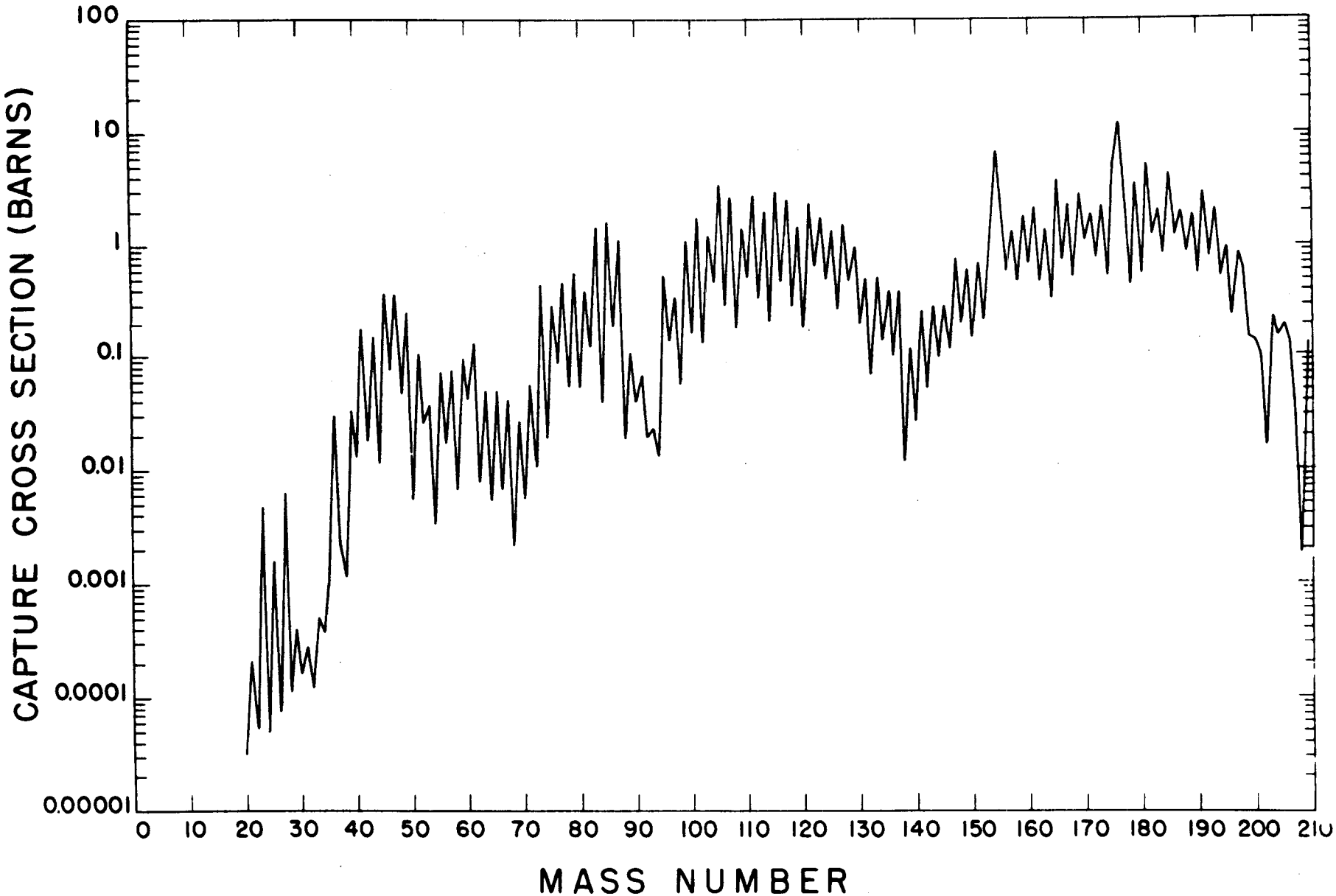
CAPTURE CROSS SECTION (BARNS)
100
10
1
0.1
0.01
0.001
0.0001
0.00001
0 10 20 30 40 50 60 70 80 90 100 110 120 130 140 150 160 170 180 190 200 210
MASS NUMBER

Figure 15.2

If the abundance of the nuclide with mass number A is N(A) and the number of neutrons injected into the abundance unit is N(n), then the rate of change of the abundances is:

$$\frac{dN(A)}{dN(n)} = \frac{N(A-1)\ \sigma(A-1) - N(A)\ \sigma(A)}{\Sigma N\sigma} \tag{15.1}$$

The abundance equations were integrated with the aid of an electronic computer. All nuclei were initially considered to lie on the capture path except certain ones with large abundances such as Fe^{54} and Ni^{58}, whose rate of feeding into the capture path was followed independently.

The abundances produced by the capture of 5, 10, 15, 20, 30, 50, 80, and 125 neutrons (injected per initial silicon atom) are shown in Figures 15.3 through 15.10.

The neutrons are initially captured mostly by the nuclei in the iron peak, centered about A = 56. As the capture progresses, a few nuclei capture many neutrons and are moved up to high mass numbers. This "tail" rapidly grows until the abundances of the heavy nuclei become much larger than the initial values. The ratios of the evolved to initial abundances of these nuclei will be called their overabundance factors.

After the injection of 5 neutrons per initial silicon atom the nuclei around A = 70 have become quite overabundant, but heavier nuclei have only small overabundance factors. By 10 neutrons the heavy nuclei have become overabundant by factors of the order of 100. The overabundance factors continue to grow as more neutrons are added until by 50 neutrons factors of many thousand are reached. For still more neutrons the overabundance factors decline. They reach a minimum for 125 neutrons. At this point the nuclei originally in the iron peak have been transformed into lead and bismuth and the overabundance factors are maintained by capture in lighter nuclei.

The reason that the neutron capture does not build up nuclei heavier than lead and bismuth is that above bismuth the capture path enters a region where the nuclei have extremely short half-lives for alpha-particle emission. Hence any nuclei which get that far immediately decay back to lead isotopes.

It should be noticed that at all times during the neutron capture the general level of abundances below A = 140 is between a factor of 2 and a factor of 10 higher than the general level above A = 140. This is a very significant point to which we shall refer when analysing the cosmic abundances of the nuclides.

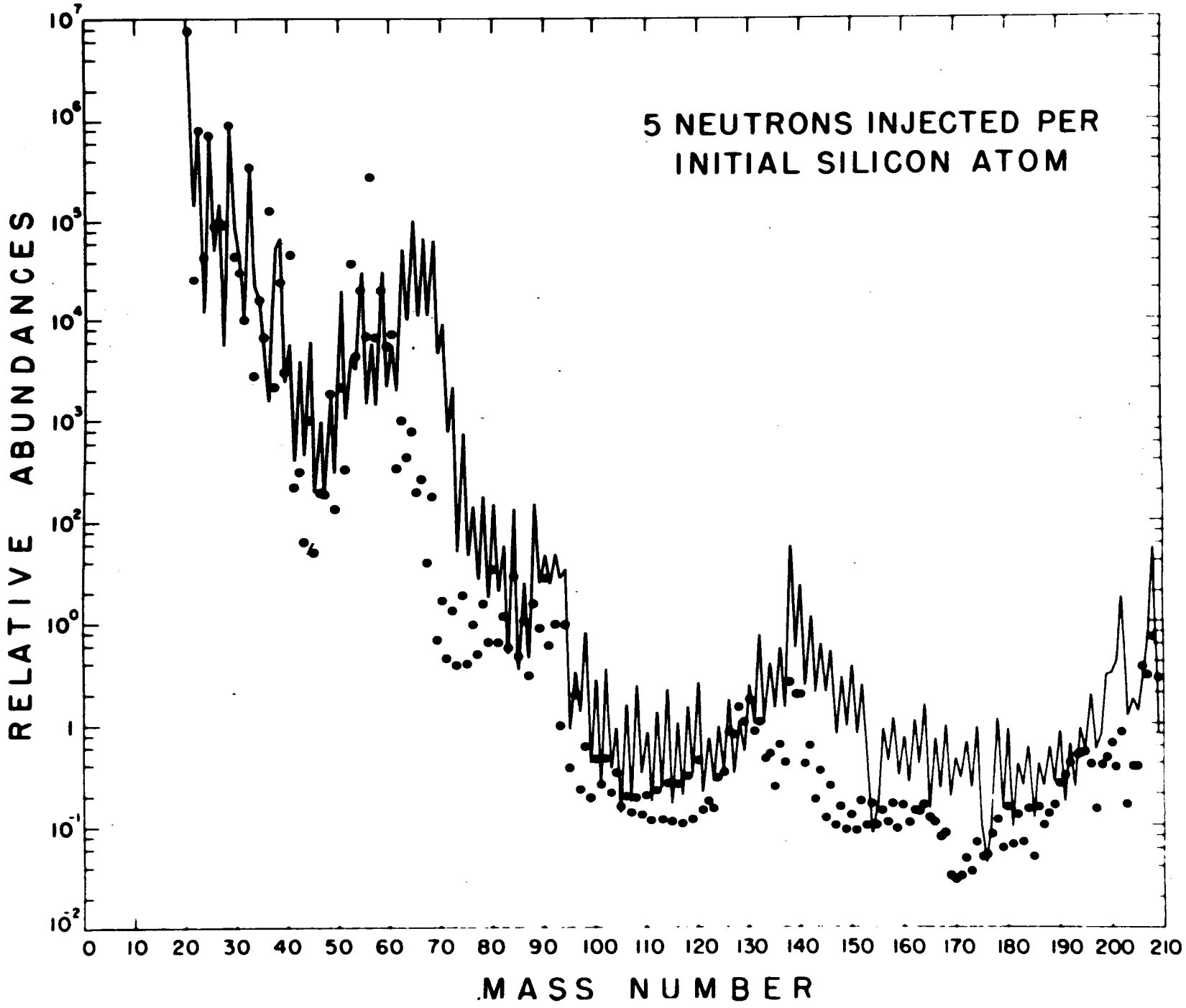
5 NEUTRONS INJECTED PER
INITIAL SILICON ATOM
RELATIVE ABUNDANCES
10^7
10^6
10^5
10^4
10^3
10^2
10^0
1
10^{-1}
10^{-2}
0 10 20 30 40 50 60 70 80 90 100 110 120 130 140 150 160 170 180 190 200 210
MASS NUMBER

Figure 15.3

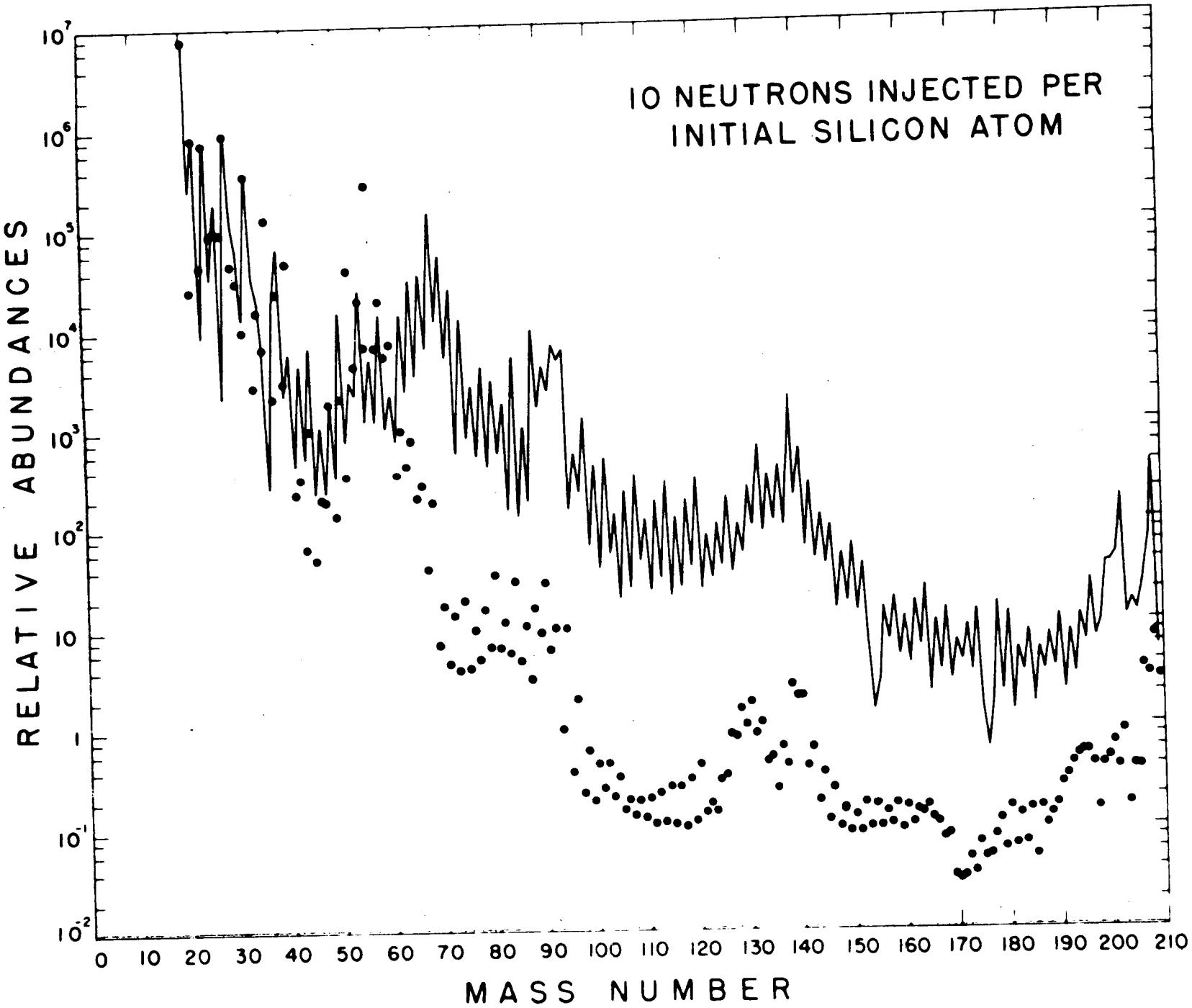
10 NEUTRONS INJECTED PER
INITIAL SILICON ATOM
RELATIVE ABUNDANCES
MASS NUMBER
10^7
10^6
10^5
10^4
10^3
10^2
10
1
10^{-1}
10^{-2}
0 10 20 30 40 50 60 70 80 90 100 110 120 130 140 150 160 170 180 190 200 210

Figure 15.4

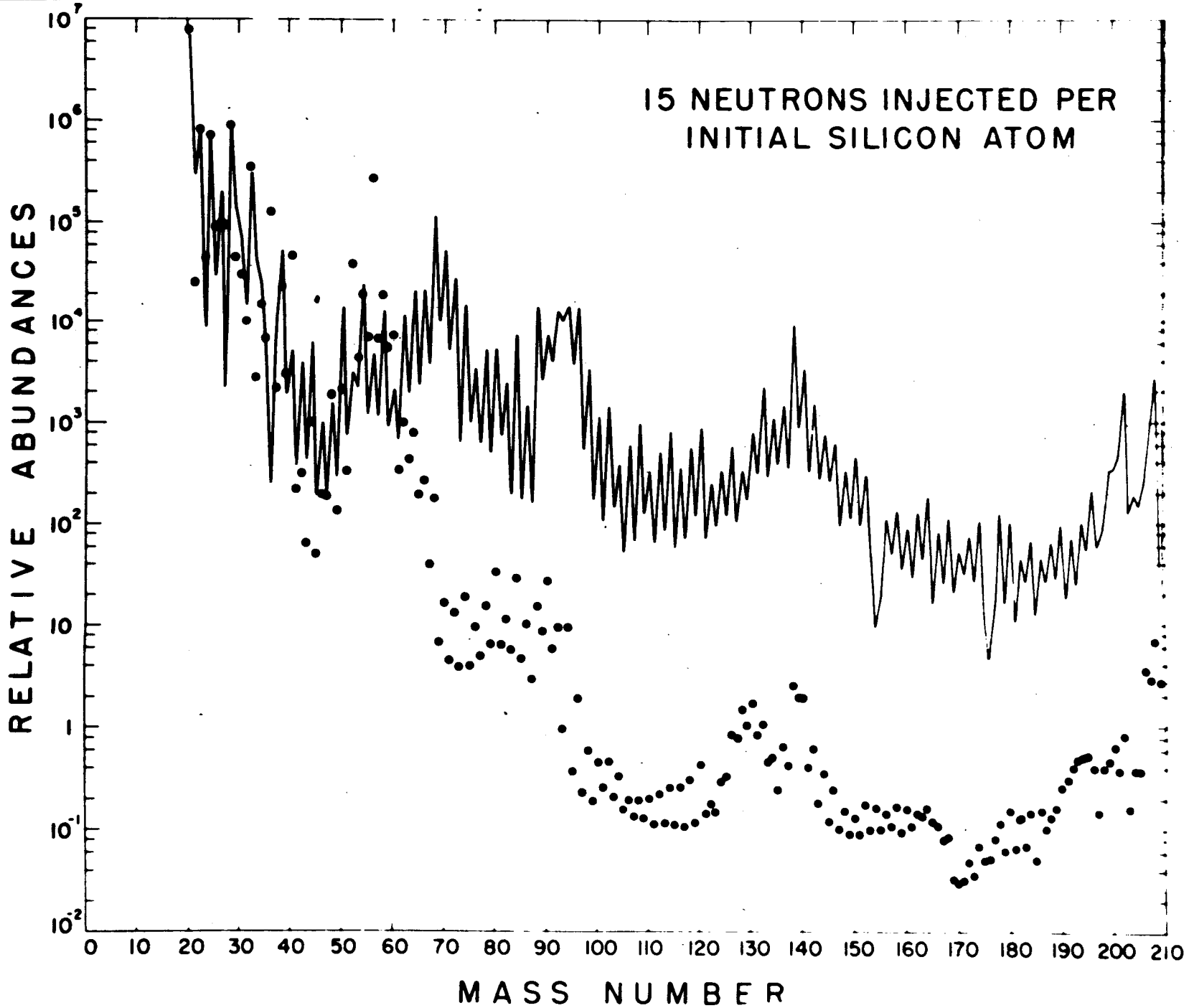
15 NEUTRONS INJECTED PER
INITIAL SILICON ATOM
RELATIVE ABUNDANCES
MASS NUMBER
10^7
10^6
10^5
10^4
10^3
10^2
10
1
10^{-1}
10^{-2}
0 10 20 30 40 50 60 70 80 90 100 110 120 130 140 150 160 170 180 190 200 210

Figure 15.5

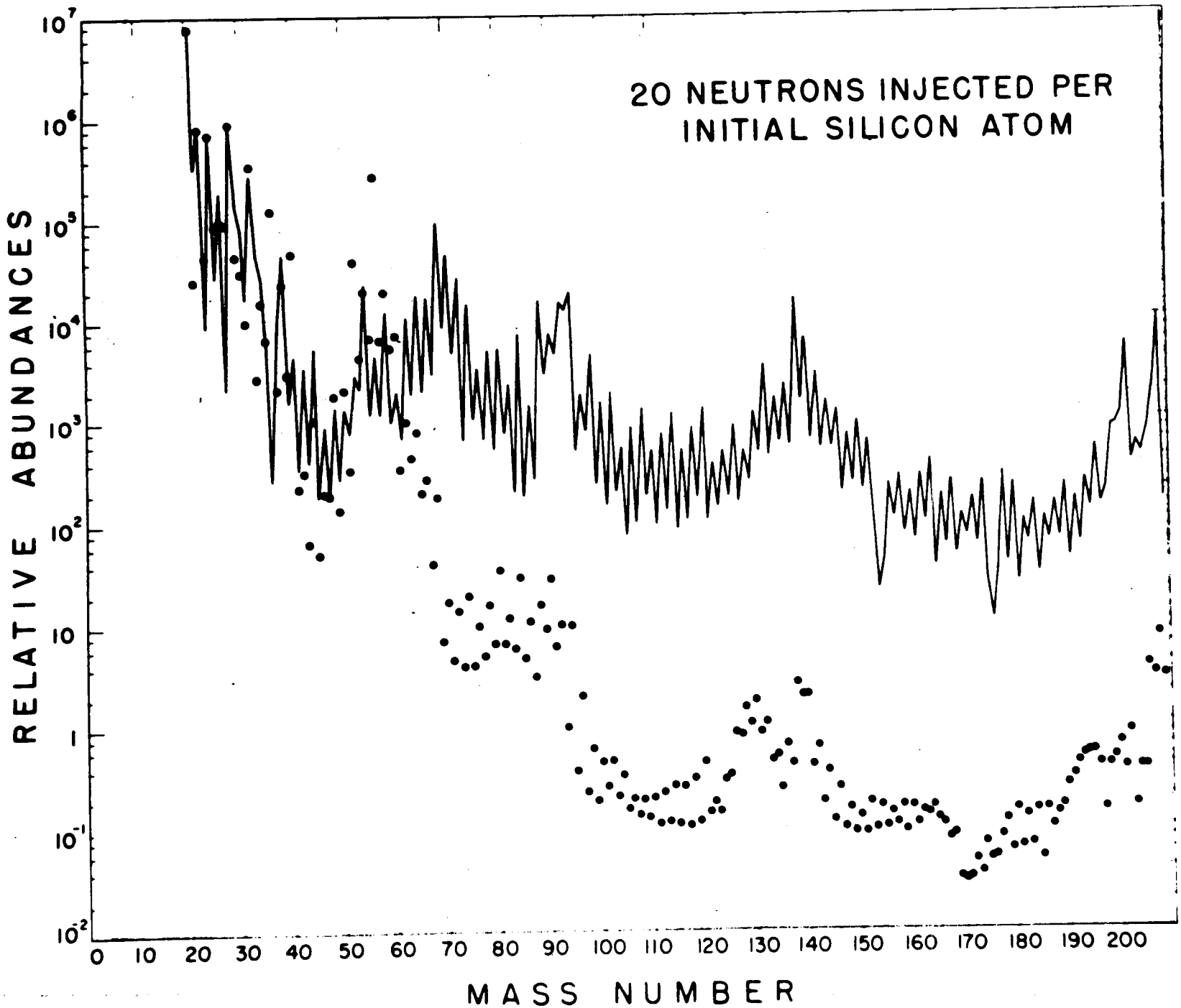
20 NEUTRONS INJECTED PER
INITIAL SILICON ATOM
RELATIVE ABUNDANCES
10^7
10^6
10^5
10^4
10^3
10^2
10
1
10^{-1}
10^{-2}
0 10 20 30 40 50 60 70 80 90 100 110 120 130 140 150 160 170 180 190 200
MASS NUMBER

Figure 15.6

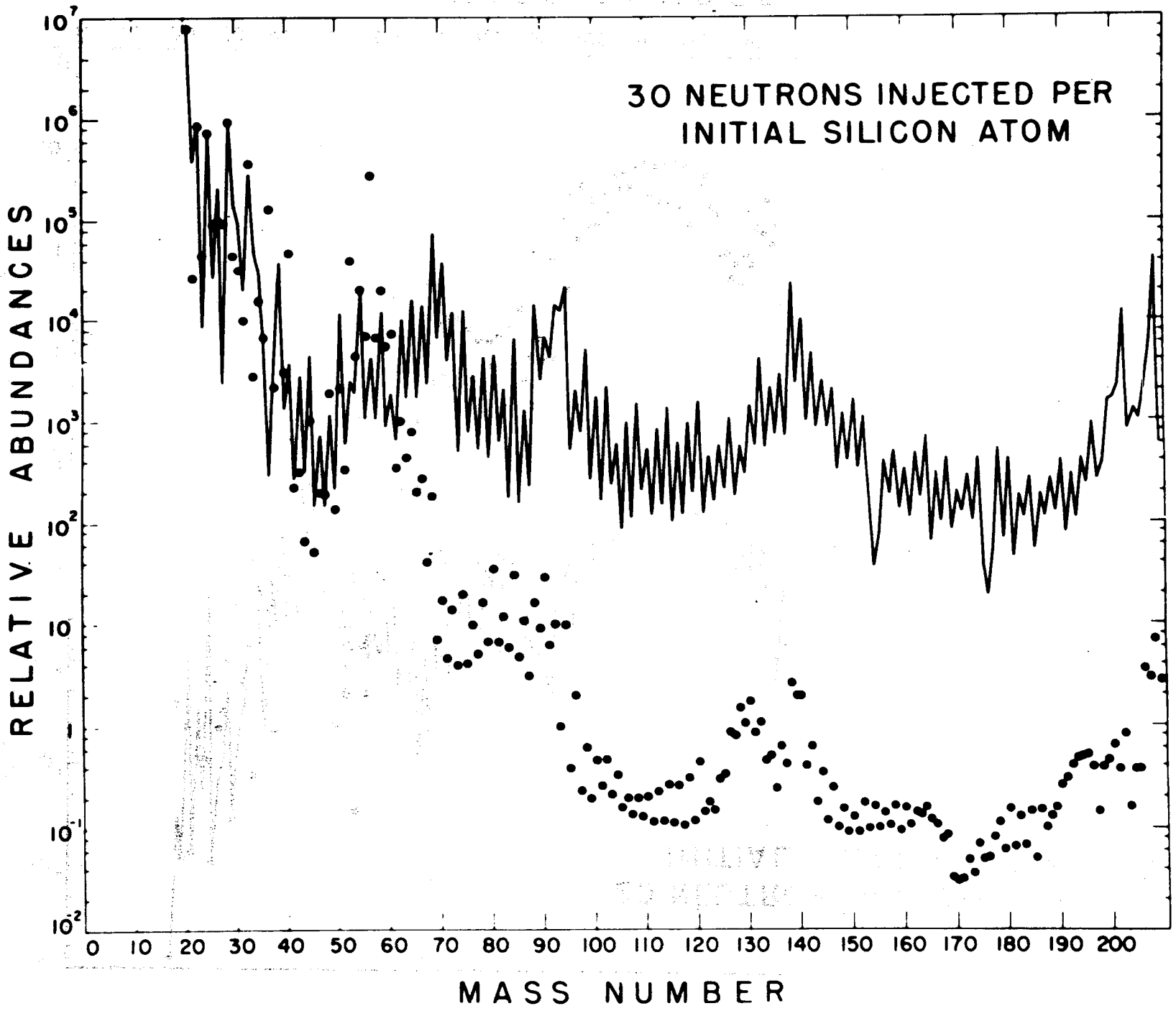
30 NEUTRONS INJECTED PER
INITIAL SILICON ATOM
RELATIVE ABUNDANCES
10^7
10^6
10^5
10^4
10^3
10^2
10
1
10^{-1}
10^{-2}
0 10 20 30 40 50 60 70 80 90 100 110 120 130 140 150 160 170 180 190 200
MASS NUMBER

Figure 15.7

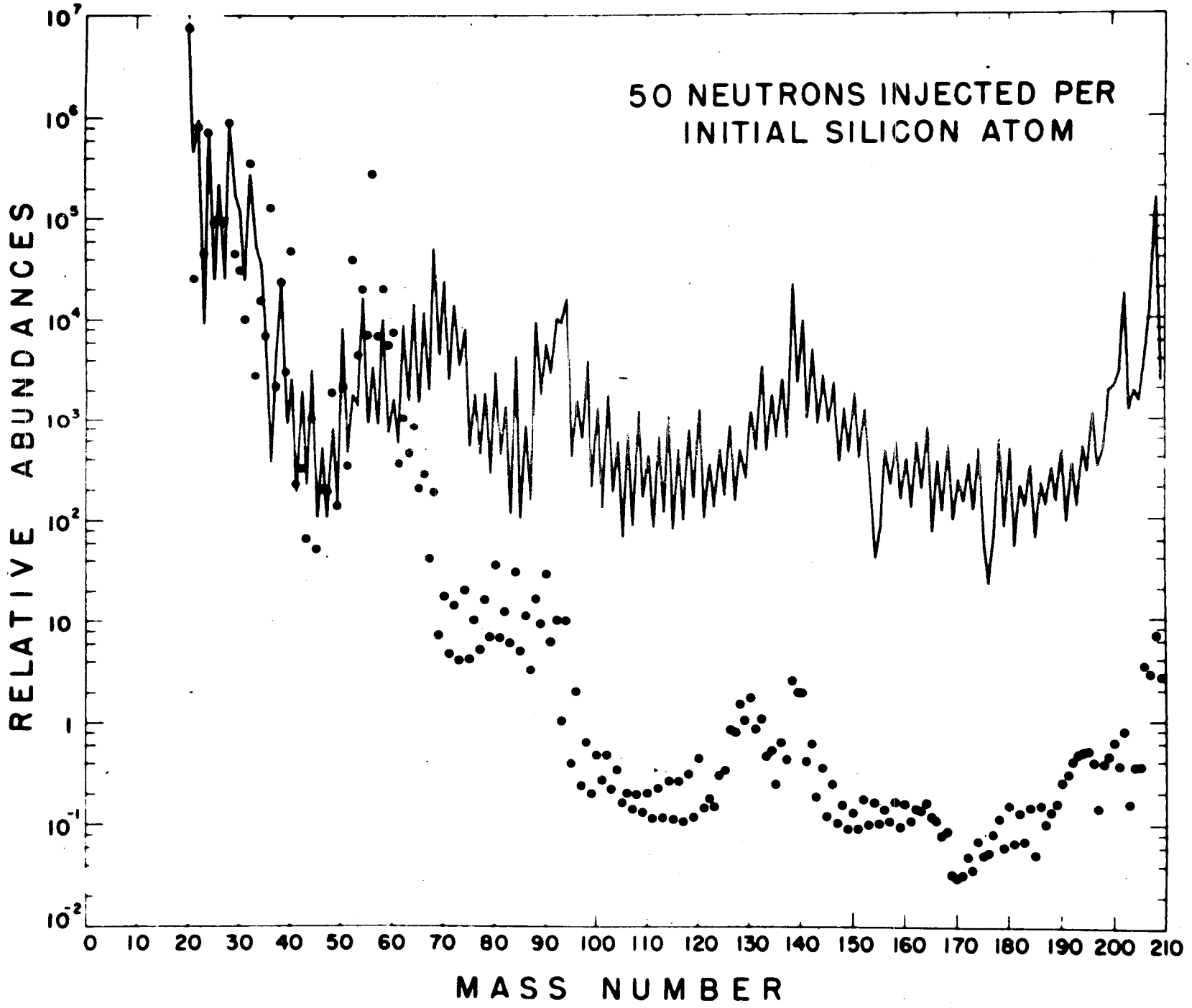
50 NEUTRONS INJECTED PER
INITIAL SILICON ATOM
RELATIVE ABUNDANCES
10^7
10^6
10^5
10^4
10^3
10^2
10
1
10^{-1}
10^{-2}
0 10 20 30 40 50 60 70 80 90 100 110 120 130 140 150 160 170 180 190 200 210
MASS NUMBER

Figure 15.8

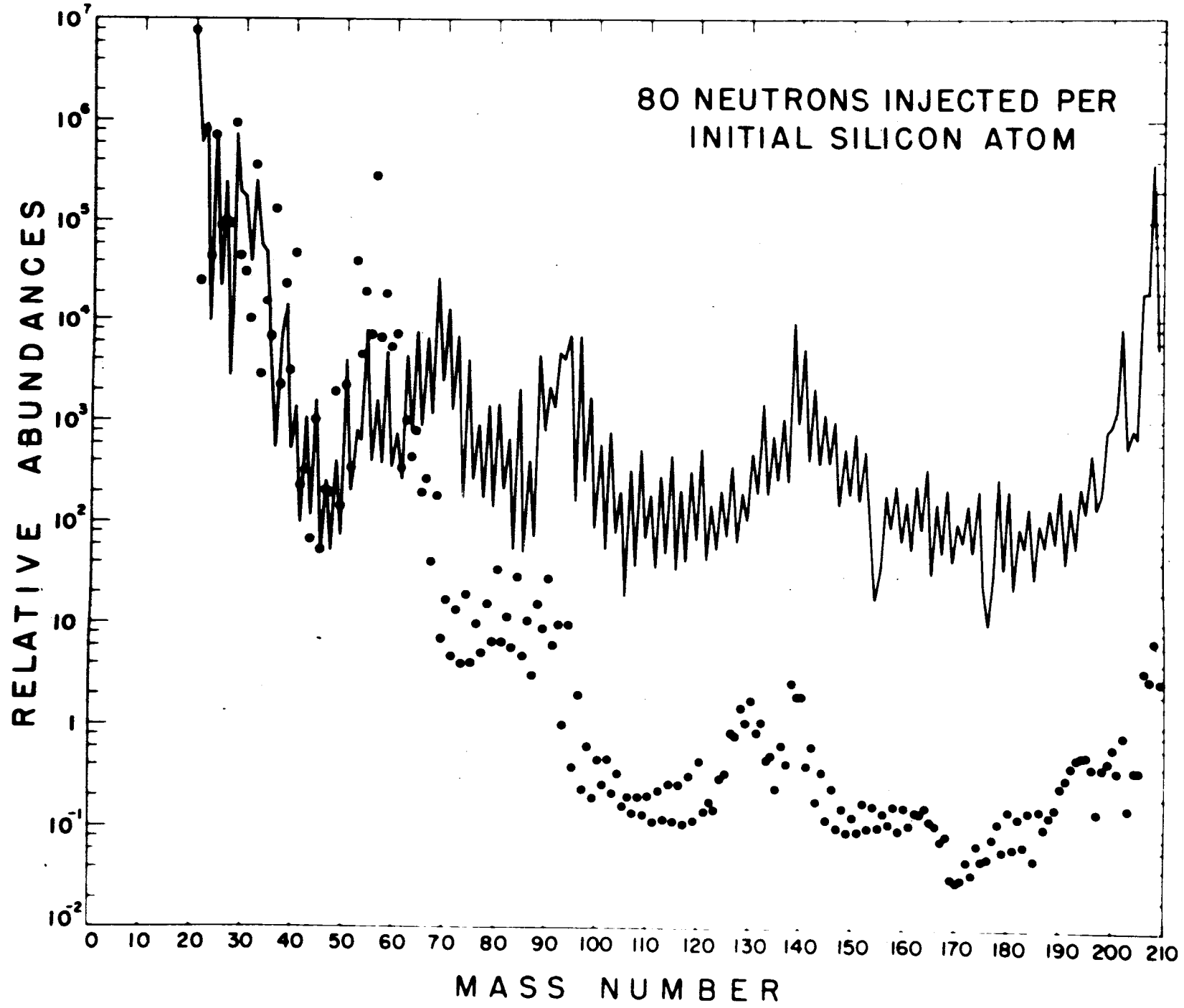
80 NEUTRONS INJECTED PER
INITIAL SILICON ATOM
RELATIVE ABUNDANCES
10^7
10^6
10^5
10^4
10^3
10^2
10
1
10^{-1}
10^{-2}
0 10 20 30 40 50 60 70 80 90 100 110 120 130 140 150 160 170 180 190 200 210
MASS NUMBER

Figure 15.9

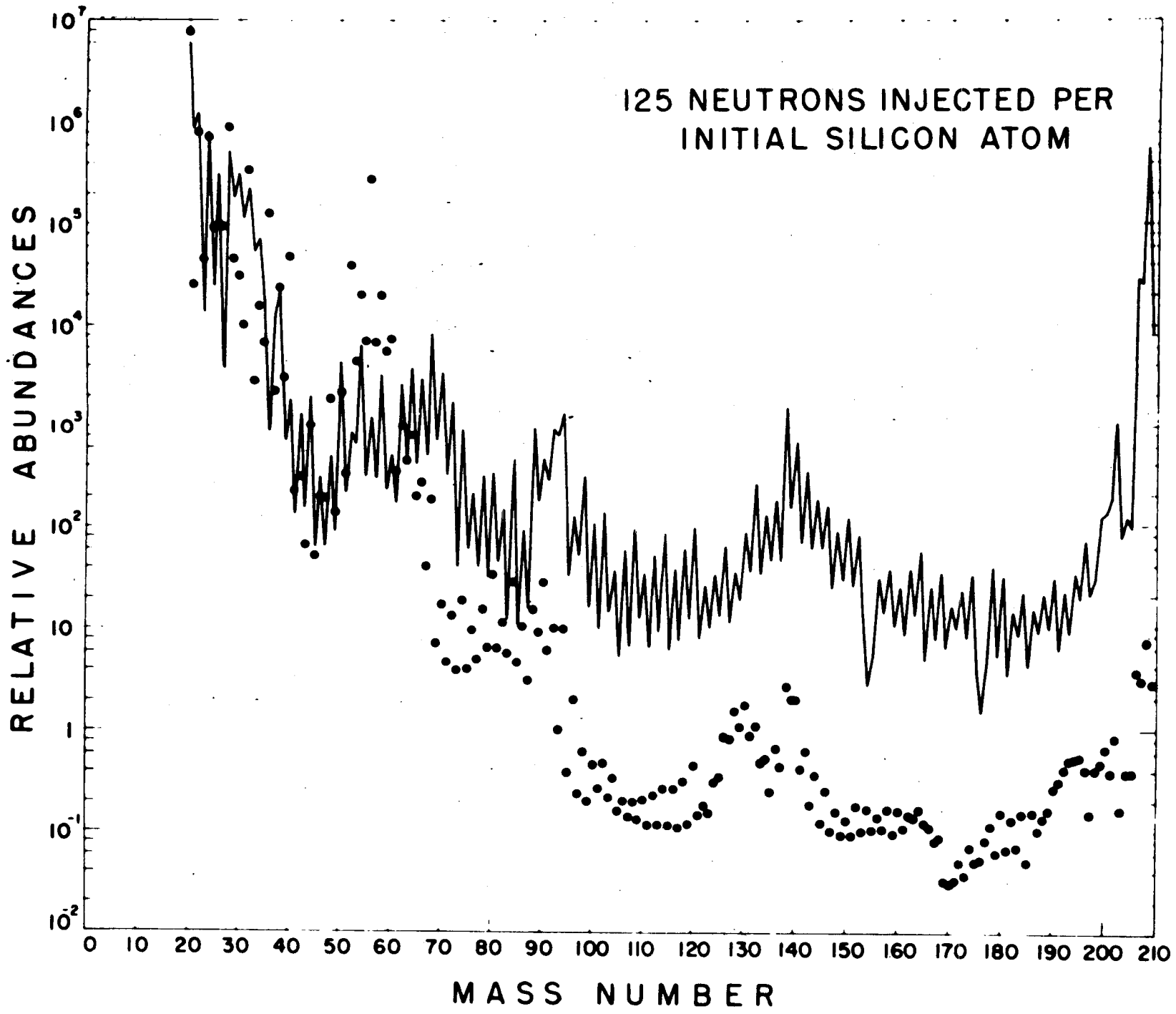
125 NEUTRONS INJECTED PER
INITIAL SILICON ATOM
RELATIVE ABUNDANCES
10^7
10^6
10^5
10^4
10^3
10^2
10
1
10^{-1}
10^{-2}
0 10 20 30 40 50 60 70 80 90 100 110 120 130 140 150 160 170 180 190 200 210
MASS NUMBER

Figure 15.10

16. A New Table of Abundances of the Elements in the Solar System

A.G.W. Cameron

Belfer Graduate School of Science
Yeshiva University
New York, New York

and

Institute for Space Studies
Goddard Space Flight Center, NASA
New York, New York

Abstract

A new table of the abundances of the elements, presumably characteristic of primitive solar matter, has been compiled. It is based as much as possible on abundances in Type I carbonaceous chondrites. Other sources, used where necessary, are ordinary chondrites, solar atmospheric abundances, and solar cosmic ray abundances. Eight elements were interpolated using criteria based on the theory of nucleosynthesis in stars. A discussion is given of some features of the abundance table which should be taken into account in theories of nucleosynthetic processes.

A basic and necessary step in the development of theories of stellar nucleosynthesis was made by Suess and Urey (1956), who selected astronomical, meteoritic, and terrestrial element abundance data and produced a table of cosmic abundances. Most of the abundance data used by Suess and Urey were of poor quality, so these authors adjusted and interpolated the abundances of the elements to produce a smooth variation in the abundances of nuclides with odd mass numbers. From the resulting abundance tables it was then possible to identify a number of different nuclear processes which could probably occur in stars and which would produce the characteristic features of the Suess-Urey table (Burbidge, Burbidge, Fowler, and Hoyle 1957; Cameron 1957).

The writer (Cameron 1959) later readjusted some parts of the Suess-Urey abundance table making use of the hindsight given by the identification of the processes responsible for nucleosynthesis to use additional criteria for the adjustment of the abundances. Apart from minor adjustments, the principal predictions were that the Sr/Zr ratio should be inverted, the rare earth abundances should be strongly modified, and the abundance of Pb should be greatly increased. Subsequent meteoritic abundance measurements have confirmed the first two of these points and have shown that the Pb abundance lies between the two values suggested.

In subsequent years a great deal of high quality meteoritic abundance data has been obtained by radiochemical techniques, and interest has arisen in the differences in abundances between various meteorite classes. The writer (Cameron 1963) made a new abundance compilation based to a much greater extent than previously on good meteorite abundance measurements. Although this table was not published,

many references to it appear in the literature, and hence the numbers obtained at that time have been included in Table I for the sake of the record.

Anders (1964) has pointed out that there are systematic differences between the abundances of certain elements of somewhat greater volatility between abundance classes; he postulated some mechanisms to account for this. These ideas have recently received additional discussion (Larimer and Anders 1967). These authors and others have pointed out that the least element depletions have occurred in Type I carbonaceous chondrites. Taking the point of view that it is probably easier to obtain uniform element depletion factors than uniform enrichment factors, the present writer has constructed a new abundance table based as much as possible on measurements in Type I carbonaceous chondrites. These meteorites are thus assumed to be the most representative source of solar system abundance data for which high quality measurements can be made.

The resulting list of abundances is given in Table I as Cameron (1967). The sources of the abundances and the assumptions made in assigning values to certain elements are given in the notes to Table I. It may be seen from these notes that the majority of the nonvolatile elements now have abundances based on Type I carbonaceous chondrite measurements. In some cases it has been necessary to use abundances measured in ordinary chondrites. The volatile elements are based on solar photospheric and cosmic ray abundance data; they have been normalized to the meteoritic data using the solar photospheric abundances of ten nonvolatile elements. There remains a significant uncertainty in this normalization factor, perhaps amounting to a few tens of per cent. Only eight elements have now been interpolated

on the basis of nuclear regularities.

It should be noted that this procedure has selected a high value of the iron abundance. This abundance has been a long-standing problem, since the solar photospheric abundance of iron (Aller 1961) is considerably lower than the meteoritic value, and the oscillator strengths of the iron lines used in the solar abundance determination are claimed to be of superior quality. These are strong iron lines. Nevertheless, it appears that the iron abundance determined from weak lines is higher than for the strong lines (L. Goldberg, private communication), and the iron abundance is anomalously high in the solar corona. Hence it has seemed best to use the meteoritic value. The question of the iron abundance is of great importance for problems of nucleosynthesis, and it is important that additional work be done in an attempt to resolve the problem.

The abundances of individual nuclides corresponding to the latest adjustment are given in Table II. Also given in this table is a classification of certain of the heavier isobars as being predominantly made by a particular mechanism of nucleosynthesis. Thus F isobars are those which have been made principally by neutron capture on a fast time scale, corresponding to the "r" process of Burbidge et al (1957). S isobars are those which have been made principally by neutron capture on a slow time scale, corresponding to the "s" process of Burbidge et al (1957). B isobars are those which are bypassed by neutron capture processes, corresponding to the "p" process of Burbidge et al (1957).

A few assumptions have been necessary for the construction of Table II in addition to those used in the construction of Table I. Thus the He^3/He^4 ratio has been taken to be 3×10^{-4} since this ratio is

usually found in primordial helium extracted from meteorites (Signer and Suess (1963). The large abundance of Ar^{40} in atmospheric argon is due to decay of terrestrial K^{40}; the estimate in Table II comes from the consideration that Ar^{40} is a product of neutron capture on a fast time scale and hence should be comparable in abundance to S^{36}, Ca^{46}, and Ca^{48}. The abundances of uranium, thorium, and K^{40} isotopes have been corrected for a decay interval of 4.5×10^9 years to make them typical of the initial solar system; other radioactive nuclides have not been corrected because the half-lives are long and the corrections small. The isotopic abundances of xenon have been taken from the analysis of xenon from the Murray carbonaceous chondrite according to the interpretation given by Cameron (1962); this assumes that the atmospheric composition of xenon is distorted by a fission xenon contribution.

The Cameron (1967) abundances are plotted as a function of mass number in Figure 16.1 Of particular interest for problems of nucleosynthesis are the odd-even ratios among the heavier nuclei and the sharp and rounded peaks corresponding to closed shells of 82 and 126 neutrons in the process of neutron capture on slow and fast time scales.

The abundances of products of neutron capture are shown separately for each element upwards from the iron region in Figures 16.2 to 16.5 Nuclides with odd mass numbers are plotted as solid circles; those with even mass numbers are plotted with crosses. If an even mass number is classed as an F isobar, the cross is surrounded by a square; if it is classed as an S isobar, the cross is surrounded by a circle. These figures are very useful if one wishes to make estimates of the relative contributions to abundances of nuclides from the fast and slow time scale processes.

It should be emphasized that the abundances of heavy elements which are now based principally upon good determinations in Type I carbonaceous chondrites are very satisfactory from the point of view of the processes of nucleosynthesis. It has been known for a long time that there is an excellent regularity in abundances of nuclides corresponding to a given process of nucleosynthesis among the rare earth elements, which are subject to very little chemical fractionation. This property is now generally true of the entire distributions of Figures 16.2 to 16.5. Odd-even ratios vary regularly, being small for fast time scale products and larger for slow time scale products. One difficulty with previous abundance determinations has been the small odd-even ratios for the isotopes of Cu and Zn. This has now been satisfactorily eliminated because of the higher Zn abundance measured in Type I carbonaceous chondrites. Other expected regularities as enumerated by Cameron (1959) are satisfactorily followed.

In Figure 16.6 are plotted the abundance trends of even mass numbers for three processes of nucleosynthesis: products of neutron capture on fast and slow time scales, and bypassed nuclei. These abundance trends have been determined from isobaric abundances and from additional behavior, such as peaks at closed neutron shells, where it is evident that the observed abundances are produced primarily by a single process.

One of the striking features of the abundance distribution of the products of neutron capture on a slow time scale is the fact that σN, the product of the average neutron capture cross section near 25 keV and the abundance, is a smooth monotonically-decreasing function of mass number (Seeger, Fowler, and Clayton 1965). Because of local variability in the neutron capture cross sections, it may be noticed in Figure 16.6

that the abundances of the S isobars scatter about a smooth curve.

At present we know much less about the set of astrophysical environments responsible for the production of the products of neutron capture on a fast time scale than we do about those responsible for the slow time scale products. Therefore it is important to examine the abundance data to determine whether additional boundary conditions can be assigned to the fast time scale processes. Several features are worthy of note. The curve drawn through the F isobar abundances is remarkably smooth, in contrast to the scatter about the S isobar curve. Hence the fast time scale abundances are not affected by the variability of individual neutron capture cross sections. Abundance smoothing processes must have been operative, either through a contribution from several values of atomic number Z to each mass number, or through frequent neutron emission following the high energy beta decays of the neutron-rich final products of the capture process. In addition, the neutron capture process must have terminated quite abruptly; otherwise fast beta decays would have produced only one capture product per mass number, and the final abundances would have been affected by cross section variations.

The fast time scale product peaks at mass numbers 130 and 195 correspond to closed shells of 82 and 126 neutrons. As discussed by Truran, Arnett, Tsuruta, and Cameron (1967), it appears that these peaks are made near the base of an ejected supernova envelope, where the material has been largely transformed into neutrons. Under the astrophysical conditions in which these peaks are made, it is expected that negligible amounts of intermediate mass numbers will be formed. Yet it can be seen in Figure 16.6 and from Table II that the abundances associated with F isobars near mass numbers 40 and 70 are much larger

than those in the closed shell peaks mentioned above. This suggests that there must be a very different fast time scale process in which a burst of neutrons can be produced and added to pre-existing intermediate elements. One possibility for producing this situation is the passage of a supernova shock wave through the helium shell in the presupernova structure, where rapid (α, n) reactions may be an effective neutron source.

Also plotted in Figure 16.6 are the abundances of the B isobars. These can be produced from a pre-existing abundance distribution either by photodisintegrations which remove neutrons and protons from nuclei, or by proton capture reactions taking place in a hydrogen-rich region briefly raised to a high temperature. The first case can arise when a supernova shock wave traverses a hydrogen-depleted region of the presupernova structure in which neutrons cannot be produced in quantity by (α, n) reactions. The second case can occur when a supernova shock wave traverses the outer hydrogen layer of the presupernova structure.

The abundance distribution of Figure 16.6 favors the proton capture process. Since this would take place in the outer layers of the presupernova structure, the heavy elements could at most have been exposed to the very small neutron flux accompanying deuterium-burning, and the abundance changes produced by this would be negligible. Hence one should expect that the abundance distribution of the proton capture products would be similar to the superposition of the abundance distributions produced by neutron capture, except that the increasing Coulomb barrier with increasing atomic number would produce a progressive decrease in proton capture rates, with a corresponding increase in the ratio of the abundances of the neutron capture to proton capture

products. It may be seen that this expectation is fulfilled. In addition, the abundances of the B isobars are relatively high up to a position slightly beyond the slow time scale closed shell peaks, beyond which they fall rapidly. This also would be expected on the proton capture mechanism.

The rise at the upper end of the B isobar distribution is given solely by an isotope of mercury. This element was interpolated in the compilation of the new abundance table, and there is great uncertainty in the interpolation. The mercury abundance was chosen as high as seemed reasonable in view of the large amounts of mercury in carbonaceous chondrites. Hence the reality of this final rise in the B isobar distribution is not at all certain.

I am indebted to Professor E. Anders for a great deal of advice on meteorite abundances during a period of several years and in connection with the present abundance compilation. I am further indebted to Dr. J.W. Truran and Dr. W.D. Arnett for many discussions of the relation between nucleosynthesis and supernova hydrodynamics which has influenced the discussion in the latter part of the paper. This research has been supported in part by the U.S. Atomic Energy Commission and the National Aeronautics and Space Administration.

References

Aller, L.H. 1961, The Abundances of the Elements, Interscience Pub., Inc., New York.

Anders, E. 1964, Space Sci. Revs., 3, 583.

Baedecker, P.A. 1967, Thesis, U. of Kentucky.

Burbidge, E.M., Burbidge, G.R., Fowler, W.A., and Hoyle, F. 1957, Revs. Modern Phys., 29, 547.

Cameron, A.G.W. 1957, Chalk River report CRL-41.

Cameron, A.G.W. 1959, Astrophys. J., 129, 676.

Cameron, A.G.W. 1962, Icarus, 1, 13.

Cameron, A.G.W. 1963, Nuclear Astrophysics, notes from lectures at Yale University, unpublished.

Gaustad, J.E. 1964, Astrophys. J., 139, 406.

Larimer, J.W. and Anders, E. 1967, preprint.

Morgan, J.W. and Lovering, J.F. 1967, preprint.

Seeger, P.A., Fowler, W.A., and Clayton, D.D. 1965, Astrophys. J. Suppl., 11, 121.

Signer, P. and Suess, H.E. 1963, in Earth Science and Meteoritics (J. Geiss and E.D. Goldberg, eds.), North-Holland Pub. Co., Amsterdam.

Suess, H.E. and Urey, H.C. 1956, Revs. Modern Phys., 28, 53.

Truran, J.W., Arnett, W.D., Tsuruta, S., and Cameron, A.G.W. 1967, paper in proceedings of the Paris Symposium on the Origin and Distribution of the Elements.

Table I. Compilations of abundances normalized to Si=10^6. Notes refer to the sources of Cameron (1967).

Element	Suess Urey	Cameron (1963)	Cameron (1967)	Notes
1 H	4.00×10^{10}	3.2×10^{10}	2.6×10^{10}	1
2 He	3.08×10^{9}	5.0×10^{9}	2.1×10^{9}	2
3 Li	100	38	45	3
4 Be	20	7	0.69	3
5 B	24	6	6.2	3
6 C	3.5×10^{6}	1.66×10^{7}	1.35×10^{7}	1
7 N	6.6×10^{6}	3.0×10^{6}	2.44×10^{6}	1
8 O	2.15×10^{7}	2.9×10^{7}	2.36×10^{7}	1
9 F	1600	$\sim 10^{4}$	3630	4
10 Ne	8.6×10^{6}	1.7×10^{7}	2.36×10^{6}	2
11 Na	4.38×10^{4}	4.18×10^{4}	6.32×10^{4}	4
12 Mg	9.12×10^{5}	1.046×10^{6}	1.050×10^{6}	5
13 Al	9.48×10^{4}	8.93×10^{4}	8.51×10^{4}	5
14 Si	1.00×10^{6}	1.00×10^{6}	1.00×10^{6}	5
15 P	1.00×10^{4}	9320	1.27×10^{4}	5
16 S	3.75×10^{5}	6.0×10^{5}	5.06×10^{5}	4
17 Cl	8850	1836	1970	4
18 Ar	1.4×10^{5}	2.4×10^{5}	2.28×10^{5}	6
19 K	3160	2970	3240	4
20 Ca	4.90×10^{4}	7.28×10^{4}	7.36×10^{4}	5
21 Sc	28	29	33	5
22 Ti	2240	3140	2300	5

Element	Suess Urey	Cameron (1963)	Cameron (1967)	Notes
23 V	220	590	900	7
24 Cr	7800	1.20×10^4	1.24×10^4	5
25 Mn	6850	6320	8800	4
26 Fe	6.00×10^5	8.42×10^5	8.90×10^5	5
27 Co	1800	2290	2300	5
28 Ni	2.74×10^4	4.44×10^4	4.57×10^4	5
29 Cu	212	861	919	4
30 Zn	486	930	1500	4
31 Ga	11.4	39	45.5	4
32 Ge	50.4	134	126	4
33 As	4.0	4.4	7.2	8
34 Se	67.6	18.8	70.1	4
35 Br	13.4	3.95	20.6	4
36 Kr	51.3	20	64.4	9
37 Rb	6.5	5.0	5.95	4
38 Sr	18.9	21	58.4	5
39 Y	8.9	3.6	4.6	5
40 Zr	54.5	23	30	7
41 Nb	1.00	0.81	1.15	10
42 Mo	2.42	2.42	2.52	3
44 Ru	1.49	1.58	1.6	3
45 Rh	0.214	0.26	0.33	3
46 Pd	0.675	1.00	1.5	11
47 Ag	0.26	0.26	0.5	12
48 Cd	0.89	0.89	2.12	4
49 In	0.11	0.11	0.217	4

Element	Suess Urey	Cameron (1963)	Cameron (1967)	Notes
50 Sn	1.33	1.33	4.22	4
51 Sb	0.246	0.15	0.381	4
52 Te	4.67	3.00	6.76	4
53 I	0.80	0.46	1.41	4
54 Xe	4.0	3.15	7.10	13
55 Cs	0.456	0.25	0.367	4
56 Ba	3.66	4.0	4.7	5
57 La	2.00	0.38	0.36	5
58 Ce	2.26	1.08	1.17	5
59 Pr	0.40	0.16	0.17	5
60 Nd	1.44	0.69	0.77	5
62 Sm	0.664	0.24	0.23	5
63 Eu	0.187	0.083	0.091	5
64 Gd	0.684	0.33	0.34	14
65 Tb	0.0956	0.054	0.052	14
66 Dy	0.556	0.33	0.36	5
67 Ho	0.118	0.076	0.090	5
68 Er	0.316	0.21	0.22	5
69 Tm	0.0318	0.032	0.035	5
70 Yb	0.220	0.18	0.21	5
71 Lu	0.050	0.031	0.035	5
72 Hf	0.438	0.16	0.16	3
73 Ta	0.065	0.021	0.022	15
74 W	0.49	0.11	0.16	11
75 Re	0.135	0.054	0.055	16

Element	Suess Urey	Cameron (1963)	Cameron (1967)	Notes
76 Os	1.00	0.73	0.71	16
77 Ir	0.821	0.500	0.43	17
78 Pt	1.625	1.157	1.13	18
79 Au	0.145	0.13	0.20	17
80 Hg	0.284	0.27	0.75	19
81 Tl	0.108	0.11	0.182	4
82 Pb	0.47	2.2	2.90	4
83 Bi	0.144	0.14	0.164	4
90 Th	--	0.069	0.034	20
92 U	--	0.042	0.0234	20

Notes to Table I

1. In Cameron (1963) the volatile elements are normalized to silicon = 10^6 in the sun, which is somewhat poorly determined. In Cameron (1967) the normalization is based on logarithmic averages of Na, Mg, Al, Si, S, K, Ca, Ti, Co, and Ni in the sun relative to meteoritic values. The solar abundances are taken from Aller (1961).
2. He and Ne are normalized to the solar oxygen abundance using solar cosmic ray data, as suggested by Gaustad (1964).
3. Based on abundances in chondrites, taken from Urey (1964).
4. Based on abundances in Type I carbonaceous chondrites, taken from Larimer and Anders (1967).
5. Based on abundances in the Orgueil and Ivuna Type I carbonaceous chondrites, taken from Urey (1964).
6. Ar^{36} was interpolated between S^{32} and Ca^{40}.
7. Based on abundances in carbonaceous chondrites, taken from Urey (1964).
8. As^{75} was interpolated between Ge^{73} and Se^{77}.
9. Kr was assigned an abundance representing a compromise between interpolations of Kr^{84} between Se^{80} and Sr^{88} and of Kr^{83} between Br^{81} and Rb^{85}.
10. Nb^{93} was interpolated between Zr^{91} and Mo^{95}.
11. Based on abundances in Type I carbonaceous chondrites, private communication from E. Anders.
12. Based on abundances in carbonaceous chondrites, taken from Larimer and Anders (1967).
13. Isotopic abundances of Xe were based on those in the Murray carbonaceous chondrite (Cameron 1962). The element was normalized

to Te and I to form a continuous abundance peak.

14. The abundances of Gd and Tb measured for Type I carbonaceous chondrites are anomalous relative to the usual chondritic pattern and have fairly large errors. Hence these abundances were based on those in ordinary chondrites (Urey 1964) but normalized to Sm.

15. The Ta abundance of 0.044 for carbonaceous chondrites (Urey 1964) appears too high relative to neighboring odd-mass nuclides. The given value was interpolated between Hf^{179} and W^{183} and is in good agreement with values in ordinary chondrites.

16. Based on abundances in Type I carbonaceous chondrites, taken from Morgan and Lovering (1967).

17. Based on abundances in Type I carbonaceous chondrites, taken from Baedecker (1967).

18. The abundance of Pt was adjusted relative to Os, Ir, and Au to form a continuous peak. The adopted value is slightly higher than in ordinary chondrites (Urey 1964).

19. The abundances of Hg in carbonaceous chondrites are anomalously high and greatly variable. Hg was interpolated with as high a value as seemed possible, specifically by interpolating Hg^{199} and Hg^{201} between Au^{197} and Tl^{203}.

20. Abundances as of 4.5×10^9 years ago based on ordinary chondrites, taken from Urey (1964).

Table II. Abundances of the nuclides corresponding to the element abundances of Cameron (1967) in Table I.

Element	A	%Abundance	Class	Abundance	
H				2.6×10^{10}	
	1	99.985			2.6×10^{10}
	2	.015			3.9×10^{6}
He				2.1×10^{9}	
	3	~0.03			6.3×10^{5}
	4	~100			2.1×10^{9}
Li				45	
	6	7.42			3.34
	7	92.58			41.66
Be	9	100		0.69	
B				6.2	
	10	19.64			1.22
	11	80.36			4.98
C				1.35×10^{7}	
	12	98.89			1.33×10^{7}
	13	1.11			1.50×10^{5}
N				2.44×10^{6}	
	14	99.634			2.44×10^{6}
	15	0.366			9000
O				2.36×10^{7}	
	16	99.759			2.36×10^{7}
	17	0.0374			8800
	18	0.2039			4.8×10^{4}

Element	A	%Abundance	Class	Abundance	
F	19	100		3630	
Ne				2.36×10^6	
	20	90.92			2.15×10^6
	21	0.257			6060
	22	8.82			2.00×10^5
Na	23	100		6.32×10^4	
Mg				1.050×10^6	
	24	78.70			8.26×10^5
	25	10.13			1.06×10^5
	26	11.17			1.17×10^5
Al	27	100		8.51×10^4	
Si				1.000×10^6	
	28	92.21			9.22×10^5
	29	4.70			4.70×10^4
	30	3.09			3.09×10^4
P	31	100		1.27×10^4	
S				5.06×10^5	
	32	95.0			4.80×10^5
	33	0.760			3.85×10^3
	34	4.22			2.14×10^4
	36	0.0136	F		69
Cl				1970	
	35	75.529			1490
	37	24.471			480

Element	A	%Abundance	Class	Abundance	
Ar				2.28×10^5	
	36	84.2			1.92×10^5
	38	15.8			3.61×10^4
	40	~0.01	F		~20
K				3240	
	39	93.10			3020
	40	0.38			12.3
	41	6.88			223
Ca				7.36×10^4	
	40	96.97			7.13×10^4
	42	0.64			470
	43	0.145			107
	44	2.06			1520
	46	0.0033	F		2.43
	48	0.185	F		136
Sc	45	100		33	
Ti				2300	
	46	7.93			182
	47	7.28			168
	48	73.94			1700
	49	5.51			127
	50	5.34			123
V				900	
	50	0.24			2.2
	51	99.76			898

Element	A	%Abundance	Class	Abundance
Cr				1.24×10^4
	50	4.31		535
	52	83.7		1.04×10^4
	53	9.55		1180
	54	2.38		297
Mn	55	100		8800
Fe				8.90×10^5
	54	5.82		5.19×10^4
	56	91.66		8.15×10^5
	57	2.19		1.95×10^4
	58	0.33		2900
Co	59	100		2300
Ni				4.57×10^4
	58	67.88		3.10×10^4
	60	26.23		1.20×10^4
	61	1.19		544
	62	3.66		1670
	64	1.08		494
Cu				919
	63	69.09		635
	65	30.91		284
Zn				1500
	64	48.89		732
	66	27.81		417
	67	4.11		61.8
	68	18.57		278
	70	0.62	F	9.3

Element	A	%Abundance	Class	Abundance	
Ga				45.5	
	69	60.4			27.5
	71	39.6			18.0
Ge				126	
	70	20.52	S		25.8
	72	27.43			34.6
	73	7.76			9.77
	74	36.54			46.0
	76	7.76	F		9.77
As	75	100		7.2	
Se				70.1	
	74	0.87	B		0.61
	76	9.02	S		6.32
	77	7.58			5.31
	78	23.52			16.5
	80	49.82			34.9
	82	9.19	F		6.44
Br				20.6	
	79	50.537			10.4
	81	49.463			10.2
Kr				64.4	
	78	0.354	B		0.228
	80	227			1.46
	82	11.56	S		7.45
	83	11.55			7.44
	84	56.90			36.6
	86	17.37			11.2

Element	A	%Abundance	Class	Abundance	
Rb				5.95	
	85	72.15			4.29
	87	27.85			1.66
Sr				58.4	
	84	0.56	B		0.327
	86	9.86			5.76
	87	7.02			4.10
	88	82.56			48.2
Y	89	100		4.6	
Zr				30	
	90	51.46			15.1
	91	11.23			3.37
	92	17.11			5.14
	94	17.40			5.32
	96	2.80	F		0.84
Nb	93	100		1.15	
Mo				2.52	
	92	15.84	B		0.399
	94	9.04	B		0.228
	95	15.72			0.396
	96	16.53	S		0.417
	97	9.46			0.238
	98	23.78			0.599
	100	9.63	F		0.242

Element	A	%Abundance	Class	Abundance	
Ru				1.6	
	96	5.51	B		0.088
	98	1.87	B		0.030
	99	12.72			0.204
	100	12.62	S		0.202
	101	17.07			0.273
	102	31.61			0.505
	104	18.58	F		0.297
Rh	103	100		0.33	
Pd				1.5	
	102	0.96	B		0.0144
	104	10.97	S		0.164
	105	22.23			0.324
	106	27.33			0.410
	108	26.71			0.400
	110	11.81	F		0.177
Ag				0.5	
	107	51.35			0.257
	109	48.65			0.243
Cd				2.12	
	106	1.215	B		0.0258
	108	0.875	B		0.0186
	110	12.39	S		0.262
	111	12.75			0.270
	112	24.07			0.510
	113	12.26			0.260

Element	A	%Abundance	Class	Abundance	
	114	28.86			0.611
	116	7.58	F		0.161
In				0.217	
	113	4.28			0.0093
	115	95.72			0.208
Sn				4.22	
	112	0.96	B		0.0405
	114	0.66	(B)		0.0278
	115	0.35	(B)		0.0148
	116	14.30	S		0.603
	117	7.61			0.321
	118	24.03			1.01
	119	8.58			0.362
	120	32.85			1.39
	122	4.72	(F)		0.199
	124	5.94	F		0.250
Sb				0.381	
	121	57.25			0.218
	123	42.75			0.163
Te				6.76	
	120	0.089	B		0.0060
	122	2.46	S		0.166
	123	0.87			0.059
	124	4.61	S		0.312
	125	6.99			0.472
	126	18.71			1.27
	128	31.79	F		2.15

Element	A	%Abundance	Class	Abundance	
	130	34.48	F		2.33
I	127	100		1.41	
Xe				7.10	
	124	0.126	B		0.00895
	126	0.115	B		0.00816
	128	2.17	S		0.154
	129	27.5			1.95
	130	4.26	S		0.303
	131	21.4			1.52
	132	26.0			1.85
	134	10.17	F		0.721
	136	8.39	F		0.595
Cs	133	100		0.367	
Ba				4.7	
	130	0.101	B		0.00475
	132	0.097	B		0.00455
	134	2.42	S		0.114
	135	6.59			0.310
	136	7.81	S		0.367
	137	11.32			0.532
	138	71.66			3.37
La				0.36	
	138	0.089			0.00032
	139	99.911			0.36
Ce				1.17	
	136	0.193	B		0.00226

Element	A	%Abundance	Class	Abundance	
	138	0.250	B		0.00292
	140	88.48			1.035
	142	11.07	F		0.129
Pr	141	100		0.17	
Nd				0.77	
	142	27.11	S		0.209
	143	12.17			0.0936
	144	23.85			0.184
	145	8.30			0.0640
	146	17.22			0.133
	148	5.73	F		0.0441
	150	5.62	F		0.0433
Sm				0.23	
	144	3.09	B		0.0071
	147	14.97			0.0344
	148	11.24	S		0.0259
	149	13.83			0.0318
	150	7.44	S		0.0171
	152	26.72			0.0614
	154	22.71	F		0.0522
Eu				0.091	
	151	47.82			0.0435
	153	52.18			0.0475
Gd				0.34	
	152	0.200			0.00068
	154	2.15	S		0.00731
	155	14.73			0.0501

Element	A	%Abundance	Class	Abundance	
	156	20.47			0.0696
	157	15.68			0.0532
	158	24.87			0.0847
	160	21.90	F		0.0745
Tb	159	100		0.052	
Dy				0.36	
	156	0.0524	B		0.000189
	158	0.0902	B		0.000325
	160	2.294	S		0.00825
	161	18.88			0.0680
	162	25.53			0.0919
	163	24.97			0.0899
	164	28.18			0.1112
Ho	165	100		0.090	
Er				0.22	
	162	0.136	B		0.000299
	164	1.56			0.00343
	166	33.41			0.0735
	167	22.94			0.0505
	168	27.07			0.0595
	170	14.88	F		0.0327
Tm	169	100		0.035	
Yb				0.21	
	168	0.135	B		0.000284
	170	3.03	S		0.00636
	171	14.31			0.0301

Element	A	%Abundance	Class	Abundance
	172	21.82		0.0460
	173	16.13		0.0339
	174	31.84		0.0670
	176	12.73	F	0.0268
Lu				0.035
	175	97.41		0.0341
	176	2.59		0.00091
Hf				0.16
	174	0.18	B	0.000288
	176	5.20	S	0.00832
	177	18.50		0.0296
	178	27.14		0.0434
	179	13.75		0.0220
	180	35.24		0.0564
Ta				0.022
	180	0.0123		0.0000027
	181	99.9877		0.022
W				0.16
	180	0.135	B	0.000216
	182	26.41		0.0423
	183	14.40		0.0230
	184	30.64		0.0490
	186	28.41	F	0.0455
Re				0.055
	185	37.07		0.0204
	187	62.93		0.0346

Element	A	%Abundance	Class	Abundance	
Os				0.71	
	184	0.018	B		0.000128
	186	1.29	S		0.0113
	187	1.64			0.0116
	188	13.3			0.0945
	189	16.1			0.1142
	190	26.4			0.1875
	192	41.0	F		0.291
Ir				0.43	
	191	37.3			0.164
	193	62.7			0.276
Pt				1.13	
	190	0.0127	B		0.000144
	192	0.78	S		0.00994
	194	32.9			0.372
	195	33.8			0.382
	196	25.3			0.286
	198	7.21	F		0.0815
Au	197	100		0.20	
Hg				0.75	
	196	0.146	B		0.00102
	198	10.02	S		0.0703
	199	16.84			0.118
	200	23.13			0.162
	201	13.22			0.0926
	202	29.80			0.2084

Element	A	%Abundance	Class	Abundance	
	204	6.85	F		0.0480
Tl				0.182	
	203	29.50			0.0537
	205	70.50			0.1283
Pb				2.90	
	204	1.97	S		0.057
	206	18.83			0.546
	207	20.60			0.596
	208	58.55			1.70
Bi	209	100		.164	
Th	232	100		0.034	
U				0.0234	
	235	23.1			0.0054
	238	76.9			0.0180

Figure Captions

Figure 16.1: Abundances of the nuclides plotted as a function of mass number.

Figure 16.2: Abundances of nuclides which can be formed by neutron capture, upwards from the iron peak region (in which all nuclides are plotted). Symbols are explained in the text.

Figure 16.3: Continuation of Figure 16.2

Figure 16.4: Continuation of Figure 16.3

Figure 16.5: Continuation of Figure 16.4

Figure 16.6: Trends among heavy nuclei of abundances attributable to neutron capture on fast and slow time scales and to bypassed processes.

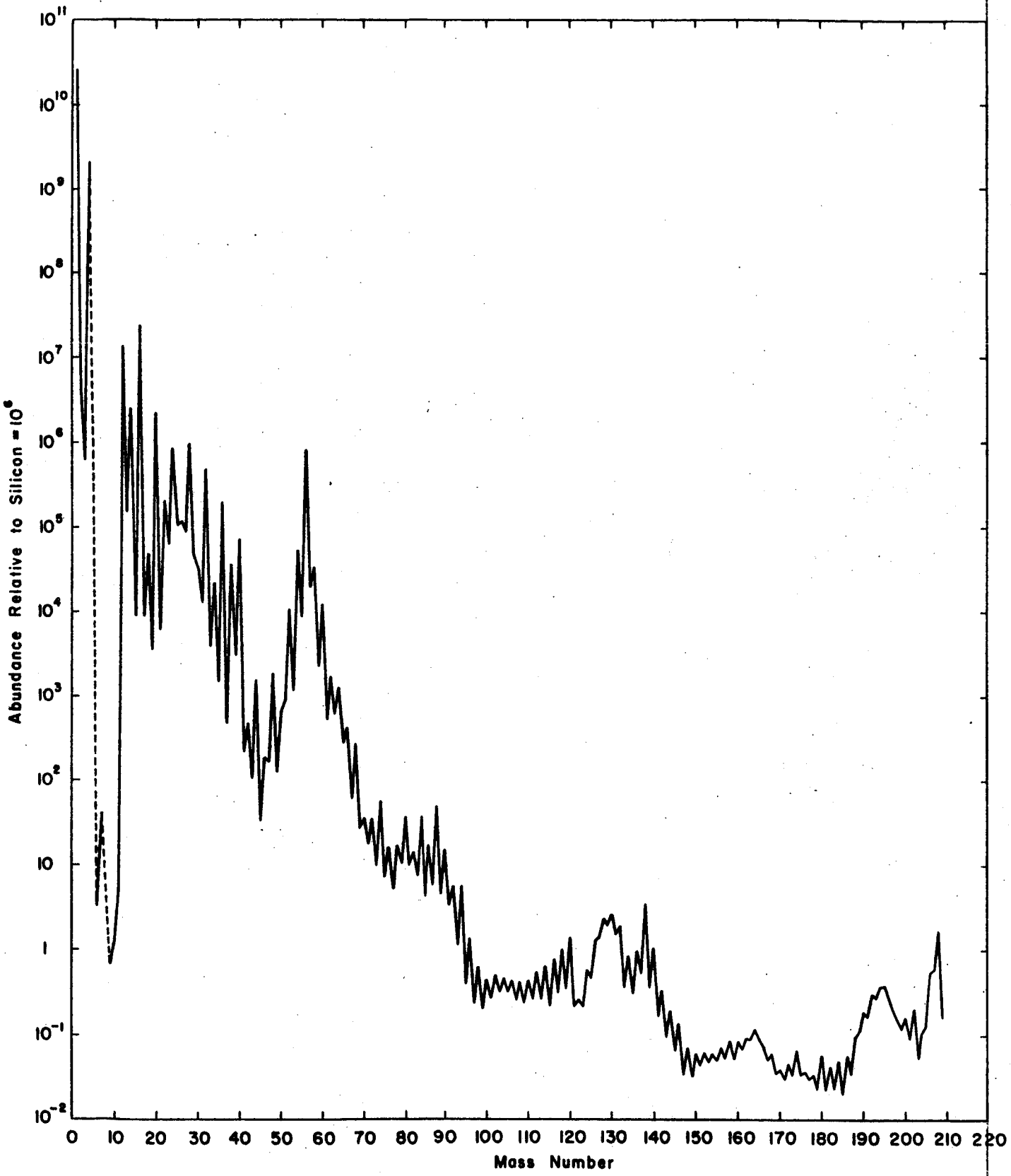
Abundance Relative to Silicon = 10^6
10^{11}
10^{10}
10^9
10^8
10^7
10^6
10^5
10^4
10^3
10^2
10
1
10^{-1}
10^{-2}
0 10 20 30 40 50 60 70 80 90 100 110 120 130 140 150 160 170 180 190 200 210 220
Mass Number

Figure 16.1

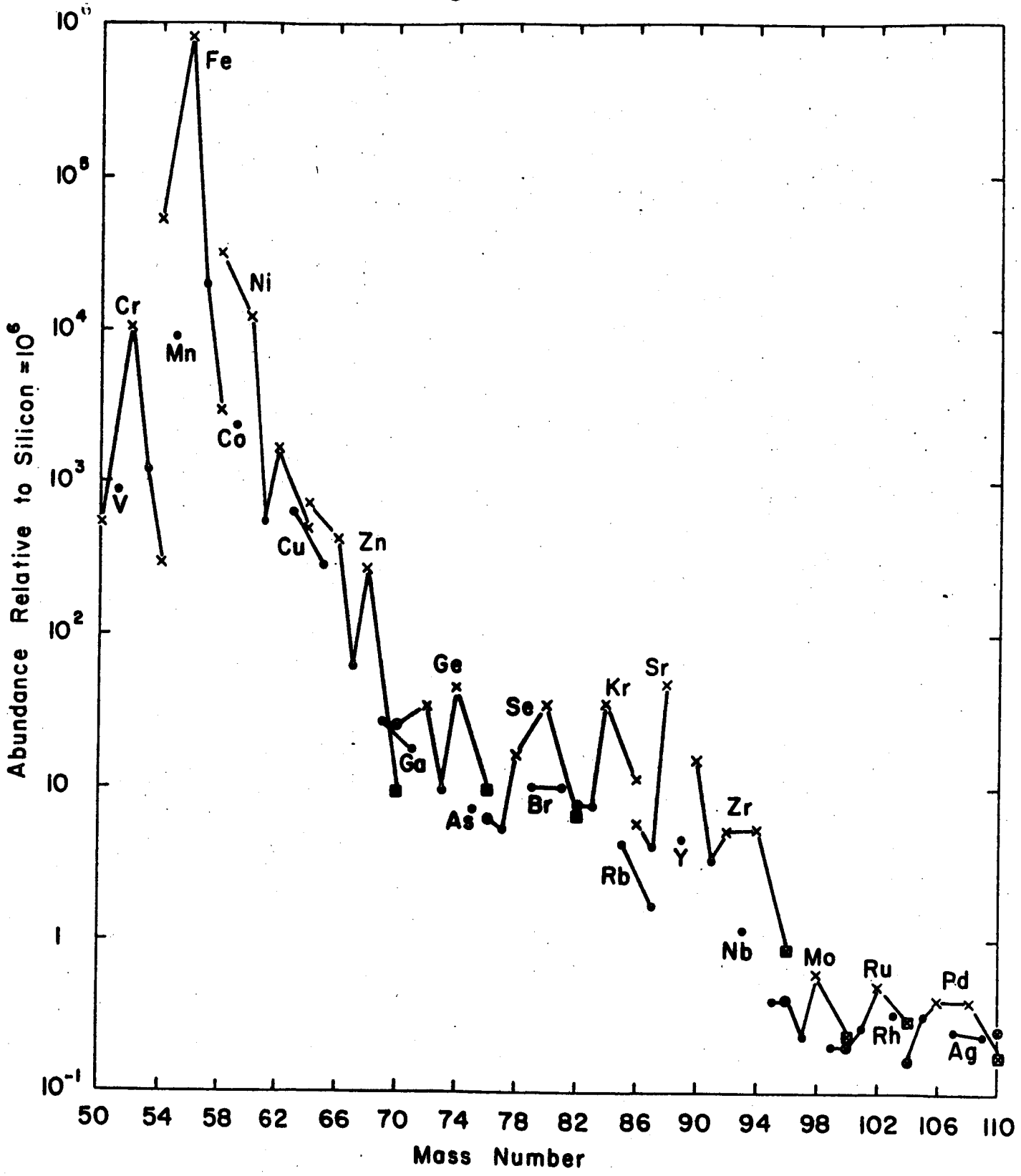
Abundance Relative to Silicon =10^6
Mass Number
Fe
Ni
Cr
Mn
Co
V
Cu
Zn
Ga
Ge
As
Se
Br
Kr
Rb
Sr
Y
Zr
Nb
Mo
Ru
Rh
Pd
Ag

Figure 16.2

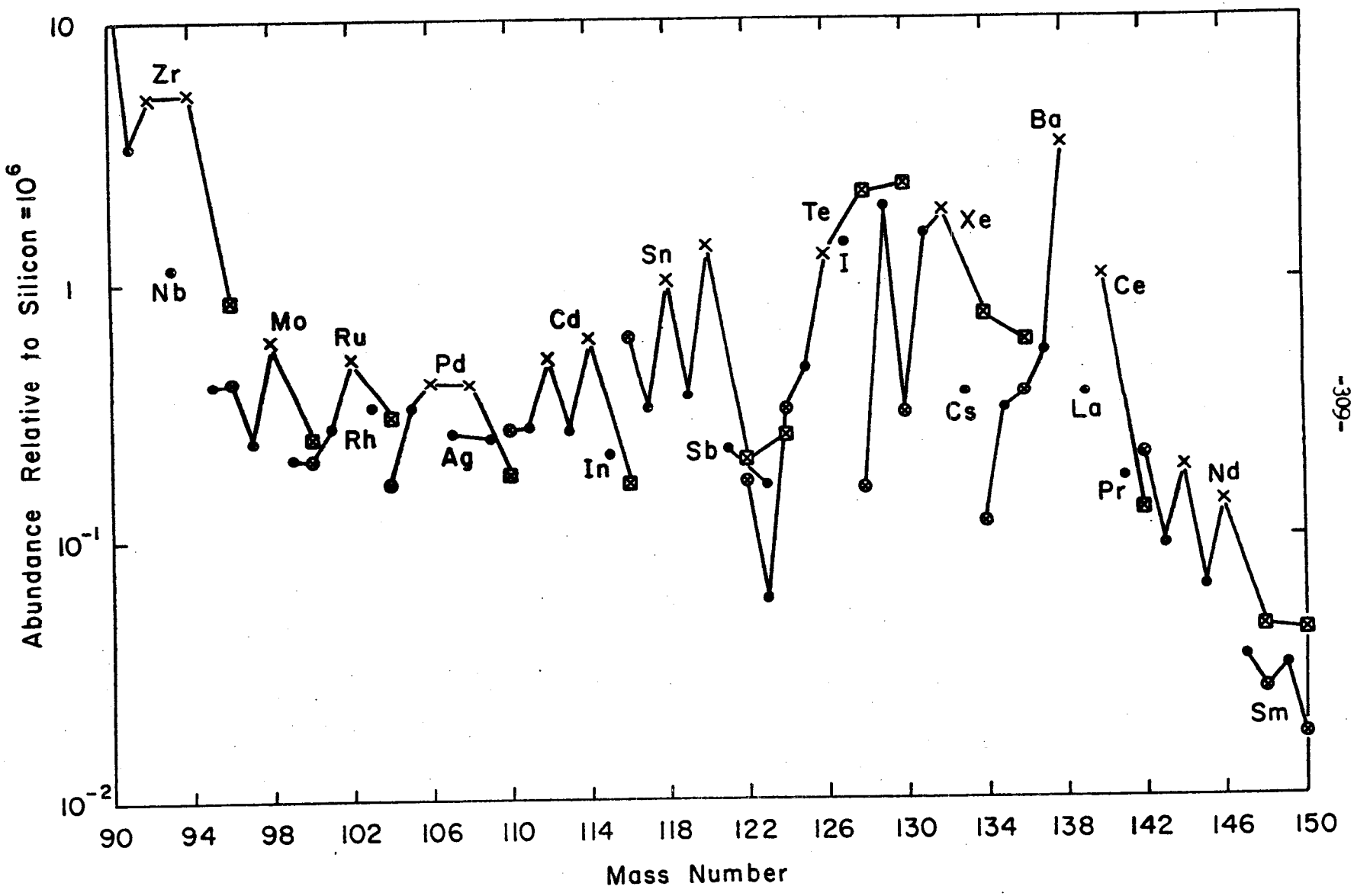
Abundance Relative to Silicon = 10^6
10
1
10^{-1}
10^{-2}
90
94
98
102
106
110
114
118
122
126
130
134
138
142
146
150
Mass Number
Zr
Nb
Mo
Ru
Rh
Pd
Ag
Cd
In
Sn
Sb
Te
I
Xe
Cs
Ba
La
Ce
Pr
Nd
Sm

Figure 16.3

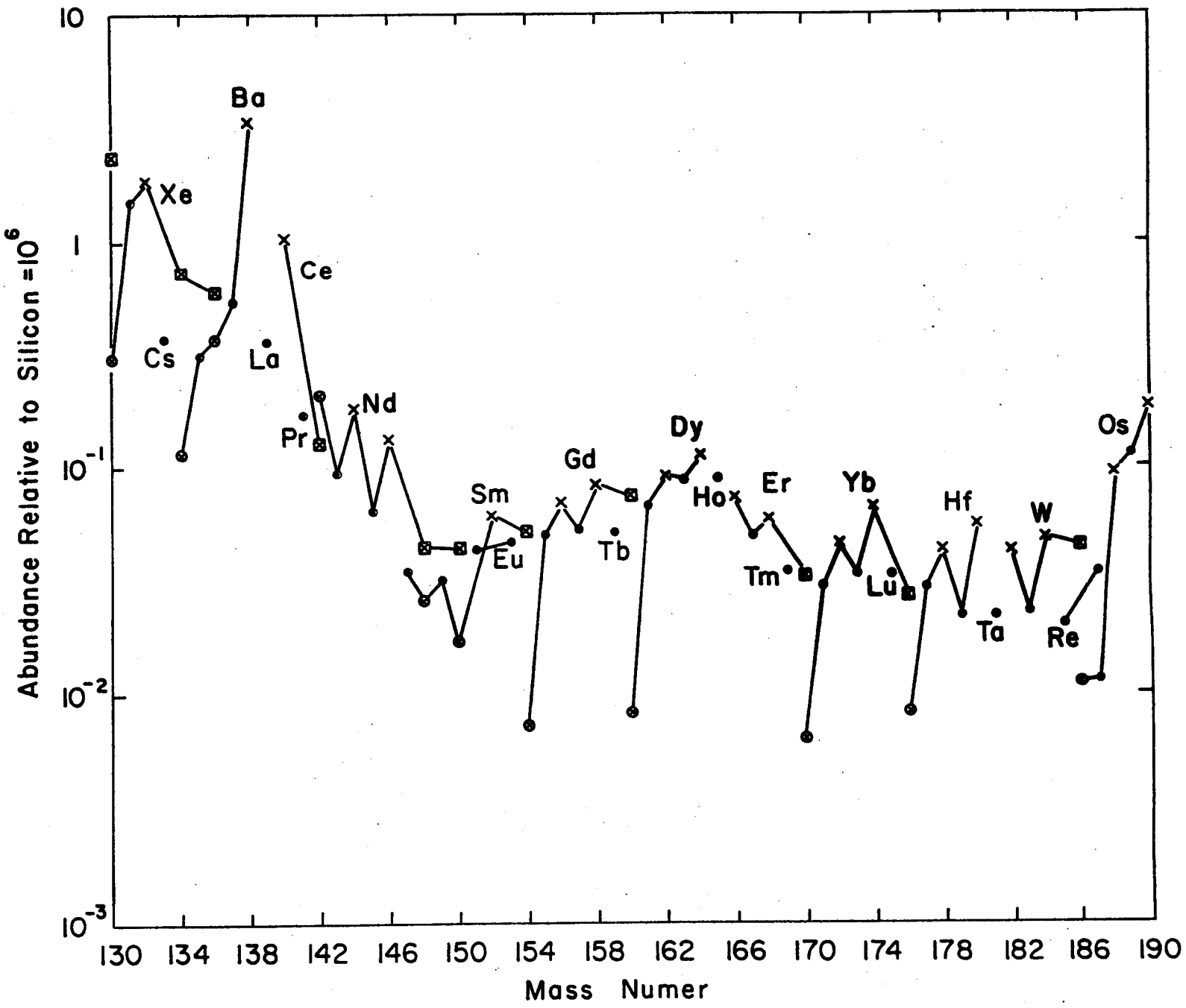
Abundance Relative to Silicon =10^6
10
1
10^-1
10^-2
10^-3
130 134 138 142 146 150 154 158 162 166 170 174 178 182 186 190
Mass Numer
Ba
Xe
Cs
La
Ce
Pr
Nd
Sm
Eu
Gd
Tb
Dy
Ho
Er
Tm
Yb
Lu
Hf
Ta
W
Re
Os

Figure 16.4

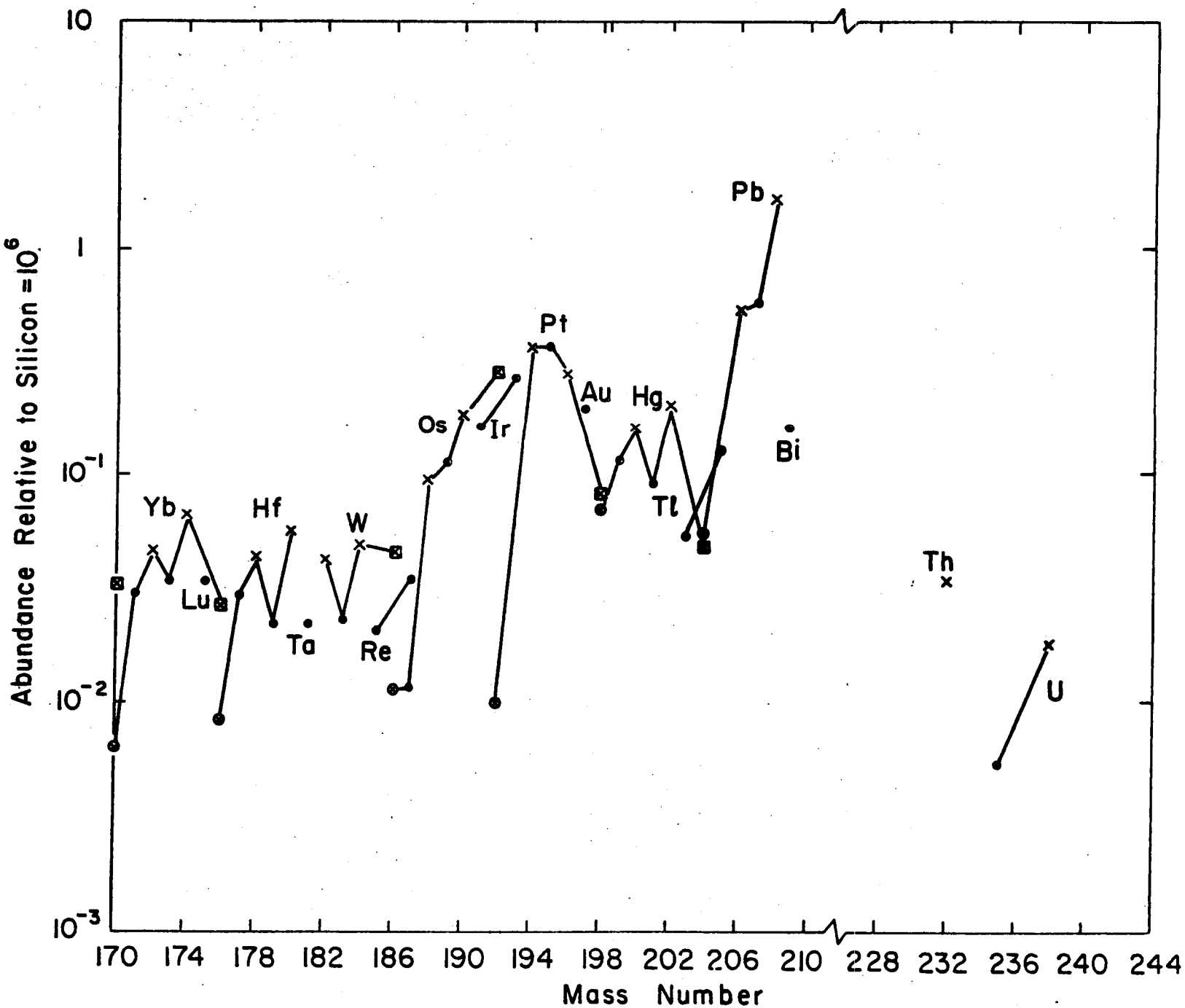
Abundance Relative to Silicon = 10^6
10
1
10^{-1}
10^{-2}
10^{-3}
Yb
Lu
Hf
Ta
W
Re
Os
Ir
Pt
Au
Hg
Tl
Pb
Bi
Th
U
170 174 178 182 186 190 194 198 202 206 210 228 232 236 240 244
Mass Number

Figure 16.5

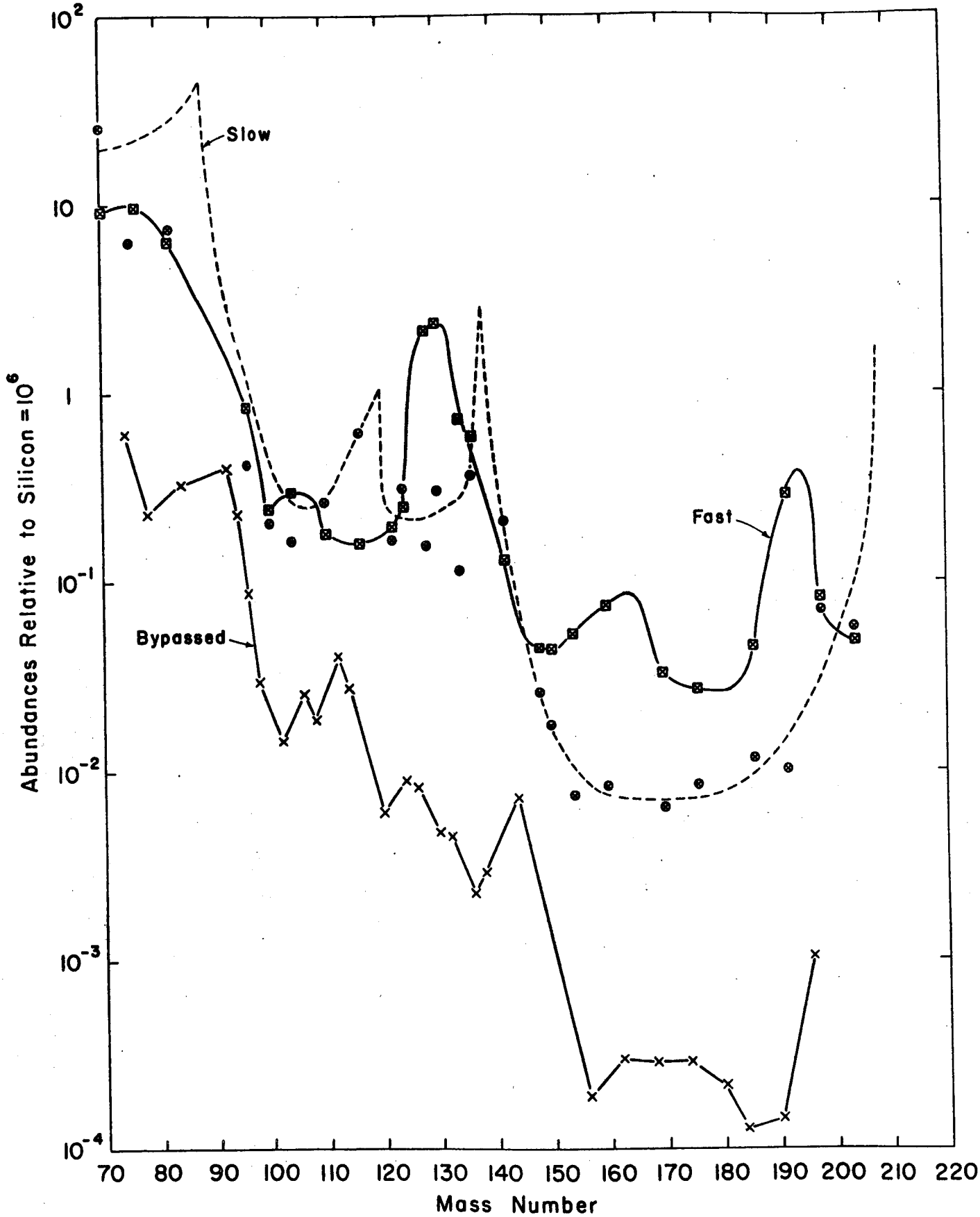
Slow
Fast
Bypassed
Abundances Relative to Silicon = 10^6
10^2
10
1
10^{-1}
10^{-2}
10^{-3}
10^{-4}
70 80 90 100 110 120 130 140 150 160 170 180 190 200 210 220
Mass Number

Figure 16.6

17. Photobeta Reactions

Before examining the restrictions that abundance analysis places upon the time scales associated with neutron capture we shall consider a process called photobeta reactions*. This process can influence the rate at which a nuclide can undergo beta decay, and it is precisely these decay rates which allow us to establish the time scales for the neutron capture process.

The basic idea behind the photobeta reaction is that nuclei in the stellar interior will have an equilibrium distribution of the populations of excited states which is weighted according to the Boltzmann factor. Now if we have a fairly high excitation energy in the nuclei, then it is generally true that the excited states of the nuclei can beta decay to neighboring nuclei at a faster rate than the ground states can decay. In the laboratory situation this process is not important because gamma emission is much faster than beta emission in the great majority of cases, but in a star there is always an equilibrium population of excited states, and then the photobeta process can become important.

The fractional population of an excited state E_i is

$$a_i(E_i) = \frac{(2J_i+1)\ \exp(-E_i/kT)}{f(T)} \tag{17.1}$$

*A.G.W. Cameron, Astrophys.J., 130, 2, p. 452.

J_i is the total momentum of the state E_i. If the temperature isnot too high,

$$f(T) \approx 2I + 1$$

where f(T) is the partition function for the nucleus and I is the spin of the ground state. Only if the fractional population of the low-lying excited states approach unity must we use equation (17.1). Hence

$$a_i(E_i) \simeq \frac{(2J_i+1)}{2I+1} \exp(-E_i/kT) \tag{17.2}$$

Now the question arises: Why do we call the beta decays from the excited states "photobeta" reactions, since the nuclei may be put into the excited states by collisions as well as photon excitation? The rates of beta decay will be independent of the particle density. They will be individual rates for a given nucleus that depend only upon the nucleus being bathed by black-body radiation at the appropriate temperature. Although collisions may participate in changing nuclei among the various excited states, their role is not an essential one. Therefore the process is equivalent to entering the state by a photon absorption and leaving the state by a beta transition of some kind.

In general, the uncertainty principle gives

$$\Gamma\tau = \hbar = \frac{\Gamma}{\lambda} \tag{17.3}$$

for the parameters of a given level of an excited nucleus, where Γ is the total width at half maximum, τ is the mean life, and λ the decay constant. Whenever we consider a resonance involved in some kind of reaction, the reaction rate is proportional to

$$\frac{\Gamma_\beta \, \Gamma_{\text{not } \beta}}{\Gamma_{\text{total}}}$$

If Γ_β is the width for the beta transition and $\Gamma_{\text{not } \beta}$ is the width for all other transitions, we use

$$\Gamma_\beta \ll \Gamma_{\text{not } \beta}$$

so

$$\Gamma_{\text{not } \beta} \simeq \Gamma_{\text{tot}}$$

and the reaction rate is approximately

$$\approx \Gamma_\beta$$

and we may write

$$\lambda_\beta = \frac{\Gamma_\beta}{\hbar} \quad . \tag{17.4}$$

It should be noted that unless $\Gamma_\beta \ll \Gamma_{\text{not } \beta}$, the method of statistical equilibrium cannot be used. The neutrinos and antineutrinos emitted in the beta transitions escape from the

stellar interior, thus making the reactions irreversible. Hence the method of statistical equilibrium can be used when the beta-decays make only small pertubations to the nuclear level formation and destruction rates.

Beta-transitions are characterized by a varying degree of forbiddenness, depending on the angular momentum carried away by the electron and the neutrino. "Allowed" transitions are those in which the nuclear spin does not change by more than one unit of angular momentum and the parity of the nuclear states is the same. There follow a number of degrees of "forbiddenness" in which successively larger changes of angular momentum can take place and in which changes of parity and no changes of parity alternate.

Beta-transition probabilities involve Fermi functions, f(Z,E), where Z is the charge of the product nucleus (negative for positron emission) and E is the energy available for the transition. It has been found that the product of f(Z,E) and the half-life t of the transition is very roughly constant for any degree of forbiddenness of the beta-transition. Log_{10} ft usually lies in the range 5-6 for allowed transitions and 6-8 for first forbidden transitions. However, values outside these ranges are not uncommon. The variations arise through the variation in the individual nuclear matrix elements

for the transitions. Transitions which are higher than first forbidden are usually too slow to be of interest in photobeta reactions.

For reasonably heavy nuclei (Z > 20) the Fermi function can be calculated from relations given by Feenberg and Trigg (1950). For electron and positron emission, it is

$$f_{\pm} = \langle R(Z,W)\rangle f^{o}(Z,W) \tag{17.5}$$

where $\langle R(Z,W)\rangle$ is a slowly varying function plotted by Feenberg and Trigg (lying in the range 1-6); Z is the charge of the product nucleus (negative for positron emission); and W is the energy of the transition in units of $m_o c^2$ = 0.51 mev, including the rest mass of the electron. It should be remembered that positron emission is possible only when the energy available for the transition exceeds the energy threshold for creation of a positron-electron pair, or 1.02 mev.

The function f^o can be written as the sum os three products, as follows:

$$f^o = U_1 f_{01} + U_2 f_{02} + U_3 f_{03} \tag{17.6}$$

For electron emission we have

$$U_1(Z) = \frac{2\pi\alpha Z}{1-\exp(-2\pi\alpha Z)} \tag{17.7}$$

$$U_2(Z) = -U_1^2(Z)\ \exp(-2\pi\alpha Z) \tag{17.8}$$

and $$U_3(Z) = U_2(Z)[2\pi\alpha Z - 3 + 2U_1(-Z)] \tag{17.9}$$

where $\alpha \approx \frac{1}{137}$ is the fine structure constant. For positron emission, the equations (17.8) and (17.9) remain the same, but equation 11.7 becomes

$$U_1\ (-Z) = -\ 2\pi\alpha Z + U_1(Z) \tag{17.7a}$$

where $U_1(Z)$ is as in equation (17.7). Feenberg and Trigg (1950) have tabulated these functions at convenient intervals. The remaining functions in equation (17.6) are

$$f_{01} = \frac{1}{30}\ (W-1)^3(W^2 + 3W + 6) \tag{17.10}$$

$$f_{02} = \frac{1}{6}\ (W-1)^3 \tag{17.11}$$

$$f_{03} = \frac{1}{8}\ (W^2-1 - 2W\ \ell nW) \tag{17.12}$$

Let us write

$$C = (ft) \tag{17.13}$$

to represent the transition constant for any given transition.

Then

$$\lambda_\beta = \frac{\ell n2}{t} = \frac{\ell n2}{C}f = \frac{\Gamma_\beta}{\hbar} \tag{17.14}$$

Then

$$\Gamma_\beta = (\ln 2)\frac{\hbar}{c}\ f. \tag{17.15}$$

The total transition rate, p_β, per nucleus is the sum of all such transition probabilities multiplied by the fractional populations of the corresponding states:

$$p_\beta = \sum_i \frac{\Gamma_{\beta i}}{\hbar}\ a_i(E_i)$$

$$= \frac{\ln 2}{(2I+1)} \sum_i (2J_i + 1)\ \frac{f_i}{c_i}\ \exp\left(\frac{-E_i}{kT}\right) \tag{17.16}$$

This equation may be used for either electron or positron emission. In the more general case the statistical weight (2I+1) should be replaced by the entire partition function.

Convenient expressions for the Fermi function for electron capture from the K shell have been given by Major and Biedenharn(1954):

$$f_K\ (Z,W) = \frac{1}{2}\pi\ g_K^2\ W_K^2\ , \tag{17.17}$$

where Z is the charge of the capturing nucleus; W_K is the transition energy in units of $m_o c^2$ = 0.51 Mev, in which the binding energy of the K shell should be taken into account for greatest accuracy; and g_K^2 is well approximated by

$$\log_{10} g_K^2 = (7.9776-10) + 0.03256Z - 10^{(0.48775-0.0380236Z)} \tag{17.18}$$

Under astrophysical conditions in which photobeta reactions are likely to be of interest, the temperature is sufficiently high that the K shells of even very heavy elements are likely to be ionized. Under such conditions the rate for the K capture must be replaced by the rate for capture of the free electrons. A very crude calculation of this rate follows.

The probability of finding a K electron inside the nucleus* is

$$\int |\Psi_e| K^2 \, dV = \frac{1}{\pi} \left(\frac{Zme^2}{\hbar^2} \right)^3 V_N \tag{17.19}$$

where Ψ_e is the electron wave function; the integral is taken over the nuclear volume; m is the electron mass; and V_N is the volume of the nucleus. For free electrons in the absence of coulomb fields, if an electron is confined to a volume V, the probability of finding it inside the nuclear volume is V_N/V. In the presence of a coulomb field this must be multiplied by a coulomb function:

$$\int |\Psi_e|^2_{free} \, dV = \frac{V_N}{V} \frac{2\pi\eta}{1-\exp(-2\pi\eta)} \tag{17.20}$$

where,

$$\eta = \frac{Ze^2}{\hbar v} \tag{17.21}$$

*J.M. Blatt and V.F. Weisskopf, Theoretical Nuclear Physics, John Wiley and Sons, New York, 1952, page 686.

and v is the velocity of the free electron. In this expression renormalization of the wave function is neglected.

If the electrons are non-degenerate, we may replace the electron velocity in equation 11.21 by the average velocity:

$$\langle v \rangle = \left(\frac{8kT}{\pi m}\right)^{\frac{1}{2}} \tag{17.22}$$

We shall identify the volume V with the volume occupied by one electron in the stellar interior. Since under most conditions of interest there are two atomic mass units per electron in the stellar interior, then

$$V = \frac{3.32 \times 10^{-24}}{\rho} \text{ cm}^3 , \tag{17.23}$$

where ρ is the density in grams per cubic centimeter.

For the relatively small electron velocities involved in most non-degenerate conditions of interest, η is sufficiently large that the exponential part of the denominator in equation (17.20)can be neglected compared to unity.

The free-electron capture rate can then be written as equal to the K capture rate multiplied by the probability of finding a free electron inside the nucleus relative to the probability of finding a K electron inside the nucleus. Remembering that the atom normally contains two K electrons, the free-electron capture probability becomes

$$\lambda_e = 6\times10^{-3}\,\frac{\rho}{Z^2}\,\lambda_K \tag{17.24}$$

where λ_K is the normal (i.e., laboratory) K electron-capture rate.

The total rate of free-electron capture by the nucleus is then given by equation 11.16, provided that f_i is calculated from equations (17.17), (17.18), and (17.24).

We shall now consider a number of individual cases which will illuminate the details of the neutron capture theory.

1) Abundance of Kr^{80}

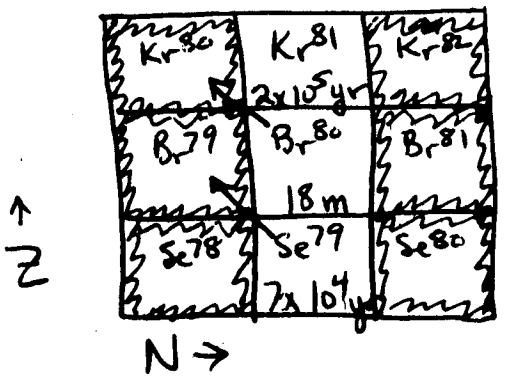

(Shading refers to stable isotopes, arrows indicate decay paths). The main capture path for neutron capture on a slow time scale passes through Se^{78}. What happens at Se^{79}? It has a rather long half-life in the laboratory, 7×10^4 years. If the mean time required for a neutron capture is short compared to the beta decay time of Se^{79}. then the capture path will continue through Se^{80}. On the other hand, if this is not the case then beta decay would give Br^{79}

and on the capture of a neutron the Br^{80} formed would beta decay to Kr^{80}. We can examine the abundance of Kr^{80} to see whether it has an abundance comparable to the abundance of the neighboring nuclei which are formed by neutron capture on a slow time scale, or whether it has an abundance comparable to the very much lower abundances of the neighboring nuclei which have been by-passed entirely by neutron capture. We also wish to see if the half-life of Se^{79} will change when we take possible photobeta reactions into account.

The abundance of Kr^{80} seems to be of the order of half of the abundance expected from neighboring even-even isobars that are formed by neutron capture on a slow time scale, which we will call half the "S" abundance. The abundance also happens to be about 6 times that of neighboring nuclei that are by-passed entirely and are presumably formed by the photonuclear reactions; we call this 6 times the "B" abundance. Evidently this is an intermediate case.

Consider the decay scheme:

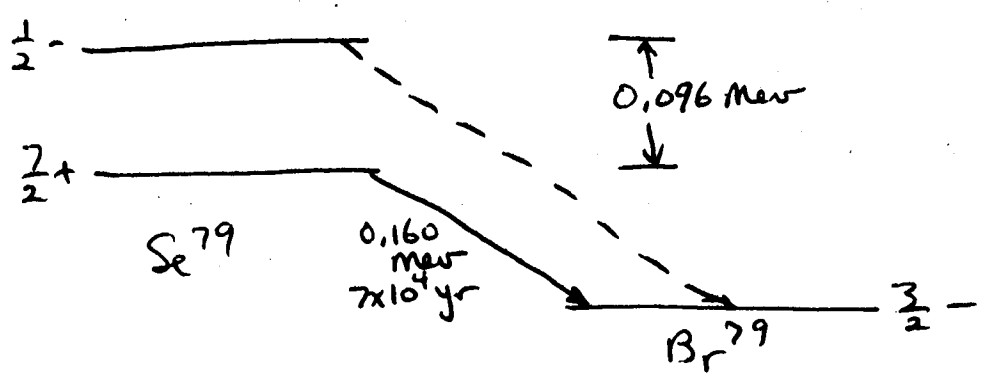

The 7/2(+) to 3/2(-) transition is first forbidden while the $\frac{1}{2}$(-) to 3/2(-) transition is allowed. Populating the excited state may speed the decay rate. To calculate, we assume

$$T_8 \sim 2.5 \sim \text{ excitation energy in a helium}$$

burning shell source in a massive star. Then, for the 0.096 Mev state,

$$\log f = -0.9.$$

We estimate that for this allowed transition

$$\log ft \approx 5.5$$

So

$$\log t \approx 6.4$$

and

$$t \approx 0.08 \text{ yr.} \sim 1 \text{ month is the half-life for}$$

decay to Br^{79} if the first excited state were the only state present. The population factor is, however,

$$a_i = 2.9\text{x}10^{-3}$$

and the effective half-life for Se^{79} decay is

$$t_{\frac{1}{2}} = \frac{0.08 \text{ years}}{2.9\text{x}10^{-3}} = 27 \text{ years,}$$

roughly. Since the abundance of Kr^{80} is about ½S, we may estimate the neutron capture lifetime of Se^{79}. Thus

$$t_n \sim 27 \text{ years.}$$

2) Abundance of Kr^{86}

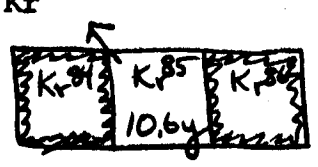

Kr^{86} has a closed shell of 50 neutrons. This is actually not a photo-beta case since the excitation energy of the first excited state is large enough so that its population is very small, at the temperatures which we consider. We discuss this in conjunction with the other cases because of the information it gives concerning the half-life of the neutron capture processes. Kr^{86} has an abundance that is of the order of 1/20 to 1/10 of S (slow time scale), and the order of 5 times the typical abundance in the neighborhood of the nuclei formed by neutron capture on a fast time scale, i.e., 5"F". Apparently there is some neutron capture in Kr^{85}. From the half-life involved and the relative abundance of K^{86} to that expected by different modes of formation, we may estimate that the neutron capture lifetime is

$$t_n \sim 150 \text{ years}$$

(not temperature sensitive since we consider an ordinary beta decay, not a photobeta reaction).

3) Abundance of Gd^{152}

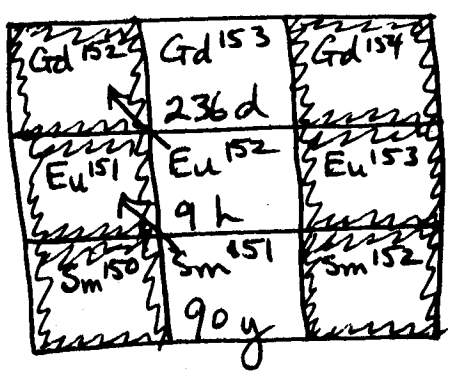

Sm^{150} lies on the slow time scale neutron capture path. We are interested in the abundance of Gd^{152} to see if there is branching of the neutron capture path, or if neutron capture is very fast compared to 90 years so that the path goes through Sm^{152}. The abundance of Gd^{152} is ~ B, the abundance of bypassed neighbors. The low lying states of Sm^{151} have unknown spins and parities; we cannot estimate whether the 90 year half-life is speeded by photobeta decay. We would not expect the half-life to be greater than that of the ground state, so we get the inequality

$$t_n \ll 90 \text{ years}$$

for the neutron capture lifetime in Sm^{151}.

Although 90 years does not seem radically different from 14 years in terms of the relative abundances involved, the cross section in this heavy rare earth region is very much larger than in a case such as Se^{79}. These values are not inconsistent with prior results.

4) Abundance of Er^{164}

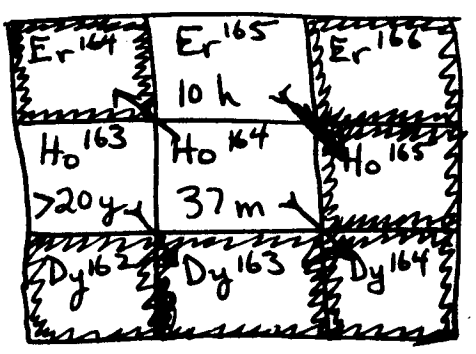

The abundance of Er^{164} is 1/3 that of its slow time scale neighbors and 15 times that of its bypassed neighbors. Hence the Er^{164} is apparently not bypassed as expected from first impressions. We consider the energy level diagram of Dy^{163}:

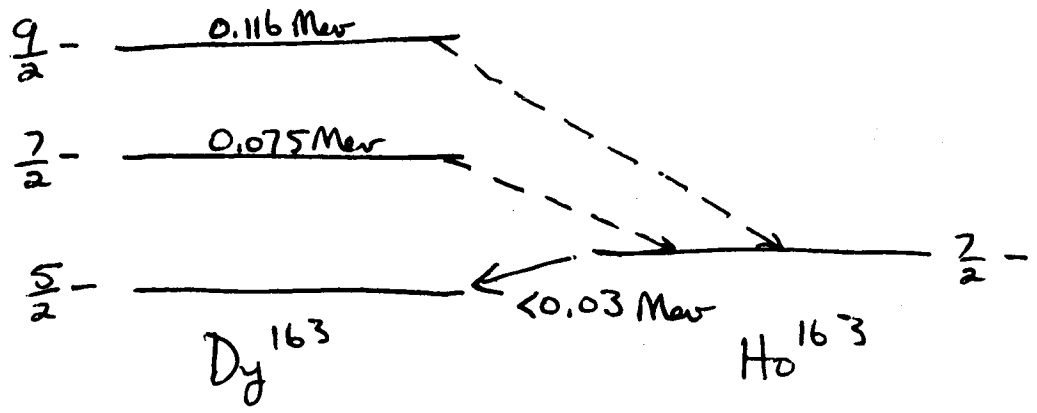

The half life of the Ho^{163} decay to the ground state of Dy^{163} is unknown. The transition energy is less than 0.03 Mev; for purposes of calculation we will use 0.01 Mev. The excited states of Dy^{163} can make allowed transitions to Ho^{163}. If we then have neutron capture to form Ho^{164}, 55% of this will decay to Er^{164}. This could explain the high abundance of Er^{164}.

	0.075 State	0.116 State
log f	~ -2.1	~ 0.9
log ft	~ 5.0	~5.0
log t	~ 7.1	~5.9
t	~ 0.4 yr	~0.025 yr
a_i	4.1×10^{-2}	7.6×10^{-4}
$t_{1/2}$	~9.6 yr	~ 33 yr

The total effective half life is

$$t_{\frac{1}{2}} = 7.5 \text{ years}$$

It appears that we should expect half of the neutron capture chain to go by way of Ho^{164}. Therefore, we say the half-life for neutron capture is

$$t_n \lesssim 7.5 \text{ years.}$$

5) Abundance of Hf^{176}

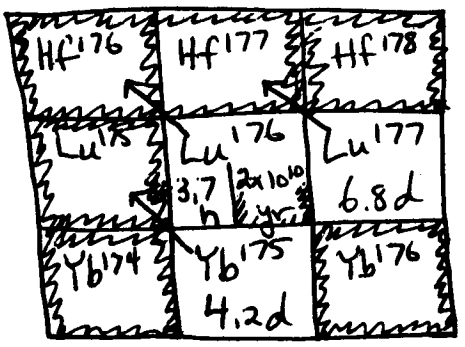

Lu^{175} lies on the neutron capture path. Lu^{176} is one of the rare exceptions in which beta decay from an excited state is faster than gamma decay to the ground state. The isomer has a half-life of 3.7 hours; the ground state, $2x10^{10}$ years. Since Lu^{175} is on the capture path, so must be Lu^{176}. Hf^{176} has an abundance of the order of 1/2 to 1 times the abundance of its slow time scale neighbors. We conclude that Lu^{176} has necessarily beta-decayed rapidly compared to neutron capture within Lu^{176}.

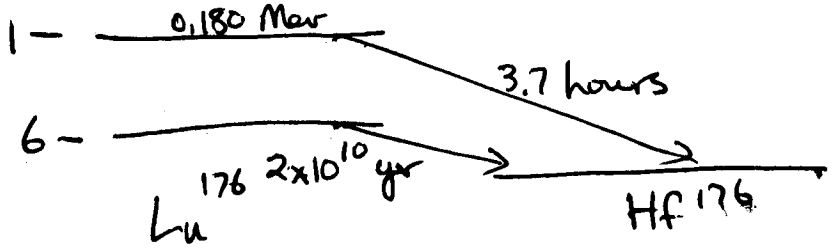

In this case,

$$a_i = 5.5\times10^{-5}$$

$$t_{\frac{1}{2}} = 7.6 \text{ yr} \quad \text{(photobeta)}$$

$$t_n \gtrsim 7.6 \text{ yr} \quad \text{(neutron capture)}$$

We must have an appreciable amount of decay through Hf^{176}.

We have enough cases to suggest that the spread in the numbers representing the neutron capture time scale is small. In the Hf case we found a lower limit and in the Er case, an upper limit. It seems the data are more homogeneously understandable if the spread in characteristic capture times has not been too great around the values we have mentioned.

6) The technetium puzzle.

There is another photobeta reaction which does not explain anything, but is instead a very considerable puzzle.

About 10 years ago Paul Merrill found lines of the element Tc in the red giant stars of spectral class S. It has subsequently been found that the abundances of all the heavy elements of the S stars seem to be increased, and the abundance of Tc seems comparable to that of its neighbors. It might be expected that some process of neutron capture on a slow time scale, taking place in the interior, has been responsible for forming an overabundance of heavy elements in these stars. Then

by some means, either a mixing of the material of the star or a stripping away of the outermost layers, the material that has been enriched in heavy elements comes to the surface. Tc has no stable isotope. Tc^{97} has a half-life of 2.6×10^6 years, and is well shielded from the neutron capture path. Tc^{99} has a half-life of 2.1×10^5 years and is on the neutron capture path. These half-lives are of the order of the time we expect the more massive stars to spend in the red giant stage.

The level diagram for Tc^{99} is

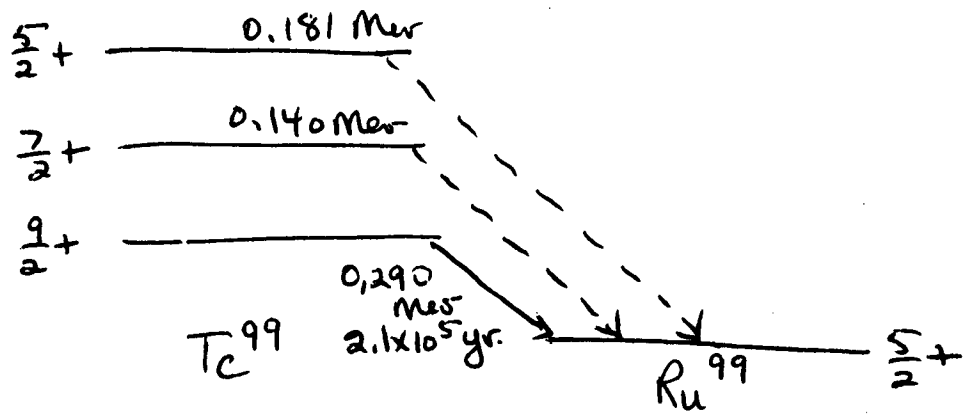

	0.140 State	0.081 State
log f	1.4	1.8
log ft	~5.5	~5.5
log t	~4.1	~3.7
t	~ 0.00043 yr	~1.45×10^{-4} yr.
a_i	~ 1.23×10^{-3}	~1.34×10^{-4} yr
$t_{\frac{1}{2}}$	~ 0.35 yr.	~ 1.08 yr.

The total half-life is

$$t_{\frac{1}{2}} = 0.26 \text{ yrs.}$$

What does this mean? The formation of Tc^{97} would require photobeta reactions in the stable nucleus Mo^{97}, but there is no known excited state of Mo^{97} that would be suitable for that purpose. The first excited state is 0.67 Mev, which is sufficiently high to give an extremely small Boltzmann factor, and consequently no significant decay to Tc^{97} is expected. Not only that, but the Tc^{97} can have an enhanced photobeta decay back to Mo^{97}. Also, Tc^{99} has a half-life that is very short compared to typical neutron capture times that we have been discussing for the sources that have given us the elements. We do not know that type S red giant stars have made any massive contribution of their elements to us, but if they have their contribution would tend toward a spread in the high neutron flux or short neutron capture half-life. This strains the interpretations we previously made. It is difficult to understand how improvement will be made if we assume the log ft values are large. It is possible, but unlikely. A flash in the neutron production which locally speeds up capture might be a possible explanation, but no very specific mechanism has been offered, and the puzzle remains.

18. Heavy Ion Thermonuclear Reactions

After the exhaustion of helium, we find that C^{12} and O^{16}

will participate in a series of thermonuclear reactions if the temperature is sufficiently high. The theory for these reactions is not as good as might be desired. One reason is that the Bessel-Clifford expansion for the coulomb wave functions is no longer applicable. Secondly, theoretical treatment of collisions between heavy ions cannot make use of the same technique applied to collisions between a light particle and a heavy nucleus. For example, it is not useful to speak of a C^{12} nucleus moving in the potential well of another C^{12} nucleus. Again, when heavy ions collide we will have contributions from a wider range of momenta than previously. Besides the problems this raises in summation over the range of angular momenta, the effects may exhibit themselves in a more basic manner. For instance, the C^{12} plus C^{12} system seems to form a quasi-molecule, that is a sort of dumbbell configuration in which the nuclear attractive forces balance the electrostatic and centrifugal repulsive forces. The cross section curve for the C^{12} plus C^{12} complex has large wiggles which are probably the result of the formation of these quasi-molecules. Our basic problem is to extrapolate experimental cross-sections to low energies despite this gross resonant structure of the quasi-molecules.

To add to our difficulties, the C^{12} nucleus has a large spread

in density at the edge. Consequently the problem does not separate into pure coulomb and pure nuclear effects easily, and our usual Wigner-Eisenbud formulation of nuclear reaction theory does not work well with naive application*.

The following reactions can take place:

Reaction		Q
$C^{12} + C^{12}$	$\rightarrow$ $Mg^{24} + \gamma$	13.930 Mev
	$Na^{23} + p$	2.238
	$Ne^{20} + \alpha$	4.616
	$Mg^{23} + n$	-2.605
	$O^{16} + 2\alpha$	-0.114

These reactions will be taking place at a temperature of the order of 700 million degrees, so a new feature appears: the exothermic production of lighter charged particles, which we expect to be rapidly reabsorbed on other nuclei. This makes the whole process quite complicated. In general, capture in the elements with low Z is favored. In particular,

$$Ne^{20}\ (\alpha,\gamma)\ Mg^{24}$$

$$Na^{23}\ (p,\gamma)\ Mg^{24}$$

have a high yield. Proton capture can form an abundance tail

*For a fuller treatment, see: A.G.W. Cameron, Astrophys. J. Vol. 130, No. 2, p. 429, September, 1959.

extending beyond Mg^{24} but declining rapidly.

The reaction forming $Mg^{24} + \gamma$ and that forming $O^{16} + 2\alpha$ can be shown to have negligibly small reaction rates. The reactions forming p's and α's should have comparable yields. A recent estimate of the reaction rate due to Fowler and given by Reeves is:

$$\log_{10} \frac{p}{\rho\, x_{12}\, f} = 26.9 - \frac{36.57}{T_9^{1/3}[1+0.08T_9]^{1/3}} - \frac{2}{3}\log_{10} T_9$$

This is uncertain by at least a factor of 10. Neutron emission is sufficiently endothermic that we do not need to worry about the direct effects of neutron emission, although some neutrons are formed.

If we are near the beginning of the carbon burning process the protons and alphas formed can react with C^{12} by

$$C^{12}(p,\gamma)N^{13}\ (\beta^+\nu)\ C^{13},\ \tau_\beta = 871 \text{ sec.}$$
$$C^{13}(\alpha,\eta)O^{16}$$

The neutrons formed may add predominantly to the heavy nuclei which, presumably, have already built up in the stellar interior by (α,n) reactions. At higher temperatures the reaction

$$N^{13}(\gamma,p)C^{12}\ ,\quad Q = -\ 1.941 \text{ Mev}$$

may occur faster than positron decay, in which case neutron production by this means is blocked. The photodisintegration

rate (calculated in a manner to be outlined later) gives:

$$\tau_p = 1.05\text{x}10^{-15} \exp\left(\frac{27.45}{T_9}\right)$$

We have

T_9	$\tau_p/(\tau_\beta+\tau_p)$
≤ 0.65	~ 1
0.7	10^{-1}
0.75	10^{-2}

where τ_p is the lifetime for photonuclear ejection of a proton and τ_β is the lifetime for beta decay. At higher temperatures the protons will be captured preferentially by the heavier nuclei. Once blocking occurs, this ratio gives fairly well the factor by which neutron production is decreased. The presence of neutrino emission may raise the temperature and accentuate this effect.

Now we consider oxygen burning.

Reaction		Q
$O^{16} + O^{16} \rightarrow$	$S^{32} + \gamma$	16.539 Mev
	$P^{31} + p$	7.676
	$Si^{31} + n$	5.417
	$Si^{28} + \alpha$	9.593
	$Mg^{24} + 2\alpha$	-0.393
	$Si^{30} + 2p$	0.424

Of the most important reactions, it is probable that protons and alphas have comparable yields while neutrons have a somewhat smaller yield. The reaction rate (again due to Fowler) gives

$$\log_{10} \frac{p}{\rho x_{16} f} = 38.0 - \frac{59.04}{T_9^{1/3}}[1+0.08T_9]^{1/3} - \frac{2}{3}\log_{10} T_9$$

The reactions will take place at $T_9 \sim 1.5$ but, as we shall see, they are strongly dependent on the neutrino emission effects. The protons, alphas and neutrons formed by these reactions are rapidly recaptured. The main products are Si^{28}, S^{32}, and other nuclei in the range $A \leq 36$. Neutrons will be of limited usefulness in neutron capture on a slow time scale because (γ,n) reactions will block the flow at points of low neutron binding energy. So we see that after heavy ion thermonuclear reactions large amounts of Mg^{24}, Si^{28}, S^{32} and lesser amounts of their neighbors are formed.

19. Photonuclear Reactions

We shall now discuss the subject of photonuclear reactions briefly. Consider the equilibrium between two constituents with number densities n_1 and n_2 and their compound nucleus n_{12}:

$$\frac{n_1 n_2}{n_{12}} = \left(\frac{2\pi\, m_1 m_2}{m_1 + m_2}\frac{k}{}\right)^{3/2} \frac{T^{3/2}}{h^3} \frac{\omega_1 \omega_2}{\omega_{12}} e^{\chi/kT}$$

where the ω's are statistical weights and χ is the energy of the compound state above the sum of masses of the constituents. Now, the probability of photodisintegration per unit time is $\lambda\ n_{12}$ while the probability of formation per unit time is

$$r = n_1\ n_2 \langle\sigma v\rangle = q\ n_1\ n_2$$

in our previous notation. In equilibrium, the rate of formation equals the rate of disintegration so

$$\lambda n_{12} = q n_1 n_2$$

$$\lambda = q\left(\frac{n_1 n_2}{n_{12}}\right)$$

$$= 1.89\text{x}10^{29} \left(\frac{A_1 A_2}{A_1 + A_2}\right)^{3/2} \frac{\omega_1 \omega_2}{\omega_{12}} \langle\sigma v\rangle\ T_6^{3/2}\ e^{-0.0116\ \chi/T_6}$$

We will apply this to the case of photodisintegration of Ne^{20}.

$$Ne^{20}(\gamma,\alpha)\ O^{16}, \quad Q = -\ 4.730 \text{ Mev}$$

From our previous examination of the inverse reaction, we know that the excited state of 4.97 Mev in Ne^{20} does not act as a resonance for α capture to form Ne^{20}, but that the two higher states do. In this case we have contributions from these two levels.

5.64 Mev level:

$$\log_{10} p = 12.7 \begin{pmatrix}+0.2\\-0.5\end{pmatrix} - 28.4/T_9$$

5.80 Mev level:

$$\log_{10} p = 13.40 - 29.3/T_9 \pm \text{(factor of 10)}$$

We will have $Ne^{20}(\gamma,\alpha)O^{16}$ taking place near $T_9 = 1.3$ or at a slightly lower temperature than for oxygen burning. The alpha particles will be captured mainly by Ne^{20} since the reaction

$$O^{16}\ (\alpha,\gamma)Ne^{20}$$

merely undoes the work of the photodisintegration reactions. Thus the main products will be O^{16} and Mg^{24}.